ACTA CHIMICA

ACADEMIAE SCIENTIARUM HUNGARICAE

ADIUVANTIBUS

V. BRUCKNER, GY. DEÁK, K. POLINSZKY,
E. PUNGOR, G. SCHAY, Z. G. SZABÓ

REDIGIT

B. LENGYEL

TOMUS 84 FASCICULUS 1

AKADÉMIAI KIADÓ, BUDAPEST

1975

ACTA CHIM. (BUDAPEST) ACASA 2 84 (1) 1–119 (1975)

ACTA CHIMICA

A MAGYAR TUDOMÁNYOS AKADÉMIA KÉMIAI TUDOMÁNYOK OSZTÁLYÁNAK IDEGEN NYELVŰ KÖZLEMÉNYEI

SZERKESZTI

LENGYEL BÉLA

TECHNIKAI SZERKESZTŐK

DEÁK GYULA és HARASZTHY-PAPP MELINDA

Az Acta Chimica német, angol, francia és orosz nyelven közöl értekezéseket a kémiai tudományok köréből.

Az Acta Chimica változó terjedelmű füzetekben jelenik meg, egy-egy kötet négy füzetből áll. Évente átlag négy kötet jelenik meg.

A közlésre szánt kéziratok a szerkesztőség címére (Budapest 112/91 Műegyetem) küldendők.

Ugyanerre a címre küldendő minden szerkesztőségi levelezés. A szerkesztőség kéziratokat nem ad vissza.

Megrendelhető a belföld számára az „Akadémiai Kiadó"-nál (1363 Budapest Pf 24. Bankszámla 215 11488), a külföld számára pedig a „Kultúra" Könyv- és Hírlap Külkereskedelmi Vállalatnál (1389 Budapest 62, P. O. B. 149. Bankszámla: 218 10990) vagy annak külföldi képviseleteinél és bizományosainál.

Die Acta Chimica veröffentlichen Abhandlungen aus dem Bereich der chemischen Wissenschaften in deutscher, englischer, französischer und russischer Sprache.

Die Acta Chimica erscheinen in Heften wechselnden Umfanges. Vier Hefte bilden einen Band. Jährlich erscheinen 4 Bände.

Die zur Veröffentlichung bestimmten Manuskripte sind an folgende Adresse zu senden:

Acta Chimica
Budapest 112/91 Műegyetem

An die gleiche Anschrift ist auch jede für die Redaktion bestimmte Korrespondenz zu richten. Abonnementspreis pro Band: $ 32.00.

Bestellbar bei dem Buch- und Zeitungs-Außenhandels-Unternehmen »*Kultúra*« (1389 Budapest 62, P. O. B. 149 Bankkonto Nr. 218 10990) oder bei seinen Auslandsvertretungen und Kommissionären.

ACTA CHIMICA

ACADEMIAE SCIENTIARUM HUNGARICAE

ADIUVANTIBUS

V. BRUCKNER, GY. DEÁK, K. POLINSZKY,
E. PUNGOR, G. SCHAY, Z. G. SZABÓ

REDIGIT

B. LENGYEL

TOMUS 84

AKADÉMIAI KIADÓ, BUDAPEST

1975

ACTA CHIMICA

TOMUS 84

FASCICULUS 1
FASCICULUS 2
FASCICULUS 3
FASCICULUS 4

INDEX

BERECZ, E.: Study of the Viscosity of Metal Chloride–H_2O and Metal Chloride–HCl–H_2O Systems 353

BEYER, H. Beiträge zur Kenntnis der Krackreaktionen, II. Kinetik der katalytischen Krackung von Propan sowie *n*-und i-Butan an H-Klinoptilolit (Contribution to the Knowledge of Cracking Reactions, II. Kinetics of the Catalytic Cracking of Propane Further of *n*- and iso-Butane) 7

BEYER, H., PAPP, J. und KALLÓ, D.: Irreversibel Strukturveränderungen von H-Faujasit, H-Mordenit und H-Klinoptilolit durch thermische Behandlung und Einwirkung von Wasser (Irreversible Structural Changes of H-Faujasite, H-Mordenite and H-Klinoptilolite by Thermal Treatment and the Action of Water) 25

BÉKÁSSY, S. s. HEISZMAN, J.

BOGNÁR, R. s. DÁVID É.

BOGNÁR R. s. FARKAS, I.

BOGNÁR, R. s. SZTARICSKAI, F.

BOSE, A. K. s. MUSHRAN, S. P.

CLAUDER, O. s. DÓRA-HORVÁTH, K.

CLAUDER, O. s. SHAMS EL-DINE, SH. A.

CZIRA, G. s. DINYA, Z.

CYVIN, J. s. CYVIN, N.

CYVIN, N. HARGITTAI, M. and CYVIN, J.: On the Ring Puckering of the Trimeric Tungsten Trioxide Molecule 55

CSER, F., and HARDY, GY.: Structural Studies on Polycenaphthylene 297

DANCSI, L. s. TAMÁS, J.

DÁVID, E., BOGNÁR, R.: The Reactivity of the Carbonyl Group in Flavonoid Compounds I. Kinetic Studies on the Formation of 2,4-Dinitrophenyl-hydrazones 335

DEÁK, GY., GÁLL-ISTÓK, K., HAZAI, L.: Synthesis of Arylidene-*bis*-(Phenyl-acetamides) (Short Communication) 477

DINYA, Z., LITKEI, GY., TAMÁS, J. and CZIRA, G.: Structural Investigation of Flavonides and Their Model Compounds, VII. Calculation and Determination of the Ionization Potential of 4-and 4'-Monosubstituted Chalcones (Short Communication) 181

DÓRA-HORVÁTH, K., CLAUDER, O.: Alkaloids Containing the Indolo [2,3-c]quinazolino [3,2-a] pyridine Skeleton, III. 3,14-Dihydrorutecarpine 93

ELKASCHEF, M. A.-F., FAROUK, M. E. ABDEL-MEGEID, MOKHTAR, K.-E. M. and GAD, F. A.: 4-Pyrones, VII. Further Reactions of 4-Pyrones 319

ELKASCHEF, M. A.-F., FAROUK M. E. ABDEL-MEGEID, SALAH, M. M. ELZEIN: Triarylmethanes, VI. Reactions of Naphtoquinone Diphenylmethides with Organometallic Compounds 187

FARKAS, I., BOGNÁR, R., MENYHÉRT, M. M., TARNAI, A. K.: Selektive Spaltung von Thioglykosiden mit Dichlormethyl-Methyläther (On the Selective Splitting of Thioglycosides with Dichloromethyl-methylether) 325

FARKAS, J. s. KISS, L.

FAROUK, M. E. ABDEL-MEGEID. s. ELKASCHEF, M. A.-F.

FEJES, P. s. KÖNIG, P.

FEKETE, E. and INCZÉDY, J.: Ion Exchange Equilibria of Some Monovalent Anions 121

Fiedorow, R. s. Wojciechowska, M.
Fuzailov, Sh. s. Tashmukhamedov
Gerecs, Á.: Acetolysis of *o*-Tetraacetyl-1-Deoxy-1-(2',4'-Di-nitrophenylhydrazino)-D-Glucopyranose (Short Communication) 467
Géczy, I.: Synthetic Linear Polymers, XXXII. Changes in the Dipole Moment of Polymer Homologous Compounds as a Function of the Molecular Weight 289
Hajós, A.: Synthesis of *Threo-* and Erythro-*β-o*-Tolylserine and Their Derivatives .. 471
Hardy, Gy. s. Cser, F.
Hargittai, M. Cyvin, N.
Harsányi, K., Héja, G. und Korbonits, D.: Basische Ester mit Antiarrhythmischer Wirkung. (Basic Esters with Antiarrhythmic Action) 217
Harsányi, K. s. Pálosi, E.
Hazai, L. s. Deák, Gy.
Hegedüs-Vajda, J. s. Tamás, J.
Heiszman, J., Payer, K., Békássy, S., Petró, J.: Complex Study of Nickel Skeleton Catalysts, I. Thermal Desorption Method and Apparatus for the Study of Hydrogenation Catalysts 431
Héja, G. s. Harsányi, K.
Héja, G. s. Pálosi, E.
Huszti, Zs., s. Kasztreiner, E.
Ikrényi, K.: Tandem Titrator 229
Inczédy, J. s. Fekete, E.
Kalló, D. s. Beyer, H.
Karabaev, A. Sh. s. Tashmukhamedov, S. A.
Kasztreiner, E. s. Sohár, P.
Kasztreiner, E., Szilágyi, G., Kosáry, J., Huszti, Zs.: Synthesis of O-Substituted Hydrosylamines 167
Kiss, A. B.: Infrared Vibrational Frequencies of Reduced Tungsten Oxides WO_{3-x} $(1 \geq x > 0)$ 393
Kiss, Á. I. s. Martin, A.
Kiss, L. and Farkas, J.: Kinetic Equations of Multistep Electrode Processes, I .. 161
Kisfaludy, L. and Schön, I: Rapid Synthesis of Oxytocin (Short Communication) . 227
Kisfaludy, L. s. Tamás, L.
Korbonits, D. s. Harsányi, K.
Kosáry, J. s. Kasztreiner, E.
Kosáry, J. s. Sohár, P.
Kovács, J., Teplán, I. and Mező, I.: Labelled Amino Acids and Their Derivatives, V. Resolution of *p*-Chloro-DL-phenylalanine. Preparation of L-Phenylalanine-4[3]H from *p*-chloro-L-phenylalanine 109
Kőnig, P. und Fejes, P.: Über die Möglichkeiten der digitalen Bestimmung der Parameter der kontakt-katalytischen Hydrierung von Äthylen, III. Die "Schätzung" der Geschwindigkeitskonstanten für den stationären Fall. (On the Possibilities of the Digital Determination of the Parameters of the Contact-Catalytic Hydration of Ethylene, III. Estimation of the Rate Constants for the Steady State) 141
Kuczynsky, W. s. Wojcieshowska, M.
Larin, P. O. s. Tashmukhamedov, S. A.
László-Parragi, M. s. Ratkovics, F.
Lévai, A., Lipták, A., Pintér, I. and Snatzke, G.: Circular Dichroism, LXVI. Chiroptical Properties of Some Mono- and Polysubstituted Phenyl Glycosides 99
Lipták, A. s. Lévai, A.
Lipták, A. s. Nánási, P.
Liszi, J.: Dipole Association of Nitrobenzene in Non-polar Solvents 125
Litkei, Gy. s. Dinya, Z.
Martin, A., and Kiss, Á. I.: Calculation of the π-Electronic Structure and Spectra of Hetero-Disubstituted Halobenzenes by the MIM and PPP Methods 259
McCorkindale, N. J. s. Paál, Z.
Menyhárt, M. M. s. Farkas, I.
Mező, I. s. Kovács, J.
Mokhtar, K.-E. M. s. Elkaschef, M. A.-F.
Mushran, S. P., Sanehi, R. and Bose, A. K.: Mechanism of Cyclohexanone Oxidation by Chloramine-T 135
Nagy, Z. s. Sámsoni, Z.
Nádor, K. s. Scheiber, P.

Nánási, P. and Lipták, A.: Carbohydrate Methyl Ethers, V. Synthesis of Phenyl-β-D-glucopyranoside Derivatives Partially Methylated on Their Sugar Moiety. Preparation of 4,6-di-O-, 2,4,6-tri-O- and 3,4,6-tri-O-Methyl-D-glucose 63
Ocskay, Gy. s. Sohár, P.
Otta, K. H. s. Zsadon, B.
Paál, Z., Thomson, J. S., Webb, G., McCorkindale, N. J.: Interactions of Unsaturated Hydrocarbons with Platinum Catalysts: Involving Reactions, Retention, Deactivation, and Regeneration 445
Papp, J. s. Beyer, H.
Payer, K. s. Heiszman, J.
Pálosi, E., Harsányi, K. und Héja, G.: 4-S-substituierte 2,6-Dinitro-aniline. (4-S-substituted 2,6-Dinitroanilines) 205
Petró, J. s. Heiszman, J.
Pintér, I. s. Lévai, A.
Prasad, R. N. s. Singh, O. P.
Puskás, M. M. s. Sztaricskai, F.
Ratkovics, F. and László-Parragi, M.: Properties of Alcohol–Amine Mixtures, VII. Conductivity of *n*-Butylamine–Alcohol Mixtures 45
Recensiones 115
Saheni, R. s. Mushran, S. P.
Salah, M. M. Elzein. s. Elkaschef, M. A.-F.
Shams El-Dine, Sh. A. and Clauder, O.: Derivatives of 1,3,4-Thiadiazole as Potential Schistosomicides 85
Sámsoni, Z. and Nagy, Z.: Objective Method for Measuring the Length of Wedge-Shaped Spectrum Lines 1
Sárkány, A. Guczi, L. und Tétényi, P.: Über den Mechanismus der an Nickelpulver katalysierten Hydrogenolyse von Butan. (On the Mechanismus of the Hydrogenolysis of Butane Over Nickel Dust Catalyst) 245
Scheiber, P. and Nádor, K.: Conformation of 3,7-Diazabicyclo[3.3.1] Nonanes 193
Schön, I. s. Kisfaludy, L.
Singh, O. P., Prasad, R. N., Tandon, J. P.: Tin(IV) Complexes of Schiff Bases Derived from *o*-Hydroxyacetophenone and Aminoalcohols 459
Singh, S. P., Tandon, J. P.: pH-Metric Studies on the Mixed-Ligand Chelates of Oxovanadium(IV) with Picolinic Acid and Some Dicarboxylic Acids 419
Snatzke, G. s. Lévai A.
Sohár, P., Kosáry, J. and Kasztreiner, E.: Diamagnetic Shielding of the Dibenzocycloheptatrien Ring System in Some Acylaminomalonic Ester Derivatives ... 201
Sohár, P., Ocskay, Gy., Vargha, L.: Distinction betwen *Syn* and *Anti* Ketoximes of 2-Aryl-Furans and Their Condensed Analogues by Their NMR Spectra 381
Srivastava, R. D., Sushil Kumar: Electrodeposition of Cobalt, II. Cathode Polarization and Grain Size of the Deposit 385
Sushil Kumar s. Srivastava, R. D.
Szabó, I. s. Szotyori, L.
Szilágyi G. s. Kasztreiner, E.
Szotyory, L. Ujhidy, A. und Szabó, I.: Reaktionskinetische Beiträge zur Untersuchung der Ringschlussreaktion von Carbäthoxy-2-(3-Chlorphenylamino)-äthylacrylat (Reaction Kinetic Contributions to the Investigation of the Ring-Closing Reaction of Carbethoxy-2-(3-chlorophenylamino)-ethylacrylate) 279
Sztaricskai, F., Bognár, R. and Puskás, M. M.: Structural Investigation of the Antibiotic Ristomycin A. Chemical Structure of the Oligosaccharide Part of Ristomycin A 75
Tamás, J., Hegedüs-Vajda, J., Dancsi, L., Kisfaludy, L.: Mass Spectra of Some α-Amynooxy Acid Derivatives 409
Tamás, J. s. Dinya, Z.
Tandon, J. P. s. Singh, O. P.
Tarnai, A. K. s. Farkas, I.
Tashmukhamedov, S. A., Karabaev, S. Sh., Fuzailov, Sh., Larin, P. O., Tillaev, R. S., and Usmanov, Kh. U.: (Synthesis and Study of Polyvinyl Alcohol–Polyvinylpyrrolidone Graft Copolymer Solutions) 343
Teplán, I. s. Kovács, J.
Tétényi, P. s. Sárkány, A.
Tétényi, P. s. Zsadon, B.
Thomson, J. S. s. Paál, Z.

Tillaev, R. S. s. Tashmukhamedov, S. A.
Újhidy, A. S. Szotyori, L.
Usmanov, Kh. U. s. Tashmukhamedov, S. A.
Varga, L. s. Sohár, P.
Webb, G. s. Paál, Z.
Wojciechowska, M., Fiedorow, R. and Kuczynski, W.: Catalytic Properties of Magnesium Fluoride 313
Zsadon, B., Otta, K. H. and Tétényi, P.: Minor Alkaloids from the Seeds of *Amsonia Tabernaemontana*: (+)—1,2-Dehydroaspidospermidine, (—)-Tetrahydroalstonine and (—)-Quebrachamine 71

Acta Chimica Academiae Scientiarum Hungaricae, Tomus 84 (1), pp. 1—6 (1975)

OBJECTIVE METHOD FOR MEASURING THE LENGTH OF WEDGE-SHAPED SPECTRUM LINES*

Z. SÁMSONI** and Z. NAGY***

*(**Institute for Nuclear Research of the Hungarian Academy of Sciences, Debrecen, and ***Central Research Laboratory of the Medical University, Debrecen)*

Received December 18, 1973

A novel method and equipment have been developed to measure accurately the length of wedge-shaped spectrum lines. The equipment, which contains two phototransistors in differential connection, permits a more accurate and objective measurement of the length of spectrum lines. By moving the spectrum in front of the photodetectors the end-point of a spectrum line is determined with a zero-instrument connected to the detectors. The photographic densities of the line and of the background in a line-free section of the spectrum are detected separately by the two phototransistors. The end of a line is assigned to the point where the instrument returns to the zero position. The length of the shift can be read directly on a digital scale to an accuracy of 0.1 mm. Experimental errors in line length can be reduced to 7—9% from 13—15%.

The logarithmic sector method [1, 2], which has long been used in spectrography and the logarithmic filter method developed recently by us [3] are readily applicable in rapid, orientative analysis. The spectra obtained under these conditions consist of wedge-shaped lines proportional in length to the logarithms of the original line intensities. Relative intensities or concentrations can therefore be determined very simply by length measurements. With this technique, however, the wedge-shaped lines, instead of having sharp boundaries, disappear gradually in the background veil of the photographic plate, and their visual evaluation is therefore subject to ambiguities, rendering the length measurement inaccurate [4—13]. The experimental error depends on various factors including the physiological state of the operator and his eyes, the actual contrast-sensitivity of the latter, the illumination of the laboratory, etc.

It has been pointed out in one of our earlier papers [14] that the performance of the logarithmic sector method can be greatly improved by length measurements based on photoelectric end-point detection. The rapid advancement in the application of semiconductors enabled us to design a relatively simple device and to develop a method whereby the determination of line length can substantially be increased in accuracy.

* Presented at the XVIIth Colloquium Spectroscopicum Internationale, Florence, Sept. 16—22, 1973.

1. Principles and design

The equipment consists of two main parts:

(i) a projector table, which contains the photodetectors and the means for length measurements, and can be mounted on the spectrum projector, and

(ii) an electrical power supply and a zero-instrument connected to an amplifier.

A magnified section of the spectrum is projected onto the photoelectric detector through a small circular diaphragm, the line to be measured is moved in front of the diaphragm in the direction of decreasing intensities, and the end of the line is located with the aid of the zero-instrument attached to the photoelectric detector. The distance between the end-point thus obtained and

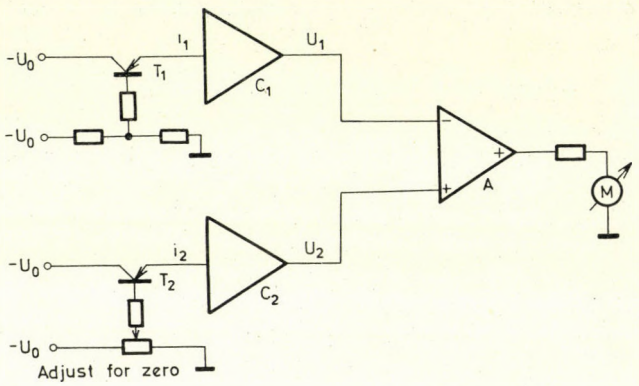

Fig. 1. Electronic block diagram of the LLL Densitometer

the base of the line, *i.e.* the length of the line, is determined with a measuring thread which can be moved in a direction perpendicular to the line. The thread is set to the base of the line and the displacement can be read on a digital scale. The measuring apparatus is built into the pane of the projector table fitted to the spectrum projector. The photodetectors are placed below, and the circular diaphragms adjustable according to the line width, above the pane.

The electronic block diagram of the equipment is shown in Fig. 1.

Phototransistors T_1 and T_2 act as photodetectors. Currents i_1 and i_2 passing through these detectors and proportional to the intensities of incident light, are converted into voltages U_1 and U_2, proportional to the intensities, using the current-voltage transducers C_1 and C_2. The difference in voltage is produced by differential amplifier A, and measured with meter M, the zero point of which can be set by adjusting the static basis current of transistor T_2.

After its purpose, the device has been named LLL Densitometer (*L*ogarithmic *L*ine *L*ength Densitometer).

The equipment has been adapted to a Zeiss SP-2 spectrum projector, but it can be mounted, of course, on any other type.

2. Measurement of line length with LLL Densitometer

The diaphragm in front of the photodetectors is adjusted according to the line widths in the spectrum projected onto the measuring table. The instrument is set to zero at a position where both detectors are exposed to direct light, *i.e.* to an exposure corresponding to the background veil of the photographic plate. Then the head enclosing the photodetectors is turned with a handle into a position where the measuring detector is exposed to the projected image of the line to be measured, and the reference detector to a line-free section of the spectrum. By moving the spectrographic plate, the visually observable end of the line is shifted to below the photodetector. The arm of the zero-instrument departs from its position. The line is now shifted further to find the point where the arm just returns to zero. (During this operation the reference detector is always exposed to a direct light which corresponds to the prevailing background veil.) The extent of shift, *i.e.* the length of the line is determined by moving the measuring thread supplied with a digital readout to the well-defined base point of the line. The equipment permits the measurement of spectral lines at most 140 mm in length to an accuracy of 0.1 mm.

The method can also be applied to the evaluation of densely spaced spectra where it cannot be ensured that the reference detector is always exposed to direct light. In such cases the reference detector is barred from the incident light, and a reference signal corresponding to the background intensity in the vicinity of the end point of the line is produced electronically. The further operations are the same as above.

3. Comparison of measurements with a mm-scale and LLL Densitometer

Recording conditions:
Spectrograph: Zeiss Q 24
Electrodes: C/Fe
Plate: Agfa Gevaert Sciencia 23 D 50 and 23 D 56
Logarithmic filter: 0.33 A/mm*, Ni–Cr metal film on a quartz lens of f = 200 mm
Diaphragms: 15, 25 and 50 μm
Exposure: 10 – 60 s
Excitation: AC-arc, 3 – 5 Amp (high-frequency ignition)
Imaging: Zeiss, three-step medium
Development: KODAK D-19, 4 min at 20°C

The performance of the LLL Densitometer was compared with that of visual evaluation using a mm-scale, for measurements on the spectrum of iron.

* $A = -\log T$

The differences in line length were measured on 10 multiplet lines in the spectra between 316.1 and 324.4 mm, which correspond to known relative intensities. The measurements were performed by two different person. A third person evaluated the same lines with an LLL Densitometer. The reference iron line at 321.7 μm, the intensity of which was taken to be 1.00, was measured ten times in all spectra, the other lines were evaluated only once. The calculated average differences in line length along with the corresponding dispersions of measurements (s) for the various intensity groups are given in Table I. The data include measurements on 10 iron lines in each of the 51 spectra taken on 12 plates.

Table I

Comparison of subjective and objective measurements of line length

Wave-length (nm)	Line intensity	Subjective visual evaluation		Objective evaluation with LLLD	
		$\pm s$ (mm)	s_{rel}%	$\pm s$ (mm)	s_{rel}%
316.2	0,36	$-18{,}7 \pm 1{,}1$	5,9	-15.5 ± 0.9	5.8
317.8	0.52	-14.3 ± 0.8	5.6	-11.7 ± 0.8	6.8
316.1	0.63	$-\ 8.4 \pm 1.0$	11.9	$-\ 6.8 \pm 0.8$	11.8
317.5	0.69	$-\ 8.4 \pm 0.9$	10.7	$-\ 6.3 \pm 0.6$	9.5
321.7	1.00	0.0 ± 0.0		0.0 ± 0.0	
32.05	1.34	2.7 ± 0.9	33.3	5.6 ± 0.7	12.5
320.0	1.65	4.2 ± 1.1	26.2	9.6 ± 0.6	6.2
324.4	1.93	8.0 ± 0.8	10.0	9.8 ± 0.7	7.2
323.9	2.22	10.3 ± 0.1	9.7	12.8 ± 0.7	5.5
322.2	4.90	26.1 ± 0.9	3.4	27.2 ± 0.9	3.3

The differences in line length, Δl, measured in two ways, are plotted against the logarithms of relative line intensities in Fig. 2.

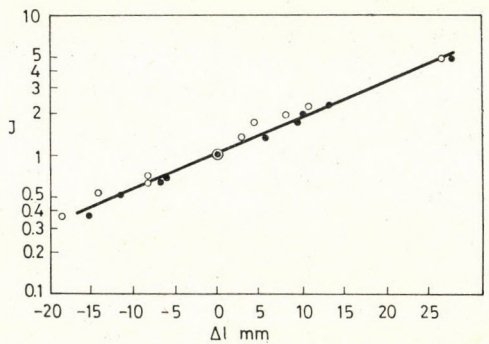

Fig. 2. The differences in line length for the multiplet lines of the iron spectrum (Fe line at 321.7 nm, I = 1.00), as a function of the relative line intensity. ● Densitometric measurements; ○ visual evaluation

Full circles in the diagram denote densitometric results, whereas empty circles indicate visually obtained data. It can be seen that the points corresponding to instrumental measurements lie closer to the theoretical straight line, and can therefore be regarded more accurate. A line is, in general, measured to be shorter by the subjective, visual method than with the instrument. The dispersion ranges of objective and subjective measurements are compared in Fig. 3, where the per cent dispersions assigned to the averages in the various intensity groups are given.

Empty blocks in the histogram refer to instrumental, shaded blocks to visual measurements.

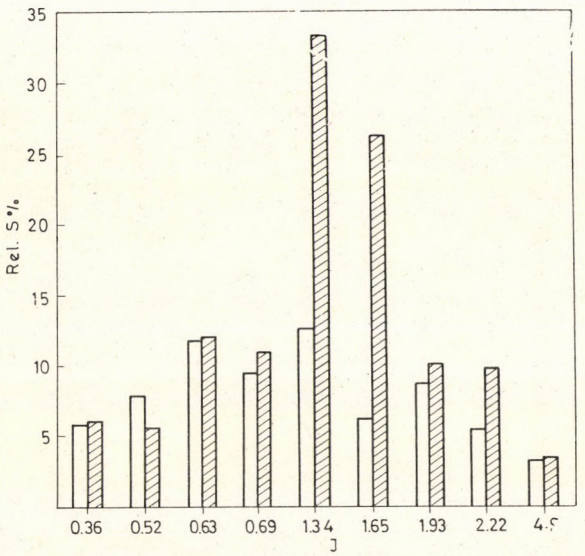

Fig. 3. Dispersion ranges ($s_{rel}\%$) of the differences in line length for the multiplets of the iron spectrum. Empty blocks: densitometric measurements; shaded blocks: visual evaluation

4. Discussion

The experience concerning the equipment and the measuring method can be summarized as follows. It is important to use clean, dust-free and unscratched spectrum plates. To increase accuracy, the diaphragm should be as wide as possible; spectra should therefore be taken preferably with a slit of 25 μm or greater. With densely spaced spectra the use of one phototransistor and electronic compensation, with lower line densities the use of two phototransistors proved to be advantageous. For an operator with some practice, it takes about 3—4 minutes to evaluate 10 lines.

A comparison of the results indicates that the objective measurements with LLL Densitometer provide more accurate results than the subjective

measurement of line length, since with the use of the equipment the relative dispersion is decreased on the average by about 30—40%.

The equipment and the measuring method permits simple, fast and objective evaluation of spectra taken with the use of a logarithmic sector of logarithmic filter, because the LLL Densitometer adapter enables to determine line lengths and to accomplish qualitative evaluation in one operation step.

REFERENCES

[1] SCHEIBE, G., NEUHAUSER, A.: Z. angew. Chemie, **41,** 1218 (1928)
[2] TWYMAN, F., SIMEON, F.: Trans. Opt. Soc. London, **31,** 169 (1929)
[3] NAGY, Z., SÁMSONI, Z., BENKŐ, K.: Magy. Fiz. Foly. **10,** 333 (1962)
[4] GREEN, M., POLK, M. L.: Appl. Spectroscopy, **8,** 126 (1954)
[5] MARTIN, L. C., BURKE, S. A., KNOWLES, E. G.: Trans. Faraday Soc., **31,** 495 (1935)
[6] NAGY, Z., SÁMSONI, Z., BENKŐ, K.: Spectrochim. Acta, **19,** 2057 (1963)
[7] NAGY, Z., SÁMSONI, Z., BENKŐ, K.: Magy. Kém. Foly. **70,** 549 (1964)
[8] NAGY, Z., SÁMSONI, Z.: Magy. Kém. Foly. **73,** 26 (1967)
[9] NAGY, Z., SÁMSONI, Z.: Magy. Kém. Foly. **74,** 239 (1968)
[10] NAGY, Z., SÁMSONI, Z.: Spectrochim. Acta, **24B,** 147 (1969)
[11] NAGY, Z.: Acta Chim. (Budapest), **77,** 1 (1973)
[12] TÖPELMANN, H., SCHUHKNECHT, W.: Z. anal. Chem., **86,** 160 (1931)
[13] TWYMAN, F.: Trans. Opt. Soc. London, **33,** 176 (1932)
[14] NAGY, Z., N. PÓLYIK, E.: Magy. Kém. Lapja, **5,** 119 (1959)

Zoltán SÁMSONI; 4001 Debrecen, ATOMKI POB 51, Hungary.
Zoltán NAGY; 4012 Debrecen DOTE Hungary.

Acta Chimica Academiae Scientiarum Hungaricae, Tomus 84 (1), pp. 7–23 (1975)

IRREVERSIBLE STRUKTURVERÄNDERUNGEN VON H-FAUJASIT, H-MORDENIT UND H-KLINOPTILOLIT DURCH THERMISCHE BEHANDLUNG UND EINWIRKUNG VON WASSER

H. BEYER, J. PAPP und D. KALLÓ

(Zentralforschungsinstitut für Chemie der Ungarischen Akademie der Wissenschaften, Budapest)

Eingegangen am 12. März 1973

Die durch thermische Vorbehandlung der NH_4-Formen von Faujasit, Mordenit und Klinoptilolit erhaltenen H-Formen und dehydroxylierten Zeolithe wurden nach unter verschiedenen Bedingungen vorgenommener Rehydratisierung differentialthermoanalytisch, thermogravimetrisch und z. T. röntgenograpisch untersucht. Es wurde festgestellt, daß die unter Wasserabspaltung verlaufende Dehydroxylierung bei allen drei Zeolithen ein irreversibler Prozeß ist und wahrscheinlich schon mit gewissen Gitterumlagerungen einhergeht. Die dehydroxylierten Formen, insbesondere die des Klinoptilolits, sind thermisch relativ instabil. Die sauren Zentren von H-Faujasit werden bei Einwirkung von bei Zimmertemperatur sorbiertem Wasser umgebildet, wobei ein noch die Faujasitstruktur zeigendes, thermisch aber außerordentlich instabiles Produkt erhalten wird. Diese bei den H-Formen von Mordenit und Klinoptilolit nicht zu beobachtende Reaktion wird auf ein Herauslösen des größten Teils des Gitteraluminiums unter der Einwirkung der aus den eigenen Protonen der H-Form gebildeten H_3O^+-Ionen zurückgeführt.

In der Wasserstoff-Form vorliegende Zeolithe sind für viele Kohlenwasserstoffreaktionen außerordentlich aktive und in vielen Fällen auch selektiv wirkende Katalysatoren (vgl. z. B. VENUTO und LANDIS [1]). Ein direkter Austausch der Kationen eines Zeoliths gegen Wasserstoffionen ist aber prinzipiell nur bei Zeolithen mit einem hohen Si/Al-Verhältnis möglich, da nur diese gegen Mineralsäuren genügend beständig sind. Im allgemeinen werden deshalb die Wasserstoff-Formen der Zeolithe durch thermische Zersetzung (Desaminierung) der Ammonium-Formen dargestellt. An die Desaminierung schließt sich bei höheren Temperaturen eine im allgemeinen mit einer Verminderung der katalytischen Aktivität einhergehende, unter Wasserabspaltung verlaufende und sich meistens mehr oder weniger mit der Desaminierung überlappende Reaktion, die sog. Dehydroxylierung an.

In erster Linie haben IR-spektrophotometrische, thermogravimetrische und differentialthermoanalytische Untersuchungen von Faujasit zu dem auf RABO *et al.* [2] sowie UYTTERHOEVEN *et al.* [3] zurückgehenden Reaktionsschema

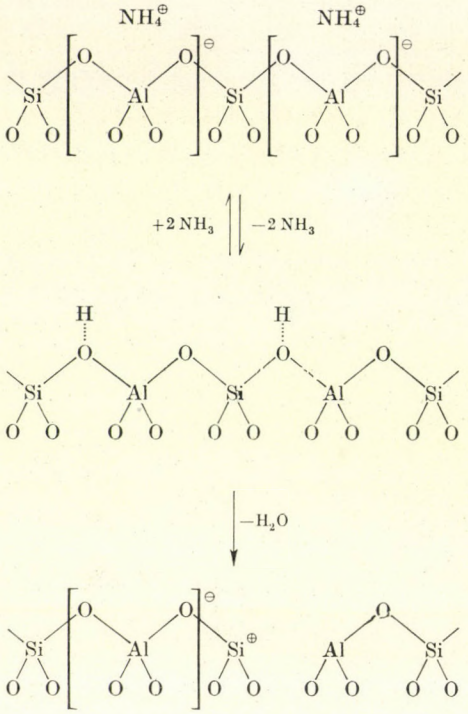

für die Ammoniak- und Wasserabspaltung geführt. Diese schematische Darstellung gibt selbstverständlich den tetraedrischen Aufbau der $SiO_{4/2}$- bzw. $AlO_{4/2}$-Gitterbausteine und deren räumliche Zuordnung zueinenander, die zu mehreren, sich durch ihre Lage im Gitter unterscheidenden Arten von Sauerstoffbrücken führt, nicht wieder.

Zwar wird das Reaktionsschema (1) in den seither in großer Zahl erschienenen Publikationen im wesentlichen akzeptiert, aber trotzdem finden sich in der Literatur sowohl viele widersprüchlich erscheinende experimentelle Angaben, die aber heute wenigstens zum Teil auf unterschiedliche Austauschgrade und Si/Al-Verhältnisse der Zeolithe sowie auf nicht gleiche Arbeitsbedingungen bei der thermischen Behandlung zurückgeführt werden können, als auch voneinander abweichende Auffassungen über Details dieses Reaktionsschemas.

Unbestritten ist, daß die Desaminierung reversibel verläuft [3, 4, 5]. Dagegen ist die Frage oft diskutiert worden, auf welche Weise die Wasserstoff-Form zu formulieren sei. Da einerseits im IR-Spektrum nicht die für H_3O^+ charakteristischen Banden, aber zwei Valenzschwingungsbanden bei etwa 3545 und 3650 cm^{-1} auftreten, die auf an verschiedenen Gitterstellen lokalisierte saure SiOH-Gruppen [Struktur B im Reaktionsschema (1)] zurückgeführt wurden [3, 4, 6, 7], andererseits aber diese Banden reversibel mit steigender Temperatur schwächer werden [8], und sich bei Resorption von NH_3 die Ammo-

nium-Form zurückbildet bzw. bei Sorption von Pyridin [4, 6] die für das Pyridiniumion charakteristischen Banden zu beobachten sind, wurde das Gleichgewicht

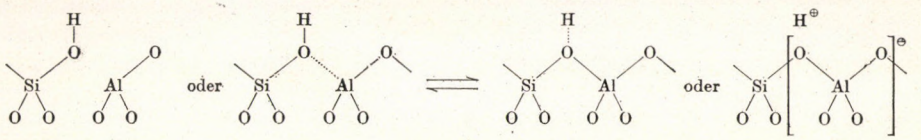

(2)

angenommen [3, 4, 8], das sich mit steigenden Temperaturen nach rechts verschiebt. BENESI [9] wiederum gibt an, daß sich die IR-Bande bei 3650 cm^{-1} auch direkt der reinen Brönstedsäure auf der rechten Seite der Gleichung (2) zuordnen lasse. OLSON und DEMPSEY [10] haben später an Hand von Röntgendiffraktionsmessungen gezeigt, daß die Al-Atome des desaminierten Zeoliths ebenfalls tetraedrisch von vier Sauerstoffatomen umgeben sind, so daß SCHOONHEYDT und UYTTERHOEVEN [11] die im Reaktionsschema (1) angegebene schematische Struktur B annehmen.

Durch IR-spektrophotometrische Untersuchungen von an H-Zeolithen sorbiertem NH_3 [3] bzw. Pyridin [4, 6, 12, 13] wurde festgestellt, daß mit steigender Vorbehandlungstemperatur, besonders ausgeprägt im Temperaturbereich über 500 °C, die Lewis-Acidität, von einem sehr geringen Wert ausgehend, auf Kosten der Konzentration der Brönsted-Zentren ansteigt. Es muß aber betont werden, daß sich die in Abhängigkeit von der Vorbehandlungstemperatur ermittelten Absolutwerte für die Konzentrationen der Lewis- und Brönsted-Zentren in den Arbeiten der einzelnen Verfasser beträchtlich unterscheiden und lediglich — aber auch nur innerhalb gewisser Temperaturbereiche — die Tendenz ihres Verlaufes übereinstimmt.

Ein derartiger Verlauf der Brönsted- und Lewis-Acidität ist nun ohne weiteres mit der Dehydroxylierung des H-Zeoliths gemäß dem zweiten Schritt des Reaktionsschemas (1) zu erklären. Für diesen Reaktionschritt spricht auch, daß in dem Temperaturbereich über 500 °C thermogravimetrisch eine Gewichtsabnahme festzustellen ist, die der nach der Stöchiometrie des Reaktionsschemas (1) zu erwartenden Wassermenge entspricht, und ein schwach endothermer Peak in der DTA-Kurve auftritt [6, 14].

Es muß nun bemerkt werden, daß sich alle bisher angeführten Arbeiten ausschließlich auf den Zeolith Faujasit (Molekularsieb Y) beziehen und über derartige Untersuchungen an anderen Zeolithen auch nur sehr wenige Publikationen vorliegen. CANNINGS [15] hat versucht, die Konzentrationen von Lewis- und Brönsted-Zentren des bei verschiedenen Temperaturen im Vakuum ausgeheizten H-Mordenits aus den IR-Banden von sorbiertem Pyridin abzuschätzen. Danach beginnt die Anzahl der Brönsted-Zentren bei 400—500 °C abzunehmen, während die zunächst wesentlich geringere Konzentration der

Lewis-Zentren bei 500 °C durch ein Maximum geht. Bemerkenswert ist, daß Banden bei 1462 und 1455 cm^{-1} zwei verschiedenen Arten von Lewis-Zentren zugeschrieben werden, und zwar der Struktur C im Reaktionsschema (1) (starke Zentren) und der auf der linken Seite der Gleichung (2) angegebenen Struktur (mittelstarke Zentren). In einer eingehenderen Untersuchung stellte KARGE [16] dagegen fest, daß H-Mordenit — im Gegensatz zum Faujasit — schon von vornherein die gleiche Anzahl von Brönsted- und Lewis-Zentren (bestimmt aus der Intensität der IR-Banden von sorbiertem Pyridin) enthält. Die Konzentration beider Zentrenarten nimmt über 500°C ab, die des Brönsted-Typs allerdings schneller. Zur Erklärung wird angenommen, daß eine thermisch aktivierte Sorption von Pyridinmolekülen an dreifach koordinierten Al-Atomen, wie sie auf der linken Seite der Gleichung (2) schematisch dargestellt sind, vor sich gehen kann. Damit erscheint aber auch vom katalytischen Standpunkt aus die reine Wasserstoff-Form von Zeolithen in einem anderen Licht als bisher, da man nunmehr auch bei diesen — und zwar abhängig von strukturellen Gegebenheiten des Zeoliths und der chemischen Natur des Reaktanden — mit Lewis-Zentren rechnen muß.

Es liegt auf der Hand, daß sich aufgrund der dargelegten Vorstellungen bei verschiedenen Temperaturen thermisch vorbehandelte NH_4-Zeolithe ausgesprochen für die Untersuchung der Rolle von Brönsted- und Lewis-Zentren bei katalytischen Reaktionen eignen sollten, und es fehlt auch nicht an derartigen Untersuchungen (z. B. TURKEVICH und ONO [17], WARD [6]). Von diesem Standpunkt aus ist es nun von außerordentlichem Interesse, inwieweit die Struktur C des Reaktionsschemas (1) stabil ist bzw. tatsächlich vorliegt und ob bzw. inwieweit der Dehydroxylierungsschritt reversibel verläuft. Es sei vorausgeschickt, und in der Diskussion wird darauf näher eingegangen, daß in der Literatur in bezug auf diese für die Deutung katalytischer Versuchsergebnisse so wichtigen Fragen völlig widersprechende Angaben zu finden sind.

Um zur Klärung dieses Sachverhaltes beizutragen, haben wir die bei verschiedenen Temperaturen vorbehandelten NH_4-Formen von Faujasit, Mordenit und Klinoptilolit auch nach der Resorption von Wasser thermogravimetrisch untersucht, denn bisher liegen nur am Faujasit ausgeführte, zudem nicht sehr eingehende und nicht mit der thermogravimetrischen Methode vorgenommene Untersuchungen über die Reversibilität des Dehydroxylierungsschrittes vor.

Material und Methode

Die Untersuchungen erstreckten sich auf folgende Zeolithe:

1. Faujasit

a) $Na_2O.Al_2O_3.5{,}6\ SiO_2$; mikrokristallines Pulver, Hersteller: Farbenfabrik Wolfen, DDR Handelsbezeichnung: Zeosorb V50, im weiteren als Faujasit-W bezeichnet.

b) $Na_2O.Al_2O_3.4{,}3\ SiO_2$; mikrokristallines Pulver, sowjetisches Erzeugnis, im weiteren als Faujasit-SU bezeichnet.

2. Mordenit

$Na_2O.Al_2O_3.10{,}5\ SiO_2$; mikrokristallines Pulver, Hersteller: Norton Chemical Process Prod. Div. Handelsbezeichnung: Zeolon 100.

3. Klinoptilolit

a) ein in Ungarn natürlich vorkommendes Gestein, das zu etwa 70% aus Klinoptilolit besteht und daneben noch Feldspat, Cristobalit und einen amorphen Anteil enthält. Das $SiO_2 : Al_2O_3$-Verhältnis beträgt 10.26. Handelsbezeichnung: Klinosorb.

b) ein in Bulgarien in einer Reinheit von etwa 60% vorkommendes Klinoptilolit-Mineral. Da sich dieses Material — abgesehen von dem etwas geringeren Klinoptilolitgehalt und einer wesentlich geringeren Festigkeit des Gesteines — ebenso wie der ungarische Klinoptilolit verhielt, wird darauf im weiteren nicht gesondert eingegangen.

Die Zeolithe wurden durch Ionenaustausch mit NH_4Cl und Auswaschen bis zur Chlorid-Freiheit in die entsprechenden Ammonium-Formen überführt und als solche untersucht. Der NH_4-Gehalt der Zeolithe wurde bestimmt, indem das beim Erhitzen der Zeolithe auf etwa 650 °C in Freiheit gesetzte NH_3 im Stickstoffstrom in Schwefelsäure überführt und diese zurücktitriert wurde. Der Austauschgrad betrug 78% bei Faujasit-W, 69% bei Faujasit-SU, 90% bei Mordenit und etwa 85% bei Klinoptilolit.

Die thermogravimetrischen (TG) und differentialthermoanalytischen (DTA) Messungen wurden mit dem »Derivatographen« der Fa. MOM bei Aufheizgeschwindigkeiten von 5,3—5,8 °C/min und mit der Zeit praktisch linearem Temperaturanstieg ausgeführt. Die Zeolithe wurden in etwa 1 mm starker Schicht auf als Probebehälter dienende Pt-Teller aufgeschüttet. Das Klinoptilolitgestein wurde pulverisiert mit Korndurchmessern unter 0,1 mm eingesetzt.

Die Versuche wurden im allgemeinen in Sauerstoffatmosphäre ausgeführt. Der bei der endothermen Zersetzung der NH_4-Form der Zeolithe entstehende Ammoniak wird unter diesen Bedingungen — wahrscheinlich katalytisch an den aus Platin bestehenden Probebehältern — verbrannt, so daß dieser Schritt an einem stark exothermen Peak in der DTA-Kurve gut erkannt werden kann.

In allen Fällen wurde zunächst der allergrößte Teil des physikalisch adsorbierten (»zeolithischen«) und kristallwasserartig gebundenen Wassers durch eine 90-minutige isotherme Ausheizung bei 180—190 °C entfernt, und erst danach wurde die Probe mit der vorgegebenen Geschwindigkeit weiter aufgeheizt. Durch diese isotherme Vorbehandlung, bei der nur im Falle des Faujasits auch schon eine — allerdings geringfügige — Zersetzung der NH_4-Form zu beobachten ist, wird eine zu starke Überlappung der Abgabe des zeolithischen Wassers mit der Freisetzung des NH_3 vermieden.

Thermische Vorbehandlungen der Zeolithe wurden ebenfalls im Derivatographen und unter gleichen Bedingungen vorgenommen. Die Proben wurden also ebenfalls 90 Minuten bei 180—190 °C ausgeheizt und danach mit der vorgegebenen Geschwindigkeit bis auf die gewünschte Vorbehandlungstemperatur aufgeheizt und sofort aus dem Ofen entnommen. Von einem Teil dieser Proben wurden auch Röntgendiffraktogramme aufgenommen.

Da sich der Ausgangszustand der Zeolithe infolge der leichten Abgabe eines Teils des physikalisch adsorbierten Wassers und einiger nicht oder nur schwer einzuhaltender Versuchsbedingungen (Luftfeuchtigkeit, Anfangstemperatur des Ofens u.a.) nicht genau festlegen läßt, wurde in dieser Arbeit das Gewicht des bis 1000 °C flüchtigen Zeolithanteils (zeolithisches Wasser, Ammoniak, Strukturwasser) auf das Gewicht des bei 1000 °C geglühten, praktisch strukturwasserfreien und bereits amorphen Zeoliths bezogen und in den Abbildungen und der Tabelle I in mg/g angegeben. In den Abbildungen sind ebenfalls die sich aus dem gesondert bestimmten NH_4-Gehalt der Zeolithe und der Stöchiometrie des Reaktionsschemas (1) ergebenden Mengen an Strukturwasser (untere gestrichelte Linie) und NH_3 + Strukturwasser (obere gestrichelte Linie) angegeben.

Ergebnisse

Die bei der Untersuchung des *Mordenits* erhaltenen Ergebnisse sind in Abb. 1 und Tab. I zusammengefaßt. Nach 90 minutiger isothermer Vorbehandlung bei 180 °C enthält Mordenit, wie aus Kurve I hervorgeht, noch etwas zeolithisches Wasser, dessen Desorption sich in der TG-Kurve mit der Abgabe des bei etwas höheren Temperaturen in Freiheit gesetzten NH_3 überlagert.

Die selbstverständlich endotherme NH_3-Abspaltung ist aber sehr gut an dem auf die katalytische Verbrennung des Ammoniaks zurückzuführenden exothermen Peak der DTA-Kurve zu erkennen. Beide Kurven zeigen, daß bei einer

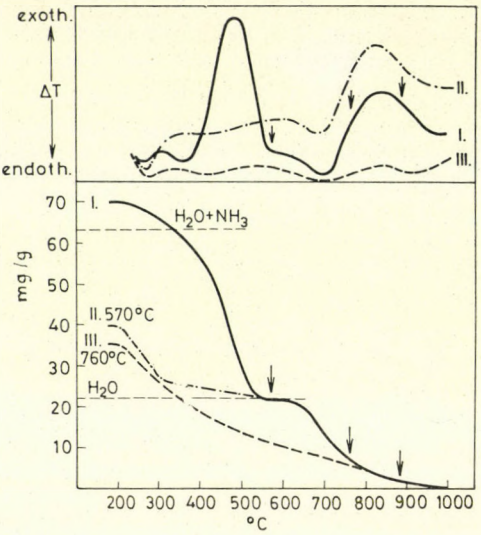

Abb. 1. DTA-Kurven (oben) und thermogravimetrische Kurven (unten) von NH_4-Mordenit nach 90-minutiger isothermer Ausheizung bei 180 °C. I: ohne weitere Vorbehandlung; II: nach Aufheizen auf 570 °C und nachfolgender Rehydratisierung bei 20 °C; III: nach Aufheizen auf 760 °C und nachfolgender Rehydratisierung bei 20 °C.

thermischen Vorbehandlung bis 570 °C die reine Wasserstoff-Form des Mordenits entsteht. Bei noch höheren Temperaturen setzt dann die Abspaltung von Strukturwasser (Dehydroxylierung) ein.

Benesi [9] hat bei der thermogravimetrischen Untersuchung von NH_4-Mordenit keine getrennten Stufen für Desaminierung und Dehydroxylierung

Tabelle I

Wassersorptionskapazität in mg/g bei Zimmertemperatur

Vorbehandl.-Temp. °C	Mordenit	Klinoptilolit
180*	114	60
570	190	67
760	174	52
880	148	—
1000	13**	—

* NH_4-Form
** Röntgenamorph

erhalten, die Kurven für Faujasit zeigen aber den gleichen Verlauf wie die, die in dieser Arbeit weiter unten mitgeteilt werden. Da BENESI einen praktisch Na^+-freien, also zu 100% ausgetauschten Mordenit (ebenfalls Zeolon 100) verwendet hat, ist es möglich, daß ein bestimmter Anteil an Metallionen — ähnlich wie beim Faujasit [13, 14, 18] — die Struktur des H-Mordenits stabilisiert.

Die bis 570 °C vorbehandelte NH_4-Form des Mordenits, also die Wasserstoff-Form, resorbiert bei Zimmertemperatur — wie aus Tab. I zu ersehen ist — wesentlich mehr Wasser als die NH_4-Form. Das ist damit zu erklären, daß innerhalb des Gitters nunmehr auch der größte Teil des Raumes für die Adsorption zur Verfügung steht, der vorher von im Vergleich zum Proton viel größeren NH_4-Ionen eingenommen wurde. Aus der thermogravimetrischen Untersuchung der rehydratisierten H-Form (Kurve II) folgt, daß nach der isothermen Vorbehandlung bei 180 °C noch die relativ große Wassermenge von 18 mg/g im Mordenit verbleibt, woraus geschlossen werden kann, daß die Bindung des zeolitischen Wassers in der H-Form stärker als in der NH_4-Form ist. Die TG-Kurve oberhalb 550 °C, also die Abgabe des Strukturwassers, deckt sich mit der der NH_4-Form.

Nach einer thermischen Vorbehandlung bis 760 °C, nachdem also bereits etwa 70% des Strukturwassers abgegeben sind, und anschließender Wasserresorption bei Zimmertemperatur ist nur eine geringfügige Abnahme der Sorptionskapazität für Wasser festzustellen (Tab. I). Die TG-Kurve (III) zeigt jedoch einen ganz anderen Verlauf als die der NH_4- bzw. H-Form, woraus folgt, daß die Dehydroxylierung unter diesen Bedingungen der Rehydratisierung ein irreversibler Vorgang ist.

Bei höheren Vorbehandlungstemperaturen ist eine Abnahme der Sorptionskapazität für Wasser und zugleich — wie aus den in Abb. 2 in Form von

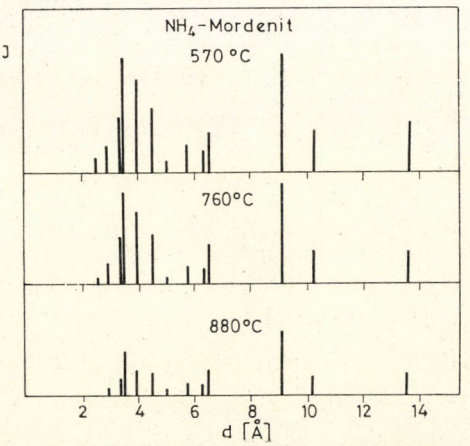

Abb. 2. Intensitäten der Hauptlinien der Röntgendiffraktogramme von thermisch vorbehandeltem und bei 20 °C rehydratisiertem NH_4-Mordenit.

Strichdiagrammen angegebenen Intensitäten der Röntgendiffraktionsbanden zu ersehen ist — ein Verlust an Kristallinität festzustellen. Der bei 1000 °C geglühte NH_4-Mordenit ist röntgenamorph.

Bei der Untersuchung des *Klinoptilolits* wurden weitgehend analoge Ergebnisse erhalten, die in Abb. 3 und Tab. I angegeben sind. An dieser Stelle

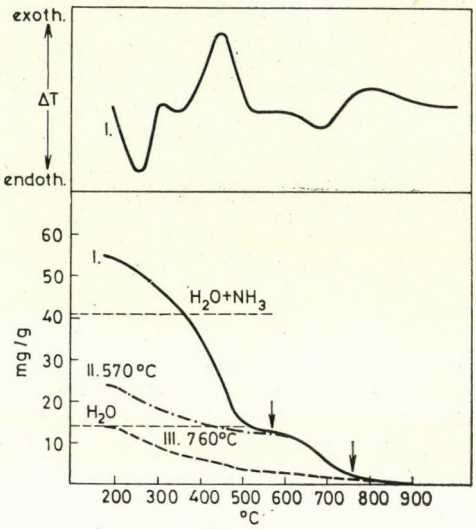

Abb. 3. DTA-Kurve (oben) und thermogravimetrische Kurven (unten) von NH_4-Klinoptilolit nach 90-minutiger isothermer Ausheizung bei 180 °C. I: ohne weitere Vorbehandlung; II: nach Aufheizen auf 570 °C und nachfolgender Rehydratisierung bei 20 °C; III: nach Aufheizen auf 760 °C und nachfolgender Rehydratisierung bei 20 °C.

sei nur vermerkt, daß die Zersetzung der NH_4-Form und die Dehydroxylierung weniger scharf voneinander getrennt und bei um 30—50 °C niedrigeren Temperaturen verlaufen als im Falle des Mordenits. Weiterhin ergibt sich aus den Wassersorptionskapazitäten in Tab. I und aus den Röntgendiagrammen in Abb. 4, daß dekationisierter Klinoptilolit weit weniger thermisch stabil ist als dekationisierter Mordenit.

Die mit *Faujasit* erhaltenen Ergebnisse sind in den Abb. 5—7 dargestellt. Die TG-Kurven der NH_4-Form beider untersuchter Faujasite (Kurve I in den Abb. 5—7) zeigen den gleichen charakteristischen Verlauf wie im Falle des Mordenits oder Klinoptilolits.

Die durch thermische Vorbehandlung bis 500 °C erhaltene Wasserstoff-Form des Faujasits resorbiert bei Zimmertemperatur — ebenso wie die des Mordenits und Klinoptilolits — mehr Wasser (350 mg/g), als bei der vorangegangenen isothermen Desorption bei 180 °C von der NH_4-Form abgegeben wurde (289 mg/g). Bei der nachfolgenden Aufheizung (Kurve IV in Abb. 5 und 6) wird aber im Gegensatz zu den mit Mordenit und Klinoptilolit erhal-

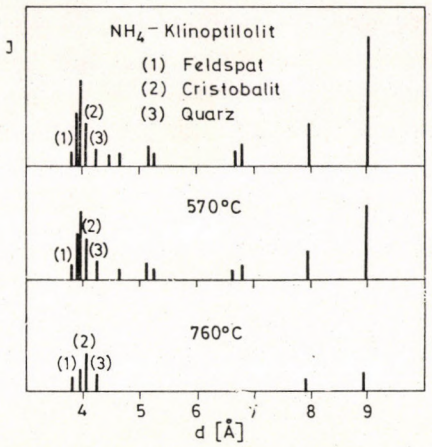

Abb. 4. Intensitäten der Hauptlinien der Röntgendiffraktogramme von thermisch vorbehandeltem und bei 20 °C rehydratisiertem NH_4-Klinoptilolit. Angegeben ist ebenfalls die jeweils intensivste Linie der drei Begleitminerale.

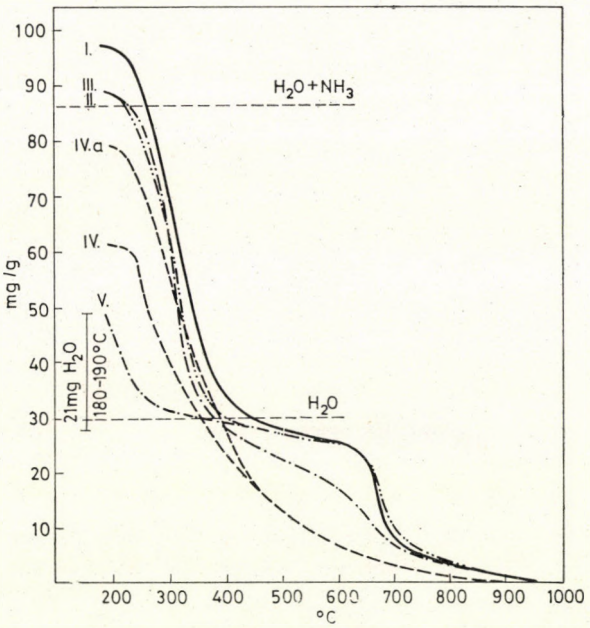

Abb. 5. Thermogravimetrische Kurven von NH_4-Faujasit-W nach 90-minutiger isothermer Ausheizung bei 180 °C. I: ohne weitere Vorbehandlung; II: nach Aufheizen auf 500 °C, NH_3-Behandlung bei 20 °C und nachfolgender H_3O-Sorption bei Zimmertemperatur; III: nach Aufheizen auf 500 °C, H_2O-Sorption bei Zimmertemperatur und NH_3-Behandlung bei 20 °C nach 24-stündigem Stehen; IV: nach Aufheizen auf 500 °C, H_2O-Sorption bei Zimmertemperatur, 24-stündigem Stehen und Aufheizen auf 180 °C; IV/a.: wie Kurve IV, nur noch anschließende Behandlung mit NH_3 bei 20 °C; V: nach Aufheizen auf 500 °C und Resorption von Wasser bei 180—190 °C.

tenen Ergebnissen nicht wieder die charakteristische Dehydroxylierungsstufe der Wasserstoff-Form, sondern eine monoton abfallende Kurve erhalten. Im Verlaufe der ausgeführten Operationen muß also eine irreversible strukturelle Veränderung eingetreten sein.

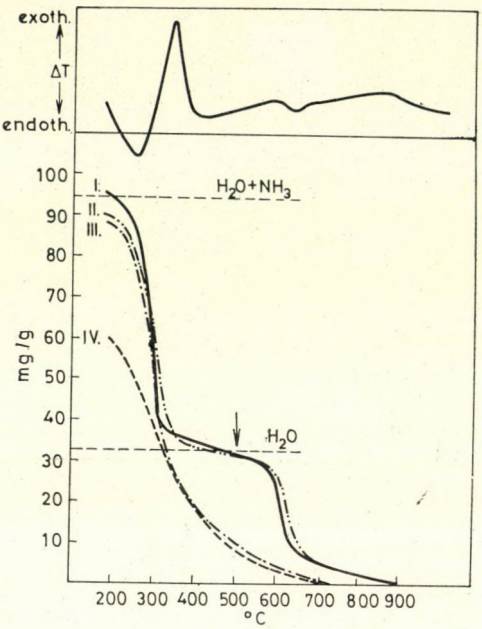

Abb. 6. DTA-Kurve (oben) und thermogravimetrische Kurven (unten) von NH_4-Faujasit-SU nach 90-minutiger isothermer Ausheizung bei 180 °C. I: ohne weitere Vorbehandlung; II: nach Aufheizen auf 500 °C, NH_3-Behandlung bei 20 °C und nachfolgender H_2O-Sorption bei Zimmertemperatur; III: nach Aufheizen auf 500 °C, H_2O-Sorption bei Zimmertemperatur und NH_3-Behandlung bei 20 °C nach 24-stüdigem Stehen; IV: wie Kurve III, nur ohne NH_3-Behandlung.

Um zu klären, wann und unter welchen Versuchsbedingungen diese Veränderungen vor sich gehen und welcher Natur sie sind, wurde eine Reihe von Versuchen vorgenommen. Die charakteristische Dehydroxylierungsstufe trat auf, wenn die durch thermische Vorbehandlung bis 500 °C zu erhaltende Wasserstoff-Form unter Ausschluß von Wasserdampf auf Zimmertemperatur abgekühlt oder bei Temperaturen von 180—190 °C (Kurve V in Abb. 5) bzw. 130 °C mit Wasserdampf gesättigt (21 bzw. 77 mg/g) und anschließend das Thermogramm aufgenommen wurde. Die strukturellen Veränderungen können somit nur in Gegenwart von Wasser und bei Temperaturen unter 130 °C eintreten, und somit liegt der Schluß nahe, daß dafür eine vollständige Ausfüllung des innerkristallinen Porenraumes mit Wasser eine notwendige Bedingung ist.

Um eine Zerstörung der Wasserstoff-Form während des Aufheizvorganges auszuschließen, wurde der entsprechend vorbehandelte H-Faujasit vor der

thermogravimetrischen Untersuchung in eine NH_3-Atmosphäre gebracht. Dadurch werden die nach der Vorbehandlung noch intakten Zentren der H-Form in die NH_4-Form überführt und somit gewissermaßen »fixiert«.

Wird die Wasserstoff-Form erst einer NH_3-Atmosphäre ausgesetzt (Rückbildung der NH_4-Form), und läßt man erst danach Wasser sorbieren, so erhält man bei der nachfolgenden thermogravimetrischen Untersuchung erwartungsgemäß nahezu den gleichen TG-Kurvenverlauf (Kurve II in Abb. 5 und 6) wie im Falle des ursprünglichen NH_4-Faujasits, nicht aber dann, wenn

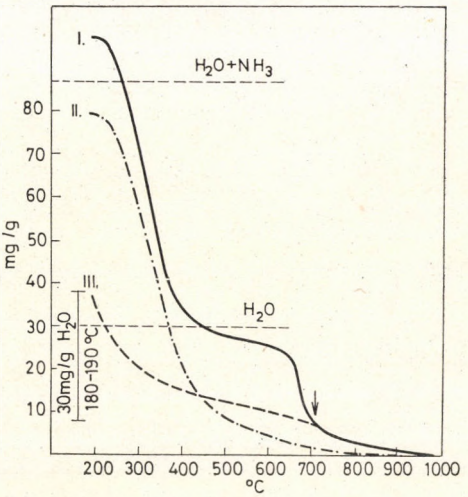

Abb. 7. Thermogravimetrische Kurven von NH_4-Faujasit-W nach 90-minutiger isothermer Ausheizung bei 180 °C. I: ohne weitere Vorbehandlung; II: nach Aufheizen auf 705 °C, H_2O-Sorption bei Zimmertemperatur und nachfolgender Behandlung mit NH_3 bei 20 °C; III: nach Aufheizen auf 705 °C und nachfolgender Resorption von Wasser bei 180—190 °C.

die Wasserstoff-Form vor der NH_3-Sorption durch 20-stündiges Stehen über 30%iger Schwefelsäure bei Zimmertemperatur mit Wasserdampf gesättigt (Kurven III in Abb. 5 und 6) oder vor der Ammoniakbehandlung auf 180 °C aufgeheizt wird (Kurve IVa in Abb. 5).

Aus dem Verlauf dieser Kurven geht hervor, daß bei Zimmertemperatur die Wasserstoff-Form des Faujasit-W weniger stark als die des Faujasit-SU durch kapillarkondensiertes Wasser angegriffen wird, daß aber bei erhöhter Temperatur auch im Falle des Faujasit-W eine TG-Kurve erhalten wird, die die Dehydroxylierungsstufe nicht mehr erkennen läßt. Ein derartiger Faujasit weist noch eine Wassersorptionskapazität von 205 mg/g auf und zeigt nur einen teilweisen Verlust an Kristallinität (Abb. 8).

Aus Abb. 7 ist zu ersehen, daß die Dehydroxylierung auch im Falle des Faujasits ein irreversibler Prozeß ist. Der bis 705 °C erhitzte, schon weitgehend dehydroxylierte NH_4-Faujasit-W kann — wie Kurve III zeigt — durch Wasser-

dampfsorption bei 180—190 °C bis zur Sättigung nicht wieder in die H-Form überführt werden, obwohl die sorbierte Wassermenge von 30 mg/g dafür ausreichend wäre. Bei 400 °C wird aus einem bei Zimmertemperatur mit Wasserdampf gesättigten Gasstrom nur sehr wenig Wasser (2—3 mg/g) resorbiert. Diese Menge ist schon aus stöchiometrischen Gründen nicht für eine Rückbildung der H-Form ausreichend. Wassersorption bis zur Sättigung bei Zimmertemperatur führt ebenfalls zu keiner Rückbildung der Wasserstoff-Form, vielmehr werden dabei auch noch bei der Vorbehandlungstemperatur von 705 °C intakt gebliebene Zentren der H-Form angegriffen (Kurve II in Abb. 7).

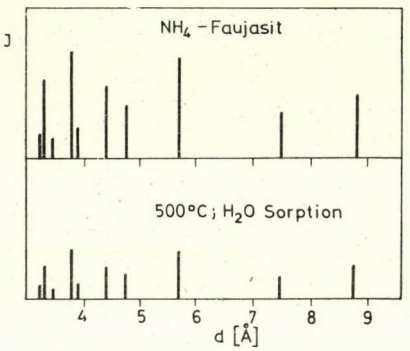

Abb. 8. Intensitäten der Hauptlinien der Röntgendiffraktogramme von NH_4-Faujasit ohne Vorbehandlung und nach Aufheizen auf 500 °C, Sorption von Wasser bei Zimmertemperatur und nachfolgendem Aufheizen auf 180 °C.

Diskussion

Die Desaminierung der in dieser Arbeit untersuchten NH_4-Zeolithe ist — wie für NH_4-Faujasit schon festgestellt wurde [3, 4, 5] — reversibel.

Die Desaminierung ist ein endothermer Prozeß [14, 19]. Die exothermen Peaks in den DTA-Kurven in Abb. 1 und 3 sind auf die Verbrennung des in Freiheit gesetzten NH_3 zurückzuführen. VENUTO, WU und CATTANACH [20] und HOPKINS [21], die bei der Desaminierung im N_2-Strom einen exothermen Peak erhielten, dürften wahrscheinlich nicht unter vollständigem Ausschluß von Sauerstoff gearbeitet haben.

HICKSON und CSICSERY [19] schließen aus DTA-Messungen, daß die Desaminierung von NH_4-Faujasit in drei Stufen (Maxima bei 275, 370 und 430 °C) vor sich geht. Thermogravimetrisch konnte die Abgabe von chemisorbiertem NH_3 in zwei Stufen beobachtet werden [5, 22].

VENUTO, WU und CATTANACH [20] sowie BOLTON und LANEWALA [14] haben für NH_4-Faujasit außerdem noch einen exothermen DTA-Peak bei etwa

550 °C gefunden, der jedoch mit der Desaminierung nicht in einen direkten Zusammenhang gebracht werden kann, da diese bereits bei 400 °C abgeschlossen ist. Bei unseren Versuchen (s. Abb. 6) wurde ein solcher exothermer Peak nicht festgestellt.

Unsere Versuche lassen auch keinen Schluß darüber zu, ob im Falle des Faujasits die NH_3-Abgabe in mehreren Schritten erfolgt, da diese sich mit der Desorption des zeolithischen Wassers überlappt und ein Teil des NH_3 schon während der isothermen Behandlung bei 180 °C in Freiheit gesetzt wird. Im Falle des Mordenits und Klinoptilolits könnte aber der vor dem — in Sauerstoffatmosphäre! — exothermen Hauptberg liegende Peak mit einem Maximum bei etwa 300 °C (Abb. 1 und 3) darauf hindeuten, daß die Bindungsenergien (Gitterplätze) nicht für alle NH_4-Ionen gleich sind.

Die charakteristische Dehydroxylierungsstufe in den TG-Kurven wird stets — wie im Falle des Faujasits schon mehrmals festgestellt wurde [6, 14, 19, 21] — von einem schwach endothermen DTA-Peak begleitet. Beim Mordenit und Klinoptilolit schließt sich diesem endothermen Peak sofort, und zwar noch im Bereich der Dehydroxylierung, ein exothermer an.

Es soll bemerkt werden, daß bei Faujasit die Dehydroxylierung mit einem schwach positiven DTA-Peak einhergeht, wenn NH_4-Faujasit nicht in 1 mm starker Schicht auf Tellern, sondern in etwa 12 mm starker Schicht in einem Tiegel eingesetzt wurde. Vermutlich hat diese Erscheinung ihre Ursache in dem zur Ausbildung des sog. »ultrastabilen Faujasits« führenden »deep-bed«-Effekt [23—26]. McDaniel und Maher [18] haben im gleichen Temperaturbereich ebenfalls einen schwach exothermen Peak festgestellt, machen aber keine Angaben über die Schichtdicke und andere in diesem Zusammenhang interessierende Versuchsbedingungen.

Es gibt mehrere Hinweise dafür, daß dehydroxylierter Faujasit thermisch relativ instabil ist. Die Gesamtzahl der sauren Zentren beginnt z. B. nach Ward [6] bei 550 °C, nach Hughes und White [12] bei 600 °C schneller abzunehmen, als nach Reaktionsschema (1) zu erwarten wäre, was auf einen beginnenden Gitterzusammenbruch oder eine Gitterumlagerung hindeutet. Die dehydroxylierte Form geht schon bei niedrigeren Temperaturen als Kationenformen in den amorphen Zustand über. Aus DTA-Kurven wurde ein Gitterzusammenbruch bei 850 °C [27] festgestellt. Es muß aber bemerkt werden, daß die Intensitäten der Röntgeninterferenzlinien schon bei wesentlich niedrigeren Temperaturen abzunehmen beginnen. In der Literatur finden sich auch Hinweise darauf, daß das Gitter schon bei Temperaturen unter 600 °C zusammenbricht [3, 18].

Das Gitter des dehydroxylierten Mordenits ist offensichtlich wesentlich thermostabiler als das des Faujasits. Die Kristallinität — und damit parallel die Sorptionskapazität — nimmt zwar mit dem Fortschreiten der Dehydroxylierung etwas ab, aber noch bei 880 °C ist die Kristallstruktur weitgehend

erhalten (Abb. 2). Allein mit dem höheren Si : Al-Verhältnis ist diese Thermostabilität wohl nicht zu erklären, denn dehydroxylierter Klinoptilolit ist bei einem Si : Al-Verhältnis von ebenfalls 5 wesentlich instabiler (Abb. 3).

Bei einer Gegenüberstellung der Temperaturbereiche, in denen das Gitter zusammenbricht, muß man selbstverständlich berücksichtigen, daß die thermische Stabilität auch weitgehend vom Austauschgrad abhängt und somit Vergleiche nur bedingt möglich sind. Beim Klinoptilolit ist noch zu beachten, welche anderen Kationen im Zeolith verblieben sind, da nach unseren Untersuchungen die Erdalkalimetall-Formen des Klinoptilolits — insbesondere die Ca-Form — überraschenderweise wesentlich instabiler sind als die dehydroxylierte Form.

Die Details der strukturellen Veränderungen, die bei der Dehydroxylierung durch das Herauslösen eines Gittersauerstoffs auftreten, sind noch nicht geklärt. Da einerseits Mordenit und Klinoptilolit nach dem Einsetzen des Dehydroxylierungsprozesses einen exothermen DTA-Peak zeigen, andererseits aber besonders beim Mordenit erst bei höheren Temperaturen merkliche Veränderungen in den Röntgendiffraktogrammen und im der Sorptionskapazität festzustellen sind, vermuten wir, daß sich die Struktur Cim Reaktionsschema (1) sofort oder doch sehr bald durch eine Umlagerung des dreifach koordinierten Al-Atoms — indem dieses vielleicht durch die Ebene der drei verbliebenen O-Atome hindurchschwingt und in eine energetisch günstigere Position kommt — stabilisert. Bei höheren Temperaturen und mit fortschreitender Dehydroxylierung bricht dann schließlich das Zeolithgitter in einem bestimmten, von der Struktur des Zeoliths abhängigen Temperaturintervall nach und nach zusammen.

Sollte die Struktur C (Reaktionsschema 1) existent sein, so wäre eine Reversibilität der Dehydroxylierung zu erwarten, auch wenn der Abstand zwischen den beiden dreifach koordinierten Zentralatomen etwas größer ist. Eine Irreversibilität wäre dagegen bei einer Umlagerung des Al-Atoms im Gitter leicht zu erklären. Somit kommt der — immer noch umstrittenen — Frage, ob bzw. inwieweit der Dehydroxylierungsprozeß reversibel ist, nicht nur hinsichtlich der Verwendung der Zeolithe als Katalysatoren, sondern auch vom theoretischen Standpunkt aus eine große Bedeutung zu.

WARD [6, 8] sowie HUGHES und WHITE [12] haben aus der Intensität der IR-Banden von an sauren Zentren sorbiertem Pyridin geschlossen, daß die im Verlaufe der Dehydroxylierung gebildeten Lewis-Zentren durch Wasser wieder in Brönsted-Zentren überführt werden. Das spricht aber nicht notwendigerweise für eine Reversibilität des im Reaktionsschema (1) angegebenen Dehydroxylierungsprozesses, da die erhaltenen Brönsted-Zentren qualitativ anderer Natur sein können. Offensichtlich ist das auch der Fall, denn die für zeolithische SiOH-Gruppen charakteristische, in der H-Form gut ausgebildete Bande bei 3640 cm^{-1} wird durch Wasser nicht rückgebildet [4, 6, 12].

BENESI [9] nimmt ebenfalls an, daß die Dehydroxylierung reversibel ist, da nach Rehydratisierung von Mordenit bzw. Faujasit (dehydroxyliert bei 700 bzw. 800 °C) die während der Dehydroxylierung verloren gegangene katalytische Aktivität für die Spaltung von *n*-Butan bzw. Disproportionierung von Toluol vollständig bzw. teilweise zurückgewonnen wird. Die nach der Rehydratisierung festzustellenden Selektivitätsveränderungen sprechen aber auch in diesem Falle dafür, daß nicht die ursprüngliche H-Form zurückerhalten wird. Durch Rehydratisierung eines bei 690 °C dehydroxylierten Klinoptilolits lassen sich nur 3% des während der Dehydroxylierung eingetretenen Aktivitätsverlustes (katalytische Krackung von Propan) rückgängig machen, wobei auch Selektivitätsverschiebungen zu beobachten sind [28].

BOLTON und LANEWALA [14] vertreten ebenfalls die Meinung, die Dehydroxylierung sei reversibel, und zwar dann, wenn ein bei 600°C dehydroxylierter Faujasit beim Abkühlen auf 400 °C — also in dem Temperaturbereich, in dem die Dehydroxylierung vor sich geht — einer Wasserdampf enthaltenden Atmosphäre ausgesetzt wird. Diese Annahme beruht auf der experimentellen Feststellung, daß durch diese Behandlung die NH_3-Sorption und die Ionenaustauschkapazität teilweise restauriert wird. Abgesehen davon, daß diese zwei Eigenschaften nicht spezifisch für die ursprüngliche H-Form des Faujasits und somit wenig geeignet für derartige Reversibilitätsuntersuchungen sind, kann die beschriebene Behandlung des Faujasits zu einem Herauslösen von Al-Atomen aus dem Gitter führen [26, 29], wodurch der sog. ultrastabile Faujasit entsteht.

In der vorliegenden Arbeit wurde gezeigt, daß aus den drei untersuchten dehydroxylierten Zeolithen die ursprünglichen Wasserstoff-Formen weder durch Resorption von Wasser bei Zimmertemperatur, noch durch Erhitzen bis 400 °C in einem bei Zimmertemperatur mit Wasserdampf gesättigten Gasstrom, noch durch Behandlung mit einer wäßrigen NH_3-Lösung (in der die für eine eventuelle Rückbildung der NH_4-Form erforderlichen Ionen $[NH_4]^+$ und OH^-] in ausreichendem Maße enthalten sind) rückgebildet werden können. Damit soll selbstverständlich nicht gesagt sein, daß die dehydroxylierten Zeolithe mit Wasser nicht in irgendeiner anderen Weise reagieren können. Die oben besprochenen Veränderungen mehrerer Eigenschaften sprechen ebenso wie der Verlauf der TG-Kurven der rehydratisierten Zeolithe für eine solche Reaktion, in deren Verlauf aber nicht die Oberflächenstruktur der ursprünglichen Wasserstoff-Form zurückgebildet wird.

CATTANACH, WU und VENUTO [5] geben ebenfalls an, daß alle Versuche, die Wasserstoff- oder Ammonium-Form aus dehydroxyliertem Faujasit durch Reaktion mit Wasser bei höheren Temperaturen oder durch Zugabe von NH_3 und H_2O bei Zimmertemperatur zurückzuerhalten, erfolglos verliefen und im allgemeinen zu einem völligen Verlust der Kristallinität und der Sorptionskapazität führten.

In mehreren Arbeiten finden sich Hinweise auf die außerordentliche Instabilität des H-Faujasits gegenüber Wasser [5, 6, 23, 27, 30]. Bisher ist aber noch nicht näher untersucht worden, unter welchen experimentellen Bedingungen diese zu einem amorphen Produkt führende Reaktion mit Wasser vor sich geht.

In der vorliegenden Arbeit konnte gezeigt werden, daß die H-Form von Faujasit bei 130—200 °C gegenüber bei diesen Temperaturen sorbiertem Wasser völlig stabil ist. Dagegen sind die an der charakteristischen Dehydroxylierungsstufe in der TG-Kurve zu erkennenden sauren Zentren nicht mehr festzustellen, wenn die H-Form bei Zimmertemperatur oder etwas darüber liegenden Temperaturen die maximale Menge an Wasser aufnimmt. Das dabei erhaltene Produkt ist noch weitgehend kristallin (Abb. 8), das Gitter ist aber derart thermoinstabil, daß es schon bei Temperaturen oberhalb 250 °C zusammenbricht. Beim Einbringen dieses Produktes in eine Na-Ionen enthaltende Lösung werden Al-Ionen ausgetauscht. Diese Befunde lassen sich gut mit dem von KERR [23] für diese Reaktion angenommenen Schema vereinbaren, nach dem Al-Atome — ähnlich wie bei den zur Bildung von ultrastabilen Faujasit führenden Verfahren, aber in wesentlich größerem Maße — durch Hydrolyse von Al—O—Si-Bindungen aus dem Gitter herausgelöst werden. Es ist ja auch bekannt, daß Faujasit zunehmend instabiler wird, wenn mehr als 50% des Gitteraluminiums entfernt werden [31].

Für die Sprengung der Al – O—Si-Bindung ist aber offensichtlich nicht nur Wasser erforderlich, da bei höheren Temperaturen und im sorbierten Zustand in ausreichender Menge vorliegendem Wasser keine Hydrolyse festzustellen ist. Wir nehmen an, daß bei völliger Ausfüllung des innerkristallinen Porengefüges mit Wasser die Protonen der H-Form H_3O^+-Ionen bilden können und Al gewissermaßen durch die so als wäßrige Säure fungierende H-Form selbst aus dem Gitter herausgelöst wird. Damit wäre auch zu erklären, warum die H-Form des an Al ärmeren, also gegen Säure beständigeren Faujasit-W gegenüber Wasser stabiler ist und die H-Formen von Mordenit und Klinoptilolit, deren Gitter säurebeständig sind, bei Sättigung mit Wasser keine Veränderungen zeigen.

LITERATUR

[1] VENUTO, P. B., LANDIS, P. S.: Advanc. Catalysis **18,** 259 (1968)
[2] RABO, J. A., PICKERT, D. E., STAMIRES, D. N., BOYLE, J. E.: Actes du 2e Congrès Intern. de Catalyse, 1960, S. 2055
[3] UYTTERHOEVEN, J. B., CHRISTNER, L. G., HALL, W. K.: J. Phys. Chem. **69,** 2117 (1965)
[4] LIENGME, B. V., HALL, W. K.: Trans. Faraday Soc. **62,** 3229 (1966)
[5] CATTANACH, J. C., WU, E. L., VENUTO, P. B.: J. Catalysis **11,** 342 (1968)
[6] WARD, J. W.: J. Catalysis, **9,** 225 (1967)
[7] UYTTERHOEVEN, J. B., JACOBS, P., MAKAY, K., SCHOONHEYDT, R.: J. Phys. Chem. **72,** 1768 (1968)
[8] WARD, J. W.: J. Catalysis **9,** 398 (1967)
[9] BENESI, H. A.: J. Catalysis **8,** 368 (1967)

[10] OLSON, D. H., DEMPSEY, E.: J. Catalysis **13,** 364 (1969)
[11] SCHOONHEYDT, R. A., UYTTERHOEVEN, J. B.: J. Catalysis **19,** 55 (1970)
[12] HUGHES, T. R., WHITE, H. M.: J. Phys. Chem. **71,** 2192 (1967)
[13] WARD, J. W.: J. Catalysis **11,** 251 (1968)
[14] BOLTON, A. P., LANEWALA, M. A.: J. Catalysis **18,** 154 (1970)
[15] CANNINGS, F. R.: J. Phys. Chem. **72,** 4691 (1968)
[16] KARGE, H.: Z. Phys. Chem. Neue Folge **76,** 133 (1971)
[17] TURKEVICH, J., ONO, Y.: Advanc. Catalysis **20,** 135 (1969)
[18] MCDANIEL, C. V., MAHER, P. K.: in "Molecular Sieves", Society of Chemical Industry, London, 1968, S. 186
[19] HICKSON, D. A., CSICSERY, S. M.: J. Catalysis **10,** 27 (1968)
[20] VENUTO, P. B., WU, E. L., CATTANACH, J.: Anal. Chem. **38,** 1266 (1966)
[21] HOPKINS, P. D.: J. Catalysis **12,** 325 (1968)
[22] KERR, G. T.: Thermochim. Acta **3,** 113 (1971)
[23] KERR, G. T.: J. Catalysis **15,** 200 (1969)
[24] JACOBS, P., UYTTERHOEVEN, J. B.: J. Catalysis **22,** 193 (1971)
[25] JACOBS, P., UYTTERHOEVEN, J. B.: J. Catalysis **27,** 161 (1972)
[26] WARD, J. W.: J. Catalysis **27,** 157 (1972)
[27] KERR, G. T.: J. Phys. Chem. **73,** 2780 (1969)
[28] BEYER, H.: Acta Chim. (Budapest) (im Druck)
[29] KERR, G. T.: J. Phys. Chem. **71,** 4155 (1967)
[30] PERI, J. P.: Preprints of the 5th Intern. Congr. on Catal., North-Holland Publ. Comp., Amsterdam, 1972
[31] KERR, G. T.: J. Phys. Chem. **72,** 2594 (1968)

Hermann BEYER
János PAPP
Dénes KALLÓ

Zentralforschungsinstitut für Chemie der Ungarischen Akademie der Wissenschaften, 1025 Budapest, Pusztaszeri út 59—67. Ungarn.

Acta Chimica Academiae Scientiarum Hungaricae, Tomus 84 (1), pp. 25—43 (1975)

BEITRÄGE ZUR KENNTNIS DER KRACKREAKTIONEN, II

KINETIK DER KATALYTISCHEN KRACKUNG VON PROPAN SOWIE *n*- UND *i*-BUTAN AN H-KLINOPTILOLIT

H. BEYER

(Zentralforschungsinstitut für Chemie der Ungarischen Akademie der Wissenschaften, Budapest)

Eingegangen am 20. November 1973

Die kinetische Untersuchung der katalytischen Krackung von Paraffinen ist äußerst problematisch, da die zahlreichen Folgereaktionen der als primäre Reaktionsprodukte auftretenden Olefine ein sehr komplexes Reaktionsgeschehen ergeben. Die damit zusammenhängenden Schwierigkeiten wurden umgangen, indem die Versuche in einem Zirkulationsreaktor ausgeführt und die gebildeten Olefine aus der Gasphase des Zirkulationssystems durch selektive Absorption ständig entfernt wurden.

Als Katalysator wurde ein natürlich vorkommendes, zu etwa 61% aus Klinoptilolit-Kristalliten bestehendes Gestein verwendet. Der durch Ionenaustausch in die NH_4-Form überführte Klinoptilolit wurde zwischen 460 und 690 °C thermisch vorbehandelt und gelangte so als H-Klinoptilolit mit unterschiedlichem Dehydroxylierungsgrad zur Untersuchung. Mit zunehmender Dehydroxylierung geht ein steigender Verlust an Kristallinität der Klinoptilolit-Kristallite einher, während sich die »Sekundärstruktur« des Gesteins nicht wesentlich ändert.

Krackung und Dehydrierung der untersuchten Paraffine verlaufen stets, unabhängig von der Vorbehandlungstemperatur des Katalysators, nach einer Kinetik erster Ordnung. Die scheinbaren Aktivierungsenergien der primären Reaktionen sind unabhängig von der Vorbehandlungstemperatur und für einen gegebenen Reaktanden nahezu gleich. Krack- und Dehydrieraktivität des Katalysators gehen mit steigender Vorbehandlungstemperatur bei 500 °C durch ein Maximum. Bei oberhalb des Maximums liegenden Vorbehandlungstemperaturen tritt eine Verschiebung der Selektivität zugunsten der Dehydrierreaktion ein. Das Verhältnis der Geschwindigkeiten, mit denen die 1- und 2-Bindung von *n*-Butan gespalten werden, ist unabhängig von der Vorbehandlungstemperatur. Der Katalysator weist eine sterisch bedingte Selektivität für *n*-Paraffine auf.

Aus den experimentellen Befunden wird geschlossen, daß die Dehydrierreaktion und die Krackreaktionen über einen gemeinsamen aktiven Oberflächenkomplex verlaufen, der durch Chemisorption des Reaktanden an den bei der Dehydroxylierung entstehenden sauren Lewiszentren zustande kommt, an der Spaltung von C–C-Bindungen aber noch ein in Nachbarschaft zum Lewiszentrum befindliches saures Brönstedzentrum beteiligt ist.

Die Untersuchung der Kinetik der primären Krackreaktionen stößt im allgemeinen deswegen auf Schwierigkeiten, weil die primär gebildeten Olefine zahlreiche Neben- und Folgereaktionen eingehen, wodurch das Reaktionsgeschehen außerordentlich komplex und kompliziert wird. Die in solchen Fällen übliche Auswertung der kinetischen Kurven durch Extrapolation auf die Zeit Null führt dabei nicht zum Ziele, da die störenden Folgereaktionen meist um mehrere Größenordnungen schneller als die primären Krackreaktionen verlaufen und Reaktionsprodukte ergeben, die auch bei den primären Reaktionen auftreten.

In der ersten Mitteilung dieser Reihe [1] wurde darauf hingewiesen, daß diese störenden Folgereaktionen im Prinzip ausgeschaltet werden können, wenn mit einem Zirkulationsreaktor gearbeitet wird und die gebildeten Olefine laufend aus der Gasphase entfernt werden. Am Beispiel der Krackung von Propan wurde eine Methode beschrieben, bei der die als primäre Reaktionsprodukte gebildeten Olefine in einem in dem Zirkulationskreis eingebauten Hydrierreaktor zu den gesättigten Verbindungen aufhydriert werden. Ein Nachteil dieses Verfahrens ist, daß damit die mit der Krackung stets parallel verlaufende Dehydrierung des Reaktanden nicht untersucht werden kann.

Bei den der vorliegenden Mitteilung zugrunde liegenden Untersuchungen wurden die Olefine durch Absorption in Silbersulfat gelöst enthaltender konzentrierter Schwefelsäure aus der Gasphase des Zirkulationssystems entfernt und die Kinetik der einzelnen primären Krackreaktionen anhand des zeitlichen Verlaufs der Partialdrücke der paraffinischen Reaktionsprodukte und des gebildeten Wasserstoffs untersucht. Da ein noch einigermaßen übersichtliches Reaktionsgeschehen am ehesten bei der Krackung kurzkettiger Paraffine zu erwarten ist, wurden die Butane und Propan als Reaktanden eingesetzt.

Bis vor etwa einem Jahrzehnt fanden für die katalytische Krackung von Kohlenwasserstoffen fast ausschließlich amorphe Alumosilikate als Katalysatoren Verwendung, seitdem gewinnen aber Zeolithe wegen ihrer in vielen Fällen außerordentlich hohen Aktivität und Selektivität auf diesem Gebiet immer mehr an Interesse und Bedeutung. Allerdings beschränken sich bisher die diesbezüglichen Untersuchungen im wesentlichen auf Faujasit [z. B. 2—10] und Mordenit [z. B. 2, 3, 6, 9, 11]. Daneben sind noch vereinzelt einige andere, meist synthetische Zeolithe bei der Krackung paraffinischer Kohlenwasserstoffe eingesetzt worden, so z. B. Erionit [12, 13], Offretit [2, 12, 14], Gmelinit [2], Chabasit [2], Stilbit [2] und die Zeolithe T [12] und L [6] sowie A und X [15].

Von den Zeolithen, die in der Natur weit verbreitet, in großen Lagern und in relativ hoher Reinheit vorkommen und somit auch vom technischen Standpunkt aus von Interesse sind, ist Klinoptilolit noch nicht näher hinsichtlich seiner katalytischen Eigenschaften in bezug auf die Krackung von Paraffinen untersucht worden.

Nachdem wir in früheren Arbeiten [1, 16] gezeigt haben, daß Paraffine an H-Klinoptilolit katalytisch gekrackt werden, sind in der vorliegenden Arbeit die bei thermischer Vorbehandlung dieses Katalysators eintretenden strukturellen Veränderungen und die damit einhergehenden Veränderungen der katalytischen Eigenschaften Gegenstand der Untersuchung.

Apparatur und Versuchsausführung

Die in der vorangegangenen Mitteilung [1] angegebene Apparatur und Arbeitsweise wurden bis auf folgende Modifikationen beibehalten:

1. Der Hydrierreaktor wurde durch ein Sorptionsgefäß ersetzt. Als Sorptionsmittel wurde auf Bimsstein aufgebrachte konzentrierte Schwefelsäure verwendet. Um unter den Versuchsbedingungen auch Äthylen weitgehend (bis zu Partialdrücken von weniger als 10^{-2} Torr) entfernen zu können, erwies es sich als notwendig, 20 Gew.% Silbersulfat in der Schwefelsäure zu lösen und das Sorptionsmittel auf 0 °C abzukühlen. Frisches Sorptionsmittel wurde im allgemeinen dann eingesetzt, wenn der Äthylen-Partialdruck im Zirkulationssystem einen Wert von etwa 10^{-2} Torr erreichte. Propylen und höhere Olefine waren bei dieser Versuchsführung in der Gasphase nicht nachweisbar, d. h., die Partialdrücke lagen unter 10^{-3} Torr.

2. Da keine Hydrierung der Olefine vorgenommen wurde, unterblieb der Zusatz von Wasserstoff zum Reaktanden.

3. Der aktive Katalysator wurde ebenfalls durch thermische Zersetzung der NH_4-Form eines in Ungarn natürlich vorkommenden Klinoptilolits erhalten, die thermische Behandlung wurde jedoch im Reaktor selbst durch im allgemeinen 2stündiges Ausheizen im Vakuum (bis zu einem Druck von 10^{-3} Torr) vorgenommen. Die Ausheiztemperatur wurde jeweils nach Beendigung der bei verschiedenen Reaktionstemperaturen ausgeführten Krackversuche erhöht, ohne den Katalysator zu wechseln, d. h., daß dieselbe Probe, jedoch in zunehmendem Maße dehydroxyliert, zur Untersuchung gelangte.

Versuchsergebnisse

Zur Demonstration der bei Entfernung der olefinischen Reaktionsprodukte zu erreichenden Ergebnisse sind in Abb. 1 bei der Krackung von Propan an einem bei 543 °C im Vakuum ausgeheizten H-Klinoptilolit erhaltene Kon-

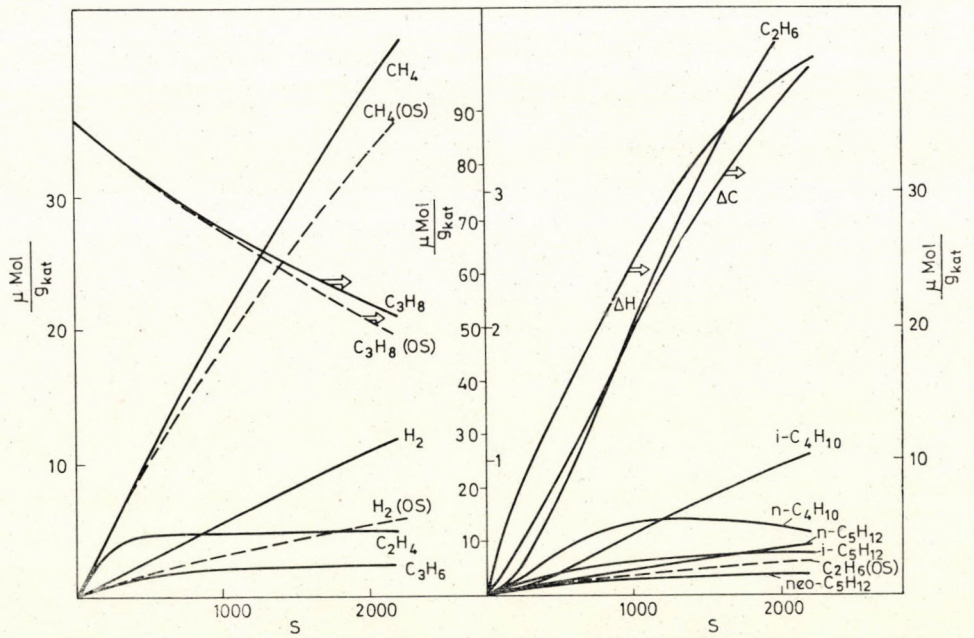

Abb. 1. Krackung von Propan an bei 543 °C vorbehandeltem NH_4-Klinoptilolit. Links: Reaktand und primäre Reaktionsprodukte. Rechts: Sekundäre Reaktionsprodukte sowie C- und H-Defizit. Ausgezogene Kurven: Verbleib der olefinischen Reaktionsprodukte im System. Gestrichelte, mit OS gekennzeichnete Kurven: Entfernung der olefinischen Reaktionsprodukte durch selektive Absorption. Reaktionstemp.: 420 °C.

versionskurven des Reaktanden angegeben und die Mengen der pro g Katalysator gebildeten Reaktionsprodukte in Abhängigkeit von der Versuchszeit dargestellt. Die gestrichelten (mit OS gekennzeichneten) Kurven wurden bei Entfernung der olefinischen Reaktionsprodukte, die ausgezogenen Kurven beim Verbleib der Olefine in der Gasphase des Zirkulationssystems erhalten. Links sind die Kurven für den Reaktanden und für die zu erwartenden primären Reaktionsprodukte, rechts die für die sekundären Reaktionsprodukte sowie der zeitliche Verlauf des Wasserstoff- und Kohlenstoffdefizits angegeben.

Wie zu ersehen ist, sind bei Entfernung der Olefine — von einer sehr geringen Äthanmenge abgesehen — keine sekundären Reaktionsprodukte

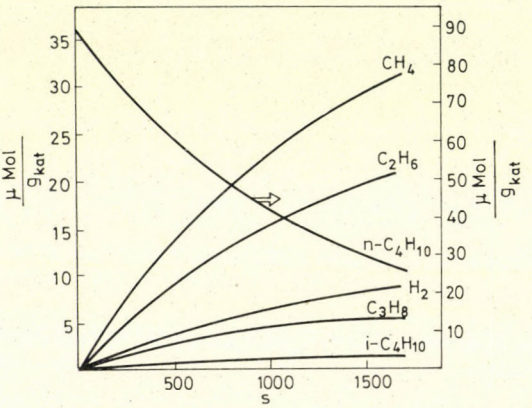

Abb. 2. Krackung von *n*-Butan an bei 510 °C vorbehandeltem NH_4-Klinoptilolit und Entfernung der olefinischen Reaktionsprodukte aus dem System. Reaktionstemp.: 408 °C.

nachweisbar. Die Kurven der primären Reaktionsprodukte Wasserstoff und Methan lassen sich zudem durch die Geschwindigkeitsgleichung erster Ordnung genau beschreiben. Während der Reaktion bleibt der Druck im Zirkulationssystem konstant und eine Produktablagerung ist in Übereinstimmung mit früheren Ergebnissen [1] nicht festzustellen. Im Krackreaktor verlaufen also praktisch nur die zu Methan und Äthylen führende Krackung und die Wasserstoff und Propylen ergebende Dehydrierung von Propan.

Dagegen laufen beim Verbleib der Olefine im Zirkulationssystem unter sonst gleichen Versuchsbedingungen mehrere Folgereaktionen ab, die — wie aus den beträchtlichen H- und C-Defiziten zu ersehen ist — zur Ablagerung kohlenstoffreicher Verbindungen auf der Katalysatoroberfläche und damit zu einer schon nach relativ kurzer Versuchszeit wahrnehmbaren Desaktivierung des Katalysators führen.

Prinzipiell die gleichen Feststellungen wurden auch bei der Krackung von *n*-Butan gemacht. Durch Entfernung der Olefine können zu *i*-Butan und Propan führende Neben- bzw. Folgereaktionen zwar weitgehend, aber doch nicht — wie aus Abb. 2 zu ersehen ist — völlig ausgeschaltet werden. Außer

den in Abb. 2 angegebenen Reaktionsprodukten wurden bei diesem Versuch bis zum Versuchsende noch 0,28 μMol (0,4% des Gesamtumsatzes) *i*-Pentan und 0,1 μMol (0,14%) *n*-Pentan per g Katalysator gebildet.

Da Propan und *i*-Butan, also die Produkte der Neben- bzw. Folgereaktionen (die Pentane sind wegen der sehr geringen Konzentrationen zu vernachlässigen), unter den Reaktionsbedingungen ebenfalls — wenn auch langsamer — reagieren und Methan und Wasserstoff ergeben, sind die experimentell bestimmten Partialdrücke dieser Verbindungen zu korrigieren. Diese Korrektur wurde zusammen mit der Auswertung der Meßwerte mittels einer elektronischen Rechenmaschine auf folgende Weise vorgenommen.

Die Krackung von Propan und *i*-Butan sowie die Dehydrierung von Propan verlaufen kinetisch — wie in dieser Arbeit noch gezeigt wird — nach erster Ordnung. Für die Dehydrierung von *i*-Butan konnte zwar die Reaktionsordnung nicht genau bestimmt werden, für diese Korrekturberechnungen kann aber auch diese Reaktion als in erster Näherung nach erster Ordnung verlaufend angesehen werden. Es gilt also

$$n_i(t) = k_{i,j} \int_0^t p_j(t) \cdot dt,$$

wobei sich der Index i auf die Reaktionsprodukte Methan und Wasserstoff und der Index j auf die Reaktanden bezieht, die in diesem Falle Produkte von Folge- bzw. Nebenreaktionen der *n*-Butankrackung sind. Die durch Krackung bzw. Dehydrierung dieser Produkte gebildeten Wasserstoff- und Methanmengen wurden berechnet, indem die bei der *n*-Butankrackung experimentell erhaltenen Partialdruck–Zeit-Kurven von Propan und *i*-Butan numerisch integriert und die erhaltenen Integralwerte mit den entsprechenden — in getrennten Versuchen ermittelten — Geschwindigkeitskonstanten $k_{i,j}$ multipliziert wurden. Diese Wasserstoff- und Methanmengen wurden von den bei der *n*-Butankrackung experimentell erhaltenen Werten abgezogen. Die sich aufgrund der Stöchiometrie ergebenden umgesetzten Propan- und *i*-Butanmengen wurden zu den experimentell erhaltenen Werten addiert. In Abb. 2 sind für diese vier Verbindungen die bereits korrigierten, sich also nur auf die Umsetzung von *n*-Butan beziehenden Werte angegeben.

Bei dieser Korrektur wurde der Einfluß des in wesentlich höheren Konzentrationen vorliegenden primären Reaktanden (*n*-Butan) auf die Kinetik der Krackung und Dehydrierung der Reaktionsprodukte (Propan und *i*-Butan) vernachlässigt. Dies ist zulässig, da unter den Reaktionsbedingungen die Bedeckung der aktiven Zentren — wie aus Massenbilanzen hervorgeht und worauf auch die Kinetik erster Ordnung hindeutet — sehr gering ist.

Die Krackung der 1- bzw. 2-Bindung* sowie die Dehydrierung des

* Unter 2-Bindung ist die zwischen den C-Atomen 2 und 3 des *n*-Butans liegende Bindung, unter 1-Bindung dagegen die zwischen den C-Atomen 1 und 2 bzw. 2 und 4 zu verstehen.

n-Butans können bei unserer Versuchstechnik anhand der Kurven, die den zeitlichen Verlauf der Methan- bzw. Äthan- und der Wasserstoffbildung beschreiben, verfolgt werden. Diese Reaktionen verlaufen — unabhängig von der Vorbehandlung des Katalysators — stets nach erster Ordnung. Nach 5—6 ohne Regenerierung aufeinanderfolgenden Versuchen ist noch keine ins Gewicht fallende Vergiftung des Katalysators festzustellen. Im Verlaufe der Reaktion steigt der Druck im Reaktionssystem um etwa 3 Torr an, was darauf zurückzuführen ist, daß *n*-Butan unter den Versuchsbedingungen merklich, und zwar wesentlich stärker als die leichteren Reaktionsprodukte, vom Sorptionsmittel gebunden und mit Abnahme des Partialdruckes wieder desorbiert wird. Die Geschwindigkeitskonstanten wurden deshalb in diesem Falle nicht (wie in [1]) aus der Steigung der nach der linearisierten Form der Geschwindigkeitsgleichung erster Ordnung dargestellten Geraden, sondern durch graphische Differentiation der Kurven ermittelt, die den zeitlichen Verlauf der Bildung der entsprechenden Reaktionsprodukte beschreiben.

Für die Bildung von Propan und *i*-Butan ergibt sich ein von den primären Krackreaktionen abweichendes kinetisches Bild. Die Bildung von Propan verläuft langsamer, die von *i*-Butan schneller als nach einer Kinetik erster Ordnung zu erwarten wäre. Hierbei spielt aber offensichtlich auch eine Vergiftung des Katalysators bzw. ein autokatalytischer Prozeß eine Rolle, denn bei den ohne Regenerierung aufeinanderfolgenden Versuchen nimmt die gebildete Propanmenge ständig ab, die *i*-Butanmenge dagegen zu.

Zunächst liegt der Gedanke nahe, daß das gebildete Propan durch Hydrierung eines Teils des primär gebildeten Propylens noch während des Durchgangs durch den Krackreaktor entsteht. Diese Möglichkeit muß aber u. a. schon deswegen ausgeschlossen werden, weil zwar hinsichtlich der Propanbildung, nicht aber für die Dehydrierung des Reaktanden eine Vergiftung des Katalysators festzustellen ist. Bei der Bildung des *i*-Butans spielt anscheinend der Partialdruck des in der Gasphase des Zirkulationssystems verbleibenden Restäthylens eine Rolle. Untersuchungen über die zur Bildung von Propan und *i*-Butan führenden Nebenreaktionen sind Gegenstand der folgenden Mitteilung.

Wird *i*-Butan als Reaktand eingesetzt, so verläuft nur die Methan als primäres Reaktionsprodukt ergebende Krackung nach einer Kinetik erster Ordnung. Die Wasserstoffbildung verläuft etwas schneller und ist kinetisch nicht auswertbar, da die Menge des gebildeten Wasserstoffs bei den ohne Regeneration aufeinanderfolgenden Versuchen von Versuch zu Versuch immer etwas größer wird. Auf die möglichen Ursachen für dieses von Propan und *n*-Butan abweichende Verhalten wird später noch eingegangen. Es sei noch vermerkt, daß ebenfalls wie bei der *n*-Butankrackung Neben- bzw. Folgereaktionen auch zur Bildung von Propan (3—4% des Gesamtumsatzes), des isomeren *n*-Butans und von *i*-Pentanspuren führen. Die durch Weiterreaktion dieser Sekundär-

produkte entstehenden Mengen der auch als primäre Reaktionsprodukte auftretenden Verbindungen Wasserstoff und Methan wurden auf die bei der *n*-Butankrackung schon dargelegte Weise berechnet und bei der Auswertung berücksichtigt.

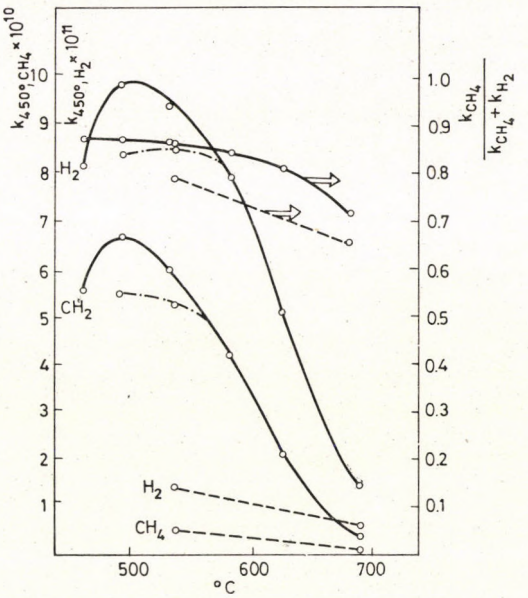

Abb. 3. Geschwindigkeitskonstanten der Krackung (CH_4) und Dehydrierung (H_2) von Propan bei einer Reaktionstemperatur von 450 °C an deamminiertem NH_4-Klinoptilolit (linke Ordinate) und Krackselektivität (rechte Ordinate) in Abhängigkeit von der Vorbehandlungstemperatur. Strich-Punkt-Kurven: nach Rehydratation des bei 536 °C vorbehandelten Katalysators. Gestrichelte Geraden: nach Rehydratation des bei 690 °C vorbehandelten Katalysators.

In Abb. 3 sind die experimentell ermittelten Geschwindigkeitskonstanten der Dehydrierung (H_2) und Krackung (CH_4) von Propan bei einer Reaktionstemperatur von 450 °C sowie die Krackselektivität in Abhängigkeit von der Vorbehandlungstemperatur des Klinoptilolit-Katalysators dargestellt. Der bis zu einer Temperatur von 690 °C ausgeheizte Klinoptilolit wurde bei Zimmertemperatur mit Wasserdampf gesättigt und nach darauffolgendem Ausheizen bei 536 und 690 °C nochmals als Katalysator eingesetzt. Die bei diesen Versuchen erhaltenen Geschwindigkeitskonstanten sind in Abb. 3 zur Kennzeichnung der Zusammengehörigkeit durch gestrichelte Geraden verbunden. Die Strich-Punkt-Kurven beziehen sich auf einen Klinoptilolit-Katalysator, der zunächst bei 536 °C ausgeheizt und danach bei Zimmertemperatur mit Wasserdampf gesättigt wurde.

In Abb. 4 sind die Geschwindigkeitskonstanten der Dehydrierung (H_2) und Krackung von *n*-Butan (ausgezogene Kurven: CH_4 = Spaltung der 1-Bindung; C_2H_6 = Spaltung der 2-Bindung) sowie der Krackung von *i*-Butan

(gestrichelte Kurve) bei einer Reaktionstemperatur von 450 °C in Abhängigkeit von der Vorbehandlungstemperatur des Katalysators dargestellt. Außerdem sind noch die Selektivitätskurven für die *n*-Butanreaktionen angegeben, die den Anteil der beiden Krackreaktionen am Gesamtumsatz bzw. den Anteil

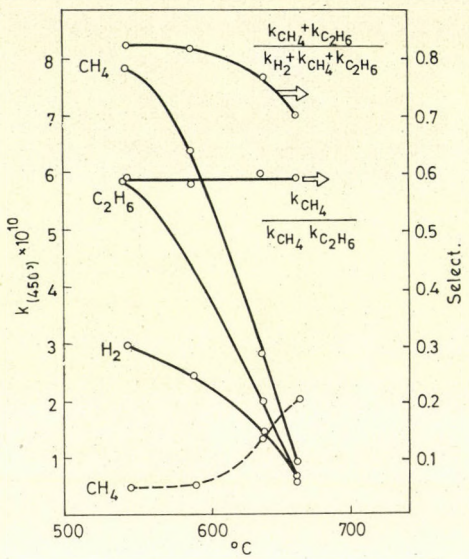

Abb. 4. Geschwindigkeitskonstanten der Krackung der 1-Bindung (CH_4) und 2-Bindung (C_2H_6) sowie der Dehydrierung (H_2) von *n*-Butan und der Krackung von *i*-Butan (CH_4, gestrichelte Kurve) bei einer Reaktionstemperatur von 450 °C an deamminierten Klinoptilolit (linke Ordinate) und Krackselektivität (rechte Ordinate) in Abhängigkeit von der Vorbehandlungstemperatur.

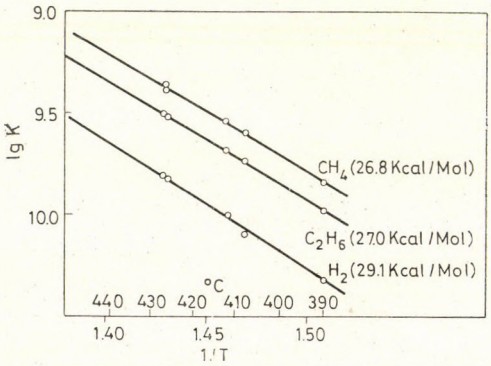

Abb. 5. Arrhenius-Diagramme für Dehydrierung (H_2) und Krackung der 1-Bindung (CH_4) und 2-Bindung (C_2H_6) von *n*-Butan an bei 543 °C vorbehandeltem NH_4-Klinoptilolit.

der an der 1-Bindung angreifenden Krackreaktion an der durch Krackung umgesetzten *n*-Butanmenge wiedergeben.

Die Geschwindigkeitskonstanten wurden jeweils für mehrere Reaktionstemperaturen bestimmt und der Arrhenius-Gleichung entsprechend aufgetragen. In Abb. 5 sind als Beispiel die Arrhenius-Diagramme für die Dehydrierung

und die Krackung der beiden Kohlenstoff-Bindungen des *n*-Butans an einem bei 543 °C vorbehandelten NH_4-Klinoptilolit wiedergegeben. Aus diesen Diagrammen wurden die scheinbaren Aktivierungsenergien der einzelnen Parallelreaktionen mit einer Genauigkeit von im allgemeinen 1—2 kcal/Mol ermittelt. In Tab. I sind die für die scheinbaren Aktivierungsenergien der einzelnen Reaktionen erhaltenen Werte angeführt.

Tabelle I

Reaktand	Vorbehandl.-Temp. °C	Aktivierungsenergie in kcal/Mol		
		Dehydrierung	Krackung	
			1-Bindung	2-Bindung
C_3H_8	462	37,6	34,4	
	494	34,3	33,0	
	532	36,6	34,3	
	581	33,7	32,3	
	624	33,4	31,7	
	690	32,0	33,4	
	536*	33,9	31,1	
	690*	33,0	32,5	
	496**	34,8	32,1	
	536**	34,1	32,8	
n-C_4H_{10}	543	29,1	26,8	27,0
	587	28,5	26,9	26,0
	635	28,0	27,2	26,3
	660	29,2	27,2	27,3
i-C_4H_{10}	543	nicht bestimmbar	21,2	
	587		19,4	
	635		20,2	
	660		20,8	

* Nach Ausheizen bei 690 °C, nachfolgender Wasserdampfadsorption bei Zimmertemperatur und erneutem Ausheizen bei der angegebenen Temperatur

** Nach Ausheizen bei 536 °C, nachfolgender Wasserdampfadsorption bei Zimmertemperatur und erneutem Ausheizen bei der angegebenen Temperatur

Das als Katalysator verwendete Klinoptilolit-Gestein enthält an kristallinen Komponenten — wie die Röntgendiffraktogramme zeigen — neben Klinoptilolit noch geringere Mengen von Quarz, Feldspat und Cristobalit. Montmorillonit ist offensichtlich nicht oder nur in geringen Mengen zugegen, da der dafür charakteristische diffuse, breite Peak bei kleinen Reflexionswinkeln nicht zu beobachten ist.

Der Mindestgehalt des Gesteins an Klinoptilolit kann abgeschätzt werden, wenn man annimmt, daß der beim Austausch gegen NH_4-Ionen maximal zu erreichende Austauschgrad von 1,64 mVal pro g wasserfreie deamminierte Substanz einem 100%igen Austausch entspricht und das Gestein — wofür die Röntgenuntersuchungen sprechen — außer Klinoptilolit keine ins Gewicht fallenden Mengen ionenaustauschender Begleitminerale enthält. Unter Zugrun-

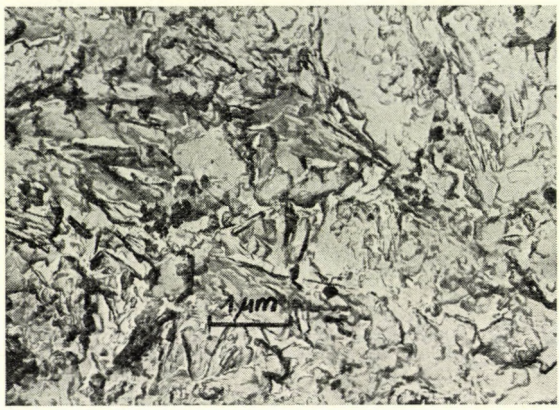

Abb. 6. Elektronenmikroskopische Aufnahme der Oberfläche von thermisch nicht vorbehandeltem NH_4-Klinoptilolit.

delegung der Formel $Me_2O \cdot Al_2O_3 \cdot 10{,}8\,SiO_2$, die aus der chemischen Zusammensetzung eines praktisch reinen Klinoptilolits erhalten wurde (siehe [17]), errechnet sich somit der Klinoptilolit-Gehalt der wasserfreien NH_4-Form zu etwa 61%.

Das Klinoptilolit-Gestein ist — wie die in Abb. 6 wiedergegebene, nach dem Kohlehülleabdruckverfahren angefertigte elektronenmikroskopische Aufnahme der NH_4-Form erkennen läßt — ein Agglomerat von meist länglichen, unregelmäßigen Kristalliten mit Teilchengrößen von etwa 0,05 bis 1 μm. Mit steigender Vorbehandlungstemperatur, also zunehmender Dehydroxylierung werden zwar die Ecken und Kanten der Kristallite zunehmend unschärfer, Größe und Verteilung dieser Agglomerat-Teilchen ändern sich aber nicht wesentlich. Das ist aus der in Abb. 7 als Beispiel wiedergegebenen elektronenmikroskopischen Aufnahme der bei 700 °C vorbehandelten NH_4-Form zu erkennen.

In Übereinstimmung damit ist die mit einem Quecksilberporosimeter gemessene Makroporenverteilung (interkristallines Porenvolumen) praktisch unabhängig von der Vorbehandlungstemperatur. Durch Tempern der NH_4-Form bei 700 °C wird das Maximum der Porenverteilungskurve lediglich von 210 Å auf etwa 240 Å (Porendurchmesser) verschoben.

Die bei —196 °C aufgenommenen Krypton-Adsorptionsisothermen ändern sich — wie aus Abb. 8 zu ersehen ist — ebenfalls nicht wesentlich mit der Vor-

behandlungstemperatur. Die aus diesen Isothermen nach BET berechneten Oberflächengrößen liegen zwischen 39,8 und 31,4 m^2/g. Da Krypton bei —196 °C nicht in das Innere der Klinoptilolit-Kristallite einzudringen vermag,

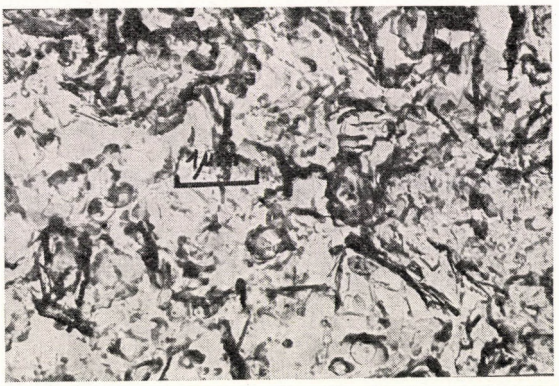

Abb. 7. Elektronenmikroskopische Aufnahme der Oberfläche von bei 700 °C vorbehandeltem NH_4-Klinoptilolit.

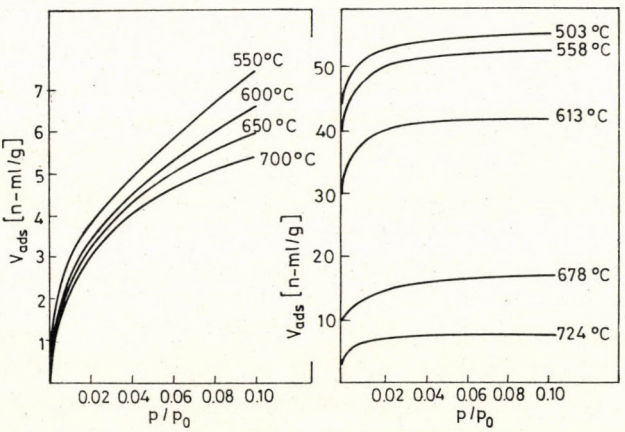

Abb. 8. Krypton- (links) und Stickstoff-Adsorptionsisothermen (rechts) an bei verschiedenen Temperaturen vorbehandeltem NH_4-Klinoptilolit. Adsorpt-.Temp.: —196 °C.

handelt es sich hierbei um die Oberfläche des Makroporenraumes, also hauptsächlich um die äußere Oberfläche der Klinoptilolit-Kristallite.

Die bei —196 °C aufgenommenen, in Abb. 8 ebenfalls wiedergegebenen N_2-Adsorptionsisothermen zeigen den für die Adsorption in Zeolithen charakteristischen Verlauf. Die Sorptionskapazität nimmt mit steigender Vorbehandlungstemperatur stark ab, was eine Zerstörung der Klinoptilolit-Struktur anzeigt. In Übereinstimmung damit stehen röntgendiffraktometrische Unter-

suchungen. In Abb. 9 ist die Peakfläche der intensivsten Reflektion (020-Ebene) in Abhängigkeit von der Vorbehandlungstemperatur dargestellt. Wie zu ersehen ist, tritt mit steigender Vorbehandlungstemperatur ein in den Ausmaßen mit der Verminderung der N_2-Adsorptionskapazität vergleichbarer Verlust an Kristallinität ein.

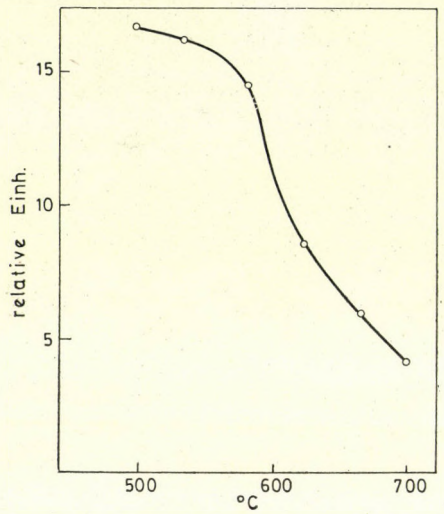

Abb. 9. Röntgendiffraktogramm-Peakfläche der intensivsten (020) Reflexion am NH_4-Klinoptilolit in Abhängigkeit von der Vorbehandlungstemperatur.

All diese Beobachtungen zusammenfassend kann gesagt werden, daß bei der thermischen Behandlung der als Katalysator eingesetzten NH_4-Form des ungarischen Klinoptilolits die Kristallstruktur der Klinoptilolit-Kristallite schon bei relativ niedrigen Temperaturen (dehydroxylierter Mordenit ist z. B. wesentlich thermostabiler [18]) fast vollständig zusammenbricht, die »Sekundärstruktur« des Gesteins aber praktisch unbeeinflußt bleibt.

Diskussion

Bei der thermischen Behandlung von NH_4-Zeolithen entsteht — wie Uytterhoeven u. Mitarb. [19—21], Ward [22, 23] und viele andere am Faujasit des Y-Typs und Karge [24] am Mordenit durch IR-spektroskopische und thermoanalytische Untersuchungen eindeutig festgestellt haben — nach den folgenden schematischen Reaktionsgleichungen zunächst unter Abspaltung von Ammoniak die Zentren des Brönsted-Typs (A) enthaltende Wasserstoff-Form des Zeoliths, die bei höheren Temperaturen unter Wasserabspaltung in die saure Zentren des Lewis-Typs (B) und basische Brönstedzentren (C) aufweisende sog. dehydroxylierte Form übergeht:

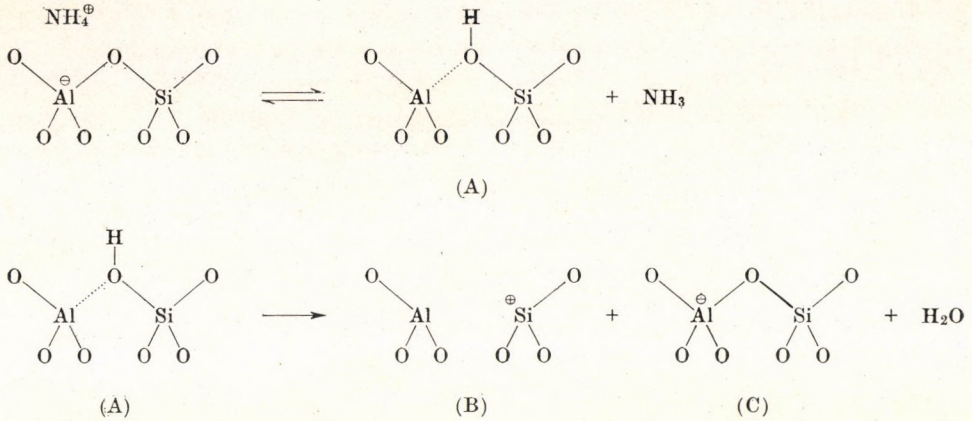

Sowohl beim Faujasit als auch beim Mordenit, aber auch beim Klinoptilolit [18] überlappen sich die Temperaturbereiche, in denen diese beiden Reaktionen ablaufen, nur wenig. Es ist also zu erwarten, daß gewisse Schlüsse über die chemische Natur der aktiven Zentren zu ziehen sind, wenn die katalytische Aktivität und Selektivität in Abhängigkeit von der thermischen Vorbehandlung der NH_4-Zeolithe untersucht wird.

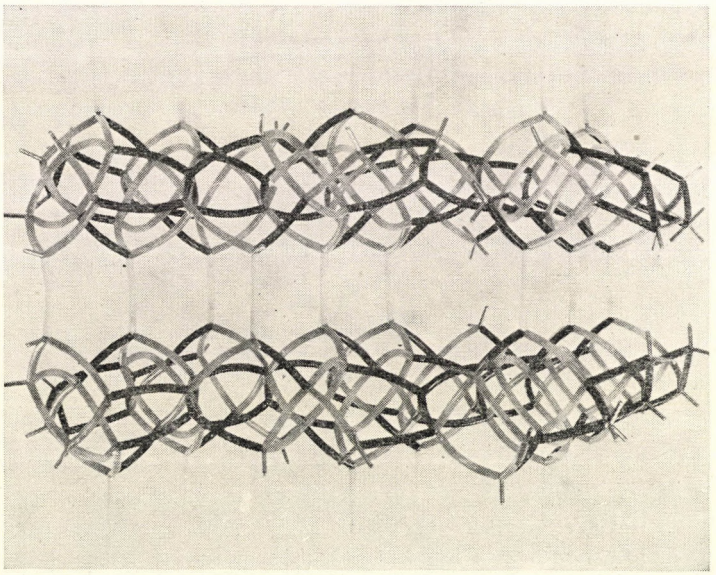

Abb. 10. Kristallgitter des mit Klinoptilolit isostrukturellen Heulandits [25].

Klinoptilolit ist bekanntlich isostrukturell mit Heulandit, und man darf deshalb die in Einzelheiten aufgeklärte Kristallstruktur dieses Zeoliths [25] — die in Abb. 10 dargestellt ist — auch dem Klinoptilolit zugrunde legen.

Die relative Instabilität des H-Klinoptilolits bei thermischer Behandlung ist nun aufgrund dieser Struktur leicht zu erklären, wenn man annimmt, daß bei der Dehydroxylierung — entweder infolge einer entsprechenden Verteilung der Al- und Si-Atome in Gitter oder durch bei den betreffenden Temperaturen leicht vorstellbare Oberflächendiffusion von O^{2-}-Ionen — vornehmlich die Brückensauerstoffatome aus dem Kristallverband heraustreten, die die in der Heulandit-Struktur vorliegenden Schichten miteinander verbinden. In einem solchen Falle ist zu erwarten, daß bereits der Austritt von relativ wenigen Gittersauerstoffatomen eine beträchtliche Instabilität des Gitters parallel zu den Schichten zur Folge hat.

Es ist wiederholt festgestellt worden, daß die katalytische Aktivität von NH_4-Zeolithen mit steigender Vorbehandlungstemperatur durch ein Maximum geht. TURKEVICH und ONO [26] beobachteten bei der Krackung von 2,3-Dimethylbutan an Y-Faujasit ein Maximum bei etwa 450 °C, während HOPKINS [6] bei der Krackung von *n*-Hexan und *n*-Heptan an deamminiertem NH_4—Y und NH_4—L Aktivitätsmaxima bei etwa 550 °C konstatierte. Bei der Alkylierung von Benzol [27] und der Disproportionierung von Toluol [3] an Y-Faujasit wurde eine maximale Aktivität bei Vorbehandlungstemperaturen von etwa 600 °C gefunden. HICKSON und CSICSERY [28] beobachteten bei der Isomerisierung von 1-Methyl-2-äthyl-benzol und Diäthylbenzol an Y-Faujasit ein Maximum bei etwa 650 °C. Im Falle des Mordenits liegen die Aktivitätsmaxima (Disproportionierung von Toluol, Krackung von *n*-Butan und *n*-Pentan) bei noch höheren Temperaturen, und zwar bei nahezu 700 °C [3].

Aus Abb. 3 ist zu ersehen, daß ein solches bei etwa 500 °C liegendes Aktivitätsmaximum auch bei der Krackung und Dehydrierung von Propan an getempertem NH_4-Klinoptilolit auftritt. Als einfachste Erklärung für die Ausbildung dieser Maxima wäre anzunehmen, daß saure Brönstedzentren (A) katalytisch aktiv sind, denn die Zahl dieser Zentren muß ja infolge des konsekutiven Verlaufs der Reaktionen (1) und (2) mit steigender Temperatur durch ein Maximum gehen. Diese Annahme ist aber nicht haltbar, da — wie IR-spektrophotometrische [29, 30] und thermogravimetrische [18] Untersuchungen gezeigt haben — die Deamminierung von NH_4-Klinoptilolit bereits bei Temperaturen um 400 °C praktisch beendet ist und bei einer Temperatur von 500 °C, bei der das Aktivitätsmaximum liegt, schon eine merkliche Dehydroxylierung eingesetzt hat.

Auch im Falle des Faujasits liegen — worauf mehrere Autoren hinweisen — die Aktivitätsmaxima bei beträchtlich höheren Temperaturen als das Maximum der Oberflächenkonzentration der Brönstedzentren, und zwar in einem Temperaturbereich, in dem bereits eine partielle Dehydroxylierung vorliegt (s. auch [31]). HOPKINS [6] nimmt deshalb an, daß ausschließlich oder zumindest vorwiegend die am stärksten sauren, also erst bei relativ hohen Temperaturen gebildeten Brönstedzentren aktiv sind. Wäre eine solche Inho-

mogenität in der Säurestärke Ursache für das Auftreten der Aktivitätsmaxima, so sollten Unterschiede in den scheinbaren Aktivierungsenergien der ablaufenden Reaktionen zu beobachten sein. Aus Tab. I ist jedoch zu ersehen, daß die scheinbare Aktivierungsenergie für die Propankrackung innerhalb der Fehlergrenzen unabhängig von der Vorbehandlungstemperatur ist. Die Aktivierungsenergie für die Dehydrierung des Propans scheint sogar mit steigender Vorbehandlungstemperatur geringfügig abzunehmen, allerdings nicht nur in dem in diesem Zusammenhang interessierenden Bereich bis 500 °C.

Wahrscheinlicher ist deshalb die von LUNSFORD [32] sowie TURKEVICH und ONO [26] vertretene Auffassung, daß ein Zusammenwirken von Brönsted- und Lewiszentren anzunehmen sei. Nach Lunsford wirken die Defektstellen des Typs B (Reaktion 2) induktiv auf benachbarte Hydroxylgruppen und erhöhen deren Säurestärke. Als katalytisch aktiv werden nur die so induktiv aktivierten Brönstedzentren angesehen. Der Verlauf der Aktivitätskurven läßt sich dann damit erklären, daß die Zahl dieser aktiven Zentren im Temperaturbereich unterhalb des Maximums durch die Oberflächenkonzentration der Defektstellen, oberhalb des Maximums dagegen durch die der noch verbliebenen Brönstedzentren limitiert wird.

Für diese Annahme spricht, daß das Aktivitätsmaximum stets in dem Temperaturbereich auftritt, in dem die Zeolithe bereits partiell dehydroxyliert sind. Die verschiedenen Literaturangaben lassen leider keine weitergehenden, quantitativen Beziehungen zwischen katalytischer Aktivität und Dehydroxylierungsgrad erkennen und lassen auch keine genauen Vergleiche untereinander zu, da z. T. beträchtliche Unterschiede in den den Dehydroxylierungsgrad mitbedingenden Faktoren, nämlich in Zusammensetzung und Austauschgrad der Zeolithe einerseits und bestimmten Temperungsbedingungen (Druck, Zeitdauer) andererseits bestehen. Hinzu kommt, daß bisher — und darauf hat auch schon WARD [33] hingewiesen — dem bei höheren Temperaturen eintretenden partiellen oder totalen Zusammenbruch der Kristallstruktur dehydroxylierter Zeolithe keine oder zu wenig Beachtung geschenkt wurde.

Es muß aber bemerkt werden, daß bei einigen katalytischen Reaktionen an H-Zeolithen, z. B. bei der Cumolkrackung [26, 34], kein Maximum im Bereich der partiellen Dehydroxylierung auftritt. Für die Buten-Doppelbindungsisomerisierung an H-Klinoptilolit [30, 35] wurde gezeigt, daß Aktivität und Oberflächenkonzentration der Brönstedzentren parallel verlaufen. Bei diesen Reaktionen sind also — im Gegensatz zu den ein Aktivitätsmaximum aufweisenden Reaktionen — offensichtlich nur die Brönstedzentren (A) als aktive Zentren und ein reiner Carboniumionen-Mechanismus anzunehmen.

Wenn wir nun im folgenden den Versuch unternehmen, aus den dargelegten Versuchsergebnissen Rückschlüsse auf einen möglichen Reaktionsmechanismus oder zumindest auf Teilschritte des Mechanismus zu ziehen, so muß unbedingt auch der — wie aus den Abb. 3, 4 und 9 zu ersehen ist — weit-

gehend parallele Verlauf des Aktivitäts- und Kristallinitätsverlustes nach dem Aktivitätsmaximum Berücksichtigung finden. Weiterhin ist dem Umstand Beachtung zu schenken, daß die Krackaktivität mit steigender Vorbehandlungstemperatur schneller als die Dehydrieraktivität abnimmt, was sich in einer Verschiebung der Selektivität des Katalysators zuungunsten der Krackreaktion äußert.

Nicht nur das Aktivitätsmaximum, sondern auch diese Selektivitätsverschiebung lassen einen Zweizentren-Mechanismus als sehr wahrscheinlich erscheinen. Die angeführten experimentellen Befunde können widerspruchslos erklärt werden, wenn für die Dehydrierung die Defektstellen (B), für die Krackung jedoch die Kombination eines sauren Brönstedzentrums (A) mit einer benachbarten Defektstelle (B) als katalytisch aktive Zentren angesehen werden. Die Anzahl der für die Krackaktivität verantwortlichen kombinierten Zentren ist natürlich zunächst mit zunehmender Dehydroxylierung praktisch nur von der Oberflächenkonzentration der Defektstellen und nicht von der der Brönstedzentren abhängig. Erst wenn die Dehydroxylierung ziemlich weit fortgeschritten ist, beginnt die statistische Wahrscheinlichkeit, daß sich in Nachbarschaft einer neu entstehenden Defektstelle noch ein Brönstedzentrum befindet, schnell geringer zu werden. Damit erklärt sich die nicht mit einer Selektivitätsverschiebung einhergehende Aktivitätszunahme im Temperaturbereich unterhalb des Maximums und die Selektivitätsverschiebung bei höheren Dehydroxylierungsgraden. Auf den mit zunehmender Dehydroxylierung fortschreitenden Zusammenbruch des Gitters und der damit verbundenen Verringerung der aktiven Defektstellen des Typs B ist offensichtlich zurückzuführen, daß auch die Dehydrieraktivität ein Maximum durchläuft.

In Übereinstimmung damit steht, daß nach Ausheizen des Katalysators bei 536 bzw. 690 °C (Punkt-Strich-Kurve bzw. durch gestrichelte Geraden verbundene Meßpunkte in Abb. 3) und nachfolgender Rehydratation durch Adsorption von Wasserdampf bei Zimmertemperatur die maximale Aktivität nicht wieder erreicht wird, denn der partielle Gitterzusammenbruch kann natürlich nicht durch Rehydratation rückgängig gemacht werden. Es hat jedoch den Anschein, daß zumindest ein Teil der B- und C-Zentren, die in den nach einer Vorbehandlung bei 690 °C noch intakten Bereichen der Kristallstruktur vorliegen, wieder in Brönstedzentren des Typs A überführt werden können, denn nach Rehydratation und nachfolgendem Ausheizen bei 536 °C nimmt die Geschwindigkeit der Krackreaktion um etwa 30% zu, während die der Dehydrierung um einige Prozente abnimmt (s. Abb. 3).

Zweifellos interessant ist die Feststellung, daß das Verhältnis der sich auf die Spaltung der 1-und 2-Bindung von *n*-Butan beziehenden Geschwindigkeitskonstanten innerhalb der Fehlergrenzen unabhängig von der thermischen Vorbehandlung des Katalysators ist. Das weist darauf hin, daß die an den verschiedenen Bindungen eines Kohlenwasserstoffmoleküls ansetzenden Spalt-

reaktionen an gleichartigen aktiven Zentren ablaufen, erklärt jedoch noch nicht, daß die für die Spaltung der sich in der Festigkeit unterscheidenden beiden Bindungen erforderlichen Aktivierungsenergien gleich sind. Diese Übereinstimmung ist höchstwahrscheinlich einem der Oberflächenreaktion vorangehenden, geschwindigkeitsbestimmenden Reaktionsschritt, also der Chemisorption des Reaktanden bzw. der Bildung des »aktiven Oberflächenkomplexes« zuzuschreiben. Das bedeutet, daß die Aktivierungsenergien der Oberflächenreaktionen im Vergleich zu der des Sorptionsschrittes sehr gering sind.

Die experimentelle Feststellung, daß sowohl bei der katalytischen Umsetzung des Propans als auch bei der des *n*-Butans Dehydrierung und Krackung ebenfalls jeweils annähernd die gleiche scheinbare Aktivierungsenergie erfordern, deutet darauf hin, daß Krack- und Dehydrierreaktionen über den gleichen »aktiven Oberflächenkomplex« verlaufen. Daraus und aus den oben angeführten Überlegungen über die Natur der aktiven Zentren folgt, daß der aktive Oberflächenkomplex durch Chemisorption des Reaktanden an der Defektstelle des Typs B gebildet wird, bei der Aufspaltung einer C–C-Bindung des Komplexes aber — im Gegensatz zur Dehydrierung — noch ein saures Brönstedzentrum (A) am Mechanismus beteiligt ist.

Mit diesen Schlußfolgerungen ist auch die Kinetik der Krack- und Dehydrierreaktionen verträglich. Ausgehend vom Langmuirschen Adsorptionsmechanismus ist bekanntlich leicht abzuleiten, daß die Bruttoreaktion nach erster Ordnung verläuft, wenn die Chemisorption des Reaktanden der geschwindigkeitsbestimmende Schritt ist und eine geringe Bedeckung der aktiven Zentren vorliegt.

Seit langem ist bekannt, daß an den herkömmlichen Krackkatalysatoren Paraffine mit tertiären C-Atomen wesentlich schneller als die geradkettigen Paraffine mit gleicher C-Atomzahl gekrackt werden [36]. In Übereinstimmung damit ist die scheinbare Aktivierungsenergie für die Krackung von *i*-Butan an H-Klinoptilolit geringer als die für die *n*-Butanspaltung. Das ist zu erwarten, da ja das am tertiären C-Atom gebundene Wasserstoffatom reaktionsfähiger als ein H-Atom eines sekundären C-Atoms ist. Trotzdem wird aber an H-Klinoptilolit — wie aus Abb. 4 zu ersehen ist — *n*-Butan viel schneller als *i*-Butan gekrackt. Es liegt auf der Hand, daß diese Selektivität darauf zurückzuführen ist, daß zwar geradkettige, nicht aber verzweigte Paraffine in das durch die zeolithische Kristallstruktur gegebene Porensystem der Klinoptilolit-Kristallite einzudringen vermögen. Die Krackung von *i*-Butan verläuft also nur an der mit etwa 30 m^2/g relativ kleinen äußeren Oberfläche der Kristallite, und zwar mit einer Geschwindigkeit, die um mehr als eine Größenordnung geringer als die der *n*-Butankrackung ist.

Während nun aber die Aktivität der *n*-Butankrackung mit steigender Vorbehandlungstemperatur abnimmt, zeigt die entsprechende Kurve für *i*-Butan gerade einen entgegengesetzten Verlauf. Daraus folgt, daß mit zuneh-

mendem Zusammenbruch des Kristallgitters mehr aktive Zentren für *i*-Butan zugänglich werden, da die scheinbare Aktivierungsenergie gleich bleibt und somit eine qualitative Veränderung der aktiven Zentren auszuschließen ist. Leider lassen unsere gegenwärtigen Kenntnisse über die Art des partiellen Gitterzusammenbruchs und die damit einhergehenden Veränderungen der Oberflächenstrukturen des Klinoptilolits vorerst nur rein spekulative Erklärungen dieses Effektes zu, auf die hier aber nicht eingegangen werden soll.

Die Kinetik der Dehydrierung von *i*-Butan konnte — wie schon erwähnt — nicht bestimmt werden. Offensichtlich reagiert das als primäres Dehydrierprodukt entstehende *i*-Butylen noch während des Durchgangs durch den Krackreaktor oder am Katalysator in größeren Mengen chemisorbiert bleibend zu einem bereits ins Gewicht fallenden Teil unter Wasserstoffentwicklung weiter. Es könnte sich dabei z. B. um einen Ringschluß und Dehydrierung der cyclischen Verbindungen handeln. Es liegt auf der Hand, daß solche Folgereaktionen, die aus sterischen Gründen nicht im Kanalsystem, sondern nur an der äußeren Oberfläche der Klinoptilolit-Kristallite ablaufen können, selbstverständlich nur bei der Untersuchung von *i*-Paraffinen zu wesentlichen Komplikationen führen.

Deamminierter Klinoptilolit dürfte auch vom technischen Standpunkt aus von Interesse sein, da damit — im Gegensatz zu den bisher in Krackanlagen verwendeten Katalysatoren — die *n*-Paraffine weitgehend selektiv gekrackt werden und somit zu erwarten ist, daß die oft erwünschten verzweigten Kohlenwasserstoffe in größeren Ausbeuten erhalten werden. Hinzu kommt, daß diese Selektivität des Katalysators einfach durch Tempern bei bestimmten Temperaturen in sehr weiten Grenzen variierbar ist. Schließlich sei noch bemerkt, daß das in Ungarn vorkommende Klinoptilolit-Gestein mit minimalen Selbstkosten in praktisch beliebigen Mengen abgebaut werden kann und eine für die direkte Verwendung als Katalysator ausreichende Festigkeit aufweist.

*

Frau E. CZÁRÁN bin ich für die Anfertigung der elektronenmikroskopischen Aufnahmen und den Herren J. KIRÁLY und J. VALYON für die Bestimmung der Krypton-Adsorptionsisothermen und der Makroporen-Verteilungskurven zu Dank verpflichtet.

Herrn Prof. Dr. G. SCHAY und Herrn Dr. D. KALLÓ sowie Herrn Dr. H. KARGE (Fritz-Haber-Instut, Berlin) danke ich für eingehende, klärende Diskussionen und für die kritische Durchsicht des Manuskriptes.

LITERATUR

[1] BEYER, H.: Acta Chim. (Budapest) **73,** 313 (1972)
[2] MIALE, J. N., CHEN, N. Y., WEISZ, P. B.: J. Catal. **6,** 279 (1966)
[3] BENESI, H. A.: J. Catal. **8,** 368 (1967)
[4] TUNG, SHAO E., MCININCH, E.: J. Catal. **10,** 166 (1968)
[5] TUNG, SHAO E., MCININCH, E.: J. Catal. **10,** 175 (1968)
[6] HOPKINS, P. D.: J. Catal. **12,** 325 (1968)
[7] BOLTON, A. P., BUJALSKI, R. L.: J. Catal. **23,** 331 (1971)

[8] PICKERT, P. E., RABO, J. A., DEMPSEY, E., SCHOMAKER, V.: Proc. Third Intern. Congr. Catal. (Amsterdam 1964) S. 714
[9] TOPCHIEVA, K. V., ROMANOVSKII, B. V., PIGUZOVA, L. I., HO-SI THOANG, BIZREH, Y. W.: Proc. Fourth Intern. Congr. Catal. (Moscou 1968) II, S. 135
[10] RABO, J. A., ANGELL, C. L., SCHOMAKER, V.: Proc. Fourth Intern. Congr. Catal. (Moscou 1968) II, S. 96
[11] ADAMS, C. E., KIMBERLIN, C. N., SHOEMAKER, D. P.: Proc. Third Intern. Congr. Catal. (Amsterdam 1964) S. 1310
[12] CHEN, N. Y.: Preprints Fifth Intern. Congr. Catal. (Miami Beach 1972)
[13] CHEN, N. Y., LUCK, S. J., MOVER, E. B.: J. Catal. **13,** 329 (1969)
[14] WHYTE, T. E., WU, E. L., KERR, G. T., VENUTO, P. B.: J. Catal. **20,** 88 (1971)
[15] WEISZ, P. B., FRILETTE, R. W., MAATMANN, R. W., MOWER, E. B.: J. Catal. **1,** 307 (1962)
[16] BEYER, H., KALLÓ, D., SCHAY, G.: Rev. Roum. Chim. **17,** 29 (1972)
[17] MUMPTON, F. A.: Amer. Mineralogist **45,** 351 (1960)
[18] BEYER, H., PAPP, J., KALLÓ, D.: Acta Chim. (Budapest) (im Druck)
[19] UYTTERHOEVEN, J. B., CHRISTNER, L. G., HALL, W. K.: J. Phys. Chem. **69,** 2117 (1965)
[20] UYTTERHOEVEN, J. B., JACOBS, P., MAKAY, K., SCHOONHEYDT, R.: J. Phys. Chem. **72,** 1768 (1968)
[21] SCHOONHEYDT, R. A., UYTTERHOEVEN, J. B.: J. Catal. **19,** 55 (1970)
[22] WARD, J. W.: J. Catal. **9,** 225 (1967)
[23] WARD, J. W.: J. Catal. **11,** 251 (1968)
[24] KARGE H.: Z. phys. Chem. Neue Folge **76,** 133 (1971)
[25] MERKLE, A. B., SLAUGHTER, M.: Amer. Mineralogist **52,** 273 (1967)
[26] TURKEVICH, J., ONO, Y.: Adv. Catal. **20,** 135 (1969)
[27] VENUTO, P. B., HAMILTON, L. A., LANDIS, P. S., WISE, J. J.: J. Catal. **5,** 81 (1966)
[28] HICKSON, D. A., CSICSERY, S. M.: J. Catal. **10,** 27 (1968)
[29] KARGE, H.: Privatmitteilung
[30] DETREKŐY, E. J., JACOBS, P. A.: Third Intern. Conf. on Molecular Sieves, Zürich 1973
[31] RABO, J. A., POUTSMA, M. L.: Adv. Chem. Ser. **102,** 284 (1971)
[32] LUNSFORD, J. H.: J. Phys. Chem. **72,** 4163 (1968)
[33] WARD, J. W.: Award Symposium on Structure-Reactivity Relationship in Zeolite Catalyst Systems, Los Angeles 1971
[34] TSUTSUMI, K., TAKAHASHI, H.: J. Catal. **24,** 1 (1972)
[35] DETREKŐY, E. J., JACOBS, P. A., KALLÓ, D., UYTTERHOEVEN, J. B.: J. Catal. (im Druck)
[36] GOOD, G. M., VOGE, H. H., GREENSFELDER, B. S.: Ind. Engng. Chem. **39,** 1032 (1947)

Hermann BEYER; 1025 Budapest, Pusztaszeri út 59/67. Ungarn.

Acta Chimica Academiae Scientiarum Hungaricae, Tomus 84 (1), pp. 45—53 (1975)

PROPERTIES OF ALCHOL–AMINE MIXTURES, VII

CONDUCTIVITY OF *n*-BUTYLAMINE–ALCOHOL MIXTURES

F. RATKOVICS and M. LÁSZLÓ-PARRAGI

(Electrochemistry Departmental Research Group of the Hungarian Academy of Sciences, Chemical Industrial University, Veszprém)

Received February 4, 1974

A study was made at 0 and 20 °C of the specific conductivity, as a function of the composition, in mixtures of *n*-butylamine with methanol, ethanol, 1-propanol and 1-butanol. In these mixtures the conductivity exhibits a maximum in the amine mole fraction range 0.05—0.15. It was found that of the alcohol–amine associates formed in the mixtures, the electrolytic dissociation of complexes containing several alcohol and only one amine molecule is of primary importance as regards the conduction of current. With the rise of temperature the specific conductivity increases in mixtures containing little amine, and decreases in those containing little alcohol. On the basis of the difference between the association properties of alcohols and amines, this phenomenon is interpreted by the assumption of the Grotthus conduction mechanism.

The formation and properties of the mixed associates developing in mixtures of primary amines and normal primary alcohols have already been studied by various methods. It turned out from these studies, and mainly from those employing thermodynamic methods, that the presence of association complexes of the type AB or A_iB_j must on all accounts be reckoned with in such mixtures [1—3]. Examination of the static dielectric properties of the *n*-propylamine–1-propanol and *n*-butylamine–1-butanol mixtures revealed that the dielectric loss factor ($\tan \delta$) exhibits a sharp maximum in the concentration range between amine mole fractions of 0.1 and 0.2 [4]. On this basis it may be presumed that the specific conductivity, which can be measured more easily by classical electrochemical methods, also varies similarly as a function of the composition. The present paper gives an account of these investigations.

Experimental

Mixtures of *n*-butylamine with methanol, ethanol, 1-propanol and 1-butanol were measured at 20 and 0 °C in the complete concentration range from pure alcohol to pure amine.

Prior to use the amines (Fluka, analytically pure) were freed from water by distillation over magnesium. The alcohols used (Reanal, analytically most pure) were water-free.

The specific conductivities of the mixtures were determined in a thermostatable cell with a Radelkis OK 102/1 conductometer. In the range under consideration the apparatus operates at a frequency of 80 Hz; its highest sensitivity is 0.05 μS/scale division. The mixtures of various concentrations were prepared by mixing the components according to volume. The experimental results are given in Tables I—IV, where C is the amine concentration in mole/l, and X_{amine} is the mole fraction of the amine.

Discussion

It can be seen from the data in Tables I—IV that in the four systems examined the specific conductivity varies in a similar way as a function of concentration. In spite of the fact that the magnitude of the conductivity decreases rapidly with the increase of the molecular weight of the alcohol component, therefore, in the evaluation of the results it is possible to talk in general of

Table I

Specific conductivity of methanol–n-butylamine mixtures

C mole/l	X_{amine}	$\varkappa$,μS cm^{-1}	
		at 20 °C	at 0 °C
0	0	1.66	3.32
0.481	0.020	182.98	174.96
1.082	0.046	225.93	214.85
1.683	0.075	188.57	166.27
2.754	0.133	123.15	136.00
5.050	0.290	45.19	50.06
6.733	0.450	21.26	25.25
7.855	0.589	6.97	7.31
8.978	0.766	0.66	0.77
10 100	1.000	0.178	0.40

Table II

Specific conductivity of ethanol–n-butylamine mixtures

C mole/l	X_{amine}	$\varkappa$,ν S cm^{-1}	
		at 20 °C	at 0 °C
0	0	0.678	1.11
0.918	0.056	12.45	9.00
1.680	0.105	14.23	10.00
2.330	0.151	12.05	11.05
2.880	0.192	10.60	10.60
3.880	0.270	9.12	9.13
5.050	0.372	6.28	6.34
6.220	0.485	3.34	3.47
8.080	0.700	0.578	1.11
8.180	0.854	0.267	0.713
10.100	1.000	0.178	0.400

Table III

Specific conductivity of 1-propanol–n-butylamine mixtures

C mole/l	X_{amine}	$\varkappa$,μS cm^{-1}	
		at 20 °C	at 0 °C
0	0	0.76	0.67
0.918	0.070	4.45	3.56
1.680	0.131	5.12	3.92
2.330	0.184	5.03	3.96
2.880	0.232	4.72	3.56
3.880	0.320	3.87	3.03
5.050	0.430	2.45	2.13
6.220	0.546	1.25	1.30
8.080	0.750	0.36	0.64
9.180	0.880	0.27	0.67
10.100	1.000	0.178	0.40

Table IV

Specific conductivity of 1-butanol–n-butylamine mixtures

C mole/l	X_{amine}	$\varkappa$,μS cm^{-1}	
		at 20 °C	at 0 °C
0	0	0.31	0.51
0.918	0.085	1.60	1.49
1.680	0.133	1.69	1.58
2.330	0.218	1.65	1.58
2.880	0.270	1.56	1.53
3.880	0.367	1.20	1.16
5.050	0.480	0.80	0.79
6.220	0.598	0.53	0.70
8.420	0.820	0.27	0.55
9.320	0.917	0.31	0.46
10.100	1.000	0.178	0.40

(It should be noted that the conductivities of the pure alcohols measured in this work are somewhat larger than the literature values, probably because of the slight contamination of the chemicals. However, this does not affect the findings relating to the observed phenomena).

alcohol–primary amine mixtures. The results measured at 20 °C are compared in Figure 1. The specific conductivity can be seen to have a maximum in the concentration range 1—2 mole/l. Inspection of the concentrations relating to

these specific conductivity maxima, or more appropriately the concentrations expressed in the mole fractions of the amine, it can be seen that the position of the maximum on the mole fraction scale is shifted towards higher amine contents with the increase of the molecular weight. This is shown in Table V.

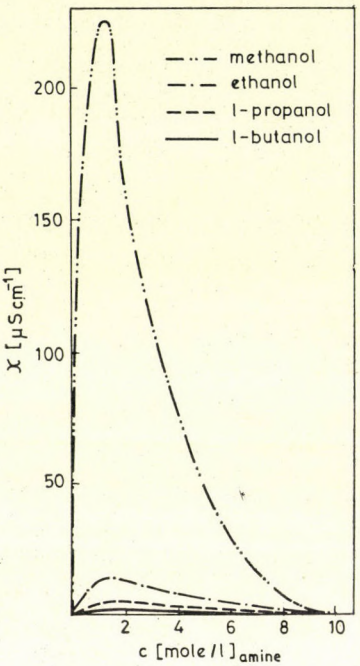

Fig. 1. Specific conductivity of *n*-butylamine–alcohol mixtures at 20 °C

The temperature dependence of the specific conductivity reveals that in the range of low and medium amine concentrations the conductivity increases with the increase of the temperature, whereas for mixtures with higher amine

Table V

Composition of mixtures exhibiting maximum specific conductivity at 20 °C

Component accompanying *n*-butylamine	Mixture with max. specific conductivity	
	C mole/l	X_{amine}
Methanol	1.2	0.05
Ethanol	1.7	0.11
1-Propanol	1.8	0.14
1-Butanol	1.6	0.15

contents the conductivity falls as the temperature rises. This can be seen in Figures 2—5. These observations can be interpreted by consideration of the association properties of alcohols and amines. Our hypothesis, which provides a qualitative explanation for the experimental results presented, and at the

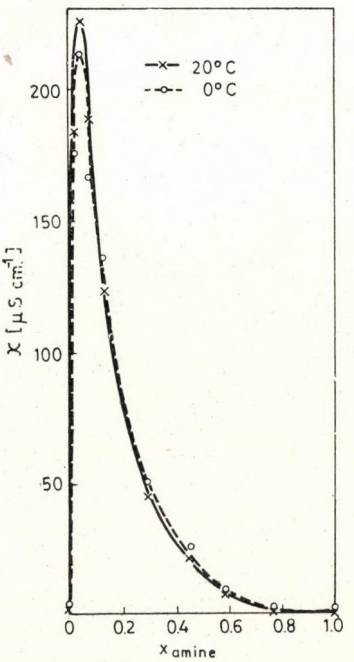

Fig. 2. Specific conductivity of *n*-butylamine–methanol mixtures

same time is not in contradiction with other experimental results relating to alcohols, amines and their mixtures, is as follows.

In the liquid phase, pure alcohols consist of association complexes of cyclic and chain form. It was earlier shown that in such systems the greatest possible average degree of association is approximately 4, and this theoretical conclusion was further confirmed experimentally [3, 5]. It was also found that in the liquid phase *n*-butylamine similarly contains associated molecules, but the average degree of association in this system at 20 °C is only about 1.5.

Study of the mixed associates has so far shown that, although association complexes of the type AB, $A_i B$, AB_i and $A_i B_j$ may all be present, on proceeding from the pure alcohol towards the pure amine the average degree of association decreases monotonously as a function of the composition. We feel that this finding can justifiably be generalized to each of the mixtures examined. It follows simply from stoichiometric reasons and from what has been said that (denoting the alcohol by A, and the amine by B) of the mixed associates that of type $A_i B$ must predominate in mixtures of low amine content.

The maximum concentration of the association complex of type AB is to be expected in the equimolecular mixture, or at a concentration close to this, while in all probability the complex AB_i will be present in significant amount at concentrations close to the pure amine. The amounts of complexes of the

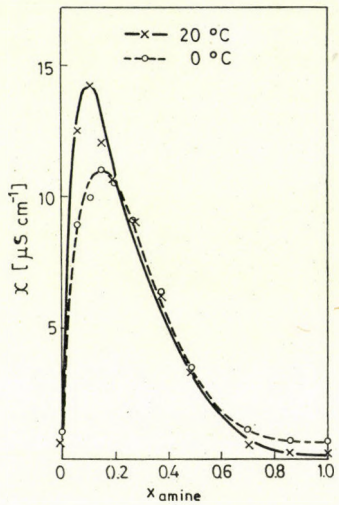

Fig. 3. Specific conductivity of *n*-butylamine–ethanol mixtures

type A_iB_j can not be too great, for if the combining of the amine and alcohol associates were to be appreciable, then the monotonous decrease of the average

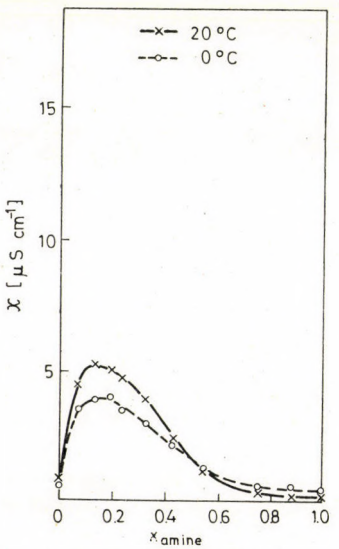

Fig. 4. Specific conductivity of *n*-butylamine–1-propanol mixtures

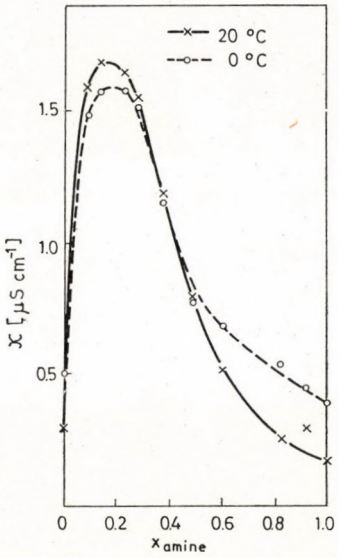

Fig. 5. Specific conductivity of *n*-butylamine–1-butanol mixtures

degree of association as a function of the composition would not be understandable. It appears from this physical picture and from the experimental results that the maxima in the specific conductivities of the mixtures, at amine mole fractions of 0.05—0.15, can be explained primarily by the electrolytic dissociation of associates of the type A_iB. A similar result is arrived at if the possible structures of the associates are considered. The assumed structure of the cyclic dimers is [6, 7]

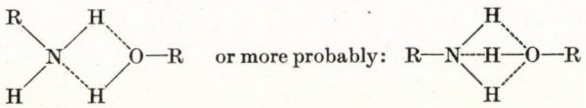

It is difficult to conceive that an amine molecule would combine *via* a triple hydrogen bond to an association complex consisting of several alcohol molecules. We consider it more likely that the coupling takes place in the following way:

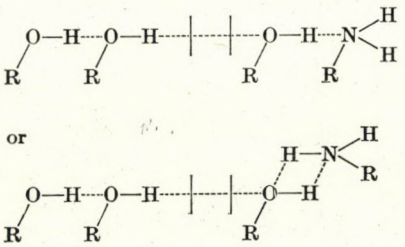

In all probability these associates possess a lower dissociation energy than the cyclic dimers, and it thus seems an acceptable assumption that the associates of the type A_iB play a decisive role in the development of the conductivity.

It must not be forgotten that, according to the Nernst—Thomson rule, the degree of dissociation of weak electrolytes is the higher, the greater the dielectric factor (relative permittivity) of the solvent, and this decreases from the pure alcohol towards the amine [4]. It is probable, therefore, that the concentration of the associates capable of dissociation and the specific conductivity exhibit maxima at different compositions. If it is assumed that this effect is quite considerable, then the experimental results can be interpreted merely *via* the formation of cyclic dimers. This was pointed out in the discussion of the dielectric properties of *n*-butylamine–1-butanol mixtures [4]. Nevertheless, as indicated in the literature [8], the Nernst—Thomson rule can be expected to hold approximately only if the electrolyte also consists of ions in the solid state. This is not so in the present case, and thus this rule can not be relied upon sufficiently either. Here the electrolyte decomposes to ions by reaction with the solvent, and can therefore be classified as a potential electrolyte. Since the dissociation of potential electrolytes is a chemical process, the dissociation depends much more on the chemical properties of the solvent than on its dielectric constant.

To summarize, it can be said that the concentration dependence of the specific conductivity of *n*-butylamine–alcohol mixtures can very probably be explained by the presence of association complexes of the type A_iB, containing several alcohol molecules. We consider that the dissociation of the cyclic dimers of type AB occurs to a much lower extent. The assumed mechanism of the association and electrolytic dissociation is thus:

$$(ROH)_n + RNH_2 \rightleftharpoons (ROH)_{n-1}RO^-H_3N^+R \rightleftharpoons RNH_3^+ + (ROH)_nRO^-$$

If this stoichiometric equation is compared with the earlier [4] assumed equation:

$$ROH + RNH_2 \rightleftharpoons RNH_3^+ \, ^-OR \rightleftharpoons RNH_3^+ + RO^-$$

it is seen that there is no fundamental difference between the two conceptions. The present conception is more general, and includes the earlier one too.

It is also wished to deal with the temperature dependence of the conductivity. It was seen in Figures 2—5 that the specific conductivity increases with the increase of temperature at low amine concentrations, but decreases for mixtures containing only a little alcohol. With the rise of temperature the amount of mixed associates certainly decreases (the heat of mixing, interpreted as the heat of the association reaction, is exothermic), and thus in low amine-containing solutions the dissociation must increase considerably as the temper-

ature rises. In other words, this means that the electrolytic dissociation of the associates of type A_iB is an endothermic process. In mixtures containing little alcohol the change of the equilibrium of the electrolytic dissociation does not compensate (and in principle it may even strengthen) the effect caused in the conductivity of the mixture by the shift in the association equilibrium in the case of a change of temperature.

Such a change in the conductivities of the pure amine and mixtures containing much amine can be justified if the conduction in these proceeds similarly to the Grotthus conduction mechanism, and so the proton exchange is accelerated as a result of the larger association complexes present at the lower temperature. This effect does not come about in the alcohols and the solutions containing much alcohol, for besides the special association conditions of the alcohols the average degree of association depends only very slightly on the temperature [5].

REFERENCES

[1] RATKOVICS, F., LISZI, J., LÁSZLÓNÉ, A.: Magy. Kém. Foly. **79**, 273 (1973)
[2] RATKOVICS, F., LÁSZLÓNÉ, A.: Magyar Kém. Foly. **79**, 276 (1973)
[3] RATKOVICS, F., SALAMON, T., DOMONKOS, L.: Magyar Kém. Foly. **80**, 155 (1974)
[4] LISZI, J., SALAMON, T., RATKOVICS, F.: Magyar Kém. Foly. **79**, 468 (1973)
[5] RATKOVICS, F., SALAMON, T., DOMONKOS, L.: Magyar Kém. Foly. **80**, 159 (1974)
[6] HUYSKENS, P., HUYSKENS, Z. T.: Bull. Soc. Chim. Belges **69**, 267 (1960)
[7] HUYSKENS, T. Z., HUYSKENS, P., von TIPPELN, P.: Bull. Soc. Chim. Belges **70**, 386 (1961)
[8] ERDEY-GRÚZ, T., SCHAY, H.: Elméleti fizikai kémia, II. (Theoretical Physical Chemistry, II.) Tankönyvkiadó, Budapest 1954

Ferenc RATKOVICS
Mária LÁSZLÓ-PARRAGI
Veszprémi Vegyipari Egyetem
8200 Veszprém, Schönherz Z. u. 10. Hungary.

Acta Chimica Academiae Scientiarum Hungaricae, Tomus 84 (1), pp. 55–61 (1975)

ON THE RING PUCKERING OF THE TRIMERIC TUNGSTEN TRIOXIDE MOLECULE

B. N. CYVIN,* M. HARGITTAI,** S. J. CYVIN* and I. HARGITTAI**

(The University of Trondheim, The Norwegian Institute of Technology, Division of Physical Chemistry, Trondheim, Norway and ** Central Research Institute for Chemistry, Hungarian Academy of Sciences, Budapest)*

Received February 8, 1974

Calculated $K = [\langle(\Delta x)^2\rangle + \langle(\Delta y)^2\rangle]/(2r)$ values from spectroscopic data of very approximate nature reveal that shrinkage effects cannot be the origin of the apparent ring puckering of W_3O_9 molecules determined in an electron diffraction study.

The electron diffraction study [1] of tungsten trioxide vapors shows the trimeric species to be prevailing under the experimental conditions with a nozzle temperature of 1400 °C in agreement with the findings of mass spectrometric investigations [2, 3]. The most important conclusion from the electron diffraction work by HARGITTAI *et al.* [1] is that the trimeric $(WO_3)_3$ molecules have a six-membered ring structure (Fig. 1). An average value of 1.77 ± 0.02 Å for the length of the tungsten–oxygen bonds was determined. The experimental data could be better approximated with nonplanar ring models than with planar ones. Figure 2 shows the experimental radial distribution together with theoretical ones calculated for nonplanar (C_{3v}) and planar (D_{3h}) ring configurations. The ring puckering of the C_{3v} model is characterized by the puckering angle ε in Fig. 3. The electron diffraction study emphasized that "the model with C_{3v} symmetry may be only one of a number of configurations of the six-membered ring structure of W_3O_9. Perhaps the structure of W_3O_9 may also be described with a planar ring and D_{3h} symmetry with large shrinkage effects caused by the enormous bending vibrations expected at this temperature."

It was the aim of the present work to calculate shrinkages or rather the quantities

$$K = \frac{\langle(\Delta x)^2\rangle + \langle(\Delta y)^2\rangle}{2r}$$

for the W_3O_9 ring structure to examine whether an average structure free from shrinkage (this would correspond approximately to the r_α parameters characterized by distances between average positions of the nuclei [4]) could be expected to be planar or nearly planar. In addition to the K values containing the effect of the perpendicular vibrations, the mean parallel amplitudes (l values) have been calculated and are presented here. The latter are expected to be useful for future electron diffraction reinvestigations of the trimeric

tungsten trioxide molecule. For a detailed description of the calculation procedures used the reader is referred to CYVIN's book [5].

From the beginning, however, the very approximate nature of the present calculations must be emphasized. The most important difficulty arises from

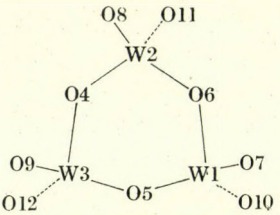

Fig. 1. Numbering of atoms in the W_3O_9 molecular model

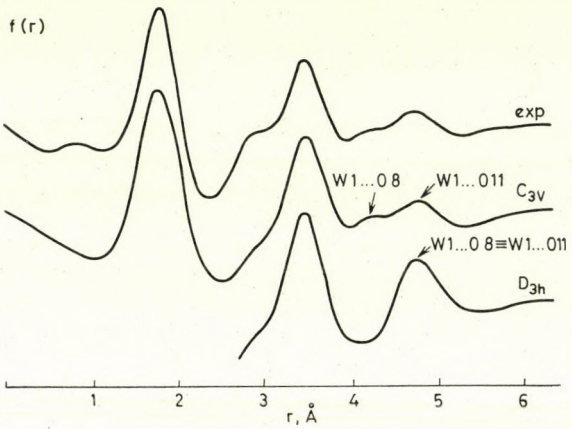

Fig. 2. Experimental (E) and theoretical (C_{3v} and D_{3h}) radial distributions of W_3O_9

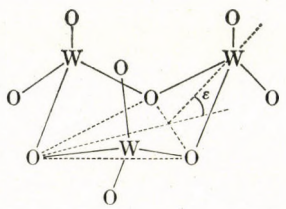

Fig. 3. The puckering angle (ε) of the C_{3v} model of W_3O_9 determined to be 15—20° from electron diffraction data [1]

the scarcity of reliable vibrational frequencies. On the basis of a matrix isolation infrared spectroscopy study, for $(WO_3)_3$ itself WELTNER and MCLEOD [6] present only three frequencies (out of the expected 17 active for the puckered ring model) as positively identified, and even these three are not characterized as to type, species and degeneracy. It might have been possible, however, to

transfer force constants from similar molecules if reliable spectra had been available. Frequencies for WO_3 and W_3O_9 (g, D_{3h}) from JANAF Tables [7] do not seem to be unambiguous enough and have not been used here. The frequencies for WO_2 [6, 7] seem to be reliable and those for tetrahedral WO_4^{2-} [7, 8] were also considered adequate because of the relative stability of this ion as compared to the mixtures of the gaseous oxides.

The above considerations clearly stress the limitations of the present calculations. On the other hand, the effects we are looking for, are relatively large, as the variations of the W1...O8 and W1...O11 distances illustrate. In the case of the planar ring these two types of distances are equivalent

Table I

Observed and calculated frequencies (cm^{-1}) for $(WO_3)_3$
(the geometrical parameters used are given in the text)

Observed*	Calculated	
	Puckered ring force field 2	Planar ring force field 2
1024	1029 (E)	1035 (E')
941	951 (A_1)	980**(A_1')
	941 (E)	947**(A_1')
	931**(A_2)	942 (E')
932	928 (A_1)	932**(A_2')
860	887 (E)	885 (A_2'')
874	879 (A_1)	885**(E'')
826	827 (E)	832 (E')
487	507 (A_1)	389**(E'')
	402 (E)	380 (A_2'')
	330 (A_1)	304**(A_1')
	292 (E)	279 (E')
	249 (E)	263**(A_2')
	248**(A_2)	260 (E')
	245 (A_1)	242**(A_1')
	212**(A_2)	226**(A_1'')
	208 (E)	192 (E')
	192 (E)	192**(E'')
	119 (A_1)	107**(E'')
	86 (E)	64 (A_2'')

* Observed by WELTNER and MCLEOD [6] who give the following frequencies: 1024, (941), (932), 874, (860), (848), (826), (776) and 487 (all in cm^{-1}) with the values in parenthesis marked W_3O_9 or W_4O_{12}

** Inactive in infrared

($r \approx 4.5$ Å). For the nonplanar ring models the W1...O8 and W1...O11 distances are not equivalent. According to the experimental data (*cf.* the radial distribution in Fig. 2), the splitting is about 0.5 Å or more. Accordingly, an order of magnitude estimate of the shrinkages was expected to be revealing.

The calculations were performed on the basis of the data mainly for WO_2 and WO_4^{2-} and also of intuition and experience. The influence of different force fields and different geometrical parameter sets has also been checked. Force field 1 is close to having diagonal elements only, while force field 2 has some reasonable interaction terms.

In spite of the very loose foundation, the calculated frequencies above 500 cm^{-1} showed, especially for the puckered ring model, remarkably good correspondence to those of WELTNER and MCLEOD [6]. Table I tentatively

Table II

Calculated frequencies (cm^{-1}) for $(WO_3)_3$
(the geometrical parameters used are given in the text)

Puckered ring			Planar ring		
	Force field 1	Force field 2		Force field 1	Force field 2
A_1:	977	951	A_1'**:	950	980
	950	928		788	947
	881	879		250	304
	686	507		229	242
	301	330	A_2'**:	1031	932
	259	245		429	263
	140	119	E':	1031	1035
A_2**:	1035	931		944	942
	406	248		827	832
	345	212		373	279
E:	1057	1029		257	260
	944	941		162	192
	898	887	A_1''**:	368	226
	868	827	A_2'':	889	885
	551	402		584	380
	352	292		68	64
	328	249	E''**:	827	885
	263	208		611	389
	229	192		313	192
	89	86		112	107

** Inactive in infrared

Table III

Tentative l and K values (Å) *for* $(WO_3)_3$, *planar ring model*
(the geometrical parameters used are given in the text)

Distance	Equilibr. distance	Force field 1 1400 °C		Force field 2			
				l		*K*	
		l	*K*	25 °C	1400 °C	25 °C	1400 °C
W—O 1—5	1.870	0.066	0.019	0.038	0.065	0.004	0.019
W=O 1—7	1.680	0.058	0.045	0.036	0.058	0.011	0.058
W...W 1—2	3.455	0.103	0.002	0.037	0.083	0.000	0.002
W...O 1—4	3.708	0.122	0.013	0.048	0.094	0.003	0.013
W...O 1—8	4.535	0.217	0.013	1.105	0.239	0.003	0.016
O ...O 7—10	2.744	0.185	0.066	0.079	0.166	0.016	0.088
O ...O 4—5	2.967	0.102	0.021	0.051	0.087	0.004	0.022
O ...O 4—7	4.875	0.220	0.025	0.105	0.232	0.005	0.029
O ...O 4—8	2.920	0.119	0.045	0.077	0.160	0.009	0.051
O ...O 7—8	5.135	0.468	0.009	0.218	0.508	0.002	0.012
O ...O 7—11	5.822	0.165	0.015	0.098	0.215	0.004	0.020

Table IVa

Tentative l and K values (Å) *for* $(WO_3)_3$, *puckered ring*
(the geometrical parameters used are given in the text)

Distance	Equilibr. distance	Force field 1 1400 °C		Force field 2			
				l		*K*	
		l	*K*	25 °C	1400 °C	25 °C	1400 °C
W—O 1—5	1.870	0.066	0.018	0.038	0.067	0.004	0.018
W=O 1—7	1.680	0.058	0.043	0.036	0.058	0.008	0.059
W...W 1—2	3.455	0.103	0.001	0.045	0.100	0.000	0.002
W...O 1—4	3.609	0.108	0.008	0.053	0.107	0.002	0.008
W...O 1—8	4.205	0.271	0.015	0.118	0.303	0.003	0.019
O ...O 7—10	2.744	0.174	0.046	0.082	0.160	0.009	0.071
O ...O 4—5	2.757	0.124	0.025	0.064	0.124	0.005	0.025
W...O 1—11	4.781	0.126	0.006	0.060	0.154	0.001	0.010
O ...O 4—7	4.542	0.245	0.015	0.110	0.272	0.003	0.019
O ...O 4—10	4.976	0.188	0.008	0.087	0.200	0.002	0.012
O ...O 4—8	2.961	0.118	0.044	0.062	0.157	0.008	0.051
O ...O 4—11	2.961	0.118	0.025	0.061	0.157	0.005	0.032
O ...O 7—8	4.300	0.507	0.025	0.218	0.558	0.005	0.032
O ...O 7—11	5.697	0.246	0.014	0.111	0.287	0.003	0.020
O ...O 10—11	5.798	0.214	0.009	0.098	0.281	0.002	0.014

correlates the observed frequencies with those calculated for the puckered and planar rings using force field 2. The frequency values are arranged in descending order. WELTNER and MCLEOD observed the spectrum above 280 cm^{-1} only, and, accordingly, there is no hint as to the reliability of our lowest frequencies. Table II gives our calculated frequencies with the two force fields for each molecular model. Tables III and IV (a, b) give the l and K values calculated

Table IVb

Tentative l and K values (Å) *for* $(WO_3)_3$, *puckered ring*
(the geometrical parameters used are as follows: $r(W{=}O) = 1.73$ Å, $r(W{-}O) = 1.82$ Å, $<O{=}W{=}O = 120°$, $<O{-}W{-}O = 85°$ and $<W{-}O{-}W = 144°$)
Calculated frequencies (cm^{-1}):
944, 912, 867, 536, 374, 253, 135
953, 218, 187
1047, 937, 893, 800, 410, 318, 242, 209, 178, 93

Distance			1400 °C	
			l	K
W—O	1—5	1.820	0.067	0.015
W=O	1—7	1.730	0.059	0.054
W...W	1—2	3.462	0.098	0.001
W...O	1—4	3.439	0.115	0.006
W...O	1—8	4.178	0.285	0.019
O...O	7—10	2.996	0.132	0.066
O...O	4—5	2.459	0.131	0.020
W...O	1—11	4.739	0.166	0.011
O...O	4—7	4.348	0.237	0.020
O...O	4—10	4.739	0.211	0.013
O...O	4—8	2.937	0.161	0.046
O...O	4—11	2.937	0.161	0.029
O...O	7—8	4.178	0.520	0.031
O...O	7—11	5.699	0.276	0.020
O...O	10—11	6.623	0.309	0.014

with these force fields for the planar and two different puckered models, respectively. The geometrical parameters used in the calculations the results of which are presented in Tables I, II, III and IVa are as follows

for puckered and planar rings:

$$r(W{=}O) = 1.68 \text{ Å}$$
$$r(W{-}O) = 1.87 \text{ Å}$$
$$<O{=}W{=}O = 109.5°$$
$$<W{-}O{-}W = 135°$$

and for the puckered ring in addition $<O—W—O = 95°$. The geometrical parameters used for obtaining the results of Table IVb are presented in the same Table.

From the calculated K values (and without further calculation of r_α parameters or new radial distributions) it can be seen that the shrinkage effects are by far not large enough to be the origin of the apparent ring puckering of the $(WO_3)_3$ molecules.

*

Financial support to BNC from the Norwegian Research Council for Science and the Humanities is gratefully acknowledged.

REFERENCES

[1] HARGITTAI, I., HARGITTAI, M., SPIRIDONOV, V. P., EROKHIN, E. V.: J. Mol. Structure, **8**, 31 (1971)
[2] ACKERMAN, R. J., RAUH, R. G.: J. Phys. Chem., **67**, 2596 (1963)
[3] KAZENAS, E. K., TSVETKOV, YU. V.: Zh. Fiz. Khim., **41**, 3112 (1967)
[4] See *e.g.* K. KUCHITSU, S. J. CYVIN: Representation and Experimental Determination of the Geometry of Free Molecules. Molecular Structures and Vibrations (Ed.: CYVIN, S. J.). Elsevier, Amsterdam 1972
[5] S. J. CYVIN: Molecular Vibrations and Mean Square Amplitudes. Universitetsforlaget, Oslo and Elsevier, Amsterdam 1968
[6] WELTNER, W., JR., MCLEOD, D., JR.: J. Mol. Spectroscopy, **17**, 276 (1965)
[7] JANAF Thermochemical Tables. Second edition (Project dir.: STULL, D. R., PROPHET, H.) U.S. Department of Commerce, Washington, D.C., 1971
[8] K. S. KRASNOV, V. S. TIMOSHININ, T. G. DANILOVA, S. V. KHANDOZHKO: Molekularnye Postoyannye Neorganicheskikh Soedinenii. Khimiya, Leningrad 1968

Bjørg N. CYVIN, Sven J. CYVIN — N-7034 Trondheim–NTH Division of Physical Chemistry, The University of Trondheim, The Norwegian Institute of Technology, Norway

Magdolna HARGITTAI, István HARGITTAI — H-1088 Budapest, Puskin utca 11—13, Hungary.

Acta Chimica Academiae Scientiarum Hungaricae, Tomus 84 (1), pp. 63—69 (1975)

CARBOHYDRATE METHYL ETHERS, V*

SYNTHESIS OF PHENYL-β-D-GLUCOPYRANOSIDE DERIVATIVES PARTIALLY METHYLATED ON THEIR SUGAR MOIETY. PREPARATION OF 4,6-DI-O-, 2,4,6-TRI-O- AND 3,4,6-TRI-O-METHYL-D-GLUCOSE

P. NÁNÁSI and A. LIPTÁK

(Department of Biochemistry, L. Kossuth University, Debrecen)

Received December 18, 1973

Phenyl-2-O-methyl-β-D-glucopyranoside (**4**),phenyl-3-O-methyl-β-D-glucopyranoside (**5**), phenyl-4-O-methyl-β-D-glucopyranoside (**6**), phenyl-4,6-di-O-methyl-β-D-glucopyranoside (**9**), phenyl-2,4,6-tri-O-methyl-β-D-glucopyranoside (**17**) and phenyl-3,4,6-tri-O-methyl-β-D-glucopyranoside (**18**) have been synthesized. Compounds **4**, **5** and **6** were obtained from the corresponding partially methylated sugar acetates according to the HELFERICH method, after saponification. The synthesis of compounds **9**, **17** and **18** was carried out by methylating the products of the acid hydrolysis of C_2- and C_3-substituted benzylidene derivatives and subsequently debenzylating the methylated products by catalytic hydrogenation. The hydrolysis of compounds **9**, **17** and **18** afforded 4,6-di-O-methyl-D-glucose (**19**), 2,3,6-tri-O-methyl-D-glucose (**20**) and 3,4,6-tri-O-methyl-D-glucose (**21**), respectively, in good yield.

For the investigation of the mechanism of the action of emulsin, we have prepared phenyl β-D-glucopyranoside derivatives partially methylated on their sugar moiety. These investigations have shown at the same time that syntheses carried out through the β-phenylglucosides are more favourable than the methods described so far in the literature, owing to the convenient way of preparation of the intermediates and to the high yields of the individual steps.

Four isomers of the mono-O-methyl ethers of phenyl-β-D-glucopyranoside may exist. Of these, the 2-O- [1], the 3-O- [3, 4] and the 6-O-methyl [1, 5] derivatives are known from the literature. The 2-O- and 3-O-methyl ethers were obtained by the Koenigs–Knorr reaction of the corresponding acylhalo sugars subsequent to saponification.

The simplified synthesis of these two isomers and of the so far unknown phenyl-4-O-methyl-β-D-glucopyranoside was made possible by our finding that partially methylated sugar acetates can be prepared in a simple way by methylation with diazomethane and that the products obtained, quite independently of their anomeric configuration when treated by the HELFERICH method [6] in the presence of *p*-toluenesulfonic acid, afford mixtures of anomers of phenyl-tri-O-acetyl-mono-O-methyl-D-glucopyranoside rich in β-anomers. Of these mixtures, the β-anomer can be separated simply by crystallization.

By this method we have prepared the corresponding phenyl-tri-O-acetyl-mono-O-methyl-β-D-glucopyranosides (**1**—**3**), from 1,3,4,6-tetra-O-acetyl-2-O-

* Part IV: LIPTÁK, A., SELIGMANN, O.: Ber. (In press)

methyl-α-D-glucopyranose (*a*) [7], from 1,2,4,6-tetra-O-acetyl-3-O-methy-β-D-glucopyranose (*b*) [8] and from 1,2,3,6-tetra-O-acetyl-4-O-methyl-β-D-glucopyranose (*c*) [7]. The saponification of these compounds according to ZEMPLÉN gave the desired phenyl-mono-O-methyl-β-D-glucopyranosides (**4**—**6**).

Of the theoretically possible six isomeric phenyl-β-D-glucopyranoside-di-O-methyl ethers, the syntheses of the 2,3- [4], 2,4- [9], 2,6- [1], 3,4- [1] and 3,6- [1] isomers are already known.

The lacking sixth isomer, 4,6-di-O-methyl-D-glucopyranoside (**8**), was synthesized from phenyl-2,3-di-O-benzyl-β-D-glucopyranoside (*d*), described by MICHEEL *et al.*, [10]. On methylating *d* according to KUHN [11], we obtained phenyl-2,3-di-O-benzyl-4,6-di-O-methyl-β-D-glucopyranoside (**7**) the catalytic hydrogenation of which afforded the glucopyranoside **8**.

The syntheses of **2** of the theoretically possible four tri-O-methyl isomers, phenyl-2,3,4- [1, 12] and phenyl-2,3,6-tri-O-methyl-β-D-glucopyranoside [1], which also confirm their structures have been described recently.

The synthesis of the other two isomers was made possible by the successful preparation of phenyl-4,6-O-benzylidene-2-O-methyl- (**9**) and phenyl-4,6-O-benzylidene-3-O-methyl-β-D-glucopyranosides (**10**) in good yield by treating compounds **4** and **5**, with benzaldehyde and zinc chloride. By treating compounds **9** and **10** with benzyl chloride in the presence of solid potassium hydroxide, protective groups against acid hydrolysis were introduced in positions **2** and **3**, respectively (compounds **11** and **12**), and subsequently benzylidene acetal was removed by hydrolysis with dilute acid. Thus we obtained phenyl-3-O-benzyl-2-O-methyl-β-D-glucopyranoside (**13**) and phenyl-2-O-benzyl-3-O-methyl-β-D-glucopyranoside (**14**).

On methylating compounds **13** and **14**, respectively, we obtained the corresponding mono-O-benzyl-tri-O-methyl derivatives (**15** and **16**) which, after removal of the benzyl groups by catalytic hydrogenation, afforded the phenyl-2,4,6-tri-O- (**17**) and phenyl-3,4,6-tri-O-methyl-β-D-glucopyranosides (**18**).

On the basis of its physical constants, compound **17** proved to be identical with phenyl-tri-O-methyl-β-D-glucopyranoside obtained by RICHTMYER [13] by partial methylation of phenyl-β-glucopyranoside. Thus, the synthesis carried out by us confirms also the structure.

The hydrolysis of compounds **8**, **17** and **18** with 0.25 *M* sulfuric acid afforded 4,6-di- (**19**), 2,4,6-tri- (**20**) and 3,4,6-tri-O-methyl-D-glucose (**21**) in very good yield. These three glucose methyl ethers proved to be identical with authentic samples as regards their crystallographic and physical constants and chromatographic properties. The structures of the compounds prepared are shown in Fig. 1.

The ^{1}H–NMR spectra of all the six phenyl-β-D-glucopyranoside methyl ethers (**4**, **5**, **6**, **8**, **17** and **18**) recorded in deuterochloroform and deuterochloroform-deuterium oxide unequivocally prove their structures. The H-1

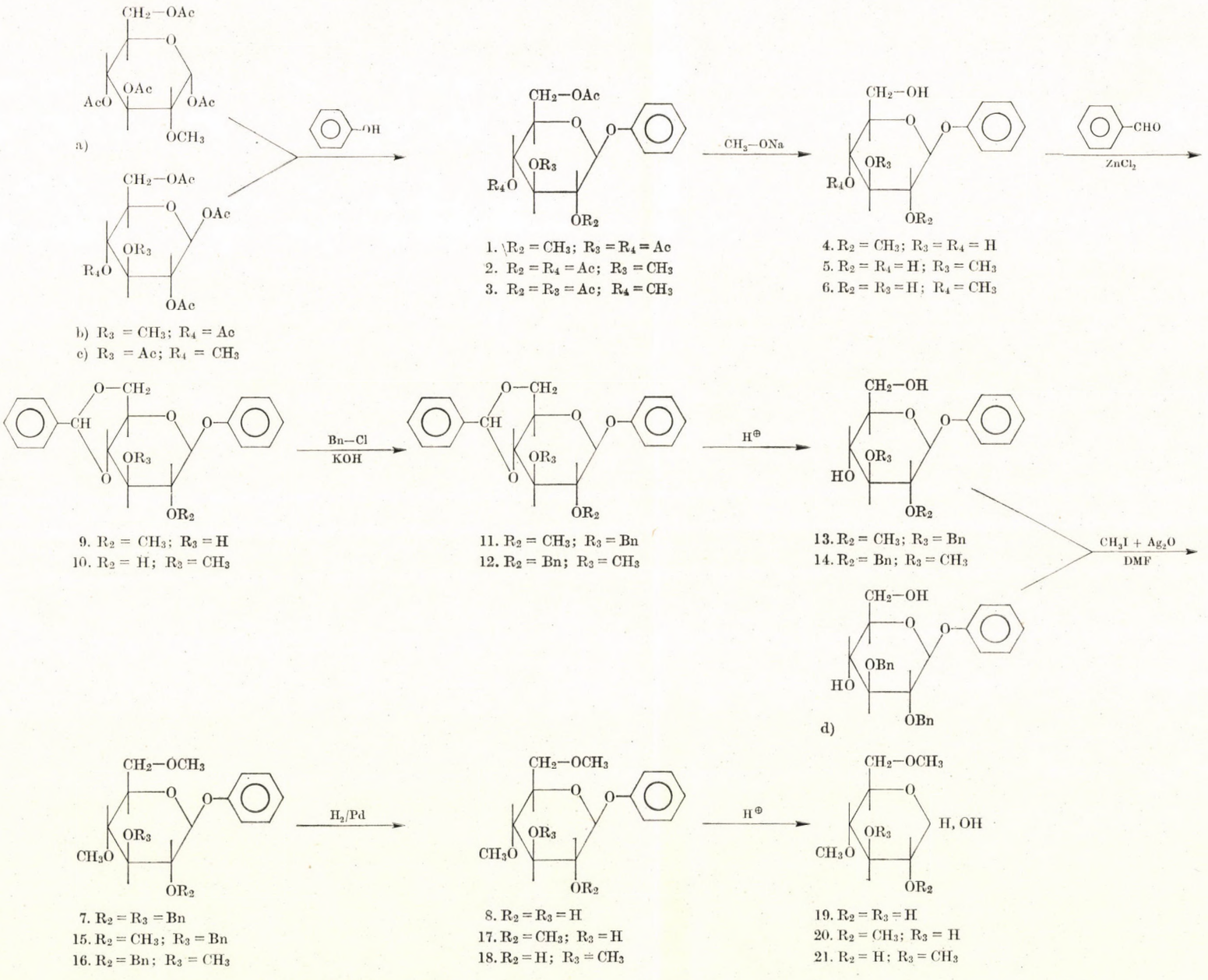

Fig. 1. **Structures of the compounds synthesized and the routes of synthesis. Ac = acetyl; Bn = benzyl; DMF = dimethylformamide**

signals appear in the $\delta = 4.95 - 4.98$ ppm range as doublets with a coupling constant $J_{1,2}$ of 7.5 Hz, pointing to a trans-diaxial structure, *i.e.* to a β-anomeric configuration.

The chemical shifts of the OCH_3 protons, in the C_2 and C_3 isomers are identical for the β-anomeric configuration ($\delta = 3.68 - 3.74$ ppm), thus they cannot be distinguished in this way. The C_4–OCH_3 protons show absorption at $\delta = 3.55 - 3.57$ ppm, and the C_6–OCH_3 protons at $\delta = 3.42 - 3.44$ ppm, thus they can readily be distinguished both from one another and from the C_2 and C_3 isomers.

Experimental

Melting points were determined with a Küstner instrument and are uncorrected. Specific rotation was measured on a Bellingham-Stanley instrument. Kieselgel G (Merck) was used in thin- layer chromatography. NMR spectra were recorded on a Varian A-60 A instrument, using tetramethylsilane ($\delta = 0$) as internal standard.

Phenyl-3,4,6-tri-O-acetyl-2-O-methy -β-D-glucopyranoside (1)

10.0 g of 1,3,4,6-tetra-O-acetyl-2-O-methyl-α-D-glucopyranose (*a*) [7] was converted with 10.35 g of phenol and 140 mg of *p*-toluenesulfonic acid in vacuum at 100 °C into a homogeneous melt and kept at this temperature for two hours. After cooling, the melt was dissolved in 300 ml benzene, the unreacted phenol extracted by shaking with 1.0 *M* sodium hydroxide and the residue washed with water until neutral reaction. The benzene solution was dried over sodium sulfate, evaporated in vacuum to a syrup and the residue crystallized from 30 ml ethanol. Yield: 6.15 g (56.4%), m.p. 92—94 °C, $[\alpha]_D^{20}$: −56.2°. (*c* = 0.2%, in chloroform).

$C_{19}H_{24}O_9$ (396.4) Calcid. C 57.57; H 6.10; Found C 58.10; H 6.12%.

Phenyl-2,4,6-tri-O-acetyl-3-O-methyl-β-D-glucopyranoside (2)

10.0 g of 1,2,4,6-tetra-O-acetyl-3-O-methyl-β-D-glucopyranose (*b*) [8] was treated with 10.35 g of phenol and 140 mg of *p*-toluenesulfonic acid as described for **1**. The crude product was recrystallized 3 times from 15 ml portions of ethanol. Yield: 4.30 g (39.4%), m.p. 147—148 °C, $[\alpha]_D^{20}$: −52.8 °C (*c* = 0.3%, in chloroform). From Ref. [3], m.p. 144—145 °C, $[\alpha]_D$: −37.6° (in chloroform).

$C_{19}H_{24}O_9$ (396.4) Calcd. C 57.57; H 6.10; Found C 57.42; H 6.06%.

Phenyl-2,3,6-tri-O-acetyl-4-O-methyl-β-D-glucopyranoside (3)

3.3 g of 1,2,3,6,-tetra-O-acetyl-4-O-methyl-β-D-glucopyranose (*c*) [7] was treated with 3.4 g of phenol and 45 mg of *p*-toluenesulfonic acid as described for **1**. The syrup, obtained on processing the melt, was recrystallized 3 times from 8 ml portions of ethanol. Yield: 1.84 g (51.0%), m.p. 86—88 °C, $[\alpha]_D^{22}$: −40.8° (*c* = 0.5%, in chloroform). From Ref. [14]: m.p. 85—89 °C, $[\alpha]_D$: −39.9° (*c* = 3.03%, in chloroform).

$C_{19}H_{24}O_9$ (396.4). Calcd. C 57.57; H 6.10; Found C 57.12; H 6.18%.

Phenyl-2-O-methyl-β-D-glucopyranoside (4)

7.90 g of phenyl-3,4,6-tri-O-acetyl-2-O-methyl-β-D-glucopyranoside (**1**) was saponified in 70 ml of anhydrous methanol with 0.5 ml of 1.0 *M* sodium methylate according to ZEMPLÉN. After allowing the mixture to stand for 14 hrs the solution was neutralized with a small amount of glacial acetic acid then evaporated to dryness in vacuum. The crystalline residue was recrystallized from 11 ml of water. Yield: 3.75 g (72.9%), m.p. 162 °C, $[\alpha]_D^{22}$: −46.0° (*c* = 0.2%, in water). Literature: m.p. 167—168 °C, $[\alpha]_D$: −63.0 (*c* = 1.0%, in ethanol).

$C_{13}H_{18}O_6$ (270.3). Calcd. C 57.78; H 6.71; Found C 57.09; H 6.61%.

Phenyl-3-O-methyl-β-D-glucopyranoside (5)

10.5 g of phenyl-2,4,6-tri-O-acetyl-3-O-methyl-β-D-glucopyranoside (**2**) was saponified in 100 ml of anhydrous methanol at room temperature with 1.5 ml 1.0 *M* sodium methylate. After evaporating the reaction mixture to dryness the residual crystalline crude product was recrystallized from 19 ml water. Yield: 6.76 g (94.4%), m.p. 151—153 °C; $[\alpha]_D^{22}$: −58.2° (*c* = 0.5%, in water). From Ref. [4]: m.p. 150—150.2 °C; $[\alpha]_D$: −65.5° (*c* = 20%, in water)

$C_{13}H_{18}O_6$ (270.3). Calcd. C 57.78; H 6.71; Found C 58.18; H 6.91%.

Phenyl-4-O-methyl-β-D-glucopyranoside (6)

2.0 g of phenyl-2,3,6-tri-O-acetyl-4-O-methyl-β-D-glucopyranoside (**3**) was saponified in 30 ml of anhydrous methanol at room temperature with 0.4 ml 1.0 *M* sodium methylate. After neutralization and evaporation the crude product was repeatedly recrystallized from 5 ml portions of water. Yield: 0.97 g (72.0%), m.p. 173 °C; $[\alpha]_D^{22}$: −52.2° (*c* = 0.22%, in water).

$C_{13}H_{18}O_6$ (270.3). Calcd. C 57.78; H 6.71; Found C. 58.11; H 6.69%.

Phenyl-2,3-di-O-benzyl-4,6-di-O-methyl-β-D-glucopyranoside (7)

3.00 g of phenyl-2,3-di-O-benzyl-β-D-glucopyranoside (*d*) [10] was shaken in 25 ml of dimethylformamide for 24 hrs with 9.80 g methyl iodide and 4.30 g silver oxide. On diluting the mixture with 150 ml chloroform, the silver halide formed precipitate was filtered off and the filtrate was washed 3 times with 20 ml portions of a 1% potassium cyanide and then 3 times with 20 ml portions of water. On drying over sodium sulfate the liquid was evaporated in vacuum to a syrup, which was then dissolved in 3 ml ethyl acetate and diluted with 12 ml of petroleum ether until it turned turbid. Small silky crystals. Yield: 2.90 g (90.0%), m.p. 56—57 °C, $[\alpha]_D^{20}$: −54.6° (*c* = 0.5%, in chloroform).

$C_{28}H_{32}O_6$ (464.5). Calcd. C 74.40; H 6.94; $-OCH_3$ 13.38; Found C 73.48; H 7.08; $-OCH_3$ 13.52%.

Phenyl-4,6-di-O-methyl-β-D-glucopyranoside (8)

The solution of 2.70 g of phenyl-2,3-di-O-benzyl-4,6-di-O-methyl-β-D-glucopyranoside (**7**) in 50 ml of ethanol was hydrogenated for 24 hrs with 200 mg of palladium on charcoal. The course of hydrogenation was followed by thin-layer chromatography in 9:1 benzene–methanol. The R_f value of the initial compound (**7**) was 0.91, whereas that of the end product (**8**) was 0.30.

The catalyst was removed by filtration and the filtrate evaporated to dryness in vacuum. The solid residue was dissolved in 3 ml ethyl acetate and the solution diluted with 60 ml of cyclohexane, affording white needle crystals. Yield: 1.35 g (81.8%), m.p. 130—131 °C, $[\alpha]_D^{20}$: −60.1° (*c* = 0.5%, in chloroform).

$C_{14}H_{20}O_6$ (284.3). Calcd. C 59.15; H 7.09; Found C 59.86; H 7.12%.

Phenyl-4,6-O-benzylidene-2-O-methyl-β-D-glucopyranoside (9)

3.24 g of phenyl-2-O-methyl-β-D-glucopyranoside (**4**) was shaken for 16 hrs with 13 ml benzaldehyde in the presence of 3.60 g zinc chloride catalyst. The reaction mixture was then diluted with 100 ml of ice-water, the crystalline precipitate filtered and washed twice with 20 ml portions of water then twice with 20 ml portions of petroleum ether until it was free of benzaldehyde. On crystallization from 115 ml methanol, yield: 3.86 g (90.0%), m.p. 210—212 °C, $[\alpha]_D^{20}$: −67.5° (*c* = 0.3%, in chloroform).

$C_{20}H_{22}O_6$ (358.4). Calcd. C 67.02; H 6.19; Found C 67.85; H 6.21%.

Phenyl-4,6-O-benzylidene-3-O-methyl-β-D-glucopyranoside (10)

3.00 g of phenyl-3-O-methyl-β-D-glucopyranoside (**5**) was suspended in 12 ml benzaldehyde and after the addition of 3.3 g zinc chloride shanken for 12 hrs. The jellified reaction mixture was diluted with 50 ml of ice-water, the crystalline precipitate filtered and washed

3 times with 20 ml portions of water then 3 times with 20 ml portions of petroleum ether until it was free of benzaldehyde. On crystallization from 145 ml ethanol, yield: 3.77 g (95.0%), m.p. 211 °C, $[\alpha]_D^{20}$: −46.2° ($c = 0.2\%$, in pyridine).

$C_{20}H_{22}O_6$ (358.4). Calcd. C 67.02; H 6.19; Found C 67.02; H 6.32%.

Phenyl-3-O-benzyl-4,6-O-benzylidene-2-O-methyl-β-D-glucopyranoside (11)

3.00 g of phenyl-4,6-O-benzylidene-2-O-methyl-β-D-glucopyranoside (**9**) was benzylated for 6 hrs at 100—105 °C with 19.1 ml benzyl chloride in the presence of 9.3 g powdered potassium hydroxide. After cooling, the reaction mixture was diluted with 25 ml water, the precipitate filtered and washed twice with 20 ml portions of water then 3 times with 15 ml portions of petroleum ether. The crude product was recrystallized from 250 ml methanol. Yield: 1.55 g (42%), m.p. 180—182 °C, $[\alpha]_D^{20}$: −72.5° ($c = 0.1\%$, in chloroform).

$C_{27}H_{28}O_6$ (448.5). Calcd. C 72.30; H 6.29; Found C 72.84; H 6.29%.

Phenyl-2-O-benzyl-4,6-O-benzylidene-3-O-methyl-β-D-glucopyranoside (12)

3.58 g of phenyl-4,6-O-benzylidene-3-O-methyl-β-D-glucopyranoside (**10**) was treated with 23 ml benzyl chloride and 11.2 g powdered potassium hydroxide as described for **11**. The crystalline crude product was recrystallized from 350 ml methanol. Yield: 4.25 g (94.7%), m.p. 184—185 °C, $[\alpha]_D^{20}$: −56.2° ($c = 0.4\%$, in pyridine)

$C_{27}H_{28}O_6$ (448.5). Calcd. C 72.30; H 6.29; Found C 72.16; H 6.27%.

Phenyl-3-O-benzyl-2-O-methyl-β-D-glucopyranoside (13)

2.30 g of phenyl-3-O-benzyl-4,6-O-benzylidene-2-O-methyl-β-D-glucopyranoside (**11**) was boiled for 1 hr in 50 ml ethanol containing 0.5 ml concentrated hydrochloric acid. The hot solution was neutralized with sodium hydrogen carbonate and subjected to steam distallation. The residue was evaporated to dryness in vacuum, and the crude product recrystallized twice from 50 ml portions of cyclohexane. Yield: 1.20 g (64.7%), m.p. 108—111 °C, $[\alpha]_D^{20}$: −62.8° ($c = 0.3\%$, in chloroform).

$C_{20}H_{24}O_6$ (360.4). Calcd. C 66.65; H 6.71; Found C 67.03; H 6.78%.

Phenyl-2-O-benzyl-3-O-methyl-β-D-glucopyranoside (14)

The solution of 3.00 g of phenyl-2-O-benzyl-4,6-O-benzylidene-3-O-methyl-β-D-glucopyranoside (**12**) in 30 ml ethanol was boiled for 1 hr after the addition of 0.3 ml concentrated hydrochloric acid. After neutralization with sodium hydrogen carbonate the mixture was subjected to steam distillation. After cooling the distillation residue, the crude product was obtained in a crystalline form. Recrystallization from 180 ml cyclohexane. Yield: 1.62 g (67.2%), m.p. 122 °C, $[\alpha]_D^{20}$: −63.1° ($c = 0.2\%$, in ethyl acetate).

$C_{20}H_{24}O_6$ (360.4). Calcd. C 66.65; H 6.71; Found C 66.92; H 6.41%.

Phenyl-3-O-benzyl-2,4,6-tri-O-methyl-β-D-glucopyranoside (15)

720 mg of phenyl-3-O-benzyl-2-O-methyl-β-D-glucopyranoside (**13**) was methylated in 20 ml dimethylformamide with 6 ml methyl iodide and 6 g silver oxide, and subsequently processed as described for **7**. The solid crude product was crystallized from 3 ml petroleum ether. Yield: 520 mg (68.0%), m.p. 69—71 °C, $[\alpha]_D^{20}$: −59.2° ($c = 0.3\%$, in chloroform).

$C_{22}H_{28}O_6$ (388.4). Calcd. C 68.02; H 7.27; Found C 67.86; H 7.18%.

Phenyl-2-O-benzyl-3,4,6-tri-O-methyl-β-D-glucopyranoside (16)

1.44 g of phenyl-2-O-benzyl-3-O-methyl-β-D-glucopyranoside (**14**) was methylated in 25 ml of dimethylformamide with 10 ml methyl iodide and 10 g silver oxide, and subsequently processed as described for **7**. The syrup-like crude product was crystallized from 4 ml petroleum ether. Yield: 1.38 g (89.0%), m.p. 60 °C, $[\alpha]_D^{20}$: −58.6° ($c = 0.4\%$, in chloroform).

$C_{22}H_{28}O_6$ (388.4). Calcd. C 68.02: H 7.27; Found C 68.39; H 7.24%.

Phenyl-2,4,6-tri-O-methyl-β-D-glucopyranoside (17)

The solution of 500 mg of phenyl-3-O-benzyl-2,4,6-tri-O-methyl-β-D-glucopyranoside (**15**) in 10 ml of ethanol was hydrogenated in the presence of 100 mg palladium on charcoal until the initial substance disappeared. The progress of the reaction was followed by thin-layer chromatography. The R_f value of the initial substance was 0.87 whereas that of the end product was 0.62 (in 9:1 benzene–methanol). After removing the catalyst by filtration the solution was evaporated to dryness in vacuum and the residue crystallized from 8 ml petroleum ether. Yield: 320 mg (84.0%), m.p. 107—110 °C, $[\alpha]_D^{20}$: −54° ($c = 0.1\%$ in chloroform). From Ref. [13]: m.p. 108—109 °C, $[\alpha]_D^{20}$: −57.5° ($c = 2\%$, in chloroform).

$C_{15}H_{22}O_6$ (298.3). Calcd. C 60.38; H 7.43; Found C 61.02; H 7.34%.

Phenyl-3,4,6-tri-O-methyl-β-D-glucopyranoside (18)

1.16 g of phenyl-2-O-benzyl-3,4,6-tri-O-methyl-β-D-glucopyranoside (**16**) was hydrogenated in 75 ml methanol in the presence of 50 mg palladium on charcoal until the initial substance disappeared. The crystalline crude product obtained on precessing the mixture was dissolved in 3 ml of benzene and diluted with 25 ml of petroleum ether. Yield: 604 mg (67.5%), m.p. 84—85 °C, $[\alpha]_D^{20}$: −42.9° ($c = 0.3\%$, in chloroform).

$C_{15}H_{22}O_6$ (298.3). Calcd. C 60.38; H 7.43; Found C 60.04; H 7.28%.

4,6-Di-O-methyl-D-glucose (19)

710 mg of phenyl-4,6-di-O-methyl-β-D-glucopyranoside (**8**) was hydrolyzed in 70 ml 0.25 *M* sulfuric acid for 10 hrs at 100 °C. The hot reaction mixture was neutralized with barium carbonate, and the filtrate evaporated in vacuum. The residue was crystallized from ethyl acetate. Yield: 410 mg (82.0%), m.p. 159—160 °C, $[\alpha]_D^{20}$: +112° ($c = 0.45\%$, in water). According to literature [15]: m.p. 156—158 °C, $[\alpha]_D^{20}$: +101° (in water).

2,4,6-Tri-O-methyl-D-glucose (20)

600 mg of phenyl-2,4,6-tri-O-methyl-β-D-glucopyranoside (**17**) was treated in 60 ml 0.25 *M* sulfuric acid in the way described for **19**. The crude product was crystallized from petroleum ether. Yield: 346 mg (78.0%), m.p. 123—124°C, $[\alpha]_D^{20}$: +110° ($c = 0.25\%$, in methanol). From Ref. [13]: m.p. 123—126 °C, $[\alpha]_D^{20}$: +111° ($c = 2\%$, in methanol).

3,4,6-Tri-O-methyl-D-glucose (21)

447 mg of phenyl-3,4,6-tri-O-methyl-β-D-glucopyranoside (**18**) was treated in 45 ml 0.25 *M* sulfuric acid in the way described for **19**. The crude product was crystallized from petroleum ether. Yield: 246 mg (74.0%), m.p. 77 °C, $[\alpha]_D^{20}$: +89° ($c = 0.2\%$, in water). From Ref. [16]: m.p. 76—77 °C, $[\alpha]_D^{20}$: +92° ($c = 2\%$, in water).

The NMR spectra were recorded in the Institute for Pharmacognosy of the Munich University. Thanks are due to Prof. H. WAGNER for his permission to use the instrument, and to O. SELIGMANN for help in evaluating the spectra. One of us (A. L.) is indebted to the Alexander von Humboldt Foundation for a fellowship.

REFERENCES

[1] Part IV. LIPTÁK, A., SELIGMANN, O.: Ber. (In press)
[2] BARDOLPH, M. P., COLEMAN, G. H.: J. Org. Chem., **15**, 169 (1950)
[3] HELFERICH, B., LANG, O.: Z. physiol. Chem., **216**, 123 (1933)
[4] MCCLOSKEY, C. M., COLEMAN, G. H.: J. Org. Chem., **10**, 184 (1945)
[5] HELFERICH, B., GÜNTHER, E.: Z. physiol. Chem., **231**, 62 (1935)
[6] HELFERICH, B., SCHMITZ-HILLEBRECHT, E.: Ber., **66**, 378 (1933)
[7] MASTRONARDI, J. O., FLAMETTI, S. M., DEFERRARI, J. O., GROS, E. G.: Carbohydrate Res., **3**, 177 (1966)
[8] FREUDENBERG, R., HIXON, R.: Ber. **56**, 2125 (1923)

[9] VAN CLEVE, J. M., SCHAEFER, W. C.: J. Amer. Chem. Soc., **77,** 5341 (1955)
[10] MICHEEL, F., KLEMER, A., FLITSCH, R.: Ber., **91,** 663 (1958)
[11] KUHN, R., TRISCHMANN, H., LÖW, I.: Angew. Chem., **67,** 32 (1955)
[12] NÁNÁSI, P., LIPTÁK, A., NAGY, G.: Acta Chim. Acad. Sci. Hung., **65,** 97 (1970)
[13] RICHTMYER, N. K.: J. Amer. Chem. Soc., **61,** 1831 (1949)
[14] WOLLWAGE, P. C., SEIB, P. A.: J. Chem. Soc., **3143** (1971)
[15] FREUDENBERG, K., PLANKENHORN, E.: Ber., **73,** 621 (1940)
[16] SUNDBERG, R. L., MCCLOSKEY, C. M., REEVES, D. E., COLEMAN, G. H.: J. Amer. Chem. Soc., **67,** 1080 (1945)

Pál NÁNÁSI
András LIPTÁK } 4010 Debrecen, 10. Hungary.

Acta Chimica Academiae Scientiarum Hungaricae, Tomus 84 (1), pp. 71—74 (1975)

MINOR ALKALOIDS FROM THE SEEDS OF *AMSONIA TABERNAEMONTANA*: (+)-1,2-DEHYDROASPIDOSPERMIDINE, (—)-TETRAHYDROALSTONINE AND (—)-QUEBRACHAMINE

B. ZSADON, K. H. OTTA and P. TÉTÉNYI*

*(Department of Chemical Technology, Eötvös Loránd University, Budapest, and * Research Institute for Medicinal Plants, Budakalász)*

Received January 25, 1974

The following minor alkaloids have been isolated from the ripe seeds of *Amsonia tabernaemontana* Walt. in addition to the major alkaloid, tabersonine (**I**): (+)-1,2-dehydroaspidospermidine (**III**) (134 mg/kg), (—)-tetrahydroalstonine (**II**) (125 mg/kg) and (—)-quebrachamine (**IV**) (12 mg/kg). At first, the developing crop contains only a few tabersonine and also (+)-vincadifformine (**V**). The latter undergoes complete decomposition into (+)-1,2-dehydroaspidospermidine in the crop during the formation and ripening of the seeds. This process is accompanied by a great increase in the concentration of tabersonine in the seeds.

In 1954, JANOT *et al.* [1] isolated tabersonine (**I**), an indole alkaloid [3] with hypotensive activity [2], as the main alkaloid from the seeds of *Amsonia tabernaemontana* Walt. PLAT [4] also isolated (—)-tetrahydroalstonine (**II**) from the seeds, in addition to tabersonine. As reported by us [5] earlier, tabersonine was found to be the major alkaloid in the ripe seeds of *Amsonia tabernaemontana* grown in Hungary, too.

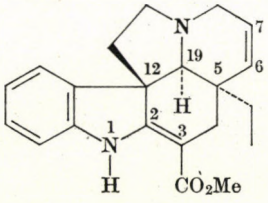

I

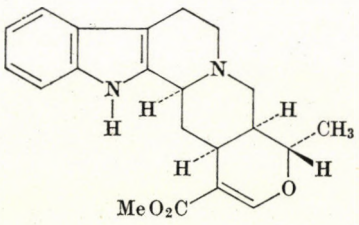

II

In the course of our recent work aiming at the isolation of the minor alkaloids, (+)-1,2-dehydroaspidospermidine (**III**) (134 mg/kg), (—)-tetrahydroalstonine (**II**) (125 mg/kg) and (—)-quebrachamine (**IV**) (12 mg/kg) have been obtained, in addition to tabersonine (**I**) (9.4 g/kg), from the ripe seeds of *Amsonia tabernaemontana* grown in Hungary. For identification, the alkaloids isolated earlier from the leaves of this plant [6, 7] were used as reference sub-

stances. The minor alkaloids now isolated from the seeds were found to be identical in every respect with the authentic samples.

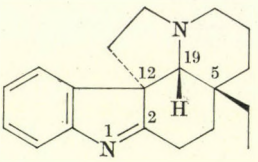

III

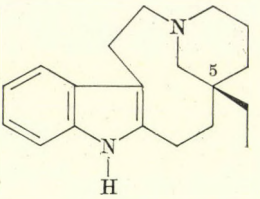

IV

Of the minor alkaloids, (+)-1,2-dehydroaspidospermidine (**III**) isolated in the largest amount is an alkaloid of the aspidospermine type, its structure being very similar to that of the major alkaloid, tabersonine (**I**); however, the configuration of its centres of asymmetry (C_5, C_{19} and C_{12}) is just the opposite. In order to reveal the connection between the biosynthesis of the two alkaloids, the alkaloid composition of the crop has been examined in consecutive periods during the biological development of the plant. It was found that the developing crop contained initially tabersonine in a very low (hundredth per cent) concentration and, among other alkaloids, also (+)-vincadifformine (**V**) was present. The latter is an alkaloid of the aspidospermine type belonging to the antipode series of tabersonine, similarly to (+)-1,2-dehydroaspidospermidine. In the course of ripening, (+)-vincadifformine (**V**) suffered decomposition giving rise to (+)-1,2-dehydroaspidospermidine (**III**), while the concentration of tabersonine (**I**) increased by several orders of magnitude in the crop, and reached a maximum value in the ripe seeds after the total conversion of (+)-vincadifformine. (Within the seeds, tabersonine is concentrated in the germ; its concentration measured in the germ of the ripe seed was about 2%.) At the same time, no (+)-vincadifformine could be detected any longer in the ripe seeds.

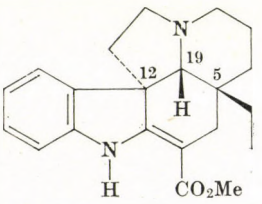

V

In view of the above observation, the biosynthetic pathways of tabersonine (**I**) and (+)-1,2-dehydroaspidospermidine (**III**) can well be differentiated from each other and it is also clearly seen that the biosynthesis of tabersonine during the development and ripening of the seeds is accompanied by the conversion of (+)-vincadifformine into (+)-1,2-dehydroaspidospermidine.

It is worth noting here that alkaloids of the aspidospermine and quebrachamine type comprising centres of asymmetry with opposite configuration also occur in great variety in the leaves of *Amsonia tabernaemontana* [6, 7, 8, 9, 10, 11], in which the major alkaloid is (+)-vincadifformine [8]. The latter compound is converted into (+)-1,2-dehydroaspidospermidine in the leaves, too, during the periods of flowering and development of the crop, as confirmed unambiguously in our earlier experiments [8, 12]. Nevertheless, in the leaves not all (+)-vincadifformine is converted into (+)-1,2-dehydroaspidospermidine, and the concentration of tabersonine remains there very low all the time.

Experimental

The investigations were carried out on plants of *Amsonia tabernaemontana* grown in the Research Institute for Medicinal Plants, Budakalász, Hungary.

All m.p.s are uncorrected. The optical rotation values were measured with a Schmidt-Haensch polarimeter, the ultraviolet spectra were recorded with an Optica Milano CF 4R spectrophotometer. During isolation, thin-layer chromatography was used for detection of the alkaloids.

Isolation of the alkaloids

The seeds were beaten out from the ripe crop collected in November, 1972. 1 kg of the ground air dried material was subjected to exhaustive extraction with methanol in a Soxhlet type extracter for 10 hrs. The methanolic extract was concentrated to 1 l volume at reduced pressure, then mixed with 3 l of 2% sulfuric acid and the residual methanol was removed at room temperature under reduced pressure. In order to purify the diluted acid solution, it was shaken with 2×200 ml of benzene, then made alkaline and the alkaloids were extracted with 5×200 ml of benzene.

The benzene solution containing the alkaloids was dried, concentrated to a volume of 50 ml under reduced pressure, then mixed with 50 ml of *n*-heptane and subjected to chromatographic separation on a column packed with 200 g of neutral aluminium oxide (Brockmann activity II). Using 2 l of a benzene–heptane (1:1) mixture, 9.4 g of pure *tabersonine* base was eluted. For identification, it was crystallized from ethanol, m.p. 88 °C, $[\alpha]_D^{20}$ −360° (in ethanol, $c = 0.2$), UV spectrum (in methanol): λ_{max} 226, 298 and 328 nm. No m.p. depression occurred in admixture with authentic tabersonine [5].

The alkaloids retained on the aluminium oxide column were eluated with 1 l of benzene/ether (1:1) mixture. The evaporation residue of the eluate was a resinlike mixture (900 mg), which contained several components of alkaloid character. This mixture was dissolved in 100 ml of benzene and the benzene solution extracted with 5×50 ml of 2% sulfuric acid solution. The alkaloids appeared in the sulfuric acid phase, while the non-basic coloured components remained in the benzene phase. The sulfuric acid solution was made alkaline and the alkaloids were extracted with 5×50 ml of benzene.

The alkaloid mixture purified in the above manner (350 mg) was subjected to chromatographic separation on a column packed with 15 g of silica gel. The first portion (80 ml) of benzene eluated 13 mg of a mixture which contained some tabersonine, besides, components of non-alkaloid character.

The evaporation residue of the next benzene eluate (120 ml)was 12 mg of pure (−)-*quebrachamine*, $[\alpha]_D^{20}$ −110° (in ethanol, $c = 0.2$). UV spectrum (in methanol): λ_{max} 228, 286 and 293 nm; $\log \varepsilon = 4.53$, 3.84 and 3.83, respectively. M.p. (from *n*-heptane) 147 °C; no depression occurred in mixed m.p. determination with an authentic sample of (−)-quebrachamine [6].

The elution was then continued with a 1:1 mixture of benzene and ether. The evaporation residue of the first eluate fraction (110 ml) gave 125 mg of pure (−)-*tetrahydroalstonine;* this was crystallized from ethanol, m.p. 228 °C, $[\alpha]_D^{20}$ −107° (in chloroform, $c = 0.5$). UV spectrum (in methanol): λ_{max} 226, 282 and 290 nm, $\log \varepsilon = 4.61$, 3.90 and 3.82, respectively.

No melting point depression was observed in admixture with authentic (—)-tetrahydroalstonine [7].

The next fraction (180 ml) of the benzene/ether (1:1) mixture was also evaporated to obtain 134 mg of a colourless viscous oil; this proved to be pure (+)-1,2-*dehydroaspidospermidine*, $[\alpha]_D^{20}$: +250° (in ethanol, $c = 0.5$). UV spectrum (in methanol): λ_{max} 222, 228 (sh) and 262 nm; log $\varepsilon = 4.57$, 4.45 and 3.99, respectively. After reduction with sodium borohydride in hot ethanolic solution [6], (—)-quebrachamine was obtained as the main product, while at 0 °C (+)-aspidospermidine [6] was formed.

Finally a coloured mixture (26 mg) could still be eluated from the silica gel column with methanol, which did not contain any of the alkaloids mentioned above.

REFERENCES

[1] JANOT, M. M., POURRAT, H., LE MEN, J.: Bull. Soc. Chim. France, **1954,** 707
[2] MORIN, H., LE MEN, J., POURRAT, H.: Ann. Pharm. Fr., **13,** 123 (1955)
[3] PLAT, M., LE MEN, J., JANOT, M. M., WISLON, J. M., BUDZIKIEWICH, H.: Tetrahedron Letters, **1962,** 271
[4] PLAT, M.: Theses (Paris), 1963. Serie A, No. 4043
[5] ZSADON, B., HUBAY, R., EGRY, É., RÁKLY, M., SÁRKÖZI, M.: Magy. Kém. Foly. **76,** 466 (1970); ZSADON, B., RÁKLY, M., HUBAY, R.: Acta Chim. Acad. Sci. Hung. **67,** 71 (1971)
[6] ZSADON, B., EGRY, É., SÁRKÖZI, M.: Acta Chim. Acad. Sci. Hung. **67,** 77 (1971)
[7] ZSADON, B., TAMÁS, J., SZILASI, M.: Magy. Kém. Foly. **79,** 341 (1973)
[8] ZSADON, B., KAPOSI, P.: Tetrahedron Letters, **1970,** 4615; ZSADON, B., KAPOSI, P.: Acta Chim. (Budapest). **71,** 115 (1972)
[9] ZSADON, B., TAMÁS, J.: Chem. Ind. **1972,** 32; ZSADON, B., TAMÁS, J., SZILASI, M., KAPOSI, P.: Acta Chim. (Budapest). **78,** 207 (1973)
[10] ZSADON, B., TAMÁS, J., SZILASI, M.: Chem. Ind. **1973,** 229
[11] PANAS, J. M., MORFAUX, A. M., OLIVIER, L., LE MEN, J.: Ann. Pharm. Fr., **30,** 273 (1972)
[12] ZSADON, B., OTTA, K.: Acta Chim. (Budapest). **69,** 87 (1971)

Béla ZSADON
Klára H. OTTA
} H-1088 Budapest, Múzeum krt 6—8, Hungary

Péter TÉTÉNYI; H-2011 Budakalász, Pf. 11. Hungary.

Acta Chimica Academiae Scientiarum Hungaricae, Tomus 84 (1), pp. 75—84 (1975)

STRUCTURAL INVESTIGATION OF THE ANTIBIOTIC RISTOMYCIN A

CHEMICAL STRUCTURE OF THE OLIGOSACCHARIDE PART OF RISTOMYCIN A

F. SZTARICSKAI, R. BOGNÁR and M. M. PUSKÁS

(Chemical Research Group for Antibiotics of the Hungarian Academy of Sciences, Debrecen)

Received February 14, 1974

The glycoside antibiotic ristomycin A produced by *Proactinomyces fructiferi* var. *ristomycini* contains one molecule of D-mannose and a tetrasaccharide side chain connected separately to the aglycone moiety. The tetrasaccharide consists of the units D-glucose, D-mannose, L-rhamnose and D-arabinose attached to one another according to structure **V**.

Ristomycin was isolated in 1963 by BRAZHNIKOVA *et al.* [1] from a culture of *Proactinomyces fructiferi* var. *ristomycini*. The antibiotic is highly effective against Gram-positive microorganisms [2, 3], moreover, it can affect pathogenic organisms resistant to penicillin, streptomycin or erythromycin.

It has been pointed out by LAVROVA *et al.* [4] that ristomycin consists of a mixture of two biologically active variants: ristomycin A and B, which they have isolated in the form of the crystalline sulfates.

In their physical, chemical and biological properties, ristomycin A and B have proved to be very similar to the previously known antibiotics ristocetin A and B [5, 6].

The hydrolysis of ristomycin A or its aglycone with 6 *N* hydrochloric acid gave three unknown amino acids — *a*, *b* and *c*. According to quantitative analysis, the antibiotic molecule contains 1 mole of *a* and only one mole of the total [7] of *b* and *c*.

The structure of amino acid *a* has been proved by IR and NMR spectroscopy and chemical degradation [8, 10]. According to our investigations, amino acid *a*, called *ristomycinic acid*, is a new aromatic di-aminodicarboxylic acid, built up of a D-(—)-α-amino-4-hydroxyphenylacetic acid and an α-amino-2,6-dihydroxy-3-methylphenylacetic acid connected by a diphenyl ether linkage at their 5- and 4-positions, respectively.

On the basis of NMR spectroscopic studies and analogies with the structure of ristomycinic acid, a similar structure was suggested by LOMAKINA *et al.* [10, 11] for amino acid *b*.

The hydrolysis of ristomycin A with 2% or 1 *N* hydrochloric acid gave D-glucose, D-mannose, L-rhamnose and D-arabinose (molar ratio 1 : 2 : 1 : 1), whereas the hydrolysate of ristomycin B contained D-glucose, D-mannose and L-rhamnose in the molar ratio 1 : 1 : 1 [6, 13].

When ristomycin A was hydrolyzed with 0.5 *N* hydrochloric acid at 100 °C for 4 hrs, in addition to the simple sugars mentioned earlier, a new deoxyamino sugar could be isolated which was named *ristosamine*. According to structural investigations it proved to be 2,3,6-trideoxy-3-amino-L-ribohexopyranose [9].

The present work is a report on the results of our structural studies on the oligosaccharide part of ristomicin A which is composed of simple neutral sugar components.

The cleavage of peracetylristomycin A ($C_{153}H_{189}O_{72}N_9$) with hydrogen bromide in glacial acetic acid or with 1,1-dichlormethyl methyl ether, followed by treatment with acetic anhydride and silver acetate and subsequent saponification according to ZEMPLÉN's method, revealed that the products contained again only simple sugars — D-glucose, D-mannose, L-rhamnose, D-arabinose, as shown by paper chromatography.

In 1967 BRAZHNIKOVA *et al.* [12], then LOMAKINA *et al.* [13] hydrolyzed ristomycin A with 0.1 *N* hydrochloric acid at 100 °C for 1 hr and separated, by means of a Sephadex G 25 column, the following glycosides and oligosaccharides: D-Man-aglycone, D-Man-aglycone-D-Glu, aglycone-D-Glu-L-Rha, D-Glu-D-Man (**I**), D-Glu-L-Rha (**II**), L-Rha-D-Glu-D-Man (**III**) and D-Glu-D-Man-D-Ara (**IV**).

In the same way from ristomycin B the following components were obtainable: D-Man-aglycone, D-Man-aglycone-D-Glu and D-Glu-L-Rha (**II**) disaccharide.

This result gave information about the carbohydrate sequence, and the conclusion was drawn that both in ristomycin A and B the sugar moieties are attached to the aglycone at two places.

In our experiments, work-up of the acetolysis product of ristomycin A on a Kieselgel G column led to the isolation of an octaacetyl-disaccharide and a decaacetyl-trisaccharide. The octaacetyl-disaccharide after saponification in absolute methanol with sodium methoxide was found identical with the disaccharide **I** appearing among the products of partial hydrolysis. This sugar was named *ristobiose*. The structure determination of this glucosido-mannose will be outlined in the following discussion.

First, the disaccharide **II** was identified. Our paper chromatographic examinations proved its identity with rutinose [14], known to occur frequently in nature in glycoside form (Table I). The disaccharide **II** isolated from ristomycin A gave, on acetylation in acetic anhydride in the presence of sodium acetate or pyridine, a white amorphous product which, after recrystallization from absolute ethanol, was in every respect (m.p., mixed m.p., $[\alpha]_D^{20}$, thin-layer chromatography, IR spectrum) identical with an authentic sample of rutinose heptaacetate (**IIa**).

It follows from the identity of the disaccharide **II** with rutinose and from

the results of GORIN and PERLIN [14] that, in the tetrasaccharide side chain of ristomycin A, L-rhamnose is atteched to D-glucose by an α-glycosidic linkage at position C-6.

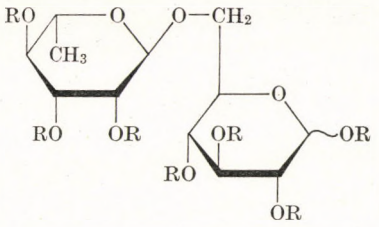

II rutinose R = H
IIa heptaacetylrutinose R = $COCH_3$

When ristomycin A ($C_{107}H_{143}O_{49}N_9$) itself was oxidized with periodic acid and the isolated product hydrolized with acid, none of the sugar components of the antibiotic could be detected in the hydrolysate. This proves that the glucose unit (presumably with a pyranose structure), representing the centre of branching in the tetrasaccharide side chain of the antibiotic, also contains a vicinal diol group oxidizable with periodic acid.

Since the C-6 atom D-glucose is occupied by L-rhamnose, D-mannose can only be linked to C-2 or C-4 (A or B in Fig. 1). A decision between these alternatives was achieved by the investigation of ristobiose (**I**) and the trisaccharide with structure L-Rha-D-Glu-D-Man, which we named *ristotriose* (**III**).

The hydrolysis of decamethylristotriose (**IIIa**), prepared by the KUHN methylation [15] of **III** gave a mixture in which, by means of TLC, three partially methylated sugars were detected: 2,3,4-tri-O-methyl-L-rhamnose, 2,3,4,6-tetra-O-methyl-D-mannose, and 3,4-di-O-methyl-D-glucose (Table II).

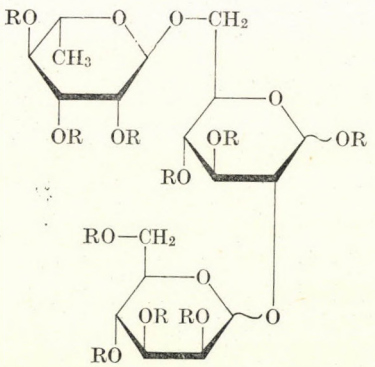

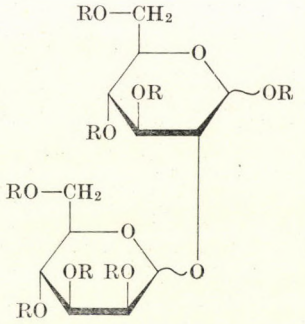

III: ristotriose R = H
IIIa: decamethylristotriose R = CH_3

I: ristobiose R = H
Ia: octamethylristobiose R = CH_3

It follows that in ristotriose (**III**), D-mannose is linked to D-glucose in the C-2 position. This is also proved by the fact that in the hydrolysate of octamethylristobiose (**Ia**), prepared by permethylation, besides 2,3,4,6-tetra-O-methyl-D-mannose, only 3,4,6-tri-O-methyl-D-glucose can be found (Table II);

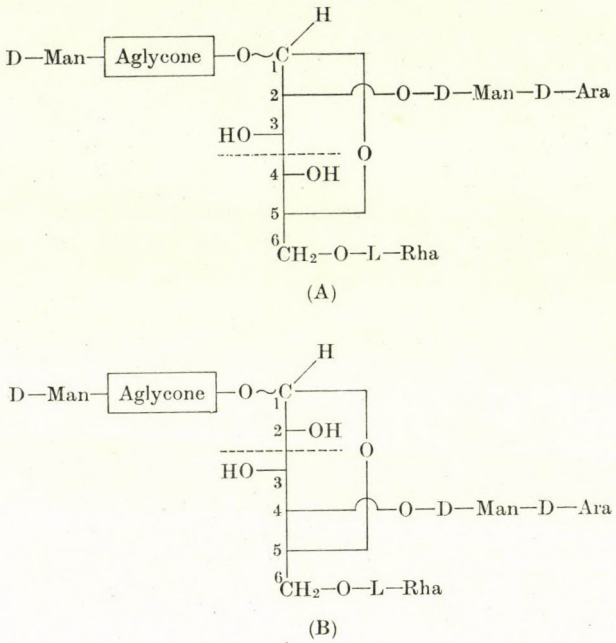

Fig. 1. Possibilities A and B for the linkage of D-mannose to D-glucose in the tetrasaccharide side chain, as deduced from periodic acid oxidation

it is further shown by our observation that phenylosazones cannot be obtained from **I** and **III** with phenylhydrazine [10, 16].

In enzymic hydrolysis, ristobiose (**I**) was hydrolyzed four times slower than cellobiose by emulsin. This presumably indicates that **I** has the 2-O-α-D-mannosido-D-glucose structure. The other trisaccharide, with structure D-Glu-D-Man-D-Ara (**IV**) has so far been obtained only in the form of decaacetyl-trisaccharide (**IVa**) by the acetolysis of ristomycin A.

The NMR spectrum (in $CDCl_3$ solution at 100 MHz) of the decaacetyl-D-Glu-D-Man-D-Ara-trisaccharide (**IVa**) shows doublets at δ 6.37 ppm ($J = 3.6$ Hz) and 5.78 ppm ($J = 7.7$ Hz). These signals can be unequivocally assigned to the anomeric protons of the reducing end glucose unit in the α and β configuration, respectively (literature values [17] δ 6.34 ($J = 3.3$ Hz) for α-, and δ 5.76 ($J = 6.9$ Hz) for β-D-glucopyranose pentaacetate). The $\alpha : \beta$ ratio is about 1 : 2.5. Also, the fact that there are more (at least 12) acetyl methyl signals in the δ 1.9—2.2 ppm region can only be explained on the basis of an anomeric

mixture. The complexity of the remaining spectral regions does not allow to deduce any kind of information concerning the interglycosidic linkages.

However, from the partial structures of the splitting products — ristotriose and 2,3,4-tri-O-methyl-L-rhamnose found in the hydrolysate of permethylated ristomycin A — it can be assumed that one of the terminal groups in the tetrasaccharide chain of the antibiotic is D-arabinose and the other is L-rhamnose. In particular, if D-arabinose were attached to D-glucose, then the latter would not be amenable to periodic acid oxidation. Similar considerations also rule out a 1 → 3 linkage of D-arabinose to D-mannose.

The exact linkage position of the arabinose unit was only determined after the permethylation of ristomycin A. The only effective way of preparing permethylated ristomycin A ($C_{128}H_{185}O_{70}N_9$) was the method of HAKOMORI [18]. The completeness of permethylation was checked by determination of the methoxyl content. In the hydrolysate of the permethylated antibiotic TLC showed the presence of 2,3,4,6-tetra-O-methl-D-mannose, 2,3,4-tri-O-methyl L-rhamnose, 3,4-di-O-methyl-D-glucose, 3,4,6-tri-O-methyl-D-mannose, and 2,3,5-tri-O-methyl-D-arabinose. The presence of these two latter products proves that in the tetrasaccharide side chain of ristomycin A the terminal arabinose unit occurs in the furanoside form and is affixed to D-mannose by a 1 → 2 linkage. This statement is in agreement with reported data [20, 21] indicating the extreme instability of arabinofuranosides.

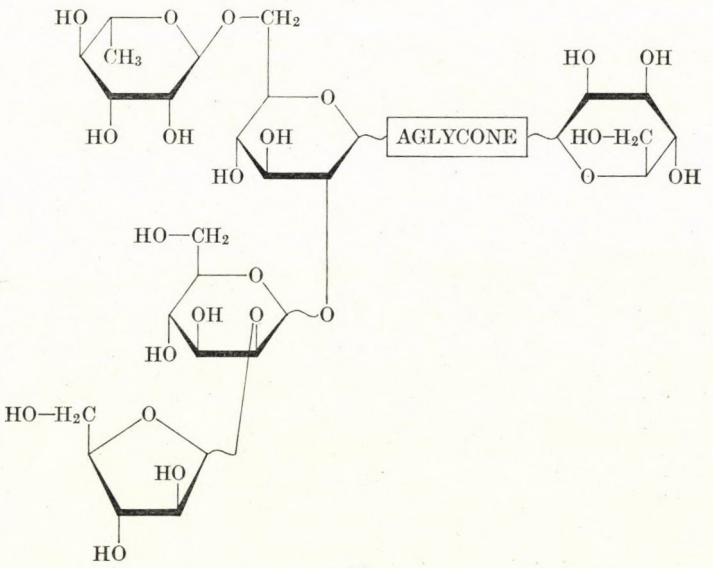

V

On the basis of these and previous experimental results, structure V can be suggested for the part of the antibiotic ristomycin A built up of the neutral sugar components.

In the knowledge of the molar ratios [6, 13] of the simple carbohydrates in ristomycin B and on the basis of composition of the products of partial hydrolysis [12, 13], it can be assumed that the oligosaccharide side chain of the component B of common biological origin and produced by the same strain, differs from that of ristomycin A only by the absence of the 2-O-β-D-arabino-furanosyl-D-mannosyl part.

Experimental

Preparation of the di- and trisaccharides from ristomycin A

The di- and trisaccharides of ristomycin A have been isolated *via* hydrolysis with hydrochloric acid in a different way from the Soviet researchers [12] as follows.

In small portions ristomycin A (25.00 g) was dissolved in 500 ml of preheated 0.1 *N* hydrochloric acid and refluxed for 1 hr. The solution, after cooling, was neutralized to pH 4.0 with 200 ml of Dowex 2×3 (OH^-) ion-exchange resin and the filtrate was poured slowly into 2500 ml of acetone, with stirring. The precipitate was filtered off, and the filtrate was passed slowly through a column of Dowex 50×4 (H^+) ion-exchange resin. Fractions 1—8 (100 ml each) were collected, and 100—150 μl of each of them was applied on chromatographic paper and sprayed with aniline hydrogen phthalate reagent (105 °C, 10 min). Fractions 3—5 produced the most intense colour. The possible presence of aglycone was checked in every fraction by means of Pauly reagent, but the reaction was found negative in every sample.

The combined fractions 3—5 were then neutralized to pH 7.0—7.5 with Dowex 2×4 (OH^-) ion-exchange resin, and the solution was evaporated to 15 ml in vacuum. On dilution of the remaining syrup to 150 ml with acetone, the mono- and oligosaccharides separated as white precipitate. Only small quantity of rhamnose could be detected in the acetonic mother liquor by means of paper chromatography, using the solvent system ethyl acetate–acetic acid–1-butanol–water (7:3:3:3).

The filtered precipitate was dissolved in 12 ml of the former solvent system, to which some methanol and a few drops of distilled water had been added. The solution was applied to a cellulose column (75×2.3 cm) and developed with the solvent system used for paper chromatography (rate of flow 20 ml/hr = 4—5 ml/cm^2/hr); 10—15 ml fractions were collected. According to paper chromatography, fractions 1—10 contained only monosaccharides. Fractions 21—27, 34—46 and 51–70 gave, after evaporation in vacuum and precipitation with acetone containing 5—10% ether, two different disaccharides having miscellaneous R_f values and a trisaccharide.

Rutinose (121.4 mg) was isolated from fractions 21—27. $[\alpha]_D^{20}$ —5.2° (c = 1, water). $C_{12}H_{22}O_{10}$ (326.29). Calcd. C 44.17; H 6.79 Found C 42.76, 42.73; H 6.86, 7.38%.
Ristobiose (80 mg) was isolated from fractions 34—36. $[\alpha]_D^{20}$ +54.3° (c = 1, water). $C_{12}H_{22}O_{11}$ (342.29). Calcd. C 42.11; H 6.47. Found C 41.62, 41.20; H 6.64. 6.35%.
Ristotriose (56 mg) was isolated from fractions 51—70. $[\alpha]_D^{20}$ +36.6° (c = 1, water). $C_{18}H_{30}O_{15}$ (486.42). Calcd. C 44.45; H 6.21. Found C 43.79, 43.82; H 6.73 6.68%.

Paper chromatographic investigation of the di- and trisaccharides isolated from ristomycin A

The homogeneity of the di- and trisaccharides isolated from ristomycin A was checked by paper chromatography using 100 μg each of 1% aqueous solutions. The compositions were checked after hydrolysis by paper chromatographic comparison with standard sugars. For this purpose 1.0 mg each of the di- and trisaccharide was dissolved in about 10 mg of 2 *N* H_2SO_4 and hydrolyzed at 100 °C in a sealed capillary tube for 2 hrs. From the hydrolysates volumes containing 30—40 μg of the sugars were applied to chromatographic paper. The chromatographic results are included in Table I.

Table I

Paper chromatographic data for the di- and trisaccharides isolated from ristomycin A

Sample		*RG*			
I	0.39				
II	0.62				
Rutinose	0.62				
III	0,25.				
IV	0.20				
IV-hydrolysate		1.00	1.20	1.49	
III-hydrolysate		1.00	1.20		2.19
II-hydrolysate		1.00			2.16
I-hydrolysate		1.00	1.20		
D-Glucose		1.00			
D-Mannose			1.20		
D-Arabinose				1.47	
L-Rhamnose					2.16

Solvent system: ethyl acetate–acetic acid–water (44:20:10). Detecting agent: 2% aniline hydrogen phthalate solution in 1-butanol (105 °C, 10 min). Paper: Schleicher and Schüll 2043b Mgl.

Acetolysis of ristomycin A

(A.) Crystalline ristomycin sulfate (2.0 g) was suspended, with cooling, in a mixture of acetic anhydride (18.0 ml) and conc. sulfuric acid (0.2 ml) cooled to 0 °C, and the reaction mixture was then allowed to stand for 14 days at room temperature. After the first day the antibiotic dissolved to give a dark cherry-red solution. The solution was diluted with 10 ml of glacial acetic acid and poured on 500 g of ice. The orange-yellow precipitate was filtered off, washed acid-free with distilled water, and dried at room temperature in a vacuum desiccator over calcium chloride–potassium hydroxide to give 2.12 g of the product. It was powdered, extracted with three 50 ml portions of hot absolute benzene, and the combined benzene solutions were evaporated to dryness in vacuum.

The mixture of sugar acetates obtained in this way was dissolved in 5.0 ml of absolute benzene containing 6% absolute methanol and, in order to remove the aglycone, the solution was passed through a Kieselgel G (Merck, according to Stahl) column (13 cm long, 2 cm in diameter) at a flow rate of 3 ml/hr. The sugar acetates left the column in 40 ml of eluate, which was evaporated to dryness in vacuum at 35 °C, and the residue was dried at room temperature over phosphorus pentoxide, to give 245.6 mg of the product.

(B.) When the acetolysis of ristomycin A (10 g) dried over phosphorus pentoxide (to constant weight) was made according to method *(A)*, only the decaacetyl-D-Glu-D-Man-D-Ara trisaccharide (**IVa**) could be isolated (212.8 mg), $[\alpha]_D^{20}$ +125° (c = 1, absolute methanol).

$C_{37}H_{50}O_{25}$ (894.77). Calcd. C 49.66, H 5.63. Found C 49.88, 50.38; H 5.64, 5.61%.

The decaacetyl-trisaccharide on saponification according to ZEMPLÉN [22] gave D-Glu-D-Man-D-Ara trisaccharide (**IV**). After hydrolysis with 2 N H_2SO_4, D-glucose, D-mannose and D-arabinose were identified in the hydrolysate by paper chromatography (details described above).

Deacetylation and isolation of I

The sugar acetates (245.6 mg) obtained from the acetolysis of ristomycin A were dissolved in 10 ml of methanol, then deacetylated by ZEMPLÉN's method [22] in the presence of sodium methoxide to give 138.8 g of a product which, according to paper chromatography, contained D-glucose, D-arabinose, L-rhamnose and the disaccharide **I**. Compound **I** (133.4 mg) was separated from the monosaccharides by chromatography on a cellulose column with the solvent system ethyl acetate–acetic acid–1-butanol–water (7:3:3:3); $[\alpha]_D^{20}$ +80° ($c = 1$, water).*

$C_{12}H_{22}O_{11}$ (342.29). Calcd. C 42.11; H 6.47. Found C 41.70, 41.30; H 6.35, 6.64%.

In the 2 *N* sulfuric acid hydrolysate of **I** D-glucose (*RG* 1.00) and D-mannose (*RG* 1.20) were detected by paper chromatography. According to paper chromatography, the non-hydrolyzed **I** (*RG* 0.40) proved to be identical with the disaccharide of structure D-Glu-D-Man isolated from ristomycin A after partial hydrolysis [12, 13].

Octaacetate of the disaccharide I

Compound **I** (45.0 mg) was acetylated at 100 °C in a mixture of acetic acid anhydride and sodium acetate to yield 25.0 mg of the octaacetate of **I**, which was recrystallized from 50% ethanol; m.p. 69—71 °C (Kofler), $[\alpha]_D^{20}$ +61.7° ($c = 6.0$, methanol).

Enzymic hydrolysis of the disaccharide I

Compound **I** (5.0 mg) and 3.0 mg of emulsin were dissolved in 1.0 ml of distilled water and hydrolyzed in a thermostat at 37 °C. Aliquots of the solution, each containing 10 μg of the hydrolysate, were chromatographed on Kieselgel-G thin-layer in the solvent system ethyl acetate–acetic acid–water (44:20:10).In the hydrolysate of **I**, monosaccharides could only be detected after 140 hrs. Under similar conditions the standard cellobiose hydrolyzed completely within 42 hrs.

Identity of the disaccharide II with rutinose

(A.) Compound **II** (32.0 mg) was dissolved in 0.2 ml of acetic anhydride. After the addition of 50.0 mg of sodium acetate, the mixture was heated at 100 °C for 2 hrs. The reaction mixture was then poured into ice-water and the white precipitate (25.0 mg) was filtered off and crystallized from absolute ethanol; m.p. 167 °C (Kofler); $[\alpha]_D^{25}$ −39.0° ($c = 1.0$, pyridine). Authentic rutinose heptaacetate has m.p. 167—169 °C; $[\alpha]_D^{25}$ −43.0° ($c = 1.0$ pyridine). Mixed m.p. determination gave no depression (m.p. 168—170 °C, Kofler).

The IR spectrum (KBr) of the product was identical with that of authentic rutinose heptaacetate. Chromatography on Silicagel-G thin-layer in absolute benzene containing 5% methanol using detection with 50% H_2SO_4 (150 °C, 10 min). also showed identical R_f values for the acetylated product of disaccharide **II** and an authentic sample of rutinose heptaacetate.

(B.) Compound **II** (20.0 mg) was dissolved in a mixture of 0.30 ml pyridine and 0.30 ml acetic anhydride, and allowed to stand at room temperature for 25 hrs. The reaction mixture was poured into ice-water and worked up as described in *(A)* to give 25.3 mg of the product. Recrystallization from absolute ethanol gave m.p. 165—167 °C (Kofler); $[\alpha]_D^{25}$ −45.0° ($c = 1.0$, pyridine), mixed m.p. with rutinose heptaacetate was 165—170 °C.

Permethylation and hydrolysis of the disaccharide I

Compound **I** (51.30 mg) was methylated according to HAKOMORI [18] with methyl iodide in dimethyl sulfoxide in the presence of sodium hydride to give 70.2 mg (80.41%) of the octamethyl-disaccharide (**Ia**).

The IR spectrum of the compound had no hydroxyl band [19] at 3500 cm^{-1}.

Compound **Ia** prepared as described above was subjected to methanolysis in a sealed ampoule in 1 ml of 5% methanolic hydrogen chloride at 100°C for 2 hrs. After the ampoule had been opened, the methanol was evaporated in vacuum, the methyl-glycosides were dissolved in 1 ml of 0.5 *N* HCl and after the ampoule had been sealed, hydrolyzed at 100 °C for

The specific rotation of 2-O-α-D-mannosido-D-glucose recently synthesized by DICK *et. al.* [Carb. Res. **36,** 319 (1974)] was identical that of ristobiose.

3 hrs. The contents of the ampoule were neutralized to pH 6.0 by means of a small quantity of Dowex 1×4 (HCO_3^-) ion-exchange resin, and 2—5 μl of the solution was chromatographed on Kieselgel-G thin-layer in the solvent systems given in Table II; for comparison standard sugar methyl ethers were used .

In the hydrolysate of **Ia** 3,4,6-tri-O-methyl-D-glucose (*R*TMG 0.73 and 0.71 in solvent systems A and B, respectively) and 2,3,4,6-tetra-O-methyl-D-mannose (*R*TMG 0.94 and 0.95 in solvent systems A and B, respectively) were detected.

Permethylation and hydrolysis of the trisaccharide III

Compound **III** (97.5 mg) was methylated with methyl iodide according to KUHN [15] in dimethylformamide in the presence of active silver oxide. Methylation was repeated four times to give 42.3 mg of the decamethyl-trisaccharide (**IIIa**). The IR spectrum of the compound had no hydroxyl band [19] at ~3500 cm^{-1}.

The hydrolysis of **IIIa** was accomplished in the same as that of **Ia**. The chromatographic data are presented in Table II.

Table II

Thin-layer chromatographic comparison of the partially methylated monosaccharides obtained from **Ia** *and* **IIIa**

Name	*R*TMG	
	A	B
Ia-hydrolysate	0.73	0.71
	0.94	0.95
IIIa-hydrolysate	1.13	1.15
	0.95	0.96
	0.34	0.21
2,3,4,6-tetra-O-methyl-D-glucose	1.00	1.00
2,3,4,6-tetra-O-methyl-D-mannose	0.95	0.96
2,3,4-tri-O-methyl-L-rhamnose	1.11	1.15
3,4,6-tri-O-methyl-D-glucose	0.73	0.71
2,3-di-O-methyl-D-glucose	0.46	0.30
2,4-di-O-methyl-D-glucose	0.41	0.28
3,4-di-O-methyl-D-glucose	0.34	0.21

Thin-layer: Kieselgel-G (Activated for 1 hr at 105 °C). Solvent systems: *A* benzene–acetone (1:4) + 1% of conc. ammonium hydroxide; *B* methyl ethyl ketone saturated with 1% ammonium hydroxide. Detecting agent: 2% aniline hydrogene phthalate solution in 1-butanol (105 °C, 10 min)

In the hydrolysate of **IIIa** 3,4-di-O-methyl-D-glucose (*R*TMG 0.34 and 0.21 in solvent systems A and B, respectively), 2,3,4,6-tetra-O-methyl-D-mannose (*R*TMG 0.95 and 0.96 in solvent system A and B, respectively) and 2,3,4-tri-O-methyl-L-rhamnose (*R*TMG 1.13 and 1.15 in solvent systems A and B, respectively) were detected.

Preparation and hydrolysis of permethylristomycin A

Ristomycin A sulfate (2.30 g) was methylated three times according to HAKOMORI [18] with methyl iodide in dimethyl sulfoxide in the presence of sodium hydride to give 270 mg of permethylristomycin A. Repeated methylation did not increase the methoxyl content of the compound.

$C_{128}H_{185}O_{49}N_9$ (2662). Calcd. N 4.74; OCH_3 24.75. Found N 4.66, 4.60; OCH_3 25.30, 25.00%.

The hydrolysis of permethylristomycin A was effected as described for **Ia** and **IIIa**. The partially methylated monosaccharides formed as a result of the hydrolysis were detected by the procedure described in Table II. The hydrolysate of permethylated ristomycin A contained, in addition to the hydrolysis products of **IIa**, 3,4,6-tri-O-methyl-D-mannose (*R*TMG 0.69 and 0.73 in solvent systems A and B, respectively) and 2,3,5-tri-O-methyl-D-arabinose (*R*TMG 1.05 and 1.04 in solvent systems A and B, respectively).

*

The authors wish to express their appreciation to Mr. L. SZILÁGYI for the exploratory NMR work at 100 MHz.

REFERENCES

[1] BRAZHNIKOVA, M. G., LOMAKINA, N. N., LAVROVA, M. F., TOLSTYKH, I. V., YURINA, M. S., KLYUEVA, L. M.: Antibiotiki **8,** 392 (1963)
[2] GAUZE, G. F., KUDRINA, E. S., UKHOLINA, R. S., GAVRILINA, G. V.: Antibiotiki **8,** 387 (1963)
[3] SHORIN, V. A., PEVZNER, N. S., SHAPOVALOVA, S. P.: Antibiotiki **8,** 396 (1963)
[4] LAVROVA, M. F., LOMAKINA, N. N., BABENKO, G. A., BRAZHNIKOVA, M. G.: Antibiotiki **9,** 885 (1964)
[5] PHILIP, J. E., SHENCK, J. R., HARGIE, M. P.: Antib. Ann. 699 (1956—57)
[6] BRAZHNIKOVA, M. G., LOMAKINA, N. N., SZTARICSKAI, F., PUSKÁS, M., MAKLEIT, S., BOGNÁR, R.: Kém. Közl. **27,** 143 (1967)
[7] BRAZHNIKOVA, M. G., LOMAKINA, N. N., LAVROVA, M. F., MURAVYEVA, L. I., GAVRILINA, G. V.: Directed Biosynthesis. Nauka, Moscow 1966 p. 252
[8] LOMAKINA, N. N., ZENKOVA, V. A., BOGNÁR, R., SZTARICSKAI, F., SHEINKER, YU. N., TURCHIN, K. F.: Antibiotiki **13,** 675 (1968)
[9] BOGNÁR, R., SZTARICSKAI, F., MUNK, M., TAMÁS, J.: J. Org. Chem. **39,** 2971 (1974)
[10] LOMAKINA, N. N., BOGNÁR, R., BRAZHNIKOVA, M. G., SZTARICSKAI, F., MURAVYEVA, L. I.: 7th International Symposium on the Chemistry of Natural Products, Abstract. Zinate, Riga 1970 p. 625
[11] LOMAKINA, N. N., YURINA, M. S., SHEINKER, YU. N., TURCHIN, K. F.: Antibiotiki **17,** 488 (1972)
[12] BRAZHNIKOVA, M. G., LOMAKINA, N. N., MURAVYEVA, L. I: 5th International Congress of Chemotheraphy, Abstract. Vienna 1967 p. 759
[13] LOMAKINA, N. N., MURAVYEVA, L. I., PUSKÁS, M.: Antibiotiki **13,** 867 (1968)
[14] ZEMPLÉN, G., GERECS, Á.: Ber. **67,** 2049 (1934);
ZEMPLÉN, G., GERECS, Á.: Ber. **68,** 1318 (1935);
ZEMPLÉN, G., GERECS, Á.: Ber. **70,** 1098 (1937);
GORIN, P. A. J., PERLIN, A. S.: Can. J. Chem. **37,** 1930 (1959);
KAMIYA, S., HAMA, M.: Agr. Biol. Chem. **31,** 261 (1967)
[15] KUHN, R., TRISCHMANN, H., LÖW, I.: Angew. Chem. **67,** 32 (1955)
[16] BOGNÁR.: 7th International Symposium on the Chemistry of Natural Products, Pre-Symposium 4. Chemistry and Mode of Action of Antibiotics. Riga 1970 p. 22
[17] LEMIEUX, R. U., STEVENS, J. D.: Can. J. Chem. **43,** 2059 (1965)
[18] HAKOMORI, S.: J. Biochem. (Tokyo) **55,** 205 (1964)
[19] BISHOP, C. T.: Can. J. Chem. **35,** 1010 (1957)
[20] WHISTLER, R. L.: Methods in Carbohydrate Chemistry **5,** 271, 285. Academic Press, New York and London 1965
[21] SMITH, F., MONTGOMERY, R.: Chemistry of Plant Gums and Mucilages. Reinhold Publishing Corp., New York 1959 p. 80
[22] ZEMPLÉN, G., GERECS, Á., HADÁCSI, I.: Ber. **69,** 1827 (1936)

Ferenc SZTARICSKAI
Rezső BOGNÁR
M. Mária PUSKÁS
4010 Debrecen, Hungary.

Acta Chimica Academiae Scientiarum Hungaricae, Tomus 84 (1), pp. 85—91 (1975)

DERIVATIVES OF 1,3,4-THIADIAZOLE AS POTENTIAL SCHISTOSOMICIDES

SH. A. SHAMS EL-DINE* and O. CLAUDER

(Institute of Organic Chemistry, Semmelweis Medical University, Pharmaceutical Faculty, Budapest)

Received February 14, 1974

Some 1,3,4-thiadiazole derivatives were prepared on isometric basis in analogy with the corresponding antischistosomal thiazole compounds.

Although many nitro-substituted heterocyclic compounds, *e.g.* nitrothiazoles, nitroimidazoles and nitrofurans have antiprotozoal and antibacterial properties, only very few of them are endowed with antischistosomal activity [1, 2]. Some years ago, LAMBERT, WILHELM *et al.* [3—5] reported their success in the introduction of a new potent clinical agent for schistosomiasis, niridazole [1-(5-nitro-2-thiazolyl)-2-imidazolidinone] (**I**).

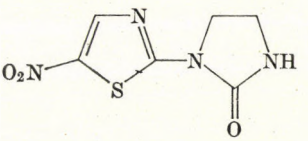

I

Since that time, several 5-nitrothiazolyl derivatives and related compounds were synthesized and tested for schistosomicidal activity [6—9]. The structure-activity relationship as well as their mode of action were investigated [9, 10]. It has been reported that there are two types of antischistosomal effects of nitroheterocyclic compounds [10]. One is observed with many structurally unrelated compounds and is limited to reversible damage to the female reproductive system. The other type of action is initiated by a reduction in phosphorylase phosphatase activity, followed by a hepatic shift and the eventual partial or complete elimination of the parasite. This second type of effect is exerted by compounds which have specific structural and conformational characteristics in common, *e.g.* niridazole; among these compounds are *trans-*

* To whom all correspondence should be addressed; present adress: Pharmaceutical Chemistry Department, Faculty of Pharmacy, Alexandria.

5-amino-3-[2-(5-nitrofuryl)vinyl]-1,2,4-oxadidazole (**II**) [11] and 1-[3-[(4-nitroso1-naphthyl)amino]propyl] piperidine (**III**) [12].

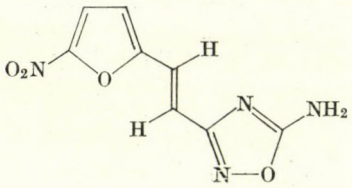

II

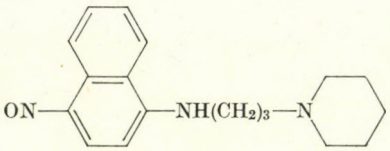

III

The bioisosterism known to exist between the thiazole and 1,3,4- thiadiazole rings prompted us to prepare 1-(5-nitro-1,3,4-thiadiazol-2-yl)-2-imidazolidinone (**IV**) and some related compounds in analogy to niridazole and its derivatives, especially since the thiadiazole ring remained unexplored regarding the antischistosomal activity.

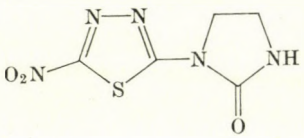

IV

The preparation of **IV** was first thought of to be achieved *via* the following route:

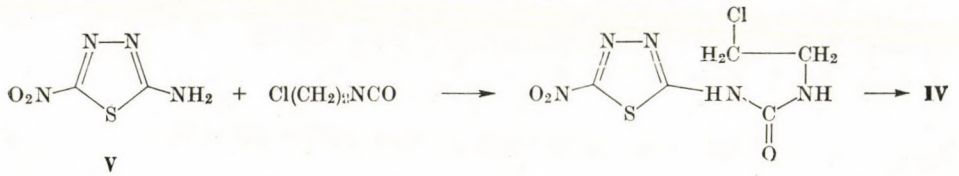

V

Compound **V** was first claimed in the literature as prepared by the nitration of 2-amino-1,3,4-thiadiazole (**VI**) with fuming nitric acid at 40 °C [13]. However, the product has the same melting point (177 °C, d.) as 2-nitramino-1,3,4-thiadiazole (**VII**) prepared by KANAOKA under similar conditions [14]. In our work, when the same procedure was applied to compound **VI**, the results proved that the product was **VII**. It is acidic in nature and dissolves in sodium carbonate solution with effervescence. The IR spectrum shows the following characteristics.

1. The two strong bands at 3320 and 3130 cm^{-1} found in the spectrum of the starting material **VI** (N—H str. of NH_2) disappears and is replaced by a strong band at 3100 cm^{-1} (N—H str. of —NH—).

2. The strong band at 3140 cm^{-1} assigned to C—NO_2 sym. str. (compared with other nitrothiadiazoles prepared in this work) is absent.

3. The strong band at 890 cm^{-1} (C—H of the ring) is still present [15]. This confirms the work of KANAOKA [14].

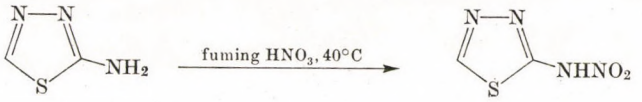

VI **VII**

VII was also obtained when **VI** was treated in a similar way to that followed in the preparation of 2-amino-5-nitrothiazole [16].

On the other hand, several attempts to prepare **VI** *via* molecular rearrangement of compound **VII** by heating with sulfuric acid at 60 °C for 13 hrs [17] or at 120 °C for 2 hrs [18] were unsuccessful. The product obtained melted above 300 °C with decomposition [19]; its IR spectrum had the strong band at 890 cm^{-1} assigned to C—H. These results can be explained by the electron deficiency of the thiadiazole ring [17].

Thus, the following route was suggested for the preparation of compound **IV**:

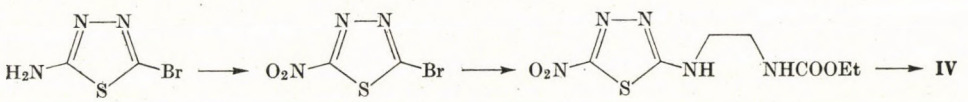

VIII **IX** **X**

Compound **VIII** was first prepared by BACK *et al.* [20] *via* the bromination of **VI** in 40% HBr; however, the product was not isolated but diazotized *in situ* to 2,5-dibromo-1,3,4-thiadiazole. In the present work, **VIII** was prepared by treating **VI** with bromine in acetic acid; it was isolated as a crystalline product and subjected to microanalysis. The IR spectrum of this product shows the following bands assigned to the primary amino group; 3350 v.s. 3100 v.s. 1600 s., and 1305 m cm^{-1}; in addition, the two bands at 1225 m and 890 v.s. cm^{-1} assigned to C—H are absent. Further confirmation of the structure was obtained by preparing the N-acetyl derivative (**XI**) of this product.

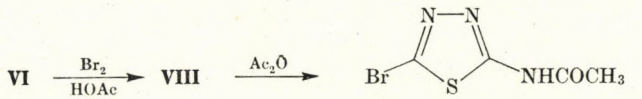

XI

The preparation of compound **IX** was first described in a U. S. patent [21], and this was accomplished by treating **VIII** with sodium nitrite and copper

metal powder in hydrochloric acid. In our work further improvement of the method of preparation and isolation of the product have been achieved. The IR spectrum of this compound has two bands at 1540 v.s. and 1340 v.s. cm^{-1} assigned to C—NO_2.

Preparation of compound **X** was accomplished by the action of N-carbethoxyethylenediamine **XII** on compound **IX**. The IR spectrum shows a strong band at 3350 cm^{-1} assigned to N—H str. of the secondary amino and monosubstituted carbamate groups; amide I band appears at 1695 v.s. cm^{-1} and amide II band appears at 1550 v.s. cm^{-1}, mixed with C—NO_2 asym. str.

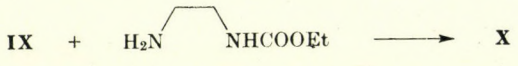

XII

A Hungarian patent described the preparation of 1-(2-thiazolyl)-2-imidazolidinone **XIII** by heating N-[2-[(2-thiazolyl)aminolethyl]-ethyl]urethane **XIV** with sodium ethoxide in absolute ethanol [22].

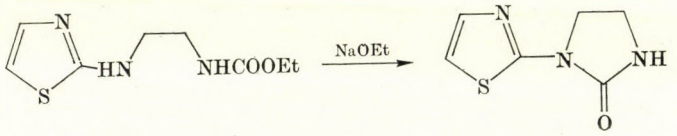

XIV **XIII**

However, the presence of the nitro group on the electrondeficient thiadiazole ring which may lead to its substitution by the strong nucleophilic ethoxyl radical [23], in addition to the possibility of ring cleavage [24], have led us to avoid the use of this procedure to prepare compound **IV**. A new method was applied which consisted in heating **X** at a temperature above its melting point for several hours. (Refluxing a solution of **X** in dimethylformamide for several hours did not bring the reaction to completion).

The preparation of N-[2-[(5-nitro-1,3,4-thiadiazol-2-yl)-amino]ethyl]-acetamide **XV** was accomplished by treatment of compound **IX** with N-acetylethylenediamine **XVI**. The IR spectrum shows amide I band at 1660 v.s. cm^{-1} and amide II band at 1570 v.s. cm^{-1}.

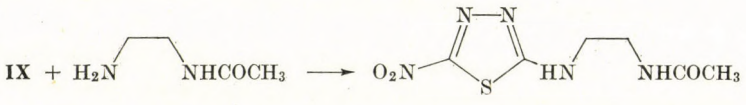

XVI **XV**

N-[2-[(5-Nitro-2-thiazolyl)amino]ethyl]ethyl-urethane (**XVIII**) was prepared by the action of **XII** on 2-bromo-5-nitrothiazole (**XVIII**). The IR spectrum has amide I band at 1680 v.s. cm^{-1} and amide II band at 1590 v.s. cm^{-1}.

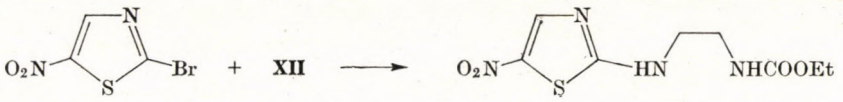

XVIII XVII

Compounds **XV** and **XVII** were prepared to examine their antischistosomal activity in comparison with compounds **IV** and **X**. Investigation of the activity of these compounds is in progress and the results will be discussed elsewhere.

Experimental

M.p.'s are uncorrected. The IR spectra were obtained with a UNICAM SP. 1200 spectrophotometer.

2-Nitramino-1,3,4-thiadiazole (VII)

A mixture of 1.01 g (0.01 mole) of **VI** and 0.8 ml nitric acid was added gradually to 6 g sulfuric acid at a temperature below 30 °C. The solution was stirred for 3 hrs at room temperature, poured into 10 ml ice-cold water, and the yellow precipitate produced was filtered off, washed with ice-cold water and dried to yield 0.73 g of **VII**, m.p. 175—177 °C (d).

2-Amino-5-bromo-1,3,4-thiadiazole (VIII)

A solution of 10 g (0.1 mole) of **IV** in 30 ml glacial acetic acid was mixed gradually with 17.6 g (0.11 mole) bromine in 6 ml glacial acetic acid, with shaking. The mixture was allowed to stand for 3 days at room temperature and then poured into 200 ml water with continuous stirring. The precipitated solid was filtered off, washed with water and recrystallized from 80% ethanol using charcoal to give white needles melting at 184—185 °C; yield 85%.

$C_2H_2N_3SBr$. Calcd. C 13.35; H 1.12; N 23.35; S 17.78; Br 44.4%. Found C 13.50; H 1.10; N 23.80; S 17.10; Br 44.3%.

2-Acetamido-5-bromo-1,3,4-thiadiazole (XI)

3.6 g (0.02 mole) of the amine **VI** was heated gently with 15 ml acetic anhydride until dissolution. The solution was refluxed for 30 min cooled and then poured into 100 ml cold water with continuous stirring. The precipitate was filtered off, washed with water and crystallized from 50% ethanol to obtain white needles, m.p. 245—247 °C, yield 75%.

$C_4H_4N_3OSBr$. Calcd. C 21.62; H 1.80; N. 18.90; S. 14.40; Br 36.36%. Found C 22.10; H 2.00; N 19.20; S 14.00; Br 35.90%.

2-Nitro-5-bromo-1,3,4-thiadiazole (IX)

1.3 g (0.02 mole) of copper metal powder suspended in a solution of 2.1 g (0.03 mole) sodium nitrite in 20 ml water. This suspension was treated with two drops of hydrochloric acid and stirred for 15 min. 1.8 g (0.01 mole) of the amine **VI** was dissolved in a mixture of 2 ml hydrochloric acid and 4 ml water by warming on a steam bath, and the solution was added dropwise during a 15 min period to the previously prepared suspension with vigorous stirring. During addition, the mixture became green, gas evolved and a yellowish green solid separated. The mixture was stirred for 2 hrs, filtered and the precipitate dried in a desiccator.

The solid was extracted repeatedly with ether, the ether extract was dried over Na_2SO_4, filtered, and the ether evaporated to leave 1 g of dark yellow crystals. Repeated recrystallization from a mixture of ether and petroleum ether (60—80 °C) produced 0.9 g (43%) of yellow crystals, m.p. 102—103 °C.

N-[2-[(5-Nitro-1,3,4-thiadiazol-2-yl)amino]ethyl]ethyl urethane (X)

2.7 g (0.02 mole) of N-carbethoxyethylenediamine (**XII**) was added dropwise to a magnetically stirred solution of 2.1 g (0.10 mole) of **IX** in 20 ml tetrahydrofuran. Stirring was continued for 2 hrs, and the solvent was evaporated under reduced pressure to leave a reddish brown oily residue which was then placed on a silica gel column. Development of the column with a mixture of benzene and acetone (8:2) gave a yellow crystalline product; this was recrystallized from chloroform-petroleum ether (60—80 °C); m. p. 140—142 °C, yield 1.7 g (65%).

$C_7H_{11}N_5O_4S$. Calcd. C 32.18; H 4.25; N. 26.81. Found C 32.05; H 4.40; N 26.53%.

1-(5-Nitro-1,3,4-thiadiazol-2-yl)-2-imidazolidinone (IV)

2.6 g (0.01 mole) of **X** was heated at 160—170 °C for 5 hrs. After cooling the brown residue was suspended in ethanol and the suspension was filtered. The solid was repeatedly washed with hot ethanol and then dried to yield 0.9 g (42%) of a brown amorphous product which did not melt when heated to 320 °C.

$C_5H_5N_5O_3S$. Calcd. C 27.91; H. 2.34; N. 32.50. Found C 27.50; H 2.50; N 32.10%.

N-[2-[(5-Nitro-1,3,4-thiadiazol-2-yl)amino]ethyl] acetamide (XV)

2 g (0.02 mole) of N-acetylethylenediamine (**XVI**) was added to a stirred solution of 2.1 g (0.01 mole) of **IX** in 20 ml ethanol during 20 min. The resulting reddish yellow solution was stirred at room temperature for 1 hr, then the yellow precipitate which separated was filtered off and washed with cold ethanol. A second crop was obtained by concentration of the filtrate and washings under reduced pressure. The product was recrystallized from ethanol as yellow needled melting at 228—230 °C with decomposition; yield 73%.

$C_6H_9N_5O_3S$. Calcd. C 31.17; H 3.92; N 30.29. Found C 31.13; H 4.00; N 30.22%.

N-[2-[(5-Nitro-2-thiazolyl)amino]ethyl]ethyl urethane (XVIII)

A magnetically stirred solution of 2.1 g (0.01 mole) of **XVIII** in 50 ml of a mixture of ethanol and ether (1:1) was mixed with 2.7 g (0.02 mole) of **XII** adding the compound dropwise in a 20 min period. The mixture was stirred for 1 hr and then allowed to stand overnight to give a yellow precipitate; a second crop was obtained from the mother liquor. Recrystallization from a mixture of ethanol and ether gave 1.6 g (60%) of yellow crystals, m.p. 165—167 °C.

$C_8H_{12}N_4O_4S$. Calcd. C 36.92; H 4.60; N 21. 53. Found C 37.00; H 4.80; N 21.50%.

REFERENCES

[1] Miura, K., Reckendorf, H. K.: Progr. Med. Chem. **5,** 320 (1967)
[2] Schnitzer, R. J.: in "Experimental Chemotography" (R. J. Schnitzer and F. Hawking, eds), Vol. 1, Academic Press, New York 1963 p. 289
[3] Lambert, C. R., Wilhelm, N., Striebel, H., Kradolfer, F., Schmidt, P.: Experientia **20,** 452 (1964)
[4] Schmidt, P., Wilhelm, M.: Angew. Chem., Internat. Ed. Engl., **5,** 857 (1966)
[5] Wilhelm, M., Marquardt, F. H., Meier, K., Schmidt, P.: Helv. Chim. Acta **49,** 2443 (1966)
[6] Bruderer, H., Ruegg, R.: S. African Pat. 6804, 729; C. A. **71,** 112923a (1969)
[7] Werbel, L. M., Rattaglia, R.: J. Med. Chem. **14,** 1, 10 (1971)
[8] Islip, P.: Brit. Pat. 1, 245, 916; C. A. **75,** 104839 (1971)
[9] Westland, R. D., Werbel, L. M., Dice, J. R., Holmes, J. L., Zahn, B. G.: J. Med. Chem. **14,** 10, 916 (1971)

[10] ROBINSON, C. H., BUEDING, E., FISCHER, J.: Molec. Pharmacol. **6,** 604 (1970)
[11] BRUER, H.: J. Med. Chem. **12,** 708 (1969)
[12] WERBEL, L. M., ELSLAGER, E. F., WORTH, D. F.: J. Med. Chem. **11,** 950 (1968)
[13] TOWNE, E. B., DICKEY, J. B.: U.S. 2, 790, 791; C.A. **51,** 13402e (1957)
[14] KANAOKA, M.: J. Pharm. Soc. Japan **75,** 1149 (1955); C.A. **50,** 5647 (1956)
[15] RAO, C. N. R., VENKATARAGHAVAN, R.: Can. J. Chem. **42,** (1), 43 (1964)
[16] BRADFORD, L., JENISON, J. D.: Swiss. Pat. 487, 923; C.A. **73,** 66560w (1970)
[17] DICKEY, J. B., TOWNE, E. B., WRIGHT, G. F.: J. Org. Chem. **20,** 499 (1955)
[18] NOVIKOV, S. S., KHMEL'NITSKU, L. I., LEBEDEV, O. V., SEVAST'YANOVA, V. V., EPISHINA, L. V.: Khim. Geterotsikl. Soedin (4), 503 (1970); C. A. **73,** 66491 (1970)
[19] SAIKACHI, H., KANAOKA, M.: Yakugaka Zasshi **81,** 1333 (1961); C.A. **56,** 7304h (1962)
[20] BACK, B., CHRISTENSEN, C. H., HANSEN, T. S., PEDERSEN, E. J., NIELSEN, J. T.: Acta Chem. Scand. **19,** 2434 (1965)
[21] TOMCUFCIK, A. S., OLD TAPPAN, N. J., NEWMANN, H., VALLEY, N. Y. S., HOFFMAN, A. M., RIDGE, P., EVANS, E. L., TEANECK, N. J.: U.S. Pat. 3, 497, 597; C.A. **72,** 121547e (1970)
[22] FUCHS, O., NEMES, A., DUMBOVICH, B., SZENTPÉTERI, A., PALÁGYI, T.: Ger. offen. 2,033.611 (cl. c 07d); C.A. **74,** 87982w (1971)
[23] HERTOG, H. J., JOUWERSMA, C., VAN DER WAL, A. A., WELLEBRANDS-SCHOGT, E. E. C.: Rec. Trav. Chim. **68,** 282 (1949)
[24] SANDSTRÖM, J.: in "Advances in Heterocyclic Chemistry" (A. R. KATRITZKY and A. J. BOULTON eds), Vol. 9, Academic Press, New York 1968 p. 189.

Sh. A. SHAMS EL-DINE; University of Alexandria, Pharmaceutical Faculty, Alexandria

Ottó CLAUDER; 1092 Budapest, Hőgyes E. u. 7, Hungary.

Acta Chimica Academiae Scientiarum Hungaricae, Tomus 84 (1), pp. 93—97 (1975)

ALKALOIDS CONTAINING the INDOLO [2,3-c] QUINAZOLINO [3,2-a]PYRIDINE SKELETON, III*

3,14-DIHYDRORUTECARPINE

K. HORVÁTH-DÓRA and O. CLAUDER

(Institute of Organic Chemistry, Faculty of Pharmaceutical Sciences, Semmelweis Medical University, Budapest)

Received March 29, 1974

3,14-Dihydrorutecarpine ③ was prepared from tryptamine ④ by means of acylation with isatoic anhydride ⑤ followed by ring closure with ethyl formate. The oxidation and N_{14} methylation of ③ yielded rutecarpine ⑧ and evodiamine ⑨, respectively. Rutecarpane ⑩ and rutecarpene ⑪ have also been prepared from 3,14-dihydrorutecarpine ③.

In our earlier paper [1] the synthesis and reduction of rutecarpine was treated. It was stated that in rutecarpine the C_3—N_{14} double bond cannot be reduced selectively because of the extensive conjugation involving the whole ring system. Its hydrogenation can be achieved only after decreasing the extent of conjugation, for example, after the reduction of the lactam C=O group. Therefore 3,14-dihydrorutecarpine ③ could only be synthesized up to now.

Similarly to the synthesis of rutecarpine, it was already prepared through the condensation reaction of N-formyltryptamine ① and anthranilic acid ②[1]. (Fig. 1.)

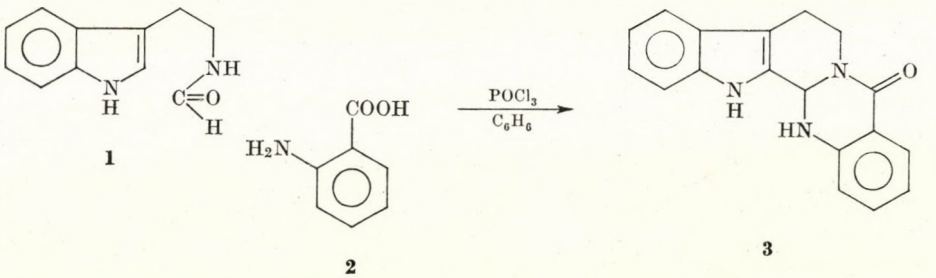

Fig. 1

A novel synthetic method have also been developed for the compound. Tryptamine ④ was acylated with isatoic anhydride ⑤ [2] in melt, yielding N-anthranoyl-tryptamide ⑥. This substance was already prepared by ASAHINA and ISHIMAVA [3] in $ZnCl_2$—HCl reduction of *o*-nitrobenzoyltryptamide ⑦. Then N-anthranoyl-tryptamide ⑥ was subjected to ring-closure with ethyl formate in a fusion reaction again, and 3,14-dihydrorutecarpine ③ was obtained. (Fig. 2.)

* Part II: HORVÁTH-DÓRA, K., CLAUDER, O.: Acta Pharm. Hung. **44**, Suppl. 80 (1974)

LUCKNER [4, 5] assumed that dihydrorutecarpine (3) is a key compound in the biosynthesis of rutecarpine (8) and evodiamine (9). According to JOHNE and GRÖGER [6, 7], the N-methylation reaction necessary for the biosynthesis of evodiamine (9) proceeds already in the anthranilic acid, rather than in the

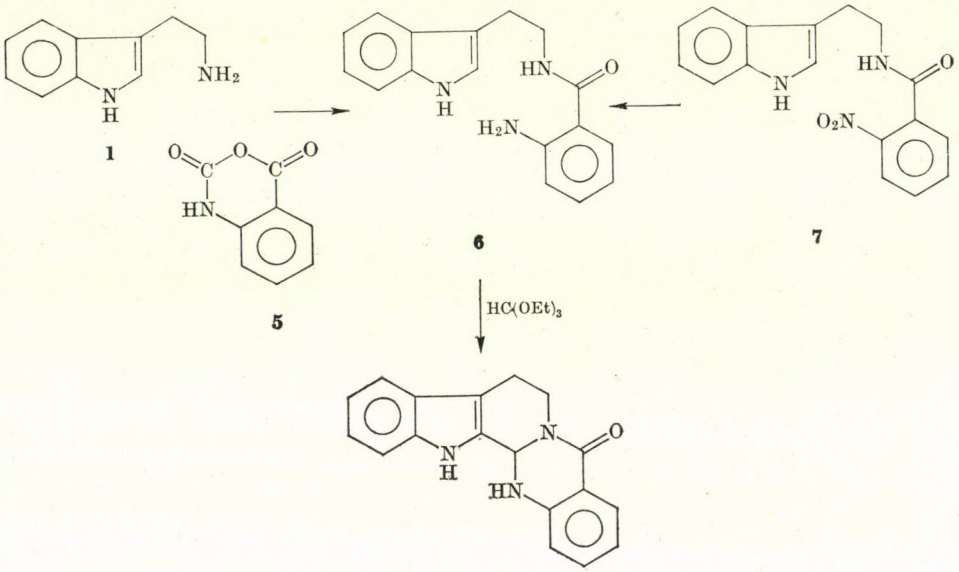

Fig. 2

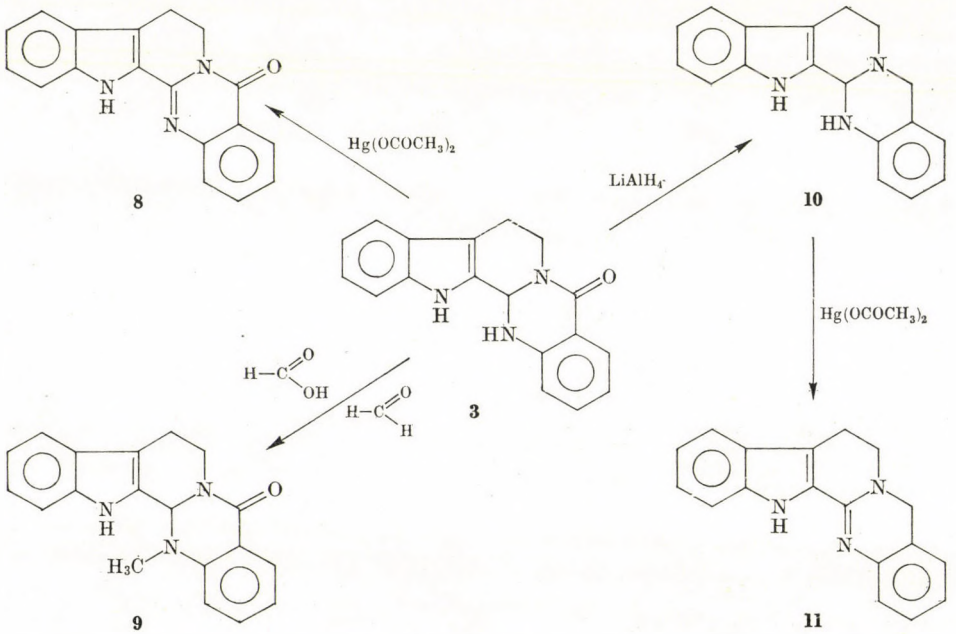

Fig. 3

dihydrorutecarpine (3). It can certainly be stated that, even if it has no important role in the biosynthesis, both alkaloids can be prepared from it under laboratory conditions.

Oxidation of 3,14-dihydrorutecarpine (3) with mercuric acetate yielded rutecarpine (8), while the N_{14} methylation reaction carried out with formic acid and formaldehyde resulted in evodiamine (9). Evodiamine (9) was identified on the basis of literature data (m.p., spectroscopic characteristics, etc.). [8, 9, 10].

In the reduction of 3,14-dihydrorutecarpine (3) with $LiAlH_4$ involving the hydrogenation of the C=O bond, rutecarpane (10) was formed. Oxidation of rutecarpane (10) with mercuric acetate yielded rutecarpene (11). Rutecarpane (10) and rutecarpene (11) have already been prepared earlier [1] by the reduction of rutecarpine (8) under various conditions. (Fig. 3.)

Experimental

Isatoic anhydride (5)

The substance was prepared from anthranilic acid (2) (5.0 g, 0.036 mole) and ethyl chlorocarbonate (15 ml, 0.0125 *M*) according to the prescriptions given in Ref. [2]. Yield: 88% (5.15 g). M.p. 246—248 °C (Lit. m.p. 243 °C [2]).

UV (etanol): λ_{max} (log ε): 242 (3.85); 315 nm (3.51).

IR: (KBr): 3300—2700 cm^{-1} (ν NH cyclic dimer), 1775, 1735 cm^{-1} (ν CO lactone), 760 cm^{-1} (γ CH *o*-disubst.).

N-Athranoyl-tryptamide (6)

Tryptamine base (4) (1.0 g, 0.0625 mole) and isatoic anhydride (5) (1.0 g, 0.00625 mole) were ground together thoroughly in a porcelain mortar then kept on a paraffin bath at 100 °C for 1 hr. The material first settled then foamed. After 1 hr treatment, it was crystallized from absolute ethanol (10 ml). White crystals (1.5 g; yield: 86%). After recrystallization from ethanol, m.p. 156—157 °C (Lit. m.p. 157.5 °C) [3].

UV (ethanol): λ_{max} (log ε): 248 (4.03), 272 (3.79), 282 (3.82), 290 (3.80), 322 nm (3.59).

IR (KBr): 3470, 3390 cm^{-1} (ν NH_2), 3300 cm^{-1} (ν NH indole), 1630 cm^{-1} (ν CO acid amide).

3,14-Dihydrorutecarpine (3)

N-Anthranoyl tryptamide (9) (1.5 g, 0.0054 mole) was refluxed with freshly distilled ethyl formate (0.0225 mole, 3.0 ml) on a paraffin bath at 180 °C for 20 hrs. The excess ethyl formate was distilled in vacuum. The oily residue was crystallized from acetone. 1.40 g of the product was obtained. (Yield: 77%.) After recrystallization from ethanol, m.p. 178—179 °C.

UV (ethanol): λ_{max} (log ε): 272 (4.11), 290 nm (3.98).

IR (KBr): 3350 cm^{-1} (ν NH), 1660 cm^{-1} (ν CO acid amide), 745 cm^{-1} (γ CH *o*-disubst.).

Rutecarpine (8)

3,14-Dihydrorutecarpine (3) (0.15 g, 0.0005 mole) was blended thoroughly with 3% acetic acid (6 ml). Mercuric acetate (0.40 g, 0.0013 mole) and EDTA disodium salt (0.45 g) in 3% acetic acid (6 ml) were added to the suspension, then it was refluxed on a paraffin bath at 110 °C in N_2 atmosphere for 5 hrs. The reaction mixture clarified first then a rubber-

like material separated. The colour of the solution turned yellow. After cooling the solution was made alkaline to pH = 8 with 2 *M* NH_4OH, then extracted with 1×20 ml, then 3×10 ml of chloroform. After drying it was evaporated to dryness in vacuum. A yellowish beige oil was obtained; it could be crystallized from ethanol. 0.13 g of the product was obtained (yield 75%). M.p. 256—258 °C.

UV (ethanol): λ_{max} (log ε): 278 (3.88), 290 (3.92), 332 (4.48), 345 (4.54), 364 nm (4.44).

IR (KBr): 3350 cm^{-1} (ν NH indole), 1660 cm^{-1} (ν CO acid amide), 765, 725 cm^{-1} (γ CH *o*-disubst.).

Evodiamine ⑨

98% Formic acid (3 ml) was poured onto 3,14-dihydrorutecarpine ③ (0.08 g, 0.00025 mole) while cooling with water and stirring. The substance was dissolved forming a yellow solution. 35% formaldehyde was added to it (4 ml). The solution became almost colourless. It was stirred then on a water bath at 80 °C in N_2 atmosphere for 5 hrs. The colour of the solution deepened and turned orange. Concentrated hydrochloric acid (1 ml) was added to it under cooling with ice, then evaporated in vacuum. Chloroform (30 ml) was poured onto the residue and made alkaline with 2*M* NH_4OH while cooling in ice. The aqueous phase was extracted with 3×20 ml of chloroform. After drying the chloroform solution was evaporated in vacuum, yielding a beige dry foam. Purification was accomplished on a Kieselgehl H preparative layer. Developing mixture: benzene : ethyl acetate : methanol (4:2:1). 0.03 g of product was obtained in 40% yield. M.p. 270—271 °C.

UV (ethanol): λ_{max} (log ε): 268 nm (4.08), (acetonitrile): 272 (4.06), 280 (4.02), 291 (3.90), 335 nm (3.30).

IR (KBr): 3250 cm^{-1} (ν NH indole), 1660 cm^{-1} (ν CO acid amide), 745 cm^{-1} (γ CH *o*-disubst.).

Rutecarpane ⑩

Absolute ether (5 ml) was poured onto 3,14-dihydrorutecarpine ③ (0.05 g, 0.00016 mole), then $LiAlH_4$ (0.03 g, 0.0008 mole) was added to it under continuous stirring. Then the mixture was refluxed on a water bath and stirred continuously for 20 hrs. It was decomposed with water (1 ml) then filtered. The precipitate was washed thoroughly with ether. After drying the ether, it was distilled off, and a white solid residue was obtained (0.04 g). Yield: 93%. After recrystallization from acetone: m.p. 165—168 °C.

UV (ethanol): λ_{max} (log ε): 283 nm (4.04).

IR (KBr): 3400 cm^{-1} (ν NH indole), 3250 cm^{-1} (ν NH *sec.* amine), 745 cm^{-1} (ν CH *o*-disubst.).

Rutecarpene ⑪

3% Acetic acid (3 ml) was poured onto rutecarpane ⑩ (0.05 g, 0.00018 mole) and boiled for 5 minutes under continuous stirring. The substance did not dissolve completely. After cooling the solution, mercuric acetate (0.20 g, 0.0006 mole) and a solution of the disodium salt of EDTA (0.22 g) in 3% acetic acid (3 ml) were added to it. The mixture was kept on a paraffin bath at 110 °C under N_2 atmosphere for 8 hrs. The colour of the solution turned yellow and yellow crystals separated. The mixture was made alkaline with 2*M* NH_4OH while cooling with ice then extracted with 1×20 ml, then 3×10 ml of chloroform. The chloroform phase was dried then evaporated. 0.04 g of product was obtained. Yield: 83%. After recrystallization from ethanol, m.p. 205—207 °C.

UV (ethanol): λ_{max} (log ε): 336 nm (4.28).

IR (KBr): 1640 cm^{-1} (ν C=N), 760, 740 cm^{-1} (γ CH *o*-disubst.).

REFERENCES

[1] CLAUDER, O., HORVÁTH-DÓRA, K.: Acta Chim. (Budapest) **72,** 221 (1972)
[2] CLARK, WAGNER, E. C.: J. Org. Chem. **9,** 60 (1944)
[3] ASAHINA, Y., ISHIMASA: J. Pharm. Soc. Japan **1926,** 61; C.A. **1927,** I. 1469
[4] LUCKNER, M.: International Symposium on Chemistry and Biology of Rutaceae Components, Szeged, Hungary, 1971, April 15—17
[5] LUCKNER, M.: Herba Hung. **10,** 27 (1971)
[6] JOHNE, S., GRÖGER, D.: International Symposium on Chemistry and Biology of Rutaceae Components, Szeged, Hungary, 1971, April 15—17
[7] JOHNE, S., GRÖGER, D.: Herba Hung. **10,** 65 (1971)
[8] CHATTERJEE, A., BOSE, S., GHOSH, C.: Tetrahedron **7,** 257 (1959)
[9] GOPINATH, K. W., GOVINDACHARI, T. R., RAMADAS, RAO, U.: Tetrahedron **8,** 293 (1960)
[10] NAKASATO, A., ASADA (NOMURA) S., MARUI, K.: Jakugaku Zashi **82,** 619 (1962)

Klára HORVÁTH-DÓRA
Ottó CLAUDER
} 1092 Budapest, Hőgyes E. u. 7, Hungary.

Acta Chimica Academiae Scientiarum Hungaricae, Tomus 84 (1), pp. 99—107 (1975)

CIRCULAR DICHROISM, LXVI*

CHIROPTICAL PROPERTIES OF SOME MONO- AND POLYSUBSTITUTED PHENYL GLYCOSIDES

A. LÉVAI[a]**, A. LIPTÁK[b], I. PINTÉR[a]*** and G. SNATZKE[a]

([a]Lehrstuhl für Strukturchemie, Ruhr-Universität Bochum, [b]Biochemical Institute, L. Kossuth University, Debrecen)

Received April 9, 1974

In contrast to compounds with the center of chirality bound to the phenyl ring *via* a C-atom, for phenyl glycosides the substitution pattern of the aryl ring is in general without any influence upon the sign of the Cotton effects, as long as these substituents are not very strong perturbers. Both the $^1B_{2u}$ and the $^1B_{1u}$ band CD are negative for β-glycosides and positive for the α-anomers. In the case of *o*-substituted compounds steric and/or electronic effects may, however, change the sign of some CD bands of the aromatic chromophore.

Numerous papers have been published on the Optical Rotatory Dispersion (ORD) and Circular Dichroism (CD) of purine and pyrimidine nucleosides but the chiroptical behaviour of the phenyl glycosides have not received so much attention [1—5]. Though several substituted compounds have been investigated [3—5], they mostly contained either more than one group in the phenyl ring or such substituents which act as strong perturbers, like C(=O)R or NO_2. In view of some rules which have been proposed for the correlation between chiroptical properties and substitution patterns within the aromatic ring [6, 7] it seemed interesting to measure the CD spectra of some simpler phenylglycosides which have been synthesized by known methods [8, 9]. The data are summarized in Table I.

Discussion

The determination of the configuration at the anomeric C-atom is usually achieved with the help of HUDSON's isorotation rule [10] and from coupling constants $J_{1',2'}$ in the NMR spectra of glycosides [11]. According to his rule, β-glycosides in the D-series are more levorotatory or less dextrorotatory than the corresponding α-anomers. This rule is based on the fact that the acetal chromophore of 2-alkoxytetrahydropyrane shows a positive plain ORD curve

* Part LXV: SNATZKE, G., GRAF, W., SCHLATTER, H.-R., LÜTHY, CH.: Helv. Chim. Acta, **57**, 1055 (1974)

** Permanent address: Institute of Organic Chemistry, L. Kossuth University, Debrecen, Hungary

*** Permanent address: Central Research Institute for Chemistry of the Hungarian Academy of Sciences, Budapest

Table I

Circular dichroism data of different phenyl glycosides

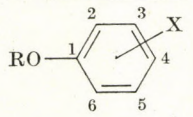

	R: Sugar component X: Substituents in benzene ring	λ_{max} ($\Delta\varepsilon$)
	α-Series	
I	R: Tetra-O-methyl-D-glucose X: —	273 (+0.42), 266 (+0.55), 261 (+0.42), 218 (+2.36)
II	R: Hepta-O-acetyl-D-maltose X: —	272 (+0.51), 265 (+0.65), 260 (+0.50), 232 (−0.08), 216 (+3.46)
III	R: Hepta-O-acetyl-D-cellobiose X: —	272 (+0.45), 265 (+0.58), 259 (+0.43), 230 (−0.19), 217 (+2.91)
IV	R: 4',6'-O-Benzylidene-D-glucose X: —	273 (+0.34), 266 (+0.44), 260 (+0.38), 216 (+4.96)
V	R: 2',3'-Di-O-methyl-4',6'-O-benzylidene-D-glucose X: —	273 (+0.42), 266 (+0.54), 260 (+0.47), 216 (+6.38)
VI	R: D-Glucose X: 4-CH_3	283 (+0.28), 275 (+0.37), 221 (+1.84)
VII	R: Tetra-O-acetyl-D-glucose X: 4-CH_3	281 (+0.29), 274 (+0.40), 236 (−0.06), 220 (+3.55)
VIII	R: D-Galactose X: 4-CH_3	282 (+0.29), 275 (+0.40), 270 (+0.36), 222 (+3.24)
IX	R: Tetra-O-acetyl-D-galactose X: 4-CH_3	280 (+0.32), 273 (+0.45), 268 (+0.39), 220 (+4.77), 194 (+17.00)
X	R: Tetra-O-acetyl-D-glucose X: 4-C_2H_5	280 (+0.26), 273 (+0.35), 268 (+0.30), 237 (−0.08), 221 (+3.68), 193 (+14.50)
XI	R: D-Galactose X: 4-C_2H_5	281 (+0.30), 274 (+0.41), 268 (+0.35), 222 (+3.40)
XII	R: Tetra-O-acetyl-D-galactose X: 4-C_2H_5	280 (+0.34), 273 (+0.47), 267 (+0.42), 261 (+0.29), 221 (+5.00)
XIII	R: D-Glucose X: 3-CH_3	277 (+0.67), 270 (+0.77), 220 (+2.00)
XIV	R: Tetra-O-acetyl-D-glucose X: 3-CH_3	276 (+0.65), 269 (+0.73), 235 (−0.07), 220 (+2.83)
XV	R: D-Glucose X- 2-CH_3	275 (+0.68), 269 (+0.77), 215 (+1.82)

XVI	R: Tetra-O-acetyl-D-glucose X: 2-CH_3	275 (+0.37), 269 (+0.38), 234 (−0.10), 220 (+3.00)
XVII	R: D-Glucose X- 4-Br	284 (+0.17), 276 (+0.26), 226 (+2.34)
XVIII	R: Tetra-O-methyl-D-glucose X: 4-Br	283 (+0.23), 275 (+0.36), 225 (+3.39)
XIX	R: Tetra-O-acetyl-D-glucose X: 4-Br	282 (+0.17), 275 (+0.26), 269 (+0.22), 225 (+3.26)
XX	R: D-Glucose X: 4-NO_2	303 (+1.27), 278 (+0.97), 219 (+0.70)
XXI	R: Tetra-O-acetyl-D-glucose X: 4-NO_2	290 (+1.91), 223 (+0.57)
	β-Series	
XXII	R: D-Glucose X: —	273 (−0.35), 266 (−0.39), 261 (−0.32), 217 (−1.46)
XXIII	R: 2',3'-Di-O-methyl-D-glucose X: —	273 (−0.54), 266 (−0.61), 261 (−0.48), 217 (−2.10)
XXIV	R: Tetra-O-methyl-D-glucose X: —	273 (−0.61), 266 (−0.73), 260 (−0.51), 217 (−2.14)
XXV	R: Hepta-O-acetyl-D-maltose R: —	272 (−0.66), 265 (−0.81), 259 (−0.56), 215 (−1.14)
XXVI	R- Hepta-O-acetyl-D-cellobiose X: —	272 (−0.49), 265 (−0.59), 259 (−0.38), 214 (−2.09)
XXVII	R: Hepta-O-acetyl-D-lactose X: —	272 (−0.67), 265 (−0.81), 259 (−0.58), 215 (−1.95)
XXVIII	R: 4',6'-O-Benzylidene-D-glucose X: —	273 (−0,49), 266 (−0.56), 261 (−0.45), 220 (−0.44)
XXIX	R: 2',3'-Di-O-methyl-4',6'-O-benzylidene-D-glucose X: —	272 (−0.54), 266 (−0.61), 260 (−0.46), 221 (−0.69)
XXX	R: D-Glucose X: 4-CH_3	282 (−0.35), 274 (−0.42), 222 (−1.98)
XXXI	R: Tetra-O-methyl-D-glucose X: 4-CH_3	281 (−0.45), 273 (−0.47), 222 (−1.65)
XXXII	R: Tetra-O-acetyl-D-glucose X: 4-CH_3	280 (−0.34), 273 (−0.39), 218 (−2.38)
XXXIII	R: D-Glucose X: 4-C_2H_5	281 (−0.36), 274 (−0.44), 268 (−0.37), 222 (−2.23)
XXXIV	R: Tetra-O-acetyl-D-galactose X: 4-C_2H_5	280 (−0.40), 273 (−0.48), 267 (−0.36), 220 (−1.32)

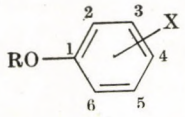

	R: Sugar conponent X: Substituents in benzene ring	λ_{max} ($\Delta\varepsilon$)
XXXV	R: D-Glucuronic acid methyl ester X: 4-CH_3	281 (−0.37), 274 (−0.48), 269 (−0.43), 224 (−2.61)
XXXVI	R: Tetra-O-acetyl-D-glucose X: 3-CH_3	275 (−0.75), 268−0.80), 220 (−2.14)
XXXVII	R: D-Isorhamnose X: 2-CH_3	275 (−0.51), 269 (−.55), 220 (−1.80)
XXXVIII	R: Tri-O-acetyl-D-isorhamnose X: 2-CH_3	275 (−0.34), 268 (−0.36), 262 (−0.28), 220 (−2.71)
XXXIX	R: D-Glucose X: 2-CH_3	275 (−0.54), 269 (−0.62), 221 (−2.52)
XL	R: Tetra-O-acetyl-D-glucose X: 2-CH_3	275 −0.35), 268 (−0.37), 220 (−3.41)
XLI	R: 6'-Deoxy-6'-iodo-tri-O-acetyl-D-glucose X: 2-CH_3	275 (−(0. 55), 268 (−0.60), 262 (−0.49), 218 (−3.52)
XLII	R: D-Glucose X: 4-Br	283 (−0.25), 276 (−0.29), 224 (−1.72)
XLIII	R: Tetra-O-methyl-D-glucose X: 4-Br	283 (−0.25), 276 (−0.28), 224 (−2.05)
XLIV	R: Tetra-O-acetyl-D-glucose X: 4-Br	282 (−0.24), 275 (−0.29), 268 (−0.22), 219 (−1.58)
XLV	R: D-Glucose X: 2,4-$(CH_3)_2$	282 (−0.14), 274 (−0. 14), 220 (−2.53)
XLVI	R: Tetra-O-acetyl-D-galactose X: 2-$[CH(CH_3)_2]$,5-CH_3	278 (−0.54), 270 (−0.57),225 (−2.86)
XLVII	R: D-Glucose X: 3-CH_3, 4-Cl	284 (−0.37), 276 (−0.44), 227 (−2.04)
XLVIII	R: Tetra-O-acetyl-D-glucose X: 3-CH_3, 4-Cl	283 (−0.39), 275 (−0.46), 270 (−0.37), 224 (−2.12)
XLIX	R: D-Glucose X: 2,4,5-$(Cl)_3$	295 (−0.56), 288 (−0.62), 234 (−0.63)
L	R: Tetra-O-acetyl-D-glucose X: 2,4,5-$(Cl)_3$	294 (−0.14), 285 (−0.18), 234 (−3.98)

LI	R: D-Glucose X: 2-Benzyl, 4-Cl	286 (−0.42), 278 (−0.50), 272 (−0.42), 266 (−0.20) 258 (−0.08), 253 (−0.05), 230 (−4.95), 201 (+6.76)
LII	R: Tetra-O-acetyl-D-glucose X: 2-Benzyl, 4-Cl	285 (−0.36), 278 (−0.42), 268 (−0.19), 259 (−0.05) 230 (−5.95), 203 (+14.14)
LIII	R: Methyl-tri-O-acetyl-D-glucuronate X: 2-(CH_3CO)	273 (−0.69), 266 (−0.84), 260 (−0.64), 255 (−0.39) 228 (+0.62), 218 (−0.31), 210 (+1.06)
LIV	R: D-Glucose X: 4-NO_2	318 (−0.76), 218 (−1.04)
LV	R: Tetra-O-methyl-D-glucose X: 4-NO_2	307 (−1.09), 219 (−1.34)
LVI	R: Tetra-O-acetyl-D-glucose X: 4-NO_2	325 (−0.98), 216 (−2.03) 210 (−3.04)
LVII	R: D-Glucose X: 2-NO_2	342 (−1.47), 305 (+0.27), 279 (−0.63), 254 (+1.15) 210 (−3.24)
LVIII	R: Tetra-O-methyl-D-glucose X: 2-NO_2	345 (−0.75), 304 (+0.26), 278 (−0.29), 254 (+0.36),
LIX	R: Tetra-O-acetyl-D-glucose X: 2-NO_2	317 (+1.49), 281 sh (−1.02), 253 (−2.55), 228 sh (−1.51) 210(−3.04)
LX	R: Tetra-O-acetyl-D-glucose X: 2,6-$(Cl)_2$, 4-NO_2	320 (+0.47), 222 (−1.97)
	Other glycosides	
LXI	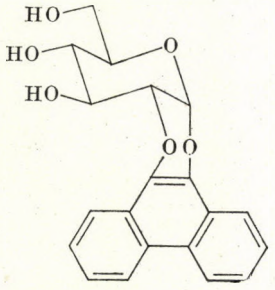	364 (−0.25), 348 (−0.21), 310 (+3.55), 298 (+2.87), 259 (−2.08), 240 (+1.03), 225 (−13.37)

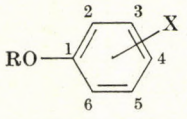	R: Sugar component X: Substituents in benzene ring	λ_{max} ($\Delta\varepsilon$
LXII	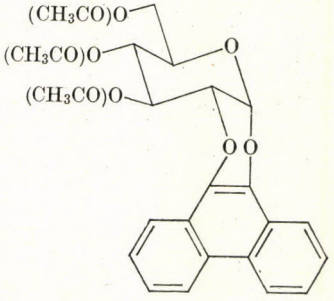	361 (−0.14), 345 (−0.10), 316 (+0.18), 307 (+2.98), 295 (+2.30), 264 (−1.90), 239 (+0.88), 215 (−18.19)
LXIII	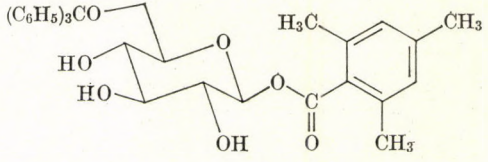	252 (−0.69), 226 (+0.90)

for the (S)-, and a negative one for the (R)-configuration, which then contributes either positively or negatively to the rotation at the NaD line [12].

This rule is violated, however, when there are such chromophores in the molecule which themselves show at longer wavelengths Cotton effects of opposite sign to that of the corresponding "background rotation" due to the acetal chromophore. The most prominent examples of such an exception are the pyrimidine glycosides [13].

The aromatic chromophore gives rise to only a very weak Cotton effect within the $^1B_{2u}$ absorption band, its sign depending on the substitution pattern of the ring. For derivatives and analogues (**LXIV**) of mandelic acid the unsubstituted and the *m*-substituted compounds give Cotton effects of opposite signs to those of the *p*- and *o*-substituted isomers [6]. However, in the case of phenylalanine and its three hydroxy derivatives (**LXV**) *p*-substitution does not change the sign of this Cotton effect, whereas the *m*- and *o*-hydroxy derivatives show sign inversion [14]. This latter result is in agreement with theoretical calculations [14] in which it is assumed that the OR group is the main perturber and the alkyl group can be neglected. The same result can, however, also be obtained by taking into consideration only the "spectroscopic moments" of the individual substituents and neglecting their magnitudes [7]. The difference between KORVER's [6] and HOOKER and SCHELLMAN's [14] results could be explained by assuming that the "insulation" of the chromophore from the center of chirality by a CH_2 group gives the theoretically predicted correlation between substitution pattern and sign, whereas in the case of direct connection between the benzene ring and the center of chirality, the different degrees of hyperconjugation may change the conformational equilibria. This will in turn influence the sign of the Cotton effect.

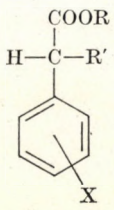

LXIV

R: H, CH_3
R': OH, OCH_3, CH_2OH
X: H, F, Cl, Br, OCH_3 (o, m, p)

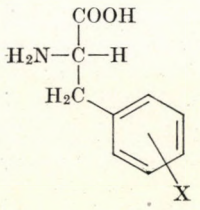

LXV

X: H, OH (o, m, p)

As can be seen from Table I, the sign of the Cotton effect of substituted phenylglycosides follows neither the pattern obtained for mandelic acid derivatives [6], nor that of the tyrosines [14]: the CD curve within the $^1B_{2u}$ and also the $^1B_{1u}$ transition is nearly uninfluenced by this substitution. Also, minor

changes in the sugar moiety (methylation, acetylation, 4',6'-benzylidene derivative formation, epimerization at C(4'), replacement of the OH at C(6') by hydrogen or iodine, or oxidation to the uronic acid, glycoside formation at C(4') do not bring about drastic changes in the CD. From the synthesis and enzymatic cleavage of these glycosides, as well as from NMR coupling constants the configuration at the anomeric C-atom is known unequivocally, so this lack of change of sign of the Cotton effect cannot be due to a wrong assignment from a violated Hudson rule.

An explanation for this surprising fact may be given in the following way. The empirical q-value [15], which is a measure of the spectroscopic moment, is 4 to 6 for alkyl groups, chlorine and bromine, and 21 for OCH_3; the main influence upon the electric transition moment vector will thus come through the glycosidic linkage, and the same must hold for the Cotton effects. It seems as if in the case when the chiral center is linked to the phenyl chromophore through a perturber of medium strength like oxygen, the substitution pattern (provided that the other substituents are only weak perturbers) is without pronounced influence upon the Cotton effect within the $^1B_{2u}$ and $^1B_{1u}$ absorption bands. One can therefore safely determine the configuration at C(1') of substituted phenyl-D-glycosides from the CD: the $^1B_{2u}$ and the $^1B_{1u}$ band CD are positive for the α- and negative for the β-glycosides. These Cotton effects have thus the same signs as the background rotation caused by the Cotton effect of the acetal chromophore, so they reinforce each other. It must be emphasized, however, that any extrapolation of this rule to phenylglycosides substituted by strong perturbers should not be tried without experimental proof.

As noticed earlier [5], in the CD-spectra of many acetylated α-phenylglycosides a very small but distinct negative Cotton effect appears at about 230 nm in between the two positive ones at around 275 and 220 nm.

TSUZUKI *et al.* [3] have described the chiroptical data of several nitrophenylglycosides and their acetates. Some of these compounds and their methyl ethers were also available to us and we could not always reproduce the CD curves published. For some of these compounds (especially the p-nitrophenylglycosides) the anisotropy factor $g' = \frac{\Delta\varepsilon}{\varepsilon}$ is in the order of 10^{-4} and smaller, and we have noticed that (at least with the dichrograph) artifacts may be measured if the optical density is too high. Instead of the whole CD band the instrument records correctly only the beginning of the steep rise and the end of the band, but instead of climbing to the maximum it returns to the base line in between. The CD curves given in Ref. [3] for the p-nitrophenylglycosides resemble very much those we have obtained with solutions of too high optical density. These apparent three Cotton effects merge into a single broader one if this "artifact" is eliminated by reducing either the con-

centration of the solution or the cell path. We could, however, confirm the findings [3] that the long-wavelength Cotton effect of the α-glucoside is positive and that of the β-anomer is negative. Furthermore, between 210 and 220 nm another Cotton effect of the same sign as around 310 nm could be detected.

If two additional chlorine atoms are introduced in *o*-, *o'*-position (**LX**), the sign and magnitude of the short-wavelength CD remain unchanged whereas the long-wavelength CD, to which mainly the nitro chromophore contributes, is inverted.

In the case of the *o*-nitro compounds our measurements agree with the literature data [3]. It is interesting to note that the [3] sign inversion of the CD bands, observed upon by acetylating the OH groups of the glucose moiety, does not take place for the methylated glucoside **LVIII**. Other than mere steric reasons (*e.g.* orbital interaction between the acetoxy and the nitro chromophores) must therefore be responsible for this fact. The CD data of some more complicated arylglycosides are also listed in Table I, however, a detailed discussion must await the measurement of more analogues.

Experimental

All CD spectra were recorded on a Model 185 Roussel–Jouan dichrograph in acetonitrile solution at concentrations of about 1 mg/cm^3 in 2.00 to 0.01 cm cells at 20 °C.

G. S. thanks the Deutsche Forschungsgemeinschaft and the Fonds der Chemischen Industrie for financial support of this work, Prof. B. HELFERICH, and Mr. S. MÜLLER (Bonn University) for many glycosides.

REFERENCES

[1] STICZAY, T., PECIAR, C., BAUER, S.: Tetrahedron Letters, 2407 (1968)
[2] STICZAY, T., PECIAR, C., BAUER, S.: Tetrahedron, **25,** 3521 (1969)
[3] TSUZUKI, Y., KOYAMA, M., AOKI, K., KATO, T., TANABE, K.: Bull. Chem. Soc. Jap., **42,** 1052 (1969)
[4] TSUZUKI, Y., KATAOKA, S., FUNAYAMA, M., SATSUMABAYASHI, K.: Bull. Chem. Soc. Jap., **44,** 526 (1971)
[5] LÉVAI, A., TŐKÉS, A. L., BOGNÁR, R., STICZAY, T., PECIAR, C., BAUER, S.: Magyar Kém. Foly., **79,** 197 (1973)
[6] KORVER, O.: Tetrahedron, **26,** 5507 (1970)
[7] For a detailed discussion *cf.* SNATZKE, G., KAJTÁR, M., SNATZKE, F. in Fundamental Aspects and Recent Developments in Optical Rotatory Dispersion and Circular Dichroism, (CIARDELLI, F., SALVADORI, P., eds). Heyden, London 1973
[8] CONCHIE, J., LEVVY, G. A., MARSH, C. A.: Adv. Carb. Chem., **12,** 157 (1957)
[9] PIGMAN, W.: The Carbohydrates. Academic Press, New York 1957
[10] HUDSON, C. S.: J. Amer. Chem. Soc., **31,** 66 (1909)
[11] KOTOWYCZ, G., LEMIEUX, R. U.: Chem. Rev. **73,** 669 (1973)
[12] KLYNE, W., MOSE, W. P., SCOPES, P. M., HOLDER, G. M., WHALLEY, W. B.: J. Chem. Soc. (C), 1273 (1967)
[13] LEMIEUX, R. U., HOFFER, M.: Canad. J. Chem. **39,** 110 (1961)
[14] HOOKER, T. M., SCHELLMAN, J. A.: Biopolymers, **9,** 1319 (1970)
[15] PETRUSKA, J.: J. Chem. Phys., **34,** 1120 (1961)

Albert LÉVAI
András LIPTÁK } H-4010 Debrecen, Hungary
István PINTÉR; H-1025 Budapest, Pusztaszeri út, 57—69, Hungary.
Günther SNATZKE; D-463 Bochum, BRD.

Acta Chimica Academiae Scientiarum Hungaricae, Tomus 84 (1), pp. 109—114 (1975)

LABELLED AMINO ACIDS AND THEIR DERIVATIVES, V*

PRESOLUTION OF *p*-CHLORO-DL-PHENYLALANINE. REPARATION OF L-PHENYLALANINE-(4-^{3}H) FROM *p*-CHLORO-L-PHENYLALANINE

J. KOVÁCS,** I. TEPLÁN*** and I. MEZŐ***

*(** Institute of Isotopes of the Hungarian Academy of Sciences, Budapest, and *** Institute of Biochemistry, Semmelweis University Medical School)*

Received April 25, 1974

The resolution of acetyl-*p*-chloro-DL-phenylalanine was accomplished with L-(+)-threo-1-(*p*-nitrophenyl)-2-aminopropanediol-(1,3). Catalytic hydrogenation and catalytic tritiation of *p*-chloro-L-phenyl-alanine yielded L-phenylalanine, and L-phenyl-alanine-(4-^{3}H) having a molar activity of 8.76 Ci/mmol, respectively

Radioactive amino acids for use in biological research are usually prepared in optically active forms. In modern biochemical research, optically active amino acids with high specific activities, labelled with tritium in definite positions are particularly important. Of the amino acids of biological importance, phenylalanine labelled with tritium could be prepared by a limited number of suitable methods only.

Labelling of L-phenylalanine can be achieved by catalytic exchange of hydrogen for tritium in the aromatic ring located farther from the optically active center [1], by catalytic saturation of the double bond that can be formed in α–β position in the alkyl chain [2, 3], or by a hydrogen–tritium exchange reaction accomplished at the α-carbon atom, which can be carried out *e.g.*, by the so-called racemization technique [4]. The latter two techniques yield, of course, a racemic product, whose antipodes must be separated by an appropriate resolution method.

In isotope exchange reactions, thus in the case of amino acids labelled by the racemization technique [4], only very low specific activities can be achieved, which strongly limit their application.

GERDAY and VERLY [2] elaborated a procedure for the preparation of L-phenylalanine with high specific activity tritiated in the alkyl side-chain. 2-(Chloroacetylamino)cinnamic acid was subjected to catalytic tritiation with subsequent enzymic resolution, yielding L-phenylalanine-(2,3-^{3}H). The procedure is not suitable for preparative work, because of the small-scale operational characteristics of enzymic methods and of the low yield.

* Part IV: Acta Chim. (Budapest), **73**, 23 (1972)

** Present address: Frédéric Joliot Curie National Research Institute for Radiology and Radiohygiene, Budapest

The above facts suggest that L-phenylalanine with high specific activity can be prepared most appropriately by catalytic tritiation of the chemically uniform, optically active phenylalanine derivative substituted by halogen atom in the aromatic ring.

BIRKOFER and HEMPEL [1] carried out bromination of L-phenylalanine with subsequent catalytic triation in alkaline medium and assumed that 2,4-dibromo-L-phenylalanine and labelled phenylalanine of high specific activity were obtained, respectively. In repeating their experiments, the bromination step was found to yield various halogenated amino acid derivatives which could not be separated by means of crystallization. Thus the preparation of phenylalanine labelled with tritium in specific positions could not be achieved. Our experimental findings were supported by the work of FAULSTICH *et al.* [5], in which the authors studied the bromination of phenylalanine in detail. The isomers formed in the reaction were separated on a column by the chromatographic technique and identified. In this way, the preparation of L-phenylalanine labelled with tritium in known positions could be achieved after catalytic tritiation of the derivatives separated.

Since direct bromination of phenylalanine does not yield a uniform product and the isolation of the isomers is troublesome, a different approach was searched for. In the procedure described in the present paper *p*-chloro-DL-phenylalanine was synthesized. A chemical method was elaborated for resolving *p*-chloro-DL-phenylalanine; up to now, only the enzymic technique suggested by TONG *et al.* [6] has been given in the literature for this purpose. The enzymic resolution technique developed by them is suitable for the preparation of small amounts of amino acid derivatives only. Our research project and the information on the biological activity of *p*-chloro-DL-phenylalanine available in the literature [7—12] required the elaboration of a reproducible large-scale chemical method for the separation of the antipodes of *p*-chloro-DL-phenylalanine.

The experiments were accomplished in analogy to the procedures suggested for the resolution of phenylalanine. Carbobenzoxy-*p*-chloro-DL-phenylalanine and acetyl-*p*-chloro-DL-phenylalanine were prepared for use in the resolution experiments.

The diastereomeric salt of carbobenzoxy-*p*-chloro-DL-phenylalanine formed with (—)-α-phenylethylamine was prepared first. In order to decide which of the antipodes of carbobenzoxy-*p*-chloro-DL-phenylalanine was crystallized in the resolution step, catalytic hydrogenation was applied in methanol in the presence of Pd/C. Owing to hydrogenolysis of the carbobenzoxy group, L-phenylalanine could be recovered from the salt in a single step; the hydrochloric acid liberated was bound by (—)-α-phenylethylamine. The separation of carbobenzoxy-*p*-chloro-DL-phenylalanine with (—)-α-phenylethylamine yielded the D-phenylalanine, unlike in the case of carbobenzoxy-DL-phenylalanine,

where L-phenylalanine was obtained under identical experimental conditions [13].

The most suitable and reproducible resolution procedure was that involving the preparation of the diastereomeric salt of acetyl-*p*-chloro-DL-phenylalanine and L-(+)-*threo*-1-(*p*-nitrophenyl)-2-amino-1,3-propanediol; salt formation yields a diastereomeric salt in ethanol, which is readily purified.

In order to achieve the desired degree of purity, the salt was repeatedly recrystallized from water. The diastereomeric salt was decomposed with dilute hydrochloric acid, and refluxing with 3*N* hydrochloric acid was applied in the deacetylation reaction. *p*-Chloro-L-phenylalanine was crystallized from the reaction mixture at pH 5. The specific rotation of *p*-chloro-L-phenylalanine prepared by the described procedure was identical with the value determined in the enzymically prepared product given in the literature [6]. Analogous processing of the mother liquor of separation yielded *p*-chloro-D-phenylalanine with only 80% optical purity, thus D-(—)-*threo*-1-(*p*-nitrophenyl]-2-amino-1,3-propanediol should be used in the resolution procedure when optically pure *p*-chloro-D-phenylalanine is required.

The product obtained on resolution was checked by catalytic hydrogenation of *p*-chloro-L-phenylalanine in the presence of Pd/C and potassium hydroxide in methanol–water. The product obtained on hydrogenation was chromatographically uniform, exhibiting identical specific rotation with that of an authentic L-phenylalanine sample.

Phenylalanine labelled with tritium in the aromatic ring was prepared from *p*-chloro-L-phenylalanine and its activity was found to be 8.7 Ci/mmol. Catalytic tritiation was accomplished in a manner analogous to hydrogenation, in a special vacuum apparatus constructed for tritiation reactions [14]. The product obtained after purification was uniform, according to chromatographic and radiochromatographic examination.

In parallel experiments the activities of the products obtained were 11.6 and 7.4 Ci/mmol. The variation in specific activity can presumably be attributed to the different extent of heterogeneous catalytic isotope exchange reactions between the solvent and tritium gas, owing to differences in the reaction times.

Experimental

In the TLC experiments DC-Alufolien Kieselgel (Merck) layers were used. Developing solvent systems applied:

(A) ethyl acetate : pyridine : glacial acetic acid : water = 30 : 20 : 6 : 11,
(B) ethyl acetate : pyridine : glacial acetic acid : water = 240 : 20 : 6 : 11,
(C) butanol : glacial acetic acid : water = 4 : 1 : 1.

Optical rotations were measured with a Schmidt—Haensch polarimeter.

The radioactivity measurements were carried out with a Packard Tri-Carb M 3375 liquid scintillation spectrometer.

The radiochromatograms were evaluated with a Berthold Dünnschicht Scanner LB apparatus.

The melting points were determined with a Koffler block; the data are uncorrected.

1. Carbobenzoxy-p-chloro-DL-phenylalanine

p-Chloro-DL-phenylalanine (15 g, 75 mmol) was dissolved in 2*N* sodium hydroxide (55 ml) and carbobenzoxy chloride (12 ml) and 2*N* sodium hydroxide (22 ml) were added to it cooling the reaction mixture with ice. The reaction mixture was stirred at room temperature for 2 hrs the excess of carbobenzoxy chloride was extracted with ether and the pH of the solution was adjusted to pH 1 with 6*N* hydrochloric acid. The product separated was filtered off, washed, dried and crystallized from ethanol (about 100 ml) with water. Yield 20.0 g (89%). M.p. 156—158 °C, R_f 0.8 (B).

$C_{17}H_{16}ClNO_4$ (333.77). Calcd. C 61.0; H 4.78; N 4.18; Cl 10.60. Found C 61.2; H 4.80; N 4.20; Cl 10.55.

2. Resolution of carbobenzoxy-p-chloro-DL-phenylalanine with (-)-α-phenylethylamine

Cabobenzoxy-*p*-chloro-DL-phenylalanine (9.9 g, 30 mmol) and (—)-α-phenylethylamine (5.4 g, 30 mmol) were dissolved in warm benzene (70 ml). The solution was allowed to stand for 24 hrs, then the salt separated was three times recrystallized from 96% ethanol (50 ml). Yield 3.8 g (55%). $[\alpha]_D^{25} = -39° \pm 1$ ($c = 1$, ethanol).

The salt (150 mg, 1 mmol) was hydrogenated in methanol (15 ml) in the presence of Pd/C. At the end of the reaction the solution was filtered, evaporated and the residue was applied to a Dowex 50W—X4 (H^+) ion exchange resin column. 10% Ammonium hydroxide eluent was used. The eluate was evaporated to dryness and the amino acid was crystallized at pH 5. Yield 150 mg (87%). R_f 0.6 (C). $[\alpha]_D^{25} = +31.0°$ ($c = 1.9$, water); $[\alpha]_D^{20} = +4.7°$ ($c = 1.9$, 5*N* hydrochloric acid). Specific rotation of L-phenylalanine (1): $[\alpha]_D^{22} = -34°$ ($c = 1—2$, water).

3. Acetyl-p-chloro-DL-phenylalanine

Acetyl-*p*-chloro-DL-phenylalanine was prepared from *p*-chloro-DL-phenylalanine (this compound was prepared by the Erlenmeyer azlactone synthesis) in glacial acetic acid with acetic anhydride [15]. Recrystallization was carried out from methanol/water, deviating from the procedure described. M.p. 180—183 °C. R_f 0.75 (A).

$C_{11}H_{12}ClNO_3$ (241.68). Calcd. C 54.65; H 5.01; N 5.79; Cl 14.66. Found C 54.95; H 5.02; N 5.76; Cl 14.82.

4. Acetyl-p-chloro-L-phenylalanine. L-(+)-*threo*-1-(p-nitrophenyl)-2-amino-1,3-propanediol

Acetyl-*p*-chloro-DL-phenylalanine (18.0 g, 74 mmoles) and L-(+)-*threo*-1-(*p*-nitrophenyl)-2-amino-1,3-propanediol (15.7 g, 74 mmol) were dissolved in hot anhydrous ethanol (100 ml). After the crystallization starting immediately 50 ml of ethanol was added to the warm mixture, which was then allowed to stand for 24 hrs. The salt separated was filtered off and crystallized from hot water (300 ml). In order to achieve the required degree of purity, crystallization was repeated 2—4 times, depending on the quality of the product obtained. Yield 12.8 g (75%). M.p. 212—214 °C. $[\alpha]_D^{22} = +52° \pm 3$ ($c = 1$, water).

5. Acetyl-p-chloro-L-phenylalanine

The salt of acetyl-*p*-chloro-L-phenylalanine (10.8 g, 30.5 mmol) prepared in the above manner was suspended in water (about 50 ml), then 1 *N* hydrochloric acid (120 ml) was added to it slowly. After standing for some hours, the acetyl-*p*-chloro-L-phenylalanine separated

was filtered off, washed with cold water and dried in vacuum. Yield 4.5 g (78%). M.p. 149—153 °C, R_f 0.75 (A). $[\alpha]_D^{22}$ +50° ± 1 ($c = 1$, ethanol).

$C_{11}H_{12}ClNO_3$ (241.68). Calcd. C 54.65; H 5.01; N 5.79; Cl 14.66. Found 54.43; H 5.08; N 5.71; Cl 14.80.

6. p-Chloro-L-phenylalanine

Acetyl-*p*-chloro-L-phenylalanine (4.4 g, 22 mmol) was refluxed in 3*N* hydrochloric acid for 2 hrs. The hot solution was treated with charcoal then filtered and the pH was adjust ed to 5 with concentrated ammonium hydroxide. The product separated was filtered ofafter cooling, washed with cold water and dried. Yield 2.8 g (68%). R_f 0.45 (A). $[\alpha]_D^{22} = -23°$f ±1 ($c = 0.5$, water); $[\alpha]_D^{22} = -3.5°$ ($c = 2$, 1*N* hydrochloric acid).

$C_9H_{10}ClNO_2$ (199.64). Calcd. C 44.64; H 5.12; N 6.95; Cl. 17.80. Found C 54.13; H 5.06; N 7.02; Cl 17.76.

7. L-Phenylalanine

p-Chloro-L-phenylalanine (400 mg, 2 mmol) was dissolved in a mixture of methanol containing potassium hydroxide (5 ml, 56 mg/ml) and water (10 ml), then it was hydrogenated in the presence of Pd/C (80 mg). After the consumption of the theoretically calculated amount of hydrogen (48 ml STP) the catalyst was filtered off, the solvent was evaporated and the product was charged to Dowex 50W—X4 (H^+) ion exchange column in 2*N* hydrochloric acid. 10% ammonium hydroxide was used for the elution, the amino acid was crystallized from hot water after concentration in vacuum. Yield 290 mg (86%). $R_f = 0.6$ (C); $R_f = 0.4$ (A). $[\alpha]_D^{22} = -33° \pm 2$ ($c = 1$, water).

8. L-Phenylalanine-(4-^{3}H)

p-Chloro-L-phenylalanine (40 mg, 0.2 mmol) was allowed to react with carrier-free tritium gas in methanol containing potassium hydroxide 1 ml, (43 mg/ml) in the presence of Pd/C. The amount of tritium gas consumed at 655 Torr was 9.5 Ci (3.46 ml STP).

The catalyst was filtered off, washed with hot water and the solution was evaporated in vacuo. The residue was dissolved in water and evaporated to dryness. This procedure was repeated twice again to remove the labile tritium. The residue was dissolved in 2N hydronhloric acid and the solution was applied to a Dowex 50W—X4 (H^+) ion exchange column. L-phenylalanine-(4-^{3}H) was eluted with 10% ammonium hydroxide. After evaporation of the eluent the product was dried. Yield 27 mg (81%). R_f 0.4 (A); R_f 0.6 (C).

Specific radioactivity of the product was 53.05 mCi/mg, its molar activity was 8.76 Ci/mmol. The radiochemical purity of the product was higher than 99%.

*

The authors thank Dr. Cs. Ömböly for the radioactivity measurements, Mr. A. Szabó for the technical assistance in the radioactive operations, Mrs. K. Barta and Mrs. Zs. Balogh for measuring the specific rotation and for the elemental analyses.

REFERENCES

[1] Birkofer, L., Hempel, K.: Chem Ber., **96,** 1373 (1963)
[2] Gerday, Ch., Verly, G.: J. Lab. Comp., **4,** 334 (1968)
[3] Winand, M., Bricteux-Gregoire, S., Verly, W. G.: Prep. and Bio-Med. Appl. of Lab. Molecules (Venice 1964) EURATOM 2200 e, p. 17
[4] Brundish, D. E., Elliot, D. F., Wade, R.: J. Lab. Comp., **7,** 473 (1971)
[5] Faulstich, H., Smith, H. O., Zobeley, S.: Liebigs Ann. Chem., 765 (1973)
[6] Tong, J. H., Petitclerc, C., D'lorio, A., Benoiton, N. L.: Can. J. Biochem., **49,** 877 (1971)
[7] Benoiton, N. L.: Can. J. Biochem., **50,** 151 (1972)
[8] Tagliamonte, A., Tagliamonte, P.: J. Pharm. Pharmacol., **25,** 101 (1973)
[9] Tagliamonte, A., Fratte, W.: J. Pharm. Pharmacol., **25,** 908 (1973)
[10] Tagliamonte, A., Tagliamonte, P., Gessa, F. L.: Nature, **230,** 244 (1971)

[11] REDMOND, D. E., MAAS, J. W., KLING, A.: Science, **174**, 428 (1971)
[12] BORZECKI, Z., KLEINROK, Z.: Dissert. Pharm. Pharmacol., **24**, 555 (1972)
[13] OVERBY, L. R., INGERSOLL, A. W.: J. Amer. Chem. Soc., **82**, 2067 (1960)
[14] MÁRTON, J., KOVÁCS, Á.: Acta Chim. (Budapest), **73**, 11 (1972)
[15] GREENSTEIN, J. P., WINITZ, M.: Chemistry of the Amino Acids, Vol. III. New York, London 1971, p. 1831.
[16] *Ibid.* Vol. III, p. 2156

Judit KOVÁCS; 1221 Budapest, Pentz Károly u. 5.
István TEPLÁN; 1051 Budapest, Münnich F. u. 7.
Imre MEZŐ; 1121 Budapest, Puskin u. 9. Hungary.

RECENSIONES

NONHEBEL: *Chemical Engineering in Practice*

Wykeham Publications Ltd., London 1973

In the first chapter, the various fields of chemical engineering activity are surveyed. Well-chosen statistical data (reviewing the financial figures for 20 of the 30 largest companies in the world, and the structure of the chemical industry of the United Kingdom) help outline the background of this activity.

In the second chapter (Chemical engineering operations) the fitting of the steps in industrial processes is demonstrated on some simple illustrative process diagrams as models, and indicates the frequency of application of the major chemical industrial operations. It deals with the features of catalytic processes separately.

Chapter III (Machines) described the characteristic types of machines required for "mechanical operations", more accurately, for their accomplishment (grinding machines, mills, sieves, filters, centrifuges, separation devices, cyclones, scrubbers, driers).

Chapter IV (Apparatus) reviews apparatus specific in chemical industry, such as reactors, evaporators, crystallizers, rectifiers, absorption, adsorption, extraction and ion-exchanger devices, and the apparatus designed for operation at high and very low temperatures. Beside the conventional procedures the most modern ones are described, too, thus, for example, the electrophoretic and reversed osmosis procedures are also included in the separating operations.

In Chapter V (Electrochemical operations) the operations conventionally not practised in the "kitchen art" are dealt with: acetylene production in arch, production of calcium carbide, electrolysis of brine, production of fresh water based on electrodialysis of sea water, and the performance of fuel cells is outlined, too.

The topics of Chapter VI (Biochemical processes) are, beside the classical fermentation industry, the major up-to-date preservation processes in food industry and the production of synthetic proteins. The problem of waste water treatment is also included here.

Chapter VII (Design of complete plants) proves to be the most interesting for the reader. Here the design stages of chemical industrial plants are followed, from the definition of the problem to the evaluation of the variations and the analysis of the operational and capital costs. The problems of safety measures are also treated here. The applicability of computers is another interesting topics; an unambiguously positive opinion is expressed regarding the design period. The opinions are already not so unanimous in the problem of on-line control dealt with today so often. While reviewing the advantages provided, the negative features are also indicated, mentioning even such less emphasized questions as that the operating personnel may forget the technology.

In Chapters VIII and IX (Case histories in chemical engineering I—II) the author described first the synthesis of ammonia starting from the coke-based synthesis production to the hydrocarbon decomposition (illustrated on naphtha reforming) processes, together with the modern town-gas production problems.

In the second part (The launching of a new man-made fibre), the development and technology of the production of polyester fibres are discussed.

The topics of Chapter X (The chemical engineer as manager) are the problems of management in chemical industry, primarily from technological and human points of view, including the problems of foremen, plant managers, up to the managing of great enterprises.

Chapter XI (Research and development) is devoted to the stages in technical development, and it deals in detail with the utilization of inventions, further development of existing procedures, and organization problems in reseerch.

Chapter XII (Education and careers) treats education in chemical industrial knowledge and attachment to the industrial life, and further studies. Perhaps this is the only chapter closely related to the conditions in the United Kingdom; in spite of this, it will probably be interesting for readers in other countries, too.

The purpose of the book was to provide a comprehensive picture of the engineering problems for future chemical engineers. Implicitly it also calls attention to the importance and usefulness of the individual disciplines to be studied.

It is a strikingly readable, small book providing a multilateral picture of chemical engineering operations; the problems in natural sciences, technology and economics appear together in the whole book.

Although the book is written for undergraduates, it can usefully be studied by teachers and managers who wish to obtain a general view of chemical industrial science, as well as interested researchers not engaged in technology, but being in close co-operation with the chemical industry.

K. MATOLCSY

Recent Results in Chemistry, Vol. 18

Akadémiai Kiadó, Budapest, 1974

Volume 18 of "Recent Results in Chemistry" ("A kémia újabb eredményei"), published in 1975 by Akadémiai Kiadó, comprises two treatises dealing with the investigation of surface phenomena.

The first of these is a study of 156 pages, written by Géza SCHAY and Lajos György NAGY on "Adsorption of liquid mixtures on liquid/solid and liquid/ vapour interfaces", with 315 references and 23 figures. The paper deals essentially with the adsorption of non-electrolyte liquid mixtures. Systems are investigated, for which physical exchange adsorption is to be expected. They start in their considerations from excess adsorption, and assuming a unimolecular adsorption layer, calculate from it the quantity of the preferentially adsorbed component at the interface. The authors discuss also the methods of determination of the surface excess, which make possible the plotting of the excess isotherm over the total composition range. This is in essence a mixture isotherm, representing the surface quantity of the preferentially adsorbed component at the ever completely covered interface. The authors of international renown for their activity in this field, summarize also the results of their own work in this treatise. They present the types of excess adsorption isotherms of liquid mixtures and interpreted by them. The phenomena are theoretically interpreted on the basis of phenomenological thermodynamics, which, in the exact form shown and consistent expression, is suitable for the characterization of adsorption, proceeding both on liquid/solid and vapour/liquid interfaces. Out of the practical aspects of the results the fact should be emphasized that the determination of excess isotherms offers in this way a new possibility for the determination of adsorption capacity, the knowledge of which is indispensable *e. g.* in the adsorptive separation of non-electrolyte liquids.

The second study of the volume is "Some recent methods of surface investigation" ("A felülvizsgálat néhány újabb módszere") written by Lajos György NAGY, János Soós and Lajos FÓTI, a work of 136 pages, with 236 references, further complementing bibliography and 87 figures. The authors give an excellent survey of the most modern methods. Their aim is not a review of all the methods of investigation of solid surfaces, but they wish to make acquainted the reader only with those methods, which found application very recently, and are not yet introduced in Hungary, with the exception of some special cases. The scanning electron microscopic investon igatiof the micromorphology of surfaces is illustrated by several pictures. Low-energy electron diffraction for the determination of surface structure and atomic arrangement is discussed, but regrettably a discussion of modern field emission microscopy has been omitted. On the other hand, methods for the determination of the element composition of surface layers are treated with a claim to completeness. Thus, Auger-spectroscopy, electron micro probe spectroscopy and the application of alpha-particle scattering and of ion-microprobe spectroscopy are discussed, which sometimes give also information on the bond conditions of the atoms. They deal further with Measurement and Evaluation of Surfaces by Evaporative Rate Analysis (MESERAN), which makes possible the examination of the chemical character of surfaces. For each method of investigation, the basic physical phenomena, the working principle of the instruments are briefly described, and their possible applications are illustrated by several examples. The high-level mode of discussion, which nevertheless is easy to understand, testifies the careful work of the authors.

D. KALLÓ

Electrophoresis and Isoelectric Focusing in Polyacrylamide Gel

Advances of Methods and Theories, Biochemical and Clinical Applications

Editors R. C. Allen, H. R. Maurer. Walter de Gruyter, Berlin, New York, 1974 pp. 316

30 papers written by most competent authors, (grouped in 9 chapters) presented at the first small conference of the "Blue Fingers" — experts of electrophoresis and isoelectric focusing in polyacrylamide gel.

The "Blue Fingers" are the laboratory bench experts — whose fingers are usually stained — while the "White Fingers" are the people who know the techniques just by hearsay, and their main field of interest is theory.

PAGE and PAGIF vividly investigated at present arrived at a stage where standardization is a prerequisite for routine work in biochemistry and clinical chemistry, because without standardization it is impossible compare results between laboratories — often using past and present methods.

Newly devised methods were developed, and the theoretical backgrounds of these methods has laid. The aim of the conference wes to learn more abont each others' experiences.

The extent of single chapters are 20—30 pages, with the exception of Chapter 2.

Polyacrylamide Gel Electrophoresis: Theory and Practice of Optimalization and Standardization.

— 90 pages and Chapter 9. Clinical Applications

— 40 pages.

In the opinion of the reviewer, theory and practice are well balanced throughout this book, and the most important topics got adequate spaces.

Although the book is carefully edited and very pleasingly presented some misprints remained in the text.

The book is to be welcomed as a good summary of the present state and knowledge of PAGE and PAGIF, a copy should be available not only in the biochemical research laboratories, but in the routine clinical laboratories as well.

M. PÁRKÁNY

Peter A. ROCK, George A. GERHOLD: *Chemistry.* Principles and Applications

W. B. Saunders Company, Philadelphia — London — Toronto 1974.
716 pages + 24 pages Appendix + 10 pages Index.

Though it is well known that the system of higher education in the United States is rather different from the systems developed in general in Europe, it is nevertheless thought necessary to emphasize this circumstance. Indeed, this explains that the fundamental knowledge in natural sciences must be acquired in special pre-schools in so-called colleges, prior to studies at the university in some special branches. Accordingly, the basic knowledge in chemistry must be acquired in the college by everybody, who later wishes to a tend more advanced courses in a certain branch of chemistry at university level.

The present work is an attempt for a textbook, which summarizes basic but not elementary knowledges in chemistry, without consideration of the special field of practice or research, in which the student learning from this work wishes or will be later active.

The greatest problem of the authors was to decide, what to include and in which extent and depth in the textbook.

That this statement is not only a presumption of the referee, but has been the actual concern of the authors, becomes indirectly clear from the preface, which informs us the opinion of how many experts was asked with respect to the whole work or certain parts of it.

The referee has the following opinion: the authors of the textbook took the view that theory is incomparably more important than practical knowledge, and thus, out of the whole extent of the textbook inorganic chemistry covers only 73 pages (10%), organic chemistry 29

pages (4%), biochemistry 18 pages (2.5%) and nuclear chemistry 9 pages (1.2%), that is to say, the descriptive part giving the practical facts, amounts only to 17.7%, at the end of the book. However, it is worth-while to wonder how can a student understand *e.g.* the theory of acids and bases, who wishes to acquire basic knowledge of chemistry from such book, if he does not possess yet practically any knowledge on any kind of acid or base.

However, the conceptual opinion of the referee in this matter is in no way directed specifically against the textbook in question, because the rigorous separation of theory and practice is an old tradition also in the European textbooks.

In the composing of the general chemical chapters the authors did perform a very honurable work. These chapters are written indeed in accordance with the most modern concepts, and the referee thinks that even in the present period of the rapid development of sciences the book can be used to good advantage at least for 10 years, without becoming outdated.

The authors promise in the preface to attempt to build the new knowledge logically and didactically on materials already presented. It must be established objectively that this promise is actually fulfilled, though the referee found a few statements, which do not lean on preliminaries. It must be stressed, however, that this is not characteristic of the work as a whole. The selection, order and extent of the chapters of the textbook is rather instructive and, therefore, is given in the following:

I. Quantum Chemistry
The atom (16 pages)
Atomic spectra and atomic structure (47 pages)
Molecules (17 pages)
Modern treatment of chemical bonding (42 pages)

II. States and Properties of Matter
Gases (27 pages)
Crystals (30 pages)
Stoichiometry and chemical reactions (14 pages)
Liquids and solutions (12 pages)

III. Thermodynamics
Principles of classical thermodynamics (42 pages)
Phase equilibria (20 pages)
Chemical equilibrium. Part I. Principles (27 pages)
Chemical equilibrium. Part II. Applications to homogenous equilibria (35 pages)
Chemical equilibrium. Part III. Applications to heterogenous equilibria (28 pages)
Electrochemistry (38 pages)

IV. Chemical Kinetics
Chemical kinetics. Part I. The reaction-rate law (27 pages)
Chemical kinetics. Part II. The reaction mechanism (29 pages)

V. Chemistry of the Elements
The A-group metals (16 pages)
The metalloids (16 pages)
The non-metals (37 pages)
Coordination chemistry of the transition metals (57 pages)
Organic chemistry (29 pages)
Biochemistry (18 pages)
Nuclear chemistry (9 pages).

For a better understanding of the subject discussed, each sub-chapter closes with exercises to be solved. The correct solutions are given at the end of the book. Similarly, the nice get-up of the textbook, the neat and instructive use of the figures and the careful compilation of the Appendixes deserve credit.

Appendix 1
The chemical atomic weights, 1961 (1 page)
Appendix 2
Base 10 logarithms (4 digit) (2 pages)
Appendix 3
Mathematical operations (5 pages)
Appendix 4
SI units, fundamental constants and conversion factors (7 pages)

Appendix 5
Thermodynamic data (2 pages)
Appendix 6
Answers to selected problems (6 pages)
Appendix 7
Ionic radii in Ångstroms (1 page)
Index (10 pages).

The referee cannot leave unsaid his opinion that it would be worth-while to publish the textbook in Hungarian.

D. SZABÓ

INDEX

ANALYTICAL CHEMISTRY – ANALYTISCHE CHEMIE – АНАЛИТИЧЕСКАЯ ХИМИЯ

SÁMSONI, Z. and NAGY, Z.: Objective Method for Measuring the Length of Wedge-Shaped Spectrum Lines 1

PHYSICAL AND INORGANIC CHEMISTRY – PHYSIKALISCHE UND ANORGANISCHE CHEMIE – ФИЗИЧЕСКАЯ И НЕОРГАНИЧЕСКАЯ ХИМИЯ

BEYER, H., PAPP, J. und KALLÓ, D.: Irreversible Strukturveränderungen von H-Faujasit, H-Mordenit und H-Klinoptilolit durch thermische Behandlung und Einwirkung von Wasser (Irreversible Structural Changes of H-Faujasite, H-Mordenite and H-Klinoptilolite by Thermal Treatment and the Action of Water) 7

BEYER, H.: Beiträge zur Kenntnis der Krackreaktionen, II. Kinetik der katalytischen Krackung von Propan sowie *n*- und *i*-Butan an H-Klinoptilolit (Contribution to the Knowledge of Cracking Reactions, II. Kinetics of the Catalytic Cracking of Propane further of *n*- and *iso*-Butane on H-Clinoptilolite) 25

RATKOVICS, F. and LÁSZLÓ-PARRAGI, M.: Properties of Alcohol–Amine Mixtures, VII. Conductivity of *n*-Butylamine–Alcohol Mixtures 45

CYVIN, N., HARGITTAI, M. and CYVIN, J.: On the Ring Puckering of the Trimeric Tungsten Trioxide Molecule 55

ORGANIC CHEMISTRY – ORGANISCHE CHEMIE – ОРГАНИЧЕСКАЯ ХИМИЯ

NÁNÁSI, P. and LIPTÁK, A.: Carbohydrate Methyl Ethers, V. Synthesis of Phenyl-β-D-glucopyranoside Derivatives Partially Methylated on their Sugar Moiety. Preparation of 4,6-di-O-, 2,4,6-tri-O- and 3,4,6-tri-O-methyl-D-glucose 63

ZSADON, B., OTTA, K. H. and TÉTÉNYI, P.: Minor Alkaloids from the Seeds of *Amsonia Tabernaemontana*: (+)-1,2-Dehydroaspidospermidine, (—)-Tetrahydroalstonine and (—)-Quebrachamine 71

SZTARICSKAI, F., BOGNÁR, R. and PUSKÁS, M. M.: Structural Investigation of the Antibiotic Ristomycin A. Chemical Structure of the Oligosaccharide Part of Ristomycin A 75

SHAMS EL-DINE, SH. A. and CLAUDER, O.: Derivatives of 1,3,4-Thiadiazole as Potential Schistosomicides 85

DÓRA-HORVÁTH, K. and CLAUDER, O.: Alkaloids Containing the Indolo [2,3-c]-quinazolino [3,2-a] pyridine Skeleton, III 3,14-Dihydrorutecarpine 93

LÉVAI, A., LIPTÁK, A., PINTÉR, I. and SNATZKE, G.: Circular Dichroism, LXVI. Chiroptical Properties of some Mono- and Polysubstituted Phenyl Glycosides 99

KOVÁCS, J., TEPLÁN, I. and MEZŐ, I.: Labelled Amino Acids and their Derivatives, V. Resolution of *p*-Chloro-DL-phenylalanine. Preparation of L-phenylalanine-(4-^{3}H) from *p*-Chloro-L-phenylalanine 109

RECENSIONES 115

Printed in Hungary

A kiadásért felel az Akadémiai Kiadó igazgatója. Műszaki szerkesztő: Zacsik Annamária

A kézirat nyomdába érkezett: 1974. X. 10. — Terjedelem: 11,2 (A/5) ív, 61 ábra, 1 melléklet

75.976 Akadémiai Nyomda, Budapest — Felelős vezető: Bernát György

ACTA CHIMICA
ТОМ 84—ВЫП. 1

РЕЗЮМЕ

Новый объективный метод определения длины клинообразных спектральных полос

З. ШАМШОНИ и З. НАДЬ

Был разработан новый способ и прибор для точного измерения длины т. наз., «клинообразных» спектральных полос.

Описанный прибор позволяет более точное, объективное измерение длины спектральных полос. Прибор содержит два фототранзистора с дифференциальным подключением. Проводя линию до конца перед детектором, конечная точка ее может быть определена с помощью нулевого прибора, присоединенного к фототранзисторам. Один из транзисторов чувствителен к свету актуального почернения измеряемой спектральной полосы, а другой к свету почернения фона той части спектра, где не наблюдается поглащения. Конец полосы прибор сигнализирует возвращением в нулевую позицию. Степень смещения отсчитывается непосредственно, с точностью 0,1 мм, с помощью дигитального счетчика. Ошибка измерения длины полосы в 13—15% может быть уменьшена до 7—9%.

Необратимые структурные превращения в Н-фауязите, Н-мордените и Н-клиноптилолите, протекающие под действием термообработки и под влиянием воды

Х. БЕЙЕР, Я. ПАПП и Д. КАЛЛО

Н- и дегидроксилированные цеолиты, полученные термообработкой фауязита, морденита и клиноптилолита в NH_3-форме, после регидратации, проведенной в различных условиях, были подвергнуты исследованиям с помощью дифференциалтермоаналитического, термогравиметрического и, частично, рентгеноаналитического методов. Было установлено, что в случае всех трех цеолитов процесс дегидроксилирования, протекающий с отщеплением воды, является необратимым и приводит к некоторой перестройке в решетке. Дегидроксилированные производные — особенно в случае клиноптилолита — являются термически относительно нестабильными. Кислые центры Н-фауязита при комнатной температуре и под влиянием воды превращаются в такие продукты, которые, хотя и продолжают обладать структурой фауязита, однако, становятся термически весьма нестабильными. Эта реакция, в которой алюминий кристаллической решетки растворяется под влиянием ионов H_3O^+, образующихся из протонов Н-формы, однако, не наблюдается в случае Н-морденита и Н-клиноптилолита.

О некоторых новых данных реакции крекинга, II

Кинематика каталитического крекинга пропана, н- и изобутана на Н-клиноптилолите

Х. БЕЙЕР

Исследование кинетики каталитического крекинга парафинов является весьма проблематичным, т. к. олефины, образующиеся в качестве первичных продуктов реакции, вступают в многочисленные последовательные реакции, что приводит к усложнению всего механизма реакции. Эти затруднения были преодолены таким образом, что исследования проводились в циркуляционном реакторе и образующиеся олефины непрерывно удалялись спомощью селективной абсорбции из газовой фазы циркуляционной системы.

В качестве катализатора был использован минерал, содержащий 61% кристаллита клиноптилолита. Клиноптилолит, превращенный с помощью ионного обмена в форму NH_4, подвергался предварительной термической обработке в интервале температур 460–690°C полученный H-клиноптилолит с различной степенью дегидроксилирования подвергался дальнейшим исследованиям. С возрастанием дегидроксилирования кристаллиты клиноптилолита теряют свою кристалличность, в то время как «вторичное строение» минерала не изменяется.

Крекинг и дегидрирование изученных парафинов, всегда независимо от температуры предварительной обработки катализатора, протекает по первому порядку. Кажущиеся энергии активации первичных реакций не зависят от температуры предварительной обработки и почти равны для данного реагента. Активности катализатора в крекинге и дегидрировании с повышением температуры обработки описываются кривыми с максимумом при 500°C. При температурах выше этого максимума селективность сдвигается в пользу реакции дегидрирования. Отношение скоростей расщепления 1- и 2-связей н-бутана не зависит от температуры предварительной обработки. Катализатор обладает стерической селективностью к н-парафинам.

На основе экспериментальных данных было заключено, что реакции дегидрирования и крекинга протекают через общий комплекс на поверхности, который образуется за счет хемисорбции реагирующего вещества на кислых центрах Льюиса, образующихся, в свою очередь, при дегидроксилировании. Однако, в расщеплении связи C—C участие принимает и центр Брёнштеда, находящийся в соседстве с центром Льюиса.

Свойства смесей спирт-амин, VII

Электропроводность смесей н-бутиламин — спирт

Ф. РАТКОВИЧ и А. ЛАСЛО

Удельная проводимость смесей, содержащих в качестве одного из компонентов н-бутиламин и в качестве другого компонента метанол, этанол, 1-пропанол или 1-бутанол, была исследована в зависимости от состава при температурах 0 и 20°C. Проводимость этих смесей имеет максимум в интервале молярных долей амина 0,05—0,15. Было найдено, что среди спиртово-аминных ассоциатов, образующихся в смеси, диссоциация тех, которые содержит на одну молекулу амина несколько молекул спирта, является важной с точки зрения электропроводности. При повышении температуры удельная проводимость увеличивается в смесях, содержащих небольшие количества спирта. Эти различия интерпретировались на основе различия между ассоциационными характеристиками спиртов и аминов, полагая механизм проводимости, предложенный впервые Гротусом.

Деформация кольца тримерных молекул трехокиси вольфрама

Б. Н. СИВИН, М. ХАРГИТТАИ, С. Й. СИВИН и И. ХАРГИТТАИ

Величины $K = [\langle(\Delta x^2)\rangle + \langle(\Delta y^2)\rangle]$ (2r), рассчитанные из спектроскопических данных весьма приближенного характера, указывают на то, что эффект сокращения не является причиной существующей деформации кольца молекулы W_3O_9, обнаруженной с помощью электронографического анализа.

Метиловые эфиры углеводов, V

Синтез частично метилированных на сахарном звене производных фенил β-O-глюкопиранозида; получение 4,6-ди-O-, 2,4,6-три-O- и 3,4,6-три-O-метил-D-глюкозы

П. НАНАШИ и А. ЛИПТАК

Был осуществлен синтез фенил 2-O-(*4*), 3-O- (*5*), 4-O-(*6*), 4,6-ди-O- (*9*), 2,4,6-три-O- (*17*) и 3,4,6-три-O-метил-β-D-глюкопиранозидов (*18*). Соединения *4*, *5* и *6* были получены, исходя из соответствующих парциально метилированных сахарных ацетатов за счет

омыления методом Хельферика. Синтез соединений *9*, *17* и *18* был осуществлен путем кислого гидролиза бензилиденовых производных, замещенных на C_2 и C_3 углеродных атомах, с дальнейшим метилированием и дебензилированием за счет каталитического гидрирования. Гидролиз соединений *9*, *17* и *18* с хорошим выходом дает 4,6-ди-О- (*19*) 2,3,6-три-О- (*20*) и 3,4,6-три-О-метил-D-глюкозы (*21*).

Побочные алкалоиды из зерен Amsonia tabernaemontana Walt: (+)-1,2-дигидроаспидоспермидин, (−)-тетрагидроалстонин и (−)-квебрахамин

Б. ЖАДОН, К. Х. ОТТА и П. ТЕТЕНИ

Наряду с основным алкалоидом спелых зерен *Amsonia tabernaemontana* таберсонином (I) были изолированы следующие побочные алкалоиды: (+)-1,2-дигидроаспидоспермидин (III) (134, мг(кг), (−)-тетрагидроалстонин (II) (125 мг/кг), (−)-квебрахамин (IV) (12 мг/кг).

В начале созревания плоды содержат мало таберсонина и наряду с ним (+)-винкадифформин (V). Последний во время развития и созревания плодов разлагается до (+)-1,2-дигидроаспидоспермидина. Одновременно с этим происходит значительное возрастание концентрации таберсонина.

Структурное исследование антибиотика ристомицина А

Химическое строение олигосахаридной части ристомицина А

Ф. СТАРИЧКАИ, Р. БОГНАР и М. М. ПУШКАШ

Гликозидный антибиотик ристомицин А, полученный из *Proactiomyces fructuferi var. ristomycini*, содержит одну молекулу D-маннозы и тетрасахаридную боковую цепочку, присоединенную отдельно к агликоновой части. Тетрасахарид содержит звенья D-глюкозы, D-маннозы, L-рамнозы и D-арабинозы, связанных друг с другом согласно структуре V.

Производные 1,3,4-тиациазоля как возможные скистосомициды

Ш. А. ШАМО ЭЛЬ-ДАЙН и О. КЛАУДЕР

Некоторые производные 1,3,4-тиадиазоля были синтезированы на изостерической основе по аналогии с соответствующими антискистосомальными тиазольными соединениями.

Алкалоиды с каркасом индоло[2,3-с) хиназолино[3,2-а)пиридина, III

3,14-Дигидрорутекарпин

К. ХОРВАТ-ДОРА и О. КЛАУДЕР

3,14-Дигидрорутекарпин (*3*) был получен из триптамина (*4*) ацилированием с помощью ангидрида изатокислоты (*5*) с дальнейшей циклизацией за счет этилового эфира ортомуравьиной кислоты. Окислением соединения *3* был получен рутекарпин (*8*), а метилированием на N_{14} — эводиамин (*9*). Из 3,14-дигидрорутекарпина были получены также рутекарпан (*10*) и рутекарпен (*11*).

Циркулярный дихроизм, XVI

Хироптические свойства моно- и полизамещенных фенилгликозидов

А. ЛЕВАИ, А. ЛИПТАК, И. ПИНТЕР и Г. СНАГЦКЕ

В противоположность соединениям такого типа, в которых хиральный центр присоединяется к бензольному кольцу через атом углерода, в случае фенилгликозидов заместители ароматического кольца — поскольку они не обладают сильным эффектом возмущения — не оказывают значительного влияния на знак эффекта Коттона. ЦД полос $^1B_{2u}$ и $^1B_{1u}$ является отрицательным в случае β- и положительным в случае α-аномеров. Знак определенных полос ЦД ортозамещенных соединений, однако, может быть изменен и за счет стерических и/или электростатических эффектов.

Меченые аминокислоты и их производные, V

Разделение п-хлор-ДL-фенилаланина. Получение L-фенилаланина-4-H^3 из п-хлор-L-фенилаланина

Ю. КОВАЧ, И. ТЕПЛАН и И. МЕЗЁ

Ацетил-п-хлор-DL-фенилаланин был разделен с помощью L-(+)-трео-1-(п-нитрофенил)-2-аминопропандиола-1,3. Из п-хлор-L-фенилаланина с помощью каталитического гидрирования был приготовлен L-фенилаланин, а с помощью каталитического тритирования был получен L-фенилаланин-(4-H^3) с молярной активностью 8,76 Ci/ммоль.

12 S

According to international book reviews the series
ABSORPTION SPECTRA IN THE ULTRAVIOLET AND VISIBLE REGION
started in 1959 – is highly useful in both structure research and chemical analysis.
Our Publishing House now offers you a new series on *infrared spectra!*

ABSORPTION SPECTRA IN THE INFRARED REGION

Editor of the series L. LÁNG
Introductory volume written by S. HOLLY and P. SOHÁR

Though the scientific literature has several series dealing with the same field, naturally none of them strives for completeness, and overlapping is very small. The present series is concerned with very recent spectra, including those which are not given in the original papers. The *Introductory Volume* gives a detailed discussion of the characteristic frequencies affording ample guidance for the practical spectroscopist. The most important technical information is also included.

In English . Approx. 320 pages per volume
17 × 23 cm . Loose-leaf cloth binders

AKADÉMIAI KIADÓ
Budapest

BUTTERWORTH LIMITED
London

A co-edition, — distributed in the socialist countries by *Kultura*, H-1389 Budapest P. O. B. 149; in all other countries by *Butterworth Limited*, London

ABSORPTION SPECTRA IN THE ULTRAVIOLET AND VISIBLE REGION

Series edited by L. LÁNG

According to international book reviews, this series is highly useful in both structure research and chemical analysis. This applies especially to problems of analytical character or structure determination encountered in the pharmaceutical, dye and other industries, i.e. in organic chemical industry in general. A great advantage of this collection is that the spectra published may, in many cases, directly be used for solving the particular problems in question.

The series dealing with *ultraviolet and visible spectra* was started by the Publishing House of the Hungarian Academy of Sciences in 1959, and by now the project has got as far as Vol. 18. The editors invite the users of the collection to contribute to the success of this work by submitting for publication spectra of new compounds.

Each volume contains about 400 pages spectra graphs and tables of about 190 compounds + indexes.

Cumulative index: I–V, VI–X, X–XV

AKADÉMIAI KIADÓ
Budapest

ACADEMIC PRESS
New York

The whole series is a co-edition, – distributed on the American Continent by ACADEMIC PRESS, New York, in all other countries by KULTURA, H-1389 Budapest, P. O. B. 149

JOURNAL OF THERMAL ANALYSIS

An international forum for communications on thermal investigations

Journal of THERMAL ANALYSIS has an international Editorial Board, the members of which are distinguished specialists from all over the world.

AIMS AND SCOPE

The main subjects covered are: thermogravimetry, derivative thermogravimetry, differential thermal analysis, dilatometry, differential scanning calorimetry, thermometry, evolved gas detection, evolved gas analysis, multiple techniques and miscellaneous thermal methods (including the thermal method with various instrumental techniques), instrumentation for the thermal method. Papers dealing with these subjects are published in the following sections: Original Research Papers, Short Communications, Special Reviews, Bibliography Section, Modern Instruments. The Special Reviews section is reserved for papers that have been published in greater detail in some journal for a special branch of scientific field or industry.

Papers submitted to the journal may deal with any field of chemistry, metallurgy or mineralogy, e.g. they may deal with inorganic, organic or polymeric materials and they may cover biochemical, mineralogical or metallurgical applications.

Journal of THERMAL ANALYSIS is published bimonthly comprising about 720 pages per year. Size: 17×25 cm. Subscription rate per volume: US $32.00

Journal of THERMAL ANALYSIS is published jointly by

AKADÉMIAI KIADÓ
Budapest

HEYDEN & SON LIMITED
London

RADIOCHEMICAL AND RADIOANALYTICAL LETTERS

An International Journal for RAPID Communication in Radiochemistry and Radioanalytical Chemistry

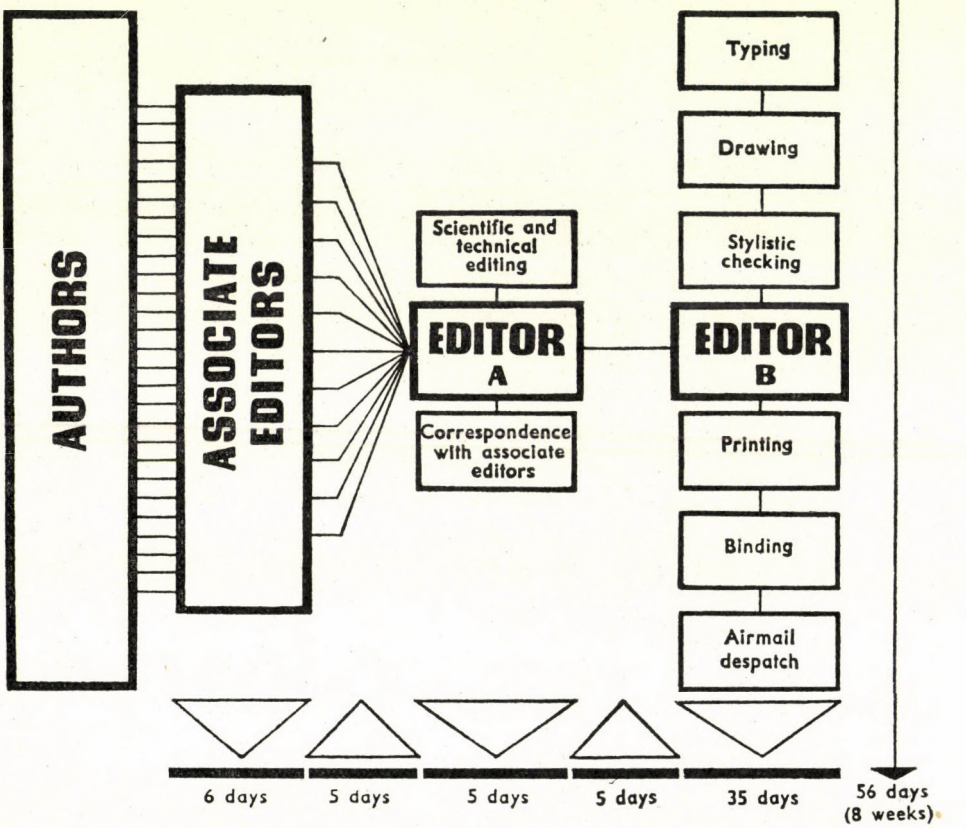

ELSEVIER SEQUOIA S.A.
LAUSANNE

AKADÉMIAI KIADÓ
BUDAPEST

JOURNAL OF RADIOANALYTICAL CHEMISTRY

International journal dealing with all aspects of nuclear analytical methods

Journal of Radioanalytical Chemistry has an international Editorial Board, whose members are distinguished specialists from all parts of the world – from Moscow ot San Diego, from Prague to Tokyo.

The main subjects covered are:

Activation analysis
Radiometric analysis
Radioreagent analysis
Radiometric titration
Isotope dilution analysis
Beta, gamma X-ray and neutron absorption and backscattering
Analytical separations involving radionuclides
Instrumentation and automation for radioanalytical chemistry

Journal of Radioanalytical Chemistry provides the reader with important and up-to-date information on research being carried out all over the world. Data and Bibliography Sections and a section entitled Laboratory of the Issue help to serve this purpose.

Journal of Radioanalytical Chemistry appears generally in three or four volumes per year of some 480 to 500 pages each, published in several issues in English, French or German. Size: 17 × 25 cm. Subscription rates per volume: US $32.00

Journal of Radioanalytical Chemistry is published jointly by

AKADÉMIAI KIADÓ
Budapest

ELSEVIER SEQUOIA
Lausanne

ACTA ALIMENTARIA

ACADEMIAE SCIENTIARUM HUNGARICAE

publishes original papers in the field of food science and technology (physico-chemistry, chemistry, analysis, biology, microbiology, enzymology, engineering, automation and economics related to fundamental principles of the production, preparation, preservation, packaging and examination of foods) in English.

Contributions to ACTA ALIMENTARIA are regularly abstracted or indexed in all reference journals.

ACTA ALIMENTARIA is as a rule a quarterly. Four issues make up a volume of some 400 to 500 pages yearly.
Subscription rate per volume: US $32.00

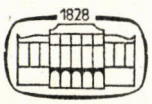

AKADÉMIAI KIADÓ
Publishing House of the
Hungarian Academy of Sciences
BUDAPEST

AKADÉMIAI KIADÓ, H-1363 Budapest, P.O.B. 24

☐ Please enter my/our subscription for ACTA ALIMENTARIA for one volume

☐ Please enter a standing order for ACTA ALIMENTARIA, beginning with

DATE . . . . . .

☐ Please send a specimen-copy free of charge

NAME . . . . . .

ADDRESS . . . . . .

The Acta Chimica publish papers on chemistry, in English, German, French and Russian.

The Acta Chimica appear in volumes consisting of four parts of varying size, 4 volumes being published a year.

Manuscripts should be addressed to

Acta Chimica
Budapest 112/91 Műegyetem

Correspondence with the editors should be sent to the same address.

The rate of subscription is $ 32.00 a volume.

Orders may be placed with "*Kultúra*" Foreign Trade Company for Books and Newspapers (1389 Budapest 62, P. O. B. 149. Account No. 218 10990) or with representatives abroad.

Les Acta Chimica paraissent en français, allemand, anglais et russe et publient des mémoires du domaine des sciences chimiques.

Les Acta Chimica sont publiés sous forme de fascicules. Quatre fascicules seront réunis en un volume (4 volumes par an).

On est prié d'envoyer les manuscrits destinés à la rédaction à l'adresse suivante:

Acta Chimica
Budapest 112/91 Műegyetem

Toute correspondance doit être envoyée à cette même adresse.

Le prix de l'abonnement est de $ 32,00 par volume.

On peut s'abonner à l'Entreprise pour le Commerce Extérieur de Livres et Journaux «*Kultúra*» (1389 Budapest 62, P.O.B. 149 Compte-courant No. 218 10990) ou à l'étranger chez tous les représentants ou dépositaires.

«*Acta Chimica*» издают трактаты из области химической науки на русском, французском, английском и немецком языках.

«*Acta Chimica*» выходят отдельными выпусками разного объема. 4 выпуска составляют один том. 4 тома публикуются в год.

Предназначенные для публикации рукописи следует направлять по адресу:

Acta Chimica
Budapest 112/91 Műegyetem

По этому же адресу направлять всякую корреспонденцию для редакции.

Подписная цена – $ 32,00 за том.

Заказы принимает предприятие по внешней торговле книг и газет «*Kultúra*» (1389 Budapest 62, P. O. B. 149. Текущий счет № 218 10990) или его заграничные представительства и уполномоченные.

Reviews of the Hungarian Academy of Sciences are obtainable at the following addresses

ALBANIA

Drejtorija Qëndrone e Párhapjes dhe Propagandimit të Librit
Kruga Konferenca e Pazes
Tirana

AUSTRALIA

A. Keesing
Box 4886, GPO
Sydney

AUSTRIA

GLOBUS
Höchstädtplatz 3
A-1200 Wien XX

BELGIUM

Office International de Librairie
30, Avenue Marnix
Bruxelles 5
Du Monde Entier
162, Rue du Midi
1000 Bruxelles

BULGARIA

HEMUS
11 pl Slaveikov
Sofia

CANADA

Pannonia Books
2, Spadina Road
Toronto 4, Ont.

CHINA

Waiwen Shudian
Peking
P. O. B. 88

CZECHOSLOVAKIA

Artia
Ve Smečkách 30
Praha 2
Poštovní Novinová Služba
Dovoz tisku
Vinohradská 46
Praha 2
Mad'arská Kultura
Václavské nám. 2
Praha 1
SLOVART A. G.
Gorkého
Bratislava

DENMARK

Ejnar Munksgaard
Nörregade 6
Copenhagen

FINLAND

Akateeminen Kirjakauppa
Keskuskatu 2
Helsinki

FRANCE

Office International de Documentation et Librairie
48, rue Gay-Lussac
Paris 5

GERMAN DEMOCRATIC REPUBLIC

Deutscher Buch-Export und Import
Leninstraße 16
Leipzig 701
Zeitungsvertriebsamt
Fruchtstraße 3—4
1004 Berlin

GERMAN FEDERAL REPUBLIC

Kunst und Wissen
Erich Bieber
Postfach 46
7 Stuttgart S.

GREAT BRITAIN

Blackwell's Periodicals
Oxenford House
Magdalen Street
Oxford
Collet's Subscription Import Department
Dennington Estate
Wellingsborough, Northants.
Robert Maxwell and Co. Ltd.
4—5 Fitzroy Square
London W. 1

HOLLAND

Swetz and Zeitlinger
Keizersgracht 471—487
Amsterdam C.
Martinus Nijhof
Lange Voorhout 9
The Hague

INDIA

Hind Book House
66 Babar Road
New Delhi 1

ITALY

Santo Vanasia
Via M. Macchi 71
Milano
Libreria Commissionaria Sansoni
Via La Marmora 45
Firenze
Techna
Via Cesi 16.
40135 Bologna

JAPAN

Kinokuniya Book-Store Co. Ltd.
826 Tsunohazu 1-chome
Shinjuku-ku
Tokyo
Maruzen and Co. Ltd.
P. O. Box 605
Tokyo-Central

KOREA

Chulpanmul
Phenjan

NORWAY

Tanum-Cammermeyer
Karl Johansgt 41—43
Oslo 1

POLAND

Ruch
ul. Wronia 23
Warszawa

ROUMANIA

Cartimex
Str. Aristide Briand 14—18
București

SOVIET UNION

Mezhdunarodnaya Kniga
Moscow G—200

SWEDEN

Almquist and Wiksell
Gamla Brogatan 26
S—101 20 Stockholm

USA

F. W. Faxon Co. Inc.
15 Southwest Park
Westwood Mass. 02090
Stechert Hafner Inc.
31. East 10th Street
New York, N. Y. 10003

VIETNAM

Xunhasaba
19, Tran Quoc Toan
Hanoi

YUGOSLAVIA

Forum
Vojvode Mišića broj 1
Novi Sad
Jugoslavenska Knjiga
Terazije 27
Beograd

24. II. 1975 **Index: 26.007**

ACTA CHIMICA

ACADEMIAE SCIENTIARUM HUNGARICAE

ADIUVANTIBUS

V. BRUCKNER, GY. DEÁK, K. POLINSZKY,
E. PUNGOR, G. SCHAY, Z. G. SZABÓ

REDIGIT

B. LENGYEL

TOMUS 84 FASCICULUS 2

AKADÉMIAI KIADÓ, BUDAPEST

1975

ACTA CHIM. (BUDAPEST) ACASA 2 84 (2) 121–228 (1975)

ACTA CHIMICA

A MAGYAR TUDOMÁNYOS AKADÉMIA KÉMIAI TUDOMÁNYOK OSZTÁLYÁNAK IDEGEN NYELVŰ KÖZLEMÉNYEI

SZERKESZTI

LENGYEL BÉLA

TECHNIKAI SZERKESZTŐK

DEÁK GYULA és HARASZTHY-PAPP MELINDA

Az Acta Chimica német, angol, francia és orosz nyelven közöl értekezéseket a kémiai tudományok köréből.

Az Acta Chimica változó terjedelmű füzetekben jelenik meg, egy-egy kötet négy füzetből áll. Évente átlag négy kötet jelenik meg.

A közlésre szánt kéziratok a szerkesztőség címére (Budapest 112/91 Műegyetem) küldendők.

Ugyanerre a címre küldendő minden szerkesztőségi levelezés. A szerkesztőség kéziratokat nem ad vissza.

Megrendelhető a belföld számára az „Akadémiai Kiadó"-nál (1363 Budapest Pf 24. Bankszámla 215 11488), a külföld számára pedig a „Kultúra" Könyv- és Hírlap Külkereskedelmi Vállalatnál (1389 Budapest 62, P.O.B. 149 Bankszámla: 218 10990) vagy annak külföldi képviseleteinél és bizományosainál.

Die Acta Chimica veröffentlichen Abhandlungen aus dem Bereich der chemischen Wissenschaften in deutscher, englischer, französischer und russischer Sprache.

Die Acta Chimica erscheinen in Heften wechselnden Umfanges. Vier Hefte bilden einen Band. Jährlich erscheinen 4 Bände.

Die zur Veröffentlichung bestimmten Manuskripte sind an folgende Adresse zu senden

Acta Chimica
Budapest 112/91 Műegyetem

An die gleiche Anschrift ist auch jede für die Redaktion bestimmte Korrespondenz zu richten. Abonnementspreis pro Band: $ 32.00.

Bestellbar bei dem Buch- und Zeitungs-Außenhandels-Unternehmen »*Kultúra*« (1389 Budapest 62, P.O.B. 149 Bankkonto Nr. 218 10990) oder bei seinen Auslandsvertretungen und Kommissionären.

Acta Chimica Academiae Scientiarum Hungaricae, 84 (2), pp. 121—124 (1975)

ION EXCHANGE EQUILIBRIA OF SOME MONOVALENT ANIONS

E. FEKETE* and J. INCZÉDY

(Institute of Analytical Chemistry, University of Chemical Engineering, Veszprém)

Received June 25, 1974

The ion exchange equilibrium constants of chlorate, bromate, hydrocarbonate, iodate, hydroxide referred to chloride were determined on Dowex 1×8 resin at 18, 28 and 38°C, and the free enthalp-change, enthalp-change and entrop-change values calculated using the equation of SALMON, derived by thermodynamic statistical theory.

The order of the adsorption strengths of the common metal cations on the sulphonic acid-type ion-exchange resin can be explained by the classical thermodynamic theory of GREGOR [1], or by the modified theory of GLUECKAUF [2], however, there are no general rules at the anion-exchange equilibria, and the adsorption strengths of the anions cannot be predicted generally on the basis of the mentioned concepts.

Since it was shown earlier [3] that at the chromatographic separations of components using an anion exchange column, the optimal conditions of the separations can be calculated if the corresponding equilibrium constants are known, the ion-exchange equilibrium constants of some monovalent ions referring to chloride ion (as reference ion) were determined at three different temperatures. At the calculation of the ion-exchange-equilibrium constants the theory of SALMON [4] was used.

According to the statistic thermodynamic theory of SALMON [4] the ion-exchange constant of the A^- anion referring to chloride is expressed by the following equation:

$$\log K_{A-Cl} = \log K_T + 437 \frac{\omega}{T} \bar{x}_{Cl} \tag{1}$$

K is the mass-action ratio expressed with molefractions of the ions, T temperature (K°), ω and K_T are constants.

$$K_{A-Cl} = \frac{\bar{x}_A x_{Cl}}{x_A \bar{x}_{Cl}} \tag{2}$$

$\bar{x}$ and x are molefractions in the resin and in the liquid phase respectively.

* Present address: Vegyiműveket Tervező Vállalat, Budapest.

Considering that in ion-exchange chromatographic separation the amount of the eluted A^- is low compared to that of eluent ion Cl^-, the K^x value used for informatory calculations can be derived from eq. (1). If $\bar{x} = 1$,

$$\log K^{x}_{A-Cl} = \log K_T + 437 \frac{\omega}{T} \tag{3}$$

Experimental

Reagent solutions. The all stock solutions were prepared from, e.g. chemicals using deionized water as solvent. For preparation of the solutions of KCl, $KClO_3$, $KBrO_3$, KIO_3, $KHCO_3$, of 0.1 *M* the amount required of the dried salt was weighed and after dissolution in ion-free water, diluted to the required volume. Carbonate-free potassium-hydroxide solution was made according to prescription and the concentration controlled by titration.

Ion-exchange resin: Dowex 1×8 (50—100 mesh) strong basic ion-exchange resin was pretreated in the usual way [5] with acid and alkali solution, converted to Cl-form with 0.5 *M* sodium-chloride solution and washed chloride-free with water. For the equilibrium experiments 0.5 g portion of the air-dried resin was used. The capacity of the air-dried resin was determined by titration of the deliberated chloride ions from the resin sample, using the solution of the anion in question for displacement. (See later.)

Equilibrium experiments [6]. Glass columns supplied with heating jacket and with upper jacketed coil were used. For feeding of the columns, tap funnels at the top of the apparatus were used. 0.50 g of the Cl-form air-dried resin was placed in the column, then solution of given composition was poured slowly on the column by means of the tap funnel. The effluent was collected in volumetric flask of 100 ml volume. The collected solution was analysed and the mole fractions of the two competing ions in the resin phase calculated. Using the data: mole fractions in the used original solution and the calculated mole fractions in the resin phase, the exchange constant of the ion in question using eq. (2) was calculated. The experiments were carried out with solutions of five different mole fractions of the ion investigated (0.15; 0.33; 0.50; 0.66; 0.83; 1.0) but of same total concentration (0.1 *M*) and at three different temperature. The solution containing the ion investigated at mole fraction 1 served for controlling the capacity of the resin sample. The analysis of the gathered effluent solution were carried out in the following ways: The chloride ions were determined in the presence of chlorate, hydrocarbonate ions argentometrically using fluoresceine as an indicator. In solutions where KIO_3, $KBrO_3$ or KOH were together with chloride, iodate, bromate, ions were determined iodometrically, while hydroxide ions by acidimetric titration.

Results and discussion

Using the K values obtained from experimental mole fraction data, $\log K$ was plotted against the inner mole fraction of the chloride ion ($\bar{x}_{Cl}$) and the $\log K_T$ as intercept of the linear curve, while the ω from the slope of the curve computed. See equation (1). The $\log K_T$ values obtained at different temperatures were plotted against $1/T$, and assuming that the enthalpy change was independent of temperature in the range investigated, using equation (4) the molar enthalpy change ΔH of the reaction from the slope calculated.

$$\log K_T = -0.434 \frac{\Delta H}{RT} + C \tag{4}$$

Table I

Calculated thermodynamic data of various anion-exchange reactions referred to chloride as reference ion

$ClO_3^- - Cl^-$

C°	K°	log. K_T	K_T	ω	ΔG	ΔH	ΔS
15	288	0.37	2.34	0.25	−0.49		
28	301	0.31	2.04	0.26	−0.43	−1.68	− 4.15
38	311	0.27	1.86	0.27	−0.38		

$BrO_3^- - Cl^-$

C°	K°	log K_T	K_T	ω	ΔG	ΔH	ΔS
18	291	−0.062	0.86	−0.050	0.082		
28	301	−0.050	0.89	−0.051	0.068	0.505	1.45
38	311	−0.038	0.92	−0.049	0.054		

$IO_3^- - Cl^-$

C°	K°	log K_T	K_T	ω	ΔG	ΔH	ΔS
18	291	−0.57	0.269	−0.145	0.76		
28	301	−0.525	0.299	−0.135	0.72	1.89	3.87
38	311	−0.48	0.331	−0.124	0.68		

$HCO_3^- - Cl^-$

C°	K°	log K_T	K_T	ω	ΔG	ΔH	ΔS
18	291	−0.288	0.515	−0.128	0.38		
28	301	−0.270	0.538	−0.134	0.37	0.754	1.28
38	311	−0.251	0.561	−0.134	0.357		

$OH^- - Cl^-$

C°	K°	log K_T	K_T	ω	ΔG	ΔH	ΔS
18	291	−1.37	0.042	0.34	1.83		
28	301	−1.20	0.063	0.41	1.65	7.08	18.0
38	311	−1.025	0.094	0.48	1.46		

R is the gas constant ($R = 1.987 \cdot 10^{-3}$ kcal. degree^{-1}). Using the general thermodynamic functions, the free enthalpy values (ΔG) and the molar entropy change were also calculated.

$$\Delta G = -2.303\, RT \log K_T \tag{5}$$

$$\Delta G = \Delta H - T\Delta S \tag{6}$$

The calculated ΔG, ΔH and ΔS values are summarized in Table I.

As can be seen the decreasing order of the adsorption strengths of the anions corresponds to the order of the increasing enthalpy change:

$$ClO_3^- > BrO_3^- > HCO_3^- > IO_3^- > OH^-$$

The corresponding ΔH values are: -1.68; $+0.505$; $+0.754$; $+1.89$; $+7.08$ kcal.mole^{-1}. The values of the entropy change show a similar tendency too.

The selectivity of the resin for all anions except hydroxide ions is increasing with the inner mole fraction of the referring chloride ion. The behaviour of the hydroxide is opposite, corresponding to the fact that its hydration affinity is larger than that of chloride ion. From the data can be also concluded that the selectivity of the resin is lower for the ions investigated at higher temperature.

REFERENCES

[1] Gregor, H. P.: J. Am. Chem. Soc. **73,** 642 (1951)
[2] Glueckauf, E.: Proc. Roy. Soc. (London) **A 214,** 207 (1952)
[3] Inczédy, J., Klatsmányi-Gábor, P., Erdey, L.: Acta Chim. Acad. Sci. Hung. **61,** 261 (1969)
[4] Salmon, J. E.: Trans. Faraday Soc. **65,** 2879 (1969)
[5] Inczédy, J.: Analytical Applications of Ion Exchangers. Pergamon Press Oxford, 1966
[6] Birch, B. J., Redfern, J. P., Salmon, J. E.: Trans. Faraday Soc. **63,** 2362 (1967)

Ernő Fekete; Vegyiműveket Tervező Vállalat, 1146 Budapest, Erzsébet királyné u. 1/c.
János Inczédy; Veszprémi Vegyipari Egyetem, 8200 Veszprém, Schönherz Z. u. 10. Hungary.

Acta Chimica Academiae Scientiarum Hungaricae, 84 (2), pp. 125—133 (1975)

DIPOLE ASSOCIATION OF NITROBENZENE IN NON-POLAR SOLVENTS

J. Liszi

(Electrochemical Research Group of the Hungarian Academy of Sciences, Department of Physical Chemistry, Industrial Chemistry University, Veszprém)

Received 5 February, 1974

The molar polarization of nitrobenzene was studied in carbon-tetrachloride, *n*-heptane and benzene solutions. It was found that the dipole association of nitrobenzene increases with the increase of the nitrobenzene concentration. The results could be described satisfactorily by the Sugden equation.

The electrostatic interactions occurring between polar molecules can lead to dipole association. The monomer molecules in the associations can figure in parallel or antiparallel arrangements. In the event of an antiparallel arrangement the dipole moments of the monomer molecules are in opposing directions, while in a parallel arrangement they lie in the same direction. For a completely antiparallel arrangement the orientation polarization becomes zero, the associated dipoles mutually eliminate the effects of each other, and the polarization will be equal to the sum of the electron and atom polarizations. The distortion polarization is not affected by the dipole-environment of the molecule [1].

The phenomenon of dipole association can also be observed in solutions of nitrobenzene in non-polar substances. In the present work a study was made of nitrobenzene–carbon tetrachloride, nitrobenzene–*n*-heptane and nitrobenzene–benzene mixtures. The relative permittivities and densities of the mixtures were measured at 20°C as a function of composition. Our conceptions relating to dipole association are based on molar polarization data.

Experimental

The relative permittivities of the mixtures were determined with a Radelkis OH-301 universal dielectrometer, at a constant frequency of 3 MHz. In our experience the relative permittivities of these systems at 20 °C with a frequency of 3 MHz agree with the static relative permittivities. The thermostable measuring cells provided by Radelkis were used in this work.

The densities of the pure substances were determined with a pycnometric method, and in the knowledge of these, the densities of the mixtures were

measured with an Austrian DMA OZC digital densimeter. The principle of this latter instrument is as follows: the natural frequency relating to vacuum of the resonator in the instrument changes if a gas or liquid enters the resonator. The change depends on the density of the entering medium. The instrument shows a period-time corresponding to the given frequency, and the density can be calculated from the period-time. The constant of the instrument can be determined from known density data, and thus it was necessary to perform the pycnometric determination of the densities of the pure substances.

The mixtures of various compositions were prepared by mixing known weights of the components. Our experimental results are given in Tables I, II and III. The symbols in the Tables are as follows: x_A = mole fraction of nitrobenzene, ε = relative permittivity, and ϱ = density.

Table I

Relative permittivities and densities of nitrobenzene–carbon tetrachloride mixtures at 20 °C as a function of composition

x_A	ε	ϱ (g.cm^{-3})
0	2.23	1.5942
0.1115	4.95	1.5495
0.2008	7.61	1.5103
0.2969	10.38	1.4740
0.3985	13.60	1.4327
0.4981	16.64	1.3959
0.5986	20.19	1.3558
0.6995	23.69	1.3168
0.7994	27.21	1.2781
0.8991	31.05	1.2393
1	34.74	1.1982

Discussion

The data in Tables I—III were used to calculate the molar polarizations of the mixtures as a function of composition. The equation used was

$$P = \frac{\varepsilon - 1}{\varepsilon + 2} \cdot \frac{x_A M_A + x_B M_B}{\varrho} \tag{1}$$

where P is the molar polarization, M the molecular weight, and x the mole fraction; index A refers to nitrobenzene, and index B to the apolar substance. The molar polarization data are given in Tables IV, V and VI and in Figs 1, 2

Table II

Relative permittivities and densities of nitrobenzene–n-heptane mixtures at 20 °C as a function of composition

x_A	ε	ϱ (g.cm^{-3})
0	1.90	0.6841
0.1050	3.44	0.7235
0.1996	4.98	0.7635
0.2991	7.29	0.8069
0.3951	9.85	0.8514
0.4944	12.29	0.9002
0.6348	17.55	0.9758
0.6944	20.00	1.0096
0.7993	24.48	1.0728
0.8979	29.74	1.1356
1	34.74	1.1982

Table III

Relative permittivities and densities of nitrobenzene–benzene mixtures at 20 °C as a function of composition

x_A	ε	ϱ (g.cm^{-3})
0	2.28	0.8737
0.1049	4.82	0.9133
0.1994	7.23	0.9475
0.2987	9.95	0.9826
0.3974	13.10	1.0150
0.4960	16.59	1.0473
0.5947	20.00	1.0788
0.6946	23.74	1.1090
0.7939	27.42	1.1382
0.8914	31.00	1.1665
1	34.74	1.1982

and 3. The Tables also list the molar polarizations of nitrobenzene, calculated *via* the relation

$$P_A = \frac{P - x_B P_B}{x_A} \tag{2}$$

with the assumption of the additivity of the molar polarization.

Table IV

Molar polarization (P) of nitrobenzene–carbon tetrachloride mixtures, and molar polarization (P_A) of nitrobenzene in the mixture, as a function of composition at 20 °C

x_A	P (cm³.mole⁻²)	P_A (cm³.mole⁻²)
0	28.1	—
0.1115	55.2	271.0
0.2008	67.2	223.1
0.2969	74.5	184.4
0.3985	77.6	152.4
0.4981	83.3	139.1
0.5986	86.4	125.4
0.6995	88.7	114.8
0.7994	90.7	106.4
0.8991	92.5	99.8
1	94.3	94.3

Table V

Molar polarization (P) of nitrobenzene–n-heptane mixtures, and molar polarization (P_A) of nitrobenzene in the mixture, as a function of composition at 20 °C

x_A	P (cm³.mole⁻²)	P_A (cm³.mole⁻²)
0	33.7	—
0.1050	63.5	317.1
0.1996	78.1	256.0
0.2991	89.7	220.6
0.3951	95.7	190.6
0.4944	97.7	163.2
0.6348	99.4	137.2
0.6944	99.2	128.0
0.7993	97.8	113.8
0.8979	96.2	103.3
1	94.3	94.3

Table VI

Molar polarization (P) of nitrobenzene–benzene mixtures, and molar polarization (P_A) of nitrobenzene in the mixture, as a function of composition at 20 °C

x_A	P (cm³.mole⁻²)	P_A (cm³.mole⁻²)
0	26.7	—
0.1049	50.7	255.8
0.1994	62.0	203.6
0.2987	69.7	170.7
0.3974	75.7	150.0
0.4960	80.3	134.8
0.5947	83.9	122.8
0.6946	87.0	113.6
0.7939	89.7	106.1
0.8914	92.1	100.0
1	94.3	94.3

The molar polarization of the mixture exhibits a similar tendency for all three systems: compared to the ideal behaviour a positive excess, molar polarization appears. This tendency is strongest in the *n*-heptane system, where the molar polarization passes through a maximum as a function of composition.

The variation with concentration of the molar polarization of nitrobenzene is even more characteristic. In these systems P_A falls rapidly with the increase of the mole fraction of nitrobenzene; this is indicative of a strong decrease in the dipole concentration.

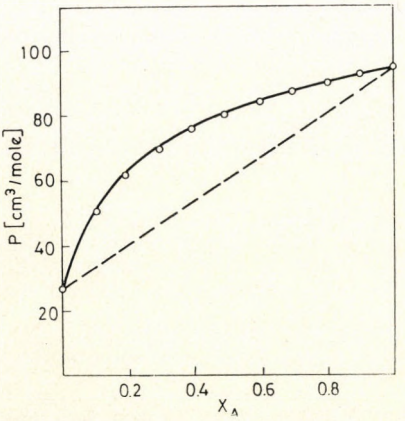

Fig. 1. Molar polarization of nitrobenzene–carbon tetrachloride mixtures at 20 °C, as a funtion of composition

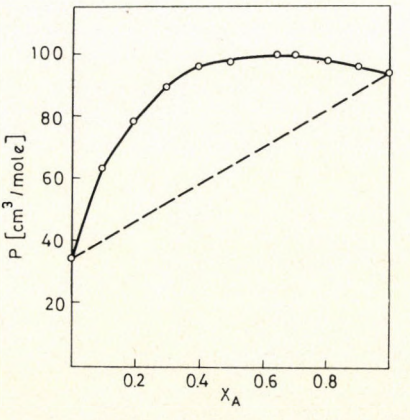

Fig. 2. Molar polarization of nitrobenzene–*n*-heptane mixtures at 20 °C as a function of composition

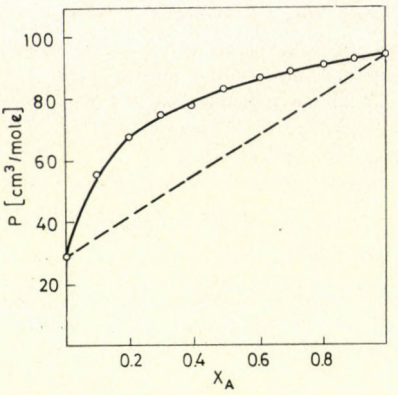

Fig. 3. Molar polarization of nitrobenzene–benzene mixtures at 20 °C, as a function of composition

Solvent effect

The most striking consequence of the phenomenon known in the literature as the solvent effect [1] is the difference of the dipole moments calculated from the gas-phase and liquid-phase measurements. This difference can be explained by the interaction of the molecules of the solvent and the solute. In concentrated solutions, however, the environment of the molecules of solute consists not only of solvent molecules but of other solute molecules too. For this reason it is usual to calculate the dipole moment from molar polarization data extrapolated to 'infinity dilute' solution [2]. The dipole-moment values calculated in this way, however, depend on the nature of the solvent. In many cases 'extrapolation to the gas phase' can be performed by the empirical formula of SUGDEN [3]:

$$P_A = \lambda + P_{\text{vap}} - P_{\text{or}} \frac{\varepsilon - 1}{\varepsilon + 1} \tag{3}$$

where P_A is the molar polarization of the substance of interest in the solution, P_{vap} is the corresponding value in the vapour phase, P_{or} is the orientation polarization of the substance, ε is the relative permittivity of the mixture, $(\varepsilon - 1)/(\varepsilon + 2)$ is the 'volume polarization' and λ is a constant.

The application of equation (3) to the systems under consideration is shown in Fig. 5. The dashed line indicates the extrapolated value. The measured data for the three systems lie on a straight line. The values extrapolated to pure solvent are also given in the Figure. In carbon tetrachloride solution, *n*-heptane solution and benzene solution the values of $P_{A\infty} = 410$, 438 and 409 cm³/mole, respectively. According to FAIRBROTHER [4] and JENKINS and SUTTON [5], the value of the constant λ in equation (3) is dependent on the

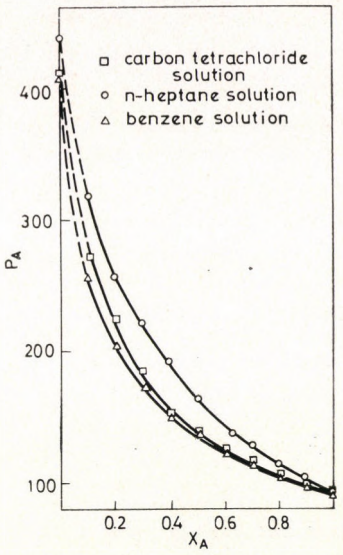

Fig. 4. Molar polarization of nitrobenzene as a function of composition in the systems under examination. The dashed line indicates extrapolated values

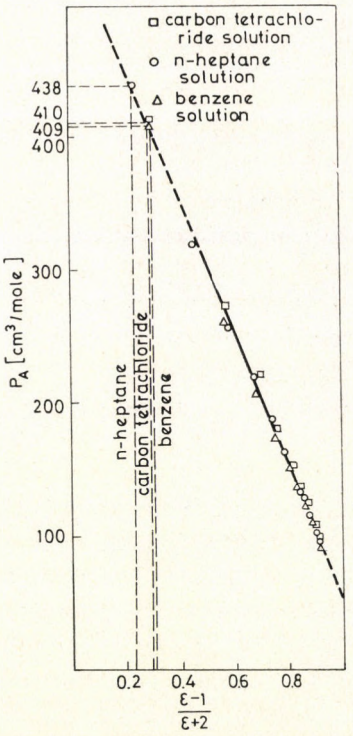

Fig. 5. Molar polarization of nitrobenzene as a function of the volume polarization. The dashed line indicates extrapolated values

solvent and the temperature. Identical λ values were found for the three systems studied in the present work. When extrapolated to $(\varepsilon - 1)/(\varepsilon + 2) = 1$, the value of the straight line in Fig. 5 is $P_e + P_a + \lambda$, where P_e and P_a are the electron and atom polarizations of nitrobenzene. From the literature [2] $P_e = 29.24$ cm³/mole, and $P_a = 3.8$ cm³/mole. Hence, from these values and Fig. 4, $\lambda = 18$ cm³/mole.

The slope of the straight line defined by equation (3) is the orientation polarization. The measurements on carbon tetrachloride, *n*-heptane and benzene solutions indicate that the orientation polarization of nitrobenzene, P_{dir}, is 509 cm³/mole. If this value is accepted as valid for the vapour phase too, then the permanent dipole moment of nitrobenzene can be calculated from the Debye equation [2]:

$$P_{\text{or}} = \frac{4\pi N_A}{3} \cdot \frac{\mu^2}{3kT} \tag{4}$$

where N_A is the Avogadro number, μ is the permanent dipole moment, k is the Boltzmann constant, and T is the absolute temperature. From equation (4) $\mu = 4.24$ D, which can be taken as identical with the value (4.2 D) determined experimentally in the vapour phase [2]. This latter result similarly confirms the validity of equation (3).

Equation (3) thus describes the molar polarization of nitrobenzene in mixtures of variable relative permittivity, making possible extrapolation to the vapour phase and hence the determination of the permanent dipole moment of nitrobenzene. As regards the explanation of the strong decrease of P_A, it may be assumed that the nitrobenzene molecules, possessing a high permanent dipole moment, form dipole associations with antiparallel arrangements. In the following we consider the extent of dipole association in pure nitrobenzene. For this certain simplifying assumptions are applied:

1. In pure nitrobenzene the molecules are present in the form of monomers and of dimers in antiparallel arrangement.

2. The molar polarization of the dimers is twice the sum of the atom and electron polarizations determined in the gas phase (and thus relating to monomer molecules).

3. The molar polarization of the monomers is the value obtained from equation (3) with extrapolation to the limiting case $(\varepsilon - 1)/(\varepsilon + 2) = 0$.

4. The molar polarization is an additive property in the sense that the sum of the molar polarizations of the components, weighed by the mole fractions, gives the molar polarization of the mixture.

With these assumptions, the molar polarization of pure nitrobenzene is

$$P_m = \frac{x_1}{1 + x_2} P_1 + \frac{x_2}{1 + x_2} P_2 \tag{5}$$

where P_m is the molar polarization of nitrobenzene, P is the molar polarization of the component, and x is the mole fraction; index 1 refers to the nitrobenzene monomer, and index 2 to the dimer. If the values $P_1 = 543$ cm^3/mole and $P_2 = 2.33$ cm^3/mole are substituted into equation (5), we obtain

$$x_1 = 0.215 \qquad \text{and} \qquad x_2 = 0.785$$

With the above approximations, therefore, it turns out that at 20 °C pure nitrobenzene contains 78.5% dimer in the antiparallel arrangement.

REFERENCES

[1] PARTINGTON, J. R.: An Advanced Treatise on Physical Chemistry, Vol. V. Longmans, Green and Co., London, New York, Toronto, (1954)
[2] HILL, N. E., VAUGHAN, W. E., PRICE, A. H., DAVIES, M.: Dielectric Properties and Molecular Behaviour. Van Nostrand Reinhold Co., London, New York, Toronto, Melbourne, 1969
[3] SUGDEN, S.: Nature **133,** 415 (1934)
[4] FAIRBROTHER, J.: J. Chem. Soc. **1934,** 1846; Trans. Faraday Soc. **30,** 474 (1934)
[5] JENKINS, F. A., SUTTON, L. E.: J. Chem. Soc. **1935,** 609

János LISZI; 8201 Veszprém VVE Fiz. Kém. Tsz. Hungary.

Acta Chimica Academiae Scientiarum Hungaricae, 84 (2), pp. 135—140 (1975)

MECHANISM OF CYCLOHEXANONE OXIDATION BY CHLORAMINE-T

S. P. MUSHRAN,* R. SANEHI and A. K. BOSE

(Chemical Laboratories, University of Allahabad, Allahabad, India)

Received March 6, 1974

Kinetic studies on the oxidation of cyclohexanone by chloramine-T in alkaline media are reported. A first-order dependence on chloramine-T, cyclohexanone and the alkali was observed. No effect of *p*-toluenesulfonamide was evident. A negligible effect of ionic strength and a strong negative effect of methanol point to a mechanism involving interaction of the enolate ion of cyclohexanone with chloramine-T in the rate-determining step. Various thermodynamic parameters and the isolation of the product 1,2-cyclohexanedione are in agreement with the proposed mechanism.

The kinetics of oxidation of cyclohexanone have been studied by a number of authors using various oxidizing agents [1—8]. The present work is an investigation of the kinetics and mechanism of cyclohexanone oxidation by the less widely used but potent oxidant chloramine-T in alkaline media.

Experimental

The materials employed were of the highest purity available. An E. Merck sample of cyclohexanone and a Koch-Light (England) sample of *p*-toluene sulfonamide were used. The chloramine-T solution was prepared as reported earlier [9]. All other reagents were of analytical grade and bidistilled water was used throughout the experiments. The reaction stills were blackened from the outside. The progress of the reaction was followed by determining unreacted chloramine-T indirectly, using ascorbic acid [10].

Stoichiometry

Different sets of experiments were carried out with varying chloramine-T to cyclohexanone ratios in presence of 0.02*M* NaOH at 55 °C for 48 hrs. From the results shown in Table I, it is concluded that 1 mol of cyclohexanone consumes 2 mol of chloramine-T according to the following stoichiometric

* Correspondence should be addressed to this author.

equation, yielding 1,2-cyclohexanedione, which was detected by a conventional method [11].

$$2\,CH_3C_6H_4SO_2N\,NaCl + \underline{CH_2(CH_2)_4{-}CO} + H_2O =$$

$$= 2\,CH_3C_6H_4SO_2NH_2 + \underline{OC{-}(CH_2)_4{-}CO} + 2\,NaCl \qquad (1)$$

Table I

Stoichiometric data

$10^3_{(M)}$ [CAT]$_0$	10^3 [cyclohexanone] (M)	$10^3_{(M)}$ [CAT]	Stoichiometric ratio [CAT]: [Cyclohexanone]
0.5	0.0	0.5	—
1.0	0.5	0.0	2 : 1
1.5	0.5	0.5	2 : 1
2.0	0.5	1.0	2 : 1
2.5	0.5	1.5	2 : 1
3.0	0.5	2.0	2 : 1

[NaOH] = 0.02 M

Results

The oxidation of cyclohexanone by chloramine-T was studied over a wide range of reactant concentrations at constant alkali concentration (Table II). A pseudo first-order dependence on chloramine-T was observed at all

Table II

Effect of reactant concentrations on the rate

$10^3\times$ [Chloramine-T] (M)	$10^2\times$ [Cyclohexanone] (M)	$k_1\times10^5$ (s^{-1}) at	
		35 °C	40 °C
0.6	0.6	4.15	5.80
0.8	0.6	4.34	6.22
1.0	0.6	5.14	6.29
1.2	0.6	4.80	6.45
1.6	0.6	4.99	6.77
2.0	0.6	5.14	6.91
1.0	0.4	3.37	4.30
1.0	0.8	6.60	8.71
1.0	1.0	7.41	9.02
1.0	1.2	9.25	11.3
1.0	1.6	11.7	15.2

[NaOH]=0.02 M

initial concentrations of the reactants (Fig. 1). A linear increase of the pseudo first-order-rate constant (k_1) was observed with increasing cyclohexanone concentration. The second-order-rate constants calculated as $k_2 = k_1/[\text{cyclohexanone}]$ give concordant values and thus establish a first-order dependence on the cyclohexanone concentration.

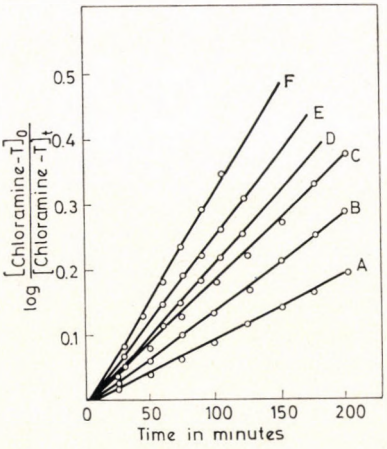

Fig. 1. First-order-rate plots at 35 °C, [Chloramine-T] = $1.0\times10^{-3}M$; [NaOH] = = $0.02M$ and [Cyclohexanone] = 4, 6, 8, 10, 12 and $16\times10^{-3}M$ in A, B, C, D, E and F, respectively

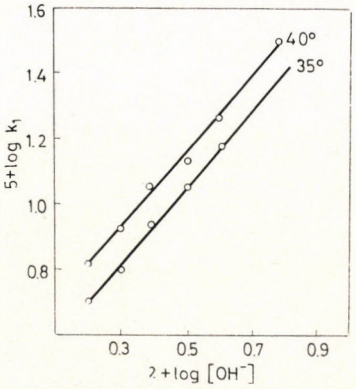

Fig. 2. Plots of log k_1 against log [OH^-]. [Chloramine-T] = $1.0\times10^{-3}M$; [Cyclohexanone] = $6\times10^{-3}M$

The oxidation of cyclohexanone by chloramine-T was found to be strongly dependent on the alkali concentration. At constant ionic strength ($\mu = 0.2$), an increase in alkali concentration increases the rate constants linearly. The plot of log k_1 against log [OH^-] is a straight line (Fig. 2) with a slope of unity establishing first-order dependence in [OH^-].

The variation of ionic strength has an insignificant effect (Table III) on the rate constants, while the effect of methanol addition is negative (Table IV). *p*-Toluenesulfonamide, the reduction product of chloramine-T, however, had no effect on the reaction rate.

The energy of activation (E_{act}), the frequency factor (A) and the entropy of activation (ΔS^+) were found to be 9.83 kcal.mol^{-1}, 5.96×10^6 l^2.mol^{-2}s^{-1} and −28.7 e.u., respectively, from rate measurements carried out at five different temperatures (Table V).

Table III

Effect of ionic strength on the reaction rate at 35 °C

Ionic strength	$k_1 \times 10^5$ (s^{-1})
0.02	5.14
0.04	5.22
0.06	5.37
0.08	5.49
0.10	5.83
0.12	5.87
0.42	6.83

[Cyclohexanone] = $0.6+10^{-2}$ M; [Chloramine-T] = 1.0×10^{-3} M and [NaOH] = = 0.02 M

Table IV

Effect of methanol on the reaction rate at 35 °C

Methanol (%)	$k_1 \times 10^5$ (s^{-1})
None	5.14
5	4.41
10	3.84
15	3.16
20	2.58
25	1.69

[Cyclohexanone] = 0.6×10^{-2} M; [Chloramine-T] = 1.0×10^{-3} M and [NaOH] = = 0.02 M

Table V

Effect of temperature on the reaction rate

Temperature (°C)	$k_1 \times 10^5$ (s^{-1})	$10k$ ($l^2 \times mol^{-2} \times s^{-1}$)	$A \times 10^{-6}$ ($l^2 \times mol^{-2} \times s^{-1}$)	$S^{\ddagger}$ (e.u.)
35	5.14	7.15	6.05	−28.7
40	6.45	8.97	5.91	−28.7
45	8.25	11.5	5.90	−28.7
50	10.6	14.7	5.96	−28.7
55	13.4	18.6	5.97	−28.7

[Cyclohexanone] = 0.6×10^{-2} M; [Chloramine-T] = 1.0×10^{-3} M and [NaOH] = = 0.02 M

Discussion

The base catalyzed oxidation of ketones clearly shows that the enolate ion is involved in the oxidation by chloramine-T.

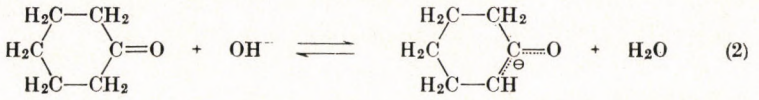

(2)

Cyclohexanone keto form Cyclohexanone enol anion

In aqueous alkaline solutions, chloramine-T (CAT) hydrolyzes [12] to *p*-toluenesulfochloramide (CAT') and *p*-toluenesulfonamide (TSA) as follows:

$$\underset{\text{CAT}}{CH_3C_6H_4SO_2N \cdot NaCl} + H_2O \rightleftharpoons \underset{\text{CAT'}}{CH_3C_6H_4SO_2N \cdot HCl} + NaOH \qquad (3)$$

$$\underset{\text{CAT'}}{CH_3C_6H_4SO_2N \cdot HCl} + NaOH \rightleftharpoons \underset{\text{TSA}}{CH_3C_6H_4SO_2NH_2} + NaClO \qquad (4)$$

It is, therefore, obvious that one of the three oxidizing species of chloramine-T, *viz.* CAT itself or CAT' or the ClO^- ion may react with the enolate ion in the rate-controlling step. Now, if ClO^- ion is the main oxidizing species, the reaction would involve an interaction between two similarly charged ions and thus would correspond to a positive ionic strength effect which is contrary to our experimental observations. Thus the possibility that the ClO^- ion is the reacting species, is completely ruled out.

The negligible effect of ionic strength points to the involvement of at least one neutral molecule in the rate-controlling step. Further, the positive dielectric constant effect observed shows that the rate-controlling step must involve the interaction of a neutral molecule and a negatively charged ion. Thus, the mechanism of the oxidation of cyclohexanone (*S*) by chloramine-T may be represented by the following two schemes satisfying the above requirements.

Scheme I with CAT' as an oxidizing species:

$$S + OH^- \underset{k_{-3}}{\overset{k_3}{\rightleftharpoons}} SOH^- \qquad \text{fast} \qquad (2)$$

$$CAT + H_2O \underset{k_{-4}}{\overset{k_4}{\rightleftharpoons}} CAT' + NaOH \qquad \text{fast} \qquad (3)$$

$$CAT' + SOH^- \xrightarrow{k_5} \text{Intermediate (X)} \qquad \text{slow} \qquad (5)$$

$$X + CAT \xrightarrow{k_6} \text{Products} \qquad \text{fast} \qquad (6)$$

By applying the steady-state approximation to all the intermediates formed, the following rate law is obtained:

$$-\frac{d[CAT]}{dt} = \frac{k_3 k_4 k_5 [CAT][S][H_2O]}{k_{-3}k_{-4} + k_3 k_5 [S]} \tag{7}$$

The rate low derived (7) from scheme I predicts a zero-order dependence in hydroxide-ion concentration which is contrary to the experimental results. Thus the possibility that the reacting species is CAT' and the oxidation process proceeds according to Scheme I, is also completely ruled out

Scheme II with CAT as an oxidizing species:

$$S + OH^- \underset{k_{-3}}{\overset{k_3}{\rightleftharpoons}} SOH^- \qquad \text{fast} \tag{2}$$

$$SOH^- + CAT \xrightarrow{k_7} \text{Intermediate (X)} \qquad \text{slow} \tag{8}$$

$$X + CAT \xrightarrow{k_8} \text{Products} \qquad \text{fast} \tag{9}$$

By applying the steady-state approximation to SOH^- and X and making the assumption that $k_{-3} \gg k_7$ [CAT], the following rate is obtained:

$$-\frac{d[CAT]}{dt} = \frac{2k_3 k_7}{k_{-3}} [CAT][S][OH^-] \tag{10}$$

The above derived rate (10) from Scheme II predicts a first-order dependence in cyclohexanone, chloramine-T and $[OH^-]$ ion concentration, which is in agreement with the experimental observations. Thus, the oxidizing species in this case is undoubtedly chloramine-T itself and the oxidation process does proceed through Scheme II.

*

The authors thank the Council of Scientific and Industrial Research, New Delhi, for financial assistance.

REFERENCES

[1] Littler, J. S.: J. Chem. Soc. **1961,** 827; **1961,** 832
[2] Rangaswamy, M., Santappa, M.: Proc. Indian Acad. Sci. Sect. A. **66,** 174 (1967)
[3] Waters, W. A.: J. Chem. Soc. **1946,** 1151
[4] Cecil, R., Littler, J. S., Easton, G.: J. Chem. Soc. (B) **1970,** 626
[5] Littler, J. S., Sayce, I. G.: J. Chem. Soc. **1964,** 2545
[6] Luyanitskii, I. Ya.: Kinetika i Kataliz **5,** 235 (1964)
[7] Subbaaman, L. R., Santappa, M.: Z. Physik. Chem. **48,** 172 (1966)
[8] Best, P. A., Littler, J. S., Waters, W. A.: J. Chem. Soc. **1962,** 822
[9] Agrawal, M. C., Mushran, S. P.: Z. Naturforsch. **276,** 401 (1972)
[10] Bottger, K., Bottger, W.: Z. analyt. Chem. **70,** 225 (1927)
[11] Feigl, F.: Spot Tests in Organic Analysis p. 325. Elsevier Publishing Co., New York, 1966
[12] Dietzel, R., Taüfel, K.: Apotheker-Ztg. **44,** 989 (1929)

S. P. Mushran
R. Sanehi
A. K. Bose
Chemical Laboratories, University of Allahabad, Allahabad, India.

Acta Chimica Academiae Scientiarum Hungaricae, 84 (2), pp. 141—159 (1975)

ÜBER DIE MÖGLICHKEITEN DER DIGITALEN BESTIMMUNG DER PARAMETER DER KONTAKT-KATALYTISCHEN HYDRIERUNG VON ÄTHYLEN, III

DIE »SCHÄTZUNG« DER GESCHWINDIGKEITSKONSTANTEN FÜR DEN STATIONÄREN FALL

P. KŐNIG und P. FEJES

(Institut für Isotope der Ungarischen Akademie der Wissenschaften, Budapest und Institut für Angewandte Chemie der József-Attila-Universität, Szeged)

Eingegangen am 22 März, 1974

Die Verfasser suchen in ihrer Mitteilung nach einer Antwort auf die Frage, ob der HORIUTI—POLÁNYIschе Mechanismus der kontakt-katalytischen Hydrierung des Äthylens mit den Ergebnissen der in der Fachliteratur beschriebenen kinetischen Versuche in Einklang zu bringen ist. Mit der Anwendung der Methode der stationären Annäherung haben sie die numerische Lösung der im I. Teil der Veröffentlichungen abgeleiteten Differentialgleichung den experimentellen kinetischen Kurven nach dem Prinzip der nicht-linearen kleinsten Fehlerquadrate — gemäß der im II. Teil der Mitteilungen erwähnten Methode — angepaßt.

Die strenge statistische Analyse der Ergebnisse der Optimalisierung hat die Erkennung der Gültigkeitsgrenzen des Modells bzw. seine Weiterentwicklung ermöglicht. Daraus ergeben sich zwei alternative Näherungen, von denen die eine die Kinetik der untersuchten Reaktion bei einer bestimmten Gemischzusammensetzung richtig beschreibt, die Wirkung bedeutender Änderungen der Gemischzusammensetzung aber nicht zu widerspiegeln vermag, während die andere die leztere Erscheinung richtig widerspiegelt, sich aber den einzelnen kinetischen Kurven nicht mit einer den strengen statistischen Forderungen entsprechenden Genauigkeit anpaßt. Es ist anzunehmen, daß die Grundhypothesen des assoziativen Mechanismus richtig sind, aber eine übermäßige Vereinfachung der tatsächlichen Sorptionsverhältnisse darstellen.

Einleitung

In der Entscheidung der Frage, ob die von uns über einen Reaktionsmechanismus gebildeten Modellvorstellungen zutreffend sind oder nicht, kann die Schätzung der Parameter der aufgrund des Modells konstruierten theoretischen reaktionskinetischen Funktionen ein wertvolles Mittel bilden. Der Vergleich der experimentellen und der mit Hilfe der geschätzten Parameter errechneten Kurven, d. h. die Untersuchung der Güte des Ausgleichs sowie der Zuverlässigkeit und chemischen Realität der geschätzten Parameter an sich vermögen zwar keine hinreichenden Beweise zur Akzeptierung irgendeines mechanistischen Modells liefern, zeigen aber — mit entsprechender Umsicht durchgeführt — die Untauglichkeit des Modells an, ja sie können sogar Hinweise auch betreffs der Weiterentwicklung des Modells oder der Planung des kritischen Versuchs bieten.

In der vorliegenden Arbeit versuchen wir, die kinetischen Parameter der kontakt-katalytischen Hydrierung des Äthylens an Nickel, unter Verwendung der Modellvorstellung von HORIUTI—POLÁNYI [1], auf die oben erwähnte

Weise [2] zu schätzen. Es wird der Versuch einer statistischen Bewertung der Ergebnisse der Parameterschätzung unternommen und geprüft, welche Bedeutung diese Ergebnisse hinsichtlich der Richtigkeit des zitierten Modells besitzen.

Im Interesse des Gelingens der Parameterschätzung müssen wir den Versuchen gegenüber die den Gegenstand des Verfahrens bilden, ziemlich strenge Forderungen stellen. Solche — einen relativ großen Druckbereich umfassende, viele zusammengehörige P- und t-Meßpunkte in Tabellenform, unter genauer Bekanntgabe der experimentellen Bedingungen dartuende — Arbeiten haben wir in der Literatur nur zwei gefunden [3, 4]. In beiden Versuchen wird Äthylen auf Nickelpulver bei 0 °C hydriert. Die Versuchsbedingungen veranschaulicht Tabelle I.

Tabelle I

Die charakteristischen Daten der zur Optimierung verwendeten kinetischen Versuche

	Versuch 1 [3]	Versuch 2 [4]
Menge des Katalysators, mg	273	3
Reduktionstemperatur des Katalysators, °C	400	480
Spezifische Oberfläche, m^2/g	2,9	—
Reaktorvolumen, cm^3	161	65
Anfangszusammensetzung für Äthylen, p_1^0, kN/m^2	4,58	14,30
Anfangszusammensetzung für Wasserstoff, p_2^0, kN/m^2	8,93	14,08
Zahl der Meßpunkte	19	31
Halbwertszeit der Reaktion, s	36,6	4290
Instrument für die Druckmessung	Quecksilbermanometer	Bourdon-Röhre mit Torsionsfaden

Nach unseren Erfahrungen führt die iterative Optimierung nur von einer bestimmten Umgebung des Minimums ausgehend zum Erfolg, und dieser Parameterbereich ist nicht allzu groß. Daher ist die richtige Wahl des Anfangswertes des Parametervektors auf spekulativem Wege eine hoffnungslose Aufgabe. Mit iterativer Simulierung des Versuches aber läßt sich ziemlich schnell ein Parametervektor finden, bei dem der Verlauf der berechneten und der gemessenen Kurve ein ähnlicher ist und das genügt schon, um mit der iterativen Optimierung beginnen zu können.

Der gute Anfangswert setzt den Zeitanspruch der Parameterschätzung weitgehend herab. Aus dem gleichen Grunde ist es von wesentlicher Bedeutung, die zur Optimierung verwendete Methode richtig zu wählen. Wir haben auch mehrere Varianten der einzig in Betracht kommenden Gradientenmethode ausprobiert, wie z. B. die Methoden von GAUSS—NEWTON, MAROUARDT bzw.

DAVIDON—FLETCHER—POWELL [5] und von diesen das auf der sich an die Namen der letzteren Autoren knüpfenden Methode beruhende »Flepomin-Verfahren« [6] als am entsprechendsten befunden. Das Besondere an diesem Vorgehen ist, daß die Inverse der HESSschen Matrix iterativ von einer beliebigen positiv definitiven Matrix — in unserem Fall von der Einheitsmatrix ausgehend — angenähert wird. Diese Näherung erfüllt sich streng nur in unmittelbarer Umgebung des Minimums, welcher Umstand die Konvergenz der Iteration nicht beeinflußt, doch ist eine so errechnete Kovarianz-Matrix — und daher auch der Konfidenz-Intervall der optimalen Parameter — mit Vorbehalt zu behandeln. Im weiteren haben wir, wenn die Abweichung nicht besonders angegeben ist, die Werte des Konfidenz-Intervalls beim Zuverlässigkeitsniveau 0,95 mittels Invertierung der auf die übliche Weise ([2], S. 222) aufgebauten (HESSschen) Matrix berechnet.

Außer den erwähnten Tatsachen wird der Zeitbedarf der digitalen Parameterschätzung durch die Fehlergrenze der in die Prozedur THEORY eingebauten Integrier-Methode MERSN (S. [2]) und die Wahl der zur Terminierung der Iteration vorgeschriebenen Bedingungen bestimmt. Beide Probleme stellen auch an sich Optimumaufgaben dar; zu lockere Bedingungen führen zu fehlerhaften Ergebnissen, zu strenge verzögern die Optimierung zeitlich sehr. Die Fehlerschranke haben wir bei einem Wert von 10^{-4} festgesetzt. Die üblichen terminierenden Bedingungen, wonach die Veränderung der Zielfunktion bzw. sämtliche Parameter unterhalb einer gewissen Schranke zu liegen kommen, haben sich nicht als zuverlässig erwiesen. Es ist nämlich vorgekommen, daß die Konvergenz fern vom Minimum lokal dermaßen verlangsamt war, daß die obigen Bedingungen ein Minimum anzeigten. Deshalb haben wir im allgemeinen die Iteration dann beendet, wenn über die erwähnten Bedingungen hinaus die parallelen Ableitungen der Zielfunktion nach den Parametern kleiner ausfielen als die vorgegebene Fehlerschranke der Integrierung.

Die Parameterschätzung erfolgte an einer Rechenmaschine des Typs ICT 1905 und die übrigen Berechnungen an der Klein-Rechenmaschine KFKI-TPAi-8k.

Die Ergebnisse der Parameterschätzung

Die den Gegenstand der Parameterschätzung bildenden experimentellen Daten sind in Form von zusammengehörigen Gesamtdruck- und Zeit-Wertpaaren gegeben. Was die statistische Verteilung der Meßfehler anbelangt, müssen wir mit Vermutungen vorliebnehmen. In Kenntnis des Instrumentes für die Druckmessung nehmen wir an, daß der Fehler vom gemessenen Druckwert unabhängig und normal verteilt ist. Die einzelnen Meßpunkte wurden mit identischem statistischem Gewicht berücksichtigt.

Die Anfangswerte sowie die optimalisierten Werte der Parameter für das in der Mitteilung [1] behandelte Modell (im weiteren Modell *A*) sind in

Tabelle II

*Die optimalen Parameter des Modells A**

	Versuch 1		Versuch 2	
	Anfangswert	Optimum	Anfangswert	Optimum
Parameter φ_1	3	4,33 ± ... (4,96)**	3	14 600 ±7 ·10⁶ (3380)**
Parameter φ_2	0,5	1,73 ± ... (4,26)	0,57	7,35 ±0,93 (0,91)
Parameter φ_3	0,02	0,0682 ± ... (0,0189)	0,67	7 710 ±4 · 10⁶ (1970)
Parameter φ_4	100	100 ± ... (5)	7,9	21,7 ±1,4 (1,5)
Zielfunktion $S(\varphi)$	540	20,37	5910	7,185
Streuung $s = \sqrt{\frac{S(\hat{\varphi})}{m-n}}$		1,166		0,516
Zahl der Iterationen	5		74	

* Die Umstände der beiden Versuche sind verschieden (s. Tab. I), deshalb sind die als unmittelbares Resultat ihrer Optimalisierung erhaltenen Parameter miteinander nicht vergleichbar. Auf den Vergleich der aus ihnen errechenbaren Reaktionsgeschwindigkeitskonstanten kommen wir in Tabelle VI zu sprechen.

** In Klammern: die Werte des durch das Flepomin-Programm gelieferten Konfidenzintervalls bei einem Zuverlässigkeitsniveau von 95%.

Beim Versuch 1 war die Invertierung der HESSschen Matrix wegen ihrer Singularität erfolglos.

Tabelle II angeführt. Die Konfidenz-Intervalle der letzteren beziehen sich auf ein Zuverlässigkeitsniveau von 95%.

Wie ersichtlich, sind die optimalen Parameter in sehr abweichendem Maße bestimmt. Besonders beim Versuch 2 ist der Widerspruch zwischen dem Durchschnittsfehler des Ausgleichs und dem Konfidenzintervall der Parameter φ_1 und φ_2 auffallend. Wenn die Eigenwerte der zum Optimum gehörigen Kovarianz-Matrix nach der Methode von HOUSEHOLDER [7] bestimmt werden, ergibt sich der größte Eigenwert in der Größenordnung von 10^{14}, was darauf hindeutet, daß die HESSsche Matrix nahezu singulär, d. h. das Problem überbestimmt ist. Auffallend ist auch, daß es zum Auffinden des Optimums des besser konditionierten Versuches 2 bedeutend mehrerer Iterationen bedurfte als im ersten Experiment. Es schien nicht wahrscheinlich, daß dies nur die Folge der ungünstigeren Wahl des Anfangswertes des Parametervektors ist, deshalb untersuchten wir die »Spurenlinie« der Optimalisierung, d. h. die Werte der Parameter und der Zielfunktion nach den einzelnen Schritten der Iteration (Tabelle III).

Diese Daten zeigen, daß mit fortschreitender Iteration nur die Parameter φ_1 und φ_3 eine wesentlichere Änderung erfahren, und zwar so, daß ihr Verhältnis konstant bleibt. Die im Laufe der Iteration unveränderten Parameterkombi-

Tabelle III

Veränderungen der Zielfunktion und der Parameter während der Optimalisierung laut Modell A in Versuch 2

Zahl der Iterationen	$S(\varphi)$	φ_1	φ_2	φ_3	φ_4	φ_3/φ_1
0	5910	3	0,57	0,67	7,9	0,223
5	8,41	8,04	6,51	3,77	21,2	0,468
10	8,19	7,39	6,22	3,40	20,3	0,461
20	7,61	13,4	6,74	6,64	21,3	0,469
30	7,36	35,7	7,06	18,6	21,8	0.521
40	7,25	112	7,09	59,9	21,7	0,535
50	7,22	1 162	7,14	626	21,8	0,539
60	7,19	11 040	7,26	5880	21,7	0,533
70	7,19	14 700	7,33	7710	21,7	0,525
74	7,19	14 700	7,35	7710	21,7	0,525

nationen, mit den tatsächlichen Reaktionsgeschwindigkeitskonstanten [1] ausgedrückt, sind:

$$\varphi_2 \equiv \sqrt{k_{-2}/k_2} \equiv \frac{1}{\sqrt{K_2}}; \qquad \varphi_4 \equiv \frac{RT}{v} K_3 k_4; \qquad \varphi_3/\varphi_1 \equiv \frac{k_{-2}/K_3 k_4}{k_2/k_1} \equiv$$

$$\equiv \frac{k_1}{K_2 K_3 k_4}, \tag{1}$$

wo K_2 die Gleichgewichtskonstante der Wasserstoffadsorption bedeutet. Mit anderen Worten: in den stabilen Parameterkombinationen kommen k_2 und $k^-{}_2$, d. h. die Geschwindigkeitskonstanten der Wasserstoffad- und desorption nicht vor, sondern nur ihr Verhältnis, die Gleichgewichtskonstante der Sorption. Die chemische Ursache hierfür dürfte darin liegen, daß die Geschwindigkeit der Ad- und Desorption des Wasserstoffs um eine Größenordnung größer ist als die der übrigen Prozesse, infolgedessen weicht die Oberflächenbedeckung Θ_2 für Wasserstoff vom Gleichgewichtswert sehr wenig ab.

In dem bisher benutzten kinetischen Modell kann die chemische Realität, das $\Theta_2 = \Theta_{2,\text{Gleichgewicht}}$ so berücksichtig werden, daß man anstatt der Gleichung (10) in Mitteilung [1]

$$f_2(P, \Theta, \mathbf{k}) = k_2 p_2 (1 - \Theta_1 - \Theta_2)^2 - k_{-2}\Theta_2^2 = 0 \tag{2}$$

schreibt. Die Lösung der Gleichungen (10) in der Arbeit [1] mit dieser Substitution ist folgende:

$$\Theta_1 = \psi_1 \frac{P - p_2^0}{P - p_1^0} \tag{3}$$

$$\Theta_2 = \frac{P - p_1^0 - \psi_1 (P - p_2^0)}{\varphi_2 \sqrt{P - p_1^0} + P - p_1^0}. \tag{4}$$

Die zu lösende Differentialgleichung ist

$$\frac{dP}{dt} = -\psi_3 \Theta_1 \Theta_2^2. \tag{5}$$

Die Bedeutung der in den Gleichungen des im weiteren B genannten Modells vorkommenden Parameter ist folgende:

$$\psi_1 \equiv \frac{k_1}{K_2 K_3 k_4} \equiv \frac{\varphi_3}{\varphi_1}; \quad \psi_2 \equiv \frac{1}{\sqrt{K_2}} \equiv \varphi_2; \quad \psi_3 \equiv \frac{RT}{v} K_3 k_4 \equiv \varphi_4; \tag{6}$$

dies sind gerade jene Kombinationen der Parameter des Modells A die sich im Laufe der Iteration als konstant erwiesen.

Die optimalen Parameter des so abgeleiteten Modells B — auf analoge Weise wie oben bestimmt — liefern die in Tabelle IV angeführten Daten.

Ein Vergleich dieser Daten mit den entsprechenden Daten in Tabelle II bzw. III läßt feststellen, daß die optimalen Werte der neu eingeführten Parameter einerseits wirklich in guter Näherung zu der durch die Zusammenhänge (6) bestimmten Relation mit den entsprechenden optimalen Parametern des Modells A stehen, und andererseits in nahezu gleichem Maße bestimmt sind. Auffallend ist, daß der wesentliche Unterschied zwischen den Werten des mit auf zwei verschiedenen Wegen berechneten Konfidenz-Intervalls geschwunden ist.

Statistische Bewertung der Ergebnisse der Parameterschätzung

Der Erfolg der Optimalisierung und der numerische Wert der optimalen Reaktionskonstanten an sich sind von geringerem Wert und gestatten nicht, zu entscheiden, ob das mathematische Modell dem chemischen Vorgang ent-

Tabelle IV

*Die optimalen Parameter des Modells B**

	Versuch 1	Versuch 2
Parameter ψ_1	0,0244 ±0,0020 (0,0020)**	0,526 ±0,050 (0,052)**
Parameter ψ_2	3,68 ±2,50 (2,50)	7,35 ±0,89 (0,93)
Parameter ψ_3	103 ±23 (24)	21,7 ±1,4 (1,4)
Streuung s	1,129	0,506
F-Test $F\ (N_1, N_2)_{0,95}$	$F(16,8) = 5,48$ [9]	$F(28,\infty) = 2,15$ [9]
s_1^2/s_2^2	$s^2/s_{K,1}^2 = 1,58$	$s^2/s_{K,2\max}^2 = 2,89$
		$s^2/s_{K,2\min}^2 = 25,6$
Abbe-Probe $r_{0,95}$	0,603 [13]	0,695 [13]
r	0,877	0,312

* Siehe die Fußnote von Tabelle II.

spricht. Mit der statistischen Aufarbeitung der Ergebnisse müssen wir uns vor allem davon überzeugen, wie gut der Ausgleich ist, d. h. in welchem Maße das mathematische Modell die experimentelle Kurve zu reproduzieren vermag und dann die Zuverlässigkeit der optimalen Parameter von statistischem, wie auch von chemischem Gesichtspunkt prüfen.

Die Streuung des Ausgleichs (s, siehe Tabelle IV) und die Standarddeviation des Versuchs (σ) müssen miteinander in enger Beziehung stehen. Ist der Ausgleich nur so fehlerhaft wie die Messung, so beträgt der Erwartungswert von »s« σ. Sofern uns eine Schätzung s_K der Standarddeviation des Experiments von unabhängigen Versuchen zur Verfügung steht, empfiehlt WILLIAMS den sog. FISHERschen F-Test zum Vergleich der beiden Streuungswerte [8]. In unserem Fall kennen wir die Streuung s_K der Experimente nicht, können aber in Kenntnis der Versuchsbedingungen eine grobe Schätzung versuchen. Versuch 1 teilt nach dem Ablauf der Reaktion 9 Meßdaten für den Gleichgewichtsdruck mit. Ihre Streuung $s_{K,1}(8) = 0{,}9$ (in Klammern die Zahl der Freiheitsgrade). Nachdem wir hier den Fehler der Zeitrechnung unberücksichtigt ließen, kann die Unsicherheit der Punkte der kinetischen Kurve nur größer als diese sein. Im Versuch 2 sind die Ergebnisse von 7 Parallelmessungen zur Demonstrierung der Konstanz der Stabiltät des Katalysators mitgeteilt. Die Streuung der Druckwerte beträgt hier $s_{K,2}(6) = 0{,}3$. Der Fehler der Druckmessung am Torsionsmanometer beträgt 0,1 Einheit (13 Nm^{-2}) und so die Streuung der Druckwerte an der kinetischen Kurve

$$0{,}1 < \sigma_2 < 0{,}3 \,.$$

Das Ergebnis des F-Tests ist in Tabelle IV ausgeführt. Während beim Versuch 1 auch betreffs der minimalen Streuung gilt, daß

$$F_{0,95} > s_1^2/s_{K,k}^2$$

ist, mit anderen Worten die Wahrscheinlichkeit dessen, daß der Fehler der Anpassung signifikant größer ist als die Streuung der individuellen Druckwerte, kleiner als 5% beträgt, ist dies beim Versuch 2 nicht einmal für die geschätzte obere Schranke der Standarddeviation erfüllt.

Die Streuung ist ein Durchschnittswert und verrät als solcher absolut nichts darüber, wie sich der Anpassungsfehler zwischen den einzelnen Meßpunkten verteilt. Ist der Versuch in der Tat gleichwertig mit einer Exposition des mathematischen Modells, so können wir fordern, daß die einzelnen Meßpunkte ideal, ungeordnet um die auf sie angepaßte theoretische Funktion zu liegen kommen. In der Untersuchung der Erfüllung dieser Forderung ist das gewöhnlich verfolgte Verfahren — die gemeinsame Darstellung der Meßpunkte und der mit den optimalen Parametern berechneten theoretischen Funktion

(Abb. 1) — subjektiv und oft irreführend. Eine wesentlich wertvollere Information liefert in dieser Hinsicht die Analyse der Residualwerte der Fehlerfunktion [10, 11]. Werden die Residualwerte der Fehlerquadrate in der Abhängigkeit der berechneten Werte der abhängigen Variablen dargestellt, so können wir uns über die Anwendbarkeit des Modells, ja sogar über die Natur der eventuell vorkommenden Unzulänglichkeiten ein Bild machen.

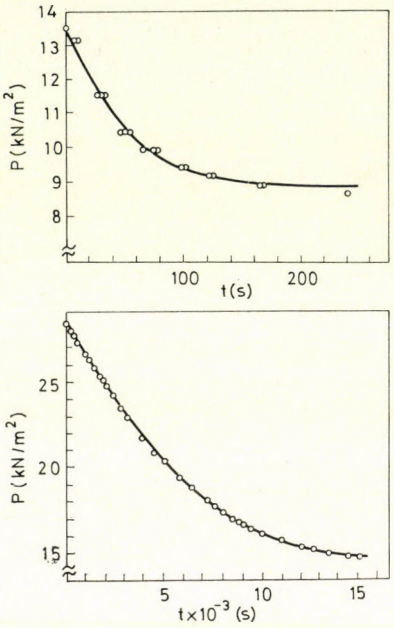

Abb. 1. Vergleich der Meßpunkte und der mittels der optimalen Parameter errechneten theoretischen Funktion

Es scheint allgemeiner und anschaulicher zu sein, wenn statt dessen durch Standardisierung der Unterschiede $(y_i - f_i)$ eine mit Erwartungswert Null und Streuung Eins charakterisierte Variable eingeführt und in der Abhängigkeit von der Reaktionskoordinate dargestellt wird. Auf diese Weise werden nämlich die unter verschiedenen Bedingungen erhaltenen Meßergebnisse miteinander vergleichbar (Abb. 2). Wie ersichtlich, zeigen die Meßpunkte im Versuch 2 einen entschiedenen Gang, einen systematischen Trend, während dies im Versuch 1 nicht der Fall ist.

Aber auch dieses demonstrative Verfahren ist nicht frei von den Fehlern der subjektiven Beurteilung. Das Kriterium des Fehlens des systematischen Trends der aufeinanderfolgenden Beobachtungen wurde von ABBE in die mathematische Statistik eingeführt [12]. Wir bilden den folgenden Ausdruck:

$$r = \frac{1}{2\Phi} \sum_{i=1}^{n-1} (q_{i+1} - q_i)^2 ,$$

wo Φ die Zahl der Freiheitsgrade und n die Zahl der Meßpunkte bedeuten.

Ist dieser Wert größer als ein Tabellenwert r_p, d. h. $r > r_p$, so ist p die Wahrscheinlichkeit des Fehlens des systematischen Trends [13]. Im Falle de

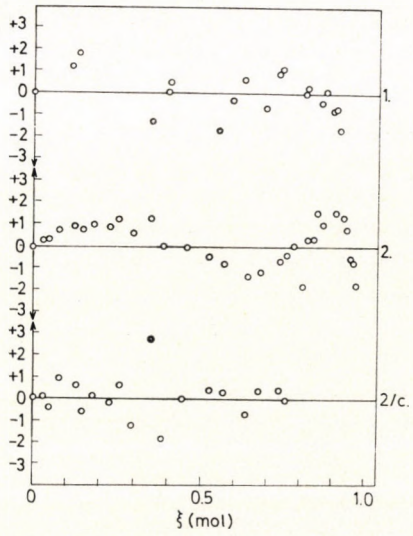

Abb. 2. Darstellung der standardisierten Residualwerte in Abhängigkeit von der Reaktionskoordinate

optimalisierten Messungen haben wir das Ergebnis dieser Untersuchungen in Tabelle IV dargetan. Wie wir sehen, erfüllt Versuch 2 auch diese Bedingung nicht.

Die Ursache dessen, daß die statistische Bewertung der beiden Versuche hinsichtlich der Beurteilung des hypothetischen Modells zu widersprechenden Ergebnissen führt, kann einerseits darin liegen, daß die Hypothese nicht zutrifft, der erste Versuch aber zu ungenau ist, um dies nachweisen zu können, oder andererseits darin, daß — obwohl die Hypothese zutrifft — wir im Versuch 2 die Grenzen ihrer Gültigkeit überschritten haben. Abbildung 2 ist zu entnehmen, daß ein beträchtlicher Teil der Meßpunkte den großen Konversionen zugehört. Stellen wir aus der theoretischen Funktion (3—4) die mit Hilfe der optimalen Parameter aus Versuch 2 errechenbaren Oberflächenkonzentrationen dar (Abb. 3), so ist festzustellen, daß die Voraussetzung der stationären Näherung, wonach $\partial\Theta/\partial t \approx 0$ sein sollte, nur bis zu einem Wert der Reaktionskoordinate von etwa $\xi = 0{,}8$ erfüllt wird. Versuch 2 enthält genügend Meß-

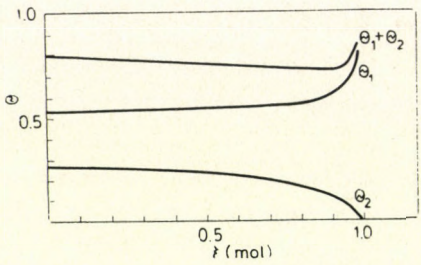

Abb. 3. Die Veränderung der mit den optimalen Parametern aufgrund der Zusammenhänge (3) und (4) berechneten Oberflächenkonzentration des Äthylens (Θ_1) und Wasserstoffs (Θ_2) mit fortschreitender Reaktion

punkte, um unter Weglassung der zu dem größeren Wert der Reaktionskoordinate gehörenden Punkte die Optimalisierung wiederholen zu können. In Tabelle V sind die optimalen Parameter und die Werte der statistischen Charakteristika des Optimums dargestellt, zu denen wir gelangen, wenn wir jeweils die letzten 4 Meßpunkte des Versuchs nacheinander weglassen.

Wie ersichtlich, erfahren die Werte der Parameter unter $= 0{,}76$ — den Erwartungen gemäß — keine nennenswerte Änderung und unterhalb dieser Grenze ist die Anpassung auch in statistischer Hinsicht entsprechend; sie erfüllt sowohl die Kriterien von FISCHER als auch die der ABBEschen Probe. Die Wirkung des Weglassens der zu einem größeren Wert als $\xi = 0{,}76$ gehörenden Punkte auf die Verteilung der q_i-Werte der Optimalisierung veranschaulicht das Diagramm 2/c in Abbildung 2.

Tabelle V

Die Veränderung der optimalen Parameter des Modells B und der den statistischen Charakteristika des Optimums beim Versuch 2 während der Optimalisierung der verschiedenen Konversionen entsprechenden Kurvenstücke

ξ	Φ	Optimale Parameter			s	$F/(s_1^2/s_2^2)$	r/r_p
		ψ_1	ψ_2	ψ_3			
0,97	28	0,526±0,050	7,35 ±0,89	21,7±1,4	0,506	0,084	0,449
0,92	24	0,704±0,003	4,50 ±0,06	29,9±2,4	0,332	0,203	0,951
0,83	20	0,788±0,001	2,56 ±0,01	40,6±3,1	0,245	0,387	1,82
0,76	16	0,847±0,002	0,935±0,007	58,5±1,4	0,110	2,07	2,67
0,56	12	0,845±0,004	1,091±0,187	56,4±3,9	0,123	1,74	2,90
0,34	8	0,827±0,016	1,96 ±0,37	54,5±6,8	0,112	2,34	2,52
0,18	4	0,835±0,015	0,366±0,091	44,4±0,3	0,065	5,68	3,23

ξ = Konversion; Φ = Zahl der Freiheitsgrade

Die Untersuchung der optimalen Reaktionsgeschwindigkeitskonstanten

Einen wesentlichen Schritt der Parameterschätzungsverfahren bildet die Berechnung der Konfidenzintervalle für die als optimal befundenen Parameter. Die einzelnen Verfahren sind auch in dieser Hinsicht nicht gleichwertig. Die sich aus der Benutzung des Flepomin-Programms ergebenden Probleme wurden bereits weiter oben erwähnt. Eine noch größere Schwierigkeit bedeutet der Umstand, daß die optimalen Parameter φ und ψ von den wirklichen Reaktionsgeschwindigkeitskonstanten abgeleitete, zusammengesetzte Parameter darstellen, wir aber in erster Linie die letzteren zum Gegenstand unserer Untersuchungen machen müssen. Die Standarddeviation der Funktionen der optimalen Parameter kann durch Verwendung der Standarddeviationen der unabhängigen Variablen aufgrund der Formel

$$\sigma_{kj}^2 = \sum_{i=1}^{m} \left(\frac{\partial k_j(\varphi)}{\partial \varphi_i} \right)^2 \sigma_{\varphi i}^2$$

— wo m die Zahl der Parameter ist — berechnet werden [14]. Dieses Verfahren führt aber in der Praxis nicht zu einem befriedigenden Ergebnis, weil die Streuungen $s\varphi$ der unabhängigen Variablen φ nur als grobe Schätzungswerte des Erwartungswertes $\sigma\varphi$ zu betrachten sind. Ein zweckentsprechenderes Verfahren ist, die Kovarianzmatrix aus den partiellen Ableitungen nach den tatsächlichen Konstanten der Zielfunktion aufzubauen, und daraus die Konfidenzintervalle der Reaktionskonstanten zu ermitteln.

Die optimalen Werte der Reaktionskonstanten, zusammen mit den auf die letztere Weise bestimmten Konfidenzintervallen, finden sich in Tabelle VI.

Tabelle VI

Vergleich der optimalen Reaktionskonstanten der Modelle A und B

*Modell A**

No.	ξ mol	$k_1 \cdot 10^4$ $\frac{\text{mol} \cdot m^2}{N \cdot s}$	$k_2 \cdot 10^4$ $\frac{\text{mol} \cdot m^2}{N \cdot s}$	k_{-2} $\frac{\text{mol}}{s}$	$(k_2/k_{-2}) \cdot 10^3$ $\frac{m^2}{N}$	$K_3 k_4$ $\frac{\text{mol}}{s}$
1	0,92	1,09	4,70	0,187	2,51	2,70
2	0,97	0,335	491	354	0,138	0,460
			Modell B			
					$K_2 \cdot 10^3$ m^2/N	
1	0,92	0,367 ± 0,798			0,551 ± 0,129	2,72 ± 45
2	0,97	0,335 ± 0,118			0,139 ± 0,034	0,460 ± 0,029
2/b	0,92	1,65 ± 0,23			0,369 ± 0,044	0,634 ± 0,018
2/c	0,76	90,3 ± 0,1			8,59 ± 0,01	1,241 ± 0,001

* Die HESSche Matrix ist nahezu singulär, nicht invertierbar, daher kann der Konfidenzintervall nicht angegeben werden.

Vergleichen wir die Reaktionskonstanten der beiden unter wesentlich abweichenden Bedingungen durchgeführten Messungen unter Berücksichtigung ihrer Zuverlässigkeit, so müssen wir feststellen, daß die Übereinstimmung hinsichtlich der einer gleichen Konversion zugehörigen Werte *B*1 und *B*2/*b* gut zu nennen ist. Als charakteristisch für den Prozeß aber müssen die in der Zeile *B*2/*c* befindlichen Werte betrachtet werden, mit denen sich die experimentelle Kurve zwischen den Werten $\xi = 0 - 0{,}76$ mit gleicher Genauigkeit beschreiben läßt.

Diese Tatsachen sprechen unbedingt dafür, daß das untersuchte Modell unter bestimmten Reaktionsbedingungen die Ergebnisse des Versuches zu repräsentieren vermag. Eine allgemeingültige Folgerung könnte aber nur durch die Auswertung von mehreren, bei unterschiedlicher Zusammensetzung und Temperatur durchgeführten Experimenten gezogen werden.

Die Mitteilung [4] gibt außer den erwähnten Daten — leider in Gestalt eines ausgeglichenen Diagramms — das Resultat von zwei bei 0 °C durchgeführten Messungen bekannt, bei denen das Verhältnis p_1^0/p_2^0 von 4 : 1 bis 1 : 4 reicht. Legt man über die Diagramme ein Netz und behandelt man die Schnittpunkte als »Meß«-Ergebnisse, so kann die Parameterschätzung ähnlich wie zuvor erfolgen (Tabelle VII).

Tabelle VII

Ergebnisse der aufgrund des Modells B durchgeführten Optimalisierung der in der Mitteilung [4] *angegebenen ausgeglichenen Kurvenschar*

Zahl der Messung	Gemischzusammensetzung p_1^0 kN/m²	Gemischzusammensetzung p_2^0 kN/m²	k_1 mol · m² / N · s	K_2 m² / N	K_3k_4 mol / s	s
11	12,52	52,99	0,232	0,257	0,412	1,42
12	13,44	40,16	$1{,}34 \cdot 10^{5}$	$3{,}02 \cdot 10^{5}$	0,286	1,09
13	13,32	27,87	$2{,}21 \cdot 10^{3}$	$1{,}01 \cdot 10^{4}$	0,214	1,06
14	14,30	14,08	$1{,}25 \cdot 10^{-5}$	$9{,}23 \cdot 10^{-5}$	0,418	0,799
15	27,10	13,48	$8{,}48 \cdot 10^{-7}$	$2{,}56 \cdot 10^{-7}$	83,8	1,83
16	39,96	13,60	$4{,}06 \cdot 10^{-7}$	$7{,}80 \cdot 10^{-7}$	17,9	1,71
17	53,48	13,40	$2{,}69 \cdot 10^{-7}$	$1{,}08 \cdot 10^{-7}$	9,08	1,34

Dieselbe Methode haben wir für die Meßwerte des früher schon bearbeiteten Experiments Nr. 2 angewendet (s. Zeile 14). Auf diese Weise kann der Fehler der oben erwähnten Methode in Betracht gezogen werden. Vergleicht man die in der 14. Zeile der Tabelle VII und in Zeile *B*2 in der Tabelle VI angeführten Werte miteinander, so sieht man deutlich, daß die Methode — obwohl bezüglich ihrer Anwendbarkeit im großen und ganzen diskutabel — für die Bestimmung von Tendenzen zweifellos geeignet ist.

Diese Tendenzen sind hinsichtlich der Gültigkeit des Modells *B* nicht im geringsten günstig. Dieses Modell — das im wesentlichen das HORIUTI—POLÁNYIsche mechanische Modell auf die beschriebene Weise [1] vereinfacht darstellt — vermag weder die reaktionskinetische Wirkung des Wasserstoff-, noch die des Äthylenüberschusses widerzuspiegeln.

Das Verhalten des Modells auf die Wirkung der Änderung der Zusammensetzung des Reaktionsgemisches kann auch geprüft werden, indem man die Anfgangsgeschwindigkeiten bei derselben Zusammensetzung für den experimentellen bzw. theoretischen Fall vergleicht. Zu diesem Zweck haben wir die aus den Diagrammen der Versuche 11—17 abgelesenen Druckwerte mit der WHITACKERschen Methode [15] numerisch deriviert und die so ermittelten Anfangsgeschwindigkeiten in Abbildung 4 als Funktion der Gemischzusammensetzung dargestellt; die Kurve wurde mit Exp. bezeichnet. Die Kurve *B* gibt die Gestaltung der bei der äquimolaren Zusammensetzung mit den optimalen *B*2/*c*-Parametern aus dem Modell *B* berechneten Anfangsgeschwindigkeiten an. Wie wir sehen, entspricht die letztere den experimentellen Ergebnissen nur in einer sehr engen Umgebung der äquimolaren Zusammensetzung.

Aufgrund unserer bisherigen Untersuchungen ist nicht festzustellen, ob der Widerspruch zwischen Modell und experimentellen Tatsachen der Unrichtigkeit der ursprünglichen HORIUTI—POLÁNYIschen Vorstellung oder aber der von uns angewandten Vereinfachung zuzuschreiben ist. Von den letzteren dürfte am ehesten die Vermutung, wonach die Oberflächenkonzentration des halbhydrierten Äthylradikals $\Theta_3 < 1$ ist ([1], S. 210), einer Korrektur bedürfen. Diese Vereinfachung haben wir, gestützt auf die später von MIYAHARA auch experimentell untermauerte Hypothese HORIUTIS eingeführt, wonach die Oberfläche des Nickels während der Hydrierungsreaktion praktisch unbedeckt ist [16, 17]. Diese Feststellung steht in krassem Widerspruch zu der aufgrund des Modells berechneten Oberflächenkonzentration (s. Abb. 3). Gleichzeitig haben CORMACK und Mitarbeiter [18] sowie MATSUZAKI und TADA [19] gezeigt, daß am Nickel unter den auch von uns experimentell untersuchten Bedingungen, die Oberflächenkonzentration des Kohlenwasserstoffs — in Übereinstimmung mit unseren Ergebnissen — $\Theta_1 \approx 0{,}5$ ist. Es liegen auch konkrete experimentelle Beweise dafür vor, daß ein ansehnlicher Teil des vom Nikkelkatalysator adsorbierten Olefins in halbhydrierter Form zugegen is [20, 21].

Die Berücksichtigung dessen, daß die Oberflächenkonzentration des halbhydrierten Äthylradikals $\Theta_3 > 0$ beträgt, ist unter Beibehaltung der übrigen Vereinfachungshypothesen auf zweierlei Arten möglich:

1. In der Mitteilung [1] ist das Reaktionsschema (5a)—(5d) unverändert gültig, doch ziehen wir die Reaktionen 2 und 3 nicht zusammen (Modell *C*);

2. Die experimentelle Tatsache, daß das Äthylen auf aktivem Nickel praktisch keinen Wasserstoff austauscht [3], berücksichtigen wir *anstatt* der Annahme $v(1)a \approx 0$ durch Einführung der Annahme $v(2) \approx 0$ (Modell *D*).

Diese beiden Näherungen des Problems lassen sich mathematisch folgendermaßen beschreiben:

Modell C

Die Gleichungen (9c), (9d) bzw. (2) in der Arbeit [1] werden den neuen Bedingungen entsprechend umformuliert:

$$dN_1 = k_1 p_1(1 - \Theta_1 - \Theta_2 - \Theta_3)^2 - K_3 k_4 \Theta_1 \Theta_2^2 \approx 0 \tag{7}$$

$$dN_2 = k_2 p_2(1 - \Theta_1 - \Theta_2 - \Theta_3)^2 - k_{-2}\Theta_2^2 \approx 0, \tag{8}$$

$$\text{wo} \qquad \Theta_3 = K_3 \Theta_1 \Theta_2 \qquad \text{und} \qquad k_2/k_{-2} = K_2. \tag{9}$$

Die Lösung von (7, 8) unter Berücksichtigung von (9) lautet:

$$\Theta_2 = \frac{P - p_1^0 - \psi_1 (P - p_2^0)}{\psi_2 \sqrt{P - p_1^0} + P - p_1^0 + \psi_4 (P - p_2^0)}, \tag{10}$$

mit $\psi_4 = k_1/K_2 k_4$.

Die Deutung der übrigen Parameter, der Ausdruck für Θ_1 sowie die zu lösende Differentialgleichung, stimmen mit den entsprechenden Ausdrücken des Modells *B* überein (3, 5, 6).

Modell D

Die (7—9) entsprechenden Gleichungen:

$$dN_1 = k_1 p_1(1 - \Theta_1 - \Theta_2 - \Theta_3)^2 - k_{-1}\Theta_1 - k_3 \Theta_1 \Theta_2 \approx 0 \tag{11}$$

$$dN_2 = k_2 p_2(1 - \Theta_1 - \Theta_2 - \Theta_3)^2 - k_{-2}\Theta_2^2 \approx 0 \tag{12}$$

$$dN_3 = k_3 \Theta_1 \Theta_2 - k_4 \Theta_2 \Theta_3 \approx 0 \tag{13}$$

mit $k_2/k_{-2} = K_2$.

Die Lösungen von (11—13):

$$\Theta_2 = \frac{k_3\sqrt{z} - k_{-1}(1+\sqrt{z}) + \sqrt{k_3^2 z - k_{-1}[4y(k_3/k_4+1) + 6k_3(z+\sqrt{z}) - k_{-1}(1+\sqrt{z})]}}{2y(k_3/k_4+1) + k_3(1+\sqrt{z})} \tag{14}$$

$$\Theta_1 = \frac{y\Theta_2^2}{z(k_{-1} + k_3 \Theta_2)} \tag{15}$$

$$\Theta_3 = \frac{k_3 y \Theta_2^2}{z k_4 (k_{-1} + k_3 \Theta_2)} \tag{16}$$

mit $y = k_1(P - p_2^0)$ und $z = K_2(P - p_1^0$

Die zu lösende Differentialgleichung ist

$$\frac{dP}{dt} = -\frac{RT}{v} k_4 \Theta_2 \Theta_3 . \tag{17}$$

Die optimalen Parameter der beiden Modelle und die statistischen Charakteristika des Optimums befinden sich in Tabelle VIII, sowohl für den vollständigen 2. Versuch, als auch für den, den Konversionen zwischen 0 und 0,76 entsprechenden, die stationären Verhältnisse besser widerspiegelnden Bereich.

Zwischen den Modellen *A*, *B*, *C* und *D* kann mittels Vergleichs der Streuungswerte — trotz ihrer beträchtlichen Abweichungen — kein Unter-

Tabelle VIII

Ergebnisse der Optimalisierung des Bereichs bis $\xi = 0{,}97$ sowie bis $\xi = 0{,}76$ im Versuch 2 aufgrund der Modelle C und D

		$\xi = 0{,}97$	$\xi = 0{,}76$
Modell C	$k_1 \frac{\text{mol} \cdot m^2}{N \cdot s}$	$(3{,}39 \pm 1{,}36) \cdot 10^{-5}$	$(1{,}43 \pm 2{,}16) \cdot 10^{-2}$
	k_2 m^2/N	$(2{,}89 \pm 0{,}74) \cdot 10^{-5}$	$(2{,}76 \pm 4{,}13) \cdot 10^{-3}$
	K_3	$2{,}51 \pm 0{,}59$	$1{,}50 \pm 0{,}16$
	k_4 mol/s	$0{,}908 \pm 0{,}158$	$4{,}08 \pm 0{,}43$
	Streuung:	0,508	0,113
	$F_{0,95}/(s_1^2/s_{K,2\min}^2)$	0,084	1,21
	$r/r_{0,95}$	0,454	2,72
Modell D*	$k_1 \frac{\text{mol} \cdot m^2}{N \cdot s}$	$(2{,}48 \pm 2{,}66) \cdot 10^{-2}$	$(1{,}48 \pm 0{,}47) \cdot 10^{-3}$
	k_{-1} mol/s	$(2{,}63 \pm 2{,}86) \cdot 10^{2}$	$11{,}5 \pm 1{,}1$
	K_2 m^2/N	$(9{,}92 \pm 3{,}30) \cdot 10^{-7}$	$(4{,}10 \pm 1{,}85) \cdot 10^{-6}$
	k_3 mol/s	$1{,}51 \pm 0{,}28$	$0{,}742 \pm 0{,}240$
	k_4 mol/s	$1{,}26 \pm 0{,}18$	$0{,}725 \pm 0{,}229$
	Streuung:	0,453	0,282
	$F_{0,95}/(s_1^2/s_{K,2\min}^2)$	0,106	0,268
	$r/r_{0,95}$	0,540	0,689

* Die Parameter k_1 und k_{-1} sind weitgehend korreliert. Die Iteration ist im Minimumbereich dermaßen verlangsamt, daß sie aufgegeben werden mußte, bevor sich die eingangs erwähnte Voraussetzung — wonach die Ableitungen der Zielfunktion nach den Parametern kleiner werden müssen als der Integrationsfehler — hätte erfüllen können.

schied gemacht werden, da sie sich auf die Ergebnisse desselben Versuches beziehen und so als sicher anzunehmen ist, daß die Statistik ihrer Streuungen keiner F-Verteilung entspricht [22]. Beim Vergleich der Streuungen mit den experimentellen Fehlern dagegen ist festzustellen, daß bei Berücksichtigung des Bereiches bis $\xi = 0{,}76$ des Versuches, von den drei Modellen das Modell D der F-Probe nicht genügt. Zu einem ähnlichen Ergebnis gelangen wir auch mit der ABBEschen Probe. Es zeigt sich, daß vom statistischen Gesichtspunkt aus die Modelle B und C gleichwertig sind, während das Modell D die kinetische Kurve bei einem so hohen Konfidenzniveau nicht zu repräsentieren vermag.

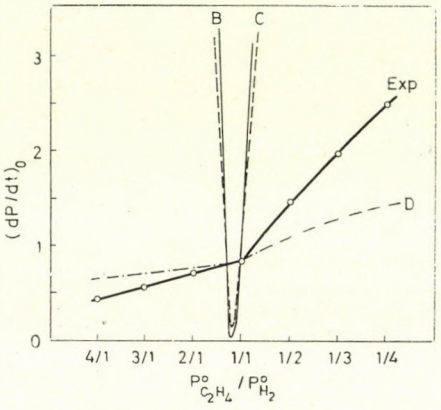

Abb. 4. Abhängigkeit der gemessenen und der aufgrund der einzelnen Modelle berechneten Anfangsgeschwindigkeiten von der Zusammensetzung des Reaktionsgemisches

Zu einer gerade entgegengesetzten Schlußfolgerung gelangen wir dagegen, wenn wir untersuchen, wie sich die mit den zu $\xi = 0{,}76$ gehörenden optimalen Parametern berechnete Anfangsgeschwindigkeit der Hydrierung in der Abhängigkeit von der Zusammensetzung des Reaktionsgemisches gestaltet. Aus Abbildung 4 erhellt, daß die Modelle B und C auch von diesem Gesichtspunkt praktisch gleichwertig sind, während das Modell D die Tendenz der Zusammensetzungsabhängigkeit der Anfangsgeschwindigkeit richtig wiedergibt.

Schlußfolgerungen

Unter Zugrundelegung des »assoziativen« Mechanismus der heterogenkatalytischen Hydrierung des Äthylens von HORIUTI—POLÁNYI lassen sich mehrere stationäre Modelle ableiten, die sich voneinander in der Beschaffenheit der vereinfachenden Hypothesen bzw. im Maße der Vernachlässigungen unterscheiden. Im Gegensatz zu der allgemein angewandten Praxis in der Fachliteratur haben wir bei keinem einzigen Modell die Existenz eines elemen-

taren geschwindigkeitsbestimmenden Reaktionsschrittes vorausgesetzt. Was das Verhältnis der einzelnen elementaren Reaktionen anbelangt, bedienten wir uns — im Interesse der Vereinfachung des Modells — nur dann vorläufiger Hypothesen, wenn die Literaturdaten dies eindeutig unterstützten. Die numerischen Werte der optimalen Parameter und ihre Zuverlässigkeit, sowie die bei der Optimalisierung beobachteten anderweitigen Erscheinungen dagegen haben es uns ermöglicht, betreffs des Verhältnisses der Geschwindigkeiten der einzelnen elementaren Reaktionen, nachträglich Informationen einzuholen und das Modell in diesem Sinne zu modifizieren. Die auf diese Weise iterativ entwickelten Modelle *B*, *C* und *D* beschreiben die Ergebnisse der kinetischen Versuche entsprechend den allgemein üblichen Forderungen. Die Kontrollberechnungen, die mit dem dissoziativen Modell von FARKAS [23] sowie mit dem bei der Hydrierung von Olefinen auf Palladiumkatalysator von UGO und CARRÁ erwiesenen RIDEAL—ELEYschen Modell [24] durchgeführt worden sind, ergaben eine viel schlechtere Anpassung der theoretischen Kurven an die experimentellen Punkte.

Die Analyse der Ergebnisse aber hat gezeigt, daß die Anpassung an die *einzelnen* kinetischen Kurven nur im Falle der Modelle *A*—*C* die strengsten statistischen Forderungen erfüllt, während die Abhängigkeit der Anfangsgeschwindigkeit von der Zusammensetzung des Reaktionsgemisches nur das hinsichtlich des zuvor erwähnten Gesichtspunktes nicht entsprechende Modell *D* richtig widerspiegelt.

Im Rahmen der Vorstellung von HORIUTI—POLÁNYI ist es also nicht gelungen, ein die am Nickel stattfindende Hydrierung des Äthylens in jeder Hinsicht richtig beschreibendes Modell zu finden. Es scheint nicht vollkommen ausgeschlossen zu sein, daß das Modell *D*, nach Aufhebung der hier angewendeten Vereinfachungen, sowohl den zeitlichen Verlauf als auch die Abhängigkeit der Anfangsgeschwindigkeit der Reaktion zu beschreiben fähig sein wird; trotzdem muß es mit Vorbehalt behandelt werden, da dieses Modell mit den in der Literatur beschriebenen Tatsachen im Widerspruch steht, wonach die Ausbildung einer halbhydrierten Äthylenschicht sowohl auf Nickel [21] als auch auf Platin [25] relativ schnell stattfindet. Aufgrund unserer Untersuchungen ist offenbar, daß dieses negative Ergebnis die Folge des assoziativien Modells und nicht der Unzulänglichkeit des rechentechnischen Appara tes ist. Aufgrund des Vergleichs der zu den verschiedenen Zusammensetzungens des Reaktionsgemisches gehörenden optimalen Sorptions- und Geschwindigkeitskonstanten (s. Tabelle VII) ist als wahrscheinlich anzunehmen, daß die an der Katalysatoroberfläche herrschenden Sorptionsverhältnisse wesentlich komplizierter sind als das von dem Modell widerspiegelte Bild.

Im Lichte der neueren Untersuchungen können an der Katalysatoroberfläche sowohl der Kohlenwasserstoff als auch der Wasserstoff in mehrererlei Sorptionszuständen anwesend sein. Obwohl am Nickel die assoziative Chemi-

sorption des Äthylens vorherrscht, konnte doch auch die dissoziative Chemisorption nachgewiesen werden [21], und an den Platinmetallen wird dieser letztere Typ unter gewissen Umständen überwiegend werden [26]. Das Äthylen wird in beiden Fällen an zwei Oberflächen-Metallatomen gebunden, und dies bedeutet, daß selbst an der mit Äthylen bedeckten Oberfläche unbedingt dem Wasserstoff zugängliche, aktive Leerstellen zurückbleiben. Diesen Umstand benutzten ROGERS, LIH und HOUGEN, als sie Propylen und Butylen an Platinkatalysator hydrierten, als Grundlage dafür, um ihre Versuche — unter Berücksichtigung der kompetitiven und nichtkompetitiven Adsorption des Wasserstoffs — auszuwerten [27]. Ihre Meßergebnisse wurden auch von MEZAKI [28] und KOLBOE [29] rechnerisch nachgeprüft; von ersterem aufgrund des assoziativen Mechanismus, unter der Annahme, daß die nichtkompetitive Wasserstoffadsorption gleichzeitig auch eine nichtdissoziative ist und von letzterem unter Annahme einer dissoziativen Olefinsorption an zwei energetisch unterschiedlichen aktiven Zentren. Die rechentechnische Methode von KOLBOE behandeln MEZAKI und DRAPER skeptisch, anerkennen aber die Berechtigung des aus der dissoziativen Adsorption beruhenden Modells [30].

Obwohl alle Autoren die Ergebnisse des erwähnten Versuchs mit Hilfe digitaler Parameterschätzung bewerteten, erlaubt es der einzige mitgeteilte statistische Parameter — die residuale Fehlerquadratsumme — nicht, einen Unterschied zwischen den empfohlenen Modellen zu machen. Die experimentelle Arbeit umfaßt einen sehr breiten Zusammensetzungs- und Temperaturintervall, teilt aber keine wiederholten Messungen mit; somit kann in Unkenntnis des tatsächlichen Meßfehlers eigentlich auch nicht entschieden werden, ob die Modelle wirklich den Versuch repräsentieren. Dazu kommt noch, daß alle Autoren ihre kinetische Gleichung aufgrund der Konzeption von HOUGEN—WATSON mit der a priori Voraussetzung *eines einzigen* geschwindigkeitsbestimmenden Reaktionsschrittes ableiteten, welcher Umstand höchstwahrscheinlich eine übermäßige Vereinfachung des tatsächlichen Zustandes ist. Fraglich ist ferner, ob es zulässig ist, den kompetitiv und nichtkompetitiv sorbierten Wasserstoff als zwei unabhängige Spezies zu behandeln und die kinetische Formel der Hydrierung *als Summe zweier Reaktionsgeschwindigkeiten* aufzuschreiben, wo doch an der Metalloberfläche der Wasserstoff aller Wahrscheinlichkeit nach *eine einzige* mobile Phase bildet, bzw. — wenn man auch die Existenz des in molekulärem Zustand sorbierten Wasserstoffs zuläßt — liegt doch der Gedanke nahe, daß dieser nicht nur über die Gasphase mit dem atomar chemisorbierten Wasserstoff in Wechselwirkung steht.

Alle diese Einwände ändern nichts an unserer Überzeugung, daß in der Erforschung des Mechanismus der kontakt-katalytischen Hydrierung der Olefine die komplexe Behandlung jener Weg ist, den wir weiter verfolgen müssen. Hierzu stehen aber in der Fachliteratur nicht hinreichend Informationen zur Verfügung, obwohl die Hydrierung des Äthylens zu den am gründ-

lichsten untersuchten katalytischen Reaktionen gehört. Die Präzisität der Meßergebnisse bzw. die Art der Publikationen machen die überwiegende Zahl der Daten von vornherein zur Verarbeitung mit Rechenmaschinen ungeeignet und die wenigen übrigbleibenden Versuche verteilen sich einerseits unter mehreren Katalysatoren, andererseits umfassen die jeweiligen Versuchsbedingungen (Gemischzusammensetzung, Temperatur, Druck usw.) nur einen sehr engen Intervall. In dieser Beziehung bilden nur die zuvor erwähnten Experimente von ROGERS, LIH und HOUGEN [27] eine Ausnahme, deren Wert aber durch das Fehlen von Parallelversuchen beträchtlich herabgesetzt wird. Zur Erzielung bedeutender neuer Ergebnisse bedarf es also umfassender, präziser und zweckmäßig gewählter Versuche. Die Rechentechnik stellt zwar ein empfindliches und vielseitiges Mittel in der Erforschung der Reaktionsmechanismen dar, wirklich wirksam aber kann sie nur werden, wenn sie mit der Versuchsplanung gekoppelt zur Anwendung gelangt.

LITERATUR

[1] FEJES, P., KÖNIG, P.: Acta Chim. (Budapest) **71,** 205 (1972)
[2] FEJES, P., KÖNIG, P.: Acta Chim. (Budapest) **71,** 217 (1972)
[3] GUCZI, L., TÉTENYI, P.: Z. Phys. Chem. **237,** 356 (1968)
Meßergebnisse: persönliche Mitteilungen
[4] TOYAMA, OSAMU: Rev. Phys. Chem. Japan, **11,** 353 (1937)
[5] KOWALIK, I., OSBORNE, M. R.: Methods for Unconstrained Optimization Problems, Elsevier, NY. (1968)
[6] WELLS, M.: Communications of the ACM, **8,** 169 (1965)
FLETCHER, R.: Communications of the ACM, **9,** 686 (1966)
[7] ICL Scientific subroutines p. 121 (1968)
[8] WILLIAMS, E. I.: Regression Analysis, Chap. 5. John Wiley, New York (1959)
[9] HODGMAN, C. D.: Handbook of Chemistry and Physics, p. 222. The Chemical Rubber Publ. Cleveland (1960)
[10] ANSCOMBE, F. I., TUKEY, I. W.: Technometrics **5,** (2), 141 (1963)
[11] BOX, G. E. P.: Ann. N.Y. Acad. Sci. **86,** (3) 792 (1960)
[12] ABBÉ, E.: Werke, Bd. 2. pp. 55—81. Iena (1906)
[13] LINNIK, YU. V.: Method of Least Squares, pp. 109—113, 360. Pergamon (1961)
[14] WORTHING, A. G., GEFFNER, I.: Treatment of Experimental Data. Wiley (1943)
[15] WHITACKER, S., PIGFORD, R. L.: Ind. Eng. Chem. **52,** 185 (1960)
[16] HORIUTI, I.: I. Res. Inst. Catalysis, Hokkaido Univ. **6,** 250 (1958)
[17] MIYAHARA, K., TERATANI, S., TSUMURA, A.: I. Res. Inst. Catalysis, Hokkaido Univ. **12,** 98 (1965)
[18] CORMACK, D., THOMSON, S. I., WEBB, G.: J. Catal. **5,** 224 (1966)
[19] MATSUZAKI, I., TADA, A.: J. Catal. **13,** 215 (1969)
[20] ERKELENS, I., LIEFKENS, TH. I.: J. Catal. **8,** 36 (1967)
[21] HIROTA, K., HIRONAKA, Y.: J. Catal. **4,** 602 (1965)
[22] DRAPER, N. R., SMITH, H.: Applied Regression Analysis, Chap. 10. Wiley, N.Y. (1966)
[23] FARKAS, A.: Trans. Faraday Soc. **35,** 906 (1939)
[24] UGO, R., CARRÁ, S.: Inorganica Chimica Acta Reviews 49, **1967**
[25] BLOCK, I., THIMM, H., ZEI, M. S.: Int. Symposium on Heterogen Catal. VARNA 1971; Abstracts
[26] HIROTA, K., HIRONAKA, Y.: Bull. Chem. Soc. Jap. **39,** 2638 (1966)
[27] ROGERS, G. B., LIH, M. M., HOUGEN, O. A.: A.I.Ch.E. Journal **12,** 369 (1966)
[28] MEZAKI, R.: J. Catal. **10,** 238 (1968)
[29] KOLBOE, S.: J. Catal. **24,** 40 (1972)
[30] MEZAKI, R., DRAPER, N. R.: J. Catal. **28,** 179 (1973)

Péter KŐNIG; 1121 Budapest, Konkoly Thege M. út
Pál FEJES; 671 Szeged, Ungarn.

Acta Chimica Academiae Scientiarum Hungaricae, 84 (2), pp. 161—166 (1975)

KINETIC EQUATIONS OF MULTISTEP ELECTRODE PROCESSES, I

L. KISS and J. FARKAS

(Department of Physical Chemistry and Radiology, L. Eötvös University, Budapest)

Received May 9, 1974

The equation of the polarization curve has been deduced and analyzed for metal ionization and metal-ion reduction proceeding in m steps, for the case when the process is influenced only by charge transfer. The concentration of the intermediate at the electrode surface has been calculated as a function of the electrode potential and of the current density passing through the electrode.

In an earlier communication [1] a method has been given for the calculation of the polarization curves of metal ionization and metal ion neutralization processes taking place by charge transfer in several successive steps (multistep process), for the case when the kinetics of the process are influenced both by diffusion and charge transfer. In the course of these investigations, the following processes have been studied:

$$M \underset{k_{k1}}{\overset{k_{a1}}{\rightleftharpoons}} M^{z_1+} + n_1 e \qquad \text{(I)}$$

$$M^{z_1+} \underset{k_{k2}}{\overset{k_{a2}}{\rightleftharpoons}} M^{z_2+} + n_2 e \qquad \text{(II)}$$

. . . . . .

$$M^{z(i-1)+} \underset{k_{k_i}}{\overset{k_{ai}}{\rightleftharpoons}} M^{zi+} + n_i e \qquad (i)$$

. . . . . .

$$M^{z(m-1)+} \underset{k_{km}}{\overset{k_{am}}{\rightleftharpoons}} M^{zm+} + n_m e \qquad (m)$$

where M is the metal, M^{z_i+} are ions with charge number z_i ($i = 1, 2, \ldots i, \ldots m$), n_i is the number of elementary charges transferred in the individual steps, and k_{ai} and k_{ki} are rate constants depending on the electrode potential.

The conditions under which the diffusion of the components does not influence the kinetics of processes (I) — (m) have been given. Under consideration of the fulfilment of these conditions, the present communication gives the polarization curves of processes (I) — (m), and the concentrations of the intermediate ions at the electrode surface when current passes through the electrode, for the case when these are not influenced by diffusion.

If we assume that the solution contains an excess of indifferent electrolyte, and that the intermediates do not react with each other or with other components of the solution at the surface of the electrode, then, after a steady state has been reached for electrode process (I) — (m), the following equation can be written for the current density j:

$$j = j_1 + j_2 + \ldots j_i + \ldots + j_m = \frac{z_m}{n_i} j_i \tag{1}$$

where

$$\begin{aligned} j_1 &= k_{a_1} c_{00} - k_{k_1} c_{10} \\ j_2 &= k_{a_2} c_{10} - k_{k_2} c_{20} \\ &\vdots \\ j_i &= k_{a_i} c_{(i-1)0} - k_{k_i} c_{i0} \\ &\vdots \\ j_m &= k_{a_m} c_{(m-1)0} - k_{k_m} c_{m0} \end{aligned} \tag{2}$$

where j_i is the current density due to the i-th electrode process, c_{00} is the concentration (activity) of the metal at the electrode surface, which is taken as unity in the case of a pure solid metal electrode, c_{i0} is the concentration of the M^{zi+} ion at the electrode surface, $c_{m\infty}$ is the concentration of the M^{zm+} ion in the bulk of the solution (under the conditions selected, $c_{m0} = c_{m\infty}$).*

From the set of equations (2), a linear inhomogeneous system of equations can be derived under consideration of Eq. (1), which can be solved for the unknown $j, c_{1,0}, c_{2,0}, \ldots c_{i0}, \ldots c_{(m-1)0}$.

Using this method, the following expression is obtained for the polarization curve of electrode process (I) — (m) proceeding in m steps:**

$$j = z_m \frac{1 - \prod_{i=1}^{m} \frac{k_{ki}}{k_{ai}} c_{m\infty}}{\sum_{i=1}^{m} \left[n_i \prod_{j=0}^{i-1} k_{kj} \left(\prod_{l=1}^{i} k_{al} \right)^{-1} \right]_i} \tag{3}$$

where $k_{k_0} = 1$. Thus relationship (3) relates to the case when the diffusion of the components does not influence the rate and only transfer polarization

* If the electrode is made of an amalgam, $c_{00} \neq 1$, and the diffusion of the metal does not affect the kinetics of the process if $c_{00} = c_{\infty}$, *where* $c_{0\infty}$ is the concentration of the metal in the bulk of the amalgam.

** In the following, k_{a_1} in the equations of the polarization curves should be understood as its product with a metal concentration of unity while, when compared with other rate constants, k_{a_1} is expressed in its own unit current density concentration.

occurs. A similar relationship has been deduced by HURD [2] for a multistep redox process with $n_i = 1$. Certain problems connected with the polarization curves of processes of the type (I) — (m) have been discussed also by LOSEV [3] for the case of $n_i = 1$.

In the case of a multistep process with transfer polarization, only the φ *vs.* lg j plot (where φ is the electrode potential) gives a straight line if the rate constants for one of the steps are small compared to those of the other steps [4], or if strong cathodic or anodic polarization is used. If the rate constants of the k-th step are low compared those of the other steps, *i.e.*:

$$(k_{k_k} + k_{a_k}) \ll (k_{k_i} + k_{a_i}) \qquad i = 1, 2 \ldots m; \qquad i \neq k \tag{4}$$

the following expressions are obtained for the apparent anodic (α') and cathodic (β') transfer coefficients:

$$\alpha'_k = n_k \alpha_k + \sum_{i=1}^{k-1} n_i \tag{5}$$

$$\beta'_k = n_k (1 - \alpha_k) + \sum_{i=k+1}^{m} n_i \tag{6}$$

where α_k is the true transfer coefficient of the k-th step of electrode process (I) — (m). If the rate constants are of the same order of magnitude and the polarization of the electrode is sufficiently strong to attain the straight section of the φ *vs.* lg j curve, or in any other case when the anodic or cathodic polarization is sufficiently high, the apparent transfer coefficients are:

$$\alpha' = n_1 \alpha_1 \qquad \beta' = n_m (1 - \alpha_m) \tag{7}$$

where α_1 and α_m are the true transfer coefficients of the first and the (m)-th step. In this case, the kinetics of the electrode process are determined by the first step of metal ionization (anodic process) or metal ion reduction cathodic process.

It can be seen therefore from relationships (5) and (6) that if the linear sections on both the anodic and cathodic polarization curves are due to the relatively low rate constants of the same reaction step, the following expression is valid for the sum of the apparent transfer coefficients:

$$\alpha'_k + \beta'_k = z_m , \tag{8}$$

similarly as in the case of the single-step mechanism. If this condition is not fulfilled, then

$$\alpha'_k + \beta'_k \neq z_m \tag{9}$$

If the electrode process is not a multistep process, the approximate value of the ratio α'/β' is always 1. In the case of a stepwise mechanism, the ratio α'/β' can only be equal or nearly equal to 1 if

$$\sum_{i=1}^{k-1} n_i = \sum_{i=k+1}^{m} n_i \tag{10}$$

and if the Eqs (7) are valid, and $n_1 = n_m$.

The above considerations concerning α' and β' are suitable to establish the existence of a stepwise mechanism.

On the basis of relationships (3)—(6), it can also be established that if the kinetics of the process proceeding *via m* successive charge-transfer steps is not influenced by diffusion, a maximum of m different linear sections can be observed on the anodic and cathodic φ *vs.* lg j curves [4.] The slopes of the straight lines increase with increasing polarization, and the magnitude of the apparent transfer coefficient decreases. The transfer coefficients of the linear sections permit to determine, using relationships (5) and (6), which of the reaction steps is rate-determining in the individual potential ranges. The number of linear sections found experimentally is generally less than m, owing to the fact the that feasible electrode potential (current density) range is not sufficiently wide.

Losev *et al.* [3, 5, 6] found in their study of bismuth amalgam, in accordance with the above, three linear sections on the cathodic polarization curve, while two linear sections could be separated on the anodic polarization curve.

Under the conditions discussed earlier, *i.e.* if relationships (1) and (2) are valid, the concentration of the intermediates at the electrode surface can be calculated. For a process occuring in two one-electron steps, this concentration has been given by Losev *et al.* [7]. In the general case discussed above, the following expression is obtained for the concentration of the k-th intermediate (c_k) at the electrode surface:

$$c_{k0} = \frac{j}{z_m} \sum_{i=k+1}^{m} \left[n_i \left(\prod_{p=k+1}^{i} k_{ap} \right)^{-1} \prod_{s=k}^{i-1} k_{ks} \right]_i + \prod_{s=k+1}^{m} k_{ks} \left(\prod_{p=k+1}^{m} k_{ap} \right)^{-1} c_{m\infty} \tag{11}$$

where $k_{k_k} = 1$.

Let us now investigate the possible variation of c_{k0} with the anodic polarization. For the sake of simplicity, the case of $c_{m\infty} = 0$ will be considered. Then, from Eq. (11):

$$\left(\frac{\partial c_{k0}}{\partial \varphi} \right) = A \left(\frac{\partial j}{\partial \varphi} \right) + j \left(\frac{\partial A}{\partial \varphi} \right), \tag{12}$$

where

$$A = \frac{1}{z_m} \sum \left[n_i \left(\prod_{p=k+1}^{i} k_{ap} \right)^{-1} \prod_{s=k}^{i-1} k_{k_s} \right]_i$$

from expression (11).

Under the condition given and with the notations used, j, A and $\left(\frac{\partial j}{\partial \varphi}\right)$ are always positive for anodic polarization, while $\left(\frac{\partial A}{\partial \varphi}\right)$ is always negative. Accordingly, c_{k0} increases with anodic polarization if

$$\left| A \left(\frac{\partial j}{\partial \varphi} \right) \right| > \left| j \left(\frac{\partial A}{\partial \varphi} \right) \right|, \tag{13}$$

while it decreases if

$$\left| A \left(\frac{\partial j}{\partial \varphi} \right) \right| < \left| j \left(\frac{\partial A}{\partial \varphi} \right) \right| \tag{14}$$

c_{k0} does not change with anodic polarization if

$$\left| A \left(\frac{\partial j}{\partial \varphi} \right) \right| = \left| j \left(\frac{\partial A}{\partial \varphi} \right) \right| \tag{15}$$

It can be seen from the above relationships, and particularly from Eqs. (13) and (14), that at low anodic polarization, the realization of condition (13), *i.e.* the increase of c_{k0} with anodic polarization, is to be expected, because the value of A is relatively high and that of j small. At higher anodic polarization, condition (14) can be realized, *i.e.* in this case the concentrations of the M^{z_k+} ions at the electrode surface decrease with anodic polarization. Condition (15) may be realized, when the anodic polarization is sufficiently strong and the condition $n_1\alpha_1 = n_{(k+1)}\alpha_{(k+1)}$.

As can be seen from relationship (11), condition (14), *i.e.* the decrease of c_{k0} with anodic polarization, can be realized only in the case of $k = (m - 1)$, when the anodic polarization is sufficiently high, and $n_1\alpha_1 < n_m\alpha_m$ [3, 6]. If this latter condition is not fulfilled, $c_{(m-1)0}$ can only increase $(n_1\alpha_1 > n_m\alpha_m)$ or remain constant $(n_1\alpha_1 = n_m\alpha_m)$ under the given conditions when the anodic polarization is changing. It should be mentioned, however, that when the process is influenced also by diffusion, the value of $c_{(m-1)0}$ can decrease also in the case of $n_1\alpha_1 = n_m\alpha_m$ [8, 9].

REFERENCES

[1] Л. Киш, Й. Фаркаш: Электрохимия. **7,** 1744 (1971)
[2] Hurd, R. M.: J. Electrochem. Soc. **109,** 327 (1962)
[3] В. В. Лосев: Итоги науки «Электрохимия» том 6. стр. 65
[4] Mauser, H.: Zeitschr. f. Elektrochemie **62,** 419 (1958); D. M. Mohilner: J. Phys. Chem. **68,** 623 (1964)

[5] В. В. Городецкий, В. В. Лосев: Электрохимия, **3,** 1192 (1967)
[6] Losev, V. V.: Electrochim. Acta **15,** 1095 (1970)
[7] В. В. Лосев, В. В. Городецкий: Электрохимия, **4,** 1103 (1968); А. М. Молодов, В. В. Лосев: Итоги науки, «Электрохимия», **7,** 65 (1971)
[8] Kiss, L., Farkas, J., Fóthi, Á.: Magy. Kém. Foly. **79,** 483 (1973); Acta Chim. (Budapest) **82,** 153 (1974)
[9] Kiss, L., Farkas, J., Fóthi, Á.: Magy. Kém. Foly. **78,** 202 (1972); Acta Chim. (Budapest) **74,** 123 (1972)

László Kiss
József Farkas } 1088 Budapest, Puskin u. 11—13. Hungary.

Acta Chimica Academiae Scientiarum Hungaricae, 84 (2), pp. 167—180 (1975)

SYNTHESIS OF O-SUBSTITUTED HYDROXYLAMINES

E. KASZTREINER, G. SZILÁGYI, J. KOSÁRY and ZS. HUSZTI

(Research Institute for Pharmaceutical Chemistry, Budapest)

Received February 5, 1973; in revised form, March 5, 1974

In the course of the preparation of O-substituted hydroxylamines possessing histidine decarboxylase-inhibiting action, a novel procedure of dephthaloylation has been worked out: the N-(substituted-oxy)-phthalimides were dephthaloylated by primary amines instead of the hydrazine method known from the literature.

Advantages of the procedure consist in its wide utility, mild conditions, high yields and in the fact that the method is useful in synthesizing also O-substituted hydroxylamines containing groups sensitive to hydrazine, in favourable yields.

In a study of the reaction mechanism, N-alkyl-N'-(substituted oxy)-phthalamide intermediates were successfully isolated. The following factors influencing the reaction were studied: solvent, dilution, basicity of the primary amines and steric relations. Of the compounds prepared, 2-hydroxy-5-carbomethoxybenzyloxyamine will be the subject of clinical trial.

In the living organism, histamine is formed from histidine by decarboxylation and this process is catalyzed by the enzyme-histidine decarboxylase [1]. As several diseases are evoked by histamine formed in pathologically high amounts, our endeavour was the research of a histidine-decarboxylase inhibitor that might be therapeutically useful for reduction of the histamine level. Of the compounds described in the literature, Brocresine (3-hydroxy-4-brombenzyloxyamine) [2] is one of the best known substances for this purpose. Other hydroxylamine derivatives were reported by HAMOR *et al.* [3].

Several O-substituted hydroxylamines have been prepared for investigation of this effect. Among the known methods [4], the following one [5] seemed to be the most useful: reaction of an RX halide with N-hydroxyphtalimide, and isolation of the $RONH_2$(**II**) endproduct after dephthaloylation of the N-(substituted-oxy)-phthalimide **I** obtained.

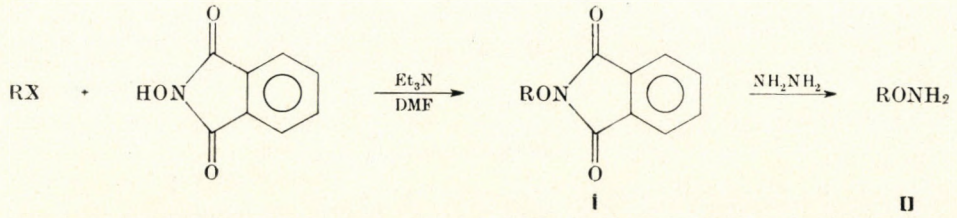

I **II**

Advantages of this method are that the intermediates (**I**) are well-crystallizable and the phthaloyl protecting group can be split off by means of

hydrazine within a few hours. On the other hand, the use of the hydrazine has the disadvantage that, because of its great nucleophilicity, it may also react with other functional groups (ester groups, mobile halogen atoms). Furthermore, the yield of the hydrazinolysis declines significantly when the scale of the experiments is increased.

Therefore, we carried out the dephthaloylation under milder conditions. Aliphatic primary amines proved to be very useful for this purpose and this method could be generally employed for the synthesis of compounds of type **II**. In the reaction of equimolar amounts of **I** and the primary amine, N-alkylphthalimide (**III**) is formed [6] in addition to the desired end product (**II**); however, if an excess of the amine is used, **III** reacts further and N,N'-dialkylphtalamide (**IV**) is obtained.

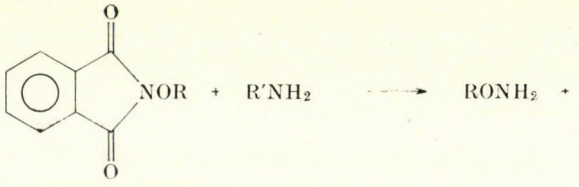

I **II**

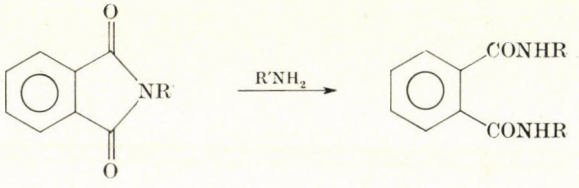

III **IV**

The overall reaction proceeds according to the mechanism of nucleophilic substitutions. (See on the next p.)

In the first step, the lone electron pair of the nitrogen atom of the amino group attacks on the electrophilic carbon atom of the imide (**I**) and the 'carbinolamine' 'A' is formed in a reversible process. The imide bond of this carbinolamine is split in an irreversible process to give an N-alkyl-N'-(substituted oxy)-phthalamide of type **V**. In this substance the amine, because of its greater nucleophilicity, starts an intramolecular attack on the electrophilic carbon atom of the hydroxamic acid bond and gives rise to the 'carbinolamine' 'B' in a reversible process; this intermediate is then stabilized by eliminating $RONH_2$ (**II**) in an irreversible reaction. Simultaneously, N-alkylphthalimide (**III**) is formed that reacts further with the excess of the primary amine to yield N,N'-dialkylphthalamide (**IV**).

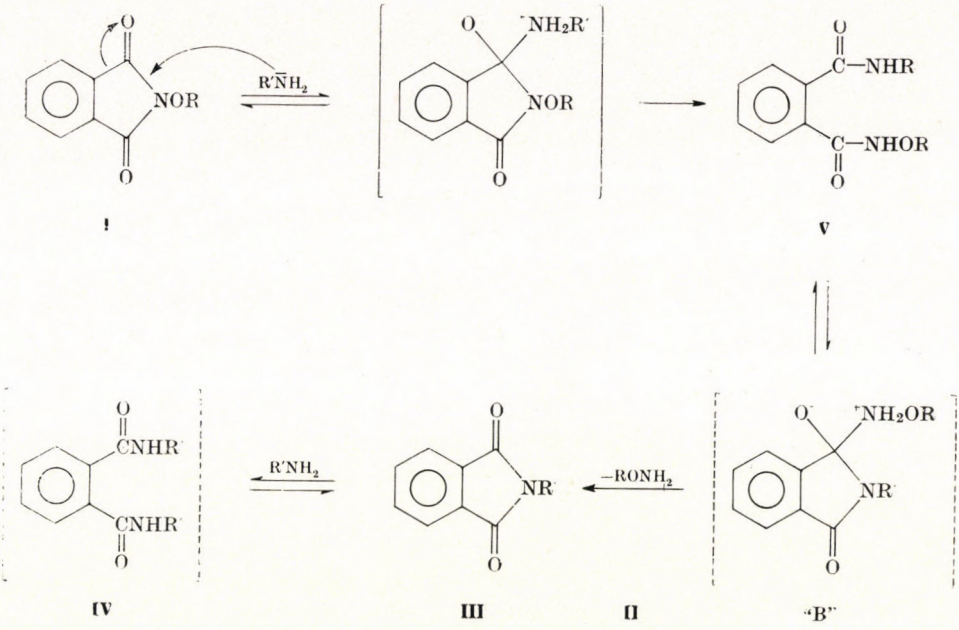

I V

IV III II "B"

This reaction can also be effected with salts formed from primary amines and organic acids, however, it fails with the salts consisting of primary amines and inorganic acids. In the course of the reaction, the salt of **II** with an organic acid as well as N-alkylphthalimide are obtained even in the case when a molar excess of the amine salt is present. In the reaction steps, the substances **II**, **III**, **IV** and **V** were isolated and their structures verified by spectroscopy. The carbinolamines 'A' and 'B' could not be isolated so far.

During the study of the reaction, the role of some factors have been investigated in detail.

Role of the solvent

When the reaction is carried out without solvent or in a polar solvent (alcohols), the products **II** and **III** (or **II** and **IV**) are obtained. When the solvent is non-polar, *e.g.* benzene, the rate of the dephthaloylation reaction decreases in the temperature interval from 8 to 12 °C to such a degree that the N-alkyl-N'-(substituted oxy)-phthalamides of type **V** are isolated in nearly quantitative yield:

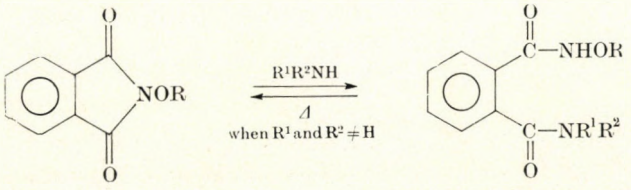

I V

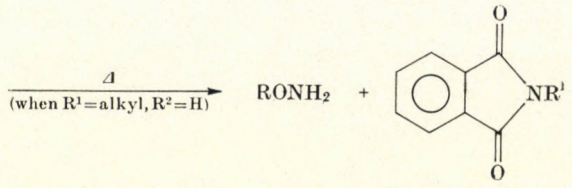

II III

These compounds are stable under the usual conditions for a long time, but on pyrolysis (above the melting point) or on heating in a solvent they undergo further transformation and give rise to the products **II** and **III**. When the reaction is carried out in polar, aprotic solvent (*e.g.* in nitromethane), then similarly, substances of type **V** are obtained. It is to be noted that the interaction of **I** with secondary amines (*e.g.* morpholine, piperidine) also leads to compounds of type **V** in a high yield. However, on heating these latter substances, the starting material (**I**) is recovered.

The reaction takes a different course when **I** and a primary amine are allowed to react in methanol (or ethanol), but *at a great* (200-fold) *dilution ratio*, at a temperature between 5 and 10 °C. In this case, solvolysis becomes prominent, and the esters of N-(substituted oxy)-phthalamic acids are obtained:



I VI

The primary amine does not play a part in this reaction, for **VI** can also be prepared from **I** and the appropriate alcohol, in the absence of any primary amine. Compounds of type **VI** are relatively stable, but at temperatures above the melting point they give back the starting substance (**I**) with the elimination of the alcohol.

Role of the primary amine

The main driving force of the reaction is the difference between the basicities of the entering and leaving amine. (The dissociation constants of aliphatic primary amines and oxyamines differ by about 5 orders of magnitude.)

When the reaction is carried cut at atmospheric pressure, in aqueous or alcoholic solution, with ammonia or primary aliphatic or alicyclic amines (*e.g.*

n-butyl-, allyl-, *n*-amyl-, cyclopropyl-, cyclohexylamine), *i.e.* with strong bases, then the reaction proceeds rapidly and easily. The same holds true of the highly basic secondary amines (morpholine, piperidine). Here the reaction comes, of course, to an end at **V**.

The rate of reaction is not significantly influenced by an increase in the length of the carbon chain. However, with amines containing bulky alkyl groups (benzhydrylamine, *t*-butylamine), the time of reaction is considerably longer — probably owing to steric hindrance — and compounds of type **V** are isolated only in a low yield.

Accomplishment by primary amines of the dephthaloylation offers several advantages:

(*a*) If the end product **II** or its salt is insoluble in the reaction medium, dephthaloylation is effected by such amines where **III** remains dissolved after the reaction is over (*e.g.* *n*-butylamine). At the end of the reaction, **II** (or its salt prepared by the addition of an acid) is then isolated by filtration;

(*b*) when, hovewer, **II** remains dissolved after accomplishment of the reaction, the primary amine and its quantity should be chosen such that **III** or **IV** forming along with **II** will be precipitated from the mixture (N-cyclopropylphthalimide, N,N'-dicyclopropylphthalamide) and **II** is then obtained from the filtrate;

(*c*) the mildness of the method is shown by the fact that it is useful also in the synthesis of such products of type **II** where there is a branching on the carbon atom next to the oxyamine group **II** *c* and *g* [7], although the yields are moderate in this case;

(*d*) even in the presence of groups sensitive to hydrazine (*e.g.* ester group, mobile halogen), the hydroxylamine derivatives are obtained by our method based on aminolysis in a nearly quantitative yield.

It should be noted that the reactions of N-substituted phthalimides with primary amines [8—14], for removal of the protecting phthaloyl group are known from the literature. It is, however, evident that the reaction of **I** with primary amines is in some respects different from the interaction of N-alkylphthalimides with amines. The reaction of **I** with primary amines proceeds under much milder conditions than the ring cleavage of N-alkylphthalimides by amines. An additional difference is that **I** can be brought into reaction with the salts consisting of aliphatic primary amines and organic acids; N-alkylphthalimides do not react in this way.

To our knowledge, no other results have been published on the alcoholic solvolysis of N-alkyl-phthalimides. In the meantime, BROWN *et al.* reported [15] that 1-(2-aminoxyethyl)-cytosine and 1-(2-aminoxyethyl)-N(4)-methyl-cytosine were prepared from the corresponding phthalimido compounds by ammonia or methylamine, respectively, under pressure and this procedure was used for N-methoxy-, N-butoxy- and N-benzyloxyphthalimide, too. How-

ever, the reaction was not investigated in detail and it was only supposed that the cleavage by methanolic ammonia of N-alkoxy-phthalimides could be generally used for the synthesis of alkoxyamines.

Table I shows the substances prepared by this method [16]. It is evident that the procedure is equally suitable for the synthesis of O-alkyl, O-(substituted benzyl)- and O-(heterocyclylmethyl)-hydroxylamines.

Although the method proved to be generally useful in our experiments, in some cases the hydrazinolysis turned out to be more reasonable for obtaining the endproduct **II** (**II***m*, *n*). These and the substances prepared only by hydrazinolysis (**II***o*, *p*) are shown in Table II. Data of the corresponding intermediates (**I**) are found in Table III and those of type **V** in Table IV.

The majority of our compounds displayed an inhibiting effect against the histidine-decarboxylase enzymes. The most active substances inhibited the rat-stomach-histidine decarboxylase at a concentration of 5×10^{-6}—10^{-7} mole *in vitro*. *In vivo*, they proved to be effective in a dose of 15—45 mg/kg of body-weight and significantly reduced the histamine level of ratstomach and ratlung. Of the substances mentioned above, **II***e* (2-hydroxy-5-carbomethoxy-benzyl-oxy-amine) had an antiinflammatory action, too, and the toxicological data also proved favourable [17, 18].

Experimental

M.p.'s were determined on a Kofler block and are uncorrected.

Preparation of N-(substituted-oxy)-phthalimides (I)

To a mixture of N-hydroxyphthalimide (0.093 mole), the appropriate halide compound (0.1 mole) and dimethylformamide (120 ml), a solution of abs. triethylamine (0.103 mole) in dimethylformamide (30 ml) was added by drops at 5—10 °C, with stirring and cooling in ice-water, during about 3 hrs. The reaction mixture was allowed to stand 3 days and then poured into 10% hydrochloric acid (600 ml) or into 600 ml of water, if the substituent R contained a basic nitrogen atom. The crystals which precipitated were filtered off, washed with water and recrystallized.

Preparation of O-substituted hydroxylamines (II)

1. *By aminolysis*

Method A:

The N-(substituted-oxy)-phthalimide (0.1 mole) was made to react with the primary amine (0.1 mole) in ethanol (200 ml) and the pH of the mixture was then adjusted to Congo blue by ethanolic hydrogen chloride solution. The precipitation of **II** hydrochloride was completed by adding ether and the salt was filtered off and dried. From the filtrate, the N-alkyl-phthalimide could be isolated in a nearly quantitative yield. In addition to elemental analyses, the products were identified by IR and NMR spectra. The salts obtained were usually recrystallized from dry or aqueous methanol or ethanol.

Method B:

A mixture of the N-(substituted-oxy)-phthalimide (0.05 mole) and cyclopropylamine (0.1 mole) was heated at 60 °C. After cooling, the mixture was triturated with 1*N* HCl and the acid-insoluble part (N,N'-dicyclopropylphthalamide, yield 95 to 97%) was filtered off. The pH of the acidic filtrate was adjusted to 7 to 7.5 by adding $KHCO_3$. The precipitated material was isolated by filtration (if solid) or by extraction with chloroform (if oil); subsequently, the appropriate salt was prepared.

2. *By hydrazinolysis*

A mixture of N-(substituted-oxy)-phthalimide (0.2 mole), hydrazine hydrate (0.2 mole) and ethanol (200 ml) was boiled, with stirring, for 2 hrs. The reaction mixture was let to stand overnight, the precipitated crystals (phthaloylhydrazine) were filtered off and washed with ethanol. The ethanolic solution was acidified to Congo blue by ethanolic hydrogen chloride and precipitation of the oxyamine hydrochloride was completed by adding ether. The crystals were filtered off, washed and dried. Usually, the end-products were obtained in moderate to good yields.

Preparation of 4-nitrobenzyloxyamine by aqueous ammonia

A mixture of N-(4-nitrobenzyloxy)-phthalimide (0.03 mole) and 6% aqueous ammonium hydroxide solution (150 ml) was stirred at room temperature for 6 hrs. The mixture was then acidified to Congo blue and, after filtration, phthalamide could be isolated in a yield of 95%. The filtrate was made alkaline with K_2CO_3, extracted with ether and the etheral phase was dried ever K_2CO_3. After removal of the drying agent, 4-nitrobenzyloxy-amine hydrochloride precipitated from the ethereal solution on the addition of ethanolic hydrogen chloride solution.

Reaction of N-(substituted-oxy)-phthalimides with amines in aprotic solvents

(A) *In benzene*

A mixture of the N-(substituted benzyloxy)-phthalimide (0.1 mole), the appropriate amine (0.1 mole) and abs. benzene (400 ml) was stirred at about 10°C for 6 hrs. and allowed to stand overnight. The crystals which precipitated were filtered off, washed with benzene and ether and dried.

(B) *In nitromethane*

A solution of *n*-butylamine (0.74 g; 0.01 mole) in nitromethane (10 ml) was added dropwise to a mixture of N-(4-nitrobenzyloxy)-phthalimide (2.98 g; 0.01 mole) and nitromethane (60 ml), with stirring, at 20 °C within 15 min. The mixture was stirred at room temperature for 24 hrs, the crystals which precipitated were filtered off, washed with nitromethane and ether, and dried to give N-(n-butyl)-N'-(4-nitrobenzyloxy)-phthalamide (3.03 g; 82.4%).

Pyrolysis of N-(n-butyl)-N-(4-nitrobenzyloxy)-phthalamide

N-(*n*-Butyl)-N'-(4-nitro-benzyloxy)-phthalamide (7.42 g; 0.02 mole) was heated for 15 min in an oil bath at 140—150 °C. The oil obtained was dissolved in chloroform, extracted four times with aqueous hydrochloric acid and dried over $MgSO_4$.

After evaporation of the solvent, the residue was distilled fractionally to yield 3.62 g (89.0%) of N-(*n*-butyl)-phthalimide [19].

The aqueous acidic solution was saturated with K_2CO_3, extracted with ether and the ethereal phase dried over K_2CO_3. From the ethereal solution, 4-nitrobenzyloxyamine hydrochloride was precipitated by ethanolic hydrogen chloride in a yield of 3.0 g (89.5%), m.p. 207—210 °C [3, 6].

Reaction of N-(4-nitrobenzyloxy)-phthalimide with benzhydrylamine

A mixture of N-(4-nitro-benzyloxy)-phthalimide (2.98 g; 0.01 mole) benzhydrylamine (1.84 g; 0.01 mole) and 60 ml of ethanol was boiled, with stirring, for 5 hrs. and let to stand overnight. The precipitated crystals were filtered off, washed with cold ethanol and dried to give 1.85 g (82%) of N-(4-nitro-benzyloxy)-phthalimide, m.p. 195—198 °C [1].

The filtrate was evaporated under reduced pressure, the residue dissolved in ether and treated with ethanolic hydrogen chloride to yield 0.65 g (83.5%) of 4-nitrobenzyloxyamine hydrochloride, m.p. 208—210 °C [3, 6].

Reaction of N-(4-nitrobenzyloxy)-phthalimide with n-butylammonium acetate

A solution of N-(4-nitro-benzyloxy)-phthalimide (2.98 g; 0.01 mole) and *n*-butylammonium acetate (0.02 mole) in ethanol (80 ml) was refluxed for 3 hrs. (The solution of *n*-butylammonium acetate was prepared by dissolving 1.46 g of *n*-butylamine in 15 ml of ethanol and titrating potentiometrically with glacial acetic acid until the end-point.) About 80% of the

Table I

O-Substituted hydroxyl-

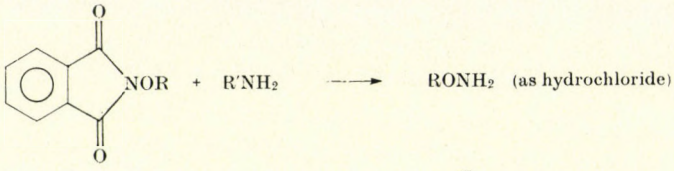

I II

II	R [ ]	Method*	R' in $R'NH_2$	Reaction time hrs	Reaction temp. °C	Yield+ %
a	$CH_3CH{=}CHCH_2$	A	cyclo-C_3H_5	0.4	60	87.9
b	3-NO_2-4-$ClC_6H_3CH_2$ [21]	A	nC_4H_9	0.65	78	94.8
c	3-NO_2-4-ClC_6H_3CHMe	A	nC_4H_9	72	24	47.2
d	4-$nC_8H_{17}O$-3,5-$(OCH_3)_2$-$C_6H_2CH_2$	A	nC_4H_9	2	40	76.4
		B	cyclo-C_3H_5	0.65	60	79.3
e	2-OH-5-CO_2CH_3-$C_6H_3CH_2$	A	nC_4H_9	4	65	84.0
		B	cyclo-C_3H_5	0.3	60	91.2
f	2-OH-3-NO_2-5-CO_2CH_3-$C_6H_2CH_2$	A	nC_4H_9	24	24	85.5
g	Pyridyl-3-CHMe	A	nC_4H_9	72	24	59.5
h	3-NO_2-4-$OHC_6H_3CH_2$	A	$C_6H_5CH_2$	0.4	78	83.0
i	3-OH-4-$NO_2C_6H_3CH_2$	A	nC_4H_9	4	65	68.0
j	3-NO_2-4-$BrC_6H_3CH_2$	A	nC_4H_9	0.4	78	81.0
k	3-NO_2-4-$CH_3OC_6H_3CH_2$	A	nC_5H_{11}	0.5	65	79.0
l	4-OCH_3-3,5-$Cl_2C_6H_2CH_2$	A	nC_4H_9	0.4	78	82.0
q	Dibenzo[a,e]cycloheptatrien-5-yl	A	nC_4H_9	0.4	78	85.5
r	$C_6H_5CH_2$ [20]	A	nC_4H_9	72	24	81.0
		A	nC_4H_9	1	60	89.0
s	3-$NO_2C_6H_4CH_2$ [3]	A	nC_4H_9	0.65	78	87.9
		A	$CH_2{=}CHCH_2$	0.65	65	79.2
t	4-$NO_2C_6H_4CH_2$ [3]	A	nC_4H_9	0.65	78	89.5
			H	8	24	79.0
u	Pyridyl-2-CH_2 [3]	A	nC_4H_9	1	78	94.0
v	Pyridyl-3-CH_2 [3]	B	cyclo-C_3H_5	0.3	100	72.1
		B	nC_5H_{11}	0.3	60	81.5
		A	nC_5H_{11}	24	24	99.0
		B	nC_4H_9	0.3	60	83.3

Notes: * For methods A and B, see Experimental
+ Preparative yields
≠ Sulfate
× Isolated as base; hydrobromide m.p. 182—185°C
[] Known in the literature

amine hydrochlorides

M.p. °C	Formula	Analysis, %							
		Found				Calculated			
		C	H	N	Cl⁻	C	H	N	Cl⁻
161—164	$C_8H_{20}N_2O_6S$≠	35.45	7.54	10.43	11.90	35.50	7.42	10.30	11.75
114—117	$C_8H_{10}Cl_2N_2O_3$	38.12	4.03	11.12	27.94	38.07	3.95	11.14	28.05
oil	$C_{19}H_{30}ClNO_4$	61.34 61.42	8.12 8.31	3.79 3.74	13,22 12.97	61.30	8.09	3.77	13.05
146—149	$C_9H_{11}NO_4$[x]	54.71 54.76	5.71 5.68	7.07 7.12		54.82	5.64	7.10	
196—200	$C_9H_{11}ClN_2O_6$	39.10	4.22	10.01	12.60	38.84	4.07	10.08	12.70
157—162	$C_7H_{12}Cl_2N_2O$			7.12	32.70			6.95	33.20
182—185	$C_7H_9ClN_2O_4$	38.37	4.06	12.78	15.90	38.07	4.08	12.71	16.10
198—200	$C_7H_9ClN_2O_4$	37.80	4.14	12.68	15.80	38.07	4.08	12.71	16.10
179—184	$C_7H_8BrClN_2O_3$			10.02	12.70			9.85	12.90
176—179	$C_8H_{11}ClN_2O_4$	41.44	4.15	12.02	15.60	41.32	4.28	11.95	15.85
195—197	$C_8H_{10}Cl_3NO_2$			5.44	40.70			5.39	41.20
275 (dec.)	$C_{15}H_{14}ClNO$	69.49	5.44	5.32	13.63	69.41	5.39	5.39	13.65

Table II

O-Substituted hydroxyl-

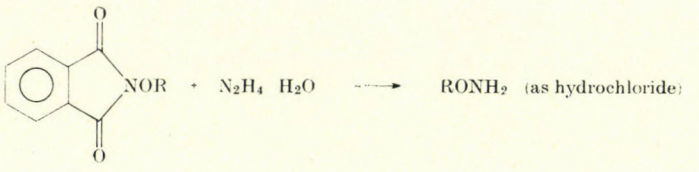

I II

II	R	Yield, %	M.p., °C	Formula
m	2,3-$(OH)_2$-5-CO_2CH_3-$C_6H_2CH_2$	72.9	330 (dec.)	$C_{13}H_{17}NO_{11}^+$
n	2-OH-5-$CON(Et)_2$-$C_6H_3CH_2$	82.5	41 (dec.)	$C_{12}H_{18}N_2O_3^+$
o	8-OH-quinolyl-5-CH_2	41.6	219—222	$C_{10}H_{12}Cl_2N_2O_2$
p	Uracil-5-CH_2	59.5	263—265 (dec.)	$C_5H_8ClN_3O_3$

Note: $^+$ Hydrogen tartarate

ethanol was evaporated in vacuum, the residue was shaken with dilute aqueous HCl, the oil which separated was extracted with chloroform (3×60 ml) and dried over $MgSO_4$. After removal of the drying agent, the filtrate was evaporated and then distilled fractionally to give 1.3 g (65.0%) of N-(*n*-butyl)-phthalimide [19].

The aqueous acidic solution was triturated with K_2CO_3 extracted with 4×80 ml of ether and the ethereal solution dried over K_2CO_3. 4-Nitrobenzyloxyamine hydrochloride was precipitated from the solution as described above, to obtain 1.5 g (75.0%) of the product, m.p. 207—290°C [3, 6].

Reaction of N-(4-nitrobenzyloxy)-phthalimide with anilinium acetate

A mixture of N-(4-nitro-benzyloxy)-phthalimide (2.98 g; 0.01 mole) aniline (0.95 g; 0.01 mole) and glacial acetic acid (1 ml) was heated for 1 hr. on a steam bath. The yellow mixture containing a precipitate was triturated with cold ethanol (5 ml), the crystals were filtered off, washed and dried to give 1.9 g (86.3%) of N-phenylphthalimide [22]. By treatment of the filtrate with ethanolic hydrogen chloride and on the addition of ether, 1.66 g (81.2%) of 4-nitrobenzyloxyamine hydrochloride was obtained, m.p. 207—210°C [3, 6].

Solvolysis of N-(4-nitrobenzyloxy)-phthalimide in methanol

(A) *In the presencee of n-butylamine* (in a 200-fold dilution)

A solution of *n*-butylamine (0.74 g; 0.01 mole) in methanol (10 ml) was added to N-(nitrobenzyloxy)-phthalimide (2.98 g; 0.01 mole) dissolved in methanol (600 ml), at 3—5 °C, with stirring, during 10 min. The reaction mixture was stirred at 5—10 °C for 4 hrs. and then stored in a refrigerator for 2 days. The pearly crystals which precipitated were filtered off,

amine hydrochlorides

Analysis, %							
Found				Calculated			
C	H	N	Cl⁻	C	H	N	Cl⁻
43.10	4.82	3.84	Oxygen 48.61	43.06	4.73	3.86	Oxygen 48.50
48.83	6.83	6.83	Oxygen 37.24	48.61	6.25	7.23	Oxygen 37.15
45.49	4.59	10.68	26.84	45.62	4.56	10.64	26.99
31.08	4.16	21.59	18.19	31.00	4.14	21.71	18.37

washed with methanol and dried to yield 2.5 g (76.0%) of methyl N-(4-nitrobenzyloxy)-phthalamate.

The substance had m.p. 163—165 °C with the loss of methanol, then it became crystalline again to form N-(4-nitrobenzyloxy)-phthalimide which, in turn, melted at 193—195 °C [3].

(B) *Without n-butylamine*

N-(4-Nitrobenzyloxy)-phthalimide (2.98 g; 0.01 mole) was stirred with anhydrous methanol (600 ml) at 5—10 °C for 24 hours. The crystals were filtered off, washed with methanol and dried to give 1.75 g (58.7%) of N-(4-nitrobenzyloxy)-phthalimide, m.p. 193—194° C [3, 6]. The filtrate was evaporated and the residue taken up in ether; the crystals obtained were filtered off and dried to yield 1.1 g (79.5%) of methyl N-(4-nitrobenzyloxy)-phthalamate; m.p. first 163—165 °C, and then 193—194 °C after resolidification. The substance was identical with that obtained in reaction A.

*

The authors are obliged to Dr. SOHÁR for the spectroscopical investigations, to Dr. E. TOLDY and Dr. L. SZABÓ for the analyses, and to Mrs. Mihály MEDVEHÁZI, V. PAP and S. OROSZ for the useful technical assistance.

Table III

N-(Substituted-oxy)-phthalimides

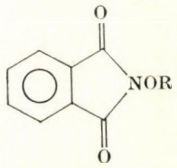

I

I	R	Yield, %	M.p., °C	Formula	Analysis, %					
					Found			Calculated		
					C	H	N	C	H	N
a	$CH_3CH=CHCH_2$	87.0	110—113	$C_{12}H_{11}NO_3$	66.42	5.18	6.51	66.45	5.14	6.45
b	$3\text{-}NO_2\text{-}4\text{-}Cl_6H_3CH_2$	90.5	194—195	$C_{15}H_9ClN_2O_5$			8.42			8.44
c	$3\text{-}NO_2\text{-}4\text{-}ClC_6H_3CHMe$	74.9	153—157	$C_{16}H_{11}ClN_2O_5$			8.04			8.11
d	$4\text{-}nC_8H_{17}O\text{-}3,5\text{-}(OCH_3)_2C_6H_2CH_2$	78.3	105—107	$C_{25}H_{31}NO_6$			3.31			3.27
e	$2\text{-}OH\text{-}5\text{-}CO_2CH_3\text{-}C_6H_3CH_2$	57.2	204—206	$C_{17}H_{13}NO_6$	62.48	4.08	4.35	62.55	4.01	4.28
f	$2\text{-}OH\text{-}3\text{-}NO_2\text{-}5\text{-}CO_2CH_3\text{-}C_6H_2CH_2$	93.5	210—213 (dec.)	$C_{17}H_{12}N_2O_8$	55.42	3.29	7.57	55.07	3.23	7.55
g	Pyridyl-3-CHMe	67.4	102—105	$C_{15}H_{12}N_2O_3$	67.29	4.65	10.34	67.05	4.48	10.45
h	$3\text{-}NO_2\text{-}4\text{-}HOC_6H_3CH_2$	79.6	190—193	$C_{15}H_{10}N_2O_6$	57.40	3.21	8.92	57.34	3.18	8.94
i	$3\text{-}OH\text{-}4\text{-}NO_2C_6H_3CH_2$	66.5	190—191	$C_{15}H_{10}N_2O_6$	57.27	3.24	9.01	57.34	3.18	8.94
j	$3\text{-}NO_2\text{-}4\text{-}BrC_6H_3CH_2$	87.4	196—200	$C_{15}H_9BrN_2O_5$			7.34			7.43
k	$3\text{-}NO_2\text{-}4\text{-}CH_3OC_6H_3CH_2$	89.5	196—197	$C_{16}H_{12}N_2O_6$	59.24	3.86	8.66	59.32	3.74	8.64
l	$4\text{-}OCH_3\text{-}3,5\text{-}Cl_2C_6H_2CH_2$	84.8	167—169	$C_{16}H_{11}Cl_2NO_4$			3.96			3.95
m	$2,3\text{-}(OH)_2\text{-}5\text{-}CO_2CH_3\text{-}C_6H_2CH_2$	84.5	189—191 (dec.)	$C_{17}H_{13}NO_7$	59.51	3.95	4.02	59.55	3.80	4.08
n	$2\text{-}OH\text{-}5\text{-}CON(C_2H_5)_2\text{-}C_6H_3CH_2$	84.2	166—169 (dec.)	$C_{20}H_{20}N_2O_5$	65.18	5.50	7.65	65.20	5.45	7.61
o	$8\text{-}OH\text{-}quinolyl\text{-}5\text{-}CH_2$	89.3	214—216 (dec.)	$C_{18}H_{12}N_2O_4$	67.38	3.79	8.91	67.51	3.75	8.76
p	$Uracil\text{-}5\text{-}CH_2$	92.3	228—231	$C_{13}H_9N_3O_5$	54.12	3.15	14.53	54.28	3.13	14.62
q	Dibenzo[a,e]cycloheptatrien-5-yl	73.6	224—227	$C_{23}H_{15}NO_3$	79.36	4.38	3.99	79.52	4.32	4.03

Table IV

N-alkyl-N'-(substituted-oxy)-phthalamides

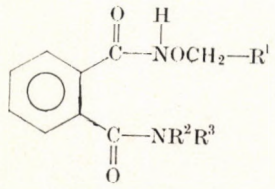

V

V	R^1	R^2	R^3	Yield, %	M.p., °C	Formula	Analysis, %					
							Found			Calculated		
							C	H	N	C	H	N
ra	C_6H_5-	nC_4H_9-	H	81.2	105—107	$C_{19}H_{22}N_2O_3$	70.02	6.77	8.56	69.93	6.79	8.40
rb	C_6H_5-	cyclo-C_3H_5-	H	84.9	102—104	$C_{18}H_{18}N_2O_3$	69.68	5.84	9.01	69.43	5.95	8.94
rc	C_6H_5-	Morpholino-	|	75.2	108—110	$C_{19}H_{20}N_2O_4$	67.05	5.88	8.25	66.85	5.98	8.16
s	3-NO_2-C_6H_4-	nC_4H_9-	H	68.2	104—107	$C_{19}H_{21}N_3O_5$	61.54	5.67	11.30	61.63	5.79	11.24
ta	4-$NO_2C_6H_4$-	-$CH_2CH(CH_3)$-C_6H_5	H	71.2	153—154	$C_{24}H_{23}N_3O_5$	66.52	5.28	9.69	66.47	5.32	9.70
tb	4-$NO_2C_6H_4$-	nC_4H_9-	H	82.5	135—137	$C_{19}H_{21}N_3O_5$	61.56	5.65	11.35	61.63	5.79	11.24
tc	4-NO_2-C_6H_4-	Piperidino-		78.4	151—154	$C_{20}H_{21}N_3O_5$	62.54	5.48	10.92	62.59	5.49	10.95
u	Pyridyl-2-	nC_4H_9-	H	78.6	117—119	$C_{18}H_{21}N_3O_3$	66.14	6.42	12.80	66.05	6.43	12.85
v	Pyridyl-3-	nC_4H_9-	H	77.3	94— 97	$C_{18}H_{21}N_3O_3$	66.01	6.45	12.81			

REFERENCES

[1] RAPOPORT, S. M.: Medizinische Biochemie **1965,** 465 (3rd edition), VEB Verlag Volk und Gesundheit, Berlin
[2] LEVINE, R. J., SATO, T. L., SJOERDSMA, A.: Biochem. Pharmacol. **14,** 139 (1965); LEVINE, R. J.: Science **154,** 1017 (1966)
[3] HAMOR, G. H., BRESLOW, D. M., FISCH, G. W.: J. Pharm. Sci. **59,** 1752 (1970)
[4] ILVESPÄÄ, A. O., MARXER, A.: Chimia **18,** 1 (1964)
[5] MARTIN, D. G., SCHUMANN, E. L., VELDKAMP, W., KEASLING, H.: J. Med. Chem. **8,** 456 (1965)
[6] SZILÁGYI, G., KASZTREINER, E., KOSÁRY, J., SOHÁR, P.: Hung. Pat. 162,578 (1970)
[7] NICOLAUS, B. J. R., PAGANI, G., TESTA, E.: Helv. Chim. Acta **45,** 1381 (1962)
[8] BARBER, H. J., WRAGG, W. R.: Nature **158,** 514 (1946)
[9] SPRING, F. S., WOODE, J. C.: Nature **158,** 754 (1946)
[10] WOLFE, S., HASAN, S. K.: Can. J. Chem. **48,** 3572 (1970)
[11] NEFKENS, G. H. L.: Recueil **79,** 688 (1960)
[12] LALIBERTE, R., BERLINGUET, L.: Can. J. Chem. **38,** 1933 (1960)
[13] DATTA, N. K., TALUKDAR, P. B.: J. Indian Chem. Soc. **43,** 461 (1966)
[14] ENDRES, W.: Arch. Pharm. **305,** 671 (1972)
[15] BROWN, D. M., COE, P. F., GREEN, D. P. L.: J. Chem. Soc. C, **1971,** 867
[16] KASZTREINER, E., VARGHA, L., SZILÁGYI, G., HUSZTI, Zs., BORSY, J., MÉSZÁROS, E., ELEK, S., POLGÁRI, I.: Hung. Pat. 158,573 (1969);
KASZTREINER, E., VARGHA, L., SZILÁGYI, G., HUSZTI, Zs., BORSY, J., SZAKÁLY, J., ELEK, S., POLGÁRI, I.: Hung. Pat. 161,866 (1970);
KASZTREINER, E., VARGHA, L., HUSZTI, Zs., BORSY, J., SZILÁGYI, G., SZAKÁLY, J., ELEK, S., POLGÁRI, I.: Hung. Pat. 161,867 (1970)
[17] HUSZTI, Zs., KASZTREINER, E., KÜRTI, M., FEKETE, M., BORSY, J.: Biochem. Pharm. **22,** 2253 (1973)
[18] HUSZTI, Zs., KASZTREINER, E., SZILÁGYI, G., KOSÁRY, J., BORSY, J.: Biochem. Pharm. **22,** 2267 (1973)
[19] SACHS, F.: Chem. Ber. **31,** 1225 (1898)
[20] BAUER, L., SHOEB, A., AGWADA, V. C.: J. Org. Chem. **27,** 3153 (1962)
[21] MAMALIS, P., JEFFRIES, L., PRICE, S. A., RIX, M. J., OUTRED, D. J.: J. Med. Chem. **8,** 684 (1965)
[22] GRAEBE, C.: Chem. Ber. **29,** 2802 (1896)

Endre KASZTREINER
Géza SZILÁGYI
Judit KOSÁRY
Zsuzsa HUSZTI

1325 Budapest, P.O. Box 82. Hungary.

Acta Chimica Academiae Scientiarum Hungaricae, 84 (2), pp. 181—185 (1975)

STRUCTURAL INVESTIGATION OF FLAVONIDES AND THEIR MODEL COMPOUNDS, VII

CALCULATION AND DETERMINATION OF THE IONIZATION POTENTIAL OF 4- AND 4'-MONOSUBSTITUTED CHALCONES

(SHORT COMMUNICATION)

Z. DINYA,* GY. LITKEI,* J. TAMÁS** and G. CZIRA**

(Department of Organic Chemistry, L. Kossuth University, Debrecen and Central Research Institute of the Hungarian Academy of Sciences, Budapest**)*

Received February 19, 1973

Applying mass spectrometric and quantum-chemical methods, the first ionization potential (I_p) of monosubstituted 4- and 4'-chalcones has been determined. A direct linear equation is proposed between I_p values and energy coefficient of the highest occupied molecular orbital. This equation can be generalized for aromatic and unsaturated ketones. The peculiarity of functional $I_p - \sigma^+$ for 4- and 4'-R substituents has been interpreted and the results have been brought into connection with the conjugation behaviour of molecules.

In an earlier communication [1], the quantum chemical calculation of the first (vertical) ionization potential of 4-substituted acetophenones has been reported. Calculations were performed on the basis of KOOPMANS' [2—5] theorem, using the HMO method [6], and a very good agreement was obtained between the calculated and measured values.

The present communication reports on the mass spectrometric and the theoretical determination of the ionization potential of monosubstituted 4-(*I*; R' = H) and 4'-(*I*; R = H) chalcones:

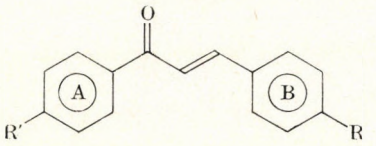

I

No similar investigation of these compounds has been reported in the literature.

Experimental and computational procedure

The preparation and physical constants of the compounds investigated have been reported [7]. The mass spectrometric determination of the ionization potentials was done by the 'semilog plot' technique [8], using a Model AEI MS-902 mass spectrometer. Ion acceleration voltage was 8 kV, the ionizing

electron current 10 μA. Benzene was used as reference substance, the ionization potential of which was taken as 9.40 eV [9].

Computations were carried out by the HMO [6, 7] and the ω-SCF-LCAO-MO [10—12] methods according to a program written for an ODRA 1204 computer.

On the basis of KOOPMANS' theorem [2—5], the first ionization potential of a molecule is the negative value of the energy of the highest occupied molecular orbital (HOMO):

$$I_p = -E^{\mathrm{HOMO}} \tag{1}$$

E^{HOMO} can be given in the following form:

$$E^{\mathrm{HOMO}} = \alpha_0 + \chi^{\mathrm{HOMO}} \beta_0 \tag{2}$$

where α_0 and β_0 are constant parameters for the carbon atoms of benzene, χ^{HOMO} is the energy coefficient of the highest molecular orbital.

From Eqs (1) and (2), a direct relationship between I and χ^{HOMO} can be derived:

$$I_p = -(\alpha_0 + \chi^{\mathrm{HOMO}} \beta_0) \tag{3}$$

For given values of α_0 and β_0

$$I_p = a + b\chi^{\mathrm{HOMO}} \tag{4}$$

In the calculation of I_p for acetophenones from Eq. (4), the values of $a = 7.1$ and $b = 2.5$ given by HEILBRONNER *et al.* for aromatic hydrocarbons, have been used [6]. The computations reported in this communication are based also on an equation of type (4), but the values of a and b have been newly determined.

Results and discussion

Experimental and HMO computational results are summarized in Table I. These calculations were performed on the basis of the equation

$$I_p = 6.8 + 2.5\chi^{\mathrm{HOMO}} \ \text{(eV)} \tag{5}$$

The measured and calculated values are in excellent agreement. As compared to HMO data (Table I), the results of ω-SCF-LCAO-MO calculations ($\omega = 0.5$) are higher by 0.8—1.2 eV, so that for these calculations the equation

$$I_p = 6.1 + 2.5\chi^{\mathrm{HOMO}} \ \text{(eV)} \tag{6}$$

Table I

Measured and calculated (HMO) ionization potentials of monosubstituted 4- and 4'-chalcones

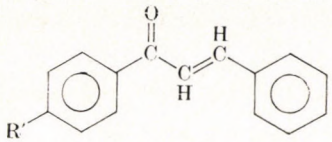

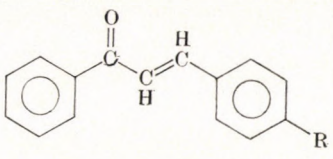

R'	I_p (exp)** (eV)	I_p^{HMO} (eV)	ΔI_p* (eV)	R	I_p (exp)** (eV)	I_p^{HMO} (eV)	ΔI_p* (eV)
$-N(CH_3)_2$	—	—	—	$-N(CH_3)_2$	—	8.10	—
$-NH_2$	8.15	8.45	0.3	$-NH_2$	—	—	—
$-OH$	8.54	8.56	0.02	$-OH$	8.20	8.23	0.03
$-OCH_3$	8.47	8.50	0.03	$-OCH_3$	8.14	8.15	0.01
$-CH_3$	8.61	8.58	−0.03	$-CH_3$	8.36	8.42	0.06
$-H$	8.59	8.58	−0.01	$-H$	8.59	8.58	−0.01
$-Cl$	8.70	8.74	0.04	$-Cl$	8.62	8.64	0.02
$-Br$	8.73	8.75	0.02	$-Br$	8.61	8.64	0.03
$-I$	—	8.77	—	$-I$	—	8.70	—
$-NO_2$	8.93	8.93	0	$-NO_2$	9.10	9.05	−0.05

*$\Delta I_p = I_{p,calc} - I_{p,exp}$ ** ± 0.05 eV

is suitable. These equations can be generalized for α,β-unsaturated aromatic carbonyl compounds. By way of example, the calculated (HMO) and measured I_p values are given for flavone (**II**) and for 2'-hydroxychalcone (**III**):

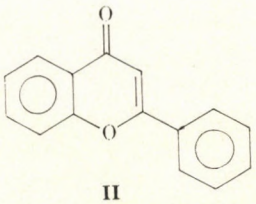

II

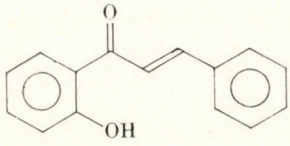

III

I_p (eV) calculated: 8.70 eV 8.52 eV

I_p (eV) measured: 8.74 $\pm$ 0.05 eV 8.41 + 0.05 eV

In these cases too there is a very good agreement between the experimental and calculated values. (In the case of 2'-hydroxychalcone (**III**), the intramolecular H-bond between 2'-OH and the carbonyl group has also been con-

sidered in the calculations.) Experimental and calculated I_p values are plotted in Fig. 1 as a function of the BROWN-σ^+ values of the substituents [13].

Both the calculated and experimental values increase linearly with the σ^+ of the substituents. The character of the effects exerted by the substituents in rings *A* and *B* on the I_p value is identical. Electron donor ($\sigma^+ < 0$) groups decrease, whereas electron-withdrawing ($\sigma^+ > 0$) substituents increase the I_p values relative to the unsubstituted chalcones. However, the substituents in

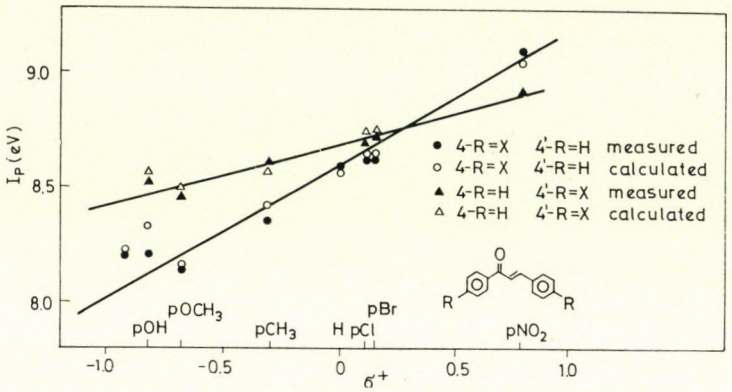

Fig. 1

rings *A* and *B* do not act in the same measure. The slopes of the straight lines are different: 0.4 in the case of 4-R and 0.18 in that of 4'-R, *i.e.* 4-R substituents have a stronger effect on I_p than the 4'-R ones. This finding supports the assumption that the vinylbenzene part is the primary charge carrier in the ionized molecule. The very moderate slope of the curves can be interpreted by the extended conjugation of the molecule. (The slope of the I_p *vs.* σ^+ straight lines for parasubstituted benzenes and acetophenones is 0.9 [14].) This is indicated also by the low I_p value (8.59 eV) of unsubstituted chalcone (*I*; R = R' = H). (For comparison: $I_{p\,\text{benzene}} = 9.4$ eV [9]; $I_{p\,\text{acetophenone}} = 9.5$ eV [14]; $I_{p\,\text{vinylbenzene}} = 9.0$ eV [14].)

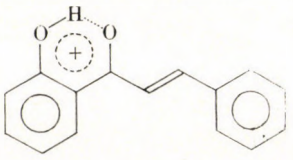

IV

In the case of 2'-hydroxychalcone (**III**), this conjugated system is still more extensive, because, owing to the 2'-OH group, a resonance-stabilized chelate system (**IV**) is to be expected [15], so that the I_p value must be low

compared to chalcone (*I*, R = R' = H). Experimental results confirm this assumption.

Our investigations were extended also to compounds of the flavone and isoflavone type. These results will be reported in the near future.

REFERENCES

[1] DINYA, Z.: Acta Chim. (Budapest) **72,** 323 (1972)
[2] KOOPMANS, T. A.: Physica **1,** 104 (1933)
[3] STREITWIESER, A.: Molecular Orbital Theory for Organic Chemists, pp. 188. John Wiley and Sons, New York, 1961
[4] PEACOCK, T. E.: Electronic Properties of Aromatic and Heterocyclic Molecules, pp. 26. Academic Press, New York, 1965
[5] TAJIMA, S., WASADO, N., TSUCHIJA, T.: Tetrahedron Letters, 139 (1970)
[6] HEILBRONNER, E., BOCK, H.: Das HMO-Modell und seine Anwendung, I—III, p. 317. Verlag-Chemie GmbH, Weinheim, 1968
[7] DINYA, Z., BOGNÁR, R.: Acta Chim. (Budapest) **73,** 453 (1972)
[8] LOSSING, F. P., TICKNER, A. W., BRYCE, W. A.: J. Chem. Phys. **19,** 1254 (1951)
[9] BAKER, A. D., MAY, D. R., TURNER, D. W.: J. Chem. Soc. (B) **22** (1968)
[10] WHELAND, G. W., MANN, D. E.: J. Chem. Phys. **17,** 264 (1949)
[11] BERGSON, G.: Arkiv för Kem. **19,** 181 (1962)
[12] JANSSEN, M. J., SANCHSTRÖM, J.: Tetrahedron **20,** 2339 (1964)
[13] BROWN, H. C., OKAMOTO, Y.: J. Amer. Chem. Soc. **80,** 4979 (1958)
[14] NSRDS-NBS. 26. Ionization Potentials, Appearance Potentials and Heats of Formation of Gaseous Positive Ions (1969). U.S. Department of Commerce, National Bureau of Standards
[15] DINYA, Z., LITKEI, GY.: Acta Chim. (Budapest) (In press)

Zoltán DINYA
György LITKEI } 4010 Debrecen, Hungary

József TAMÁS
Gábor CZIRA } 1088 Budapest, Puskin u. 11—13. Hungary.

Acta Chimica Academiae Scientiarum Hungaricae, 84 (2), pp. 187—192 (1975)

TRIARYLMETHANES, VI*

REACTIONS OF NAPHTHOQUINONE DIPHENYLMETHIDES WITH ORGANOMETALLIC COMPOUNDS

MOHAMED A.-F. ELKASCHEF, FAROUK M. E. ABDEL-MEGEID and SALAH M. M. ELZEIN

(National Research Centre, Dokki, Cairo, Egypt)

Received July 18, 1973

Reactions of 1,2-naphthoquinone diphenylmethides with organometallic compounds take place by 1,4-addition, except with 1-naphthyllithium where further substitution of the OH group by a 1-naphthyl group occurs. 1,4-Naphthoquinone 4-diphenylmethide undergoes 1,2-addition followed by migration of the OH group to C-6.

It has been shown that methylmagnesium iodide reacts with 1,4-benzoquinone 4-diphenylmethide and 1,4-naphtoquinone 4-diphenylmethide (**I**) by 1,6-addition to give α[4-(1-hydroxyphenyl)]α,α-diphenylethane and α-[4-(1-hydroxynaphthyl)]-α,α-diphenylethane (**IVa**) [2, 3], respectively. Phenylmagnesium bromide gave with these compounds, however, resins [3], but with 1,2-naphthoquinone 1-diphenylmethide (**II**) the product was 1-(2-hydroxynaphthyl) triphenylmethane (**Vb**) [4, 5] through 1,4-addition.

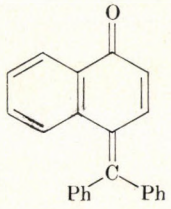

I

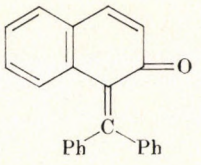

II

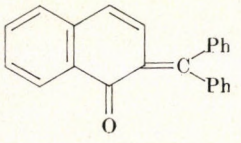

III

We found that methylmagnesium iodide and phenylmagnesium bromide react with 1,2-naphthoquinone 1-diphenylmethide (**II**) and 1,2- naphthoquinone 2-diphenylmethide (**III**) by 1,4-addition to yield α-[1-(2-hydroxynaphthyl)]α,α-diphenylethane (**Va**), α-[2-(1-hydroxynaphthyl)]-α,α-diphenylethane (**VIa**), 1-(2-hydroxynaphthyl) triphenylmethane (**Vb**), and 2-(1-hydroxynaphthyl)triphenylmethane (**VIb**), respectively. The IR spectra of these compounds are compatible with the structures assigned to them (*cf.* Experimental), and their UV spectra are similar to those of the respective carbinols (**Vc**) [6] and (**VIc**) [6]; but they give no colour with conc. H_2SO_4.

* For Part V, see Ref. [1].

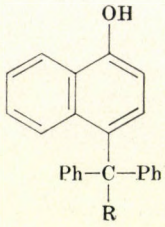

IV

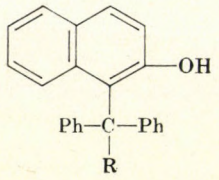

V

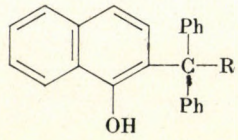

VI

a: R = Me b: R = Ph c: R = OH

Phenyllithium reacts with **II** and **III** in an analogous manner to give the same compounds (**Vb**) and (**VIb**), respectively. With 1,4-naphtoquinone 1-diphenylmethide(**I**), however, this reagent as well as 1-naphthyllithium yields 4-(1-phenylnaphthyl)- and 4-(1,1'-binaphthyl)-diphenylmethanol (**VIIa**) and (**VIIb**), respectively. The m.p. of **VIIa** differs from that of **IVb**; [5]. These compounds give a green colour with conc. H_2SO_4. The UV spectra of compounds **VIIa** and **VIIb** (*cf.* Table) and their IR spectra (*cf.* Experimental) are in support of the assigned structure.

Repeating the reaction of phenylmagnesium bromide with 1,4-naphthoquinone 1-diphenylmethide (**I**) [3], we could isolate, by the use of column chromatography, compound **VIIa**. The formation of compounds **VIIa** and **VIIb** in these reactions may be explained by a 1,2-addition to the keto group and subsequent ionization, as shown in the following reaction sequence:

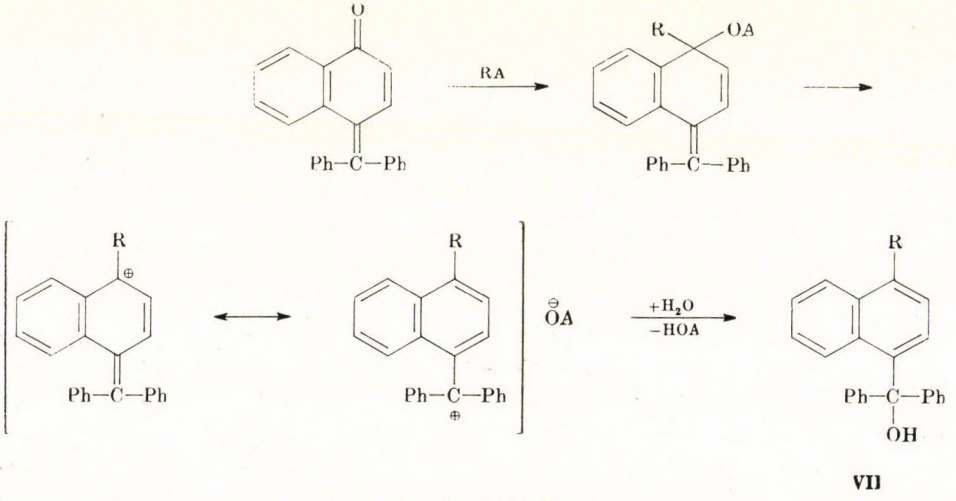

VII

A = Li or MgBr
a: R = Pb: b: R = α-naphthyl

Compounds **II** and **III** react with α-naphthyllithium to give 1-(1',2-binaphthyl)-diphenyl-1''-naphthylmethane (**VIII**) and 2-(1,1'-binaphthyl)-diphenyl-1''-naphthylmethane (**IX**), respectively.

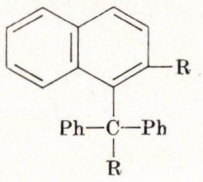

VIII

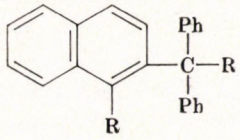

IX

R = α-naphthyl

The names for compounds VIII and IX are correct*, according to the following numbering:

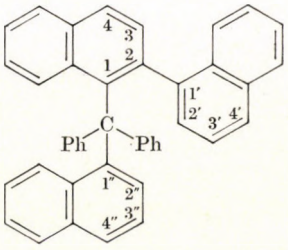

VIII

1-(1′,2-binaphthyl)diphenyl-1″-naphthylmethane

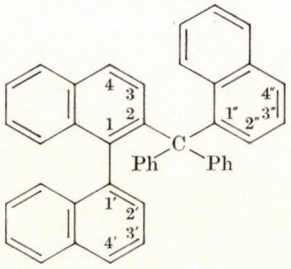

IX

2-(1,1′-binaphthyl)diphenyl-1″-naphthylmethane

This reaction may be visualized as 1,2-addition on the carbonyl group followed by the reaction of the resulting ionized compound with another molecule of α-naphthyllithium as follows:

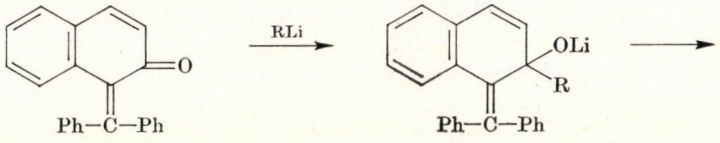

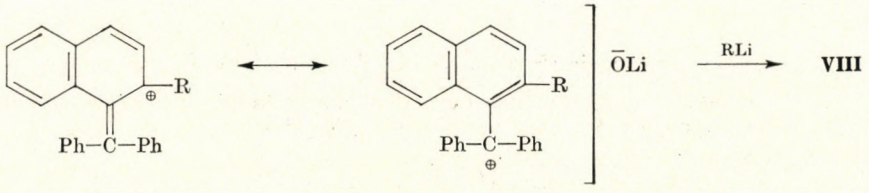

R = α-naphthyl

Compounds VIII and IX gave no colour with conc. H_2SO_4 and their IR spectra have no OH bands.

* See on page 188

Experimental

Melting points are uncorrected. The analyses were made by the Microanalytical Laboratory, N.R.C.

Reaction of methylmagnesium iodide with 1,2-naphthoquinone 1-diphenylmethide (II)

A solution of methylmagnesium iodide was prepared from methyl iodide (3.1 ml; 0.05 mole) in dry ether and a suspension of 1,2-naphthoquinone 1-diphenylmethide (3 g; 0.01 mole) was added to it. After standing overnight and 3 hrs. reflux, the mixture was treated with cold dilute hydrochloric acid. The ethereal extract of the reaction mixture was washed with 4% sodium-carbonate solution and then with water, dried over Na_2SO_4 and the solvent was evaporated. The remaining oil (**Va**) solidified under acetic acid (1.3 g; 40% of theoretical yield) and was crystallized therefrom; m.p. 141 °C.

$C_{24}H_{20}O$ (324): Calcd. C 88.89; H 6.17;
Found C 88.75; H 5.80%.
IR spectrum (CCl_4): 3485 cm^{-1} OH, 1380 cm^{-1} CH_3.

Table of electronic spectra

λ_{max} nm (log ε)

Compound					
Vb	273	283	293	310	333
	(4.00)	(3.80)	(3.63)	(3.22)	(3.27)
Vc [6]	257	385	295	320	340
	(3.75)	(3.85)	(3.75)	(3.40)	(3.45)
VIa	300	312	322	335	
	(3.73)	(3.70)	(3.62)	(3.25)	
VIb	295	302	315	322	
	(3.75)	(3.73)	(3.57)	(3.53)	
VIc [6]	290	310	320	350	
	(3.75)	(3.60)	(3.30)	(2.50)	
VIIa	295				
	(4.08)				
VIIb	298				
	(3.88)				

Reaction of methylmagnesium iodide with 1,2-naphthoquinone 2-diphenylmethide (III)

From a reaction as above, using 1,2-naphthoquinone 2-diphenylmethide (**III**) instead of **II**, α-[2-(1-hydroxynaphthyl)]-α, α-diphenylethane (**VIa**) (1.6 g; 50%) was obtained.

$C_{24}H_{20}O$ (324): Calcd. C 88.89; H 6.17;
Found C 89.15; H 6.04%.
Mol. wt. (electrothermal method: 334).
IR spectrum (in CCl_4) 3480 cm^{-1} (OH), 1385 cm^{-1} (CH_3).

Reaction of phenylmagnesium bromide with 1,2-naphthoquinone 2-diphenylmethide (III)

Phenylmagnesium bromide, prepared from bromobenzene (3 ml; 0.03 mole) in dry ether (40 ml), and 1,2-naphthoquinone 2-diphenylmethide (**III**) (3g, 0.01 mole) were mixed and

allowed to stand overnight and then refluxed for 4 hrs. After treatment as above, the remaining oil **(VIb)** solidified (2.5 g, 66%) under ethanol and was crystallized from xylene; m.p. 200 °C.

$C_{29}H_{22}Od$ (386): Calcd. C 90.16; H 5.70.
Found C 90.67; H 5.90%.
IR spectrum (CCl_4): 3490 cm^{-1} (OH).

Reaction of phenylmagnesium bromide with 1,4-naphthoquinone 4-diphenylmethide (I)

In a reaction as before, using 1,4-naphthoquinone 4-diphenylmethide **(I)** (3 g; 0.01 mole), after evaporation of the solvents, an oil was obtained; this oil **(VIIa)** was chromatographed over alumina and eluted with n-hexane. The solid residue **(VII)** (0.4 g; 11%) that remained after evaporation of the solvent was crystallized from xylene and melted at 174 °C (no depression when mixed with the product of the next experiment).

Action of phenyllithium on 1,4-naphthoquinone 4-diphenylmethide (I)

To a solution of phenyllithium, prepared from bromobenzene (3 ml; 0.03 mole) in dry ether (40 ml), a dry benzene suspension of 1,4-naphthoquinone 4-diphenylmethide **(I)** was added. After standing overnight, the reaction mixture was refluxed for 4 hrs. It was then decomposed with ice-cold dilute hydrochloric acid and extracted with ether. The ethereal extract was dried over Na_2SO_4, filtered and evaporated. The residual oil **(VIIa)** solidified (2.1 g; 54) under methanol and was crystallized from xylene; m.p. 174°C.

$C_{29}H_{22}O$ (386): Calcd. C 90.16; H 5.7
Found C 89.95; H 5.8%.
IR spectrum (nujol mull): 3600 cm^{-1} (OH).

Action of phenyllithium on 1,2-naphthoquinone 1-diphenylmethide (II)

From a reaction as before, using 1,2-naphthoquinone 1-diphenylmethide **(II)** (3 g; 0.01 mole) an oily residue **(Vb)** was obtained that solidified (1.5 g; 40%) under ethanol and was crystallized from acetic acid; m.p. 155 °C [5].

$C_{29}H_{22}O$ (386): Calcd. C 90.16; H 5.68;
Found C 89.91; H 5.75%.
IR spectrum (CCl_4): 3420 cm^{-1} (OH).

Action of phenyllithium on 1,2-naphthoquinone 2-diphenylmethide (III)

1,2-Naphthoquinone 2-diphenylmethide **(III)** (3 g; 0.01 mole) and phenyllithium (0.03 mole), in a reaction as above, gave an oil **(VIb)** that solidified (2.1 g; 54%) under methanol and was crystallized from xylene; m.p. 200 °C.

Action of 1-naphthyllithium on 1,4-naphthoquinone 4-diphenylmethide (I)

A suspension of 1,4-naphthoquinone 4-diphenylmethide **(I)** (3 g; 0.01) was added to a solution of 1-naphthyllithium (prepared from 1-bromonaphthalene, (4.2 g; 0.03 mole) in dry ether (40 ml). After standing overnight and 4 hrs. reflux, the mixture was treated with dilute hydrochloric acid and extracted with ether. The ethereal extract was washed with 4% sodium carbonate solution, then with water, dried over Na_2SO_4 and evaporated. The residual oil was subjected to steam distillation. The remaining viscous mass **(VIIb)** solidified (1.1 g; 25%) under toluene and was crystallized therefrom; m.p. 215 °C. It gave a green colour with conc. H_2SO_4 but no colour with ferric chloride solution.

$C_{33}H_{24}O$ (436): Calcd. C 90.83; H 5.50;
Found C 90.40; H 5.77%.
IR spectrum (KBr) 3420 cm^{-1} (OH).

Action of 1-naphthyllithium on 1,2-naphthoquinone 1-diphenylmethide (II)

From a reaction as before, using 1,2-naphthoquinone 1-diphenylmethide **(II)** (3 g; 0.01 mole) and 1-naphthyllithium (0.03 mole), an oily residue was obtained, that was purified by steam distillation after the usual treatment. The residual viscous mass **(VIII)** solidified (3.4 g; 66%) under ether and was crystallized from toluene; m.p. 178°C.

$C_{43}H_{30}$ (546): Calcd. C 94.51; H 5.49;
Found C 94.61; H 5.7%.

Action of 1-naphthyllithium on 1,2-naphthoquinone 2-diphenylmethide (III)

In a reaction as above 1,2-naphthoquinone 2-diphenylmethide **(III)** (3 g; 0.01 mole) gave an oily residue that was purified by steam distillation. The residual viscous mass **(IX)** solidified (3.3 g; 60%) under toluene and was crystallized therefrom; m.p. 235 °C.

$C_{43}H_{30}$ (546): Calcd. C 94.51; H 5.49;
Found C 94.31; H 5.41%.

REFERENCES

[1] ELKASCHEF, M. A-F., ABDEL-MEGEID, F. M. E., ELZEIN, S. M. M.: Acta Chim. (Budapest) **79,** 411 (1973)
[2] BAEYER, A., VILLIGER, V.: Ber. **36,** 2793 (1903)
[3] JULIAN, P. L., GIST, W. J.: J. Am. Chem. Soc. **57,** 2030 (1935)
[4] SCHÖNBERG, A., MUSTAFA, A., SHALABY, A.: J. Am. Chem. Soc. **77,** 5756 (1955)
[5] BUU-HOI, N., RIPS, R.: J. Org. Chem. **22,** 666 (1957)
[6] ELKASCHEF, M. A-F.: Egypt. J. Chem. **2,** 275 (1959)

Mohamed A.-F. ELKASCHEF
Farouk M. E. ABDEL-MEGEID
Salah M. M. ELZEIN
National Research Centre, Dokki, Cairo, Egypt.

Acta Chimica Academiae Scientiarum Hungaricae, 84 (2), pp. 193–200 (1975)

CONFORMATION OF 3,7-DIAZABICYCLO-[3.3.1] NONANES

P. SCHEIBER and K. NÁDOR

(Department of Chemistry, Veterinary University, Budapest)

Received September 10, 1973

The conformational analysis of some N,N'-dialkyl-1,5-diphenyl-diazabicyclo-(3.3.1) nonanes is described. On the basis of IR, NMR and dipole-moment data it has been shown that with an oxo group in position 9, the N,N'-dimethyl derivative exists in a chair–boat conformation, while in the case of the N,N'-di-*t*-butyl compound the boat–boat form should also be considered. In the 9-hydroxy derivatives a strong intramolecular hydrogen bond between the OH and tertiary nitrogen stabilizes one of the six-membered rings in the boat form.

Several substituted derivatives of 3,7-diazabicyclo-(3.3.1)-nonane are known [1a], which are also designated after MANNICH [1b] as 'bispidines'. Despite the great number of these compounds, only the conformation of N,N'-dimethylbispidine has been examined [2], in contrast to alicyclic, [3] 3-aza-, [4] and 9-aza- [5] -bicyclo-(3.3.1) nonanes, whose stereochemistries have been thoroughly studied. Examination of the conformation of bispidine derivatives permits to evaluate the role of nitrogen atoms in establishing a stable conformation, *i.e.* a decision concerning whether or not the chair–chair conformation of the bicyclo-(3.3.1) nonane skeleton [3] is altered upon replacement of ring CH_2 groups by nitrogen atoms bearing various substituents.

Various 1,5-diphenylbispidines symmetrically substituted at their nitrogen atoms were examined in order to determine both the conformation of the two piperidine rings in the 3,7-diazabicyclo-(3.3.1) nonane skeleton and the orientation of the substituents at the nitrogen atoms with respect to the rings. This was done by an analysis of infrared and NMR spectral, as well as dipole-moment data.

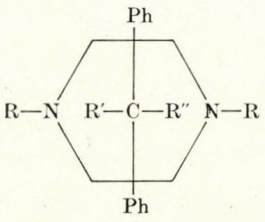

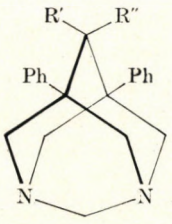

I $R = CH_3$, $R'R'' = O$
II $R = C(CH_3)_3$, $R'R'' = O$
IV $R = CH_3$, $R' = H$, $R'' = OH$
V $R = C(CH_3)_3$, $R' = H$, $R'' = OH$

III $R'R'' = O$
VI $R' = H$, $R'' = OH$

Results

Intense Bohlmann absorptions [6] appear at 2800—2700 cm^{-1} in the infrared spectrum of **I**, **II**, **IV** and **V**, which are absent in the spectrum of **III** and **VI**. These data provide useful information concerning the orientation of the unshared electron pair of the nitrogen atoms.

Table I

Dipole moments of N,N'-substituted 1,5-diphenylbispidines; benzene, 25.0 °C

Compound		Dipole moment (D)
N,N'-dimethyl-1,5-diphenylbispid-9-one	**I**	3.34
N,N'-di-t-butyl-1,5-diphenylbispid-9-one	**II**	3.86
5,7-diphenyl-1,3-diazaadamantan-6-one	**III**	1.94
N,N'-dimethyl-1,5-diphenylbispidin-9-ol	**IV**	2.66
N,N'-di-t-butyl-1,5-diphenylbispidin-9-ol	**V**	4.09

The experimentally determined dipole moments of compounds **I**—**V** are listed in Table I. The dipole moment of compound **VI**, which is less important for the discussion presented below, could not be determined because of solubility difficulties.

The dipole moment values calculated for the possible conformations of N,N'-dialkyl-1,5-diphenyl-bispid-9-ones are shown in Table II. The calculations were done by the usual vectorial addition of the corresponding bond or group moments characteristic of dipolar bonds. The bond-moment values used in the calculations are as follows: $\mu_{C=O} = 3.10$ D [7], $\mu_{NR_3} = 0.80$ D [8]. When calculating the dipole moments, the bond angles were considered to be tetrahedral.

Table II

Calculated dipole moments of the possible conformations of N,N'-dimethyl-1,5-diphenylbispid-9-one **(I)**

Conformation*	$CC_{e,e}$	$CC_{e,a}$	$CB_{e,e}$	$CB_{a,e}$	$CB_{a,a}$	$CB_{e,a}$	$BB_{e,e}$	$BB_{e,a}$	$BB_{a,a}$
Dipole Moment (D)	2.17	2.53	3.43	3.51	2.17	2.53	4.63	3.51	2.17

* The symbols C, B, *e*, *a*, indicate the chair and boat conformation of the six-membered ring, and the equatorial and axial position of the N-methyl group, respectively.

In the NMR spectrum of **I** and **II** the methylene protons give quartets at δ 3.25 and 3.40, respectively. The protons of the $R{=}CH_3$ and $R{=}C(CH_3)_3$ groups give rise to sharp absorptions at δ 2.37 and 1.2 ppm, respectively. The

NMR spectrum of **III** merely consists of three lines: the $C-CH_2-N$ and $N-CH_2-N$ protons give lines at δ 3.82 and 4.27 ppm, while the phenyl protons at δ 7.30 ppm. The NMR spectra of **IV** and **V** show considerable deviations from those of **I** and **II**. Owing to the reduction of the C=O group, the CH_2 units of the two six-membered rings are anisochronous. Accordingly, two quartets at different chemical shifts appear in the spectrum of **IV** and **V** (Table III).

Discussion

N,N'-dimethyl- and N,N'-di-t-butyl-1,5-diphenylbispid-9-one (I and II)

On the basis of comparing the experimental and calculated dipole moments, one has to take three conformations into account in the elucidation of the conformation of compound I. According to the data in Table II, the experimentally found dipole moment of 3.34 D may correspond to the $CB_{e,e}$, $CB_{a,e}$ and $BB_{e,a}$ conformations. The $CC_{e,e}$ and $CC_{e,a}$ conformations built up of the usually more stable chair conformation of six-membered rings are very unlikely; the measured dipole moment of 3.34 D is considerably greater than either one of the values calculated for the undistorted chair–chair conformations (2.72 and 2.53 D). Owing to the mutual repulsion between the unshared electron pairs, a distortion of the chair–chair-conformation skeleton, *i.e.* the symmetric receding of the two nitrogen atoms, would only slightly alter the dipole moment calculated for the undistorted $CC_{e,a}$ conformation (2.53 D). However, in the case of the $CC_{e,e}$ conformation, the dipole moment would in fact decrease, as here the unshared electron pairs of the nitrogen atoms would assume a nearly parallel orientation and the calculated dipole moment reaches its minimum ($\mu = 3.10 - 2 \times 0.80 = 1.50$ D) for the parallel orientation of the unshared electron pairs. The experimental values strongly favour a chair–boat conformation with one or two equatorial N-methyl groups, the latter being indicated by the appearance of the Bohlmann bands. The dipole moments calculated for the $CB_{e,e}$ and $CB_{a,e}$ conformations (3.43 and 3.51 D) satisfying the above requirements, are in good agreement with the experimental value of 3.34 D. Though the calculated dipole moment of the

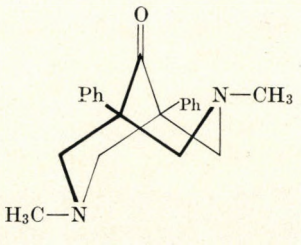

I, $CB_{e,e}$

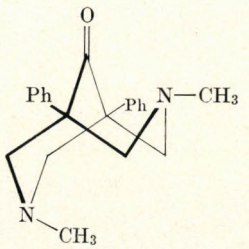

I, $CB_{a,e}$

Table III

*NMR spectral data of N,N'-Disubstituted-1,5-diphenylbispidines**

	I R=CH_3	II R=$C(CH_3)_3$	III	IV R=CH_3	V R=$C(CH_3)_3$	VI
N-R	2.37; s, 6H	1.21; s, 18H	—	2.06; s, 3H	0.97; s, 9H	—
N'-R			—	2.19; s, 3H	1.05; s, 9H	—
CH** (ring 1)	3.25; q, 8H $\Delta\nu_{AB} = 47.2$Hz $J_{AB} = 10.8$Hz	3.40; q, 8H $\Delta\nu_{AB} = 43.2$Hz $J_{AB} = 10.5$Hz	3.82; q, 8H	2.32; q, 4H $\Delta\nu_{AB} = 61.3$Hz $J_{AB} = 12.0$Hz	2.44; q, 4H $\Delta\nu_{AB} = 70.4$Hz $J_{AB} = 11.8$Hz	3.20; bs, 8H
CH_2** (ring 2)				3.05; q,4H $\Delta\nu_{AB} = 9.8$Hz $J_{AB} = 10.0$Hz	3.25; q,4H $\Delta\nu_{AB} = 16.4$Hz $J_{AB} = 10.0$Hz	
N-CH_2-N	—	—	4.27; s, 2H	—	—	3.65; s, 2H
H-9	—	—	—	4.34; s, 1H	4.24; s, 1H	3.4; s, 1H
C_6H_5	7.3; s, 10H	7.3; s, 10H	7.3; s, 10H	7.0—7.5; m, 10H	7.0—7.5; m, 10H	7.0—7.5; m, 10H

* δ-scale, TMS internal reference; $\Delta\nu_{AB}$ is calculated from the equation $\nu_A - \nu_B = \sqrt{(\nu_4 - \nu_1)(\nu_3 - \nu_2)}$; Accuracy in J in ± 0.1 Hz.
** Midpoint of quartets

$BB_{e,a}$ conformation is close to the measured value, this conformation includes two unfavourable structural units: rings in the boat conformation and axial $N-CH_3$ group, therefore, it may be ruled out. Consequently, the preferred conformation of **I** is $CB_{e,e}$ or $CB_{a,e}$ or both, but anyhow a chair–boat conformation. The two chair–boat conformations found to be probable differ only in the orientation of either of the two $N-CH_3$ groups.

The correctness of these conclusions is supported by related conformational analyses described earlier. Thus, DaRooge and Neumann [9] found the dipole moment of 3-methyl-3-azabicyclo (3.3.1)nonan-9-one, 3-methyl-3-azabicyclo-(3.2.1) octan-8-one, and N-methylpiperidone to be 2.89, 2.66 and

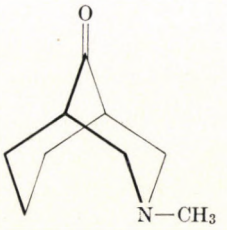

2.89 D

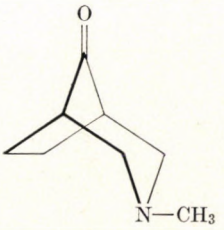

2.66 D



2.91 D

2.91 D, respectively (*cf.* Scheme). These data unambiguously indicate that in the case of N,N'-dimethyl-1,5-diphenylbispid-9-one the chair–chair conformation may be ruled out since the moment of the N-methylpiperidone ring (2.7—2.9 D) would be further decreased by the chair conformation of the other ring, in contrast to the value of 3.34 D found experimentally.

Therefore, the other ring must be attached in boat conformation to the piperidone ring in order to increase the electric dipole moment of the N-methylpiperidone skeleton from 2.7—2.9 D to 3.3—3.4 D.

In the NMR spectrum of **I** a quartet corresponding to an AB type spinsystem can be assigned to the methylene groups. The appearance of a single AB quartet indicates that, owing to rapid ring inversion, time-averaged chemical shifts are being observed. In principle a rigid chair–boat conformation would require two different quartets in the NMR spectrum, but the relatively simple pattern observed can be attributed to a rapidly equilibrating CB $\rightleftharpoons$ BC ring system.

The dipole moment of N,N'-di-*t*-butyl-1,5-diphenylbispid-9-one (**II**) is surprisingly higher than that of the corresponding N,N'-dimethyl derivative (**I**). The slight difference between the dipole moments of N-methyl- and N-*t*-butylpiperidine (0.80 D and 0.73 D) [8] cannot explain the considerable difference between the dipole moments of **I** and **II**. The nearly identical values of the dipole moments of N-methyl- and N-*t*-butylpiperidines make it possible

to use the dipole moment values calculated for the possible conformations of **I** (Table II) for the evaluation, in a first approximation, of the preferred conformation of N,N'-di-*t*-butylbispidone.

Owing to the known conformation-holding character of the tertiary butyl group, only conformations $CC_{e,e}$, $CB_{e,e}$ and $BB_{e,e}$ may be of importance in the case of **II**. Of these, a comparison of the calculated and measured dipole moments rules out $CC_{e,e}$ to leave the $CB_{e,e}$ and $BB_{e,e}$ conformations, for which the dipole moments calculated by taking into account the dipole moment of N-*t*-butylpiperidone [8], are 3.37 and 4.40 D, respectively. In the case of the $CB_{e,e}$ conformation, a distortion of the ring (towards the half-chair–boat conformation) would further decrease the dipole moment. It appears, therefore unlikely that a drastic deviation from the geometry of the regular six-membered

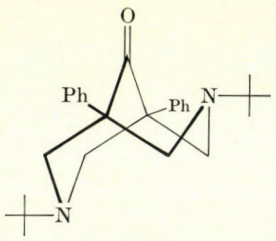

II, $CB_{e,e}$

$\mu_{calcd} = 3.37$ D

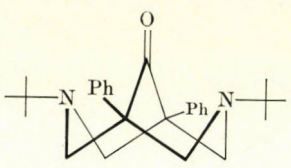

II, $BB_{e,e}$

$\mu_{calcd} = 4.40$ D

rings would cause this surprisingly high dipole moment. As the only explanation, one must assume that **II** exists also in the $BB_{e,e}$ conformation of higher dipole moment (4.40 D) and that there is an equilibrium between conformations $CB_{e,e}$ and $BB_{e,e}$, wherein $BB_{e,e}$ appears in a considerable amount (40—50%). This is a rather surprising result because no boat–boat conformation has been observed so far in the field of bicyclo-(3.3.1) nonane derivatives.

As in the case of **I**, the NMR spectrum of **II** reveals a single regular AB quartet assignable to the CH_2 groups. This means that a fast conformational equilibrium of the type CB $\rightleftharpoons$ BC takes place similarly to the case of **I**.

Conformation of N,N'-dimethyl- and N,N'-di-t-butyl-1,5-diphenyl-bispidin-9-ol

The difference between the conformation of **I** and **II** concluded mainly on the basis of dipole moment measurements, manifests itself strikingly in the NMR spectrum of **IV** and **V**. The fact that a hydrogen atom and a hydroxyl

group are attached to carbon atom 9 makes the magnetic environment of the methylene groups in the two six-membered rings different. Hence it is evident that the methylene protons of the two rings will show different chemical shifts (Table III). The quartets at δ 2.32 and 2.44 in the spectrum of **IV** and **V**, respectively (Table III), can be interpreted in terms of the boat conformation stabilized by intramolecular hydrogen bonding of one of the two rings of both

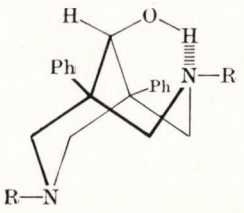

CB

IV, R = CH_3

V, R = $C(CH_3)_3$

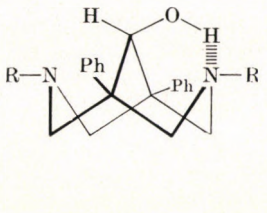

BB

IV and **V**. This assumption is supported by the very similar shifts and coupling constants of the corresponding quartet. The AB quartet for the other ring of **IV** and **V** is consistent with fast or slow ring inversion.

A further piece of evidence for the conformation of **IV** and **V** with intramolecular hydrogen bonding is supplied by infrared spectroscopic data. The spectra of both **IV** and **V**, taken in 0.1 *M* solution in CS_2, reveal single O—H absorption bands a 3325 and 3290 cm^{-1}, respectively. On dilution of the solutions (up to 0.001 *M* concentration) no absorption band appears at about 3600 cm^{-1}, which is characteristic of monomeric O—H groups, while the absorption frequency of the hydrogen-bonded O—H groups remains unchanged. Thus, the hydrogen bond is, in fact, intramolecular and rather stable.

Owing to the bond moments made obscure by the emergence of hydrogen bonds, the experimental dipole moments of **IV** and **V** (2.66 and 4.09 D, respectively) can be correlated only qualitatively with conformations. The high dipole moment found in the case of **V** can be interpreted in terms of the nearly parallel alignment of the dipolar bonds together with the corresponding bond moments. Such a dipole arrangement is satisfied in the BB conformation of **V**. The considerably lower dipole moment of 2.66 D for IV than that for **V** indicates partial compensation of the bond moments within the molecule, which may actually occur in the CB conformation of **IV**.

The two relatively sharp singlets in the NMR spectrum of **VI** (Table III) can be assigned to the methylene groups of four C—CH_2—N and one N—CH_2—N groups, which are approximately equivalent by coincidence. This spectrum, too, proves that none of **I**, **III**, **IV** and **V** assumes an adamantane-type chair–chair conformation with axial N-methyl group, because these latter give NMR spectra of quite different line structure.

Experimental

The compounds studied have been prepared by known procedures [10]. The infrared spectra were recorded in KBr pellets on C. Zeiss UR-10 and MOM 2000 type instruments.

The nuclear magnetic resonance spectra were taken at 100 MHz (Varian HA-100) and 60 MHz (AEI-RS2) in chloroform or carbon disulfide solutions, using TMS as internal reference.

The dipole moments were measured in benzene solution at 25.0°C. The instrument used and the method of evaluation have been described earlier [11].

*

The authors are indebted to Professor A. R. KATRITZKY for the valuable comments and for the NMR facilities used by one of them (P. S.) in the Chemical School, University of East Anglia, Norwich. The scholarship awarded by the Hungarian Institute of Cultural Relations and the British Council to one of the authors (P. S.) is also gratefully acknowledged.

REFERENCES

[1] (a) STETTER, H.: Angew. Chem., Intern. Ed. Eng., **1**, 286 (1962), and references therein; (b) MANNICH, C.,MOHS, P.; Ber. **63.** 608 (1930)
[2] DOUGLASS, J. E., RATLIFF, T. B.: J. Org. Chem. **33,** 355 (1968)
[3] (a) BROWN, W. A. C., MARTIN, J., SIM, G. A.: J. Chem. Soc. 1844 (1965); (b) MACROSSEN, W. D. K., MARTIN, J., PARKER, W.: J. Chem. Soc. 2589 (1965)
[4] (a) DOBLER, M., DUNITZ, J. D.: Helv. Chim. Acta **47,** 695 (1964); (b) PUMPHREY, N. W. J., ROBINSON, M. J. T.: Chem. Ind. London 1903 (1963)
[5] (a) CHEN, C.-Y., LEFÉVRE, R. J. W.: J. Chem. Soc. (B), 539 (1966); (b) AARON, H. S., FERGUSON, C. P., RADER, C. P.: J. Amer. Chem. Soc. **89,** 1431 (1967)
[6] BOHLMANN, F.: Angew. Chem. **69,** 641 (1957); Ber. **91,** 2157 (1958)
[7] LEFÉVRE, C. G., LEFÉVRE, R. J. W., RAO, B. P.: J. Chem. Soc. 2340 (1959)
[8] BISHOP, R. J., DINEEN, D., JONES, R. A. Y., KATRITZKY, A. R., SUTTON, L. E., WYATT, R. J.: J. Chem. Soc. 493 (1967)
[9] DAROOGE, M. A., NEUMANN, C. L.: unpublished results cited by E. L. ELIEL *et al.* in Conformational Analysis, p. 247. Wiley-Interscience, New York 1965
[10] KYI, ZU YOON, WILSON, W.: J. Chem. Soc. 1706 (1951)
[11] SCHEIBER, P., KRAISS, G., NESZMÉLYI, A., NÁDOR, K.: J. Chem. Soc. (B), **2149** (1971)

Pál SCHEIBER
Károly NÁDOR
1400 Budapest, P.O.B. 2, Hungary.

Acta Chimica Academiae Scientiarum Hungaricae, 84 (2), pp. 201—203 (1975)

DIAMAGNETIC SHIELDING OF THE DIBENZOCYCLOHEPTATRIEN RING SYSTEM IN SOME ACYLAMINOMALONIC ESTER DERIVATIVES

P. SOHÁR, J. KOSÁRY and E. KASZTREINER

(Research Institute for Pharmaceutical Chemistry, Budapest)

Received December 5, 1973

In the NMR spectra of diethyl-2-formylamino- and 2-acetylamino-2-(dibenzo(a,e)cycloheptene-5')-yl malonate (**III**; R = H; Me) a strong diamagnetic shift of the ethyl and acyl (formyl and acetyl, respectively) protons was observed relative to acylamidomalonic esters **II**, as a consequence of the anisotropic effect of the aromatic rings.

The dibenzocycloheptatrien derivatives **III** (R = H, Me) were obtained by treating the chloro compound **I** with malonic ester derivative **II** in dry N,N-dimethylformamide in the presence of sodium hydride, because the usual method [1] applying methanol as solvent and sodium methoxide as base failed to afford **III**. The structure of the compounds obtained was proved unambiguously by their IR and NMR spectra (Table I) as well as by the analytical results.

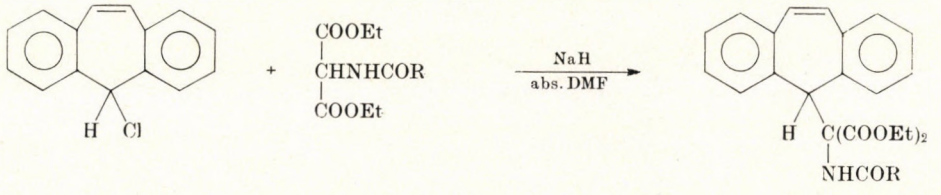

I **II** **III**

According to the NMR spectra, the protons of the ethyl and acyl groups show a strong diamagnetic shift in compound **III** as compared to **II**, owing to the anisotropic shielding effect of the π-electrons [2]. With space-filling atomic models it has been shown that in the molecules of **III** both the ethyl and acyl groups are in the anisotropic shielding cone of the double bonds of cycloheptatriene and the aromatic rings, as the group substituting the chlorine atom in compound **I** is forced into a *quasi-axial* position.

In the spectrum of the formyl compound **III** (R = H) a coupling constant of $J_{NH-CH(=O)} = 1$ Hz can be observed. A similar CH—NH coupling (7 Hz) exists in both the formamidomalonic ester **II** (R = H) and its N-acetyl analogue.

Table I

Compound	IR bands [cm^{-2}] in KBr					
	νNH	ν_{as}C=O	ν_sC=O	amide I	βNH	νC—O
II (R=H)	3330	1760	1735	1680	~1500	1270, 1240, 1210, 1095, 1030
II (R=Me)	3240	1755	1735	1635	~1540	1230, 1165, 1155, 1020, 1010
III (R=H)	3250	1758	1735	1650	~1490	1275, 1260, 1230, 1090, 1040
III (R=Me)	3380	1760	1730	1675	1505	1280, 1255, 1200, 1045, 1020

	NMR signals in $CDCl_3$ [$\delta_{TMS} = 0$ ppm]					
	δR	δCH_3(Et)*	δCH_2(Et)▽	$\delta CH^{\neq}$	δ (= $CH_{1,2}$)	δNH
III (R=H)	7.61+	1.03	3.97□	5.80	6.78	~6.8
III (R=Me)	1.55	1.01	3.95□	5.82	6.70	~6.5
II (R=H)	8.3+	1.30	4.31	5.30○	—	~7.8**
II (R=Me)	2.08	1.29	4.29	5.23○	—	~7.4○
$\Delta\delta_{II-III}$ (R=H)	0.7	0.27	0.34	—	—	~1.0
$\Delta\delta_{I-III}$ (R=Me)	0.53	0.28	0.34	—	—	~0.9

* triplet, J = 7 Hz
$\neq$ in position 5 in **III**, and methine proton in **II**
▽ quartet, J = 7 Hz
□ the methylene protons are not equivalent, therefore, the quartet shows a further AB splitting (AB part of an ABX_3 multiplet)
+ doublet, J ~ 1 Hz,
○ doublet J = 7.5Hz
** 2× doublet, J = 7.5 Hz and ~ 1 Hz

Experimental

The melting points are uncorrected. IR spectra were recorded with a Perkin-Elmer 457, and NMR spectra with a Varian A-60D spectrometer.

Diethyl-2-acylamino-2-(dibenzo[a, e]cycloheptene-5')-yl-malonate (III; R-Me)

A 50% slurry of NaH in mineral oil (1.5 g) was added to dry N,N-dimethylformamide (5 cm^3), and the stirred mixture was reacted at 5 °C with a solution of **II** (6.52 g) in N,N-dimethylformamide (10 cm^3). The reaction mixture was stirred at room temperature until no more hydrogen evolved (4 hrs). Then compound **I** [3] (7.17 g, 95% purity) was added at 0—5 °C in small portions and stirring of the reaction mixture was continued at room temperature for 5 hrs. The solution was poured into water (100 cm^3) and was extracted with ethyl acetate after acidifying with 10% HCl to pH 6. The residue, obtained after evaporating the solvent, was recrystallized from ethanol to give **III** (R = Me) (4.3 g; 63%), m.p. 132 °C.

($C_{24}H_{25}NO_5$). Calcd. C 71.0; H 6.20; N 3.44%;
Found C 70.55; H 6.22; N 3.47.

Diethyl-2-formylamino-2-(dibenzo[a, e]cycloheptene-5')-yl-malonate (III; R=H)

The reaction was carried out as described for **III** (R = Me), using **II** (R = H) as starting material. 9.0 g (76.5%) of **III** (R = H) was obtained, m.p. 135—137 °C.

($C_{23}H_{25}NO_5$), Calcd. C 70.4; H 5.85; N 3.56;
Found C 70.0; H 5.89; N 3.56%.

*

The authors wish to thank A. FÜRJES for technical assistance.

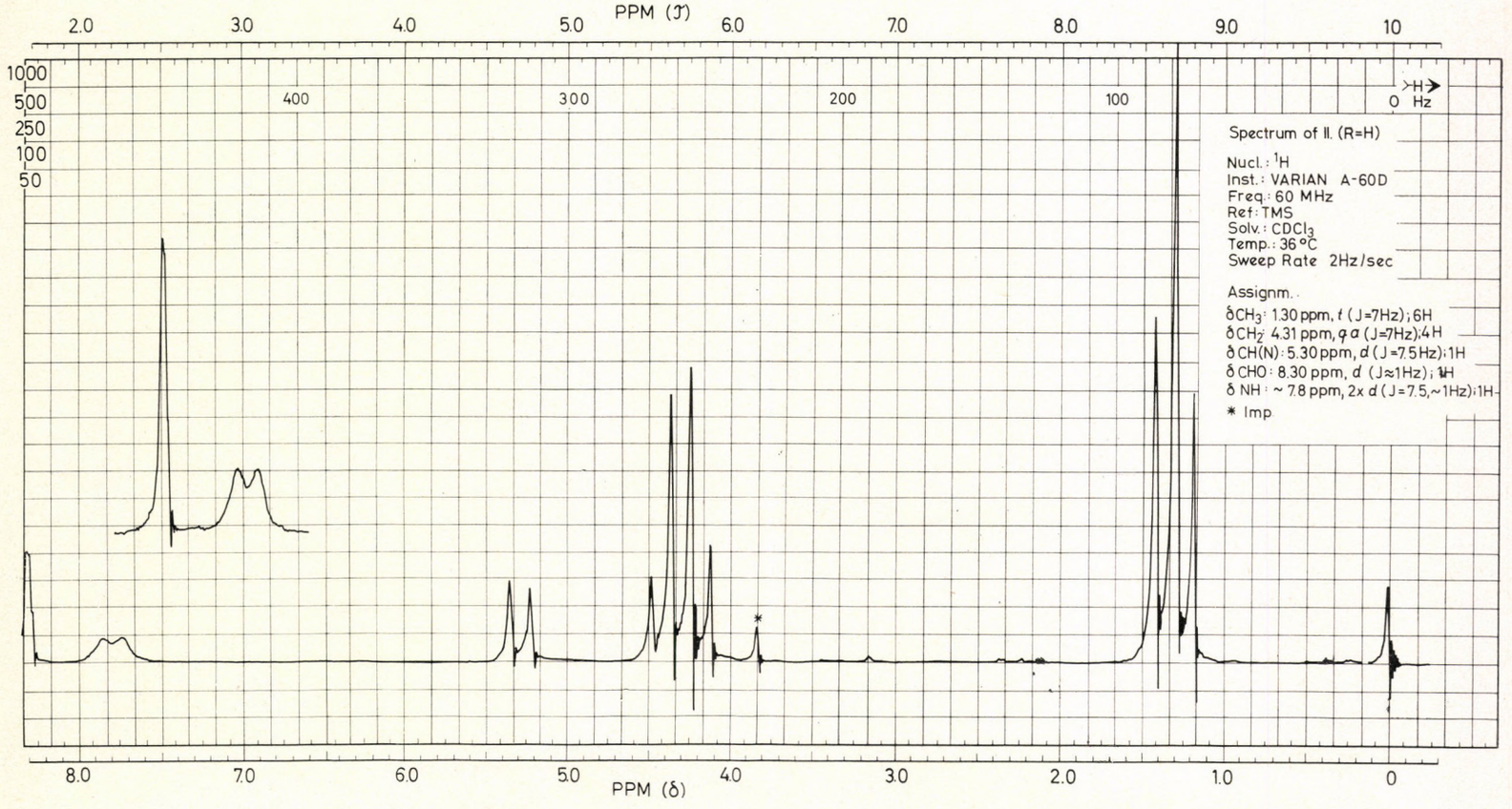
PPM (τ)
2.0
3.0
4.0
5.0
6.0
7.0
8.0
9.0
10
1000
500
250
100
50
400
300
200
100
0 Hz
Spectrum of II. (R=H)
Nucl.: 1H
Inst.: VARIAN A-60D
Freq.: 60 MHz
Ref.: TMS
Solv.: CDCl3
Temp.: 36 °C
Sweep Rate 2Hz/sec
Assignm.
δCH3: 1.30 ppm, t (J=7Hz); 6H
δCH2: 4.31 ppm, q a (J=7Hz); 4H
δ CH(N): 5.30 ppm, d (J=7.5Hz); 1H
δ CHO: 8.30 ppm, d (J≈1Hz); 1H
δ NH: ~ 7.8 ppm, 2x d (J=7.5, ~1Hz); 1H
* Imp.
8.0
7.0
6.0
5.0
4.0
3.0
2.0
1.0
0
PPM (δ)

Fig. 1

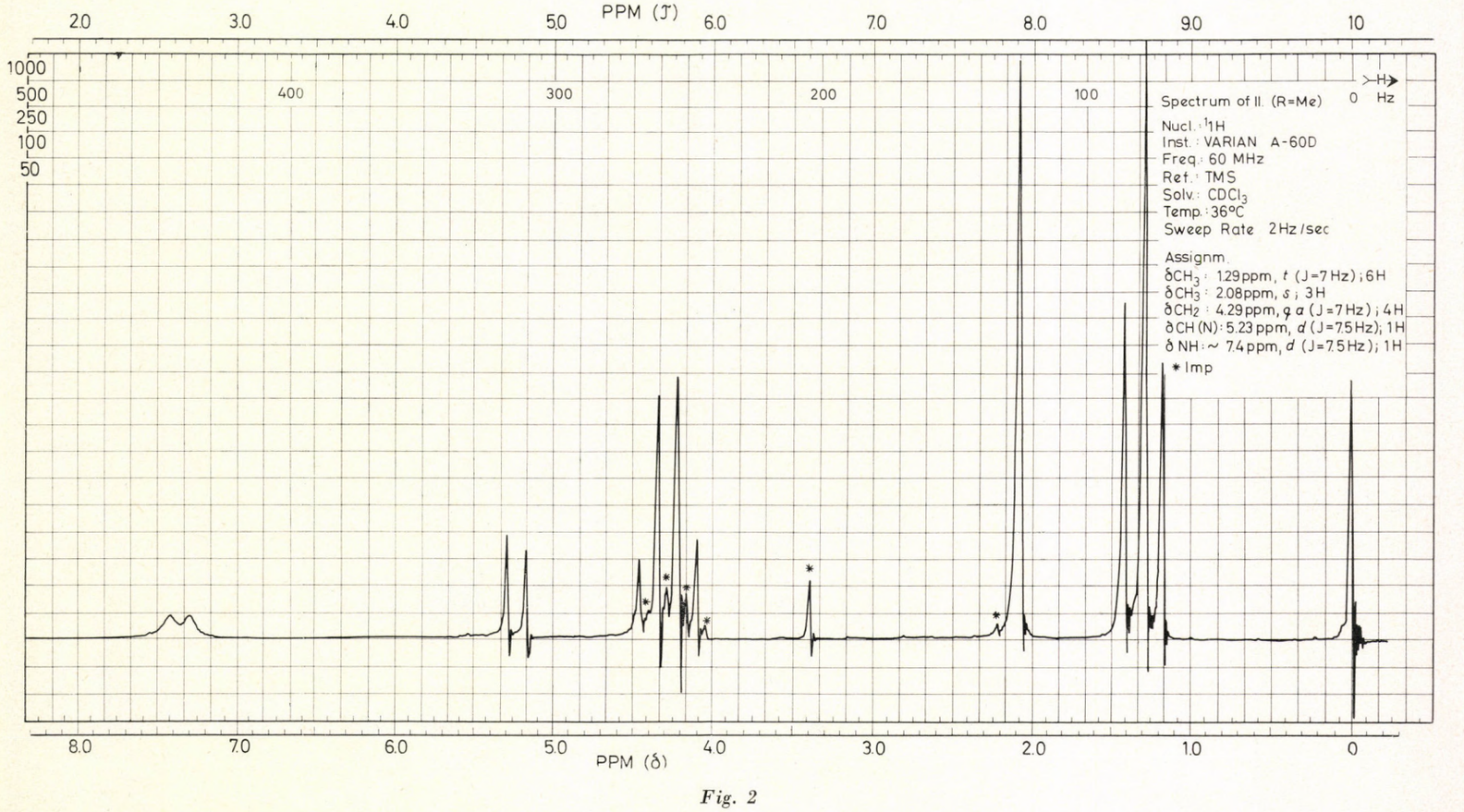
PPM (τ)
2.0
3.0
4.0
5.0
6.0
7.0
8.0
9.0
10
1000
500
250
100
50
400
300
200
100
0 Hz
Spectrum of II. (R=Me)
Nucl.: 1H
Inst.: VARIAN A-60D
Freq.: 60 MHz
Ref.: TMS
Solv.: CDCl3
Temp.: 36°C
Sweep Rate 2Hz/sec
Assignm.
δCH3: 1.29 ppm, t (J=7Hz); 6H
δCH3: 2.08 ppm, s; 3H
δCH2: 4.29 ppm, q a (J=7Hz); 4H
δ CH(N): 5.23 ppm, d (J=7.5Hz); 1H
δ NH: ~ 7.4 ppm, d (J=7.5Hz); 1H
* Imp
8.0
7.0
6.0
5.0
4.0
3.0
2.0
1.0
0
PPM (δ)

Fig. 2

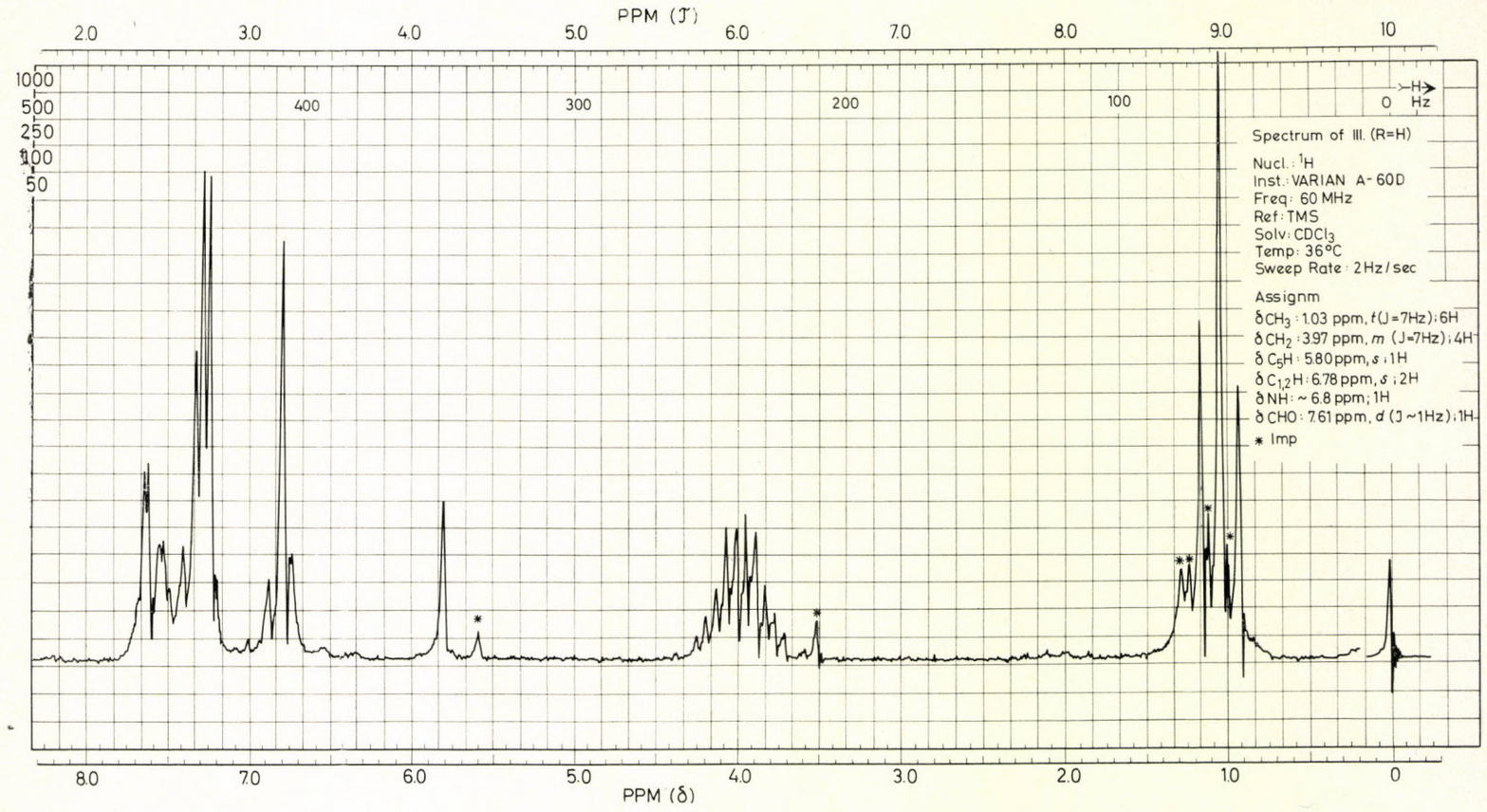
PPM (J)
2.0
3.0
4.0
5.0
6.0
7.0
8.0
9.0
10
1000
500
250
100
50
400
300
200
100
0 Hz
Spectrum of III. (R=H)
Nucl.: 1H
Inst.: VARIAN A-60D
Freq: 60 MHz
Ref: TMS
Solv: CDCl3
Temp: 36°C
Sweep Rate: 2Hz/sec
Assignm
δ CH3 : 1.03 ppm, t (J=7Hz); 6H
δ CH2 : 3.97 ppm, m (J=7Hz); 4H
δ C5H : 5.80 ppm, s ; 1H
δ C1,2H : 6.78 ppm, s ; 2H
δ NH : ~ 6.8 ppm; 1H
δ CHO : 7.61 ppm, d (J ~1Hz); 1H
* Imp
8.0
7.0
6.0
5.0
4.0
3.0
2.0
1.0
0
PPM (δ)

Fig. 3

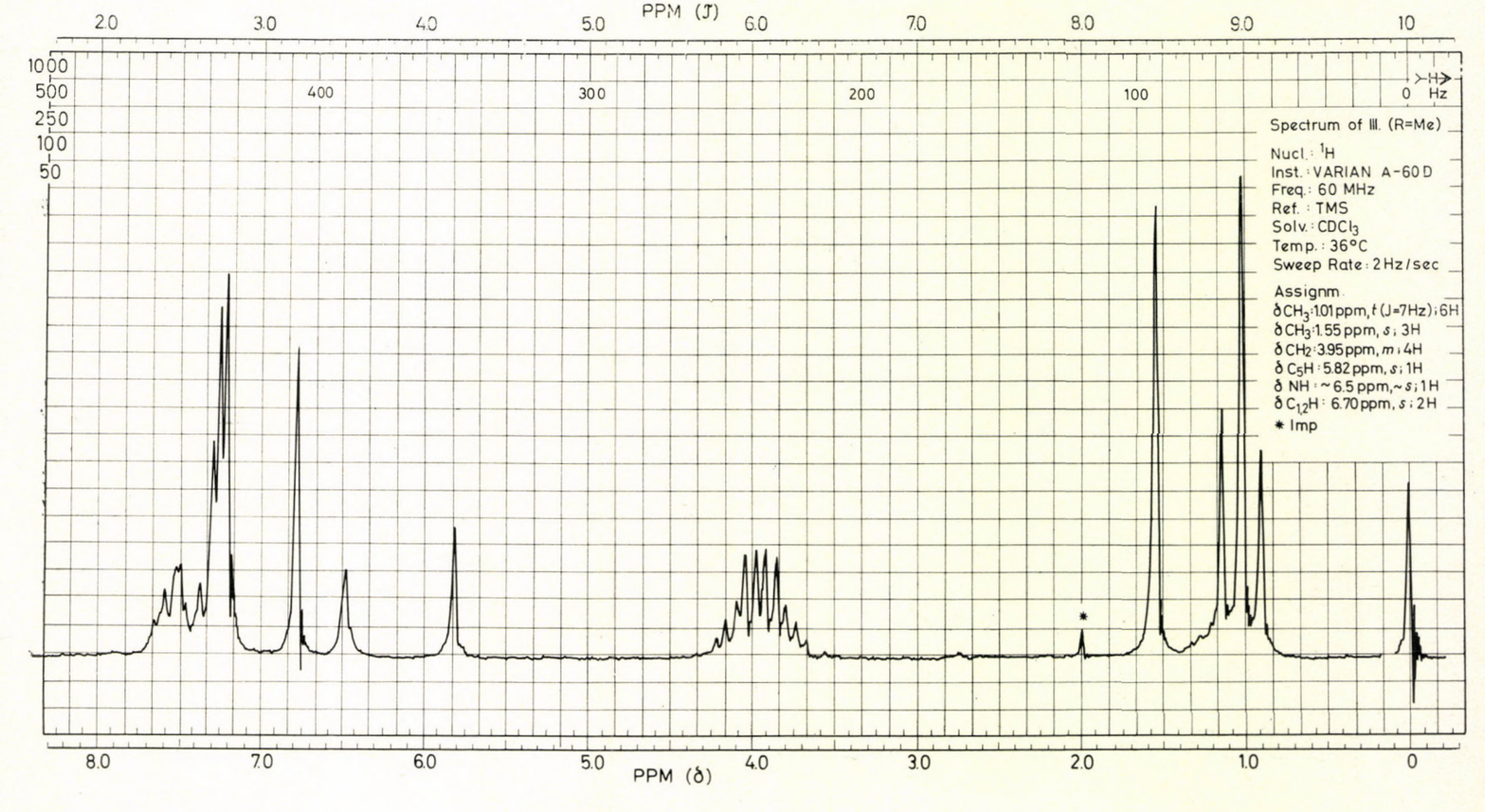
PPM (J)
2.0
3.0
4.0
5.0
6.0
7.0
8.0
9.0
10
1000
500
250
100
50
400
300
200
100
0 Hz
Spectrum of III. (R=Me)
Nucl.: 1H
Inst.: VARIAN A-60D
Freq: 60 MHz
Ref.: TMS
Solv.: CDCl3
Temp.: 36°C
Sweep Rate: 2Hz/sec
Assignm
δ CH3 : 1.01 ppm, t (J=7Hz); 6H
δ CH3 : 1.55 ppm, s ; 3H
δ CH2 : 3.95 ppm, m ; 4H
δ C5H : 5.82 ppm, s ; 1H
δ NH : ~ 6.5 ppm, ~ s ; 1H
δ C1,2H : 6.70 ppm, s ; 2H
* Imp
8.0
7.0
6.0
5.0
4.0
3.0
2.0
1.0
0
PPM (δ)

Fig. 4

REFERENCES

[1] LEONARD, F., WAJNGURT, A., TSCHANNEN, W. BLOCK, F.: J. Med. Chem. **8,** 812 (1965)
[2] JACKMAN, L. M.: Applications of Nuclear Magnetic Resonance Spectroscopy in Organic Chemistry p. 18. Pergamon Press, Oxford, 1959
[3] BERTI, G.: J. Org. Chem. **22,** 230 (1957)

Pál SOHÁR
Judit KOSÁRY
Endre KASZTREINER
1325 Budapest, P.O.B. 82. Hungary.

Acta Chimica Academiae Scientiarum Hungaricae, 84 (2), pp. 205—215 (1975)

4-S-SUBSTITUIERTE 2,6-DINITROANILINE*

E. PÁLOSI, K. HARSÁNYI und G. HÉJA

(Pharmazeutische und Chemische Werke CHINOIN)

Eingegangen am 10. Januar 1974

Es wurden in Stellung **4** mit Methylthio-, Methylsulfinyl- bzw. Methylsulfonylgruppen substituierte N,N-Dialkyl-2,6-dinitroaniline (**2**) aus S,S-Dimethyl(4-hydroxyphenyl)sulfoniumsalz (**4**) als Ausgangssubstanz hergestellt.

Wir deuten den Säurecharakter des 2,4,6-Trinitrophenols (»Pikrinsäure«) sowie den Säurederivat-Charakter der anstelle der Hydroxylgruppe Chlor bzw. eine Aminogruppe enthaltenden Verbindungen aufgrund der auf den aromatischen Ring ausgedehnten Vinylogie, der Phenylogie. Es sind neuerdings mehrere, dem Pikramid (**1a**) ähnliche Verbindungen als hervorragende Herbicide (**1b**: Planavin^R; **1c**: Oryzalin; **1d**: Treflan^R) bekannt geworden [1]; charakteristisch für sie ist, daß sie alle N,N-disubstituierte 2,6-Dinitroaniline sind, die in Stellung 4 eine stark elektronenanziehende Gruppe enthalten.

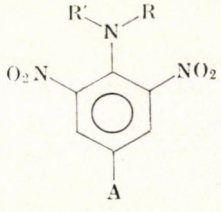

1

1a: A = NO_2: R = H
1b A = SO_2CH_3; R = n-C_3H_7
1c: A = SO_2NH_2; R = n-C_3H_7
1d: A = CF_3; R = n-C_3H_7

Zur Unterstützung dieses Zusammenhanges setzten wir uns das Ziel, N,N-disubstituierte 2,6-Dinitroaniline herzustellen, in denen der elektrische Charakter des para-Substituenten durch minimale Strukturänderungen beeinflußt werden kann. Um dieses Prinzip zu verwirklichen, versuchten wir, in Stellung 4 schwefelhaltige Gruppen einzuführen, in denen der Schwefel in ver-

* Teil der Doktorarbeit von E. PÁLOSI

schiedenen Oxydationsstufen vorliegt. Unsere zweite Zielsetzung dabei war eine Synthese, welche eine weitgehende Variierung der Substituenten der aromatischen Aminogruppe ermöglicht.

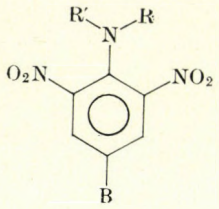

2

2a: B = SCH_3
2b: B = $SOCH_3$
2c: B = SO_2CH_3

Da mehrere Vertreter der Verbindungsgruppe **2c** bekannt sind (z. B. R und R' = n-C_3H_7; in diesem Fall ist **2c** = **1b**), untersuchten wir alternative Möglichkeiten zu ihrer Herstellung, wobei folgendes festgestellt wurde:

a) Infolge der elektrophilen Eigenschaft der 0,0'-Dinitrogruppen ist die primäre Aminogruppe mit Säureamid-Charakter nachträglich nicht alkylierbar.

b) Die primäre Aminogruppe kann mit Aminen bzw. Aminsalzen nicht in eine nukleophile Austauschreaktion gebracht werden.

c) Das in Reaktion gebrachte sekundäre Amin wird durch den Toluolsulfonsäureester von **8a**, d. h. **8b** nur mit schlechter Ausbeute aryliert (**8a** ist **2c** analog, enthält jedoch anstelle der Aminogruppe eine Hydroxylgruppe). Aus dem Methyläther von **8** (**8c**) konnte — im Gegensatz zu einzelnen Literaturangaben [2] — kein **2c** gewonnen werden. In beiden Reaktionen wurden beträchtliche Mengen von **8a**, der Verbindung mit phenolischem Hydroxyl, freigesetzt.

Aus diesen Befunden ergab sich, daß sich als Weg zu einer prinzipiell verallgemeinerungsfähigen Herstellungsweise von Verbindungen des Typs **2** allein die nukleophile Austauschreaktion von Aminen und Halogenbenzolderivaten bietet. Unter Anwendung dieser Reaktion führten wir die Synthese von Verbindungen des Typs **2c** durch [3].

Im weiteren mußten wir die Vorstellungen bezüglich der Einführung der Nitrogruppen im Endschritt verwerfen. Obwohl die Grundverbindung **2c** (R, R' = H) auf diesem Weg hergestellt wurde [4, 5], erschien das Verfahren bei **2a** (R, R' = H) aufgrund der Mitteilung von A. M. Simonow *et al.* [6] nicht aussichtsreich. Die genannten Verfasser beobachteten bei der Mononitrierung des *p*-Tosylamidothioanisols eine beträchtliche Sulfoxydbildung.

Außerdem sind bei der Nitrierung von Thiophenoläthern die Spaltung der C—S-Bindung [6, 7] und der Austausch der Thiomethylgruppe gegen eine Nitrogruppe [8] bekannte Nebenreaktionen.

Eine weitere Schwierigkeit gegenüber der Nitrierung von Acylanilinen ergab sich in unserem Fall daraus, daß wir beim Nitrieren der die gewünschte tertiäre Aminogruppe enthaltenden Verbindung auch mit einer Desalkylierungsreaktion rechnen mußten [9]. Eine derartige Reaktion beobachteten wir beim Nitrieren von 4-(N,N-Dipropylamino)-phenyl-methylsulfon **3a**; nach der Einführung einer Nitrogruppe (**3b**) erhielten wir beim weiteren Nitrieren, unter Abspaltung der einen Propylgruppe das N-Nitroderivat **3c**.

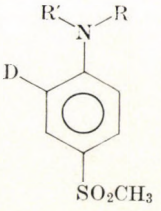

3

3a: R,R' = *n*-C_3H_7; D = H
3b: R,R' = *n*-C_3H_7; D = NO_2
3c: R = *n*-C_3H_7; R', D = NO_2

Aufgrund unserer Vorversuche und Literaturangaben wählten wir den Weg der Nitrierung des entsprechenden Sulfoniumsalzes zur Verwirklichung unserer Zielsetzung. Bekanntlich [10—12] können nämlich S,S-Dimethyl-S-phenylsulfoniumsalze mit guter Ausbeute nitriert werden.

Als Ausgangsmaterial zur Herstellung von Verbindungen des Typs **2** erschien das aus Phenol, Dimethylsulfoxyd und Salzsäuregas gewinnbare S,S-Dimethyl-(4-hydroxyphenyl)-sulfoniumchlorid **4** [13] am besten geeignet, da die Herstellung von Sulfoniumsalzen, die am aromatischen Ring in para-Stellung halogensubstituiert sind, wesentlich komplizierter ist [14].

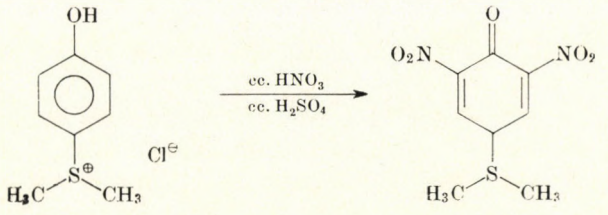

4 **5**

4 setzt sich in konzentrierter schwefelsaurer Lösung in das Sulfat um, das mit der berechneten Menge von konzentrierter Salpetersäure das S,S-Dimethyl-2,6-dinitro-4-thio-1,4-benzochinon **5** liefert. Die Verbindung **5** ist

bereits seit längerer Zeit bekannt, jedoch wurde ihre Herstellung ziemlich umständlich gelöst [8, 15].

Bei kurzzeitigem Kochen von **5** mit Halogenwasserstoffen in wäßriger Lösung entsteht quantitativ 2,6-Dinitro-4-(methylthio)phenol **6a** [8, 13b].

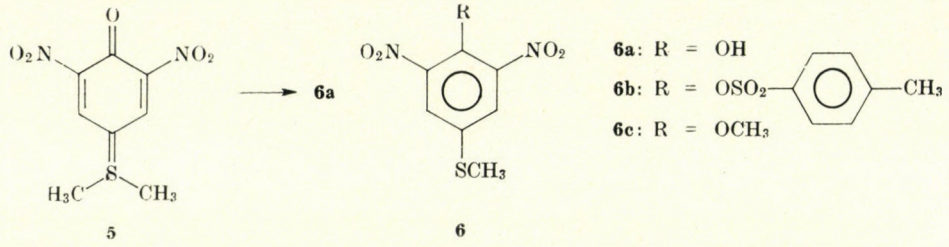

5 6

Beim Oxydieren von **6a** mit Wasserstoffperoxid in essigsaurer Lösung entsteht, in Abhängigkeit von der Menge des Wasserstoffperoxyds, entweder 2,6-Dinitro-4-(methylsulfinyl)phenol **7** oder 2,6-Dinitro-4-(methylsulfonyl)-phenol **8** mit Ausbeuten über 90%.

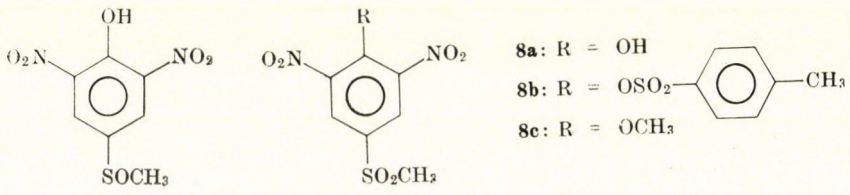

7 8

Der Austausch der phenolischen Hydroxylgruppe gegen Chlor ist ein häufiges Verfahren auf dem Gebiete der heteroaromatischen Verbindungen. In der aromatischen Reihe ist die Herstellung von Pikrylchlorid aus Pikrinsäure mit Phosphoroxychlorid in Gegenwart von Pyridin [16] sowie die Herstellung von verschiedenen Nitrochlorbenzolen aus Nitrophenolen, mit Thionylchlorid in hohem Überschuß und Dimethylformamid als Katalysator [17], bekannt.

Gegenüber den bisher bekannten Verfahren fanden wir es vorteilhafter, den Austausch der phenolischen Hydroxylgruppe mit Phosphoroxychlorid in Dimethylformamid vorzunehmen. Das chlorierende Agens ist das bekannte Addukt aus Phosphoroxychlorid und Dimethylformamid [18]. Der Vorteil des Verfahrens liegt darin, daß kein Überschuß an Phosphoroxychlorid benötigt wird; das 2,6-Dinitro-4-(methylthio)chlorbenzol **9a**, das 2,6-Dinitro-4-(methylsulfinyl)chlorbenzol **9b** sowie das 2,6-Dinitro-4-(methylsulfonyl)chlorbenzol **9c** entsteht mit fast quantitativer Ausbeute. Das überschüssige Dimethylformamid tritt nicht mit dem entstandenen Chlorbenzolderivat in Reaktion, in Gegensatz zu Beobachtungen an anderen Beispielen [19].

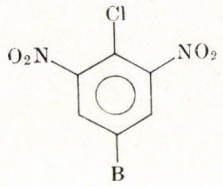

9

9a: B = SCH_3
9b: B = $SOCH_3$
9c: B = SO_2CH_3

Die Aminolyse der Verbindungen **9** liefert die entsprechenden Anilinderivative **10** mit hervorragender Ausbeute.

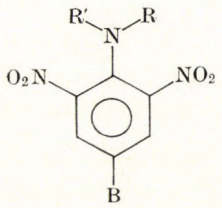

10

10a: B = SCH_3; R,R' = n-C_3H_7
10b: B = SCH_3; R,R' = $(—CH_2—)_5$
10c: B = SCH_3; R,R' = $(—CH_2—)_4$
10d: B = $SOCH_3$; R,R' = n-C_3H_7

Unter den (Methylthio)-nitroanilinen war bisher nur das 2-Nitro-4-(methylthio)anilin bekannt, das durch hydrolytische Methylierung der Thiocyangruppe erhalten wurde [20].

Wir oxydierten die 2,6-Dinitro-4-(methylthio)aniline mit recht guter Ausbeute in essigsaurer Lösung mit 1 Mol Wasserstoffperoxyd zu den entsprechenden 4-Methylsulfinylderivaten **2b**, mit überschüssigem Wasserstoffperoxyd zu den 4-Methylsulfonylverbindungen **2c**.

Das Interessante bei der letzteren Reaktion ist, daß selbst bei überschüssigem Wasserstoffperoxyd nur das Sulfon entsteht und keinerlei N-Oxydbildung zu beobachten ist. Dieser Befund ist umsomehr beobachtenswert, da — gemäß den Beobachtungen mehrerer Forscher — die Reaktivität gegenüber Wasserstoffperoxyd in essigsaurer Lösung in der Reihenfolge tert. Amin > Sulfid > Azinstickstoff > Thiolschwefel > Äthylenbindung > aromatische Bindung abnimmt [21].

In unserem Fall sind für das Ausbleiben der Bildung von N-Oxyd die stark elektrophilen Substituenten des Ringes verantwortlich. Diese machen

Tabelle I

Zeichen	Benennung	Lösungsmittel	Schmelzpunkt °C
10a	2,6-Dinitro-4-(methylthio)-N,N-dipropylanilin	Butanol	Öl
10b	1-(2,6-Dinitro-4-methylthio)-phenylpiperidin	Äthanol	99—101
10c	1-(2,6-Dinitro-4-methylthio)-phenylpyrrolidin	Äthanol	93— 94
10d	2,6-Dinitro-4-(methylsulfoxyl)-N,N-dipropylanilin	Äthanol	86— 87
1b	2,6-Dinitro-4-(methylsulfonyl)-N,N-dipropylanilin	Isopropylalkohol	150—151

das einsame Elektronenpaar des Stickstoffs der Aminogruppe unfähig, eine dative Bindung zu bilden. In Abwesenheit solcher Gruppen kann die selektive Bildung des S-Oxyds nicht gelöst werden. So erhielten z. B. KARPENKO *et al.* [22] bei der Oxydation von (*p*-Dimethylaminophenyl)-tert. butylsulfyd mit Wasserstoffperoxyd (*p*-Dimethylaminophenyl)-tert. butyl-sulfon-N-oxid.

Aus den Ergebnissen der Ausprüfung einiger unserer Verbindungen — wofür wir dem Außenhandelsunternehmen Medimpex und der Dow Chemical Co. zu Dank verpflichtet sind — konnte unsere Ansicht über den Zusammenhang zwischen Wirkung und Struktur bestätigt werden. Ein weiteres Ergebnis unserer Arbeit ist das neue, für industrielle Durchführung geeignete Syntheseverfahren des bekannten Herbicids **1b**.

*

Wir danken Herrn I. REMPORT für die Mikroanalysen und Frau Dr. T. KUBINYI sowie Frl. J. KUN und M. WUNDELE für die Teilnahme an der Durchführung der Versuche.

Experimenteller Teil

Die angegebenen Schmelzpunkte sind unkorrigiert.

2,6-Dinitro-4-(methylthio)phenyl-p-toluolsulfonat (6b)

Zu der in 30 ml trockenem Aceton gelösten, mit kaltem Wasser gekühlten Lösung von 6,2 g (0,027 mol) 2,6-Dinitro-4-(Methylthio)phenol (**6a**) und 3,8 ml Triäthylamin wird unter Rühren eine Lösung von 5,15 g (0,027 mol) Tosylchlorid in 15 ml trockenem Aceton tropfenweise zugegeben. Das Reaktionsgemisch wird bei Raumtemperatur weitere 3,5 Stunden lang gerührt. Die abgeschiedenen Kristalle (Triäthylammoniumchlorid) werden abfiltriert und das Filtrat eingedampft. Der Rückstand wird mit Wasser verrieben und filtriert. Es werden 9,53 g (92%) **6b** erhalten. Nach Umkristallisieren aus Nitromethan, Schmp. 186—187 °C.

Analyse $C_{14}H_{12}N_2O_6S_2$ (384,39)
Ber. C 43,70%, H 3,16%, N 7,30%, S 16,68%
Gef. C 43,87%, H 3,29%, N 7,10%, S 16,50%

Umkristallisiert aus	Ausbeute %	Analyse							
		Berechnet				Gefunden			
		C	H	N	S	C	H	N	S
	97								
Methanol	97	48,47	5,08	14,13	10,78	48,80	5,06	13,97	10,80
Äthanol	99	46,63	4,62	14,83	11,32	45,91	4,23	14,65	11,05
Äthanol-Wasser	82	47,03	5,81	12,76	9,73	46,93	5,67	12,40	9,79
Isopropylalkohol	91,5								

2,6-Dinitro-4-(methylsulfonyl)phenyl-p-toluolsulfonat (8b)

2,47 g (0,00645 mol) **6b** werden in 70 ml Eisessig gelöst und mit 2 ml 23%igem Wasserstoffperoxyd 2 Stunden lang auf dem Wasserbad erwärmt. Danach wird filtriert und eingedampft. Es werden 2,27 g (84,5%) **8b** erhalten. Schmp. nach Umkristallisieren aus Essigsäure 180—181°C.

Analyse $C_{14}H_{12}N_2O_9S_2$ (416,39)
Ber. C 41,32%, H 2,91%, N 6,73%, S 15,40%
Gef. C 41,48%, H 3,01%, N 6,63%, S 15,38%

2,6-Dinitro-4-(methylsulfonyl)-N,N-dipropylanilin (1b)

Ein Gemisch aus 1,25 g (0,003 mol) **8b,** 0,9 ml (0,0066 mol) Dipropylamin und 15 ml abs. Alkohol wird 1,5 Stunden lang im Sieden gehalten. Die Lösung wird im Vakuum eingedampft, der Rückstand mit 10 ml Wasser versetzt und mit 2×10 ml Chloroform ausgeschüttelt.

Zur wäßrigen Lösung werden 660 mg (0,00324 mol) S-Benzylthiuroniumchlorid zugegeben. Es werden 215 mg (21,2%) *p*-Toluolsulfonsäure-S-benzylthiuroniumsalz erhalten. Schmp. 171—173 °C.

Die chloroformische Lösung wird eingedampft und der ölige Rückstand aus Isopropylalkohol umkristallisiert. Es werden 250 mg (24,1%) **1b** erhalten. Schmp. 150—151 °C.

Das alkoholische Filtrat wird eingedampft und der Rückstand aus Äthylacetat umkristallisiert. Es werden 245 mg (31%) **8a** erhalten. Schmp. 220—222 °C.

Reaktion von 2,6-Dinitro-4-(methylthio)phenyl-p-toluolsulfonat mit Dipropylamin

3,85 g (0,01 mol) **6b** und 3,4 ml (0,025 mol) Dipropylamin werden in 50 ml Benzol gelöst und 3 Stunden lang im Sieden gehalten. Die benzolische Lösung wird eingedampft, der Rückstand in Chloroform aufgenommen, die Lösung mit 2 n Salzsäure, mit Wasser, mit 5%iger Natriumhydrogencarbonatlösung und wiederum mit Wasser gewaschen und über Natriumsulfat getrocknet. Nach dem Eindampfen der Lösung werden 1,6 g (76%) 2,6-Dinitro-4-(methyl-thio)phenol (**6a**) erhalten. Nach Umkristallisieren aus Methanol Schmp. 100—103 °C. (Literaturwert [8] Schmp. 108 °C.)

2,6-Dinitro-4-(methylsulfonyl)anisol (8c)

Zu einer aus 1,15 g (0,05 mol) Natrium und 400 ml abs. Methanol hergestellten Natriummethylatlösung werden 14 g (0,05 mol) 2,6-Dinitro-4-(methylsulfonyl)chlorbenzol (**9c**) gegeben und das Reaktionsgemisch wird 3 Stunden lang im Sieden gehalten. Nach dem Eindampfen wird der Rückstand mit Wasser behandelt. Es werden 11,05 g (80%) **8c** erhalten. Nach Umkristallisieren aus Methanol Schmp. 199—201 °C.

Analyse $C_8H_8N_2O_7S$ (276,23)
Ber. N 10,15%
Gef. N 10,16%

Aus **8c** entsteht mit Dipropylamin in methanolischer Lösung bei 8stündigem Sieden die Verbindung **8a** mit phenolischer Hydroxylgruppe (Ausbeute 95,5%).

4-(Methylsulfonyl)-N,N-dipropylanilin (3a)

a) Das Gemisch von 38 g (0,1 mol) (*p*-Chlorphenyl)-methylsulfon [23] mit 150 ml Dipropylamin und 1 g Natriumjodid wird im Rohr 25 Stunden lang bei 250 °C gehalten. Das Reaktionsgemisch wird eingedampft und der Rückstand in Chloroform aufgenommen. Die chloroformische Lösung wird mit verdünnter Salzsäure und mit Wasser gewaschen und über Natriumsulfat getrocknet. Nach dem Abdestillieren des Chloroforms wird der ölige Rückstand mit abs. alkoholischer Salzsäurelösung versetzt und die erhaltene Lösung eingedampft. Die erhaltenen Kristalle werden aus Isopropylalkohol umkristallisiert, wobei 21,3 g (73%) **3a**-Hydrochlorid erhalten werden. Schmp. 165—171 °C.

Analyse $C_{13}H_{22}ClNO_2S$ (291,84)
Ber. C 53,50%, H 7,60%, N 4,80%, Cl^- 12,15%, S 10,98%
Gef. C 53,68%, H 7,64%, N 5,02%, Cl^- 12,35%, S 11,20%

10 g des salzsauren Salzes werden in 50 ml Wasser suspendiert, mit 2 *n* NaOH alkalisch gemacht und mit Chloroform extrahiert. Nach dem Trocknen und Eindampfen werden 8,2 g öliges **3a** erhalten.

NMR ($CDCl_3$) τ = 9,1 ppm Triplett (6H) (Methyl)
8,3 Multiplett (4H) (Methylen)
6,7 Multiplett (4H) (Methylen)
7,0 Singulett (3H) (Methylsulfonylmethyl)
2,2—3,45 Multiplett (4H arom.)

b) Ein Gemisch von 2,65 g (0,015 mol) (*p*-Aminophenyl)-methylsulfon [24], 3,32 g (0,015 mol) Propyl-*p*-toluolsulfonat [25] und 1,5 g pulverisiertem Kaliumhydroxid wird 1 Stunde lang auf dem Wasserbad und anschließend 3 Stunden lang im Ölbad bei 110—120° C gehalten. Nach dem Abkühlen wird Wasser zum Reaktionsgemisch gegeben und es wird mit Chloroform extrahiert. Nach dem Eindampfen des Extraktes wird der harzige Rückstand mit Äther behandelt und die dabei abgeschiedenen Kristalle werden abfiltriert. Es werden 0,7 g des Ausgangsstoffes zurückgewonnen. Die ätherische Lösung wird eingedampft, der ölige Rückstand mit abs. alkoholischer HCl-Lösung behandelt, die Lösung eingedampft, der Rückstand aus Isopropylalkohol umkristallieiert. Es werden 1,5 g **3a**-Chlorhydrat erhalten (Schmp. 176—178 °C).

2-Nitro-4-(methylsulfonyl)-N,N-dipropylanilin (3b)

a) Zur Lösung von 0,25 g (0,001 mol) 4-(Methylsulfonyl)-N,N-dipropylanilin (**3a**) in 2,5 ml Eisessig werden 0,22 ml (0,005 mol) 95%ige Salpetersäure zugegeben. Die Lösung wird 24 Stunden bei Raumtemperatur stehen gelassen und anschließend in 25 ml Wasser gegossen. Das abgeschiedene Öl wird mit Benzol ausgeschüttelt. Die benzolische Lösung wird mit Wasser, mit Natriumcarbonatlösung und wiederum mit Wasser gewaschen und getrocknet. Nach dem Eindampfen werden 0,15 g (50%) öliges **3b** gewonnen.

NMR ($CDCl_3$) τ = 9,15 ppm Triplett (6H) (Methyl)
8,4 Multiplett (4H) (Methylen)
6,8 Triplett (4H) (Methylen)
6,92 Singulett (3H) (Methylsulfonylmethyl)
1,5—2,9 Multiplett (3H arom.) (1,2,4-trisubstituierter Benzolring)

b) Zur Lösung von 2,36 g (0,01 mol) 2-Nitro-4-(methylsulfonyl)chlorbenzol [26] und 1,06 g (0,0105 mol) Dipropylamin in 20 ml abs. Alkohol werden bei Siedentemperatur 1,06 g (0,0105 mol) Triäthylamin tropfenweise zugegeben. Die Lösung wird weitere 6 Stunden lang bei Siedetemperatur gehalten und anschließend eingedampft. Der Rückstand wird in Chloroform aufgenommen, die Lösung wird mit verdünnter Salzsäure und mit Wasser gewaschen und eingedampft. Das NMR-Spektrum des öligen Rückstandes (2,8 g **3b**, 93,5%) ist identisch mit dem Spektrum der nach a) hergestellten Verbindung.

2,N-Dinitro-4-(methylsulfonyl)-N-propylanilin (3c)

Zur Lösung von 2,55 g (0,01 mol) 4-(Methylsulfonyl)-N,N-dipropylanilin in 35 ml Eisessig werden unter Rühren bei 5—10 °C 5 ml konz. Salpetersäure tropfenweise zugegeben. Die Lösung wird 2 Stunden lang bei 50 °C gerührt und anschließend in Eiswasser gegossen.

Die abgeschiedenen Kristalle werden zweimal aus Alkohol umkristallisiert. Es werden 1,9 g (63,5%) **3c** erhalten. Schmp. 98—102 °C.

Analyse $C_{10}H_{13}N_3O_6S$ (303,28)
Ber. C 39,73%, H 4,33%, N 13,90%, S 10,85%
Gef. C 40,06%, H 4,23%, N 14,02%, S 10,99%
NMR ($CDCl_3$) τ = 9,10 ppm Triplett (3H) (Methyl)
8,30 Multiplett (2H) (Methylen)
5,4—6,05 Multiplett (2H) (Methylen)
6,80 Singulett (3H) (Methylsulfonylmethyl)
1,4—2,7 Multiplett (3H arom.)

2,6-Dinitro-4-(methylthio)phenol (6a)

114,3 g (0,6 mol) S,S-Dimethyl-(4-hydroxyphenyl)-sulfoniumchlorid **4** [13] werden in 120 ml konz. Schwefelsäure gelöst. Unter Rühren und Eis—Kochsalz-Kühlung wird — bei Temperaturen unterhalb 10 °C — tropfenweise Nitriersäure (bestehend aus 90 ml [1,2 mol] konz. Salpetersäure [Dichte 1,4] und 270 ml konz. Schwefelsäure) zugegeben. Das Reaktionsgemisch wird über Nacht stehen gelassen, dann 1,5 Stunden lang bei 90 °C gehalten und nach dem Abkühlen in Eiswasser gegossen. Die ausgeschiedenen gelben Kristalle (**5**) werden abfiltriert und mit Wasser gewaschen. Die feuchten Kristalle der Verbindung **5** werden in 540 ml konz. Salzsäure gelöst, 540 ml Wasser werden zugegeben und die Lösung wird eine Stunde lang im Sieden gehalten. Das beim Abkühlen erstarrende rote Öl wird abfiltriert und mit Wasser säurefrei gewaschen. Es werden 108 g (78%) **6a** erhalten, Schmp. 105—107 °C. (Literaturwert [8] Schmp. 108 °C.)

2,6-Dinitro-4-(methylsulfoxyl)phenol (7)

Zur Suspension von 23 g (0,1 mol) **6a** in 200 ml Eisessig werden 8,7 ml 39%iges Wasserstoffperoxyd (0,1 mol) gegeben und das Reaktionsgemisch wird 1,5 Stunden lang auf dem Wasserbad erwärmt. Anschließend wird es im Vakuum eingedampft, der Rückstand mit Wasser behandelt, die abgeschiedenen Kristalle werden abfiltriert und mit Wasser gewaschen. Es werden 23,1 g (94%) **7** erhalten. Schmp. 153—154 °C. (Literaturwert [8] Schmp. 150 °C.)

2,6-Dinitro-4-(methylsulfonyl)phenol (8a)

a) Zur Suspension von 69 g (0,3 mol) **6a** in 210 ml Eisessig werden 52,5 ml 39%iges Wasserstoffperoxyd (0,6 mol) gegeben. Das Reaktionsgemisch wird 1 Stunde lang auf dem Wasserbad erwärmt, wobei zunächst eine Lösung entsteht und alsbald die Kristalle der Verbindung **8a** abgeschieden werden. Nach dem Abkühlen werden die Kristalle filtriert und mit Wasser gewaschen. Es werden 75 g (95,5%) **8a** erhalten; Schmp. 221—222 °C. Durch Umkristallisieren aus Äthylacetat wird der Schmelzpunkt nicht verändert.

Analyse $C_7H_6N_2O_7S$ (262,20)
Ber. C 32,06%, H 2,30%, N 10,69%, S 12,23%
Gef. C 32,24%, H 2,55%, N 10,88%, S 12,16%

b) 28 g (0,1 mol) **9c** werden in 100 ml Dimethylformamid gelöst und eine Lösung von 10 g (0,25 mol) Natriumhydroxyd in 20 ml Wasser zugegeben. Die Lösung wird 1 Stunde lang im Sieden gehalten und nach dem Abkühlen mit 10%iger Salzsäure angesäuert. Nach dem Filtrieren, Waschen mit Wasser und Trocknen werden 20 g (77%) **8a** erhalten. Nach Umkristallisieren aus Äthylacetat Schmp. 220—221 °C. Die gemäß a) und b) hergestellten Substanzen **8a** sind völlig identisch.

2,6-Dinitro-4-(methylthio)chlorbenzol (9a)

23 g (0,1 mol) **6a** werden in 40 ml Dimethylformamid gelöst. Unter Rühren und Kühlen mit Eiswasser werden 9,2 ml (15,35 g; 0,1 mol) Phosphoroxychlorid tropfenweise zugegeben. Das Reaktionsgemisch wird im siedenden Wasserbad 1 Stunde lang gerührt. Nach dem Abkühlen wird es auf Eis gegossen. Die abgeschiedenen orangefarbigen Kristalle werden filtriert und mit Wasser gewaschen. Es werden 24 g (96,5%) **9a** erhalten. Schmp. 117—119 °C. Umkristallisieren aus Methanol ändert den Schmelzpunkt nicht.

Analyse $C_7H_5ClN_2O_4S$ (248,65)
Ber. Cl 14,26%, S 12,89%, N 11,27%
Gef. Cl 14,57%, S 12,94%, N 11,06%

2,6-Dinitro-4-(methylsulfoxyl)chlorbenzol (9b)

Das Gemisch von 12,55 g (0,05 mol) **9a**, 50 ml Eisessig und 4,5 ml 38%igem Wasserstoffperoxyd (0,05 mol) wird 1 Stunde lang auf dem Wasserbad erwärmt. Die Lösung wird im Vakuum eingedampft und der Rückstand mit Wasser behandelt. Nach dem Filtrieren und Trocknen werden 11,82 g (89,5%) **9b** erhalten. Aus Methanol umkristallisiert beträgt der Schmelzpunkt 127—128 °C.

Analyse $C_7H_5ClN_2O_5S$ (264,65)
Ber. C 31,77%, H 1,90%, N 10,59%, Cl 13,40%, S 12,11%
Gef. C 31,87%, H 1,75%, N 10,76%, Cl 13,39%, S 12,12%

2,6-Dinitro-4-(methylsulfonyl)chlorbenzol (9c)

a) Zur Suspension von 24,85 g (0,1 mol) **9a** in 100 ml Eisessig werden 18 ml 38,5%iges Wasserstoffperoxid (0,2 mol) zugegeben. Das Reaktionsgemisch wird 1 Stunde lang auf dem Wasserbad erwärmt. Zu dem noch warmen Gemisch werden 100 ml Wasser zugegeben. Die abgeschiedenen blaßgelben Kristalle werden filtriert und mit Wasser gewaschen. Es werden 25,8 g (92%) **9c** erhalten. Schmp. 201—203 °C. (Literaturwert [3b] Schmp. 201—203 °C.) Bei der Schmelzpunktbestimmung im Gemisch mit einer authentischen Substanz tritt keine Depression auf.

b) Zur Suspension von 26 g (0,1 mol) **8a** in 50 ml Dimethylformamid werden unter Rühren und Kühlen mit Eiswasser 9,2 ml (15,35 g; 0,1 mol) Phosphoroxychlorid tropfenweise zugegeben. Das Gemisch wird 1 Stunde lang bei Raumtemperatur und eine weitere Stunde lang auf dem siedenden Wasserbad gerührt. Nach dem Abkühlen wird die Lösung auf Eis gegossen, die abgeschiedenen Kristalle werden filtriert und mit Wasser gewaschen. Es werden 27,13 g (97%) **9c** erhalten. Schmp. 202—204 °C.

2,6-Dinitro-4-schwefelsubstituierte-N,N-Dialkylaniline (10)

Die alkoholische oder isopropylalkoholische Lösung von 1 Mol 2,6-dinitro-4-schwefelsubstituiertem Chlorbenzol und 2 Mol des entsprechenden Amins oder 1 Mol des Amins und 1 Mol Triäthylamin wird 2 Stunden lang im Sieden gehalten. Nach dem Abkühlen kristallisiert die Verbindung **10** in bestimmten Fällen. In anderen Fällen muß das Reaktionsgemisch eingedampft werden; durch Behandeln des Rückstandes mit Wasser wird **10** abgetrennt und anschließend wird umkristallisiert. Die Angaben der hergestellten Verbindungen sind in Tab. I enthalten.

2,6-Dinitro-4-(methylsulfonyl)-N,N-dipropylanilin (1b)

a) 15,6 g (0,05 mol) **10a** werden in 80 ml Eisessig gelöst und 9 ml 38%iges Wasserstoffperoxyd werden zugegeben (0,1 mol). Die Lösung wird 1,5 Stunden lang auf dem Wasserbad erwärmt und dann im Vakuum eingedampft. Der Rückstand wird mit Wasser behandelt, filtriert und mit Isopropylalkohol gewaschen. Es werden 14,30 g (83%) **1b** erhalten. Schmp. 150—151 °C.

b) Zur Lösung von 3,30 g (0,01 mol) **10d** in 16 ml Eisessig wird 1 ml 38%iges Wasserstoffperoxyd (0,01 mol) zugegeben und die Lösung wird 1 Stunde lang auf dem Wasserbad erwärmt. Das Reaktionsgemisch wird wie bei a) verarbeitet. Es werden 3,1 g (90%) **1b** erhalten. Schmp. 150—151 °C.

LITERATUR

[1] Frear, D. H.: Pesticide Index 1969, College Science Publishers, State College Pennsylvania
Dos Santos, C. A. L., De Soura, D. M.: Biologico **37**, 126 (1971); C. A. **75**, 117375 (1971); Ford, D. H., Massey, G. D.: Proc. Annual Calif. Weed Conf. **23**, 142 (1971); C. A. **75**, 117400 (1971)

[2] Borsche, W.: Ber. **56**, 1494 (1923); Boulton, J. J. K., McFarlane, N. R.: J. Chem. Soc. B. **1971**, 925; BRD-Patent No. 1 203 563 (CIBA); C. A. **61**, 16021 (1964); British Patent No. 1 241 117 und 1 228 536 (Bayer)

[3] a) Französisches Patent No. 816 727 (Soc. pour l'ind. chim. à Bâle); C. A. **32,** 2366 (1938); SCOFFONE, E., DE LA LLOSA, P. JUTISZ, M.: Bul. Soc. chim. France, **1959,** 1553; LAWRISCHTSCHEW, W. A., KRETOV, A. E.: Zh. Obschtsch. Chim. **32,** 502 (1962); belgisches Patent No. 703 611 (Gevaert-Agfa); C. A. **70,** 20 994 (1969); französisches Patent No. 1 509 499 (Eli Lilly); C. A. **70,** 57 850 (1969);
b) USA Patent 3 227 734 (Shell); C. A. **64,** 6566 (1966); USA Patent 3 321 292; C. A. **68,** 49 299 (1968); französisches Patent No. 1 453 170; C. A. **66,** 75 197 (1967); ungarisches Patent No. 154 617
[4] GILMAN, H., LINDBLAD, A. E.: J. Am. Chem. Soc. **68,** 982 (1946)
[5] LARSSON, E.: Trans. Chalmers Univ. Technol. Gothenburg No. 94, 3 (1950); C. A. **45,** 2892 (1951)
[6] SIMONOW, A. M., SAJAPIN, W. G., SIDERMAN, W. I.: Zh. Wses. Chim. Obschtschest. **15,** 232 (1970); C. A. **73,** 45 414 (1970)
[7] COMPAGNINI, A., SANTAGATI, M., MARZIANO, N., PASSERINI, R.: Ann. Chim. (Roma) **60,** 527 (1970); C. A. **74,** 53 202 (1971)
[8] ZINCKE, TH., GLAHN, W.: Ber. **40,** 3039 (1907)
[9] GLAZER, J., HUGHES, E. D., INGOLD, C. K., JAMES, A. T., JONES, G. T., ROBERTS, E.: J. Chem. Soc. **1950,** 2657
[10] KROLLPFEIFFER, F., HAHN, W.: Ber. **86,** 1049 (1953)
[11] GILOW, H. M., WALKER, G. L.: J. Org. Chem. **32,** 2580 (1967)
[12] MARZIANO, N. C., MACCARONE, E., PASSERINI, R. C.: Tetrahedron Lett. **1972,** 17
[13] a) BRD Patent No. 1 088 980 (Bayer); C. A. **55,** 25 863 (1961);
b) GOETHALS, E., DE RADZITSKY, P.: Bull. Soc. Chim. Belge **73,** 546 (1964)
[14] GILOW, H. M., BRADFORD CAMP, R. Jr., CLIFTON, E. C.: J. Org. Chem. **33,** 230 (1968)
[15] BIELIG, H. J., LÜTZEL, G., REIDIES, A.: Ber. **89,** 775 (1956)
[16] BOYER, R., SPENZER, E. V., WRIGHT, G. F.: Canad. J. Research **24,** 200 (1946); C. A. **41,** 108 (1947)
[17] IKUO MATSUMOTO: Yakugaku Zasshi **85,** 544 (1965); C. A. **63,** 6898 (1965)
[18] BREDERECK, H., GOMPPER, R., KLEMM, K., REMPFER, H.: Ber. **92,** 837 (1959)
[19] ŽEMLICKA, J., ŠORM, F.: Coll. Czech. Chem. Commun. **30,** 2052 (1965)
[20] SAWICKI, E., CARR, A.: J. Org. Chem. **22,** 503 (1957)
[21] KLEMM, L. H., MATHUR, S. B., ZELL, R., MERILL, R. E.: J. Het. Chem. **8,** 931 (1971) und die dort zitierten Literaturhinweise.
[22] KARPENKO, R. G., STOJANOWITCH, F. M., GOLDFARB, JA. L.: Zh. Org. Chim. **5,** 2000 (1969)
[23] MILLER, C. J., SMILES, S.: J. Chem. Soc. **1925,** 224
[24] DE GRAW, J. J., BROWN, V. H., CORY, M., TSAKOTELLIS, P.: J. Med. Chem. **14,** 206 (1971); FEHNEL, E., CARMACK, M.: J. Am. Chem. Soc. **72,** 1292 (1950)
[25] ROSS, A. T., GILMAN, H., BEABER, N. J.: Org. Synth. Coll. Vol. I. 145 (1956)
[26] BUNNETT, J. F., DRAPER, F. Jr., RYASON, R. R., NOBLE, P. Jr., TONKYN, R. G., ZAHLER, R. E.: J. Am. Chem. Soc. **75,** 642 (1953)

Endre PÁLOSI
Kálmán HARSÁNYI
Gergely HÉJA
1325 Budapest-Újpest 1. Pf. 110. Ungarn.

Acta Chimica Academiae Scientiarum Hungaricae, 84 (2), pp. 217—225 (1975)

BASISCHE ESTER MIT ANTIARRHYTHMISCHER WIRKUNG

K. HARSÁNYI, G. HÉJA und D. KORBONITS

(Pharmazeutische und Chemische Werke CHINOIN)

Eingegangen am 10. Januar 1974

Es wurden auf verschiedenen Wegen Ester der allgemeinen Forme Ar-$COO(CH_2)_nN^+H_2$-R (**6**) von therapeutischer Bedeutung hergestellt. Während bei Ar = 3,4,5-Trimethoxyphenyl und $n = 2$ aus dem Säureamid (**9**) unter der Wirkung von Säure der basische Ester gebildet wurde, konnte die O → N-Acylwanderung bei der Esterbase nicht durchgeführt werden.

Basische, sekundäre oder tertiäre Aminogruppen enthaltende Ester von aromatischen Carbonsäuren gelangten zuerst als Lokalanästhetika zu einer Rolle in der Heilkunde. Einige charakteristische Vertreter dieser Gruppe sind Hexylcain **1** [1], Monocain **2** [2] und Parethoxycain **3** [3]. Erst später wurde es in der therapeutischen Praxis bekannt, daß diese Lokalanästhetika das Auftreten des arryhthmischen Zustandes hemmen. Unter den Forschungsergebnissen der letzten 10 Jahre kann man von den zu dieser Verbindungsgruppe gehörenden, die Arbeit des Herzmuskels und die Durchströmung der Kranzarterie steigernden Präparaten des Hexobendin **4** [4] und das Diphenylamylate **5** [5] erwähnen.

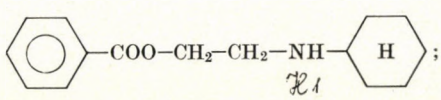

1

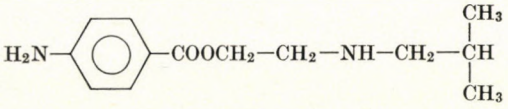

2

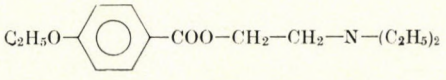

3

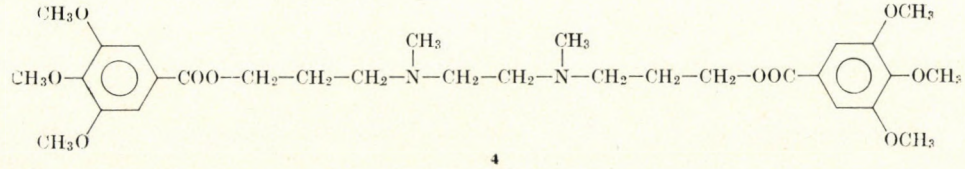

4

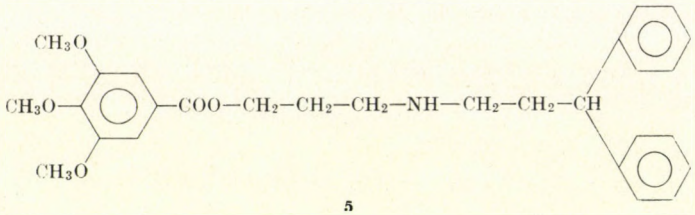

5

Als Fortsetzung unserer Forschungen auf diesem Gebiet mit 3,3-Diphenylpropylamin-Derivaten [6] setzten wir uns das Ziel, sekundäre Aminogruppen enthaltende Ester gemäß der allgemeinen Formel **6** herzustellen. In dieser Formel wurden für R — vor allem aufgrund unserer früheren Ergebnisse [6] — Aralkyl- bzw. Cycloalkylgruppen gewählt; diese wurden mit der Isopropyl-Gruppe ergänzt, die in den neuerdings in der Medizin sich einen Platz erobernden β-Blockern eine Rolle spielt. Zur Veresterung wurden vor allem aromatische Carbonsäuren, und zwar analog zu **4** und **5** Alkoxybenzoesäuren verwendet, jedoch wurden, mit Rücksicht auf die bekannte gefäßerweiternde Wirkung der Nikotinsäure [7] auch heteroaromatische Carbonsäuren einbezogen. Zwischen den Alkohol- und Aminofunktionen waren — der bisherigen Praxis (s. **1**—**5**) entsprechend — C_2—C_4 Ketten eingeschaltet.

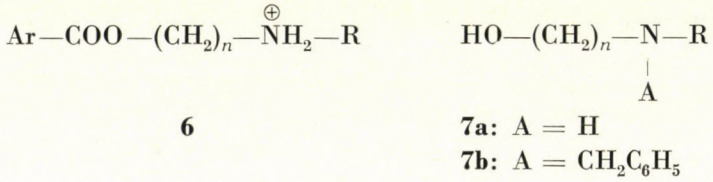

6

7a: A = H
7b: A = $CH_2C_6H_5$

Zur Herstellung der Verbindungen **I**—**XXII** wurden mehrere, im wesentlichen bekannte, Verfahren verwendet. Es soll bemerkt werden, daß sekundäre Aminogruppen enthaltende Alkohole nur dann mit Acylierungsmitteln Ester bilden, wenn ihre Aminogruppe — am einfachsten durch Salzbildung — aus der Acylierung ausgeschlossen werden. Die Salze der Aminoalkohole wurden mit Säurechlorid (Verfahren A) oder in Gegenwart von den Wasseraustritts-fördernden Mitteln, mit Säure (Verfahren B) verestert.

Nach einem bekannten Verfahren werden das Säurechlorid und das Salz des Aminoalkohols in der Schmelze in Reaktion gebracht [8]. Da der Vorgang die höhere Temperatur der Schmelze nicht benötigt, hielten wir es für günstiger, die Reaktion in Lösung (z. B. in Äthylacetat) durchzuführen, wobei das Salz des Aminoalkohols *in situ* gebildet wurde. In aromatischen Kohlenwasserstoffen als Lösungsmittel wurde die Veresterung — nach der Bildung des Säurechlorids — durch Einführen des Aminoalkohol-Salzes bewerkstelligt.

Zur unmittelbaren Veresterung mit Säuren (Verfahren B) wurden *p*-Toluolsulfonsäure in Benzol [9] oder N,N'-Carbonyldiimidazol in Tetrahydrofuran [10] verwendet.

An der Blockierung der Aminogruppe kommt außer der Salzbildung noch irgendeine leicht abspaltbare Schutzgruppe in Frage. So wurde der tertiäre Aminoalkohol **7b** verwendet, da dessen Acylierung eindeutig nur am O-Atom erfolgen kann. Das Entfernen der Benzylgruppe wurde durch Hydrogenolyse des salzsauren Salzes **8** in Eisessig [11] durchgeführt (Verfahren C).

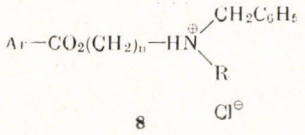

8

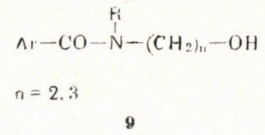

$n = 2, 3$

9

Bei den Acylderivaten von Beta- und Gamma-Aminoalkoholen ist die Acylwanderung bekannt. Ihre Richtung ist in saurem Medium das O-Acylsalz, während in basischem Medium die N-Acylverbindung (Säureamid) gebildet wird [12]. Die Umwandlung der Säureamide **9** in **6** durch Acylwanderung wurde durch Erwärmen mit salzsäurehaltigem Äthylacetat durchgeführt (Verfahren D). Obwohl wir die Auslösung des entgegengesetzten Vorganges nicht beabsichtigten, stellten wir bei der biologisch äußerst aktiven Verbindung **III** (s. Tabelle I) auch die Base dieser Verbindung her, um ihre Stabilität bzw. ihre eventuelle Umsetzung bei basischem pH zum Säureamid des Typs **9** zu untersuchen. Letzteres könnte nämlich hinsichtlich der intestinalen Resorption von Bedeutung sein. Die Base aus **III** konnte isoliert werden, jedoch gelang es weder durch Erwärmen mit Lösungsmittel, noch durch basische Katalysatoren, daraus das Säureamid **9** zu gewinnen.

Die Abhängigkeit der O → N-Acylwanderung vom Substituenten bei N- bzw. O-acylierten Derivaten von 1,2-Aminoalkoholen, im Gegensatz zum entgegengesetzten Vorgang, wurde bereits durch REASENBERG und GOLDBERG [12] beobachtet, ohne jedoch eine theoretische Erklärung des Vorgangs zu geben.

Die Stabilität der Base von **III** (Ar = 3,4,5-Trimethoxyphenyl), die Abwesenheit der O → N-acylwanderung steht in vollem Einklang mit dem Additions-Eliminationsmechanismus dieses Vorganges, welcher der bimolekularen nukleophilen Substitution, z. B. der Hydrolyse der Ester ähnlich ist. Bei letzterem Vorgang ist die Wirkung des Substituenten auf die Hydrolysegeschwindigkeit des aromatischen Carbonsäureesters wohlbekannt (sie beträgt bei *p*-NO_2-Benzoesäureester das 525fache der Geschwindigkeit beim *p*-OCH_3-Ester [13]). Diese Wirkung ergibt sich aus dem Geschwindigkeitsunterschied bei der Addition des nukleophilen Agens (OH^-) am Kohlenstoff der Estercarbonylgruppe. Bei einem weniger stark nukleophilem Agens gelangt dieser Unterschied noch mehr zur Geltung. Folglich verdankt die Base von **III** ihre Stabilität dem Trimethoxybenzoesäure-Strukturteil, da der zur O → N-Acylwanderung benötigte Additionsschritt am Aminocarbonyl-Kohlenstoff infolge der elektronstoßenden Eigenschaft der Methoxygruppe(n) nicht zustandekommen kann. Auch der entgegengesetzte Vorgang beim

Tabelle I

Die Verbindungen stehen unter Patentschutz

No.	Ar	*n*	R	Lit. *n* und R	Verfahren	Verbindungen Ausbeute %	Schmp. °C
I	3,4,5-Trimethoxyphenyl	2	Phenetyl	17	Ab	57	183—186
II	3,4,5-Trimethoxyphenyl	2	Isopropyl	17	Ab	48	169—174
III	3,4,5-Trimethoxyphenyl	2	Cyclohexyl	18	A—F	79	209—211
IV	3,4,5-Trimethoxyphenyl	2	3,4-Dimethoxy-phenyläthyl	19	Ab	41	149—151
V	3,4,5-Trimethoxyphenyl	3	Cyclohexyl	20	Ab	68	173—174
VI	3,4,5-Trimethoxyphenyl	2	Cycloheptyl		Ad	20	176—180
VII	3,4,5-Trimethoxyphenyl	2	Cyclopentyl	12	Ab	33	162—166
VIII	3,4,5-Trimethoxyphenyl	4	Cyclohexyl	21	Ad	30	148—150
IX	3,5-Dimethoxy-4-hidroxy-phenyl	2	Cyclohexyl	18	Ba	10	210—213
X	3,4-Dimethoxyphenyl	2	Isopropyl	17	Ab	40	188—190
XI	3,4-Dimethoxyphenyl	3	Isopropyl	22	Ab	35	168—172
XII	3,4-Dimethoxyphenyl	3	Cyclohexyl	20	Ab	18	176—178
XIII	3,4-Dimethoxyphenyl	2	3,4-Dimethoxy-phenyläthyl	19	Ab	23	138—140
XIV	2,4-Dichlorphenyl	2	Cyclohexyl	18	Ba	19	209—211
XV	2-Chlor-5-sulfamoyl-phenyl [23]	2	Cyclohexyl	18	Ab	3	216—219
XVI	3-Sulfamoyl-4-chlorphenyl [24]	2	Cyclohexyl	18	Ad	31	260
XVII	3-Nitro-4-chlor-5-sulfa-moylphenyl [25]	2	Cyclohexyl	18	Ba	4,5	248 Z.
XVIII	3-Pyridil	2	Phenetyl	17	Ab	54	215
XIX	3-Pyridil	2	Cyclohexyl	18	Ab	52	150
XX	3-Pyridil	2	Isopropyl	17	Ab	43	152—158
XXI	2-Furyl	2	Cyclohexyl	18	Ad	14	205—207
XXII	3-Methyl-5-phenyliso-xazol-4-yl	2	Cyclohexyl	18	Ab	25	141—144

* ΣCl

Säureamid **9** (Ar = 3,4,5-Trimethoxyphenyl) kann leicht gedeutet werden: in diesem Fall ist die Wirkung des Substituenten des aromatischen Ringes — ähnlich wie bei der sauren Hydrolyse der Ester — bei dem Protonenangriff beginnenden Vorgang unbedeutend (die Hydrolysegeschwindigkeit des *p*-NO_2-Benzoesäureesters ist das 1,12fache der Geschwindigkeit beim *p*-OCH_3-Ester [14]).

$Ar\text{-}COO\text{-}(CH_2)_n\text{-}\overset{+}{N}H_2\text{-}RX^-$

Analyse										
C		H		N		Cl^-		S		No.
Ber.	Gef.	Ber.	Gef.	Ber.	Gef.	Ber.	Gef.	Ber.	Gef.	
60,67	60,53	6,62	6,7	3,54	3,54	8,96	9,2			I
53,97	54,10	7,25	7,11	4,2	4,33	10,62	10,89			II
58,15	57,56	7,56	7,65	3,75	4,34	9,5	9,65			III
57,95	57,7	6,63	6,5	3,7	2,98	7,77	7,87			IV
58,83	59,5	7,79	7,79	3,61	3,64	9,14	8,91			V
58,79	58,26	7,79	7,9	3,61	3,31	9,14	8,9			VI
56,85	55,96	7,29	7,27	3,90	4,07	9,87	9,62			VII
59,77	59,33	8,03	7,97	3,49	3,52	8,83	8,61			VIII
56,84	57,05	7,30	7,15	3,90	4,26	9,87	9,79			IX
55,35	55,60	7,3	7,29	4,61	4,38	11,66	11,45			X
56,68	57,26	7,61	7,15	4,4	4,66	11,15	11,04			XI
60,4	60,9	7,98	8,01	3,92	4,04	9,91	9,88			XII
59,1	57,9	6,62	7,19	3,29	3,04	8,3	7,75			XIII
51,08	51,91	5,72	5,80	3,97	3,95	30,16*	30,55*			XIV
45,34	45,2	5,58	5,5	7,05	7,09	8,92	8,59			XV
45,34	45,91	5,58	5,64	7,05	7,22	8,92	8,36			XVI
				9,50	9,56	16,03*	16,47*	7,25	7,38	XVII
56,1	56,1	5,85	6,6	8,27	7,3	20,6	19,83			XVIII
52,5	51,4	6,65	6,8	8,8	8,59	22,2	21,07			XIX
54,0	53,9	7,15	7,9	11,45	11,31	14,5	15,41			XX
57,03	57,86	7,35	7,4	5,12	5,10	12,95	12,69			XXI
62,54	62,30	6,91	6,93	7,68	7,65	9,72	9,67			XXII

Die Synthese der Ester **6** wurde ferner durch Alkylierungsreaktionen, aus **10** und Aminen [15] (Verfahren E) sowie aus **11** und dem Natriumsalz der Carbonsäure [16] (Verfahren F) in dipolarem aprotischem Lösungsmittel bewerkstelligt.

$Ar—COO—(CH_2)_n—Cl$ **10**

$Cl—(CH_2)_n—\overset{\oplus}{N}H_2—R$ **11**

Die hergestellten Verbindungen sind in Tab. I zusammengefaßt. Besonders die Verbindung **III** besitzt eine in medizinischer Hinsicht nutzbare antiarrhythmische Wirkung. Angaben über die Wirksamkeit der Verbindungen sollen an anderer Stelle veröffentlicht werden.

Wir sind Herrn Professor L. SZEKERES für die pharmakologischen Untersuchungen, Herrn I. REMPORT für die Mikroanalysen und Fräulein M. WUNDELE für die Ausführung der experimentellen Arbeit zu Dank verpflichtet.

Experimenteller Teil

Die Schmelzpunkte sind unkorrigiert.

2-Cycloheptylaminoäthanol

In einem mit wasserabscheidendem Aufsatz versehenen Kolben wurden 56,1 g (0,5 mol) Cycloheptanon und 30,5 g (0,5 mol) Äthanolamin in 200 ml Chloroform gelöst und bis zum Abscheiden der berechneten Wassermenge im Sieden gehalten. Nach Abdestillieren des Lösungsmittels wurde der Rückstand im Gemisch von 200 ml Methanol und 20 ml Wasser mit 10 g Natriumborhydrid reduziert. Nach 1-tägigem Stehen wurde die Lösung in 250 ml 10%ige Salzsäure gegossen und bei vermindertem Druck eingedampft. Der Rückstand wurde in Wasser aufgenommen, mit 40%iger Natronlauge alkalisch gemacht und das abgeschiedene Öl mit Chloroform extrahiert. Nach Abdestillieren des Chloroforms wurde der Rückstand im Vakuum fraktioniert. Hauptfraktion Kp.: 120—128°C/0,8—1 Hgmm.
n_D^{26}: 1,4895, Ausbeute: 43,6 g (55%)

Verfahren A

a) 2-Cyclohexylaminoäthyl-3,4,5-trimethoxybenzoat-Hydrochlorid (III)

6,92 g 3,4,5-Trimethoxybenzoylchlorid und 5,4 g 2-Cyclohexylaminoäthanol-Hydrochlorid wurden trocken vermischt und 1 Stunde lang auf dem Wasserbad erhitzt. Nach dem Abkühlen wurde das Gemisch mit 25 ml wasserfreiem Äthanol verrieben und abgesaugt. 9,9 g (88%) **III**. Schmp. 203—208 °C. Aus wasserfreiem Äthanol umkristallisiert Schmp. 207—209 °C.

b) 2-Cyclohexylaminoäthyl-2-chlor-5-sulfamoylbenzoat-Hydrochlorid (XV)

6,3 g 2-Chlor-5-sulfamoylbenzoylchlorid und 4,4 g 2-Cyclohexylaminoäthanol-Hydrochlorid wurden in 50 ml wasserfreiem Äthylacetat bis zum Aufhören der Gasentwicklung im Sieden gehalten. Nach dem Eindampfen wurde mit Aktivkohle geklärt und umkristallisiert. 1,05 g (11%) XV. Schmp. 216—219 °C.

c) 2-Cyclohexylaminoäthyl-3,4,5-trimethoxybenzoat-Hydrochlorid (III)

2,86 g 2-Cyclohexylaminoäthanol wurden in 30 ml wasserfreiem Äthylacetat gelöst und Chlorwasserstoffgas wurde bis zum Erreichen von pH 1 in die Lösung eingeleitet. Danach wurden 4,61 g 3,4,5-Trimethoxybenzoylchlorid zugegeben und das Gemisch wurde unter Rühren 8 Stunden im Sieden gehalten. Nach dem Abkühlen wurden 6,9 g (92,5%) **III** abgeschieden Schmp. 207—209 °C.

d) 2-Cyclohexylaminoäthyl-3,4,5-trimethoxybenzoat-Hydrochlorid (III)

Auf 2,12 g 3,4,5-Trimethoxybenzoesäure wurden 10 ml Toluol gegossen und 1,19 g Thionylchlorid wurden zugegeben. Das Gemisch wurde bis zum Aufhören der Gasentwicklung im Sieden gehalten. Die erhaltene Lösung wurde zu einer Suspension von 1,8 g 2-Cyclohexylaminoäthanol-Hydrochlorid in 3 ml Toluol gegossen und bis zum Aufhören der Gasentwick-

lung im Sieden gehalten. Die nach Abkühlen ausgeschiedenen Kristalle wurden abgesaugt, mit wasserfreiem Äthanol gewaschen und aus 96%igem Äthanol unter Klären mit Aktivkohle umkristallisiert. 2,96 g (79%) **III.**

(Anstelle von Toluol wurde auch Benzol als Lösungsmittel verwendet.)

Verfahren B

a) 2-Cyclohexylaminoäthyl-3,4,5-trimethoxybenzoat-Hydrochlorid (III)

2,0 g 3,4,5-Trimethoxybenzoesäure, 1,8 g 2-Cyclohexylaminoäthanol-Hydrochlorid und 4,0 g *p*-Toluolsulfonsäure wurden in 40 ml Benzol 12 Stunden unter Rückfluß im Sieden gehalten. Nach dem Abkühlen wurde die Lösung mit 10 ml 15%iger Natriumcarbonat-Lösung und anschließend mit 10%iger Salzsäurelösung ausgeschüttelt. Aus dem salzsauren Lösung wurden 0,67 g (19%) **III** abgeschieden (Schmp. 210 °C).

b) 2-Cyclohexylaminoäthyl-3,4,5-trimethoxybenzoat-Hydrochlorid (III)

Eine Lösung von 1,05 g 3,4,5-Trimethoxybenzoesäure in 10 ml abs. Tetrahydrofuran wurde unter Kühlen tropfenweise zu einer Lösung von 0,8 g N,N'-Carbonyldiimidazol in 20 ml abs. Tetrahydrofuran gegeben. Anschließend wurde 0,5 Stunden bei Raumtemperatur und 1 Stunde bei 50 °C gerührt. Das nach dem Eindampfen zurückgebliebene Öl wurde mit 0,8 g 2-Cyclohexylaminoäthanol-Hydrochlorid in 20 ml Toluol versetzt und 15 Stunden im Sieden gehalten. Nach dem Abkühlen wurden 0,4 g (21%) **III** abgeschieden.

Verfahren C

2-(N-Benzyl-N-cyclohexylamino)äthyl-3,4,5-trimethoxybenzoat-Hydrochlorid (8,

Ar = 3,4,5-Trimethoxyphenyl, $n = 2$, R = Cyclohexyl)

2,3 g 3,4,5-Trimethoxybenzoylchlorid und 2,7 g 2-(N-Benzyl-N-cyclohexylamino)-äthanol-Hydrochlorid (**7b**, R = Cyclohexyl, $n = 2$) [26] wurden in 30 ml Toluol bis zum Aufhören der Gasentwicklung im Sieden gehalten. Der nach dem Eindampfen erhaltene Rückstand wurde zweimal aus wasserfreiem Äthanol umkristallisiert. Ausbeute 2,5 g (55%), **8**, Schmp. 180—182 °C.

Analyse:

Ber. C 64,71 H 7,38 N 3,02 Cl^- 7,64

Gef. C 64,78 H 7,52 N 2,98 Cl^- 7,41

2-Cyclohexylaminoäthyl-3,4,5-trimethoxybenzoat Hydrochlorid (III)

1,4 g 2-(N-Benzyl-N-cyclohexylamino)äthyl-3,4,5-trimethoxybenzoat-Hydrochlorid wurden in 35 ml Eisessig gelöst und in Gegenwart von Palladium-Kohle hydriert. Die Reaktion verlief sehr rasch. Nach Abfiltrieren des Katalysators wurde die Lösung eingedampft. Es wurden 1,0 g (90%) **III** erhalten.

Verfahren D

N-(2-Hydroxyäthyl)-N-cyclohexyl-3,4,5-trimethoxybenzamid (9)

(Ar = 3,4,5-Trimethoxyphenyl, $n = 2$, R = Cyclohexyl)

4,3 g 2-Cyclohexylaminoäthanol und 3,04 g Triäthylamin wurden in 50 ml abs. Pyridin gelöst. Bei 25—30 °C wurde eine Lösung von 6,92 g 3,4,5-Trimethoxybenzoylchlorid in 20 ml abs. Pyridin tropfenweise zugegeben. Das Gemisch wurde weitere 3 Stunden bei 50 °C gerührt und bei vermindertem Druck eingedampft. Der Rückstand wurde in Chloroform gelöst, mit Wasser gewaschen und wieder eingedampft. Aus Diisopropyläther wurde, unter Klären mit Aktivkohle, umkristallisiert. Es wurden 3,35 g (30%) des Benzamidderivats erhalten. Schmp. 125—128 °C.

Analyse: $C_{18}H_{27}NO_5$ (337,41)

Ber. C 64,07 H 8,07 N 4,15

Gef. C 64,25 H 8,04 N 4,25

Im IR-Spektrum meldet sich eine starke OH-Bande bei 3420 cm^{-1} und eine Amidbande bei 1620 cm^{-1}.

2-Cyclohexylaminoäthyl-3,4,5-trimethoxybenzoat-Hydrochlorid (III)

1 g N-(2-Hydroxyäthyl)-1-cyclohexyl-3,4,5-trimethoxybenzamid (**9**) wurden in 20 ml Äthylacetat gelöst und mit HCl-Gas gesättigt. Nach 1-stündigem Sieden wurden 0,75 g (66%) **III** abgeschieden.

2-Cyclohexylaminoäthyl-3,4,5-trimethoxybenzoat

40 g 2-Cyclohexylaminoäthyl-3,4,5-trimethoxybenzoat-Hydrochlorid (**III**) wurden in 200 ml Wasser bei 40—45° C suspendiert, mit 40%iger Natriumhydroxydlösung auf pH 8 eingestellt, mit Chloroform ausgeschüttelt und die organische Phase im Vakuum eingedampft. Der Rückstand wurde aus Petroläther unter Klären mit Aktivkohle umkristallisiert. Es wurden 32,1 g farblose Kristalle erhalten; Schmp. 48—50 °C. Zur Reinigung wurde die Substanz in 100 ml Dichlormethan gelöst, mit 30 ml 2 *n* Natriumhydroxydlösung durchgeschüttelt und die Dichlormethanphase wurde eingedampft. Der Rückstand wurde aus Petroläther umkristallisiert. Ausbeute 21,3 g (60%) der Base von **III**, Schmp. 51—53 °C.

Analyse $C_{18}H_{27}NO_5$ (337,41)
Ber. C 64,07 H 8,07 N 4,15
Gef. C 64,27 H 7,94 N 4,17

Im IR-Spektrum meldet sich eine intensive Cabonylbande bei 1705 cm^{-1}.

Umlagerungsversuche

1 g der Base von **III** und 0,05 g Natriummethylat wurden in 25 ml Lösungsmittel 16 Stunden auf dem Wasserbad erhitzt; es wurde keine Veränderung beobachtet. Als Lösungsmittel wurden Äthylacetat, Benzol, Pyridin, Methyläthylketon, Sulfolan, Dimethylformamid, Äthanol, Isopropyläther, N-methylpyrrolidon-2 verwendet.

Beim Rühren von 1 g der Base in 25 ml 2 *n* Natriumhydroxydlösung bei 50 °C wurde der Ester hydrolisiert.

Verfahren E

2-Cyclohexylaminoäthyl-3,4,5-trimethoxybenzoat-Hydrochlorid (III)

5,95 g Cyclohexylamin wurden in 10 ml Dimethylsulfoxyd gelöst und eine Lösung von 5,5 g 2-Chloräthyl-3,4,5-trimethoxybenzoat (**10**; Ar = 3,4,5-Trimethoxyphenyl, *n* = 2) [15] in 20 ml Dimethylsulfoxyd wurde zugegeben. Das Gemisch wurde 8 Stunden auf dem Wasserbad erwärmt und anschließend eingedampft. Der Rückstand wurde in Chloroform gelöst, mit Wasser gewaschen und die chloroformische Phase mit HCl-Gas gesättigt. Mit Äther gefällt wurden 2,3 g (31%) **III** erhalten.

Verfahren F

2-Cyclohexylaminoäthyl-3,4,5-trimethoxybenzoat-Hydrochlorid (III)

1,7 g Natrium-3,4,5-trimethoxybenzoat, 1,45 g N-(2-Chloräthyl)cyclohexylamin-Hydrochlorid (**11**; R = Cyclohexyl, *n* = 2) [27] und einige Natriumjodid-Kristalle wurden in 30 ml Dimethylformamid gelöst. Das Gemisch wurde 24 Stunden auf dem Wasserbad erwärmt, die nach dem Abkühlen abgeschiedene Substanz abfiltriert und das Filtrat eingedampft. Der Rückstand wurde aus 96%igem Äthanol unter Klären mit Aktivkohle umkristallisiert. Es wurden 0,75 g (27%) **III** erhalten.

LITERATUR

[1] Orkin, L. R., Rovenstine, E. A.: Anesthesiology **13,** 465 (1952)
[2] Büchi, J., Perlia, X., Studach, S. P.: Arzneim.-Forsch. **17,** 1012 (1967)
[3] Büchi, J., Perlia, X., Strässle, A.: Arzneim.-Forsch. **16,** 1657 (1966)
[4] Heistracher, P., Kraupp, O., Schiefthaler, Th.: Arzneim.-Forsch. **14,** 1077 (1964)
[5] Hatano, M., Sohji, Y., Kawashime, K., Kaneko, H.: Arzneim.-Forsch. **21,** 1628 (1971)
[6] Harsányi, K., Korbonits, D., Kiss, P.: Acta Chim. (Budapest) **77,** 333 (1973); Magy. Kém. Foly. **79,** 109 (1973) sowie frühere Mitteilungen

[7] KNOLL, J.: Gyógyszertan, 2. Aufl. Medicina Kiadó, Budapest 1968, p. 328
[8] PIERCE, J. S., SALSBURY, J. M., FREDERICKSEN, J. M.: U.S. Patent 2 372 116
[9] Dainippon Pharmaceutical Co. Ltd., BRD Offenlegungsschrift 1 802 656
[10] STAAB, H. A.: Angew. Chem. **74,** 407 (1962)
[11] HARTUNG, W. H.: Org. Reactions **7,** 263 (1953)
[12] REASENBERG, J. R., GOLDBERG, S. D.: J. Am. Chem. Soc. **67,** 933 (1945)
[13] INGOLD, C. K.: Structure and Mechanisms in Organic Chemistry, G. Bell and Sons Ltd., London 1953, p. 759.
[14] *ibid.*, p. 777.
[15] FRANGATOS, G., KOHAN, G., CHUBB, F. L.: Can. J. Chem. **38,** 1082 (1960)
[16] HENECKA, H., HOUBEN-WEYL, Methoden der organischen Chemie, 4. Aufl., Georg Thieme Verlag 1952. Band VIII, p. 504.
[17] COPE, A. C., HANCOCK, E. M.: J. Am. Chem. Soc. **64,** 1503 (1942)
[18] BAIN, J. P., POLLARD, C. B.: J. Am. Chem. Soc. **61,** 2704 (1939)
[19] E. Merck A. G., Neth. Pat. Appl. 6 611 733
[20] HANCOCK, E. M., HARDY, E. M., HEYL, D., WRIGHT, M. E., COPE, A. C.: J. Am. Chem. Soc. **66,** 1747 (1944)
[21] STIRLING, J. M.: J. Chem. Soc. **1960,** 255
[22] ELDERFIELD, R. C., GENSLER, W. J., BRODY, F., HEAD, J. D., DICHERMAN, S. C.: J. Am. Chem. Soc. **68,** 1579 (1946)
[23] BASU, U. P., DAS-GUPTA, S. J.: J. Indian Chem. Soc. **16,** 100 (1939); C. A. **33,** 5852
[24] JOCKMAN, G. B., PETROW, V., STEPHENSON, O., WILD, A. M.: J. Pharm. Pharmacol. **14,** 679 (1962)
[25] Lovens Kemiske Fabrik, Österreich A 5228/68
[26] Abbott Laboratories, Brit. Patent 788 137
[27] CHENEY, L. C., SMITH, R. R., BINKLEY, S. B.: J. Am. Chem. Soc. **71,** 60 (1949)

Kálmán HARSÁNYI
Gergely HÉJA
Dezső KORBONITS
1325 Budapest-Újpest 1. Pf. 110. Ungarn.

Acta Chimica Academiae Scientiarum Hungaricae, 84 (2), pp. 227—228 (1975)

RAPID SYNTHESIS OF OXYTOCIN

(SHORT COMMUNICATION)

L. KISFALUDY and I. SCHÖN

(G. Richter Chemical Works, Budapest)

Received July 29, 1974

In the structure-activity-relationship studies of biologically active peptides, the synthesis of analogs plays an important role. Rapid and simple methods are greatly needed from this point of view. We have recently reported a novel method of peptide synthesis [1], in which, with or without isolation, and simple purification of the intermediates, it is possible to control every step of the synthesis and the required time for the synthesis of medium-size peptides is approximatively one day. To demonstrate the applicability of this method, now we wish to report the novel and rapid synthesis of oxytocin in detail. The required time for the synthesis of the protected nonapeptide was 10 hrs with an overall yield of 39%.

Experimental

General. Melting points were taken on a dr. Tottoli (Büchi) apparatus and are uncorrected. The optical rotations were determined on a Perkin-Elmer 141 photoelectric polarimeter. The tlc was run on Kieselgel nach Stahl, using the following solvent systems: (1) EtOAc: (pyridine: AcOH: water = 20 : 6 : 11) = 9 : 1; (2) EtOAc : (pyridine : AcOH : water = = 20 : 6 : 11) = 4 : 1; (3) EtOAc : (pyridine : AcOH : water = 20 : 6 : 11) = 3 : 2; (4) chloroform : *n*-hexane: AcOH = 8 : 1 : 1. The amino acid analyses were performed on a BioCal 200 analyzer using Chromex UA 8 resin.

Synthesis of Z-Cys(Bzl)-Tyr(EOC)-Ile-Gln-Asn-Cys(Bzl)-Pro-Leu-Gly-NH_2. To a solution of 0.62 g (4 mmol) Gly-NH_2-HBr and 0.84 ml (6 mmol) of TEA in 6 ml DMF, 0.80 g (2 mmol) of BOC-Leu-OPFP [2] were added and after 5 min the solvent changed to 20 ml chloroform. This solution was extracted with 10% citric acid solution and with 5% $NaHCO_3$ solution, both saturated with NaCl. After drying, the solvent was evaporated and the protected dipeptide ($R_f^1 = 0.5$) was dissolved in 5 ml of freshly prepared 60% HBr/dioxane. After 5 min the dipeptide · HBr($R_f^2 = 0.15$) was precipitated and washed with dry ether then redissolved in the mixture of 20 ml chloroform and 1 ml DMF. The pH was adjusted to 8.5 by means of TEA.* To this solution was added 2.1 g (4 mmol) of BOC-Cys(Bzl)-Pro-OPFP prepared according to [2] (m.p. 74—75°C; $R_f^4 = 0.7$; analysis: calcd. C 54.1; H 4.7; N 4.9; found C 55.0; H 4.7; N 5.0%; $(\alpha)_D^{25} = -82.1°$, $c = 1$, dioxane), and the excess of active ester was removed by trituration of the evaporated reaction mixture with ether. The isolated tetrapeptide ($R_f^1 = 0.45$; m.p. 161—162 °C) was treated with 10 ml of 60% HBr/dioxane and the free tetrapeptide ($R_f^2 = 0.35$) isolated by means of dry ether was dissolved in 10 ml of DMF. To this solution 1.6 g (4 mmol) of BOC-Asn-OPFP [2] was added and after 5 min the protected pentapeptide ($R_f^5 = 0.25$) was isolated by trituration of the evaporated reaction mixture with chloroform. The deprotection was carried out by means of 13 ml HBr/dioxane and after 12 min the free peptide ($R_f^3 = 0.3$) was isolated in the usual way, then dissolved in 15 ml of DMF. To this

* Before the acylation reactions in every step, it is important to adjust the pH of the solution by means of TEA and to maintain this value during the reaction.

solution 1.65 g (4 mmol) of BOC-Gln-OPFP [2] was added, and after 25 min the solvent was removed and the protected hexapeptide ($R_f^3 = 0.5$) obtained by trituration of the residue with chloroform, was treated with 15 ml of 60% HBr/dioxane for 12 min. The free peptide ($R_f^3 = 0.25$) obtained by means of dry ether treatment, was dissolved in 15 ml of DMF and to this solution 2.4 g (6 mmol) of BOC-Ile-OPFP [2] was added. After 25 min, working in the same manner as described above, 1.05 g (55% yield based on BOC-Leu-OPFP) of isolated, protected heptapeptide ($R_f^3 = 0.6$) was obtained. 0.45 g (0.47 mmol) of the protected heptapeptide was treated with 20 ml of 50% HBr/dioxane and the free peptide ($R_f^3 = 0.2$) was isolated in the usual way then redissolved in 8 ml DMF. To this solution 1.56 g (3 mmol) of BOC-Tyr(EOC)-OPFP (m.p. 160—161°C; $R_f^4 = 0.75$; $(\alpha)_D^{25} = -23.5°$, $c = 1$, EtOAc) was added and after 25 min the resulting gel was precipitated and isolated by means of ethanol. The protected octapeptide ($R_f^3 = 0.7$) was treated with 20 ml of 50% HBr/dioxane for 13 min and the free octapeptide ($R_f^3 = 0.3$) obtained by means of dry ether was dissolved in 6 ml of DMF. In the last cycle 1.53 g (3 mmol) of Z-Cys(Bzl)-OPFP [3] was used in the acylation step for 25 min and the protected nonapeptide was isolated by means of methanol. Overall yield: 0.47 g (39%). M.p.: 257—258°C, $R_f^3 = 0.3$, $R_f^3 = 0.75$, $(\alpha)_D^{25} = -46.4°$ ($c = 1.2$ DMF).

Deprotection and oxidation. 250 mg of the protected nonapeptide obtained was selectively deprotected: first, the ethoxycarbonyl group was removed in liquid NH_3** (yield: 90.7%, $R_f^3 = 0.70$) then the other protecting groups in one step in the usual way [4]. After oxidation in the presence of H_2O_2 the crude product was once purified on CM-Sephadex column and after liophylization 51.1 mg peptide was obtained with a total activity of 17.520 IU.

REFERENCES

[1] KISFALUDY, L., SCHÖN, I., SZIRTES, T., NYÉKI, O., LÖW, M.: Tetrahedron Lett. 1785 (1974)

[2] KISFALUDY, L., LÖW, M., NYÉKI, O., SZIRTES, T., SCHÖN, I.: Liebigs Ann. Chem. 1421 (1973)

[3] KISFALUDY, L., ROBERTS, J. E., JOHNSON, R. H., MAYERS, G. L., KOVÁCS, J.: J. Org. Chem. **35,** 3563 (1970)

[4] DU VIGNEAUD, V., RESSLER, C., SWAN, J. M., ROBERTS, C. W., KATSOYANNIS, P. G.: J. Amer. Chem. Soc. **76,** 3115 (1954)

Lajos KISFALUDY
István SCHÖN
1475 Budapest 10. Pf. 27. Hungary.

** In the presence of sodium metal, a side reaction was observed, as indicated by amino-acid analysis.

INDEX

ANALYTICAL CHEMISTRY — ANALYTISCHE CHEMIE — АНАЛИТИЧЕСКАЯ ХИМИЯ

FEKETE, E. and INCZÉDY, J.: Ion Exchange Equilibria of Some Monovalent Anions . 121

PHYSICAL AND INORGANIC CHEMISTRY — PHYSIKALISCHE UND ANORGANISCHE CHEMIE — ФИЗИЧЕСКАЯ И НЕОРГАНИЧЕСКАЯ ХИМИЯ

LISZI, J.: Dipole Association of Nitrobenzene in Non-polar Solvents 125

MUSHRAN, S. P., SANEHI, R. and BOSE, A. K.: Mechanism of Cyclohexanone Oxidation by Chloramine-T 135

KŐNIG, P. und FEJES, P.: Über die Möglichkeiten der digitalen Bestimmung der Parameter der kontakt-katalytischen Hydrierung von Äthylen, III. Die „Schätzung" der Geschwindigkeitskonstanten für den stationären Fall. (On the Possibilities of the Digital Determination of the Parameters of the Contact-Catalytic Hydration of Ethylene, III. "Estimation" of the Rate Constants for the Steady State) .. 141

KISS, L. and FARKAS, J.: Kinetic Equations of Multistep Electrode Processes, I. 161

ORGANIC CHEMISTRY — ORGANISCHE CHEMIE — ОРГАНИЧЕСКАЯ ХИМИЯ

KASZTREINER, E., SZILÁGYI, G., KOSÁRY, J. and HUSZTI, Zs.: Synthesis of O-Substituted Hydroxylamines 167

DINYA, Z., LITKEI, GY., TAMÁS, J. and CZIRA, G.: Structural Investigation of Flavonides and Their Model Compounds, VII. Calculation and Determination of the Ionization Potential of 4- and 4'-monosubstituted Chalcones. (Short Communication) 181

ELKASCHEF, MOHAMED A.-F., ABDEL-MEGEID FAROUK, M. E. and ELZEIN SALAH M. M.: Triarylmethanes, VI. Reactions of Naphtoquinone Diphenylmethides with Organometallic Compounds 187

SCHEIBER, P. and NÁDOR, K.: Conformation of 3,7-Diazabicyclo-[3.3.1] Nonanes 193

SOHÁR, P., KOSÁRY, J. and KASZTREINER, E.: Diamagnetic Shielding of the Dibenzocycloheptatrien Ring System in Some Acylaminomalonic Ester Derivatives 201

PÁLOSI, E., HARSÁNYI, K. und HÉJA, G.: 4-S-Substituierte 2,6-Dinitroaniline (4-S-Substituted 2,6-Dinitroanilines) 205

HARSÁNYI, K., HÉJA, G. und KORBONITS, D.: Basische Ester mit Antiarrhythmischer Wirkung (Basic Esters with Antiarrhythmic Action) 217

KISFALUDY, L. and SCHŐN, I.: Rapid Synthesis of Oxytocin (Short Communication) .. 227

Printed in Hungary

A kiadásért felel az Akadémiai Kiadó igazgatója — Műszaki szerkesztő: Zacsik Annamária

A kézirat nyomdába érkezett: 1974. X. 29. — Terjedelem: 9,8 (A/5) ív, 53 ábra, 1 melléklet

75.1048 Akadémiai Nyomda, Budapest — Felelős vezető: Bernát György

ACTA CHIMICA

ТОМ 84—ВЫП. 2

РЕЗЮМЕ

Ионообменное равновесие некоторых моновалентных анионов

Э. ФЕКЕТЕ и Й. ИНЦЕДИ

Были определены константы ионообменного равновесия хлоратных, броматных, гидрокарбонатных, иодатных и гидроксильных ионов по отношению к хлоридным ионам. Изменения проводились на смоле Доуэкс 1×8 при температурах 18, 28 и 38°С. На основе уравнения Салмона, выведенного исходя из теории статистической термодинамики, были рассчитаны величины изменения свободной энтальпии, а также величины изменения энтальпии и энтропии.

Дипольная ассоциация нитробензола в неполярных растворителях

Й. ЛИСИ

Молярная поляризация нитробензола была исследована в четыреххлористом углероде, н-гептане и в бензоле. На основе результатов исследований можно заключить, что дипольная ассоциация нитробензола усиливается с увеличением концентрации нитробензола. Для описания результатов пригодным оказалось уравнение Сугдена.

Механизм окисления циклогексанона хлорамином-Т

С. П. МУШРАН, Р. САНЕХИ и А. К. БОУЗ

Было проведено кинетическое изучение окисления циклогексанона хлорамином-Т в щелочной среде. Была обнаружена зависимость первого порядка по хлорамину-Т, циклогексанону и щелочи. п-Толуолсульфонамид не оказывал, однако, никакого влияния. Незначительный эффект ионной силы и сильный отрицательный эффект концентрации метанола указывают на то, что реакция протекает по механизму, включающему, в качестве ступени определяющей скорость реакции, взаимодействие энольного аниона циклогексанона с хлорамином-Т. Различные термодинамические параметры, а также результаты изолирования конечного продукта — 1,2-циклогександиона — подтверждают предложенный механизм.

О возможностях дигитального определения параметров контактно-каталитического гидрирования этилена, III

Оценка констант стационарной скорости реакции

П. КЕНИГ и П. ФЕЙЕШ

Был рассмотрен вопрос о том, что механизм Хориути—Поляни, приписываемый контактно-каталитическому гидрированию этилена, в какой степени согласуется с литературными кинетическими данными. Используя метод стационарных концентраций для

компонентов, адсорбируемых на катализаторе, численное решение дифференциального уравнения, выведенного в первой части этой серии сообщений, сопоставляли с экспериментальными кинетическими кривыми, причем оценка параметров производилась с помощью метода нелинейных наименьших квадратов и на основе принципов, изложенных во второй части этой серии сообщений.

Строгий статистический анализ результатов оптимализации позволяет опознавание границ справедливости модели, а также ее дальнейшего развития. Результатом служат два возможных приближения этой проблемы, первое из которых правильно описывает кинетику изучаемой реакции при каком-то определенном составе смеси, но не способно отображать влияния значительных изменений состава, в то время как второе приближение хорошо отражает последнее, однако, не прилегает к отдельным кинетическим кривым с точностью, соответствующей строгим статистическим требованиям. Можно полагать, что основные положения ассоциативного механизма правильны, однако, приводят к чрезмерному упрощению действительных условий сорбции.

О кинетических уравнениях многостадийных электродных процессов, I

Л. КИШ и Й. ФАРКАШ

Было выведено и рассмотрено уравнение поляризационной кривой для многостадийной ионизации металлов и восстановления металлических ионов для случая перенапряжения перехода. Нами была рассчитана концентрация промежуточных продуктов у поверхности электрода в зависимости от потенциала электрода, то есть от плотности тока электрода.

Получение О-замещенных гидроксиламинов, I

Э. КАСТРЕЙНЕР, Г. СИЛАДИ, Й. КОШАРИ, Ж. ХУСТИ и М. КЮРТИ

В ходе получения О-замещенных гидроксиламинов, обладающих энзим-парализующим влиянием на гистидин-декарбоксилазу, из N-(замещенных окси)-фтальимидов был найден новый метод дефталоилирования, сущность которого заключается в том, что вместо гидразинового способа, известного в литературе, для удаления фталоил-группы были использованы первичные амины.

Преимущество данного метода заключается в возможности его широкого использования, проведении реакции в мягких условиях, высоких выходах, а также возможности использования для получения с хорошими выходами О-замещенных гидроксиаминов, содержащих группы, чувствительные к гидразину.

В ходе исследования механизма реакции удалось изолировать диамиды N-алкил- и N-(замещенный окси)-фталевой кислоты. Было исследовано влияние растворителя, разбавления, основность первичных аминов и их стерических условий на ход реакции. Среди изученных соединений 2-гидрокси-5-карбометокси-бензилоксинамин был направлен на клинические исследования.

Триарилметаны, VI

Реакции нафтохинон-дифенилметидов с органометаллическими соединениями

А. Ф. МОХАМЕД ЭЛКАСЧЕФ, Ф. М. Е. АБДЕЛЬ-МЕГЕЙД и С. М. М. ЭЛЗЕЙН

Реакция 1,2-нафтохинон-дифенилметида с органометаллическими соединениями происходит согласно механизму 1,4-присоединения. Исключение представляет 1-нафтиллитий, где наблюдается дальнейшее замещение группы OH 1-нафтилловой группой. 1,4-Нафтохинон-4-дифенилметид реагирует по механизму 1,2-присоединения с последующей миграцией группы OH к C-6.

Конформация 3,7-диазобицикло [3.3.1] нонанов, I

П. ШЕЙБЕР и К. НАДОР

Был описан конформационный анализ некоторых N,N'-диалкил-1,5-дифенил-диазабицикло [3.3.1] нонанов. На основе данных ИК и ЯМР спектроскопии, а также дипольных моментов, было показано, что N,N'-диметил производные с оксогруппой в положени и находятся в конформации стул-ванна, в то время как в случае N,N'-ди-трет-бутил производных следует считаться также и с конформацией ванна-ванна. В 9-гидрокси производных, между OH и третичным азотом образуется сильный интрамолекулярный водородный мостик, который стабилизирует одно из шестичленных колец в форме стула.

Диамагнитное смещение системы дибензоциклогептатриенового кольца в некоторых производных ациламиномалонового эфира

П. ШОХАР, Й. КОШАРИ и Э. КЕСТРЕЙНЕР

В ЯМР спектрах диэтил-2-формиламино- и 2-ацетиламино-2-(дибензо/a,e/циклогептен-5')-ил-малонатов (**III**; R = H, Me) наблюдается сильное диамагнитное смещение этильных и ацильных (формил и ацетил, соответственно) протонов — по сравнению с ациламидомалоновыми эфирами **II** — вследствие анизотропного эффекта ароматических колец.

4-S-Замещенные 2,6-динитроанилина

Э. ПАЛОШИ, К. ХАРШАНИ и Г. ХЕЙЯ

Исходя из S,S-диметил-(4-гидроксифенил)-сульфониевой соли (**4**), был проведен синтез N,N-диалкил-2, 6-динитроанилинов, замещенных в положении 4 метилтио-, метилсульфинил- и метилсульфонил-группами.

Основные эфиры с антиаритмическим эффектом

К. ХАРШАНИ, Г. ХЕЙЯ и Д. КАРБОНИЧ

Эфиры $Ap—CO_2(CH_2)_n\ NH_2—R$ (**6**), имеющие терапевтическое значение, были получены различными путями. Хотя в случае амида кислоты (Ap = 3 4, 5-триметоксифенил и $n = 2$) (**9**) под влиянием кислоты образуется основной эфир, однако, миграцию ацила O→N из основания эфира осуществить не удалось.

12 S

According to international book reviews the series
ABSORPTION SPECTRA IN THE ULTRAVIOLET AND VISIBLE REGION
started in 1959 – is highly useful in both structure research and chemical analysis.
Our Publishing House now offers you a new series on *infrared spectra!*

ABSORPTION SPECTRA IN THE INFRARED REGION

Editor of the series L. LÁNG
Introductory volume written by S. HOLLY and P. SOHÁR

Though the scientific literature has several series dealing with the same field, naturally none of them strives for completeness, and overlapping is very small. The present series is concerned with very recent spectra, including those which are not given in the original papers. The *Introductory Volume* gives a detailed discussion of the characteristic frequencies affording ample guidance for the practical spectroscopist. The most important technical information is also included.

In English . Approx. 320 pages per volume
17 × 23 cm . Loose-leaf cloth binders

AKADÉMIAI KIADÓ
Budapest

BUTTERWORTH LIMITED
London

A co-edition, – distributed in the socialist countries by *Kultura*, H-1389 Budapest P. O. B. 149; in all other countries by *Butterworth Limited*, London

ABSORPTION SPECTRA IN THE ULTRAVIOLET AND VISIBLE REGION

Series edited by L. LÁNG

According to international book reviews, this series is highly useful in both structure research and chemical analysis. This applies especially to problems of analytical character or structure determination encountered in the pharmaceutical, dye and other industries, i.e. in organic chemical industry in general. A great advantage of this collection is that the spectra published may, in many cases, directly be used for solving the particular problems in question.

The series dealing with *ultraviolet and visible spectra* was started by the Publishing House of the Hungarian Academy of Sciences in 1959, and by now the project has got as far as Vol. 18. The editors invite the users of the collection to contribute to the success of this work by submitting for publication spectra of new compounds.

Each volume contains about 400 pages spectra graphs and tables of about 190 compounds + indexes.

Cumulative index: I–V, VI–X, X–XV

AKADÉMIAI KIADÓ
Budapest

ACADEMIC PRESS
New York

The whole series is a co-edition, – distributed on the American Continent by ACADEMIC PRESS, New York, in all other countries by KULTURA, H-1389 Budapest, P. O. B. 149

The Acta Chimica publish papers on chemistry in English, German, French and Russian.

The Acta Chimica appear in volumes consisting of four parts of varying size, 4 volumes being published a year.

Manuscripts should be addressed to

Acta Chimica
Budapest 112/91 Műegyetem

Correspondence with the editors should be sent to the same address.

The rate of subscription is $ 32.00 a volume.

Orders may be placed with "*Kultúra*" Foreign Trade Company for Books and Newspapers (1389 Budapest 62, P.O.B. 149. Account No. 218 10990) or with representatives abroad.

Les Acta Chimica paraissent en français, allemand, anglais et russe et publient des mémoires du domaine des sciences chimiques.

Les Acta Chimica sont publiés sous forme de fascicules. Quatre fascicules seront réunis en un volume (4 volumes par an).

On est prié d'envoyer les manuscrits destinés à la rédaction à l'adresse suivante:

Acta Chimica
Budapest 112/91 Műegyetem

Toute correspondance doit être envoyée à cette même adresse.

Le prix de l'abonnement est de $ 32.00 par volume.

On peut s'abonner à l'Entreprise pour le Commerce Extérieur de Livres et Journaux «*Kultúra*» (1389 Budapest 62, P.O.B. 149. Compte-courant No. 218 10990) ou à l'étranger chez tous les représentants ou dépositaires.

«*Acta Chimica*» издают трактаты из области химической науки на русском, французском, английском и немецком языках.

«*Acta Chimica*» выходят отдельными выпусками разного объема. 4 выпуска составляют один том. 4 тома публикуются в год.

Предназначенные для публикации рукописи следует направлять по адресу:

Acta Chimica
Budapest 112/91 Műegyetem

По этому же адресу направлять всякую корреспонденцию для редакции.

Подписная цена — $ 32.00 за том.

Заказы принимает предприятие по внешней торговле книг и газет «*Kultúra*» (1389 Budapest 62, P.O.B. 149. Текущий счет № 218 10990) или его заграничные представительства и уполномоченные.

Reviews of the Hungarian Academy of Sciences are obtainable at the following addresses:

ALBANIA
Drejtorija Qändrone e Pärhapjes dhe Propagandimit tä Librit
Kruga Konferenca e Päzes
Tirana

AUSTRALIA
A. Keesing
Box 4886, GPO
Sydney

AUSTRIA
GLOBUS
Höchstädtplatz 3
A-1200 Wien XX

BELGIUM
Office International de Librairie
30, Avenue Marnix
1050 Bruxelles
Du Monde Entier
162, Rue du Midi
1000 Bruxelles

BULGARIA
HEMUS
11 pl Slaveikov
Sofia

CANADA
Pannonia Books
2, Spadina Road
Toronto 4, Ont.

CHINA
Waiwen Shudian
Peking
P. O. B. 88

CZECHOSLOVAKIA
Artia
Ve Smečkách 30
Praha 2
Poštovní Novinivá Služba
Dovoz tisku
Vinohradská 46
Praha 2
Mad'arská Kultura
Václavské nám. 2
Praha 1
SLOVART A. G.
Gorkého
Bratislava

DENMARK
Ejnar Munksgaard
Nörregade 6
Copenhagen

FINLAND
Akateeminen Kirjakauppa
Keskuskatu 2
Helsinki

FRANCE
Office International de Documentation et Librairie
48, rue Gay-Lussac
Paris 5

GERMAN DEMOCRATIC REPUBLIC
Deutscher Buch-Export und Import
Leninstraße 16
Leipzig 701
Zeitungsvertriebsamt
Fruchtstraße 3—4
1004 Berlin

GERMAN FEDERAL REPUBLIC
Kunst und Wissen
Erich Bieber
Postfach 46
7 Stuttgart S.

GREAT BRITAIN
Blackwell's Periodicals
Oxenford House
Magdalen Street
Oxford
Collet's Subscription Import Department
Dennington Estate
Wellingsborough. Northants.
Robert Maxwell and Co. Ltd.
4—5 Fitzroy Square
London W. 1

HOLLAND
Swetz and Zeitlinger
Keizersgracht 471—478
Amsterdam C.
Martinus Nijhof
Lange Voorhout 9
The Hague

INDIA
Hind Book House
66 Babar Road
New Delhi 1

ITALY
Santo Vanasia
Via M. Macchi 71
Milano
Libreria Commissionaria Sansoni
Via La Marmora 45
Firenze
Techna
Via Cesi 16
40135 Bologna

JAPAN
Kinokuniya Book-Store Co. Ltd.
826 Tsunohazu 1-chome
Shinjuku-ku
Tokyo
Maruzen and Co. Ltd.
P. O. Box 605
Tokyo-Central

KOREA
Chulpanmul
Phenjan

NORWAY
Tanum-Cammermeyer
Karl Johansgt 41—43
Oslo 1

POLAND
RUCH
ul. Wronia 23
Warszawa

ROUMANIA
Cartimex
Str. Aristide Briand 14—18
Bucureşti

SOVIET UNION
Mezhdunarodnaya Kniga
Moscow G—200

SWEDEN
Almquist and Wiksell
Gamla Brogatan 26
S—101 20 Stockholm

USA
F. W. Faxon Co. Inc.
15 Southwest Park
Westwood, Mass. 02090
Stechert Hafner Inc.
31. East 10th Street
New York, N. Y. 10003

VIETNAM
Xunhasaba
19, Tran Quoc Toan
Hanoi

YUGOSLAVIA
Forum
Vojvode Mišića broj 1
Novi Sad
Jugoslavenska Knjiga
Terazije 27
Beograd

13. III. 1975 **Index: 26.007**

ACTA CHIMICA

ACADEMIAE SCIENTIARUM HUNGARICAE

ADIUVANTIBUS

V. BRUCKNER, GY. DEÁK, K. POLINSZKY,
E. PUNGOR, G. SCHAY, Z. G. SZABÓ

REDIGIT

B. LENGYEL

TOMUS 84 FASCICULUS 3

AKADÉMIAI KIADÓ, BUDAPEST

1975

ACTA CHIM. (BUDAPEST) ACASA 2 84 (3) 229–351 (1975)

ACTA CHIMICA

A MAGYAR TUDOMÁNYOS AKADÉMIA KÉMIAI TUDOMÁNYOK OSZTÁLYÁNAK IDEGEN NYELVŰ KÖZLEMÉNYEI

SZERKESZTI

LENGYEL BÉLA

TECHNIKAI SZERKESZTŐK

DEÁK GYULA és HARASZTHY-PAPP MELINDA

Az Acta Chimica német, angol, francia és orosz nyelven közöl értekezéseket a kémiai tudományok köréből.

Az Acta Chimica változó terjedelmű füzetekben jelenik meg, egy-egy kötet négy füzetből áll. Évente átlag négy kötet jelenik meg.

A közlésre szánt kéziratok a szerkesztőség címére (Budapest 112/91 Műegyetem) küldendők.

Ugyanerre a címre küldendő minden szerkesztőségi levelezés. A szerkesztőség kéziratokat nem ad vissza.

Megrendelhető a belföld számára az „Akadémiai Kiadó"-nál (1363 Budapest Pf 24. Bankszámla 215 11488), a külföld számára pedig a „Kultúra" Könyv- és Hírlap Külkereskedelmi Vállalatnál (1389 Budapest 62, P. O. B. 149. Bankszámla: 218 10990) vagy annak külföldi képviseleteinél és bizományosainál.

Die Acta Chimica veröffentlichen Abhandlungen aus dem Bereich der chemischen Wissenschaften in deutscher, englischer, französischer und russischer Sprache.

Die Acta Chimica erscheinen in Heften wechselnden Umfanges. Vier Hefte bilden einen Band. Jährlich erscheinen 4 Bände.

Die zur Veröffentlichung bestimmten Manuskripte sind an folgende Adresse zu senden:

Acta Chimica
Budapest 112/91 Műegyetem

An die gleiche Anschrift ist auch jede für die Redaktion bestimmte Korrespondenz zu richten. Abonnementspreis pro Band: $ 32.00.

Bestellbar bei dem Buch- und Zeitungs-Außenhandels-Unternehmen »*Kultúra*« (1389 Budapest 62, P. O. B. 149 Bankkonto Nr. 218 10990) oder bei seinen Auslandsvertretungen und Kommissionären.

Acta Chimica Academiae Scientiarum Hungaricae, 84 (3), pp. 229—244 (1975)

TANDEM TITRATOR

K. IKRÉNYI

(Eötvös Loránd University Petrology–Geochemistry Department)

Received September 24, 1973

A titrator was developed which can expand the conductometric volumetric determinations on the fields of acid-basic, redox, precipitation, complexometric and chelatometric titrations. The construction of the differential recording conductometric titrator (Tandem Titrator) consists of a double titrant-delivery system, a differential conductivity meter, two conductometric cells and a recorder. By means of new end-point indications the tandem system makes possible the considerable elimination of matrix effects and determination of two components in a simple titration.

1. Introduction

The construction of a conductometric titrator was purposed which can extend the conductometric end-point detection on wider fields of volumetric determinations.

The conductance can be measured by direct current and alternating current. In case of d.c.-measuring technique non polarizable electrodes [1], cells with auxiliary electrodes (*e.g.* [2]), or reversible redox electrodes with low voltage [3] are used for elimination of undesirable effect of electrode polarization. KOHLRAUSCH suggested the use of alternating current for decreasing of polarization. Low-frequency a.c. compensational (bridge) method or continuously measuring conductivity meter are used for determination of admittance, however, the high-frequency conductance or susceptance also can be measured by bridge connection (*e.g.* double T-bridge [4]). The oscillometric indication is limited by the available section of function between the observed sign and concentration (*e.g.* [5] 14. tabulation). Because the conductivity of sample is not given only by the ion to be titrated, maybe the absence of end-point detection can be realized. For this reason, disregarding the d.c.- and high-frequency methods, the indicator unit of the titrator in the following is a low frequency conductivity meter where the concentration of ions and the conductivity are linear proportional in first approximation.

The conductometric titrations are not very far current on the field of applied analitical chemistry, the reason for this can be summarized in the following:

When the change of conductivity of titrating reaction is significantly less than the conductivity of sample solution to be titrated (*e.g.* redox titration in strong acidic medium, complexometric titration in buffered medium etc.), the end-point of titration can be observed poorly, or the endpoint detection does not occur.

Not only the titration reaction causes the change of conductivity during the titration but other effects too (dilution, change of temperature, change of dissociation, secondary reactions etc.) which result deformations on the linear section of titration curve, and the uncertainty of end-point evaluation can arise.

The change of conductivity in certain analytical reactions, *i.e.* the change of conductivity per gram equivalent, can be a rather low value, the indication is not sensitive (*e.g.* some ligand change reactions, molecule reactions etc.).

The temperature compensation (*e.g.* [6], [7] with aid of thermistor) and the initial conductivity compensation [7], [14] are solved by means of expedient conductometer constructions. Titration with relative concentrated titrant is used to eliminate the dilution, but this can damage the accuracy.

The overseas (*e.g.* Leeds and Nortrup Co., Industrial Instruments Inc. etc.) and the European (*e.g.* Radiometer, Metrohm) firms put in circulation titrators which can operate with the aid of conductometric indication too, but these instruments constitute a subordinate part beside the titrators based upon potentiometric indication.

The above-mentioned troubles were purposed to be eliminated on the basis of differential measurement which is easy to find at the constructions of analytical chemical instruments. Accordingly, the difference between two, approximately identical systems is measured, which systems differ from each other only at the sample or the adequate component of sample. The sign of expedient difference meter can be a differentiated sign which is a change ratio or differential ratio to the interested variable, *e.g.* the concentration of sample to be determined. On the other hand, the derivative method, which is often used in the instrument techniques (*e.g.* potentiometric titrators), results in the differential of sign in the function of time (*e.g.* R-C circuit and inductive derivative unit).

The titrimetry measuring between two titration systems originates from Cox [8], and this is used with the aid of thermometric indication according to Bark's book of reference [9].

Two fundamental constructions of automatic titrators have formed: pre-set and recording constructions. According to Robinson's [10] and Lingane's [11] initiative works numerous types of automatic titrators appeared till now. The buret of pre-set titrators differs from the traditional buret only in the use of valve which delivers the flow of titrant, and it is controlled by the measured electrochemical sign. The recording titrators have

a unit delivering uniformly the titrant which is a plunger buret in general. Although high accuracy (0.10—0.05%) is promised by the manufacturing firms in the specification of pre-set titrators, the problems of the pre-set system arise during the analytical chemical practice. The pre-set sign according to the end-point can be different in the case of different samples, therefore the value of this sign should be worked out experimentally from time to time. The use of titrators to record the titrating curve proves to be more advantageous when these problems appear. All the same, the pre-set titrators are current because they supply a lot of titrimetric exercices under satisfactory accuracy and they are cheeper than the recording titrators.

The possibility of pre-set conductometric titrator was proposed by DELAHAY [12] where the titrant delivery was controlled by the derivated conductivity sign, but the conductometric titrators are made in recording construction above all, because of mentioned problems of conductometric indications. An example of this is the titrator in the following, the experimental character of the titrator needs, as a matter of course, to be suitable for recording.

2. Instrument

A differential conductometric recording titrator was made on the above-mentioned conceptions. It consists of a double titrant-delivery unit, two conductometric electrode pairs immersing into the titrating pots, a recording conductivity meter measuring the difference between the two cells, which was named Tandem Titrator. The technical nomenclature uses the English 'tandem' word on double-series systems, the titrator in the following measures the conductivities of cells in series but contrary sign connection.

2.1. Tandem Titrator

The development of model of Tandem Titrator was carried out by the scheme in Fig. 1.

The *1* motor drives the *2* screw spindle on which the *3* threated runner feeds the *5* plungers of the *4* burets. The quantity of titrant untill the stop of titration, *i.e.* the total path of plunger feed, can be adjusted by the *6* limit switches. A deviation between the zero point of the two plungers can be produced by the *7* calibrated screw. The rate of delivery and the uniform motion of feed adjusting in advance are guaranteed by the *9* regulator unit which is connected with the *8* tachometer generator and is fed back to the motor. The burets get the titrant from the *10* pots and feed into the *11* titrating beakers. An analogous electrical sign proportional to the quantity of titrant is supplied by the *12* helical potentiometer which is driven by the *2* screw spindle with the *13* gearing (like the KATEMAN's system [13]). The

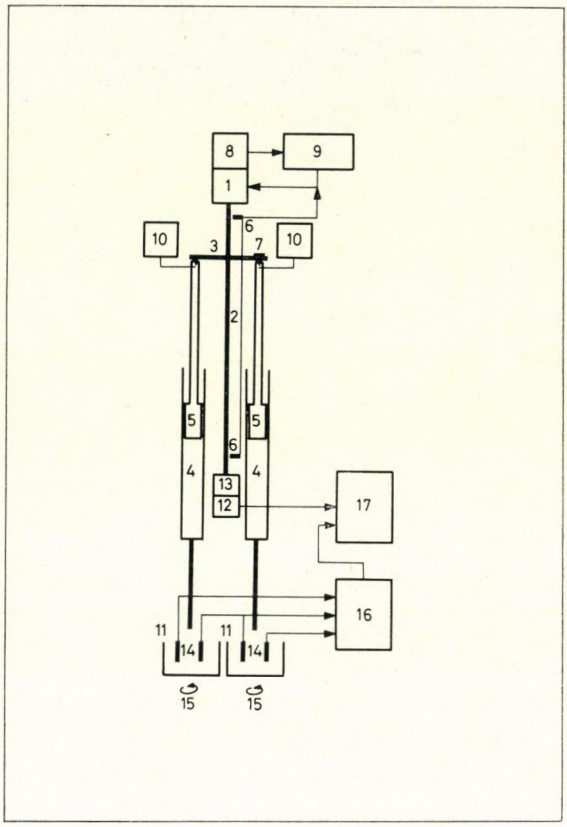

Fig. 1. Tandem Titrator

14 conductometric electrodes immerge into the titrating beakers, the cell constants of which are equal. The *15* stirrers supply the intensive and identical mixing of sample solutions. The difference between the conductivities of solution is measured by the *16* differential conductivity meter, its sign gets to the first channel of *17* recorder, the analogous voltage of titrant volume gets to the other channel from the *12* helipot.

The construction like this makes possible to registre two variables, the conductivity and the titrant volume, in the function of time on the graph, *i.e.* the kinetic investigation of the titrating reaction can be made possible. The kinetic titration curve is generally needed developing a new volumetric determination.

2.2. Interfluxional Buret

The recording titrators operate with motor-driven plunger burets in general (*e.g.* Metrohm Dosimat 415, 535, Beckman Automatic Titrator,

Radiometer Autoburette ABU 13). The burets like these have a two-way cock on their top. At the one-way position of cock the titrant can be sucked into the buret from the pot containing the titrant, at the second-way position of cock the titrant can be fed into the sample. A dead-space is formed between the cock and the upper position of plunger, wherefrom the titrant can be rinsed out only by repeated, periodic washing or elimination of plunger. The solution in the dead-space can soil, dilute the titrant. Therefore, an Interfluxional Buret was developed for the Tandem Titrator in which the solution streaming through the stem of plunger flows into the one direction, to the titrating beakers. When the titrant is changed, the previous titrant can be frontally displaced with water and with a new titrant. An example of implementation of Interfluxional Buret is shown in the Fig. 2, where the 20-ml-volume buret has a hollow stem and plunger. There are ground-glass-surface valves in the *2* plunger and before the *1* output aperture, a *3* drop of quicksilver increases the weight of valve for the fast closing. The *2* valve is closed and the *1* valve is opened during the titration, when the burets are filling, the *1* valve closes and the *2* valve opens the interflux of titrant through the stem of plunger into the buret. The Interfluxional Buret like this works in vertical installation. For the perfect operation of Interfluxional Buret not only the slight friction and good closing should be assumed but the fast, exact closing of valves too.

The reliable operation of the ground-glass plunger buret (Fig. 2) can be reached by the use of an internal lubricant. 5—25% glycerol in the titrant was mostly used as an internal lubricant. The glycerol is well soluble in aqueous and some non-aqueous media, it is generally indifferent during the acid-basic precipitation and complexometric titrations. The sulphuric and phosphoric acid were used as internal lubricants at the titration with strong oxidant because a great deal of oxidimetric titrations are effected in the strong acidic medium.

2.3. Differential Conductivity Meter

The typical problem of low-frequency conductometric titration is presented when the conductivity of medium is higher then its change during the titration. MUELLER and his collaborators developed an initial conductivity-compensation system [7] which is a T-bridge-type conductivity meter. The conductivity sign of cell can be set to zero before the titration with an amplitude-independent phase shift in the zero-compensating branch of bridge, moreover, this conductivity meter was supplied with an automatic thermistor controlled temperature compensation too.

According to the requirement of liquid chromatography, the conductivity difference of the clean eluent and of the eluate is needed to measure. By reason of DUHNE's method [14], four low-frequency conductometric cells are connected

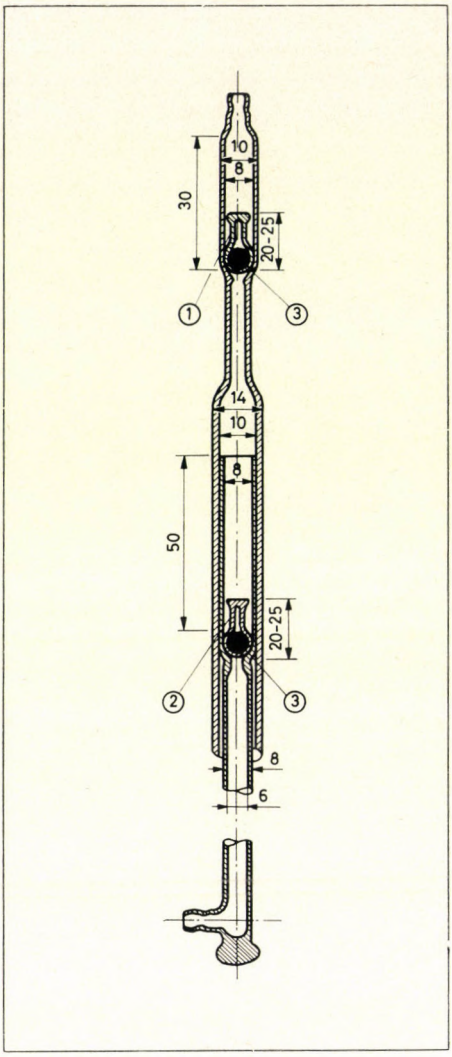

Fig. 2. Interfluxional Buret

in a Wheatstone bridge, and the output sign of the bridge is rectified, smoothed and registered.

In the case of high-frequency conductometry, the principle of differential measurement is adopted in multiple way. The CRUSE's oscillometric instrument [15] realizes to measure the frequency difference between two units, which operate one by one comparing capacitive and inductive cells.

The expedient conversion of a commercial instrument seemed to be practical instead of making a new conductivity meter. The scheme of a con-

ductivity meter is visible in the Fig. 3.1. The voltage of *1* oscillator passes through the *2* transformer to the measuring circuit. The *4* devided resistor is connected cyclically with the *3* conductometric cell. The voltage decreasing on the resistor gets through the *5* amplifier and the *6* rectifier to the *7* meter or recorder output. The stability of system is assured by the *8* negative feedback.

The scheme of the conversed instrument is shown in the Fig. 3.2. The inductive connection of oscillator is carried out by the *9* phase-inverter transformer which devides the sign of the oscillator into two equal amplitudes but contrary phase signs. These signs get to the *10* and *11* cells, the resultant current of two cells flows through the resistor which is connected between the earthing point and the centre of secondary circuit of transformer. When a variable resistor (*13*) is switched on instead of one cell with the *12* switch, the instrument works as a zero-compensating conductivity meter.

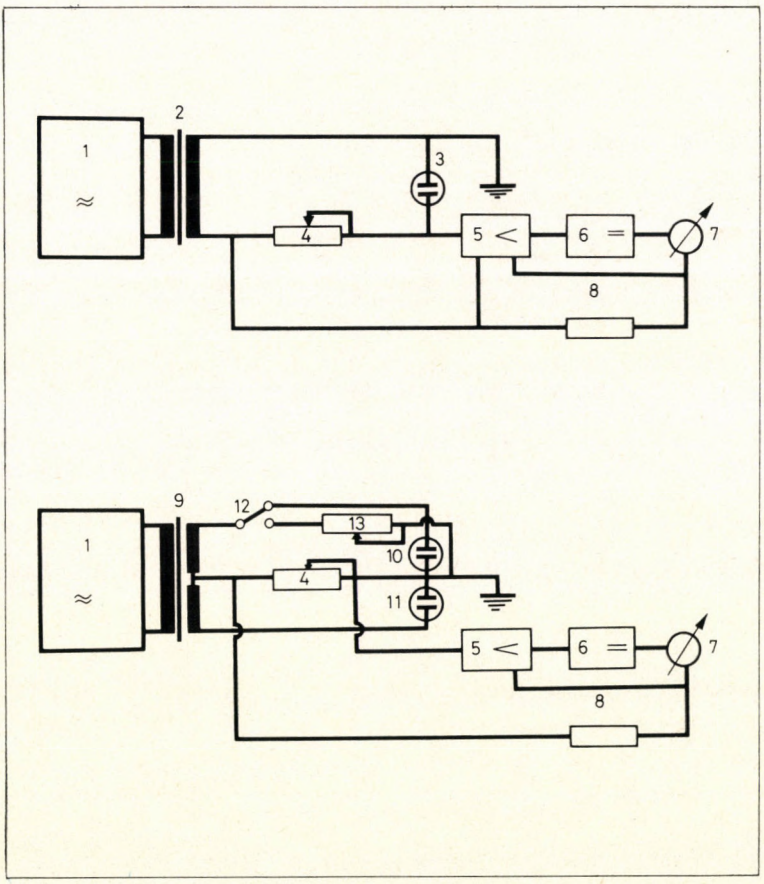

Fig. 3.1. Conductivity Meter
Fig. 3.2. Differential Conductivity Meter

2.4. Electrode Pairs

The measuring electrodes consist of two platinum, or slightly platinized platinum sheets which are insulated by plastic. The cell constants of the approximately equal electrode pairs can be equalized by platinazing. The platinazing of the electrode pair with less cell constants is being continued until the difference of conductivity proves to be of minimum value in the same solution. According to the differential measurement the formation of cells does not matter, only to keep the approximately uniform cell constant values is needed in practice.

The distance between the electrodes and the wall of beaker, and the quality of beaker influences the conductivity. This effect decreases when the distance between the electrodes and the wall increases. The titration with fixed beakers and electrodes is recommended for the accuracy.

3. Titrations with Tandem Titrator

The examples of acid-basic, precipitation, redox or complexometric titrations will be shown for demonstration of end-point detection which are made possible by the Tandem system. The titration curves in the figures are copies of the registered titrating graphs. The volumetric determinations by Tandem Titrator can be grouped according to the end-point detection in the following:

1. end-point detection by preventive elimination,
2. end-point detection by the reaction difference between the titrated media,
3. end-point detection by the concentration difference of components to be determined,
4. end-point detection by differential indication,
5. end-point detection by the concentration difference of titrants,
6. determination of two components by the adequate combinations of end-point detections during a titration (Tandem titration).

The differential conductivity meter measures the difference of conductivity between two cells without sign. It is the same for the indication of titration whether the differential conductivity increases or decreases during the titration. The general effects of the buffer influences, the changes of complex stabilities, dissociation, solubility etc. are aften so complicated that that titrating curve of tandem titrimetry doesn't consist of straights during a certain titration. But the unambiguous and significant change of sign in the end-point (break-point, step or maximum) is definitive in the respect of titration.

3.1. Titration by Preventive Elimination

The two titrating beakers contain the same aliquot parts of sample and the solutions required for titration (acid, basic, buffer, water etc.). If the ion to be titrated is preventively eliminated from the one beaker by means of a masking reagent, the registered Δ differential conductivity sign of Tandem Titrator originates only from the titrating reaction, it doesn't change during the over-titrating phase.

An example of end-point detection by preventive elimination is in the Fig. 4, where ferri ions are measured by the complexometric titration. The end-point detection like this is proposed when the titrating straights become curves according to the change of matrix in case of a traditional conductometric titration, and so the end-point detection can become doubtful. For this reason the matrix effect is decreased by the preventive elimination above all.

3.2. Titration by the Reaction Difference between the Titrated Media

The titrant can react not only with the ion to be determined but with other ions of sample solution too, however, this can be avoided by the adequate selection of matrix.

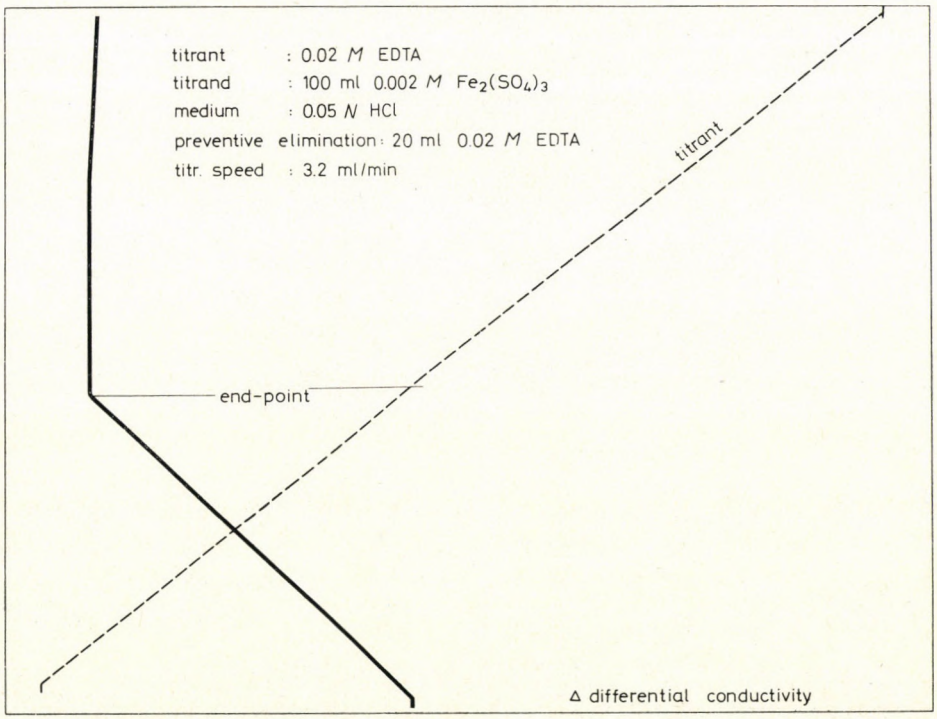

Fig. 4. End-point detection by preventive elimination

In case of example in Fig. 5 the solution contents silicate ion beside sulphate ion too. The matrix of one test solution is acidic, thus the titrant ($BaCl_2$ solution) reacts only with the ion to be titrated (sulphate ion) and in the basic medium of other solution it can also react with the other ion of matrix ($BaSiO_3$ precipitate). This difference arises as a well defined sign on the curve of differential conductivity where the different behaviour of matrixes

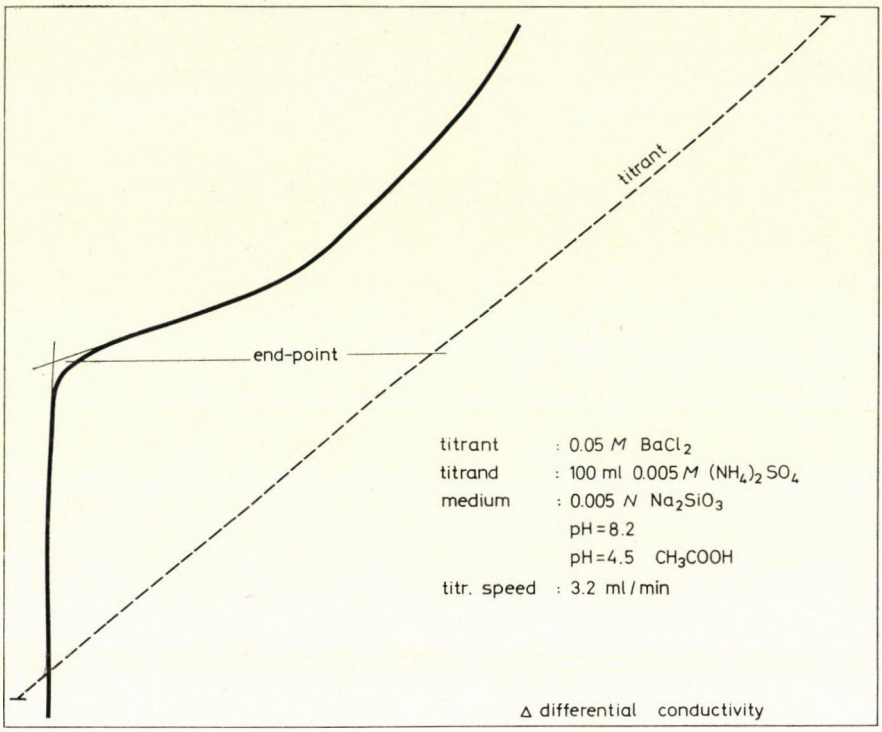

Fig. 5. End-point detection by the reaction difference of titrated media

is shown by the significant change of over-titrating phase. This phase is not always a linear straight because the conductance of solutions changes in different ways at the different matrixes (*e.g.* the second phase of titrating curve in the Fig. 5).

The difference of titrating reactions can be used to titrate two equal solutions with different quality reagents. In consequence of the theoretical and practical problems, the determination like this wasn't carried out.

3.3. Titration by Concentration Difference of Component to be Determined

At this end-point detection the samples contain the ion to be determined in known different quantities. In the case of example in Fig. 6, the one beaker includes no chloride ion, the other includes an aliquot part, so the differential

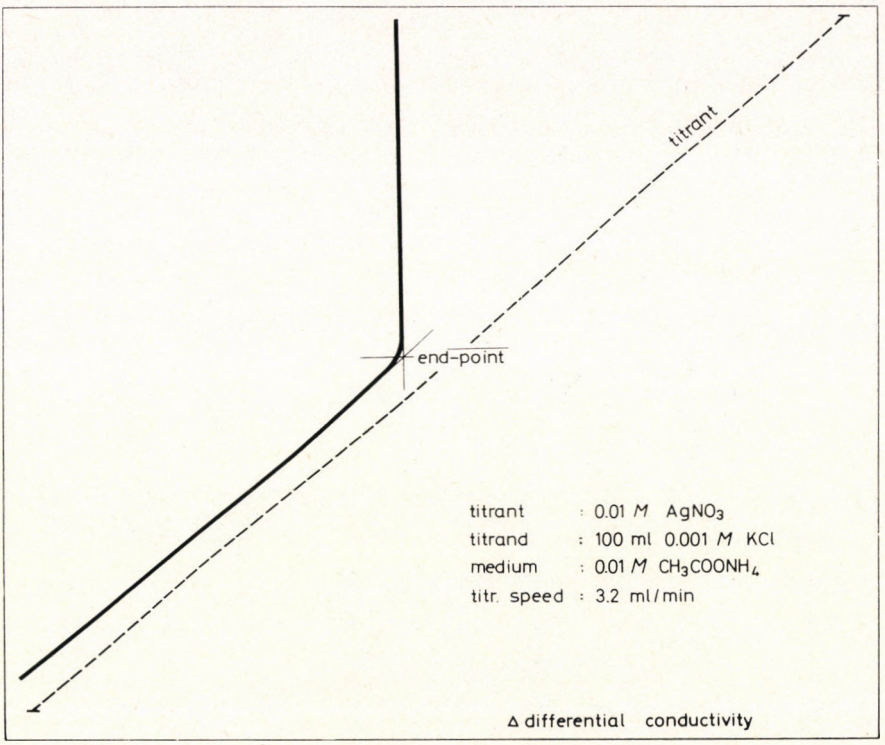

Fig. 6. End-point detection by the difference of concentration

conductance changes during the argentometric titration, but during the over-titrating phase it doesn't change.

An example of redox titration is shown in Fig. 7 where the one titrating beaker contains the double quantity of ion to be determined (ferro ion) than the other one. The end-points belonging to the two concentrations can be well evaluated on the curve of vanadatometric titration. Two parallel titrations are made by the end-point detection of additive difference, which increases the accuracy of determination. If the conductance of sample solution is strongly influenced by the matrix, the aliquot part of sample gets into the two beakers, and the adequate quantity of the ion to be determined is added into the one beaker (*e.g.* $FeSO_4$ solution constitutes the additive difference at the Fe^{2+} titration of attacked slag). In this way the second part of titration makes possible the factoring of titrant.

3.4. Titration by Differential End-point Detection

If the concentration difference mentioned with the method in point 3.2. is strongly decreased (theoretical infinitesimal small value), the differential

end-point detection is carried out. The Tandem Titrator basing on differential the principle is avaiable for registration of the titrating curve derivated by the concentration. The significant change of sign on the differential curve is expected only at the periphery of end-point, thus the more sensitive stage of instrument is useful. If the conductance curve in the function of titrant quantity

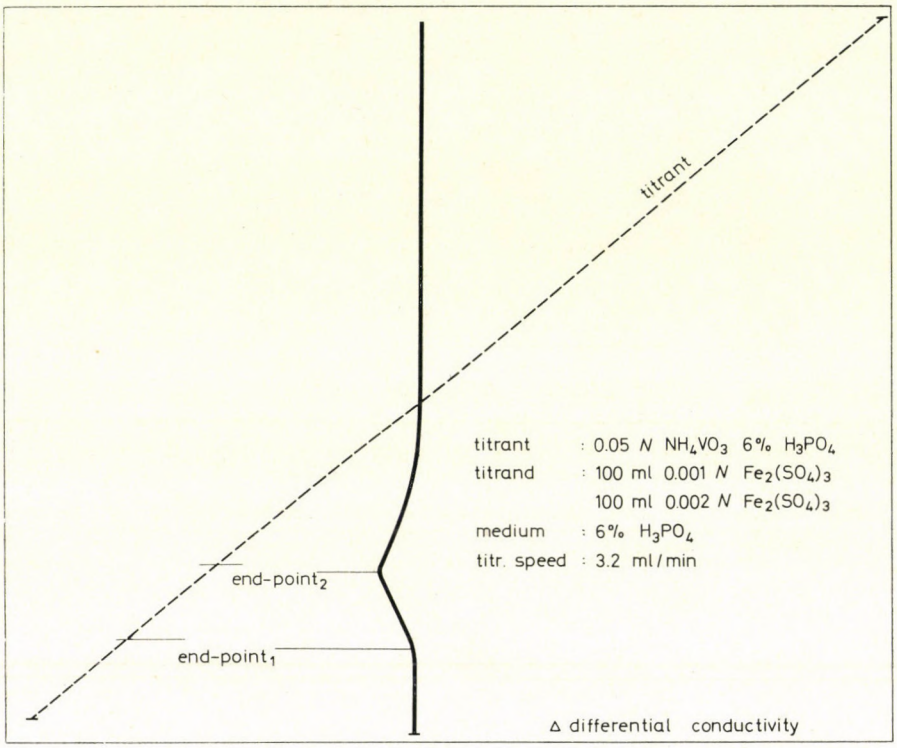

Fig. 7. End-point detection by additive difference

has a break or step change at the end-point, the derivated curve forms a step or maximum curve, respectively.

The acidimetric titrations of sodium hydroxide in the Fig. 8.1., and potassium bicarbonate in the Fig. 8.2. were carried out by hydrochloric acid with differential indication. The required titration difference is made by a screw (Fig. 1.7) which feeds a little the plunger of one buret before the titration. This buret has a preference to the other, if in this manner the difference of two, parallel shifted titrations is measured, according to the Cox's titration [8]; this procedure eliminates mostly the disturbing effects forming during the titration.

3.5. Titration by the Concentration Difference of Titrants

If the two equal samples are titrated by the titrants which have a little different concentration from each other, a reagent differential end-point detection is formed. The concentration difference between the two solutions

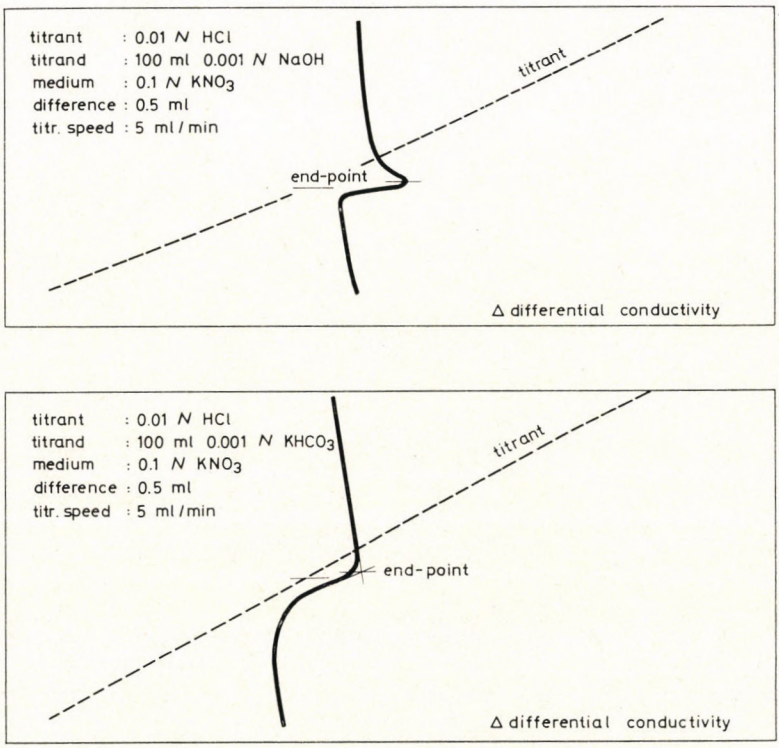

Fig. 8. End-point detection by differential indication

isn't constant, as it was seen in the previous point, but it increases during the delivery of titrants. The conductivity is differentiated not by the concentration but by a linear function of concentration.

An example of acid-basic titration on the Fig. 9 is shown for the use of reagent differential end-point detection. The conformation of differential titrating curves in the Figs. 8 and 9 can be explained by the Fig. 10. The conductances of the individual cells (k_1 and k_2) and the differential conductances (Δ_1 and Δ_2) are illustrated by the examples of acid-basic titrations, in the Fig. 10.1. in case of differential indication, and in the Fig. 10.2. in case of reagent differential end-point detection. The end-points are pointed out from the buret *2* in the Fig. 8.1., 8.2. and the buret *1* in the Fig. 9.

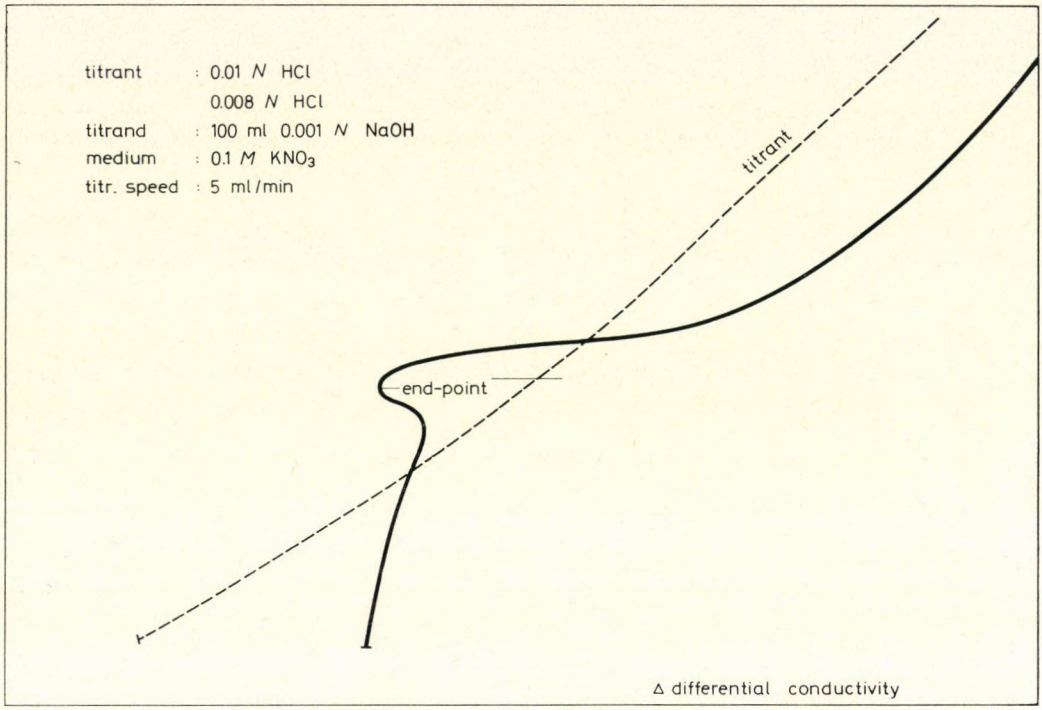

Fig. 9. End-point detection by the difference of titrant concentrations

3.6. Tandem Titration

Measurement of two components during one titration with the Tandem Titrator is named serial or tandem titration of an example of which is seen in the Fig. 11 in case of argentometric titration of a solution containing chloride and bromide ions. In one sample solution the silver chloride and bromide precipitate in the neutral medium. In the other solution the ammonium hydroxide hinders the precipitation of silver chloride (preventive elimination), only the silver bromide precipitates. The differential conductance doesn't change to the total precipitation of silver bromide (the first straight of titrating curve), hereupon there is a change of sign in consequence of the reaction difference between the chloride precipitation and the ammine-complex formation of silver, and the diverse behaviour of silver nitrate in the basic (ammonium acetate–ammonium hydroxide buffer) and weakly acidic (ammonium acetate–acetic acid buffer) media is indicated by the change of sign after the total precipitation of chloride (the third straight of curve, matrix difference).

The selection of adequate titrants and masking agents and the combination of end-point detection methods can make the Tandem Titrator available

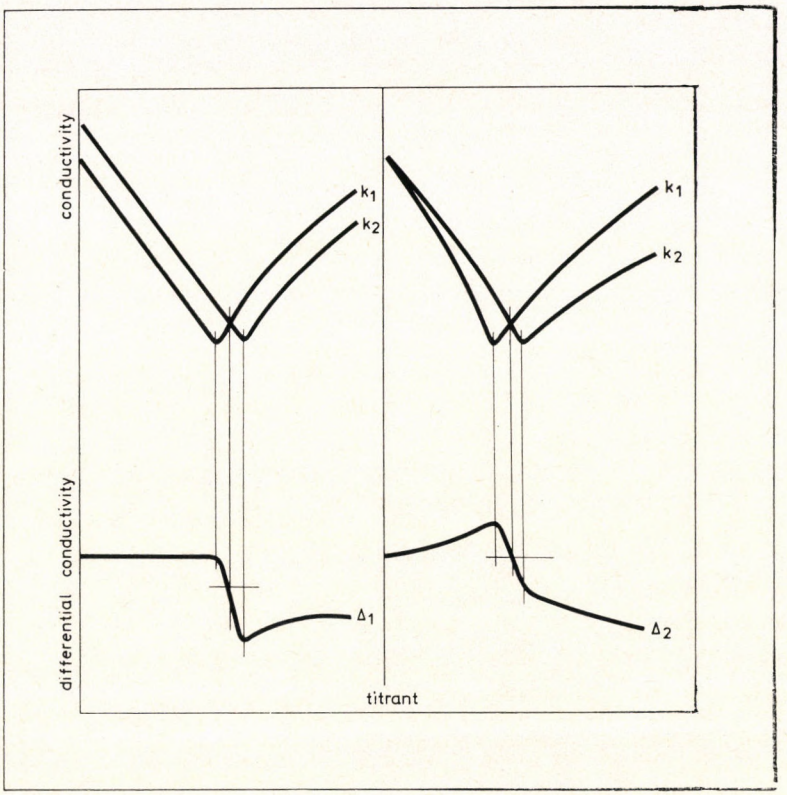

Fig. 10. Relation between the titrating curves of conductometry and Tandem titrimetry

to determine two components simultaneously during a single titration in the same solution. The method makes possible not only the faster determination but a more exact result than the individual titrations of two components.

4. Summary

A differential conductometric titrator, the Tandem Titrator, was constructed which consists of a double titrant-delivery unit, two conductometric cells, and a recording low-frequency differential conductivity meter. The titrant is fed by two interfluxional, internally lubricated ground-glass burets. The conductance difference of two cells is measured by a converted conductivity meter.

The Tandem system makes some new end-point detection possible, decreases the matrix effects, can titrate two components simultaneously and extends the conductometric methods on wider fields of titrimetry.

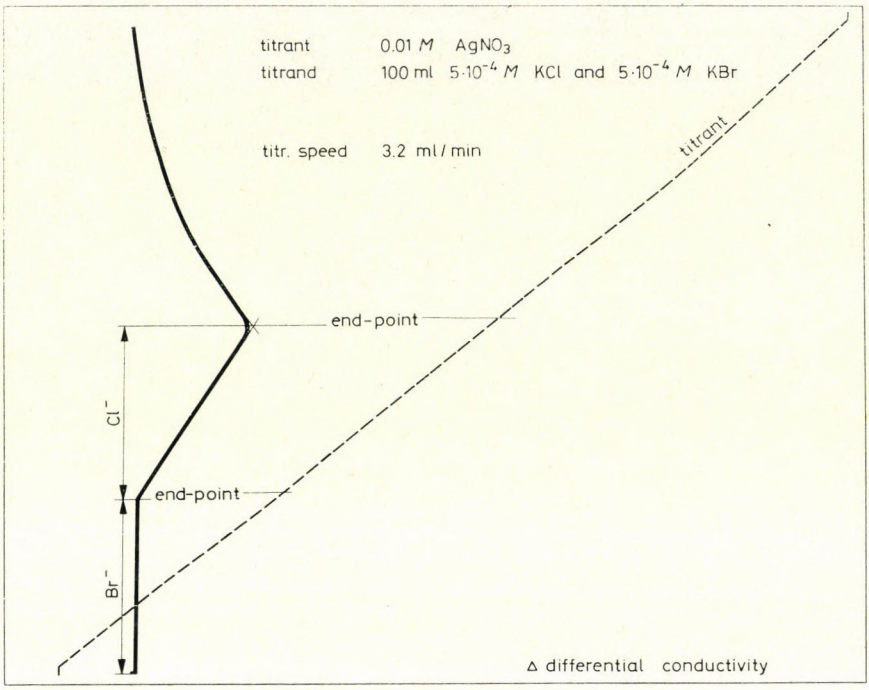

Fig. 11. End-point detection at the Tandem titration

REFERENCES

[1] Palmer, R. F., Scott, A. B.: J. Am. Chem. Soc. **72,** 4821 (1950)
[2] Taylor, R. P., Furman, N. H.: Anal. Chem. **12,** 241 (1960)
[3] Muzsnay, G., Kékedy, L.: Acta Chim. Acad. Sci. Hung. **27,** 21 (1961)
[4] Hall, L. J., Bigson, J. A.: Anal. Chem. **23,** 966 (1951)
[5] Pungor E.: Oszcillometria és konduktometria. Akadémiai Kiadó, Budapest 1963
[6] Blake, G. G.: Anal. Chim. Acta **15,** 342 (1956)
[7] Mueller, T. R., Stelzner, R. W., Fisher, D. J., Jones, H. C.: Anal. Chem. **37,** 13 (1965)
[8] Cox, D. C.: J. Am. Chem. Soc. **47,** 2138 (1925)
[9] Bark, L. S., Bark, S. M.: Thermometric Titrimetry. 31—32. Pergamon Press, London 1969
[10] Robinson, H. A.: Trans Electrochem. Soc. **92,** 445 (1947)
[11] Lingane, J. J.: Anal. Chem. **20,** 285 (1948)
[12] Delahay, P.: Anal. Chem. **20,** 1215 (1948)
[13] Kateman, G., Stornebrink, B. J.: Anal. Chem. **36,** 253 (1964)
[14] Duhne, C., Delta, O. S.: Anal. Chem. **34,** 1074 (1962)
[15] Cruse, K., Ricke, H. B., Huber, R.: Forschungberichte d. Wirtschafts- und Verkehrsministeriums Nordrhein-Westfalen. Nr. 309. Westdeutscher Verlag, Köln und Opladen 1956

Károly Ikrényi; 1088 Budapest, Múzeum krt. 4/a, Hungary

Acta Chimica Academiae Scientiarum Hungaricae, 84 (3), pp. 245—257 (1975)

ÜBER DEN MECHANISMUS DER AN NICKELPULVER KATALYSIERTEN HYDROGENOLYSE VON BUTAN

A. SÁRKÁNY, L. GUCZI und P. TÉTÉNYI

(Institut für Isotope der Ungarischen Akademie der Wissenschaften, Budapest)

Eingegangen am 6. Juni 1973

Die Hydrogenolyse von *n*-Butan und 2-Methylpropan wurde an Nickelpulver als Katalysator im Temperaturgebiet 150—260 °C untersucht. Das Molarverhältnis des Wasserstoffs zum Kohlenwasserstoff wurde bei den Versuchen zwischen 10 und 3 variiert. Die Selektivität der Reaktionskomponente wurde als Funktion des Wasserstoffpartialdrucks, der Temperatur und der katalytischen Aktivität studiert. Die Selektivität der Hydrogenolyse (S_{Pr}) wächst mit steigendem Wasserstoff-Partialdruck, mit der Abnahme der katalytischen Aktivität und der Reaktionstemperatur. Durch Propan-1-^{14}C, Zwischenproduktmarkierung wurde bestätigt, daß die nichtselektive Hydrogenolyse von *n*-Butan und 2-Methylpropan durch das Fehlen des Gleichgewichtes der Zwischenproduktadsorption erklärt werden kann. Die Versuchsergebnisse weisen darauf hin, daß an Nickel »stark« dehydrierte Kohlenwasserstoffradikale entstehen können, die an der Oberfläche schnell weiterreagieren.

1. Einleitung

Der Mechanismus des katalytischen Hydrospaltens gesättigter Kohlenwasserstoffe wurde in früheren Untersuchungen überwiegend durch Hydrospalten von Äthan [1—7] und Propan [8—12] an verschiedenen Übergangsmetallen, hauptsächlich an Ni studiert. Ein Vergleich der kinetischen Parameter zeigt, daß kein Unterschied bei der Wechselwirkung beider Kohlenwasserstoffe mit der Oberfläche aufzufinden ist, Der geschwindigkeitbestimmende Schritt ist zwar in beiden Fällen der Bruch der C–C Bindung an der Oberfläche, beim Propan können die Geschwindigkeiten der Spaltung der C–C Bindung und der Desorption des Äthans unter gewissen Versuchsbedingungen verglichen werden. Durch Radiokarbon-Markierung wurde bewiesen, daß der Mechanismus der Hydrogenolyse bei großmassigem Zerfall der Paraffinkette durch die Annahme »starker« und »schwacher« Wechselwirkungen [12] der Kohlenwasserstoffe mit dem Nickelkatalysator erklärt werden kann. KEMBALL und Mitarb. kamen zu gleichen Schlußfolgerungen an Eisen [13] bzw. an hochaktiven Platinfilmen [14].

In der vorliegenden Arbeit wird über die Hydrogenolyse von Butan berichtet. ANDERSON [8, 9] und SHEPHARD [10] fanden, daß die Hydrogenolyse von Butan und Propan an Nickelfilmen bzw. an Ni-haltigen Katalysatoren nicht selektiv ist, d. h., das Spalten in überwiegendem Maße zu Methan

als Hauptprodukt führt. HANSEL [15, 16] und KOCHLOEFL [17] stellten dagegen fest, daß die Demethylierung einiger gesättigter Kohlenwasserstoffe (z. B. *n*-Oktan, *n*-Dekan) bis zu nicht zu hoher Konversion selektiv verläuft. Die bisherigen Ergebnisse deuten darauf hin, daß die Verteilung der Zwischenprodukte bzw. die Verschiedenheit der Selektivität eng mit dem Verhältnis der unterschiedlichen Oberflächenintermediären [30] verbunden ist. Unsere Untersuchungen zielen auch darauf ab, die Gültigkeit des α-Mechanismus (Spaltung der C–C Bildung am Kettenende), wie er von KIKUCHI [18, 19], MATSUMOTO [20, 21] und KOCHLOEFL [17] an Nickel enthaltenden Katalysatoren bestimmt wurde, für trägerfreie Ni-Katalysatoren beim extensiven Hydrospalten zu kontrollieren und andererseits den Mechanismus des Hydrospaltens durch Propan-1-^{14}C-Zwischenproduktmarkierung zu erforschen.

2. Experimenteller Teil

Für die Versuche verwendeten wir ein vollständig aus Glas verfertigtes Umlaufsystem [22], wie es in früheren Mitteilungen (vgl. [7, 12]) beschrieben wurde. Der Ablauf der Reaktion und die Radioaktivität der markierten Komponenten wurden durch Radiogaschromatographie bestimmt. Proben von 1,0 ml bei jedem Partialdruck wurden an einer 6 m langen Säule, gefüllt mit Squalan (18 Gew.%) auf Chromosorb-W bei 15 °C getrennt. Die Kohlenwasserstoffe wurden durch mehrfache Destillation gereinigt. Die Reinigung des Wasserstoffs erfolgt mittels Diffusion durch eine erhitzte Palladiumhülse. Der Nickelpulver-Katalysator wurde durch die Reduktion von Nickelhydroxyd mit Wasserstoff (50 ml/min) bei 350 °C hergestellt. Die spezifische Oberfläche betrug 3,6 m^2/g.

3. Ergebnisse

Die Hydrogenolyse von *n*-Butan wurde im Temperaturgebiet 160—260 °C bei verschiedenen Mischungsverhältnissen Wasserstoff : *n*-Butan durchgeführt. Das Molverhältnis des Wasserstoffs zum Kohlenwasserstoff wurde bei den Versuchen meistens zwischen 10 und 3 variiert. Abb. 1 zeigt typische Kurven. Beide Zwischenprodukte (Propan und Äthan) weisen ein Maximum auf. Die Geschwindigkeitsgleichung der Hydrogenolyse wurde bestimmt als $W_{n-\mathrm{But}} = k' p^a_{n-\mathrm{But}} p^b_{\mathrm{H_2}}$. Die Reaktionsordnungen sind in der Tabelle I zusammengestellt. Wasserstoff hemmt bei tiefer Temperatur die Hydrospaltung des Butans. Bei 263 °C wächst die Reaktionsgeschwindigkeit in dem untersuchten Partialdruckbereich mit steigendem Wasserstoff-Partialdruck. Dieser Effekt ist noch bedeutender bei der Hydrogenolyse von *n*-Hexan [23]. Man kann auf Grund dieser Experimente weiterhin feststellen, daß die Reaktionsordnung

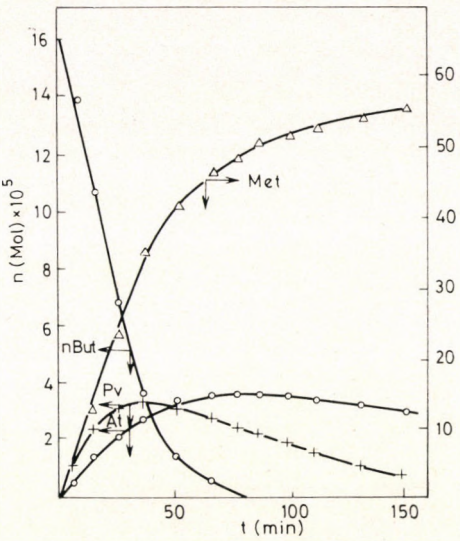

Abb. 1. Die Hydrogenolyse von *n*-Butan am Nickelpulver bei 252 °C

Tabelle I

Temperaturabhängigkeit der Reaktionsordnungen bei der Hydrogenolyse von n-Butan

T °C	P^0_H	$P^0_{n\text{-But}}$	*a*	*b*
167	20—222	5—30	0,98	—1,6
182	34—200	10—22	0,97	—0,7
182	250—350	10	—	—0,97
202	32—183	10—24	0,99	—0,03
227	34—192	12—32	0,98	0,00
245	38—201	11—43	0,97	0,00
263	42— 72	15	—	+0,13
263	122—183	15	—	0,00

bezüglich des Wasserstoffs nur in einem engen Partialdruckbereich als konstant betrachtet werden kann und mit steigendem Wasserstoff-Partialdruck noch negativer wird. Die scheinbare Aktivierungsenergie des *n*-Butan-Hydrospaltens beträgt etwa 131 $\pm$ 5 kJ · Mol^{-1} (aus den Anfangsgeschwindigkeiten im Temperaturbereich 197—250 °C bestimmt). Die Anfangsgeschwindigkeit des *n*-Butan-Hydrospaltens ist 2,8—3-mal größer als die des Propans [12] unter ähnlichen Bedingungen. Die Reaktivität des 2-Methylpropans ist 1,2—1,5-mal größer als die des *n*-Butans. Die erhaltene Aktivierungsenergie unterscheidet sich nicht bedeutend von der des *n*-Butans [12].

Die Selektivität der Hydrogenolyse des *n*-Butans wurde als Funktion des Wasserstoffpartialdrucks, der Temperatur und der katalytischen Aktivität untersucht. Die Selektivität für die Komponente S_i läßt sich folgenderweise ausdrücken [18]:

$$S_{i,\,i\neq n} = \frac{nW_{i,\,i\neq n}}{\sum_{i=1}^{n-1} iW_i}, \tag{1}$$

wobei W_i die Geschwindigkeit des i Kohlenstoffatome enthaltenden Kohlenwasserstoffes darstellt. In den Abb. 2 und 3 bzw. in Tab. II sind die auf die Anfangsgeschwindigkeiten extrapolierten Werte der Selektivitäten angeführt, die für S_{Pr} und S_{At} im Verlauf der Zeit Maximalwerte, für S_{Met} dagegen einen Minimalwert besitzen.

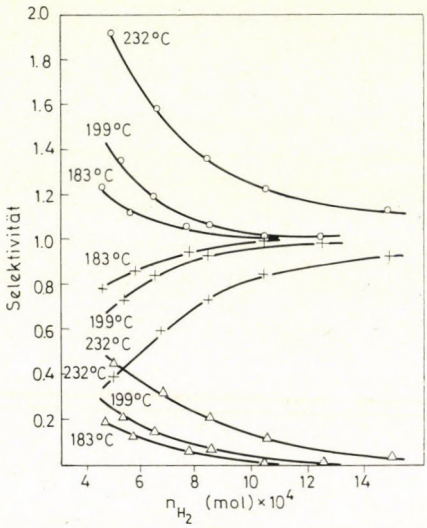

Abb. 2. Die Veränderung der Selektivität als Funktion der Wasserstoff-Konzentration ($n^0_{n\text{But}} = 1{,}47 \times 10^{-4}$ Mol, △ — Äthan, + — Propan, ○ — Methan)

Die Selektivität für das Propan wächst, für Äthan und Methan vermindert sie sich, wie Abb. 2 und 3 zeigen, mit steigendem Wasserstoff-Partialdruck und mit der Abnahme der Reaktionstemperatur.

Die Abnahme der katalytischen Aktivität verursacht eine ähnliche Wirkung, d. h., die Selektivität für das Propan Hydrospalten nimmt zu. Die Ergebnisse sind in Tab. II zusammengestellt. Die Änderung der Aktivität des Katalysators wird durch die Anfangsgeschwindigkeit der Butanabnahme charakterisiert. Aus Tab. I geht hervor, daß die Reaktionsgeschwindigkeit in bezug auf *n*-Butan, zumindest bis zu nicht zu großer Konversion, nach einer

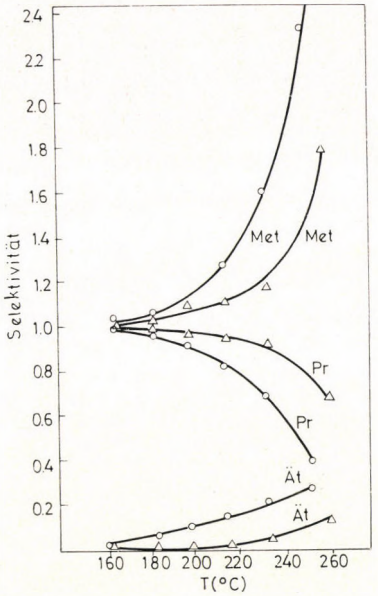

Abb. 3. Die Selektivität der Hydrogenolyse von *n*-Butan als Funktion der Temperatur ($n^0_{n\text{But}} = 1{,}47 \times 10^{-4}$ Mol, ○ — $n^0_{H_2} = 7{,}81 \times 10^{-4}$ Mol, △ — $n^0_{H_2} = 15{,}6 \times 10^{-4}$ Mol)

Tabelle II

Die Selektivität und die Anfangsverteilung der Produkte des n-Butan-Hydrospaltens als Funktion der katalytischen Aktivität

No	W°_n But Mol $s^{-1}m^{-2}$	$S^\circ_{C_3H_8}$	C_3H_8 Mol%	$S^\circ_{C_2H_6}$	C_2H_6 Mol%	$S^\circ_{CH_4}$	CH_4 Mol%	$C_2H_6^{*ber}$ Mol%
1	$2{,}34 \cdot 10^{-9}$	0,31	9,9	0,22	7,0	2,58	82,9	36,4
3	1,42	0,49	17,2	0,17	6,1	2,18	76,6	29,6
4	1,04	0,59	22,2	0,15	5,7	1,91	72,3	25,0
5	$8{,}305 \cdot 10^{-10}$	0,68	27,4	0,14	5,6	1,65	66,8	19,7
6	6,12	0,73	30,1	0,13	5,4	1,56	64,4	17,2
7	5,706	0,81	35,5	0,12	5,4	1,34	59,0	11,7
8	3,61	0,85	39,1	0,11	5,3	1,20	55,4	8,1
9	2,55	0,88	42,4	0,09	4,7	1,09	52,8	5,1
10	1,63	0,91	43,8	0,08	3,9	1,09	52,2	4,2
11	1,05	0,93	45,2	0,07	3,6	1,05	51,1	3,9
12	$7{,}23 \cdot 10^{-11}$	0,96	46,8	0,04	2,0	1,05	51,2	2,2
13	6,36	0,97	47,8	0,02	1,4	1,03	50,8	1,5
14	5,19	0,98	48,5	0,01	0,9	1,02	50,5	1,0
15	4,22	0,98	49,0	0,01	0,6	1,01	50,3	0,6

* Errechnet aus der Gleichung $C^{ber} = 0{,}5\ (C_1 - C_3)$; T = 158 °C, $n^\circ n.\text{But} = 6{,}82 \times 10^{-5}$ Mol, $r^\circ_{H_2} = 6{,}86 \times 10^{-4}$ Mol.

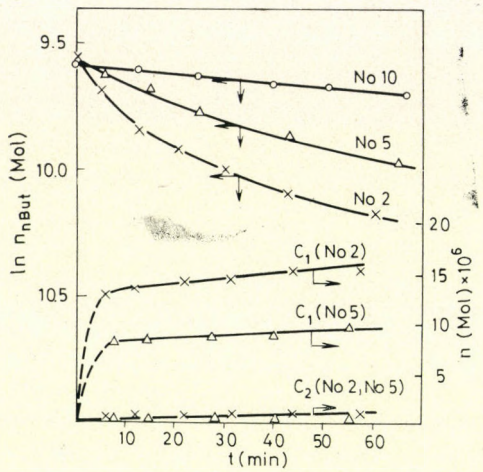

Abb. 4. Zeitabhängigkeit des Logarithmus der Butankonzentration bei 158 °C, $n^0_{H_2} = 6{,}8 \times 10^{-4}$ Mol)

Reaktion erster Ordnung abläuft. Wie aus Abb. 4 ersichtlich ist, ergab die logarithmische Transformation dennoch keinen linearen Zusammenhang, der unserer Meinung nach hauptsächlich durch Vergiftung der Oberfläche durch die Bildung von Kohlenstoffdepositen erklärt werden kann. Nach jeder Untersuchung wurde die Zirkulationsanlage bis auf etwa 10^{-5} Torr abgesaugt und die Oberfläche mit Wasserstoff abgespült. In jedem Fall erschien, wie auch die unteren Kurven der Abb. 4 zeigen, Methan und um eine Größenordnung weniger Äthan in der Gasphase. Die katalytische Aktivität erreichte den früheren Wert trotz des Abspülens der Oberfläche mit Wasserstoff nicht. Auf Grund dieser Experimente kann man nicht entscheiden, ob der irreversible, mit dem Wasserstoff wenig reaktive Teil aus graphitartigen Materialien [24, 25] oder Flächen- bzw. eindimensionalen Polymeren [26] besteht.

Zur Untersuchung des Reaktionsmechanismus wurde eine Propan-1-^{14}C-Markierung verwendet, die vor den Versuchen in 1—2 Molprozent zum Butan gemischt wurde. Die spezifische Aktivität des Propans, ϱ^0_{Pr} war 1,2mCi/mMol.

Das Hydrospalten des *n*-Butans läßt sich bei der Annahme, daß das C–C Bindungsspalten nur an den Kettenenden erfolgt, nach folgendem Schema darstellen:

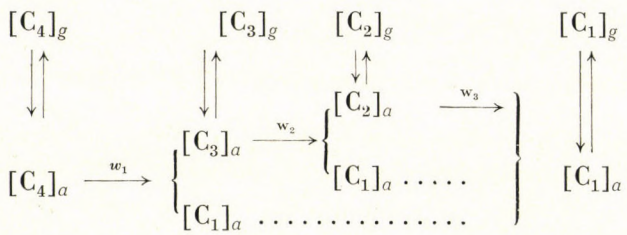

(2)

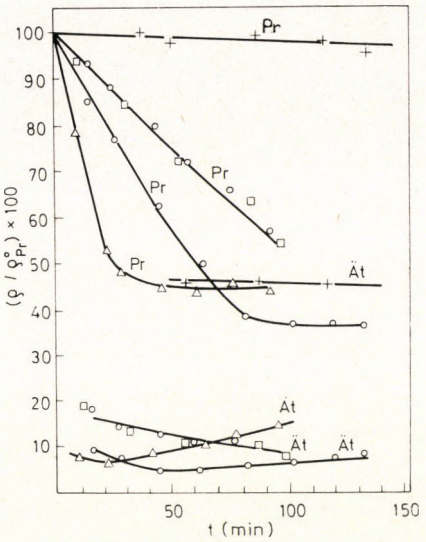

Abb. 5. Die spezifische Radioaktivität des Propans und Äthans in Hydrogenolyse von *n*-Butan als Funktion der Zeit
Bezeichnungen: ●, 218 °C; □, 221 °C; ○, 235 °C; △, 249 °C; $n^0_{n\text{But}} = 3{,}2 \times 10^{-4}$ Mol; $n^0_{H_2} = 9{,}68 \times 10^{-4}$ Mol; $n^0_{Pr} = 4{,}41 \times 10^{-6}$ Mol; +, 182 °C, $n^0_{n\text{But}} = 1{,}59 \times 10^{-4}$ Mol; $n^0_{H_2} = 16{,}32 \times 10^{-4}$ Mol; $n^0_{Pr} = 4{,}6 \times 10^{-6}$ Mol

Der Position der Markierung entsprechend $\varrho_{Ät} \simeq 1/2\varrho_{Pr}$ wenn Äthan nur aus Propan entstehen kann. Die Versuchsergebnisse sind auf Abb. 5 und 6 dargestellt. Die spezifische Radioaktivität des Propans nimmt ab, da aus *n*-Butan (bzw. aus 2-Methylpropan) laufend das unmarkierte Produkt entsteht und somit sich die Konzentration des Isotops im Propan vermindert. Parallel mit dieser Neigung ändert sich die spezifische Aktivität des Äthans, die nur bei großem Wasserstoff-Partialdruck und bei niedrigen Temperaturen an den theoretischen Wert herankommt. (Siehe Kurven in Abb. 5 wo bei T = 182 °C, $H_2/HC \simeq 10$, $S_{Pr} \simeq 1$, bzw. auf Abb. 6 wo bei T = 188 °C, $H_2/HC \simeq 12$, $S_{Pr} \simeq 1$.) Mit steigender Temperatur weicht die spezifische Radioaktivität des Äthans bedeutend von dem theoretischen Wert ab. Eine in Tendenz ähnliche Kurve bekamen wir (siehe Abb. 6) mit 2-Methylpropan-Propan-1-^{14}C-Mischung.

Der Unterschied in den spezifischen Radioaktivitäten zwischen Äthan und Propan ($\varrho_{Ät} < 1/2\varrho_{Pr}$) deutet an, dass sich das entstehende Äthan auch auf andere Weise als in einer Konsekutivreaktion bilden kann. Diese Möglichkeit versuchten wir auf Grund der Bruttogeschwindigkeiten zu prüfen. Äthan kann sich nämlich aus *n*-Butan durch das Spalten der C–C-Bindung zwischen dem zweiten und dem dritten Kohlenstoffatom auch in einem Schritt bilden. Aus der Bruttogeschwindigkeiten läßt sich im Falle $w_3 = 0$ und in

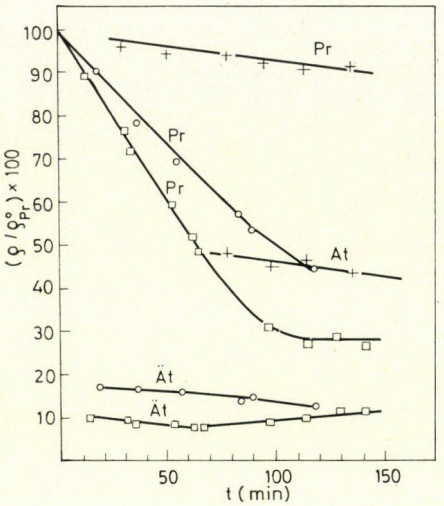

Abb. 6. Die spezifische Radioaktivität des Propans und Äthans bei der Hydrogenolyse von 2-Methylpropan
○, 225 °C; □, 238 °C; $n^0_{iB} = 3{,}22\times10^{-4}$ Mol; $n^0_{H_2} = 9{,}87\times10^{-4}$ Mol; $n^0_{Pr} = 4{,}3\times10^{-6}$ Mol;
+, 188 °C; $n^0_{iB} = 2{,}3\times10^{-4}$ Mol; $n^0_{H_2} = 28{,}2\times10^{-4}$ Mol; $n^0_{Pr} = 2{,}4\times10^{-6}$ Mol

Tabelle III

Anfangsverteilung der Komponenten bei der Hydrogenolyse von n-Butan bei $W_{El} = 0$

T°C	$n^0_{H_2}$ Mol	n^0But Mol	$\frac{-W^0_4}{\frac{1}{4}\sum_{i=1}^{3} iW^0_i}$	Anfangsverteilung in Mol%			
				CH_4	C_2H_6	C_3H_8	$C_2H_6{}^{ber}$
168	$19{,}38\cdot10^{-4}$	$5{,}31\cdot10^{-4}$	1,01	53,0	4,9	42,2	5,4
172	$7{,}55\cdot10^{-4}$	$1{,}71\cdot10^{-4}$	1,00	52,1	3,4	44,3	3,9
172	$7{,}19\cdot10^{-4}$	$1{,}63\cdot10^{-4}$	1,00	52,2	4,3	43,4	4,4
172	$6{,}63\cdot10^{-4}$	$1{,}75\cdot10^{-4}$	1,01	52,7	5,1	42,1	5,3
183	$20{,}21\cdot10^{-4}$	$5{,}35\cdot10^{-4}$	1,02	54,7	8,0	37,2	8,7
194	$7{,}39\cdot10^{-4}$	$1{,}59\cdot10^{-4}$	1,01	53,0	4,7	42,1	5,4
194	$6{,}95\cdot10^{-4}$	$1{,}71\cdot10^{-4}$	1,01	53,5	5,5	40,9	6,2
194	$24{,}93\cdot10^{-4}$	$1{,}63\cdot10^{-4}$	1,03	50,7	1,4	47,8	1,4

$C_2{}^{ber} = 0{,}5(C_1 - C_3)$

Kenntnis der Propan- sowie der Methankonzentration, dem oben angeführten Schema entsprechend, die Äthankonzentration berechnen [18].

Wenn die Reaktion nur an dem Kettenende abläuft, bildet sich mit dem Verbrauch des Butans in gleicher Menge Methan und Propan bzw. Äthan und 2 Methan. In der Tabelle III sind die auf den Zeitpunkt Null extrapolierten Werte der berechneten und der experimentell ermittelten Äthankonzentratio-

nen angeführt. Fast in jedem Fall sind die berechneten Anfangskonzentrationen des Äthans größer als die in den Versuchen bestimmten Werte, obwohl die aus der Bilanzgleichung berechneten und die experimentell bestimmten Geschwindigkeiten der Butanabnahme in Einklang waren. (Siehe die vierte Spalte in Tabelle III. Wir müssen bemerken, daß die berechneten Werte des Äthans kleiner sind, wenn direkte Äthanbildung vorkommt.) Der Unterschied zwischen den berechneten und bestimmten Werten wächst mit steigender Temperatur, vermindert sich aber, wie aus der Tabelle II hervorgeht, mit der Abnahme der katalytischen Aktivität. Die Bedingung $w_3 = 0$ wurde durch Äthan-^{14}C-Markierung kontrolliert. Etwa bis 205 °C konnten wir Methan-^{14}C nicht anweisen.

Die Möglichkeit der direkten Äthanbildung wurde auch durch Hydrospalten von 2-Methylpropan untersucht. Diese Ergebnisse sind in Tab. IV

Tabelle IV

Anfangsverteilung der Komponenten bei der Hydrogenolyse von n-Butan und 2-Methylpropan

Komponente	T °C	$-W^{\circ}_{C_4}$ Mol · m^{-2} · s^{-1}	Anfangsverteilung in Mol%		
			C_3H_8	C_2H_6	CH_4
n-C_4H_{10}	257	$2{,}21 \cdot 10^{-8}$	29,3	4,9	65,7
i-C_4H_{10}	253	$2{,}20 \cdot 10^{-8}$	30,6	4,5	64,8
n-C_4H_{10}	247	$1{,}27 \cdot 10^{-8}$	34,1	4,0	61,8
i-C_4H_{10}	242	$1{,}22 \cdot 10^{-8}$	34,8	4,1	61,0
n-C_4H_{10}	231	$4{,}87 \cdot 10^{-9}$	36,1	2,1	61,7
i-C_4H_{10}	228	$4{,}89 \cdot 10^{-9}$	37,7	1,8	60,4
n-C_4H_{10}	217	$2{,}32 \cdot 10^{-9}$	45,6	0,9	53,4
i-C_4H_{10}	218	$2{,}61 \cdot 10^{-9}$	44,1	1,3	54,6

$n^{\circ}_{C_4} = 1{,}55 \cdot 10^{-4}$ Mol, $n^{\circ}_{H_2} = 16{,}2 \cdot 10^{-4}$ Mol

angeführt. Die Spektren der bestimmten Anfangskonzentrationen unterscheiden sich nicht sonderlich von dem Komponentenspektrum des n-Butans (bezogen auf die gleichen Butanabnahme). Sie stimmen mit den früheren Untersuchungen [18—21] überein und zeigen, daß die direkte Äthanbildung aus n-Butan, d. h. die Spaltung in der β-Position nicht vorkommt.

Neben dem Hydrospalten tritt Isomerisierung des n-Butans bzw. 2-Methylpropans nicht ein. Die Annahme, daß die Isomerisierung, d. h. die Umlagerung der Paraffinkette an der Oberfläche stattfindet, aber die nachfolgende Hydrogenolyse der Isomerkette günstiger ist als die Desorption, scheint logisch zu sein. Diese Erklärung wendete KIKUCHI in seiner Arbeit [19] an. Er fand, daß sich die Isomerisation von n-Pentan an hochaktivem Iridium nicht abspielt, obwohl Iridium nach Angaben von BOUDART [27] bei der

Isomerisation von Neopentan aktiv ist. Durch Hydrospalten von Propan-1-^{14}C untersuchten wir die Möglichkeit der Umlagerung der Karbonkette mittels der spezifischen Radioaktivitäten der Komponenten im Temperaturgebiet zwischen 180—300 °C. Wenn die Isomerisierung parallel mit der Hydrogenolyse von Propan-1-^{14}C auftreten sollte, dann muß gemäß dem unteren Schema anfangs $\varrho_{\text{Ät}} = 0{,}5\varrho_{\text{Pr}}$ sein, während der Reaktion verändert sich aber das Verhältnis $\varrho_{\text{Ät}}/\varrho_{\text{Pr}}$ zwischen 0,5 und 1 abhängig von dem Propan-2-^{14}C-Teil.

$$
\begin{array}{lcccccc}
C_3\text{—}1\text{—}^{14}C & \xrightarrow[\text{genolyse}]{\text{Hydro-}} & \begin{matrix}\varrho_{\text{Ät}}/\varrho_{\text{Pr}}\\ 1/2\end{matrix} & S_{\text{Ät}} = 1 & \begin{matrix}\varrho_{\text{Met}}/\varrho_{\text{Pr}}\\ 1/2\end{matrix} & \begin{matrix}\varrho_{\text{Ät}}/\varrho_{\text{Pr}}\\ 1/2\end{matrix} & 0 < S_{\text{Ät}} < 1 \quad \begin{matrix}\varrho_{\text{Met}}/\varrho_{\text{Pr}}\\ 1/2 \leftrightarrow 1/3\end{matrix} \\
\Big\downarrow\Big\uparrow & \text{Isomeri-} & & & & & \\
 & \text{sierung} & & & & & \\
C_3\text{—}2\text{—}^{14}C & \xrightarrow[\text{genolyse}]{\text{Hydro-}} & 1 & & 0 & 1 & 0 \leftrightarrow 1/3
\end{array}
\qquad (3)
$$

Abb. 7 zeigt die typische Kurve. Die Auswertung der Versuchsergebnisse zeigt, daß das Verhältnis $\varrho_{\text{Ät}}/\varrho_{\text{Pr}}$ im Mittelwert, abgesehen vom Meßfehler,

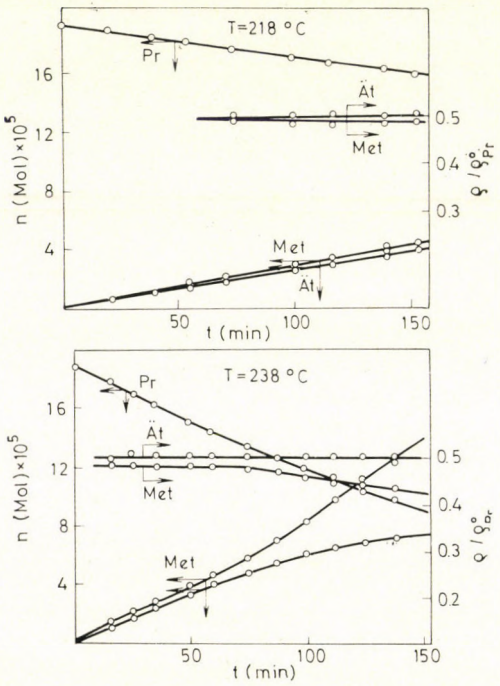

Abb. 7. Zeitabhängigkeit der Konzentration und der spezifischen Radioaktivität der Produkte der Hydrogenolyse von Propan-1-^{14}C ($n^0_{H_2} = 8{,}2 \times 10^{-4}$ Mol)

nicht größer als 0,5 ist, d. h., die Isomerisierung nicht abläuft bzw. der isomerisierte Teil in der Größenordnung des Meßfehlers liegt. Die Standardabweichung von $\varrho_{\text{Ät}}/\varrho_{\text{Pr}}$ betrug in diesen Versuchen $3—4 \times 10^{-2}$.

Diskussion

Die Temperatur, bei der die Hydrospaltung des *n*-Butans an Nickelpulver beginnt, liegt etwa bei 160 °C, sie liegt um 20 °C tiefer als beim Propan [12]. Die Reaktionsordnung bezüglich des Wasserstoffs ist bei gleicher Temperatur im Falle des *n*-Butans weniger negativ, als bei Äthan [7], Propan [12] und negativer als bei *n*-Hexan [23], was durch die Erleichterung der Adsorption mit steigender Anzahl der Kohlenstoffatome erklärt werden kann. Diese inhibierende Wirkung des Wasserstoffs wurde auch bei Austauschreaktionen [22, 28, 29] gesättigter Kohlenwasserstoffe festgestellt. Bei 263 °C erreicht die Reaktionsordnung jedoch einen positiven Wert. Wir nehmen an, daß sich die Bedeckung für Wasserstoff wegen der exothermen Adsorption mit steigender Temperatur vermindert und dadurch die Dissoziation des Wasserstoffs aus dem Kohlenwasserstoff in großem Maße auftritt. Ein Teil der entstehenden stark dehydrierten Radikale nimmt an der Reaktion nicht teil, d. h. »die arbeitende Oberfläche« vermindert sich wegen Selbstvergiftung.

Die Hydrogenolyse des *n*-Butans läuft nur bei tiefen Temperaturen und bei großen Überschüssen des Wasserstoffs (siehe Abb. 5 und 6) selektiv ab. Die Versuchsergebnisse bestätigen, daß nicht nur die Temperatur und der Partialdruck des Wasserstoffs, sondern auch das Vorleben des Katalysators die Selektivität des Hydrospaltens beeinflußen. Es wurde bestätigt, daß die Paraffinkette auch bei weitgehender Spaltung nur am Ende des Kohlenwasserstoffgerüstes erfolgt. Wir konnten keinen solchen Hinweis finden, der eine direkte Äthanbildung oder sogar Isomerisation aus *n*-Butan annehmen läßt. Bei gleichen Anfangsgeschwindigkeiten deutet die Verteilung der aus *n*-Butan bzw. 2-Methylpropan entstehenden Spaltprodukte nicht auf einen Unterschied des Reaktionsmechanismus hin. Der Unterschied in der Verteilung ist wahrscheinlich auf die verschiedenen Temperaturen zurückzuführen. Bemerkenswert ist weiterhin, daß die aus Bruttogeschwindigkeiten berechneten Anfangskonzentrationen des Äthans fast in jedem Fall größer sind als die experimentell ermittelten Werte. In diesem Fall ist der Unterschied im Reaktionsmechanismus zu suchen.

Die Abweichung der spezifischen Radioaktivität des Äthans von der des Propans bestätigt, daß die Geschwindigkeiten der Desorption und der Oberflächenreaktion bei den Zwischenprodukten [12] verglichen werden können. Diese Ergebnisse sind in Einklang damit, daß an Nickel stark dehydrierte Kohlenwasserstoffradikale entstehen können, die mit der Gasphase nicht in

Adsorptionsgleichgewicht sind, daß die unmarkierten Propanradikale an der Oberfläche mit Umgehung (der Gasphase) weiterreagieren können. Dies deutet darauf hin, daß für die an der Hydrogenolyse teilnehmenden Kohlenwasserstoffe mindestens zwei Sorptionszustände [30] angenommen werden können

$$\begin{array}{ccccc} [C_4]_g & & [C_3]_g & & [C_2]_g \\ \downarrow\uparrow & & \downarrow\uparrow & & \downarrow\uparrow \\ [C_4]_{a_1} & & [C_3]_{a_1} & & [C_2]_{a_1} \\ \downarrow\uparrow & & \downarrow\uparrow & & \downarrow\uparrow \\ [C_4]_{a_2} & \longrightarrow & [C_3]_{a_2} & \longrightarrow & [C_2]_{a_2} \longrightarrow \end{array} \qquad (4)$$

von denen die letztere $[C_i]_{a_2}$ Form eine stärkere Chemisorption mit kleinem H/C-Verhältnis, die vorletzte dagegen eine lockere Oberflächenspecies darstellt. Gemäß dem modifizierten Schema existiert das Gleichgewicht zwischen den Radikalen $[C_i]_{a_1}$ und $[C_i]_{a_2}$ nicht, wenn die Besetzung der Oberfläche durch Wasserstoff klein ist, d. h. in Form $[C_i]_{a_2}$ die Hydrogenolyse der Kohlenstoff-Bindung günstiger ist als die C–Ni-Bindungen.

Auf Grund unserer Experimente können wir weiterhin feststellen, daß die Änderung der Selektivität mit den geometrischen Überlegungen von PONEC [31] und ANDERSON [32] im Einklang steht. Mit der Abnahme der Koordinationszahl der aktiven Zentren (das heißt, mit steigendem Wasserstoff-Bedeckungsgrad oder mit der Anhäufung des Karbondeposits an der Oberfläche) wird die Formation der in großem Masse dehydrierten, in »deep« Hydrospalten teilnehmenden Kohlenwasserstoffradikale zurückgedrängt. Die niedrige Reaktionstemperatur oder der große Wasserstoff-Partialdruck begünstigt demzufolge die selektive, sich an dem Kohlenstoffkettenende abspielenden C–C-Bindungsspaltung. Die Versuchsergebnisse bestätigen, wie es mit der Propan-1-^{14}C-Zwischenproduktmarkierung bewiesen wurde, daß die Bildung des Äthans unter solchen Bedingungen auf die Einstellung des Adsorptionsgleichgewichts des Zwischenprodukts Propan zurückzuführen ist. Mit steigendem Dissoziationsgrad der Kohlenwasserstoffradikale nimmt das Maß des extensiven Hydrospaltens zu, d. h., die Sclektivität ist klein. Diese Erscheinung kann unserer Meinung nach mit der Annahme erklärt werden, daß die Geschwindigkeiten der Desorption und der Oberflächenreaktion der stark chemisorbierten Kohlenstoffradikale vergleichbar sind.

LITERATUR

[1] SINFELT, J. H., YATES, D. J. C.: J. Catal. **8,** 82 (1967)
[2] SINFELT, J. H., YATES, D. J. C.: J. Catal. **10,** 362 (1968)
[3] SINFELT, J. H., TAYLOR, W. F., YATES, D. J. C.: J. Phys. Chem. **69,** 95 (1965)
[4] TAYLOR, W. F., SINFELT, J. H., YATES, D. J. C.: J. Phys. Chem. **69,** 3857 (1965)
[5] CASTER, J. L., CUSUMANO, J. A., SINFELT, J. H.: J. Phys. Chem. **70,** 2257 (1966)

[6] SINFELT, J. H.: Catal. Rev. **3,** 173 (1970)
[7] GUCZI, L., GUDKOV, B. S., TÉTÉNYI, P.: J. Catal. **24,** 187 (1972)
[8] ANDERSON, J. R., BAKER, B. G.: Proc. R. Soc. Lond. **A271** 402 (1963)
[9] ANDERSON, J. R., BAKER, B. G.: Nature **187,** 937 (1960)
[10] SHEPHARD, F. E.: J. Catal. **14,** 148 (1969)
[11] FREEL, J., GALWEY, A. K.: J. Catal. **10,** 277 (1968)
[12] GUCZI, L., SÁRKÁNY, A., TÉTÉNYI, P.: Proc. 5th Congress on Catalysis. Vol. 2, p. 1111 (North Holland Publ. Co., Amsterdam, 1973)
[13] DOWIE, R. S., KEMBALL, C., KEMPLING, J. C., WHAN, D. A.: Proc. R. Soc. Lond. **A327,** 491 (1972)
[14] DOWIE, R. S., WHAN, D. A., KEMBALL, C.: Faraday Trans. I. **68,** 2150 (1972)
[15] HAENSEL, V., IPATIEFF, V. N.: J. Am. Chem. Soc. **68,** 345 (1946)
[16] HAENSEL, V., IPATIEFF, V. N.: Ind. Eng. Chem. **39,** 853 (1947)
[17] KOCHLOEFL, K., BAZANT, V.: J. Catal. **10,** 140 (1968)
[18] KIKUCHI, E., MORITA, Y.: J. Catal. **15,** 217 (1969)
[19] KIKUCHI, E., TSURUMI, M., MORITA, Y.: J. Catal. **22,** 226 (1971)
[20] MATSUMOTO, H., SAITO, Y., YONEDA, Y.: J. Catal. **19,** 101 (1970)
[21] MATSUMOTO, H., SAITO, Y., YONEDA, Y.: J. Catal. **22,** 182 (1971)
[22] GUCZI, L., TÉTÉNYI, P.: Acta Chim. Acad. Sci. Hung. **51,** 275 (1967)
[23] GUCZI, L., KÁLMÁN, J., SÁRKÁNY, A., TÉTÉNYI, P.: Symposium on the Mechanism of Hydrocarbon Reactions Siófok, Lake Balaton (Hungary) 5—7, June 1973
[24] BAKER, R. T. K., BARKER, M. A., HARRIS, P. S., FEATES, F. S., WAITE, R. J.: J. Catal. **26,** 51 (1972)
[25] BAIRD, T., TRYER, J. R., GRANT, B.: Nature **233,** 329 (1971)
[26] EDMONDS, T., MCCARROL, J. J., PIKETHLY, R. C.: Paper presented to Symposium on Low Temperature Carbon Formation. Glasgow, March 1973
[27] BOUDART, M., PTAK, L. D.: J. Catal. **16,** 90 (1970)
[28] GUCZI, L., SHARAN, K. M., TÉTÉNYI, P.: Monatshefte für Chemie **102,** 187 (1971)
[29] GUCZI, L., SÁRKÁNY, A., TÉTÉNYI, P.: Comm. Dept. Chemistry, Bulgarian Acad. Sci. **6,** 349 (1973)
[30] GUCZI, L., TÉTÉNYI, P.: Annuals of New York Acad. Sci. Vol. **213,** 173 (1973)
[31] PONEC, V., SACHTLER, W. M. H.: Vth ICC, Palm Beach 1972
[32] ANDERSON, J. R., MACDONALD, R. J., SHIMOYAMA, Y.: J. Catal. **20,** 147 (1971)

A. SÁRKÁNY
László GUCZI
Pál TÉTÉNYI
1525 Budapest 114, Pf. 77. Ungarn.

Acta Chimica Academiae Scientiarum Hungaricae, 84 (3), pp. 259—277 (1975)

CALCULATION OF THE π-ELECTRONIC STRUCTURE AND SPECTRA OF HETERO-DISUBSTITUTED HALOBENZENES BY THE MIM AND PPP METHODS

A. MARTIN and Á. I. KISS

(Department of Physical Chemistry, Technical University, Budapest)

Received July 2, 1973

The π-electronic structures and spectra of disubstituted benzenes containing two different halogen atoms have been calculated by the MIM and PPP methods.

The MIM energies and wavefunctions as well as the PPP spectral data, charge densities, bond orders, and π-contributions to the dipole moment of hetero-disubstituted halobenzenes are compared with the results obtained for mono- and homo-disubstituted compounds.

The same accuracy has been achieved in the calculation of hetero- and homo-disubstituted as well as monosubstituted compounds, using the same starting parameter system.

1. Introduction

Only a few calculations are to be found in the literature for the π-electronic properties of hetero-dihalobenzenes. PARISER—PARR—POPLE (PPP) calculations [1, 2] have been reported for fluoro- and chlorobenzenes [3, 4] but according to our knowledge the hetero-disubstituted halobenzenes bearing bromo and iodo substituents, have not yet been treated. Molecules in Molecules (MIM) calculations [5, 6, 7] for hetero-dihalobenzenes were not made at all.

The purpose of the present work is to investigate the applicability of the above two approximations and the parameters used for the calculation of mono- and homo-disubstituted halobenzenes [8, 9] to hetero-disubstituted derivatives.

2. MIM method

2.1. Method of calculation

The version of the MIM method used has been described previously [8]. The calculation was performed on the same model used for the homo-dihalobenzenes [9]: the benzene ring was considered as acceptor and the halogen atoms as donors. The energies of electronic transitions and the corresponding wavefunctions were calculated.

The charge transfer (CT) energies were determined by three different methods: the point charge [2], the charged sphere [1], and the MATAGA—NISHIMOTO [10] approximations.

The starting values used are collected in Tables I and II. Table I contains the valence-state ionization potentials (I_μ), electron affinities (A_μ), effective nuclear charges (Z_μ), one-center repulsion integrals ($\gamma_{\mu\mu}$) and the bond distances (r_{C_μ}). The I_μ values of the halogen atoms were calculated by

Table I

Starting parameters

μ	Z_μ (e)	I_μ (eV)	A_μ (eV)	$\gamma_{\mu\mu}$ (eV)	$r_{C\mu}$ (Å)
$\dot{C}$	3.25 [11]	11.16 [12]	0.03 [12]	11.13 [12]	1.40 [17]
$\ddot{F}$	5.20 [11]	34.00	12.61 [13]	21.39 [15]	1.30 [17]
$\ddot{Cl}$	6.10 [11]	24.37	11.34 [14]	13.03 [15]	1.70 [17]
$\ddot{Br}$	7.60 [11]	17.8	10.5 [13]	7.3 [16]	1.86 [17]
$\ddot{I}$	7.60 [11]	18.35	9.55 [13]	8.80 [16]	2.05 [17]

Table II

Diagonal elements of the interatomic matrix and interaction elements between the CT states

Donor (D)	Fluoro			Chloro		
	Point	Sphere	M. N.	Point	Sphere	M. N.
$T^1_{D_1}$, $T^1_{D_4}$	7.161	7.736	9.274	7.058	7.576	8.856
$T^2_{D_1}$, $T^2_{D_4}$	8.640	8.770	9.876	7.960	8.105	9.195
$T^1_{D_2}$, $T^1_{D_3}$	8.271	8.512	9.726	7.735	7.973	9.110
$T^2_{D_2}$, $T^2_{D_3}$	7.531	7.995	9.424	7.284	7.708	8.940
$-(T^1_{D_2} - T^2_{D_2})$, $(T^1_{D_3} - T^2_{D_3})$	0.641	0.448	0.261	0.390	0.229	0.147
Energies of benzene (eV)		4.881			6.077	

	Bromo			Iodo		
	Point	Sphere	M. N.	Point	Sphere	M. N.
$T^1_{D_1}$, $T^1_{D_4}$	6.566	7.104	8.460	5.968	6.322	7.559
$T^2_{D_1}$, $T^2_{D_4}$	7.322	7.437	8.700	6.591	6.689	7.784
$T^1_{D_2}$, $T^1_{D_3}$	7.133	7.353	8.640	6.436	6.597	7.728
$T^2_{D_2}$, $T^2_{D_3}$	6.755	7.187	8.520	6.124	6.414	7.615
$-(T^1_{D_2} - T^2_{D_2})$, $(T^1_{D_3} - T^2_{D_3})$	0.328	0.144	0.104	0.270	0.159	0.098
Energies of benzene (eV)		6.738			Ref. [19]	

means of KWIATKOWSKI's formula [18], *i.e.* the experimental first ionization potential of the corresponding alkyl halide was taken as A_μ. The details of Table I show that, contrary to the expectation, the $\gamma_{\mu\mu}$ values do not change monotonously with increasing atomic number. Wherever possible (F, Cl), the data used were taken from the HINZE—JAFFÉ tables [12] which appear to be the most reliable. The data series commonly used in the literature do not change monotonously with the atomic number of halogen atoms [16, 28]. Although monotonously changing data series can also be found in the literature [29], they require, however, entirely different $\beta_{\mu\nu}$ resonance-integral values and the results obtained are not better either. Also the effective nuclear charge does not change monotonously with the atomic number, it is identical for Br and I for both SLATER [11] and BURNS [30] charges. In this work we used the SLATER values. Table II contains the diagonal elements of the interaction matrix (the experimental energies of the first three benzene bands measured in cyclohexane solution, and the calculated CT energies) as well as the interaction elements between the CT states. The lower index of D denotes the position of substitution, while the upper index of T refers to the CT transitions belonging to the two different excited benzene states.

The resonance integral of the carbon—halogen bond ($\beta_{\mu\nu}$) was taken as a variable parameter with values —1.0, —1.5 and —2.0 eV.

2.2. Results and discussion

2.2.1. Energies of electronic transitions

As an example, the calculated energies of the first two π—π^* transitions of hetero-dihalobenzenes for some different substituent pairs for which experimental data are to be found in the literature are given in Figs 1—3 as a function of $\beta_{\mu C}$ and $\beta_{\nu C}$. The experimental energies are indicated as horizontal lines in the figures. The $\beta_{\mu C}$ denotes the resonance integral belonging to the bond involving a halogen atom of smaller atomic number, while $\beta_{\nu C}$ relates to that of greater atomic number. The results for *ortho-*, *meta-* and *para-*derivatives are given in Figs 1, 2 and, 3, respectively, and in all cases the three approximations used are indicated. It can be seen that the transition energies depend almost linearly on $\beta_{\mu C}$ and $\beta_{\nu C}$ in the interval considered. It can be established that acceptable results are obtained in the β interval between —1.0 and —2.0 eV but to give a fixed β value characteristic of a substituent, seems arbitrary. For this reason, the energies calculated by the three approximations are shown in Table III for all compounds with the values that have given the best results for the mono- and homo-disubstituted derivatives [8, 9]. This allows a comparison with the results of the mono- and homo-disubstituted derivatives on a uniform basis. The experimental data of Table III refer to cyclohexane

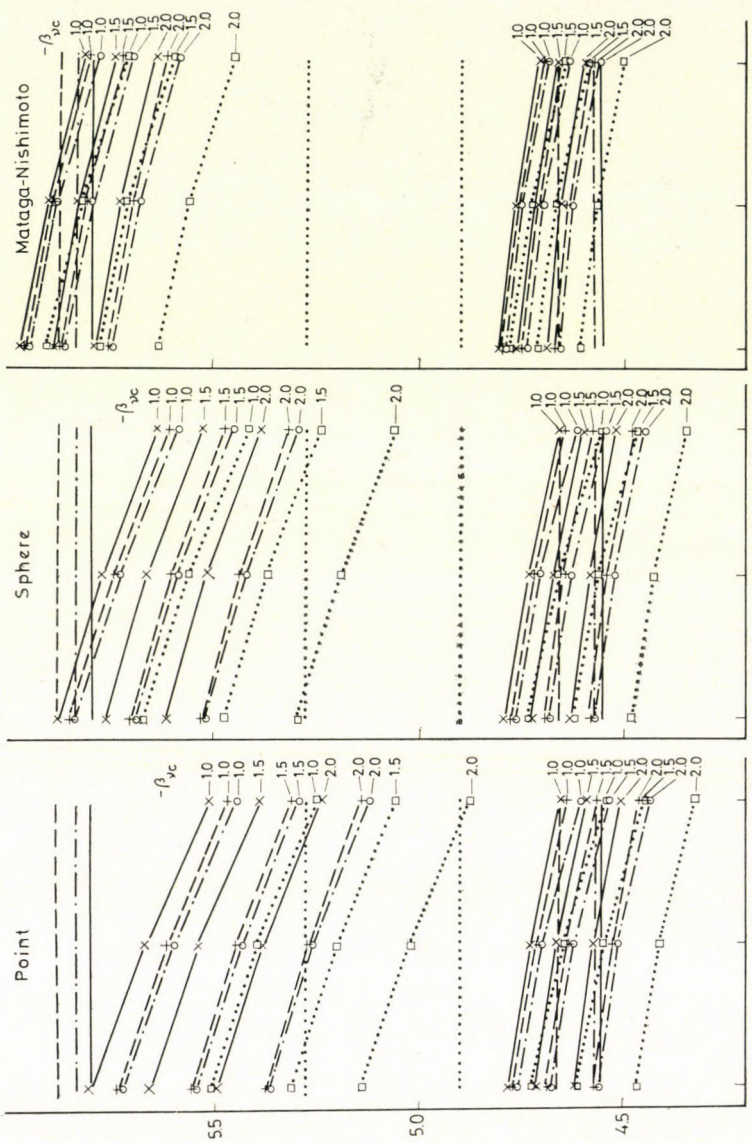

Fig. 1. ×——× *Ortho*-fluorochloro-, +- - - + *ortho*-fluorobromo-, ○-·-·-○ *ortho*-chlorobromo-, □ · · · · □ *ortho*-bromoiodo-benzenes: Energies of the first two singlet transitions as a function of $\beta_{\mu C}$ and $\beta_{\nu C}$ calculated by the point charge, charged sphere and MATAGA—NISHIMOTO approximations. The horizontal lines represent the experimental values

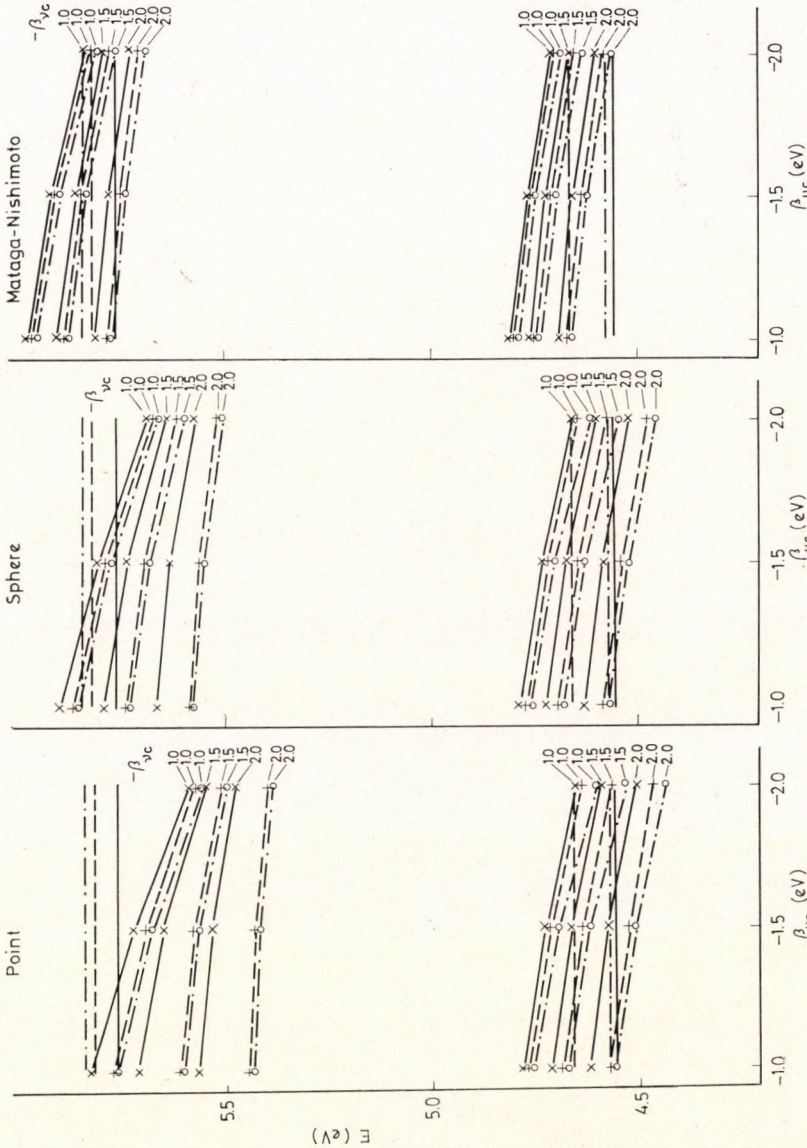

Fig. 2. Meta-derivatives. Compounds and notation are the same as in Fig. 1

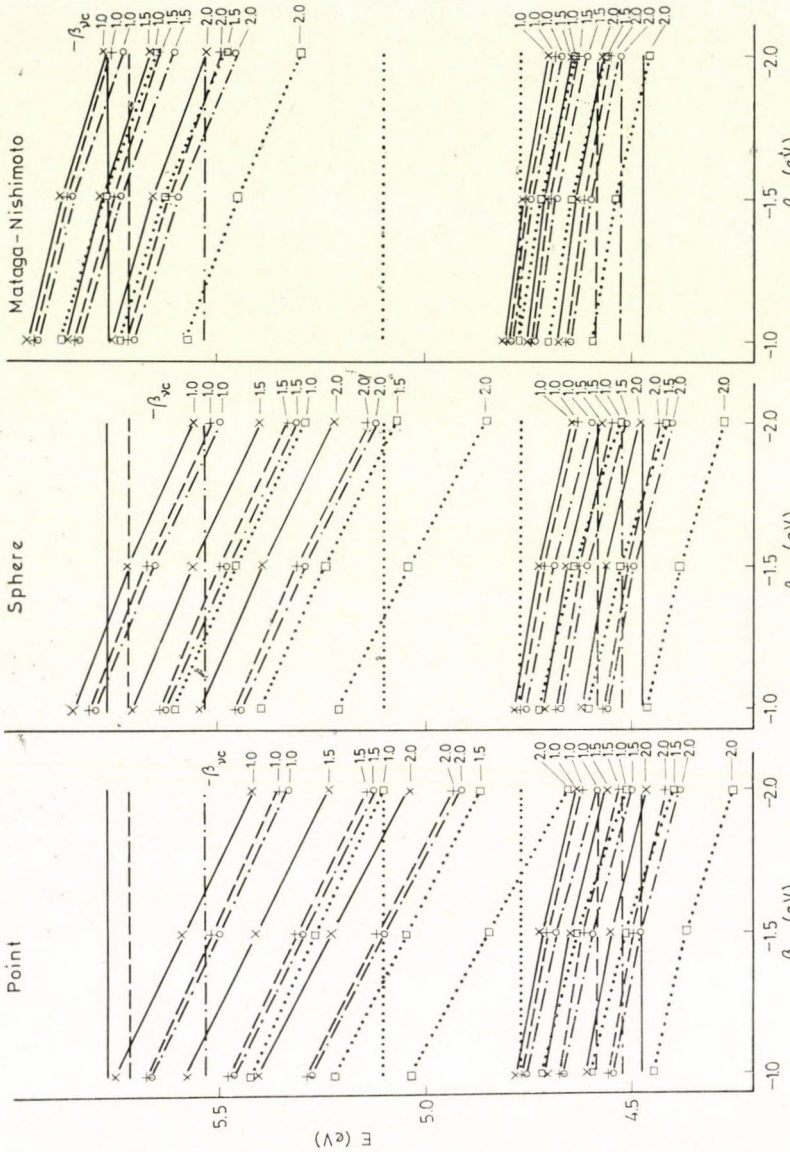

Fig. 3. Para-derivatives. Compounds and notation are the same as in Fig. 1

Table III

Energies calculated by the MIM method

Approximation	Calculated energies (eV)			Experimental energies (eV)	Ref.
	Point	Sphere	M. N.		
1	2	3	4	5	6
$(-\beta_{C-F})$ $(-\beta_{C-Cl})$ (eV)	(1.0) (1.5)	(1.0) (1.5)	(1.5) (2.0)		
1-fluoro-2-chlorobenzene	−0.296	−0.277	−0.447	(4.592)	([24])
	4.717	4.724	4.654	4.558	[20]
	5.658	5.758	5.724	5.794	
1-fluoro-3-chlorobenzene	−0.298	−0.278	−0.451	(4.592)	([24])
	4.717	4.724	4.654	4.558	[20]
	5.718	5.798	5.778	5.767	
1-fluoro-4-chlorobenzene	−0.294	−0.275	−0.443	(4.500)	([24])
	4.710	4.717	4.638	4.476	[20]
	5.582	5.704	5.653	5.767	
$(-\beta_{C-F})$ $(-\beta_{C-Br})$ (eV)	(1.0) (1.5)	(1.0) (1.5)	(1.5) (2.0)		
1-fluoro-2-bromobenzene	−0.311	−0.289	−0.460	(4.583)	([25])
	4.688	4.695	4.635	4.661	[21]
	5.552	5.693	5.692	5.876	
1-fluoro-3-bromobenzene	−0.312	−0.290	−0.463	(4.580)	([26])
	4.688	4.695	4.635	4.661	[21]
	5.616	5.737	5.751	5.821	
1-fluoro-4-bromobenzene	−0.309	−0.287	−0.455	(4.484)	([27])
	4.679	4.687	4.617	4.575	[21]
	5.473	5.634	5.616	5.713	
$(-\beta_{C-F})$ $(-\beta_{C-I})$ (eV)	(1.0) (1.0)	(1.0) (1.0)	(1.5) (1.5)		
1-fluoro-2-iodobenzene	−0.200	−0.188	−0.349		
	4.745	4.751	4.682		
	5.536	5.694	5.733		
1-fluoro-3-iodobenzene	−0.201	−0.188	−0.351		
	4.745	4.751	4.682		
	5.583	5.730	5.783		
1-fluoro-4-iodobenzene	−0.199	−0.187	−0.346		
	4.739	4.745	4.669		
	5.477	5.645	5.667		

Table III (continued)

Approximation	Calculated energies (eV)			Experimental energies (eV)	Ref.
	Point	Sphere	M. N.		
1	2	3	4	5	6
$(-\beta_{C-Cl})$ $(-\beta_{C-Br})$ (eV)	(1.5) (1.5)	(1.5) (1.5)	(2.0) (2.0)		
1-chloro-2-bromobenzene	−0.420	−0.392	−0.586		
	4.621	4.631	4.564	4.575	[21]
	5.432	5.583	5.580	5.834	
1-chloro-3-bromobenzene	−0.424	−0.396	−0.593		
	4.621	4.631	4.563	4.575	[21]
	5.573	5.682	5.689	5.848	
1-chloro-4-bromobenzene	−0.416	−0.389	−0.578		
	4.599	4.611	4.530	4.525	[21]
	5.299	5.476	5.457	5.535	
$(-\beta_{C-Cl})$ $(-\beta_{C-I})$ (eV)	(1.5) (1.0)	(1.5) (1.0)	(2.0) (1.5)		
1-chloro-2-iodobenzene	−0.313	−0.294	−0.479		
	4.674	4.683	4.608		
	5.446	5.601	5.624		
1-chloro-3-iodobenzene	−0.315	−0.296	−0.483		
	4.674	4.683	4.608		
	5.557	5.685	5.716		
1-chloro-4-iodobenzene	−0.311	−0.292	−0.473		
	4.660	4.670	4.583		
	5.340	5.512	5.518		
$(-\beta_{C-Br})$ $(-\beta_{C-I})$ (eV)	(1.5) (1.0)	(1.5) (1.0)	(2.0) (1.5)		
1-bromo-2-iodobenzene	−0.327	−0.306	−0.491		
	4.647	4.657	4.590	4.900	[21]
	5.382	5.554	5.594	5.276	
	5.964	6.149	6.297	5.904	
1-bromo-3-iodobenzene	−0.329	−0.308	−0.496		
	4.647	4.657	4.590		
	5.526	5.654	5.695		
1-bromo-4-iodobenzene	−0.325	−0.304	−0.486		
	4.630	4.641	4.563	4.768	[21]
	5.265	5.455	5.483	5.102	

solutions and the data in brackets are the O–O band energies of the lowest π–π^* transitions in vapour spectra. Since the calculation reproduces the latter values, as expected, the agreement with these is generally better. The calculated energies of the mono-halobenzenes vary with the atomic number of the halogen atom in the same order as the experimental values of the O–O bands, the experimental band maxima, however, do not follow the predicted order. The wavenumbers of O–O bands for the first π-electronic transitions in mono-halobenzenes (cm^{-1}) are F: 37 819, Cl: 37 052 [31], Br: 36 997, I: 36 760 [32]. The same order was reported by PETRUSKA [33] for the second and third bands of mono-halobenzenes as well as the first bands of homo- an hetero-disubstituted derivatives. In spite of these discrepancies we used the energies of the band maxima as experimental values since the O–O band for more complicated compounds is often not available. Consequently, the experimental values cannot be considered as accurate. For this reason a simple calculation was made to estimate the error of the experimental data used. The mean deviation of the energy of the band maximum from the O–O band was calculated for some mono- and disubstituted compounds and found to be about 4% for the first two bands.

The calculated and experimental energies of disubstituted derivatives are always smaller than those of the corresponding monosubstituted compounds. Comparison of the isomers shows that the calculated energy of the first band for the *ortho* and *meta* compounds is the same and always higher than that of the *para* isomer. This is in complete accordance with the experimental data except for 1-bromo-2-iodobenzene which seems to be a similar exception as 1,2-diiodobenzene [8] where the experimental energy of the first band is larger than that of the *meta* derivative. This anomaly of the experimental data is probably caused by steric hindrance owing to the large size of the substituents. The change in the molecular geometry and in the overlap between the bonding electrons are the results of steric interaction. With decreasing overlap, the corresponding resonance integral decreases. To verify this, calculations have been carried out with reduced β values and a modified geometry. According to the results, the distorted geometry hardly influences the calculated energies, but the reduction of β strongly increases the transition energies (one β unit changes the first band energy by about 0.5 eV). This seems to justify the above assumption.

The data of Table III show that it is possible to obtain satisfactory results for hetero-disubstituted derivatives by using β values tested with mono- and homo-disubstituted compounds. In most cases the best results are obtained with the MATAGA—NISHIMOTO approximation, whereas the largest deviations between the calculated and experimental values are generally found with the point-charge approximation. The greatest difference between the experimental and calculated energies occurs for the second band of 1-chloro-

Table IV

Wavefunctions calculated by the MIM method

Energy (eV)	Approx. $(-\beta_{C-}\mu)$ $(-\beta_{C-}\nu)$	Wave function								
		ψ_G	$\psi_{B_{2u}}$	$\psi_{E_{1u}}$	$\psi_{E_{1u}}$	$\psi_{E_{1u}'}$	$\psi_{T^1_{D_1}}$	$\psi_{T^2_{D_1}}$	$\psi_{T^1_{D_4}}$	$\psi_{T^2_{D_4}}$
1-fluoro-4-bromobenzene										
−0.455	M. N.	.976		.011		−.010	.122		.181	
4.617			.961		−.120			.126		−.216
5.616		−.046		.852		−.351	−.217		.319	
6.420	1.5		.193		.935			−.132		.266
6.514		.021		.447		.873	.104		−.161	
9.680	2.0	−.088		.198		−.243	.929		−.178	
10.113			−.143		.222			.941		−.211
9.194		−.194		−.185		.235	.255		.899	
9.045			.138		−.249			.285		.916
1-chloro-4-bromobenzene										
−0.578	M. N.	.970		.001		−.001	.168		.175	
4.530			.946		−.150			.192		−.215
5.457		−.009		.810		−.392	−.293		.322	
6.354	2.0		.240		.921			−.196		.237
6.490		.004		.506		.843	.119		−.136	
9.603	2.0	−.099		.264		−.325	.859		−.280	
9.743			−.208		.337			.813		−.427
9.159		−.222		−.135		.172	.367		.877	
8.887			.068		−.126			.514		.846
1-bromo-4-iodobenzene										
−0.486	M. N.	.973		−.009		.008	.179		.147	
4.563			.945		−.138			.214		−.206
5.483		.014		.796		−.377	−.314		.354	
6.342	2.0		.244		.901			−.227		.279
6.483		.001		.520		.827	.128		−.174	
9.242	1.5	−.145		.251		−.317	.897		−.101	
9.209			−.200		.351			.884		−.237
8.113		−.180		−.183		.271	.220		.901	
7.989			.087		−.217		3.49		.908	

1-bromo-4-iodobenzene										
−0.304	Sphere	.979		−.008		.007	.163		.120	
4.641			.944		−.108			.231		−.210
5.455		.010		.701		−.340	−.379		.500	
6.266	1.5		.266		.781			−.269		.498
6.406		.041		.643		.637	.067		−.418	
7.876	1.0	−.109		.306		−.484	.799		−.150	
7.947			−.193		.490			.820		−.222
6.808		−.166		−.047		.494	.433		.734	
6.890			.028		−.372			.449		.812
1-bromo-4-iodobenzene										
−0.325	Point	.976		−.009		.008	.175		.126	
4.630			.939		−.112			.239		−.219
5.265		.013		.613		−.338	−.435		.567	
6.232	1.5		.281		.752			−.264		.535
6.534		−.159		.280		.625	.527		.478	
7.565	1.0	−.090		.337		−.606	.688		−.195	
7.867			−.196		.517			.801		−.228
6.310		−.114		−.658		−.359	.170		.630	
6.803			.013		−.394			.481		.784

2-bromobenzene (6.89% of the experimental value). Thus the error of the calculated energy is not much greater than the uncertainty of the experimental values.

2.2.2. Wavefunctions

The wavefunctions for *para*-bromohalobenzenes calculated by the MATAGA—NISHIMOTO approximation and the results for *para*-bromoiodobenzene obtained by the point-charge and charged-sphere approximations are given in Table IV as examples. The CT states give only small contributions to the wavefunctions belonging to the first four energies. The results obtained are consistent with the experimental band assignment, *viz.*, the ground state of benzene gives the largest contribution to the ground-state configuration ψ_0, and the order of largest contribution to the excited configurations ψ_1—ψ_4 is B_{2u}, B_{1u}, E_{1u}, $E_{1u'}$. At relatively large CT energies the CT states do not mix with benzene states to such an extent that the order of the electronic transitions of benzene should change. The contribution of CT states to the first four excited configurations always increases with decreasing electronegativity of the halogen atom.

At low CT energies and β values, strong mixing between the benzene and CT states can be expected, as observed for diiodobenzenes calculated with the point-charge and charged-sphere approximations [9]. A similar mixing of states can be expected for the bromoiodobenzenes. In the point-charge approximation this mixing occurs for all three isomers at β_{IC} values of —1.0 and —1.5 eV; in the charged-sphere approximation, on the other hand, there is no mixing because of the larger starting CT energies. For this reason the point-charge approximation gives poorer results in this case.

3. PPP method

3.1. Method of calculation

The PPP method was used in the same way as before [4, 8] to determine the charge density and bond order matrix, the singlet transition energies, the polarization directions and the magnitude and direction of the π-electron contribution to the dipole moment.

The starting data are collected in Table I. For β_{CC} —2.39 eV was taken as in Ref. [8]; the $\beta_{\mu C}$ and $\beta_{\nu C}$ values are given in Table V. These β values are identical with those used for homo-dihalobenzenes, obtained as the best values in a β-variation calculation [4, 8]. The two-center repulsion integrals were calculated by the MATAGA—NISHIMOTO approximation [10].

Table V

Spectral data calculated by the PPP method

	Compound $\beta_{C\mu}$ (eV) $\beta_{C\nu}$ (eV)	Calculated			Experimental			Ref.
		E (eV)	f	α	E (eV)	lg ε	f	
	1	2	3	4	5	6	7	8
1	1-fluoro-2-chlorobenzene	4.605	0.029	33.3	4.558	3.18	0.036	[20]
		5.594	0.149	320.0	5.794	4.00	0.240	
	$\beta_{CF} = -2.20$	6.482	1.184	29.4				
	$\beta_{CCl} = -2.20$	6.581	0.861	119.8				
2	1-fluoro-3-chlorobenzene	4.635	0.017	143.9	4.558	3.00	0.024	[20]
		5.716	0.104	29.3	5.767	3.93	0.204	
	$\beta_{CF} = -2.20$	6.442	1.231	157.0				
	$\beta_{CCl} = -2.20$	6.554	0.895	249.1				
3	1-fluoro-4-chlorobenzene	4.539	0.060	90.0	4.476	3.06	0.028	[20]
		5.621	0.343	0.0	5.767	3.74	0.132	
	$\beta_{CF} = -2.20$	6.735	1.084	0.0				
	$\beta_{CCl} = -2.20$	6.761	0.903	270.0				
4	1-fluoro-2-bromobenzene	4.615	0.026	23.9	4.661	3.08	0.029	[21]
		5.548	0.171	326.8	5.876	3.95	0.216	
	$\beta_{CF} = -2.20$	6.388	1.069	32.2				
	$\beta_{CBr} = -1.80$	6.528	0.759	123.4				
5	1-fluoro-3-bromobenzene	4.640	0.015	154.4	4.661	3.00	0.024	[21]
		5.658	0.155	19.1	5.821	3.90	0.192	
	$\beta_{CF} = -2.20$	6.330	1.070	155.6				
	$\beta_{CBr} = -1.80$	6.488	0.774	248.4				
6	1-fluoro-4-bromobenzene	4.559	0.050	90.0	4.575	3.02	0.025	[21]
		5.564	0.381	0.0	5.713	3.85	0.168	
	$\beta_{CF} = -2.20$	6.672	0.922	0.0				
	$\beta_{CBr} = -1.80$	6.674	0.740	270.0				
7	1-fluoro-2-iodobenzene	4.600	0.027	198.1				
		5.397	0.216	337.8				
	$\beta_{CF} = -2.20$	6.148	0.608	53.5				
	$\beta_{CI} = -1.40$	6.346	0.539	160.0				
8	1-fluoro-3-iodobenzene	4.624	0.015	340.7				
		5.465	0.256	187.1				
	$\beta_{CF} = -2.20$	6.157	0.652	133.9				
	$\beta_{CI} = -1.40$	6.209	0.407	214.9				
9	1-fluoro-4-iodobenzene	4.546	0.044	90.0				
		5.413	0.414	0.0				
	$\beta_{CF} = -2.20$	6.259	0.169	270.0				
	$\beta_{CI} = -1.40$	6.488	0.363	0.0				

Table V (continued)

	Compound $\beta_{C\mu}$ (eV) $\beta_{C\nu}$ (eV)	Calculated			Experimental			Ref.
		E (eV)	f	α	E (eV)	lg ε	f	
	1.	2	3	4	5	6	7	8
10	1-chloro-2-bromobenzene	4.585	0.033	20.7	4.575	2.50	0.008	[21]
		5.474	0.169	306.7	5.834	4.12	0.312	
	$\beta_{CCl} = -2.20$	6.280	1.140	31.8				
	$\beta_{CBr} = -1.80$	6.483	0.712	122.2				
11	1-chloro-3-bromobenzene	4.614	0.018	160.6	4.575	2.60	0.010	[21]
		5.627	0.116	42.8	5.848	3.08	0.029	
	$\beta_{CCl} = -2.20$	6.177	1.168	150.1				
	$\beta_{CBr} = -1.80$	6.423	0.730	241.7				
12	1-chloro-4-bromobenzene	4.526	0.055	90.0	4.525	2.62	0.010	[21]
		5.478	0.464	0.0	5.535	4.13	0.324	
	$\beta_{CCl} = -2.20$	6.666	0.943	0.0				
	$\beta_{CBr} = -1.80$	6.672	0.773	270.0				
13	1-chloro-2-iodobenzene	4.571	0.033	194.9				
		5.353	0.188	321.7				
	$\beta_{CCl} = -2.20$	6.066	0.796	224.5				
	$\beta_{CI} = -1.40$	6.306	0.491	151.0				
14	1-chloro-3-iodobenzene	4.599	0.017	346.8				
		5.469	0.209	195.2				
	$\beta_{CCl} = -2.20$	5.997	0.826	141.6				
	$\beta_{CI} = -1.40$	6.173	0.394	232.0				
15	1-chloro-4-iodobenzene	4.516	0.049	90.0				
		5.354	0.484	0.0				
	$\beta_{CCl} = -2.20$	6.275	0.156	270.0				
	$\beta_{CI} = -1.40$	6.483	0.287	0.0				
16	1-bromo-2-iodobenzene	4.578	0.027	203.8	4.900	2.81	0.016	[21]
		5.316	0.188	136.7	5.276	4.00	0.240	
	$\beta_{CBr} = -1.80$	5.983	0.840	40.3	5.904	4.40	0.600	
	$\beta_{CI} = -1.40$	6.251	0.416	146.1				
17	1-bromo-3-iodobenzene	4.603	0.013	336.6				
		5.455	0.194	201.1				
	$\beta_{CBr} = -1.80$	5.873	0.838	142.2				
	$\beta_{CI} = -1.40$	6.126	0.352	235.1				
18	1-bromo-4-iodobenzene	4.533	0.041	90.0	4.768	3.13	0.032	[21]
		5.304	0.510	0.0	5.102	4.26	0.432	
	$\beta_{CBr} = -1.80$	6.264	0.159	270.0				
	$\beta_{CI} = -1.40$	6.432	0.106	0.0				

3.2. Results

3.2.1. Transition energies

The experimental and calculated spectral data for all hetero-dihalobenzenes are shown in Table V. The calculated energies are given only for the four lowest singlet transitions. The energies of the hetero-disubstituted derivatives are always lower than those of the two corresponding monosubstituted compounds. The same trend is observed for the experimental values, excepting the bromoiodobenzenes. An explanation for the extreme values of 1-bromo-2-iodobenzene is given in Section 2.2.1. A comparison of the isomers shows that the calculated energy of the first band decreases in the order *meta*, *ortho*, *para*, while the experimental energies for the *ortho*- and *meta*-derivatives are the same but for the *para* isomer lower. From Table V it is obvious that, by applying the $\beta_{\mu C}$ values used for mono- and homo-disubstituted derivatives, the energies can be obtained with nearly the same accuracy for all the compounds investigated: the greatest deviation of the first band occurs with 1-bromo-2-iodobenzene (6.57%), while for the second band with 1-chloro-2-bromobenzene (6.17%).

3.2.2. Oscillator strengths and polarization directions

Table V contains the calculated oscillator strengths together with the experimental ones obtained from the equation $f = \varepsilon/41\,700$ [22]. The calculated values are in satisfactory agreement with the experimental data.

In Table V the calculated polarization directions are given by the angles (α) measured in clockwise direction from the bond axis of the halogen substituent having the higher atomic number. The calculated polarization directions are not identical with those of the homo-disubstituted benzenes because of the hetero substitution.

3.2.3. Charge densities and bond orders

In Table VI charge densities on the halogen atoms (q_μ) and the bond orders of the carbon–halogen bonds ($p_{\mu C}$) are given. The rows of the Table give the q_μ and $p_{\mu C}$ values for a halogen atom in that compound which contains the atom given in the heading of the Table as second substituent. Similarly to the homo-dihalobenzenes, the charge density and bond-order values do not show an unambiguous correlation with the atomic number of the halogen. This is caused by the deviation of the starting parameters from the monotony. In groups of different halogen-atom pairs the charge densities and bond orders are as expected. The charge density on the substituent in *meta* position is near to that of the monosubstituted derivative, while in *ortho*-

and *para* positions it is greater. The order of charge densities is *ortho* > *para* > > *meta*.

Figure 4 shows, as examples, the molecular diagrams of the three chlorobromobenzene isomers and those of *para* halogenobromobenzenes. The charge density on the *ortho*-carbon atom is the largest while that in *meta* position is the smallest, and the other possible cases being between this two extremes: *o–o* > *o–p* > *o–m* > *p–m* > *m–m*.

3.2.4. Dipole moments

In Table VII the components of the π-electron contribution to the dipole moment (μ_y, μ_z) as well as the magnitude (μ in Debye units) and the direction (δ) of their resultant are given; δ is the angle in clockwise direction from the bond axis of the halogen substituent having the greater atomic number. The position of the molecule in a Cartesian system of coordinates is shown in Fig. 5. The calculated values show the expected changes. On comparison with the experimental data [23] it is apparent that the calculated values are smaller owing to the neglect of σ contributions, but are larger than would be expected on the basis of π-electron contributions only, considering the experimental difference between the dipole moments of alkyl and phenyl derivatives. For mono-halobenzenes both the calculated and experimental dipole moments have the maximum value for chlorobenzene, using the $\beta_{\mu C}$ values of Table V giving best fit for the spectral data. If identical $\beta_{\mu C}$ values are used, the π-electron contribution increases monotonously with the atomic number of the halogen. As the same $\beta_{\mu C}$ values were used for the calculation of both dihalo-

Table VI

Charge densities and bond orders of the

		F			Cl		
		ortho	*meta*	*para*	*ortho*	*meta*	*para*
F	q_F	1.9299	1.9249	1.9282	1.9305	1.9254	1.9288
	p_{F-C}	0.2614	0.2763	0.2671	0.2601	0.2752	0.2656
Cl	q_{Cl}	1.9236	1.9182	1.9219	1.9242	1.9187	1.9225
	p_{Cl-C}	0.2729	0.2882	0.2784	0.2717	0.2872	0.2771
Br	q_{Br}	1.9410	1.9364	1.9397	1.9415	1.9370	1.9403
	p_{Br-C}	0.2384	0.2528	0.2434	0.2371	0.2516	0.2417
I	q_I	1.9530	1.9490	1.9519	1.9535	1.9495	1.9525
	p_{I-C}	0.2114	0.2250	0.2160	0.2100	0.2238	0.2143

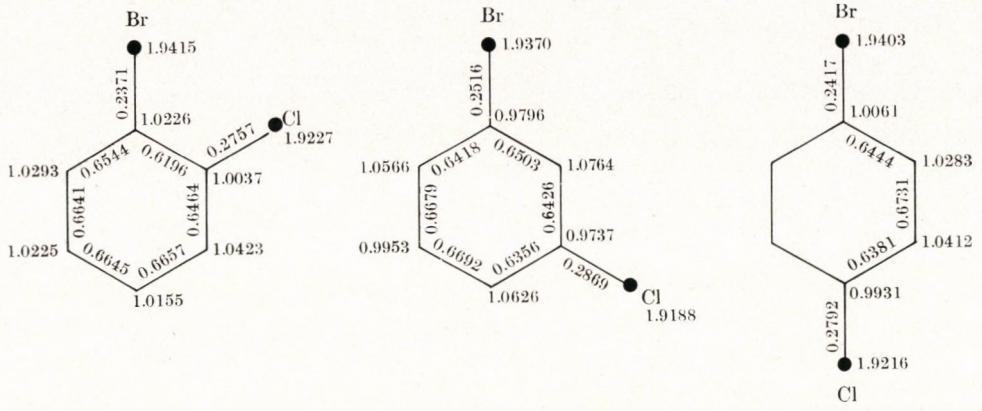

a)

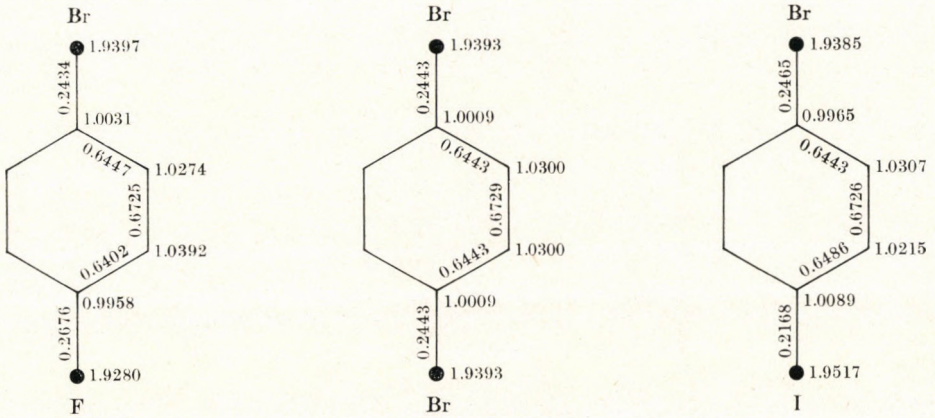

b)

Fig. 4. Molecular diagrams of some bromohalobenzenes

halogen atoms calculated by the PPP method

Br			I			mono
ortho	*meta*	*para*	*ortho*	*meta*	*para*	
1.9292	1.9256	1.9280	1.9282	1.9255	1.9273	1.9250
0.2638	0.2747	0.2676	0.2669	0.2748	0.2695	0.2756
1.9227	1.9188	1.9216	1.9215	1.9186	1.9207	1.9176
0.2757	0.2869	0.2792	0.2790	0.2871	0.2815	0.2886
1.9401	1.9368	1.9393	1.9390	1.9367	1.9385	1.9356
0.2413	0.2517	0.2443	0.2443	0.2519	0.2465	0.2537
1.9523	1.9494	1.9517	1.9513	1.9492	1.9509	1.9483
0.2139	0.2238	0.2168	0.2169	0.2242	0.2190	0.2261

Table VII

Components of the π-electron contribution to the dipole moment and the magnitude (in Debye units) and the direction of their resultant calculated by the PPP method

		ortho			*meta*			*para*			*ortho* δ	*meta* δ	*para* δ
		μ_y	μ_z	μ	μ_y	μ_z	μ	μ_y	μ_z	μ			
F	F	−1.59	0	1.59	−0.82	0.48	0.95	0	0	0	30.0	60.0	
Cl	Cl	−2.03	0	2.03	−1.05	0.61	1.22	0	0	0	30.0	60.0	
Br	Br	−1.69	0	1.69	−0.87	0.50	1.00	0	0	0	30.0	60.0	
I	I	−1.41	0	1.41	−0.72	−0.42	0.84	0	0	0	30.0	60.0	
F	Cl	−1.81	−0.13	1.82	−1.06	0.33	1.11	−0.23	−0.13	0.26	25.9	47.5	0.0
F	Br	−1.63	−0.02	1.63	−0.87	0.44	0.98	−0.04	−0.02	0.04	29.4	56.8	0.0
F	I	−1.49	0.07	1.50	−0.72	0.53	0.90	0.12	0.07	0.14	32.7	66.2	180.0
Cl	Br	−1.85	0.12	1.86	−0.87	0.72	1.12	0.20	0.11	0.23	33.6	69.7	180.0
Cl	I	−1.72	0.21	1.73	−0.72	0.81	1.08	0.36	0.21	0.41	36.9	78.4	180.0
Br	I	−1.55	0.09	1.55	−0.72	0.59	0.93	0.16	0.09	0.18	33.4	69.4	180.0
F		$\mu_y = 0.83$			$\mu_z = 0.48$			$\mu = 0.96$			$\delta = 180.0$		
Cl		$\mu_y = 1.07$			$\mu_z = 0.62$			$\mu = 1.24$			$\delta = 180.0$		
Br		$\mu_y = 0.89$			$\mu_z = 0.51$			$\mu = 1.03$			$\delta = 180.0$		
I		$\mu_y = 0.74$			$\mu_z = 0.43$			$\mu = 0.85$			$\delta = 180.0$		

benzenes and mono-halobenzenes, here too the largest π-contribution is obtained for the chloro derivatives. The corresponding experimental values, however, decrease with the atomic number.

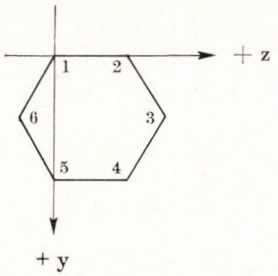

Fig. 5. Coordinate system used in the calculation of halobenzenes

REFERENCES

[1] Pariser, R., Parr, R. G.: J. Chem. Phys. **21,** 466, 767 (1953)
[2] Pople, J. A.: Trans. Faraday Soc. **49,** 1375 (1953)
[3] Mishra, P. C., Rai, D. K.: Indian J. Pure Appl. Phys. **8,** 691 (1970)
[4] Kiss, Á. I., Szőke, J.: Acta Chim. (Budapest) **74,** 59 (1972)
[5] Longuet-Higgins, H. C., Murrell, J. N.: Proc. Phys. Soc. **A68,** 601 (1955)
[6] Murrell, J. N.: Proc. Phys. Soc. **A68,** 969 (1955)
[7] Kimura, K., Nagakura, S.: Mol. Phys. **9,** 117 (1965)
[8] Kiss, Á. I., Martin, A.: Acta Chim. (Budapest) **77,** 179 (1973)
[9] Martin, A., Kiss, Á. I.: Acta Chim. (Budapest) **78,** 177 (1973)
[10] Mataga, N., Nishimoto, K.: Z. Phys. Chem. N. F. **13,** 140 (1957)
[11] Slater, J. C.: Phys. Rev. **36,** 57 (1930)
[12] Hinze, J., Jaffé, H. H.: J. Amer. Chem. Soc. **84,** 540 (1962)
[13] Dibeler, V. H., Reese, R. M.: J. Res. Nat. Bur. Stand. **54,** 127 (1955)
[14] Dibeler, V. H., Reese, R. M.: Anal. Chem. **30,** 604 (1958)
[15] Ford, B.: Theoret. Chim. Acta **10,** 342 (1968)
[16] Khetrapal, C. L., Rai, D. K.: Theoret. Chim. Acta **13,** 308 (1969)
[17] Sutton, L. E.: Tables of Interatomic Distances. Spec. Publ. No. 11, Chem. Soc., London 1958; Supplement Spec. Publ. No. 18, Chem. Soc., London 1965
[18] Kwiatkowski, J. S.: Acta Phys. Polon. **29,** 477 (1966), **30,** 529 (1966)
[19] DMS UV Atlas of Organic Compounds. Butterworths, London; Verlag Chemie, Weinheim 1968
[20] Forbes, W. F.: Can. J. Chem. **37,** 1977 (1959)
[21] Forbes, W. F.: Can. J. Chem. **39,** 1131 (1961)
[22] Allinger, N. L., Stuart, T. W., Tai, J. C.: J. Amer. Chem. Soc. **90,** 2819 (1968)
[23] Mc Clellan, A. L.: Tables of Experimental Dipole Moments. W. H. Freeman and Co., San Francisco 1963
[24] Varsányi, Gy.: Acta Chim. (Budapest) **13,** 347 (1958)
[25] Varsányi, Gy., Holly, S., Faragó, T.: Spectrochim. Acta **19,** 683 (1963)
[26] Varsányi, Gy., Holly, S., Faragó, T.: Spectrochim. Acta **19,** 675 (1963)
[27] Varsányi, Gy., Holly, S., Faragó, T.: Spectrochim. Acta **19,** 669 (1963)
[28] Dobas, I., Eichler, J.: Coll. Czech. Chem. Commun. **38,** 2602 (1973)
[29] Luckii, A. E., Gorokhova, N. I.: Teoret. Eksper. Khim. **6,** 587 (1970)
[30] Burns, G.: J. Chem. Phys. **41,** 1521 (1964)
[31] Bass, A. M., Spones, H.: J. Opt. Soc. Amer. **40,** 389 (1950)
[32] Dunn, T. M., Iredale, T.: J. Chem. Soc. **1592** (1952)
[33] Petruska, J.: J. Chem. Phys. **34,** 1120 (1961)

Antal Martin
Árpád István Kiss
1111 Budapest, Budafoki út 8, Hungary.

Acta Chimica Academiae Scientiarum Hungaricae, 84 (3), pp. 279—287 (1975)

REAKTIONSKINETISCHE BEITRÄGE ZUR UNTERSUCHUNG DER RINGSCHLUSSREAKTION VON CARBÄTHOXY-2-(3-CHLORPHENYLAMINO)-ÄTHYLACRYLAT

L. SZOTYORY, A. ÚJHIDY und I. SZABÓ

(Forschungsinstitut für Technische Chemie der Ungarischen Akademie der Wissenschaften)

Eingegangen am 26. September, 1973

Es wurde die Reaktionskinetik der Ringschlußreaktion von 1-Carbäthoxy-2-(3-chlorphenylamino)-äthylacrylat in verschiedenen Konzentrationen und bei verschiedenen Temperaturen studiert. Als Reaktionsmedium diente das Diphyl mit einem Gehalt von 10% Paraffinöl. Der Reaktionsablauf wurde durch Abwägen der nach verschiedenen Reaktionszeiten ausgeschiedenen festen Substanz verfolgt. Es wurde die zeitliche Änderung der Konzentration des Endproduktes, des 3-Carbäthoxy-4-hydroxy-7-chlorchinolins graphisch dargestellt und es wurden Maximumkurven erhalten, woraus auf konsekutive Reaktion geschlossen werden konnte. Aus diesen Kurven wurden die Geschwindigkeitskonstanten mit drei verschiedenen Methoden ermittelt. Aus den letzteren wiederum wurden die Konstanten des Arrheniusschen Zusammenhanges bestimmt. Es wurde versucht, den Unterschied zwischen den Resultaten bei Konzentrationen von 5 und 10% mit einem Salz-Effekt zu erklären.

Die in Stellung 4 mit einer Alkylamino-Gruppe substituierten Chinolin-Derivate besitzen eine bedeutende physiologische Wirkung und werden seit den vierziger Jahren als wirksame Arzneimittel gegen die Malaria verwendet [1—4]. Zu ihrer Herstellung kann im allgemeinen das Verfahren von GOULD und JACOBS [5] verwendet werden, wonach die 1-Carbäthoxy-2-arylaminoacrylester einer Ringschlußreaktion unterworfen, die entstandenen Verbindungen hydrolysiert und decarboxyliert werden und anschließend wird die Hydroxyl-Gruppe in Stellung 4 durch den gewünschten Substituenten ersetzt.

Die Ringschlußreaktion geht auf die Einwirkung von Wärme vor sich. Nach Literaturangaben [1—3, 5] liegt die optimale Temperatur der Reaktion bei 240—250 °C, deshalb verwendet man als Lösungsmittel Diphenyläther, Diphyl oder Mineralölfraktionen mit höheren Siedepunkten. Im obigen Temperaturbereich läuft die Ringschlußreaktion in 15—60 Minuten mit guter Ausbeute ab.

Im Laufe unserer Arbeit versuchten wir, durch Bestimmung von reaktionskinetischen Daten, die Richtigkeit des von RAYCHAUDHURY und BASU [6] spekulativ festgestellten Reaktionsmechanismus zu bestätigen. Außerdem hielten wir es für nötig, den zeitlichen Verlauf der Reaktion in der Umgebung der von GOULD und JACOBS [5] vorgeschlagenen Temperaturwerte festzu-

stellen, auch deswegen, weil das Produkt der Ringschlußreaktion hitzeempfindlich, und die Bestimmung der optimalen Reaktionsbedingungen nur auf diese Weise möglich ist.

Die Reaktion kann wie folgt formuliert werden:

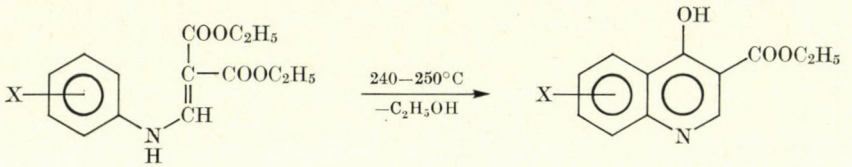

X = m-chlor: (**I**) X = 7-chlor: (**II**)

Der Substituent **X** steht in der Reaktionsgleichung für Chlor, Fluor, Methoxy- oder Phenoxy-Gruppe, für schwefelhaltige Gruppen, Amino-, Acetyl- und die Nitro-Gruppe. Die Art und Stellung dieser Gruppen am Ring können die physiologische Wirkung des Endproduktes, die Geschwindigkeit der Ringschlußreaktion sowie die gebildete Menge der Nebenprodukte stark beeinflussen.

Vom pharmakologischen Gesichtspunkt ist das Chinolin-Derivat, das Chlor in Stellung 7 enthält, eines der wirksamsten. Deshalb wurde die Ringschlußreaktion von 1-Carbäthoxy-2-(3-chlorphenylamino)-äthylacrylat geprüft, deren Endprodukt 3-Carbäthoxy-4-hydroxy-7-chlorchinolin war.

Da die Reaktion intramolekular verläuft, arbeitet man zweckmäßig in stark verdünnter Lösung, um intermolekulare Nebenreaktionen zu vermeiden. Der zeitliche Verlauf der Reaktion wurde zwischen 230—255°C in 5- und 10%-iger Lösung der Verbindung (**I**) verfolgt. Als Lösungsmittel wählten wir 10% Paraffinöl enthaltendes, frisch destilliertes Diphyl. Da das Endprodukt in Diphyl kalt unlöslich ist, die Zersetzungsprodukte dagegen löslich sind, erfolgte die Ermittlung des Umsatzes durch Wägen des während der Reaktion ausfallenden Endproduktes.

Auf Grund der IR-Spektren und dünnschichtchromatographischen Bestimmungen von (**II**) wurde festgestellt, daß die Menge der in intermolekularen Reaktionen entstehenden, unlöslichen Nebenprodukte vernachlässigbar ist.

Die Auswertung der Ergebnisse wurde dadurch erleichtert, daß die Ringschlußreaktion praktisch unumkehrbar ist. Unter bestimmten Bedingungen konnte eine Ausbeute von 97,0% an Verbindung (**II**) erreicht werden. Mit der Verlängerung der Reaktionszeit nahm aber die Ausbeute ab. Dies kann dadurch verursacht werden, wie RAYCHAUDHURI und BASU [2] nachgewiesen haben, daß das primäre Produkt (**II**) hitzeempfindlich ist. Erhitzt man dieses nämlich längere Zeit in Diphyl, so erfolgt eine teilweise Umsetzung zu 7-Chlor-1-äthyl-1,4-dihydro-4-oxochinolin-3-carbonsäure (**III**), 7-Chlor-4-äthoxy-chinolin (**IV**) bzw. 7-Chlor-1-äthyl-1,4-dihydro-4-oxo-chinolin (**V**).

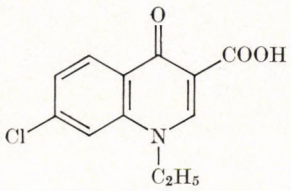

(III)

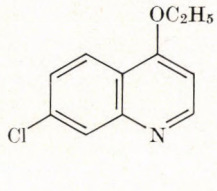

(IV)

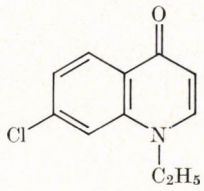

(V)

Die Bestimmung der Geschwindigkeitskonstanten der Zersetzungsreaktion bei verschiedenen Temperaturen ermöglichte einerseits die Auswertung des abklingenden Abschnittes der Kurven, die die zeitliche Konzentrationsänderung des primären Produktes zeigen, andererseits ergab sich die Geschwindigkeitskonstante der Zersetzungsreaktion direkt durch die Wiederauflösung des abgetrennten primären Produktes und durch zeitliche Verfolgung seiner thermischen Zersetzung.

Auswertung der Ergebnisse

Es wurden die im Laufe der Messungen festgestellten Werte der Konzentration des primären Produktes in Abhängigkeit von der Zeit dargestellt und wir erhielten im Falle der Konzentration 0,153 Mol/l (5%) die Kurven auf Abb. 1, bei der Konzentration 0,305 Mol/l (10%) die auf Abb. 2; über 240 °C zeigen die Kurven ein Maximum.

Bei der Auswertung der Kurven gingen wir von der Vermutung aus, daß die Reaktion konsekutiven Charakter hat, sowohl die primäre Reaktion als auch die sekundären Reaktionen I. Ordnung, und die sekundären Reaktionen mit den Zersetzungsreaktionen des primären Produktes identisch sind. Die Zersetzungsprodukte sind in Diphyl löslich. Daß die primäre Reaktion I. Ordnung ist, wird durch den intramolekularen Charakter dieser Reaktion

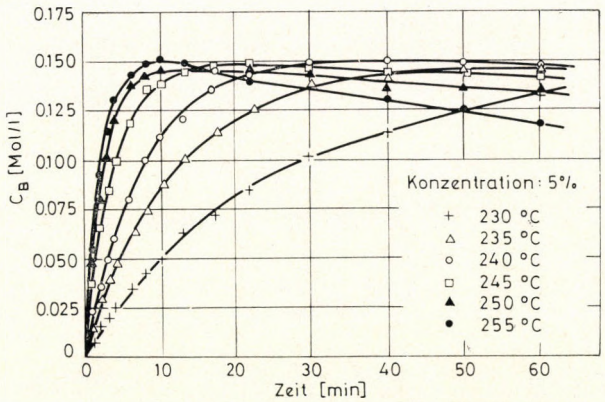

Abb. 1. Änderung der Konzentration des primären Produktes in Abhängigkeit von der Zeit, bei der Konzentration von 0,153 Mol/l (5%)

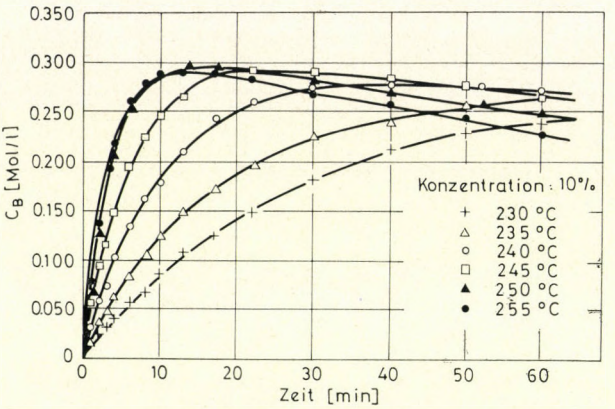

Abb. 2. Änderung der Konzentration des primären Produktes in Abhängigkeit von der Zeit, bei der Konzentration von 0,305 Mol/l (10%)

unterstützt. Nach RAYCHAUDHURI und BASU [6] ist der erste Reaktionsschritt der Zersetzungsreaktion die Spaltung der Esterbindung C–O:

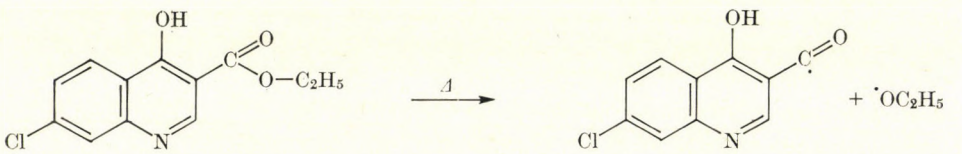

(II) **(IIa)**

Da dieser Schritt vermutlich die langsamste Phase der konsekutiven Zersetzungsreaktion ist, kann der ganze Prozeß kinetisch nach dem folgenden Schema behandelt werden:

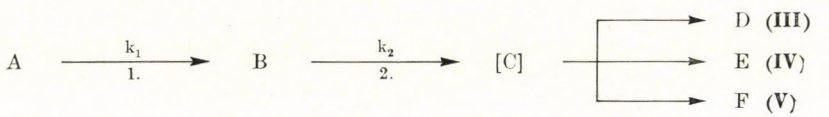

(I) **(II)** **(IIa)**

Unter Voraussetzung dessen, daß sowohl die 1. als auch die 2. Reaktion von erster Ordnung ist, gelangt man zur folgenden Reaktionsgeschwindigkeitsgleichung:

$$c_B = \frac{k_1}{k_2 - k_1} c_{A_0} \cdot [e^{-k_1 t} - e^{-k_2 t}]; \qquad (1)$$

k_1 und k_2 = Reaktionskonstanten,
c_{A_0} = Anfangskonzentration der Substanz A,
c_B = Konzentration der Substanz B im Zeitpunkt t.

Nach dem Einsetzen von $c_B = yc_{A_0}$ erhält man für die Zeitabhängigkeit der Ausbeute (y) der Substanz B den folgenden Zusammenhang:

$$y = \frac{k_1}{k_2 - k_1} [e^{-k_1 t} - e^{-k_2 t}] . \tag{2}$$

Wenn man die Derivierte der Gleichung (2) Null gleichsetzt und an Stelle von t den der maximalen Ausbeute entsprechenden Zeitwert t_0 einsetzt, so erhält man den Ausdruck:

$$\frac{dy}{dt} = \frac{-k_1^2}{k_2 - k_1} e^{-k_1 t_0} + \frac{k_2 \cdot k_1}{k_2 - k_1} e^{-k_2 t_0} = 0 . \tag{3}$$

Ersetzt man das Verhältnis k_2/k_1 durch K, so gelangt man zur transzendenten Gleichung

$$k_1 t_0 (K - 1) = \ln K . \tag{4}$$

Die Auswertung der Resultate wurde mit folgenden Methoden durchgeführt:

a) Da am Anfang der Reaktion die die Geschwindigkeit der Zersetzungsreaktion bestimmende Konzentration des Produktes (**II**) im Vergleich mit der von (**I**) gering ist, und ferner nach RAYCHAUDHURI und BASU bzw. unseren Beobachtungen die Zersetzung von (**II**) im untersuchten Temperaturintervall langsam verläuft, wurde die Zersetzungsreaktion im ersten Abschnitt (bis zur Halbwertszeit) als vernachlässigbar betrachtet. So wurde die auf Grund der die Konzentrationsänderung des Primärproduktes beschreibenden Kurve ablesbaren Halbwertszeit berechnete Geschwindigkeitskonstante als Konstante der primären Reaktion angesehen. Nach Bestimmung des den Kurvenmaxima entsprechenden Zeitwertes und Einsetzen des letzteren in die Gleichung (4), lösten wir die Gleichung dann mit einem Rechner und erhielten die Werte, die in der Tabelle I mit k_{1a} and k_{2a} bezeichnet sind. Diese Methode konnten wir natürlich nur bei den Maximumkurven anwenden.

b) Wir bestimmten den Wert von k_1 auf die unter Punkt a) erwähnte Weise und unter Verwendung des zur 60. Minute gehörenden Wertes c_B, berechneten wir mit Hilfe der Gleichung (1) die Werte von k_2 (in der Tabelle k_{2b}). So konnte jede Kurve ausgewertet werden.

c) Das einmal bereits isolierte primäre Produkt (**II**) lösten wir erneut auf und nach dem Erwärmen von verschiedener Dauer auf verschiedene Temperaturen bestimmten wir durch Zurückwägen des Rückstandes die Geschwindigkeit der thermischen Zersetzung. Unter Voraussetzung einer Reaktion erster Ordnung ermittelten wir die Geschwindigkeitskonstanten k_{2c} auf Grund des Zusammenhanges

$$c_B = c_{B_0} \cdot e^{-k_{2c} t} . \tag{5}$$

Unter Verwendung der so erhaltenen k_{2c}-Werte und der einzelnen Punkte der entsprechenden Kurven wurden mit Hilfe der Gleichung (1) die genaueren Werte der Geschwindigkeitskonstante der primären Reaktion (k_{1c}) bestimmt. Die Kurvenpunkte mußten so gewählt werden, daß sie sich auf dem ansteigenden Abschnitt der Kurven befinden, in der Nähe des Maximums, wo die Konzentration des primären Produktes durch beide Geschwindigkeitskonstanten bedeutend beeinflußt wird.

Tabelle I

Gemessene und berechnete Reaktionsgeschwindigkeitskonstanten bei verschiedenen Konzentrationen und Temperaturen

Konz. [Mol/l]	Konz. [%]	Temp. [°C]	k_{1a} [min^{-1}]	k_{2a} [min^{-1}]	k_{2b} [min^{-1}]	k_{1c} [min^{-1}]	k_{2c} [min^{-1}]
		230	0,0351	—	$0{,}672 \cdot 10^{-3}$	0,0361	$0{,}715 \cdot 10^{-3}$
		235	0,0815	—	$0{,}900 \cdot 10^{-3}$	—	—
0,153	5	240	0,1230	$7{,}231 \cdot 10^{-4}$	$1{,}034 \cdot 10^{-3}$	0,1352	$1{,}150 \cdot 10^{-3}$
		245	0,2665	$9{,}087 \cdot 10^{-5}$	$1{,}373 \cdot 10^{-3}$	—	—
		250	0,3745	$2{,}982 \cdot 10^{-3}$	$2{,}382 \cdot 10^{-3}$	0,3998	$2{,}550 \cdot 10^{-3}$
		255	0,4529	$5{,}134 \cdot 10^{-3}$	$4{,}503 \cdot 10^{-3}$	—	—
		230	0,0295	—	$1{,}740 \cdot 10^{-3}$	0,0308	$1{,}805 \cdot 10^{-3}$
		235	0,0513	—	$2{,}022 \cdot 10^{-3}$	—	—
0,305	10	240	0,0949	$1{,}414 \cdot 10^{-6}$	$2{,}367 \cdot 10^{-3}$	0,0960	$2{,}417 \cdot 10^{-3}$
		245	0,1690	$2{,}243 \cdot 10^{-3}$	$2{,}570 \cdot 10^{-3}$	—	—
		250	0,2634	$2{,}400 \cdot 10^{-3}$	$3{,}660 \cdot 10^{-3}$	0,3020	$3{,}796 \cdot 10^{-3}$
		255	0,2948	$6{,}992 \cdot 10^{-4}$	$5{,}310 \cdot 10^{-3}$	—	—

Die Abweichung zwischen den Geschwindigkeitskonstanten für die 5- und 10%ige Lösung ist vermutlich mit dem sog. »Salz-Effekt« zu erklären. Wenn die den Ringschluß ergebende zyklische, aktivierte Komplexverbindung weniger solvatiert ist als das Ausgangsmolekül, so wird der Ablauf der Reaktion durch die Konzentrationserhöhung gehemmt, da sich an der Solvatation auch die Ausgangsmoleküle beteiligen, und dadurch die Bildung eines aktivierten Komplexes erschwert wird.

Zur Unterstützung unserer Vermutung führten wir die Reaktion auch in Gegenwart von substituierten Anilin-Derivaten mit verschiedener Elektronenverteilung d. h. verschiedenen Dipolmomenten durch. Bei einer Temperatur von 240 °C, unter Anwendung einer Lösung von 0,153 Mol/l (5%ig), wobei die Menge der Anilin-Derivate im Reaktionsgemisch 25 Mol % betrug, wurden die in Abb. 3 gezeigten Kurven erhalten.

Wie ersichtlich, nahm die Reaktionsgeschwindigkeit in jedem Falle ab. Mit zunehmender Dielektrizitätskonstante bzw. Polarisierbarkeit der Anilin-

Derivate verstärkte sich der Effekt in geringem Maße. Dies scheint unsere Vorstellung über den »Salz-Effekt« zu unterstützen.

Zur Feststellung der Richtigkeit der in Tabelle I angeführten Werte der Geschwindigkeitskonstanten zeichneten wir unter Verwendung der Wertepaare k_1—k_2 für verschiedene Temperaturen die c_B-t-Kurven auf und beobachteten, in welchem Maße sie die experimentell erhaltenen Punkte annähern. Als Beispiel wird in Abb. 4 eine Reihe solcher Kurven vorgestellt, die bei 250 °C und bei einer Konzentration von 0,305 Mol/l (10%) ausgemessen wurden. Die Tendenz des Kurvenverlaufes war auch in den übrigen Fällen ähnlich.

Aus dem Ablauf der auf Abb. 4 gezeigten Kurven ist ersichtlich, daß die experimentell ermittelten Punkte am besten durch die mit der Auswertungsmethode *c* aufgezeichnete theoretische Kurve angenähert werden. Die geringe Abweichung der Kurve *b* wurde durch die Vernachlässigung der Zersetzungs-

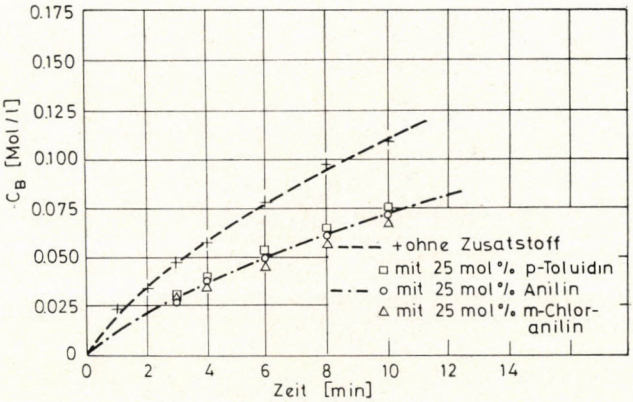

Abb. 3. Einfluß von verschiedenen Zusatzsubstanzen auf die Reaktionsgeschwindigkeit

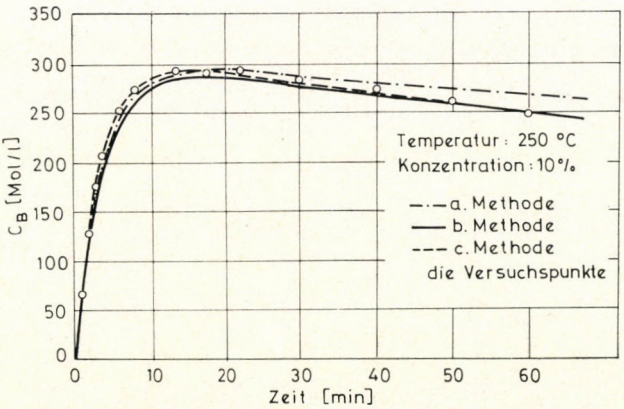

Abb. 4. Annäherung der experimentell ermittelten Punkte unter Verwendung der nach den verschiedenen Methoden erhaltenen Reaktionsgeschwindigkeitskonstanten

reaktion am Reaktionsanfang verursacht, während die verhältnismäßig starke Abweichung der mit der Methode *a* aufgezeichneten Kurve der Ungenauigkeit der Bestimmung der Maximum-Stellen zuzuschreiben ist. Die k_{1a}-Werte sind in der Regel kleiner als die k_{1c}-Werte, was gleichfalls mit der Vernachlässigung der Zersetzungsreaktion im Bereich der Halbwertszeit zu erklären ist.

Unter Verwendung der mit der Methode *c* erhaltenen Angaben wurden die Funktionen $\lg k - 1/T$ zur Bestimmung der Konstanten der Arrheniusschen Gleichung

$$k = A \cdot e^{-\frac{E^*}{RT}} \tag{6}$$

aufgezeichnet (Abb. 5).

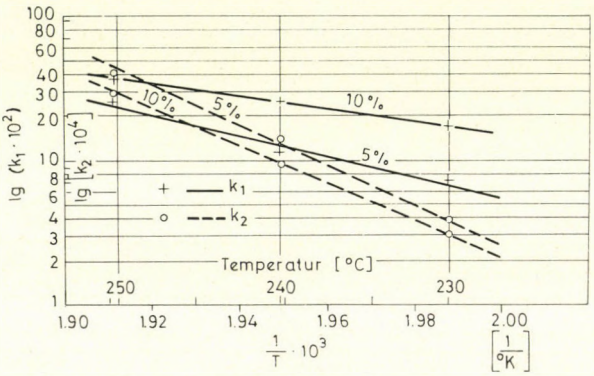

Abb. 5. Graphische Bestimmung der Arrheniusschen Konstanten

Die mit der graphischen Methode berechneten Daten sind in Tabelle II angeführt.

Tabelle II

Nach der graphischen Methode bestimmte Konstanten der Arrheniusschen Gleichung

Konz. [Mol/l]	Konz. [%]	Reaktion	A [min^{-1}]	E^* [Kcal/Mol]
0,153	5	Primär	$1{,}08 \cdot 10^{24}$	63,84
		Sekundär	$3{,}3 \cdot 10^{11}$	33,28
0,305	10	Primär	$2{,}15 \cdot 10^{22}$	59,28
		Sekundär	$9{,}7 \cdot 10^{5}$	19,60

Die angeführten Werte sind natürlich Durchschnittswerte für den Bereich von 230—250 °C, da wir die Berücksichtigung der zwar geringen aber existierenden Temperaturabhängigkeit der Konstanten A und E^* vernachlässigt haben.

Experimenteller Teil

Durchführung der Versuche

Die entsprechende Menge (90 bzw. 95 g) von 10% Paraffinöl enthaltendem Diphyl wurde in ein 200 ml fassendes hitzebeständiges, mit Schliff versehenes zylindrisches Glasgefäß eingewogen. Gas Gefäß wurde dann mit einem Deckel verschlossen, der mit Thermometer, Rührer, Gaseinleitungsrohr und Dosierstutzen ausgerüstet war. Der Rührer wurde in Gang gesetzt und das Gefäß in ein elektrisch beheiztes Ölbad getaucht. Wir ließen durch den Luftraum des Gefäßes mit einer Geschwindigkeit von 20 l/h Argongas durchströmen und erhöhten die Temperatur im Gefäß um 2—3 °C über die geplante Versuchstemperatur. Dabei wurde dafür Sorge getragen, daß die Erwärmungsgeschwindigkeit am Ende der Aufheizung etwa 2—2,5 °C/Min. betragen soll. Danach erfolgte die schnelle Zugabe des abgewogenen und auf 160 °C vorgewärmten geschmolzenen 1-Caräthoxy-2-(3-chlorphenylamino)-äthylacrylats. Nach einigen Sekunden stellte sich die gewünschte Temperatur ein, die wegen der niedrigen Wärmekapazität des Systems gut geregelt werden konnte. Die Temperatur des Gemisches wurde für die gewünschte Dauer beim entsprechenden Wert gehalten, unterdessen wurde intensiv gerührt. Zur Unterbrechung der Reaktion wurde dann schnell 50 ml kaltes 10% Paraffinöl enthaltendes Diphyl zum Gemisch gegeben. Gleichzeitig wurde das heiße Ölbad entfernt und zwecks Kühlung des Reaktionsgefäßes durch ein kaltes, stark gerührtes Ölbad ersetzt. Das abgekühlte Gemisch wurde über Nacht stehen gelassen, um die vollständige Ausfällung des Niederschlages zu erreichen. Anschließend folgten die Filtration auf einer G4-Fritte, das Waschen mit Petroläther bis zur Diphylfreiheit, Trocknen im Vakuum bei 100 °C und die Auswaage.

Versuchsmaterial

Das technisch reine 93—94%ige 1-Carbäthoxy-2-(3-chlorphenylamino)-äthylacrylat wurde aus Petroläther umkristallisiert und im Vakuum bei 45 °C getrocknet. Zur Prüfung der Reinheit des Materials wurde der Schmelzpunkt bestimmt (Schmelzpunkt: 54—56 °C).

Das als Lösungsmittel verwendete Diphyl wurde vor den einzelnen Versuchen im Vakuum frisch destilliert. Als Rohstoff für die Vakuumdestillation diente technisches Rohdiphyl oder ein Filtrat aus vorangehenden Versuchen. Das als Lösungsmittelsubstanz verwendete Paraffinöl war wasserklar und analytisch rein.

LITERATUR

[1] Surrey, A. R., Hammer, H. F.: J. Am. Chem. Soc. **68,** 113 (1964)
[2] Price, C. C., Roberts, R. M.: J. Am. Chem. Soc. **68,** 1204 (1964)
[3] Price, C. C., Leonard, N. J., Reitsema, R. H.: J. Am. Chem. Soc. **68,** 1256 (1946)
[4] Riegel, B., Lappin, G. R., Adelson, B. H., Jackson, R. I., Albisetti, C. J., Dodson, R. M., Baker, R. H.: J. Am. Chem. Soc. **68,** 1264 (1946)
[5] Gould, R. G., Jacobs, W. A.: J. Am. Chem. Soc. **61,** 2890 (1939)
[6] Raychaudhury, A., Basu, U. P.: J. Indian Chem. Soc. **47,** 25 (1970)

László Szotyory
Aurél Újhidy
István Szabó
8200 Veszprém, Schönherz Z. u. 10. Ungarn.

Acta Chimica Academiae Scientiarum Hungaricae, 84 (3), pp. 289—295 (1975)

SYNTHETIC LINEAR POLYMERS, XXXII*

CHANGES IN THE DIPOLE MOMENT OF POLYMER HOMOLOGOUS COMPOUNDS AS A FUNCTION OF THE MOLECULAR WEIGHT**

I. GÉCZY

(Research Institute for Textile Industry, Budapest)

Received November 22, 1973

The specific mean-square dipole moments of poly-(trifluorochloroethylene) and of polyene oligomeres with a phenyl end-group change linearly with the reciprocal molecular weight. Thus, under the given conditions, these polymers do not form secondary structure. The mean dipole moments of the repeating units of these polymers have the values of 0.12 D ($-CFCl-CF_2-$) and 1.02 D ($-CH=CH-$), respectively. In the cases of polyene oligomers with dimethylamine end-group, poly(γ-benzyl-L-glutamate) and phenylsiloxane ladder polymers deviations from the linearity are observed. On this basis the existence of a secondary structure can be assumed in these series of compounds.

Introduction

It has been shown earlier that the investigation of the optical rotation [1, 2] and dipole moment [3] of dissolved macromolecules as a function of the size of the molecule may give certain information as regards the molecular state and secondary structure. It was found [2] that for the detection of the secondary structure the specific rotation $[\alpha]$ and the specific mean-square dipole moment $(\overline{\mu}^2/M)$ can be conveniently used since the optical rotation is closely related to the dipole moment of the molecule [4]. It has been shown [1, 2, 3] that, in general and thus also in a number of the cases studied, there is a linear relationship between the value of $[\alpha]$ or $\overline{\mu}^2/M$ and reciprocal molecular weight. The intercepts of the straight lines thus obtained, which are characteristic of the repeating units [5], are different if the orientation and rotation of the otherwise identical repeating units differ, as *e.g.* in the case of linear and cyclic poly(dimethylsiloxanes) [6], linear maltodextrins and cyclic Schardinger dextrins [1] as well. Using the data of GOODMAN *et al.* [7—10], we have shown that deviations from the linearity [2] indicate the existence of secondary structure. This is in complete accordance with the results of GOODMAN *et al.* [7—10] obtained earlier by means of another method.

* Synthetic linear polymers XXXI: Koloriszt. Ért. **13**, 272 (1971); Acta Chim. (Budapest), **79**, 133 (1973).

** Presented at the jubilee session of the Macromolecular Committee of the Hungarian Academy of Sciences, Budapest, 11th December 1973.

Recent investigations

Since the above results concerning the specific mean-square dipole moment were based thus far only on a rather limited number of experimental data (on 8 polymer homologous series), we have now extented our considerations on the dipole moments to further polymer homologous series on the basis of literature data. The data used in the present study are listed in Table I.

Table I

Dipole moments of the members of some polymer homologous series and the data used for the calculations

Poly-(trifluorochloroethylenes):

—(CFCl—CF_2)$_p$— (fractionated samples)

$\bar{p}$	$\bar{M}$	μ(D)*	$(1/\bar{M})\times10^{-4}$	$\bar{\mu}^2$	$(\bar{\mu}^2/\bar{M})\times10^{-5}$
4.3	500	0.545	20.0	0.2970	59.4
6.0	700	0.56	14.3	0.3136	44.8
7.7	900	0.59	11.1	0.3481	38.6
9.5	1100	0.595	9.1	0.3540	32.3

* See [11]

Polyenes:

X—(CH=CH)$_p$—C(=O)H (benzene, 25°C)

X = —$N(CH_3)_2$

p	Mol. wt.	$\bar{\mu}$(D)*	$(1/M)\times10^{-4}$	$\bar{\mu}^2$	$\bar{\mu}^2/M$
1	99	6.24	101.0	38.94	0.393
2	125	7.67	80.0	58.83	0.471
3	151	8.24	66.2	67.90	0.450
4	177	8.50	56.5	72.25	0.366

* See [12]

X = —C$_6$H$_5$

p	Mol. wt.	$\bar{\mu}$(D)	$(1/M)\times10^{-4}$	$\bar{\mu}^2$	$\bar{\mu}^2/M$
1	132	3.60*	75.8	12.98	0.097
2	158	3.80**	63.3	14.44	0.091
5	236	4.16***	42.4	17.31	0.073

* See [12] ** See [13] *** See [14]

Table I (continued)

Poly(γ-benzyl-L-glutamates):

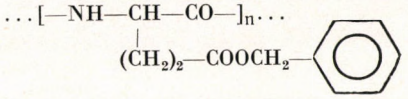

($CHCl_3$ containing 1—2% dimethylformamide, 20°C, fractionated samples)

$\bar{P}$	$\bar{M}\times10^{3}$*	$\bar{\mu}$(D)*	$(1/M)\times10^{-7}$	$\bar{\mu}^2\times10^{3}$	$\bar{\mu}^2/\bar{M}$
426	93.4	1090	107.1	1.180	12.6
639	140	1560	71.4	2.434	17.4
1096	240	2600	41.7	6.760	28.2
1379	302	3160	33.1	9.986	32.1

* See [15]

Phenylsiloxane ladder polymers:

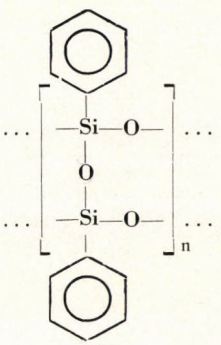

(in benzene)

$\bar{M}\times10^{5}$*	$\bar{\mu}$(D)*	$(1/\bar{M})\times10^{-7}$	$\mu^2/\bar{M}\times10^{3}$
0.89	9.0	112.40	0.9
1.27	9.0	78.74	0.7
2.14	16	46.73	1.2
2.79	25	35.84	2.4
3.67	30	27.25	2.4
4.56	50	21.93	5.1
7.08	74	14.12	7.7
8.75	80	11.43	7.4
10.7	100	9.35	9.9
16.7	130	5.99	11.3
33.5	220	2.98	15.4

* See [16—18]

In our further calculations only such data have been used for application where at least three values were available within the same polymer homologous series. A part of the data, in contrast to our earlier investigations, refers not only to homogeneous, well-defined oligomeric compounds but also to fractionated samples with an average molecular weight. Thus the relationships established up to the present can be generalized to a greater extent.

On the basis of the dipole moment values to be found in the literature we have calculated the specific mean-square dipole moment of the individual oligomeric compounds and polymer fractions. These are also given in Table I. Similarly to our method applied earlier, the values obtained were plotted against the reciprocal molecular weight. The results are shown in Figs 1—4.

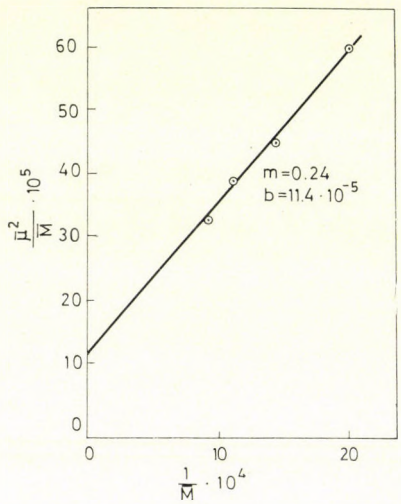

Fig. 1. Specific mean-square dipole moments of poly(trifluorochloroethylenes) as a function of the reciprocal molecular weight

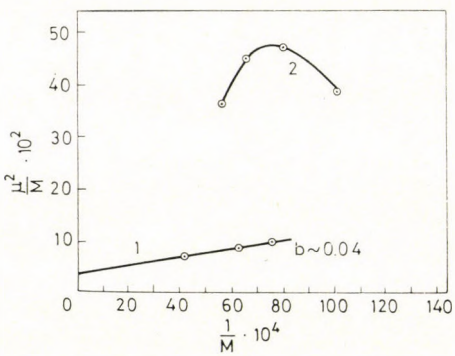

Fig. 2. Specific mean-square dipole moments of polyene oligomers as a function of the reciprocal molecular weight (phenyl end-group: curve 1; $-N(CH_3)_2$ end-group: curve 2)

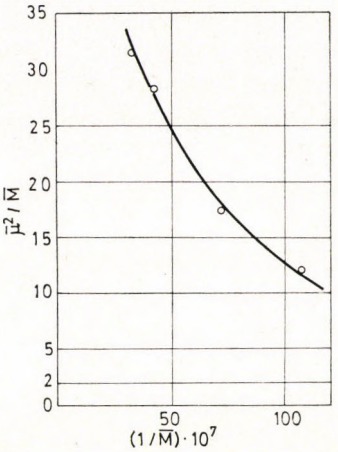

Fig. 3. Specific mean-square dipole moments of poly(γ-benzyl-L-glutamates) as a function of the reciprocal molecular weight

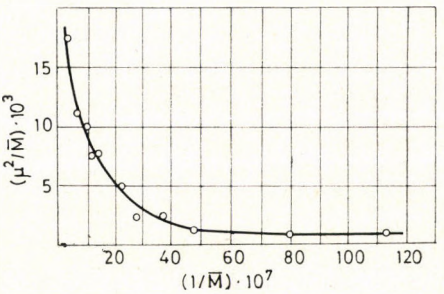

Fig. 4. Specific mean-square dipole moments of phenylsiloxane ladder polymers as a function the reciprocal molecular weight

Discussion

The Fig. 1 and the straight line number 1 of Fig. 2 indicate that the points lie with a good approximation on a line. Consequently, the relationship

$$\frac{\bar{\mu}^2}{\bar{M}} = \frac{a}{\bar{M}} + b$$

established earlier, which is essentially a special form of the equation

$$\varphi = \frac{a}{M} + b$$

where q is a specific quantity (see [3] and [5]), is also valid in the interval studied for polyene oligomers with phenyl end-group and for poly-(trifluorochlorethylene). Fig. 1 shows also the constants (slope: m and intercept: b) of relationship obtained by the method of averages. The intercept of the straight line 1 Fig. 2 was determined graphically. Its value is also given in Fig. 2.

From the straight line in Fig. 1 and from the straight line number 1 in Fig. 2 the conclusion can be drawn that in the examined interval, under the given experimental conditions, neither poly(trifluorochloroethylene) nor polyene oligomers with phenyl end-group do form secondary structure. Table II indicates the mean dipole moments ($\overline{\mu}$) of the individual repeating units for infinitely high molecular weight polymers calculated on the basis of constants b obtained from the intercepts.

Table II

Mean dipole moment of the repeating units of polymers not forming any secondary structure under the given conditions, in the case of $M = \infty$

Repeating unit	Molecular weight of the repeating unit (M_0)	Value of constant b	$\overline{\mu}$ $(= \sqrt{bM_0})$
$-(CFCl-CF_2)-$	116.5	11.4×10^{-5}	0.12 D
$-(CH=CH)-$	26.0	4×10^{-2} (benzene, 25°C)	1.02 D

A case quite different from the above is that of polyene oligomers with dimethylamine end-group (curve 2, Fig. 2). The plot here yields a curve passing through a maximum. Similarly, deviation from the linearity can be observed in the cases of poly(γ-benzyl-L-glutamate) at 20°C in chloroform containing 1—2% dimethylformamide (Fig. 3) and phenylsiloxane ladder polymers in benzene (Fig. 4). As already pointed out [2], this indicates that, under the given experimental conditions, a secondary structure is formed. The existence of this secondary structure in phenylsiloxane ladder polymers was successfully proved by experiments as well, by TSVETKOV *et al.* [16—18].

REFERENCES

[1] GÉCZY, I.: Kolor. Ért. **8,** 221 (1966); Cellulose Chem. and Techn. **4,** 245 (1970)
[2] GÉCZY, I.: Kolor. Ért. **10,** 273 (1968); Acta Chim. Acad. Sci. Hung. **66,** 77 (1970)
[3] GÉCZY, I.: Magyar Kém. Foly. **71,** 216 (1965); Acta Chim. Acad. Sci. Hung. **45,** 131 (1965)
[4] MASON, S. F.: Quart. Rev. **17,** 20 (1963)
[5] See *e.g.* GÉCZY, I.: Magyar Tud. Akad. Kémiai Tud. Oszt. Közl. **23,** 285 (1965) and references cited therein.
[6] GÉCZY, I.: Magyar Kém. Foly. **71,** 551 (1965); Polymer Rev. **2,** 556 (1966); J. Polymer Sci. (C) **16,** 2991 (1967)

[7] GOODMAN, M., SCHMIDT, E. E., YPHANTIS, D. A.: J. Amer. Chem. Soc. **84,** 1283, 1288, 1296 (1962)
[8] GOODMAN, M., LISTOWSKY, J., MASUDA, J., BOARDMAN, F.: Biopolymers **1,** 33 (1963)
[9] GOODMAN, M., BOARDMAN, F.: J. Amer. Chem. Soc. **85,** 2483 (1963)
[10] GOODMAN, M., FELIX, A. M., DEBER, C. M.: Biopolymers **1,** 371 (1963)
[11] TANIGUCHI, J.: Doshishe Kogaku Kaishi **10,** 116 (1959); C. A. **54,** 6230c (1960)
[12] HUTCHINSON, M. H., SUTTON, L. E.: J. Chem. Soc. 4382 (1958)
[13] BRANLEY, E., LE FEVRE, R. J. W.: J. Chem. Soc. 4382 (1958)
[14] KAUFMAN, M. H., ERNSBERGER, F. M., MCEVAN, W. S.: J. Amer. Chem. Soc. **78,** 4197 (1956)
[15] FROLOV, V. I.: Vysokomol. Soed. (A) **14,** 2317 (1972)
[16] TSVETKOV, V. N.: Makromol. Chem. **160,** 1 (1972)
[17] TSVETKOV, V. N., ANDRIANOV, K. A., RYUMTSEV, E. I.: Vysokomol. Soed. (A) **15,** 1248 (1973)
[18] TSVETKOV, V. N., ANDRIANOV, K. A., RYUMTSEV, E. I., SHTENNIKOVA, I. N., VITOVSKAYA, M. G., MAKAROVA, N. N., KURASHEVA, A. N.: Vysokomol. Soed. (A) **15,** 400 (1973)

István GÉCZY; 1363 Budapest, POB 21. Hungary.

Acta Chimica Academiae Scientiarum Hungaricae, 84 (3), pp. 297—312 (1975)

STRUCTURAL STUDIES ON POLYACENAPHTHYLENE

F. CSER and GY. HARDY

(Research Institute for Plastic Industry, Budapest)

Received March 1, 1974; in revised form, August 12, 1974

The densities of some oligo- and polyacenaphthylenes obtained in different ways were determined. The oligomer prepared in the iodine-initiated solid-state oligomerization had the highest density. Its X-ray powder diffractogram was resolved into its Gaussian components. The diffraction angles corresponding to the Gauss maxima were indexed as a monoclinic unit cell, using $a = 11.7$, $b = 7.62$, $c = 9.82$ Å and $\beta = 90°$ as parameters. The space group is $P2_1$.

The atomic coordinates of the threo and erythro-acenaphthylene monomeric units were computed by minimizing the conformational energies. The conformational energy of the polymer chains was built up from either *threo* or *erythro* segments computing it as a function of the dihedral angles (φ_1, φ_2) between the monomeric units of the main chain.

No regular polymer chain can be formed from merely erythro segments because of steric hindrances. The function of conformational energy of threo isotactic chain has four local minima; the deepest one corresponds to a 2_1 helix. Three regular chains of minimum energy were obtained for syndiotactic polymers having 2_1 and 4_1 helices as well as a series of symmetry centres. The 2_1 helical structure corresponds to the oligomer cell representing the absolute minimum of the energy. 2_1 helix and the series of symmetry centres are built up very similarly to each other and can be derived from the monomeric structure by small translations *i.e.*, they may be isomorphous with the monomeric structure.

The polymer consisting of a combination of *erythro* and *threo* segments has a 2_1 helix structure too but the energy of the chain is much higher then that of pure *threo* chains.

In our previous paper [1], results from structural investigations of acenaphthylene (ACN) monomer crystals were reported. The possibility of topotactic solid-state polymerization was demonstrated due to monomer molecules capable of free rotation in the lattice at room temperature. Similar results were obtained indirectly from X-ray diffraction and infrared spectroscopy [2]. It was established that the acenaphthylene polymer produced in the liquid state by radical, *i.e.* thermal initiation, showed a more irregular structure than that produced in the solid state by riadiation initiation or in the liquid state by Ziegler—Natta-type catalysts. The most regular structure was obtained in oligomers formed in the solid state by initiation with iodine.

BARRALES-RIENDA and PEPPER [3] established that in polymers prepared by thermal initiation or, in the liquid state, by initiation of BF_3, monomer units of both *threo* and *erythro* conformation were present in spite of the fact that the *erythro* conformation could not form individual polymer chains

due to steric hindrances. As they demonstrated, the polymer chains were more flexible than was expected, *i.e.*, their segmental length was smaller than that expected on the basis of dimensions of the nomomer units.

STORY and CANTY [4] drew the conclusion from spectroscopic data of polyacenaphthylene that monomer units of *threo* conformation were present in the polymer as either isotactic or syndiotactic chains. In our previous work [2], it was supposed by X-ray diffractograms and infrared spectra that the ordered oligomer was likely to have a threo isotactic structure with 2_1 or 3_1 helix.

Studying the chemically induced polymerization of ACN [5], the product was found to remain in isomorphism with the monomer up to 16—18 per cent of conversion at 60°C. The previous investigations of polyacenaphthylene have been followed in order to give a more correct interpretation of the forced isomorphism and phase diagram of the polymer/monomer system. For a more unambiguous evaluation of the experimental results, the reported X-ray diffraction and infrared spectroscopic data [2] are supplemented by density measurements and conformation analysis.

Experimental and calculation methods

Density measurements

Density of polymers was determined by flotation method in aqueous $CaCl_2$ solution. Since the polymers are fine powders, densities are given as averages of two limit values, due to certain technical reasons. The upper limit corresponds to the density of the liquid in which all polymer particles raised from the bottom of the vessel after 120 minutes, whereas the lower limit represents an unequivocal sedimentation on the bottom of the vessel after 120 minutes. A density was accepted when the difference between the two limit values did not exceed 0.008 $g \cdot cm^{-3}$. The flotating liquid was thermostated for 25 ± 0.01°C. Its density was measured by the picnometric method.

Calculation of the conformation energy

Conformation of the polymer was calculated by a computer program (POLYMER) based on the method of DE SANTIS *et al.* [7]. Atomic coordinates are presented in a polar coordinate system related to the preceding atoms according to the pattern of Fig. 1. L_i is a vector (valence) from the atom $i-1$ to the atom i; Θ_i is the valence angle between L_{i-1} and L_i; φ_i is the dihedral angle between the $L_{i-2} - L_{i-1}$ and the $L_{i-1} - L_i$ planes (*trans*-position = 0°).

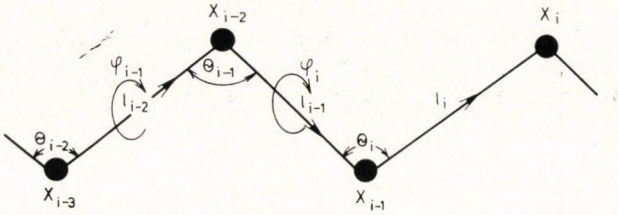

Fig. 1. Polar coordinate system of the polymer chain

Table I

Atomic coordinates of threo-dimethylacenaphthylene

i	X_i (Å)	Y_i (Å)	Z_i (Å)	L_i (Å)	Θ_i (°)	φ_i (°)	Type of atoms
1	—0.7782	—0.0068	2.1141	1.538	111.651	54.514	3
2	—1.1826	—0.0083	0.6446	1.556	111.651	0	3
3	—2.4355	—0.0360	—0.0052	1.524	108.145	115.495	2
4	—2.4644	—0.0253	—1.4259	1.412	132.793	—118.555	2
5	—1.2513	—0.0063	—2.1805	1.421	118.565	0.142	2
6	0.7782	0.0068	2.1141	1.429	120.719	179.158	2
7	1.1826	0.0083	0.6446	1.524	105.388	— 62.664	2
8	2.4355	0.0360	—0.0052	1.412	132.793	— 0.972	2
9	2.6444	0.0252	—1.4259	1.421	118.565	— 0.144	2
10	1.2513	0.0053	—2.1805	1.429	120.719	—179.158	2
11	—0.000	0.0000	—0.1089	1.402	107.113	60.341	2
12	0.0000	0.0000	—1.5178	1.416	120.213	—179.811	2
13	—1.2594	—0.7941	2.7126	1.100	101.121	—124.372	1
14	—3.3437	—0.0428	0.5719	1.076	120.153	178.802	1
15	—3.4047	—0.0129	—1.9505	1.077	120.3296	— 2.027	1
16	—1.2989	0.0053	—3.2541	1.075	119.353	— 0.172	1
17	1.2594	0.7941	2.7126	1.100	116.346	169.863	1
18	3.3437	0.0428	0.5719	1.076	120.153	—178.802	1
19	3.4047	0.0128	—1.9505	1.077	120.329	2.027	1
20	1.2989	—0.0054	—3.2541	1.075	119.353	0.172	1
21	1.3567	1.2589	2.7688	0.0	0.0	0.0	4
22	1.3567	—1.2589	2.7688	1.538	111.651	54.514	4

In Tables I and II, atomic coordinates of *threo* and *erythro* acenaphthylene monomer units are presented in a perpendicular Descartes coordinate system (Å) with the C_{11} atom in its origin or in a polar coordinate system (Fig. 1) related to the preceding atoms. Atomic coordinates of Tables I and II were calculated by a computer program (CONFORM) [1] using the WEST-

Table II

Atomic coordinates of erythro-dimethylacenaphthylene

i	X_i (Å)	Y_i (Å)	Z_i (Å)	L_i (Å)	Θ_i (°)	φ_i (°)	Type of atoms
1	−0.7809	0.0375	2.1180	1.544	119.403	173.441	3
2	−1.1826	−0.0002	0.6458	1.557	118.333	0.0	3
3	−2.4355	−0.0403	−0.0052	1.526	107.597	−120.090	2
4	−2.4644	−0.0258	−1.4259	1.413	132.737	126.196	2
5	−1.2513	−0.0057	−2.1749	1.421	118.590	− 1.974	2
6	0.7762	0.0479	2.1199	1.426	120.355	−178.416	2
7	1.1826	0.0347	0.6473	1.528	105.355	60.480	2
8	2.4355	0.0238	−0.0052	1.413	132.940	0.673	2
9	2.4644	0.0168	−1.4259	1.421	118.677	0.181	2
10	1.2513	0.0049	−2.1749	1.426	120.529	179.268	2
11	0.0000	0.0022	−0.0994	1.398	106.948	− 54.552	2
12	0.0000	0.0000	−1.5143	1.415	122.218	− 1.339	2
13	−1.2183	−0.7773	2.7044	1.095	98.724	123.142	1
14	−3.3436	−0.0424	0.5749	1.078	118.590	179.603	1
15	−3.4023	−0.0177	−1.9541	1.076	120.556	2.334	1
16	−1.2871	0.0046	−3.2527	1.078	119.795	0.033	1
17	1.2191	−0.7722	2.6979	1.097	113.547	− 63.692	1
18	3.3436	0.0343	0.5745	1.077	119.929	139.367	1
19	3.4023	0.0102	−1.9542	1.076	120.557	− 0.107	1
20	1.2871	−0.0043	−3.2527	1.078	119.795	− 0.242	1
21	−1.5222	1.2221	2.7739	0.000	0.000	0.000	4
22	1.5250	1.2112	2.8021	1.544	119.403	178.441	4

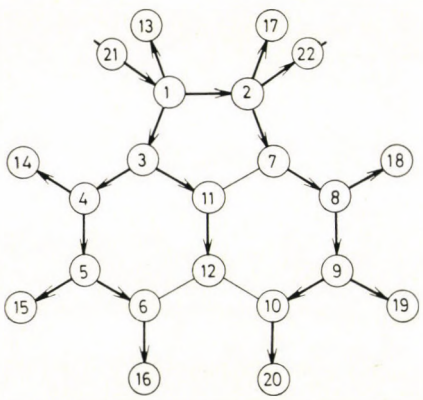

Fig. 2. Numbering of the acenaphthylene monomeric unit and the reference system of the polar coordinates

HEIMER—HENDRICKSON—WIBERG method for *threo-* and *erythro*-dimethylacenaphthylene models. Numbering of atoms and construction of the polar coordinate system is illustrated in Fig. 2.

The monomer units characterized in this way were incorporated into 6-membered chains (C_1–C_2—C_1'–C_2') and changes in the energy corresponding to a monomer unit were determined as a function of the dihedral angle for the $C_2—C_1'$ bond.

The monomer units were supposed rigid and their rotation energy around the bond, the repulsion, attraction and electrostatic energies within the molecule and between the chain segments were calculated. The individual energies were calculated by the following functions:

$$E_{\text{poly}} = \frac{1}{2} \Sigma V_{ij}^0 \{1 - \cos [n_{ij} (\varphi_{ij} - \varphi_{ij}^0)]\} +$$

$$+ \Sigma e_{ij} \left(\frac{R_{ij}^0}{R_{ij}}\right)^{12} - 2 \Sigma e_{ij} \left(\frac{R_{ij}^0}{R_{ij}}\right)^{6} + \Sigma \frac{332}{\varepsilon^\circ} \cdot \frac{q_i q_j}{R_{ij}}$$

where V_{ij}^0 the potential barrier of the rotation around the $C_2—C_1'$ bond (kcal/mole),

n_{ij} eq. 3 for the $C_2—C_1'$ bond,

φ_{ij} the dihedral angle,

φ_{ij}^0 the dihedral angle at the minimum-energy state,

R_{ij} the distance between the atoms i and j (Å),

R_{ij}^0 the sum of van der Waals radii of the atoms i and j (Å),

e_{ij} the potential corresponding to the distance of minimum energy (R_{ij}^0) between the atoms i and j (kcal/mole),

q_i, q_j the electric charge of the atoms calculated by the method of DEL RE [8] in electrons,

ε^0 the dielectric constant.

Each chain segment consists of one monomer unit in the isotactic model and a pair of monomer units relating with a mirror to each other (where φ coordinates have an opposite sign) in the syndiotactic model.

Parameters of the energy functions in the POLYMER program are summarized in the Table III.

Results

Densities and packing coefficients calculated on the basis of molecular increments of SLONIMSKII *et al.* [9] are presented in Table IV for polymers prepared in different ways. It can be stated that radical polymers or products prepared in the liquid state have lower density than those prepared in the

Table III

Parameters of the potential functions used in POLYMER and CONFORM programs

$$E_{\text{pol}} = \sum_{ij} e_{ij}\left[\left(\frac{R^0_{ij}}{R_{ij}}\right)^{12} - 2\left(\frac{R^0_{ij}}{R_{ij}}\right)^{6}\right] + \frac{332}{\varepsilon^\circ}\frac{q_i q_j}{R_{ij}} + \frac{1}{2}V^0_{ij}\{1 - \cos((\varphi_{ij} - \varphi^0_{ij}))n\}$$

$$R^0_{ij} = R^0_i + R^0_j \qquad e_{ij} = 2e_i e_j/(e_i + e_j)$$

Atom	Type	e_i (kcal/mole)	R^0_i (Å)
Hydrogen	1	0.0085	1.20
Carbon (sp^2)	2	0.0880	1.85
Carbon (sp^3)	3	0.0880	1.85

$\varepsilon^0 = 3.5$

Parameters of the CONFORM program

$$E_{\text{tot}} = \frac{1}{2}\Sigma k_e (l_{ij} - l^0_{ij})^2 + \frac{1}{2}\Sigma k_{th}(th_{ijk} - th^0_{ijk})^2 + E_{\text{pol}}$$

Type of bond	k_l (mdyn/Å)	l^0_{ij} (Å)	V^0_{ij} (kcal/mole)	$\varphi_{ij}{}^{(0)}{}_n$
1—2	5.0	1.08	—	
1—3	4.6	1.094	—	
2—2	7.0	1.396	6.0	0.2
2—3	4.5	1.509	0.46	0.3
3—3	4.4	1.512	0.138	0.3

Type of bond angle	k_{th} (mdyn Å rad^{-2})	th°
1—2—2	0.66	120.0
2—2—2	0.40	120.0
2—2—3	0.40	120.0
1—3—2	0.24	109.5
1—3—3	0.24	109.5
2—3—3	0.40	109.5
3—3—3	0.40	109.5

solid state or by ionic mechanism. A corresponding degree of regularity is also found in the diffractograms [2].

A diffractogram of an oligomer formed in the solid state by iodine initiation and multiplied by L_p is illustrated in Fig. 3. The diffractogram was graphically resolved into elementary Gaussian peaks represented by dotted lines. Locations of maxima of the 18 Gaussian peaks could be indexed according

Table IV

Densities and packing coefficients of poly- and oligoacenaphthylene

Product	Density (g cm^{-3})	Packing coefficient
Radical or thermal init. in liquid	1.154	0.6525
ZIEGLER—NATTA init. in liquid or Radiation init. in solid	1.178	0.6661
Iodine init. in solid (oligomer)	1.223	0.6919

Table V

Crystallographic data of oligoacenaphthylene

$a = 11.7$ Å	$V_{cell} = 874.0$ Å^3	Space group $= P2_1$
$b = 7.6$ Å	$\varrho m = 1.223$ g cm^{-3}	$F000 = 320$
$c = 9.8$ Å	$\varrho c = 1.229$ g cm^{-3}	$M = 86$
$\beta = 90$ deg.	$Z = 4$	

to the monoclinic crystal structure.* Table V contains the cell data of the space group, while data for the indexed lines are presented in Table VI.

On the basis of inclination angles of the axes, the elementary cell of the polymer was found to be a pseudo orthorhombic lattice consisting of four monomer units. Since 020 is the line of highest relative intensity (010 and 030 lines are missing), the cell is presumably of space group $P2_1$ and the axis 2_1 corresponds to the chain axis of the polymer. In this case, the chain period would be 3.8 Å which could not be arranged by insertion of a monomer unit into the chain. Thus the period of the chain comprises 2 monomer units together. According to NATTA [10], it can be supposed that the highly regular chain consists of syndiotactic segments.

The conformation energy of a *threo*-isotactic polymer is plotted in Fig. 4 against the dihedral angle φ_1. The curve has four local minima at 2, 150, 208 and 283.5 degrees. The energy barriers between the minima are classified into two different pairs, their magnitude makes an interchange of the two kinds of chain impossible. Even the energy barriers within the pairs of minima are quite high. Characteristic data of polymer chains corresponding to the minima are collected in Table VII. The chain of lowest energy ($\varphi_1 = 208°$) is similar

* The determination of cell parameters using only small amounts of reflections is uncertain. The degree of accuracy of the data given in Table V can be estimated by the same values of the calculated and measured densities as well as of the calculated and measured reflection angles expressed by their sinus in Table VI. The space group with the smallest symmetry was chosen, accepting only the symmetry elements found by systematic absence of reflections (2_1) $P2_1/m$ and orthorhombic $P22_12$ are also possible space groups, however, they are rather unprobable, as they are unfavourable from the point of the close packing of chains (s. A. I. KITAIGORODSKII: Organic Chemical Crystallography, Interscience, N.Y. 1961).

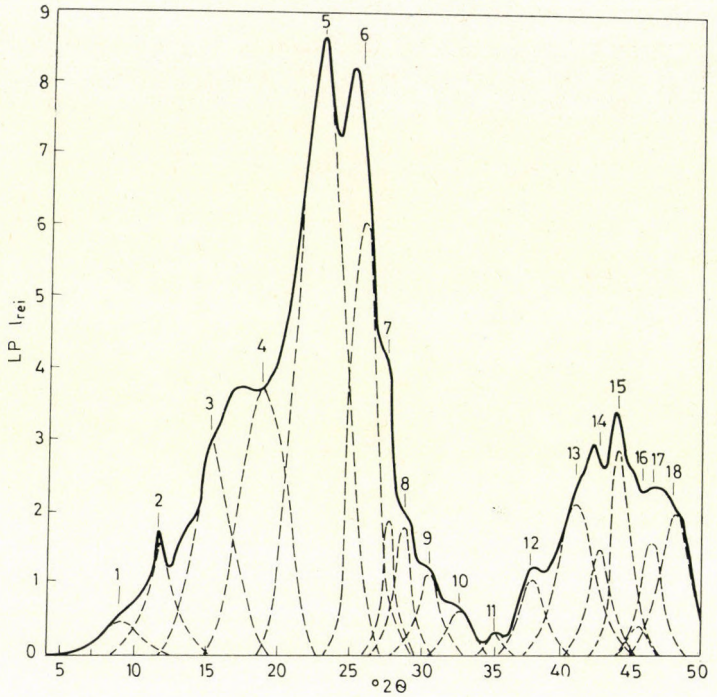

Fig. 3. X-ray diffractogram of oligoacenaphthylene prepared by iodine initiation multiplied by Lp. Dotted lines illustrate the Gaussian components of the curve

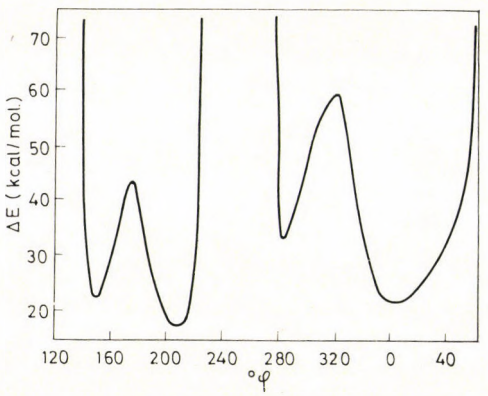

Fig. 4. Conformation energy of the isotactic *threo*-polyacenaphthylene as a function of the dihedral angle φ_1 (E_{total})

Table VI

Peak maxima and Miller indices of gaussein components in the diffractogram of oligoacenaphthylene

No.	2Θ (deg.)	$\sin^2\Theta$	index	$\sin^2\Theta$	index	$\sin^2\Theta$	index	$\sin^2\Theta$
1	8.0	0.0062	001	0.0066				
2	11.6	0.0108	101	0.0110				
3	15.2	0.0175	200	0.0176				
4	18.8	0.0266	002	0.0264				
5	23.0	0.0397	020	0.0398	112	0.0404		
6	24.8	0.0460	021	0.0463	202	0.0440		
7	27.4	0.0560	311	0.0561	212	0.0571	220	0.0573
8	29.2	0.0635	103	0.0638	221	0.0639		
9	30.6	0.0697	400	0.0697	013	0.0693		
10	32.4	0.0833	222	0.0837				
11	35.2	0.0915	130	0.0942				
12	37.8	0.1049	123	0.1035	322	0.1057	412	0.1060
13	41.2	0.1239	204	0.1232				
14	42.4	0.1310	232	0.1333	214	0.1341	303	0.1289
15	43.8	0.1392	403	0.1390	323	0.1387		
16	45.0	0.1466	304	0.1452	024	0.1453		
17	46.4	0.1535	332	0.1553	314	0.1551	521	0.1563
18	48.0	0.1655	004	0.1650	601	0.1651		

Table VII

Minimum-energy positions of polyacenaphthylene

φ_1	φ_2	E_{tot} (kcal/mole)	R° (Å)	Φ (deg.)	D (Å)	Type of helix	Note
2	—	21.67	1.939	52.06	1.912	7_1	isotactic threo
150	—	22.46	0.987	140.80	1.759	5_2	,, ,,
208	—	17.35	0.737	166.91	2.100	2_1	,, ,,
283.5	—	32.86	0.566	107.61	2.391	10_3	,, ,,
100	100	17.20	0.785	175.53	3.614	2_1	syndiotactic threo
0	90	27.04	1.196	—	3.667	c	,, ,,
60	120	21.61	2.597	89.6	2.600	4_1	,, ,,
300	332	63.22	1.207	167.53	3.807	2_1	erythrothreo

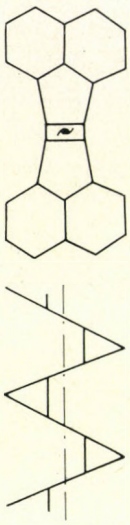

Fig. 5. Structure of the lowest-energy chain of isotactic *threo*-polyacenaphthylene

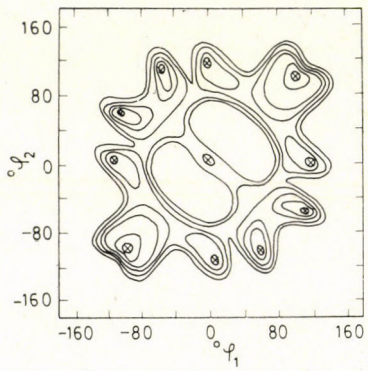

Fig. 6. Conformation energy of syndiotactic *threo*-polyacenaphthylene as a function of dihedral angles φ_1 and φ_2. Level lines refer to energy differences of 5 kcal/mole. First line corresponds to 40 kcal/mole (E_{total})

to the structure of that characterized by 2_1 helix in a previous paper (Fig. 5). However, the period of the polymer chain is considerably smaller than 3.8 Å of the diffractograms.

In Fig. 6, the conformation energy of *threo*-syndiotactic poly-ACN is plotted against dihedral angles φ_1 and φ_2. Characteristic data of the polymer chains corresponding to the minima of this symmetrical diagram are also collected in Table VII. Because of the symmetry conditions of the diagram

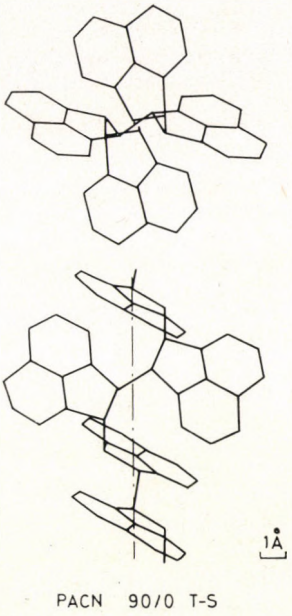

Fig. 7. Structure of the syndiotactic *threo*-polyacenaphthylene chain of dihedral angles of 0/90 deg.

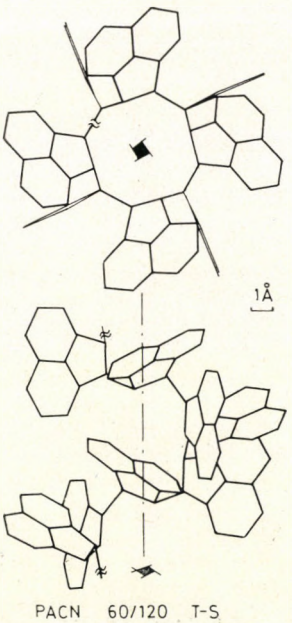

Fig. 8. Structure of the syndiotactic *threo*-polyacenaphthylene chain of dihedral angles of 60/120 deg.

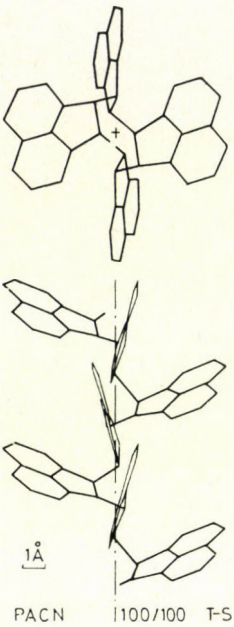

Fig. 9. Structure of the syndiotactic *threo*-polyacenaphthylene chain of dihedral angles of 100/100 deg.

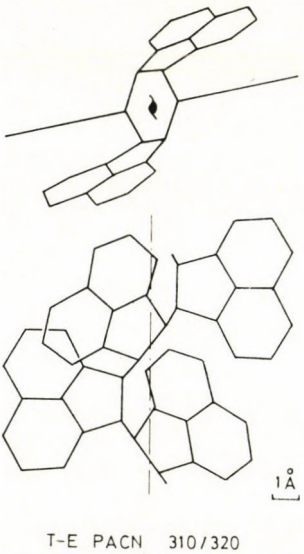

Fig. 10. Structure of a minimum-energy *erythro-threo*-polyacenaphthylene chain

(2 perpendicular mirror planes), three kinds of polymer chains correspond to the ten minima. Dihedral angles of 0/90, 0/—90; 60/120, —60/—120, 60/—120, — 60/120; and 100/100, —100/—100 refer to polymers characterized by a series of symmetry centres (Fig. 7); by 4_1 helix (Fig. 8); and 2_1 helix (Fig. 9) respectively.

For isotactic chains of *erythro* segments, no value of angle yielded a chain which had the atoms of its third—fifth monomer units not excessively close to the first one. Only a single such site was found in polymer chains consisting of pairs of *erythro* and *threo* monomer units. Its data are also included in Table VII. However, conformation energy is rather high, thus the structure of the monomer unit must be changed in the presence of such a segment. Because of the steep potential hollow, no rotation is possible around the bond. The polymer is demonstrated in Fig. 10.

Discussion

Packing coefficient of the polymer with the highest density (*i.e.* the oligomer) is comparable to that of crystalline monomer (0.6971) or, in general, the crystalline aromatic compounds. Molecular volume of the amorphous polymer calculated from the atomic volumes of SLONIMSKII [9] and that of VAN KREVELEN and HOFTYZER [11] is quite the same. The corresponding densities are 1.055 g · cm^{-3} and 1.012 g · cm^{-3} (according to SLONIMSKII and VAN KREVELEN resp.) are essentially lower than the lowest measured value. By calculating the density of the amorphous polymer from that of the oligomer, which is still crystalline [11], 1.069 g · cm^{-3} was obtained. It is only slightly higher than that estimated by the atomic volumes. It can, therefore, reasonably be supposed that the oligomer prepared by iodine initiation has a high degree of crystallinity. It seems to be proved by the good agreement between densities calculated from cell data and measured by the flotation method. On the contrary, the density of the most disordered polymer formed in the liquid state by radical initiation is even considerably higher than that estimated for the amorphous polymer.

In powder diffractograms of poly- and oligo-acenaphthylenes, two peaks are always present ($d_1 = 3.8$, $d_2 = 5.3$ Å) [2]. The former one corresponds to the translation unit of the chain period, *i.e.* to the elongation D along the helix axis with a repeated turning by Φ angle. From the result of conformational analysis those values are accepted to approximate the realities which fullfil this condition.

This condition is not met in isotactic polymers as appears from the data of Table VII, while is realized in two syndiotactic polymers (dihedral angles 0/90 and 100/100), and in the polymer built up from *threo* and *erythro* segments.

The three-polymer structure is very similar (Figs 7, 9 and 10) in spite of the great difference in the steric arrangement of the atoms. Construction of the polymer chain assigned to the minimum point of conformation-energy functions of syndiotactic polymer chains approximates the 2_1 helix, thus, it is most likely that this is the polymer chain which forms the crystal lattice of the oligomer prepared by iodine initiation. The crystal lattice having the 2_1 helix angle placed in the 2_1 axis of the lattice is shown in Fig. 11. It was checked by calculations that atomic distances between the adjacent chains were not smaller than the sum of van der Waals radii of the atoms.

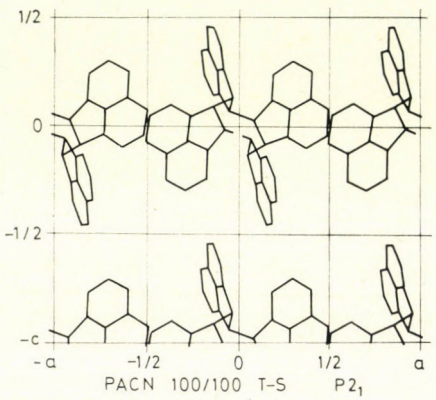

Fig. 11. Location of the lowest-energy syndiotactic *threo*-polyacenaphthylene in the unit cell of the oligomer

An additional feature of the chain shown in Fig. 9, is that it can be related directly to the crystal lattice of the monomer. This relation is conspicuous when the chain axis of the polymer is parallel to the axis x of the monomer crystal (7.679 Å) and intersects the plane $y-z$ at the point of $y = 0.25$, $z = 0.25$. In this case, monomer units of the polymer are shifted, with respect to their locations in the monomer crystal, in the plane of the molecule toward the chain axis of the polymer. This polymer chain can, therefore, remain isomorphous with the monomer crystal without any difficulties. However, the slight differences between the two structures make the existence of a whole isomorphous series impossible. Thus the isomorphism is limited in time according to the observations [5].

In the isotactic model, the polymer chains are extremely rigid. The energy barrier between two adjacent conformation state *(e.g.* between 2_1 and 4_1 helix) exceeds 20 kcal/mole. In the syndiotactic model, however, the energy barriers between the minima are as low as 5 to 10 kcal/mole. Although a polymer chain is capable of transformation from one conformation state to another in solution (sequential lengths are relatively small), the energy barrier is too

high and prevents the realization of the same conformation along the whole chain during the precipitation which would be needed for the crystallization (tertiary nucleation [12]). The 'particle size' estimated by the line widths is about 30 Å, indicating that at least one monomer unit of an average periodicity of 20 has a conformation different from that of the main chain. For an actual polymer, therefore, only the average periodicity of the chains and their fitting as cylinders appear in diffractograms (10.8 Å). The latter identity period is consistent with the plane diagonal a-c of pseudo-orthorhombic oligomer cell, suggesting a tetragonal arrangement of the ordered polymer (dihedral angle of 60/120 dg.).

The wave number of C–H valence vibrations in infrared spectra depends on the interaction between the H atoms bonded the adjacent C atoms. STORY and CANTY [4] tried to determine the conformation of the main chain of polyacenaphthylene by means of the infrared spectrum of *cis*- and *trans*-decalene. Frequencies of the C–H valence vibration of the main chain are in the range of 2800 to 3000 cm^{-1}. Polymers formed in the liquid state by ZIEGLER—NATTA catalysts show a composite band of several lines [2]. Oligomers and polymers prepared in the solid state by iodine and radiation initiation, respectively, give a relatively broad band at about 2900 cm^{-1}. This band has a higher frequency than that of *trans*-decalene (2842 cm^{-1}) but lower than that of *cis*-decalene (2924 cm^{-1}). Within the three-monomer unit H–C–C–H dihedral angle is 54 deg. while that within the polymer chain agrees in magnitude with the dihedral angle of the main chain, *i.e.* 100 deg. for 100/100 conformation. The two hydrogen atoms in the ring may vibrate at a lower frequency since the dihedral angle is smaller (is nearer to the trans-situation). On the other band, its frequency may also be higher because of the increasing effect of the five-membered monomer ring on the frequency. This is the reason of overlapping of the two bands. The vibration of higher frequency ($\nu' = 2955$ cm^{-1}) observed for less regular polymers may presumably be associated with the *erythro* segments. At the same time, the vibration frequency of $\nu' = 2855$ cm^{-1} (a shoulder for $TiCl_3$ and a peak for ZIEGLER catalysts) may correspond to the CH vibration of isotactic segments of 0/90 conformation having a dihedral angle of 208°.

By comparison of the above data, it can be stated that the polymer formed in the solid state by radiation-induced polymerization is a *threo–threo* syndiotactic chain with 2_1 helix structure — solely due to the solid-state reaction — which structure is occasionally replaced by chain segments with centres of symmetry, being similar to the 2_1 helix. The oligomer prepared in the solid state by iodine initiation is highly crystalline, consisting of microcrystals of pseudo-orthorhombic cells of monoclinic $P2_1$ space group in form of a *threo-threo* syndiotactic 2_1 helix chain.

REFERENCES

[1] CSER, F.: Acta Chim. (Budapest) **80,** 317 (1974)
[2] HARDY, GY., KOVÁCS, G., CSER, F., KOSZTERSZITZ, GY.: Acta Chim. (Budapest) **75,** 303 (1973)
[3] BARRALES-RIENDA, J. M., PEPPER, D. C.: Polymer **8,** 337 and 351 (1967)
[4] STORY, W. M., CANTY, G.: J. Res. Natl. Bur. Stand. A**68,** 165 (1964)
[5] HARDY, GY.: Solid-State Polymerization in Two-component Systems. IUPAC. Int. Symp. on Macromol. Chem., Budapest (1969) p. 571.
[6] HARDY, GY., CSER, F., KOVÁCS, G., SZATMÁRI, J., SAMAY, G.: Acta Chim. (Budapest) **79,** 143 (1973)
HARDY, GY., KOVÁCS, G., KOSZTERSZITZ, G., CSER, F.: Proc. 3rd Tihany Symp. of Radiation Chemistry. Akadémiai Kiadó Budapest, 1972, p. 601
HARDY, GY., CSER, F., TAKÁCS, E.: J. Polym. Sci. C **42,** 663 (1973)
[7] DE SANTIS, P., GIGLIO, E., LIQUORI, A. M., RIPAMONTI, A.: J. Polym. Sci. **A1,** 1383 (1963)
[8] DEL RE, G.: J. Chem. Soc. **1958,** 4031
[9] SLONIMSKII, F. L., ASKADSKII, A. A., KITAIGORODSKII, A. I.: Vysokomol. Soed. **A 13,** 494 (1970)
[10] NATTA, G., CORRADINI, P., GANIS, P.: Polym. Sci. **58,** 1191 (1962)
BIRSHTEIN, T. M., PTITSYN, O. B.: 'Conformations of Macromolecules'. Interscience, New York 1966. pp. 56—57
[11] VAN KREVELEN, D. W., HOFTYZER, P. J.: J. Appl. Polym. Sci. **13,** 875 (1969)
[12] LINDENMEYER, P. H.: Polymer. J. **3,** 507 (1972)

Ferenc CSER
Gyula HARDY } H-1950 Budapest, Hungária körút 114. Hungary.

Acta Chimica Academiae Scientiarum Hungaricae, 84 (3), pp. 313—317 (1975)

CATALYTIC PROPERTIES OF MAGNESIUM FLUORIDE

M. WOJCIECHOWSKA, R. FIEDOROW and W. KUCZYŃSKI

(Institute of Chemistry, A. Mickiewicz University, Poznań, Poland)

Received March 6, 1974; in revised form, September 22, 1974

The properties of porous magnesium fluoride obtained by the action of hydrofluoric acid on a solution of magnesium sulphate are described. Samples of magnesium fluoride calcined at various temperatures were investigated for catalytic properties in some model reactions. Some conclusions concerning the nature of acid sites on the magnesium-fluoride surface are given.

Magnesium fluoride, owing to its high thermal stability, chemical inertness, revealed, among others, by its resistance to calcination in oxygen and relatively high hardness (6 on Mohs' scale), is a substance well adapted for use as catalyst support. Despite these merits, we know of but a single paper [1] on the preparation of magnesium fluoride in porous form. That investigation was restricted, however, to the adsorptive properties of magnesium fluoride xerogel dried at 120—150°C. There is still a lack of data relating to the properties of porous MgF_2 calcined at the higher temperatures essential for catalysis. Nor are there data available on the capability of the MgF_2 surface to catalyze chemical reactions.

Magnesium fluoride catalysts for our catalytic investigation were prepared by the action of hydrofluoric acid on a solution of magnesium sulfate. After preliminary tests, we decided on a 40% $MgSO_4$ solution to which, on heating to 40°C, we added a 40% solution of hydrofluoric acid. The precipitate was left in contact with the mother liquor for 24 hrs. The remaining solution was then decanted and the precipitate washed with distilled water, dried at 105°C for 5 hrs, and divided into portions which were calcined, respectively, at 315, 400, 500, 700, 900 and 1100°C in an atmosphere of air.

The surface area of the MgF_2 preparation was determined chromatographically with a 212C Perkin-Elmer sorptometer. The carrier gas was helium, the adsorbate – nitrogen.

The catalytic activity of the MgF_2 sample was studied in the reaction of cumene cracking as well as in that of cyclohexene isomerization and the concomitant reaction of hydrogen disproportionation. The conditions of measurements were the same as those described in Ref. [2]. In all cases, the catalytic activity was expressed in terms of the product kK of the BAS-

SETT—HABGOOD equation [3]. The total surface acidity was measured chromatographically by titration with pyridine at the temperature where the catalytic activity tests were performed. However, assessment of the occurrence of Broensted acid sites was based on titration at the same temperature (315°C) with 2,6-lutidine by the method recently proposed by BENESI [4] for selective poisoning of proton centres.

The surface area of the magnesium fluoride preparations calcined in the 300—500°C range amounted to some tens of m^2/g. Upwards of 400°C, however, some slight decrease in surface area was observed (Table I). Upwards of 500°C, intense sintering of the fine pores takes place and the surface area decreases drastically. Sintering in the temperature range investigated (300 - 1100°C) is accompanied by an increase in bulk density by nearly 20%. Nevertheless, the increase in compactness of the sample apparent as an increase in bulk

Table I

Surface area and bulk density of magnesium fluoride preparations

Catalyst	Temperature [°C]	Colour	Surface area [m^2/g]	Bulk density [g/cm^3]
MF-3	315	Darkish sand-coloured	40.5	0.89
MF-4	400	Sand-coloured	40.8	0.91
MF-5	500	Light sand-coloured	33.4	0.95
MF-7	700	Orange-pink	5.0	0.99
MF-9	900	Pinkish	0.8	1.01
MF-11	1100	Light cream-coloured	0.3	1.05

Table II

Surface acidity of the investigated preparations, determined by chromatographic titration at 315°C

Catalyst	Titration with 2,6-lutidine		Titration with pyridine	
	[μmol/g]	[μmol/m^2]	[μmol/g]	[μmol/m^2]
MF-3	13.3	0.33	17.2	0.42
MF-4	8.7	0.22	49.5	1.21
MF-5	0.0	0.00	0.0	0.00
MF-7	0.0	0.00	0.0	0.00
MF-9	0.0	0.00	0.0	0.00
MF-11	0.0	0.00	0.0	0.00
A-9.5/VIII*	1.1	0.01	26.9	0.20

* Alumina with a surface area of 134 m^2/g, for details see Ref. [2].

density, is in no simple relation with its mechanical resistance. The latter property was found to increase only up to a thermal processing temperature of 700°C, whereas a further rise in temperature led to a decrease in mechanical resistance.

The surface properties of magnesium fluoride were found by us to present certain similarities with those of active alumina (Table II). The Lewis nature of their surface is, however, less marked than in the case of alumina, where proton acidity is negligible. As it is shown by titration with 2,6-lutidine (which, for steric reasons, undergoes specific adsorption at the Broensted acid sites [4]), the total surface acidity of MgF_2 contains a contribution from proton-donor centres. The latter, in the present case, may consist of an admixture of surface-hydroxyl groups introduced in the process of preparation whose ionization ability is enhanced by neighbouring electronegative fluorine atoms.

The results listed in Table III show that the most active of the magnesium fluoride preparations, namely the catalyst MF-3, is markedly less active with regard to cumene cracking than the silica-alumina catalyst of the cracking reaction. However, the cracking activity values referred to unit surface area of the catalyst suggest that the concentration of proton-donor centres on the surface of magnesium fluoride is high.

Contrary to their rather low cracking activity, the low-temperature magnesium fluoride preparations (MF-3 and MF-4) reveal a considerable activity in another model reaction of acid catalysis, *viz.* of isomerization cyclohexene to methylcyclopentenes, taking place on alumina with the participation of Lewis centres [5]. MF-4 is markedly the more active preparation of the two, whereas with regard to the amount of bonded 2,6-lutidine, the

Table III

Catalytic activity of the investigated preparations in the process of cumene cracking at 315°C

Catalyst	$kK\left[\frac{mol}{g\ s\ atm}\right]\times 10^6$	$kK\left[\frac{mol}{m^2\ s\ atm}\right]\times 10^7$
MF-3	9.32	2.3
MF-4	−0.36	0.1
MF-5	0.00	0.0
MF-7	0.00	0.0
MF-9	0.00	0.0
MF-11	0.00	0.0
A-9, 5/VIII	0.00	0.0
Standard I*	15.94	0.7

* Commercial silica—alumina catalyst, for details see Ref. [6].

Table IV

Catalytic activity of the investigated preparations in skeletal isomerization and hydrogen- disproportionation reactions at 315°C

Catalyst	Isomerization		Hydrogen disproportionation	
	$kK\left[\frac{mol}{g\ s\ atm}\right]\times10^{6}$	$kK\left[\frac{mol}{m^2\ s\ atm}\right]\times10^{7}$	$kK\left[\frac{mol}{g\ s\ atm}\right]\times10^{5}$	$kK\left[\frac{mol}{m^2\ s\ atm}\right]\times10^{7}$
MF-3	0.85	2.1	0.82	2.0
MF-4	2.67	6.5	0.51	1.3
MF-5	0.00	0.0	0.00	0.0
MF-7	0.00	0.0	0.00	0.0
MF-9	0.00	0.0	0.00	0.0
MF-11	0.00	0.0	0.00	0.0
A-9.5/VIII	2.03	1.5	0.37	0.3

situation is reversed. This would suggest that, in the case of MgF_2 too, the isomerization of cyclohexene proceeds at Lewis acid sites.

Preparations MF-3 and MF-4 were also found to be effective catalysts of the concomitant reaction of hydrogen disproportionation (transformation of cyclohexene into the corresponding saturated hydrocarbon and simultaneous formation of 'coke' — a product poor in hydrogen).

In order to characterize more closely the nature of the MgF_2 surface, we have performed assays for the presence of active sites promoting model reactions such as ethanol dehydration, oxidation of iodides to iodine, nitrous oxide decomposition and oxidative dehydrogenation of ethylbenzene. Alumina, depending on the manner of its preparation, is a catalyst of all these reactions, although the oxidation of iodide anions [2] takes place only on alumina samples containing a well defined admixture of sulfates. Magnesium fluoride turns out to be active only with respect to alcohol dehydration; hence, its surface contains no centers active in the other reactions mentioned.

Conclusions

(i) On the surface of magnesium fluoride, Lewis as well as Broensted acid sites are present; the contribution of the latter to the total acidity of the catalyst is higher than on alumina but lower than on silica-alumina catalyst.

(ii) On calcination at about 500°C the acid sites of magnesium fluoride undergo destruction; such thermal processing deprives MgF_2 of its activity as catalyst for cracking and skeletal isomerization of hydrocarbons and for hydrogen disproportionation.

REFERENCES

[1] SHENFAIN, R. YU., STAS, O. P., NEIMARK, I. E.: Kolloid Zh. **31,** 922 (1969)
[2] FIEDOROW, R., KANIA, W., KUCZYŃSKI, W., WIĘCKOWSKI, A.: Proc. Fifth Intern. Congr. Catalysis, vol. 2, p. 1455. North-Holland Publ. Co., Amsterdam 1973
[3] BASSETT, D. W., HABGOOD, H. W.: J. Phys. Chem. **64,** 769 (1960)
[4] BENESI, H.: J. Catal. **28,** 176 (1973)
[5] PINES, H., HAAG, W. O.: J. Amer. Chem. Soc. **82,** 2471 (1960)
[6] KUCZYŃSKI, W., ADAMIEC, J., WOLNIEWICZ, A.: Roczniki Chem. **44,** 1787 (1970)

Maria WOJCIECHOWSKA
Ryszard FIEDOROW
Wieńczysław KUCZYŃSKI

Instytut Chemii UAM, ul. Grunwaldzka 6, 60-780 Poznan, Poland.

Acta Chimica Academiae Scientiarum Hungaricae, 84 (3), pp. 319–324 (1975)

4-PYRONES, VII*

FURTHER REACTIONS OF 4-PYRONES

M. A.-F. ELKASCHEF, F. M. E. ABDEL-MEGEID, K.-E. M. MOKHTAR and F. A. GAD

(National Research Centre, Dokki, Cairo, Egypt)

Received February 19, 1973; in revised form, July 22, 1974

4-Alkylidene(4H)pyran has been prepared by the reaction of diazoalkanes with 4-thiopyrones. 5,6-benzoflavone with phenyl- or benzyl-magnesium halides afforded 4,4-diphenyl or 4,4-dibenzyl derivatives, while this compound with *p*-methoxyphenyl-magnesium bromide, and 2-methylchromone with phenylmagnesium bromide afforded the corresponding 4-hydroxy-compounds.

2-Styrylchromones were found to react thermally or photochemically to give maleic anhydride or naphthoquinone adducts.

4-Pyranylideneacetamides and 4-(aminoalkylidene)-pyrans are known to be potent drugs [2, 3]. We tried to prepare 4-pyranylideneacetic acid estertype compounds by reacting carbethoxymethyltriphenylphosphonium halide with 9-xanthone, 2-chloro- and 2-bromo-xanthone, 2,6-dimethyl- and 2,6-diphenyl-4-pyrone, flavone, and 5,6-benzoflavone, but obtained only the starting substances. This result was not unexpected owing to the low reactivity of the carbonyl group. When ethyl- or methyl-triphenylphosphonium iodide was tried with these same compounds, the starting ketones were also obtained together with ethyl- or methyl-diphenylphosphine oxide **Ia** or **b** [4].

4-Pyranylideneacetic acids were, however, prepared by the action of diazoacetic acid ester on thiopyrones in the presence of copper bronze and subsequent saponification of the esters obtained. Thus, 2-chloro- and 2-bromo-xanthylideneacetic acids (**IIa** and **b**, R = H) and 2-(*p*-chlorostyryl)-4-chromenylideneacetic acid (**III**, R = H) were prepared.

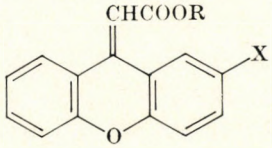

II

a: X = Cl, *b:* X = Br

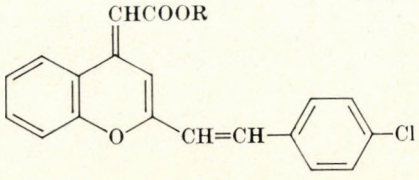

III

* Part VI, see Ref. [1].

2-Methyl-4-thiochromone with diazomethane, as usual, gave dithiol methylene ether (**IV**).

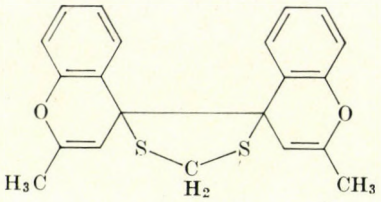

IV

The change of the carbonyl group into an ethylenic group could also be effected by changing the former into a thiocarbonyl group followed by treatment with copper bronze. Thus 2,2'-dichloro- and 2,2'-dibromo-9,9'-dixanthylidenes (**Va** and **b**) were obtained.

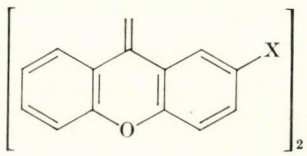

V

a: X = Cl, *b*: X = Br

2-Nitro-4-xanthione, when treated in the same way, afforded 2-nitro-4-xanthone, perhaps by atmospheric oxidation, while 2-(*p*-chlorostyryl)-4-thiochromone was recovered unchanged.

5,6-Benzoflavone, when treated with benzylmagnesium bromide, afforded 4,4-dibenzylflavone (**VIb**) instead of the expected 4-hydroxy derivative which we intended to dehydrate to the corresponding 4-benzylidene-5,6-benzoflavone.

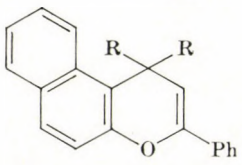

VI

a: R = Ph, *b*: R = CH_2Ph

Half of the amount of the Grignard reagent afforded both **VIb** and unchanged benzoflavone. The double substitution may be due to the increased reactivity of the initially formed, ionized Grignard complex (*A*) because of

direct attachment of the reaction center to two aryl groups and conjugation with a third phenyl group *(cf.* ionization of triarylmethanes [5]).

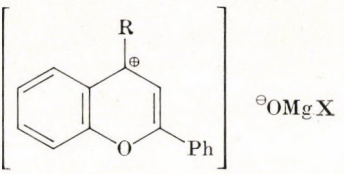

A

This explanation is supported by the reaction of phenylmagnesium bromide with 2-methylchromone (one phenyl group less) which gave 2-methyl-4-phenylchromen-4-ol (**VII**), and the action of *p*-methoxyphenylmagnesium bromide on 5,6-benzoflavone where the *p*-methoxyphenyl group will partially neutralize the positive charge on C-4 preventing further attack and enabling the formation of compound **VIII**.

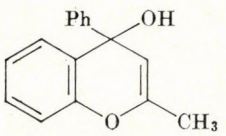

VII

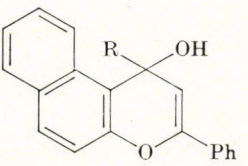

VIII

R = $C_6H_4OCH_3$ (*p*–)

2-(*o*-, *m*-, or *p*-chlorostyryl)-4-chromone, when boiled with maleic anhydride in xylene, afforded adducts **IX** *(cf.* Ref. [6]).

The *ortho*-chloro derivative, on hydrolysis with sodium hydroxide, afforded the corresponding dicarboxylic acid. From a similar reaction using naphthoquinone with 2-(*o*-chlorostyryl)-4-chromone, we obtained the corresponding adduct **X**.

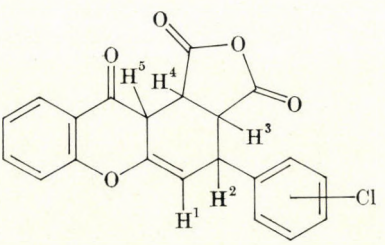

IX

The same reaction could be effected photochemically by irradiation of 2-styryl-4-chromone and maleic anhydride in the presence of benzophenone as sensitizer, leading to adduct **IX** (H instead of Cl) [6].

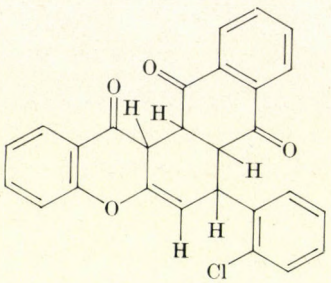

X

Experimental

Melting points are uncorrected and have been measured on a Kofler microscope. Microanalyses were performed by the Microanalytical Laboratory, N.R.C., Egypt. The IR spectra were measured in KBr. Light petroleum used, b.p. 70—80°C, unless otherwise indicated.

Reaction of carbethoxymethyltriphenylphosphonium bromide with 4-pyrones

2,6-Dimethyl-, 2,6-diphenyl 4-pyrone, 2-boromo- and 2-chloro-xanthone, 5,6-benzoflavone, N-methyl- or N-ethyl-pyridone in dry dioxane, when treated with a solution of carbethoxymethyl-triphenylphosphonium bromide [7] in absolute ethanol in the presence of sodium ethoxide, were recovered unchanged.

Reaction of methyl- and ethyl-triphenylphosphonium iodide with 4-pyrones

When a solution of flavone, 5,6-benzoflavone, xanthone, 2-chloro-, 2-bromo- or 2-nitro-xanthone in dioxan was added to a solution of methyl- or ethyl-triphenylphosphonium iodide in absolute ethanol, in the presence of lithium ethylate, only methyldiphenylphosphine oxide (m.p. and mixed m.p. [4]: 108°C) or ethyldiphenylphosphine oxide (m.p. and mixed m.p. [4]: 121°C) was isolated.

Reaction with ethyl diazoacetate

A mixture of 2-chloro-, 2-bromo-xanthone, or 2-(*p*-chlorostyryl)-thiochromone (0.015 mol) with ethyl diazoacetate (4.5 ml) in dry xylene (125 ml) was refluxed for 30 min in presence of copper bronze (3.5 g) under carbon dioxide atmosphere. The reaction mixture was filtered and evaporated to dryness. The residue was dissolved in a mixture of ethanol (125 ml) and sodium hydroxide (45 ml 8% solution), refluxed for 2 hrs, concentrated and acidified with hydrochloric acid. The corresponding carboxylic compounds were obtained.

2-Chloroxanthione gave **IIb** in 65% yield; m.p. 191°C (ethanol). $C_{15}H_9ClO_3$ (272.5). Calcd. C 66.05; H 3.30; Cl 13.03. Found C 66.53; H 3.74; Cl 13.08%. IR 1700 cm^{-1} (COOH), 3450 cm^{-1} (OH).

2-Bromocanthione gave **IIb** in 70% yield; m.p. 180—1°C (decomp.) (benzene). $C_{15}H_9BrO_3$ (317). Calcd. Br 25.24. Found Br 25.20%.

2-(*p*-Chlorostyryl)-4-thiochromone gave **III** in 42% yield; m.p. 272°C $C_{19}H_{13}ClO_3$ (324). Calcd. Cl 10.94. Found Cl 10.00%.

Reaction of diazomethane with 2-methyl-4-thiochromone

2-Methyl-4-thiochromone (0.5 g, 0.0028 mol) in dry benzene (50 ml) was added to a solution of diazomethane (from 30 g nitrosomethylurea). The reaction mixture was kept in the ice chest for 2 days and then at room temperature for another 2 days. The solvents were distilled off and the residual solid (0.3 g, 25%) was crystallized from ether (colourless crystals). 4,4'-di-(2-methylchromenylidene)-4,4'-dithiol methylene ether (**IV**) melted at 168°C. $C_{21}H_{18}O_2S_2$ (366.) Calcd. C 68.85; H 4.92; S 17.9. Found C 68.83; H 5.05; S 17.43%. IR 770 cm^{-1} (CH_2).

Action of copper bronze on thiones

A mixture of 2-chloro-, 2-bromo-, 2-nitro-xanthone or 2-(*p*-chlorostyryl)-4-thiochromone (0.008 mol) in dry xylene (100 ml) with copper bronze (2.5 g) was refluxed for 8 hrs. The reaction

mixture was filtered while hot and a solid was formed on cooling. It was crystallized from the proper solvent.

2-Chloroxanthione gave **Va** in 45% yield; m.p. 308°C [8] (xylene); IR 1085 cm^{-1} (Cl), 1620 cm^{-1} (>C=C<).

2-Bromoxanthione gave **Vb** in 40% yield; m.p. 300°C (xylene). $C_{26}H_{14}Br_2O_2$ (518). Calcd. Br 30.89. Found Br 30.21%. IR 1070 cm^{-1} (Br), 1620 cm^{-1} (>C=C<).

2-Nitroxanthione gave 2-nitroxanthone but 2-(*p*-chlorostyryl)-4-thiochromone did not react.

Reactions of Grignard reagents with 2-methylchromone and with 5,6-benzoflavone

A solution of 2-methylchromone or 5,6-benzoflavone in dry benzene was added to a cold solution of arylmagnesium halide and the reaction mixture was refluxed for 4 hrs, cooled and decomposed with a mixture of crushed ice and dilute hydrochloric acid. The mixture was extracted with ether and the ethereal extract was evaporated. The residue was crystallized from the proper solvent.

5,6-Benzoflavone (2.7 g; 0.01 mol) with (i) phenylmagnesium bromide (0.03 mol), after 4 hrs of refluxing gave 4,4-diphenyl-5,6-benzoflavone (**VIa**) (1.5 g; 37%); m.p. 190–1°C (methanol). $C_{31}H_{22}O$ (410). Calcd. C 90.73; H 5.37. Found C 90.57; H 5.26%. IR showed no OH or C=O bands.

The same reaction, when repeated using 0.015 mol of phenylmagnesium bromide, gave the starting substance.

(ii) Benzylmagnesium chloride (0.03 mol), after 4 hrs of refluxing gave 4,4-dibenzyl-5,6-benzoflavone (**VIb**) (2.0 g; 46%); m.p. 128°C (methanol). $C_{33}H_{26}O$ (438). Calcd. C 90.41; H 5.94. Found C 90.45; H 5.68%. IR showed no OH or C=O bands.

(iii) Benzylmagnesium chloride (0.015 mol), after 10 hrs of refluxing afforded **VIb** (0.5 g; 12%) and 1.6 g of unchanged 5,6-benzoflavone.

(iv) *p*-Methoxyphenylmagnesium bromide (0.03 mol), after 4 hrs of refluxing afforded 4-(*p*-methoxyphenyl)-5,6-benzoflavone-4-ol (**VIII**) (2.1 g; 55.3%); m.p. 165°C (methanol). $C_{26}H_{20}O_3$ (380). Calcd. C 82.10; H 5.26. Found C 82.27; H 5.04%. IR 3445 cm^{-1} (OH).

2-Methylchromone (3.2 g; 0.02 mol) with phenylmagnesium bromide (0.1 mol), after 4 hrs of refluxing gave 4-phenyl-2-methylchromen-4-ol (**VII**); m.p. 177°C (methanol); (0.8 g; 16%). $C_{16}H_{14}O_2$ (238). Calcd. C 80.67; H 5.88. Found C 81.03; H 5.76%. IR 3450 cm^{-1} (OH).

2-(o-, m-, and p-chlorostyryl)-4-chromone

To a solution of 2-methyl-4-chromone (1.5 g; 0.009 mol) in absolute ethanol (50 ml), chlorobenzaldehyde (1.5 g; 0.01 mol) and sodium metal (0.2 g; 0.009 mol) were added. The reaction mixture was filtered after 12 hrs. The solid was washed with alcohol and then boiled with aceticacid (5 ml) and filtered.

2-(*o*-Chlorostyryl)-4-chromone crystallized from benzene to give 69% yield, yellow crystals; m.p. 191°C. $C_{17}H_{11}ClO_2$ (282.5). Calcd. C 72.1 H 3.89; Cl 12.57. Found C 72.22; H 4.46; Cl 12.23%. IR 1080 cm^{-1} (Cl), 1620 cm^{-1} (>C=C<), 1675 cm^{-1} (>C=O<). NMR δ 6.3 (CH=CH, doublet, 15 cps), δ 6.83 (>CO–CH=C, singlet), aromatic protons higher than δ 7.0.

2-(m-Chlorostyryl)-4-chromone; m.p. 162°C (benzene) in 65% yield. (Found C 72.31; H 4.00; Cl 12.20%). IR 1085 cm^{-1} (Cl), 1670 cm^{-1} (>C=C<), 1675 cm^{-1} (>C=O<).

2-(*p*-Chlorostyryl)-4-chromone, 226°C (benzene), was obtained in 61% yield. (Found C 72.16; H 4.14; Cl 12.62%). IR 1095 cm^{-1} (Cl), 1670 cm^{-1} (>C=O<).

A solution of 2-(*o*-, *m*- or *p*-chlorostyryl)-4-chromone (0.01 mol) and maleic anhydride (4 g; 0.04 mol) in xylene (30 ml) was refluxed for 12 hrs, concentrated and cooled. The precipitate formed was isolated, washed with ethanol and crystallized from xylene.

2-(*o*-Chlorostyryl)-4-chromone gave adduct **IXa** in 43% yield; m.p. 270°C (xylene). $C_{21}H_{13}ClO_5$ (380.5). Calcd. C 66.23; H 3.42; Cl 9.33. Found C 66.70; H 3.72; Cl 8.99%. IR 1655 cm^{-1} (>C=O) 1730 and 1760 cm^{-1} (–CO–O–CO–).

Compound **IXa**, when hydrolyzed with sodium hydroxide in aqueous methanol and acidified with hydrochloric acid, affordid the corresponding dicarboxylic acid in 60% yield; m.p. 257°C (methanol). $C_{21}H_{15}ClO_6$ (398.5). Calcd C 63.80; H 3.76. Found C 63.93; H 3.73%. IR 1720 cm^{-1} (COOH), 3100 cm^{-1} wide band (OH).

2-(*m*-Chlorostyryl)-4-chromone gave adduct **IXb** in 67% yield; m.p. 240°C (xylene). (Found Cl 8.75%.) NMR δ 2.05 (H_2, doublet, 3 cps), δ 2.93 (H_3 doublet, 3 cps), δ 3.40 (H_4,

doublet, 3 cps), δ 3.91 (H_5 doublet, 9 cps), δ 7.78 (H_1, doublet, 9 cps), aromatic protons higher than δ 7.0.

2-(*p*-Chlorostyryl)-4-chromone gave adduct **IXc** in 70% yield, m.p. 230°C (decomp.) (xylene). (Found Cl 9.40%.) IR 1655 cm^{-1} (>C=O), 1785 cm^{-1} (—CO—O—CO—).

Formation of the p-naphthoquinone adduct

2-(*o*-Chlorostyryl) chromone (0.01 mol) and *p*-naphthoquinone (0.015 mol) were fused together for 10 hrs under carbon-dioxide atmosphere. The fused mass, after cooling, was extracted with xylene. The xylene was evaporated and the residual oil solidified under ether to give adduct **X** in 90% yield; m.p. 250°C (ethanol). $C_{27}H_{17}ClO_4$ (440.5). Calcd C 73.55; H 3.85. Found C 73.75; H 4.07%.

Photochemical preparation of the maleic acid anhydride adduct

2-Styrylchromone (3 g; 0.012 mol), benzophenone (3 g; 0.016 mol) and maleic acid anhydride (5 g; 0.05 mol) were irradiated with an HPK 125 W Philips lamp for 50 hrs in dioxane (350 ml). The solvent was evaporated and the residual solid (**IX**, H instead of Cl) (0.2 g; 5%) cry stallized from xylene; m.p. and mixed m.p. [6] 246°C.

REFERENCES

[1] Part VI: ELKASCHEF, M. A.-F., ABDEL-MEGEID, F. M. E., MOKHTAR, K.-E. M., ELBARNASHAWI, M. F.: Ind. J. Chem. **11,** 860 (1973)
[2] BONVICINO, G. E., ARLT Jr., H. G., PEARSON, K. M., HARDY Jr., R. A.: J. Org. Chem. **26,** 2383 (1961); C. A. **55,** 27 340c (1961)
[3] F. Hoffman-La Roche and Co. Akt.-Ges., By G. REY-BELLET and H. SPIEGELBERG, Swiss Pat. 346,892, July 30, 1960. C. A. **55,** 16 570 e—g (1961)
[4] MICHAELIS, A., SODEN, V.: Annalen **229,** 310 (1885)
[5] ELKASCHEF, M. A.-F., AHMED, A. S.: J. Chem. Soc. 2272 (1960);
ELKASCHEF, M. A.-F., NOSSEIR, M. H., M. MOHAMED, H. E.: J. Chem. Soc. 494 (1965)
[6] SCHÖNBERG, A., MUSTAFA, A., AZIZ, G.: J. Amer. Chem. Soc. **76,** 4576 (1954)
[7] WITTIG, G., HAAG, W.: Chem. Ber. **88,** 1654 (1955)
[8] SCHÖNBERG, A., MUSTAFA, A., SOBHY, E.: J. Amer. Chem. Soc. **75,** 3377 (1953)

Mohamed A.-F. ELKASCHEF; Dépt. de Chimie, Faculté des Sciènces, Université d'Alger, 2, Rue Didouche-Mourad — Alger, Algérie.

F. M. E. ABDEL-MEGEID
K.-E. M. MOKHTAR
F. A. GAD
} National Reserach Centre, Dokki, Cairo, Egypt.

Acta Chimica Academiae Scientiarum Hungaricae, 84 (3), pp. 325—334 (1975)

SELEKTIVE SPALTUNG VON THIOGLYKOSIDEN MIT DICHLORMETHYL—METHYLÄTHER

I. FARKAS, R. BOGNÁR, M. M. MENYHÁRT, A. K. TARNAI, M. BIHARI* und J. TAMÁS*

(Institut für organische Chemie, Kossuth-Lajos-Universität, Debrecen und **Zentralforschungsinstitut für Chemie der Ungarischen Akademie der Wissenschaften, Budapest)*

Eingegangen am 1. Oktober 1973

Acetylierte Alkyl- und Aryl-1-thio-β-D-gluco- und -galaktopyranoside (**1**—**13**) werden durch Dichlormethyl-methyläther/$ZnCl_2$ zu α-Acetochlor-D-glucose (**III**) bzw. α-Acetochlor-D-Galaktose (**IV**) gespalten.

Versuche mit Disacchariden zeigten, daß die Spaltung selektiv ist: die unberührte Zuckerkomponente wurde in Form ihres Acetochlor-Derivats mit guter Ausbeute isoliert.

Das einzige schwefelhaltige Nebenprodukt der Spaltung ist — je nach dem Aglykon — das entsprechende S-Alkyl- bzw. S-Arylthioformiat (**VII** und **IX**); letzteres wird jedoch unter den angewendeten Reaktionsbedingungen quantitativ zu S-Dichlormethylthiophenol (**VIII**) halogeniert. (Die Nebenprodukte wurden mittels einer kombinierten gaschromatographischen–massenspektrometrischen Methode identifiziert.) Demgemäß ist es wahrscheinlich, daß die Thioglykoside unter der Wirkung von Dichlormethyl-methyläther/$ZnCl_2$ — unabhängig von der Natur des Aglykons — einer »Glucosyl-S-Spaltung« unterworfen werden, wobei der entsprechende Acetohalogen-Zucker vermutlich über einen Sulfonium-Komplex (**X**) gebildet wird. Modellversuche zeigten, daß die aus dem Reagenten in Nebenreaktionen gebildete Salzsäure als Glykosidspalter praktisch keine Rolle spielt.

Gemäß unseren früheren Untersuchungen werden die acetylierten Alkyl- und Aryl-O-glykoside der Mono- und Disaccharide durch α-Dihalogenäther selektiv gespalten, wobei die Zuckerkomponente in Form ihres Acetohalogen-Derivats mit guter Ausbeute isoliert werden kann [1]. Das Verfahren konnte auch bei einigen natürlichen Glykosiden der Flavonoid-Reihe mit Erfolg angewendet werden [1, 2].

In der vorliegenden Arbeit berichten wir über die selektive Spaltung von Thioglykosiden mit Dichlormethyl-methyläther. Bekanntlich sind die Thioglykoside — mit Ausnahme ihrer sauren Hydrolyse [3] — reaktionsfähiger als ihre Sauerstoff-Analoga. Sie werden durch Brom oder Chlor (in organischem Lösungsmittel) leicht gespalten [4]. Diese Spaltung ist auch präparativ wertvoll, besonders für die Herstellung von β-Acetobrom-Derivaten und schwer zugänglichen Furanosyl-haloiden [5]. Die höhere Reaktivität der Glykosid-Bindung von Thioglykosiden wird auch dadurch bestätigt, daß sie sich mit Quecksilber(II)- oder Silbersalzen von Carbonsäuren in die entsprechenden 1-O-Acyl-Derivate umsetzen [6]. Demgemäß konnte erwartet werden, daß acetylierte Thioglykoside auch mit Dichlormethyl-methyläther in Reaktion treten.

Tabelle I

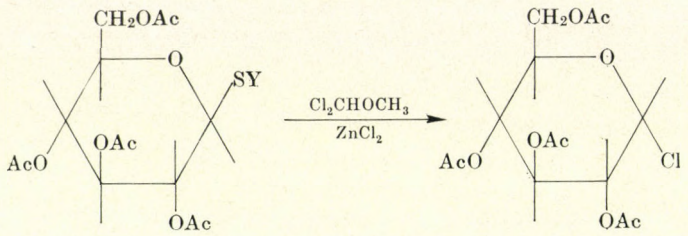

I **III**

Y		Methode	Reaktionszeit Min.	Reaktionstemp. °C	Herauspräparierte Verbindung **III**: Ausbeute, %	Schmp.* °C	$[\alpha]_D$ (in $CHCl_3$)**
$-CH_3$	**(1)**	A	55	75	66	71—73	+166,3° (c = 0,41)
CH_3CH_2-	**(2)**	A	60	70	64	73—74	+166,9° (c = 0,39)
$(CH_3)_2CH-$	**(3)**	A	60	70	55	71—72	+164,9° (c = 0,45)
$CH_3-CH_2-CH_2-CH_2-$	**(4)**	A	65	75	57	72—73	+165,3° (c = 0,41)
$(CH_3)_2CH-CH_2-$	**(5)**	A	60	70	52	71—72	+164,6° (c = 0,44)
	**(6)**	A	50	75	42	71—73	+166,2° (c = 0,40)
	**(7)**	A	60	70	46	71—72	+165,5° (c = 0,39)

* Literaturwert: 73—74 °C [10]
** Literaturwert: +167,8° [10]

Unsere Versuche zeigten erwartungsgemäß, daß acetylierte Alkyl- und Aryl-1-thio-β-D-glucopyranoside (**I**; **1**—**7**) und -1-thio-β-D-galaktopyranoside (**II**; **8**—**13**) unter der Einwirkung von Dichlormethyl-methyläther und wasserfreiem Zinkchlorid leicht gespalten werden, wobei aus dem Reaktionsgemisch α-Acetochlor-D-glucose (**III**) bzw. α-Acetochlor-D-galaktose (**IV**) mit guter Ausbeute isoliert werden kann. Die diesbezüglichen Reaktionsdaten sind in Tab. I und II zusammengefaßt.

Nach unseren Versuchsergebnissen mit Disaccharid-Derivaten (**V**; **14**—**16**) werden Thioglykoside in Gegenwart von Dichlormethyl-methyläther und $ZnCl_2$ selektiv gespalten, wobei das Acetochlor-Derivat der Zuckerkomponente (**VI**) entsteht. Unter den in Tab. III angeführten Versuchsbedingungen bleibt nämlich die Glykosidbindung des Disaccharid-Teils praktisch unberührt.

Zwecks Feststellung der Bruttogleichung der Glykosidspaltung mit Dichlormethyl-methyläther wurden die Nebenprodukte der Reaktion mit einer kombinierten gaschromatographischen—massenspektrometrischen Methode bestimmt. Bei der Spaltung von Äthyl-2,3,4,6-tetra-O-acetyl-1-thio-β-D-glucopyranosid (**2**) wurden als Nebenprodukte Salzsäure, Methylchlorid, Methylformiat und S-Äthylthioformiat (**VII**) nachgewiesen; eine Äthylchlorid-

Tabelle II

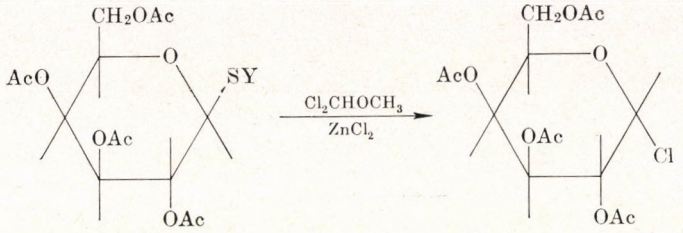

II **IV**

Y		Methode	Reaktionszeit Min.	Reaktionstemp. °C	Herauspräparierte Verbindung IV: Ausbeute, %	Schmp.* °C	$[\alpha]_D$ (in $CHCl_3$)**
CH_3—	**(8)**	A	50	75	60	81—82	+211,9° (*c* = 0,48)
CH_3CH_2—	**(9)**	A	60	70	68	81—82	+213,1° (*c* = 0,42)
$(CH_3)_2CH$—***	**(10)**	A	60	70—75	50—60	75—76	+210,6° (*c* = 0,43)
$CH_3CH_2CH_2CH_2$—***	**(11)**	A	60	75		74—76	+210,9° (*c* = 0,40)
$(CH_3)_2CHCH_2$—***	**(12)**	A	60	70		75—76	+209,8° (*c* = 0,47)
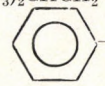 —CH_2—	**(13)**	A	50	70	61	76—78	+212,1° (*c* = 0,49)

* Literaturwerte: 75—76 °C [11]; 82—83 °C [12]
** Literaturwert: +212,25° [11, 12]
*** Sirupartiges Produkt

Tabelle III

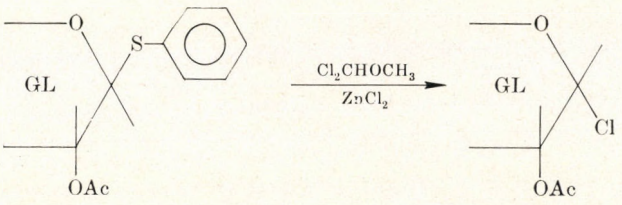

V **VI**

GL		Methode	Reaktionszeit Min.	Reaktionstemp. °C	Herauspräparierte Verbindung VI: Ausbeute, %	Schmp. °C gef.	Schmp. °C Lit.	$[\alpha]_D$ (in $CHCl_3$) gef.	$[\alpha]_D$ (in $CHCl_3$) Lit.
Cellobiosyl-	**(14)**	B	60	50—60	82	186—187	178 187—188 [13] 200—201	+72,8° (*c* = 0,2)	+73° [13]
Lactosyl-	**(15)**	C	60	50—60	57	119—120	120—121 [14]	+85,8° (*c* = 0,32)	+83,9° [14]
Maltosyl-	**(16)**	D	60	50—60	39	117—118	118—120 [15] 125	+157,4° (*c* = 0,35)	+159,5° [15]

Bildung erfolgte selbst in Spuren nicht. Die ersten drei der genannten Produkte sind Ergebnisse der nachfolgenden Reaktionen:

$$Cl_2CHOCH_3 \xrightarrow[\text{Erhitzen}]{ZnCl_2} HCl + CH_3Cl + CO$$

$$Cl_2CHOCH_3 \xrightarrow{H_2O} HCl + HCOOCH_3$$

und entstehen infolge der durch $ZnCl_2$ katalysierten Zersetzung bzw. Hydrolyse (durch das in Spuren stets gegenwärtige Wasser) des Reagenten. Als wirkliches Nebenprodukt der Glykosidspaltung kann in diesem Fall also allein das S-Äthylthioformiat (**VII**) betrachtet werden.

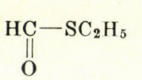

VII

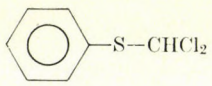

VIII

Daraus folgt, daß die Alkylthio-Gruppe ausschließlich in der Form von S-Alkylthioformiat erscheint. Der gleiche Befund ergab sich früher bei der Spaltung von Zucker-diäthylmerkaptalen mit Dichlormethyl-methyläther [7].

Bei der Reaktion von Phenyl-2,3,4,6-tetra-O-acetyl-1-thio-β-D-glucopyranosid (**7**) mit Dichlormethyl-methyläther konnte — außer den Produkten der obengenannten Nebenreaktionen — nur eine Schwefelverbindung mit der Bruttoformel $C_7H_6SCl_2$ nachgewiesen werden, die sich auf Grund von Modellversuchen und ihres Massenspektrums als S-Dichlormethylthiophenol (**VIII**) erwies. Es konnte bestätigt werden, daß **VIII** ein Umsetzungsprodukt des erwarteten S-Phenylthioformiats **IX** ist, da letztere Verbindung unter den Bedingungen der Spaltungsreaktion durch Dichlormethyl-methyläther zu **VIII** halogeniert wird:

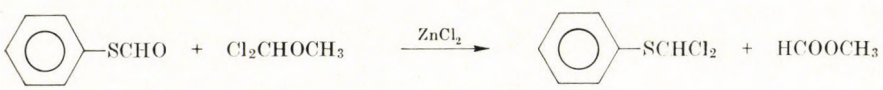

IX **VIII**

Demgemäß erscheint die Thiophenyl-Gruppe der Phenylthioglykoside — analog zu den Alkylthioglykosiden — in Form des Derivats **VIII** (bzw. **IX**).

Der Reaktionsmechanismus der Spaltung von Thioglykosiden kann also auf folgende Weise formuliert werden:

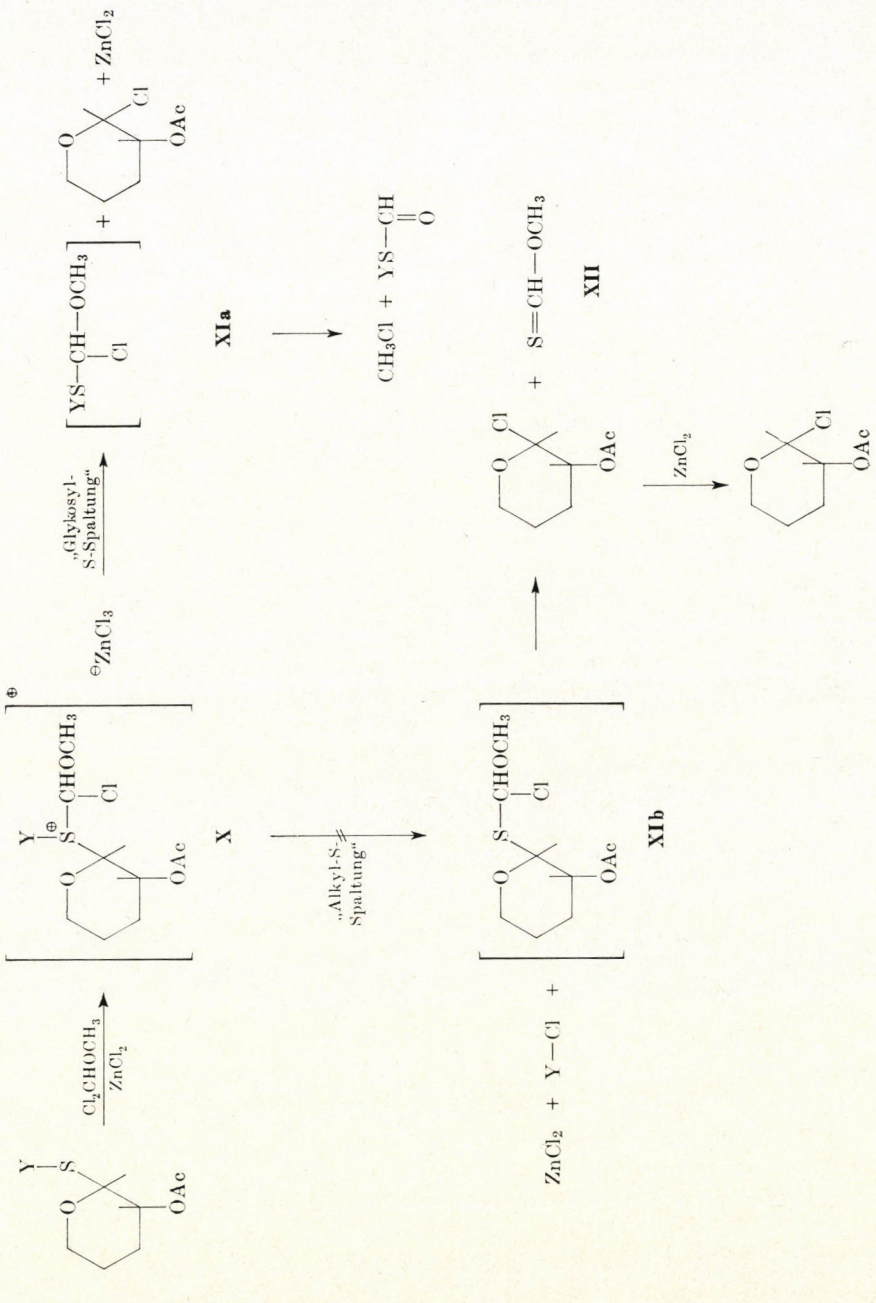
Cl2CHOCH3
ZnCl2
X
„Alkyl-S-Spaltung"
XIb
ZnCl2 + Y—Cl +
⊖ZnCl3
„Glykosyl-S-Spaltung"
XIa
CH3Cl + YS—CH
O
+ ZnCl2
XII
ZnCl2

Es kann angenommen werden, daß die Reaktion über den Sulfonium-Komplex **X** verläuft, und daß der Acetohalogen-Zucker durch »Glykosyl-S-Spaltung« gebildet wird (d. h. der nucleophile Angriff richtet sich auf das glykosidische Kohlenstoffatom). Das Intermediärprodukt **XIa**, welches den »Aglykon-Teil« enthält, wird dann in Methylchlorid und den entsprechenden Ameisensäurethiolester gespalten. Dieser Mechanismus ist unabhängig davon, ob *Y* eine Aryl- oder Alkylgruppe darstellt. Die Möglichkeit der »Alkyl-S-Spaltung« von Alkylthioglykopyranosiden kann ausgeschlossen werden, da das entsprechende Alkylchlorid nicht unter den Nebenprodukten der Reaktion erscheint und nicht einmal Spuren des Thioameisensäure-O-methyl-esters **XII** gebildet werden.

In der Glykosidspaltung mit Dichlormethyl-methyläther und $ZnCl_2$ wird in den Nebenreaktionen Salzsäure entwickelt. Deshalb versuchten wir, die Rolle der Salzsäure in der Thioglykosidspaltung zu klären. Ist die Salzsäure für die Bildung des Acetohalogen-Zuckers verantwortlich, so muß als Nebenprodukt Thioalkohol (bzw. Thiophenol) entstehen. Diese Verbindungen konnten zwar nicht unter den Nebenprodukten der Glykosidspaltung entdeckt werden; es konnte jedoch nachgewiesen werden, daß z. B. das Äthanthiol unter den Reaktionsbedingungen der Glykosidspaltung in das S-Äthylthioformiat **VII** umgesetzt wird:

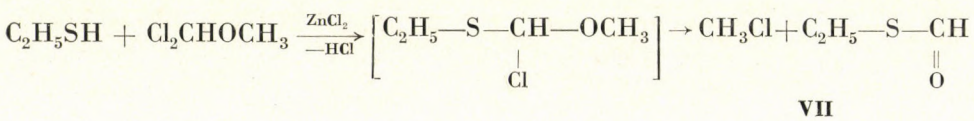

VII

während Thiophenol über S-Phenylthioformiat **IX** das S-Dichlormethylthiophenol **VIII** liefert:

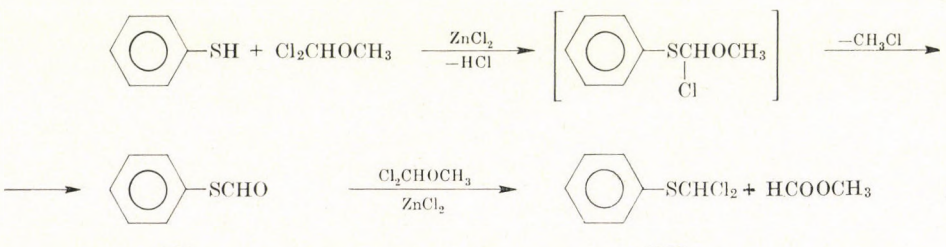

IX **VIII**

Diese Versuche bestätigen die unidirektionale selektive Zersetzung des Intermediärprodukts **XIa**, während Intermediärprodukte vom Dialkoxychlormethan-Typ, die bei der Reaktion von Alkoholen mit Dichlormethyl-methyläther entstehen, in zwei Richtungen gespalten werden, wobei zwei Alkylchloride und zwei Alkylformiate entstehen [1, 8].

Demgemäß konnte die eventuelle Rolle der Salzsäure in der Glykosidspaltung nicht geklärt werden. Zu diesem Zweck wurden Modellversuche durchgeführt. Die Verbindungen **2** und **7** wurden unter den Reaktionsbedingungen der Glykosidspaltung mit $ZnCl_2$ und trockenem gasförmigem Chlorwasserstoff in Reaktion gebracht, wobei die Thioglucoside in unveränderter Form mit einer Ausbeute von 80% zurückgewonnen wurden. (Es soll bemerkt werden, daß die Verbindung **2** in Form eines Gemisches mit ihrem α-Anomeren isoliert wurde.) Daraus konnte gefolgert werden, daß die selektive Bildung der Acetochlor-Zucker vor allem auf die unmittelbare Reaktion der Thioglykoside mit Dichlormethyl-methyläther zurückzuführen ist, während die Salzsäure als glykosidspaltendes Reagens keine oder nur eine äußerst untergeordnete Rolle spielt.

Die einfache und selektive Spaltung von Thioglykosiden mit Dichlormethyl-methyläther ist auch deshalb beachtenswert, weil sie in der Synthese von Disacchariden Anwendung finden könnte. Neuerdings wird nämlich die Synthese von reduzierenden Disacchariden über Thioglykoside als vorteilhaft angesehen; im letzten Reaktionsschritt erfolgt dabei die selektive Spaltung der Thioglykosid-Bindung [9].

Experimenteller Teil

Die Herstellung der nötigen Thioglykoside erfolgte nach bekannten Methoden. Die Synthese von **2** und **8** wurde nach SAKATA und Mitarbeitern [16] durchgeführt, während das Verfahren von PURVES [17] zur Herstellung von **7**, **14**, **15** und **16** angewendet wurde. Alle übrigen Thioglykoside wurden nach dem Verfahren von ČERNÝ und Mitarbeitern [18, 19] synthetisiert. **10**, **11** und **12** sind chromatographisch einheitliche Sirupe.

Die Reinheit der Thioglykoside und der Acetochlor-Zucker wurde dünnschichtchromatographisch geprüft (auf Silicagel G, Produkt der Firma REANAL). Zum Chromatographieren wurde ein Gemisch aus Toluol und Äther im Verhältnis von 2 : 1,5 verwendet; die Chromatogramme wurden mit 5% Schwefelsäure enthaltendem Äthylalkohol bei 145 °C entwickelt.

Spaltung der Thioglykoside

Verfahren A. 1 g Thioglykosid wird mit 2,5 ml Dichlormethyl-methyläther, in Gegenwart von 0,1 g wasserfreiem $ZnCl_2$, unter den in Tab. I und II angeführten Bedingungen in Reaktion gebracht. Anschließend wird das Reaktionsgemisch in Vakuum zur Trockne eingedampft und der Rückstand in Äther gelöst. Diese Lösung wird wiederum im Vakuum eingedampft und der zurückbleibende Sirup in Chloroform aufgenommen. Diese Lösung wird mit Eiswasser, eiskalter $KHCO_3$-Lösung und wiederum mit Eiswasser säurefrei gewaschen, mit $MgSO_4$ getrocknet und aufs neue im Vakuum eingedampft. Der sirupartige Rückstand wird aus Äther/Petroläther umkristallisiert.

Verfahren B. 1 g Thioglykosid **14** wird mit 2,5 g Dichlormethyl-methyläther und 0,1 g wasserfreiem $ZnCl_2$ auf dem Wasserbad erwärmt (Einzelheiten siehe in Tab. III). Der Halogen-Zucker wird aus dem im Vakuum eingedampften Reaktionsgemisch mit Chloroform herausgelöst und die Lösung nach dem Entsäuern und Trocknen (wie bei Verfahren A beschrieben) im Vakuum eingedampft. Der feste Rückstand wird mit Äther verrieben, abgesaugt und aus Benzol umkristallisiert.

Verfahren C. 1 g Thioglykosid **15** wird nach Verfahren B gespalten (Einzelheiten siehe in Tab. III), mit dem Unterschied, daß der nach dem Eindampfen der chloroformischen Lösung erhaltene Rückstand aus abs. Alkohol umkristallisiert wird.

Verfahren D. 1 g Thioglykosid **16** wird nach Verfahren A mit Dichlormethyl-methyläther in Reaktion gebracht (Reaktionsbedingungen s. Tab. III). Der Unterschied gegenüber

Verfahren A besteht darin, daß der nach dem Eindampfen des Reaktionsgemisches im Vakuum erhaltene Rückstand in Äther aufgenommen wird. Die Lösung wird nach dem Entsäuern und Trocknen im Vakuum einkonzentriert und anschließend soviel Petroläther zugegeben, bis eine Trübung entsteht. Die Kristallisation wird durch 24stündiges Kühlen auf 0 °C zu Ende geführt.

Untersuchung der Nebenprodukte der Glykosidspaltung

Die Analyse der die Nebenprodukte enthaltenden Lösungen wurde auf einem Massenspektrometer Typ AEI MS-20 durchgeführt, der mit einem Gaschromatographen verbunden war. Wenn es zur Identifizierung der Struktur nötig erschien, wurde auch die Bruttoformel der Ionen bestimmt, durch genaues Messen ihrer Masse auf einem Massenspektrometer Typ MS-902 hoher Auflösung. Zum Gaschromatographieren wurde eine 1,5 m hohe Glassäule verwendet; die Füllung war Diatomeenerde CQ (Korngröße 100—120 mesh), die mit 3% Silicon-Kautschuk (Typ SE-30) benetzt war.

Bestimmung der Nebenprodukte bei der Spaltung von Thioglucosid 2

1 g des Thioglucosids **2** wird mit 2,5 ml Dichloromethyl-methyläther und 0,1 g wasserfreiem $ZnCl_2$ 55 Minuten lang auf einem Wasserbad bei 75 °C gehalten. Die leichtflüchtigen Nebenprodukte der Reaktion werden mit einem über Silicagel getrockneten Stickstoffstrom aus dem Reaktionsgemisch ausgetrieben. Die mit dem Stickstoffstrom entweichenden kondensierbaren Stoffe werden anschließend in einem mit Aceton/Kohlensäureschnee gekühlten Gaswäscher kondensiert und das erhaltene Produkt bei 90 °C gaschromatographiert. Die Probe enthält in einem Verhältnis von ungefähr 50—50% Methylchlorid (charakteristische Spitzen m/e 50, 36) und Methylformiat (m/e 60, 31). Die Spektren der beiden Substanzen waren mit den Literaturangaben [20] identisch. Der Rückstand im Kolben wird in 10 ml Chloroform aufgenommen, mit Eiswasser, eiskalter $KHCO_3$-Lösung und wiederum mit Eiswasser säurefrei gewaschen, anschließend getrocknet, filtriert und im Temperaturbereich von 90—150 °C gaschromatographiert. Außer dem Lösungsmittel und Methylformiat enthält die Probe S-Äthylthioformiat **VII**.

Charakteristische Spitzen vom **VII** (70 eV): m/e 90,0140 (M^+, 100%, C_3H_6OS); m/e 62,0195 ($M^+ - CO$, 8%); m/e 61,9825 ($M^+ - C_2H_4$, 25%); m/e 61,0100 ($M^+ - COH$, 10%); m/e 60,9739 ($M^+ - C_2H_5$, 34%); m/e 46,9956 (M-43, 90%, CH_3S).

Prüfung der Nebenprodukte der Spaltung des Thioglucosids 7

1 g **7** wird mit 2,5 ml Dichloromethyl-methyläther und 0,1 g $ZnCl_2$ 1 Stunde lang auf dem Wasserbad bei 70 °C gehalten. Die flüchtigen Nebenprodukte werden wie bei **2** angegeben mit Stickstoff ausgetrieben und kondensiert. Einzelheiten der gaschromatographisch-massenspektrometrischen Untersuchung siehe bei **2**. In der Probe wurden in ungefähr gleichen Mengen Methylchlorid und Methylformiat gefunden; m/e-Angaben s. oben.

Das im Kolben zurückgebliebene Reaktionsgemisch wird im Vakuum (20 Torr, Wasserbad 40 °C) eingedampft. Der sirupartige Rückstand wird in 10 ml Chloroform aufgenommen, die Lösung wie bei **2** säurefrei gewaschen, getrocknet und im Temperaturbereich von 130—170 °C gaschromatographiert. Die Probe enthält eine einzige schwefelhaltige Verbindung mit der Bruttoformel $C_7H_6SCl_2$. Charakteristische Spitzen: m/e 194 (i, 22%); m/e 192 (M^+, 36%); m/e 159 (i, 32%); m/e 156,9869 (M-35, 100%, C_7H_6SCl); m/e 121 (157-HCl, 19%); m/e 109 (30%); m/e 77 (21%).

Die Fragmentation zeigt, daß die Verbindung S-Dichlormethylthiophenol (**VIII**) ist.

Reaktion von S-Phenylthioformiat (IX) mit Dichlormethyl-methyläther

0,3 ml S-Phenylthioformiat [21] werden mit 2,5 ml Dichlormethyl-methyläther und 0,1 g wasserfreiem $ZnCl_2$ 1 Stunde lang bei 70 °C auf dem Wasserbad gehalten. Das Reaktionsgemisch wird wie bei **7** beschrieben verarbeitet.

Die chloroformische Lösung des Rückstands enthält, nach den Ergebnissen der gaschromatographisch-massenspektrometrischen Untersuchung (ausgeführt wie bei **7**), nur S-Dichlormethylthiophenol (**VIII**) (m/e-Werte siehe oben).

Reaktion von Thiophenol mit Dichlormethyl-methyläther

0,3 ml Thiophenol werden, wie bei S-Phenylthioformiat beschrieben, mit Dichlormethyl-methyläther/$ZnCl_2$ in Reaktion gebracht; das Reaktionsgemisch wird auf analoge Weise verarbeitet.

In der chloroformischen Lösung des Rückstandes konnte allein S-Dichlormethylthiophenol (**VIII**) nachgewiesen werden. (Die Analysenbedingungen und die gefundenen m/e-Werte waren mit den bei der Verbindung **7** angeführten identisch.)

Reaktion der Verbindung 2 mit $ZnCl_2$/Salzsäure

1 g der Verbindung **2** wird in 20 ml wasserfreiem Chloroform gelöst, 0,2 g wasserfreies $ZnCl_2$ werden zugegeben und ein langsamer Strom von trockenem Chlorwasserstoffgas wird 1 Stunde lang durch das Reaktionsgemisch unter Erwärmen auf dem Wasserbad auf 70 °C geleitet. Anschließend wird die Lösung mit Eiswasser, $KHCO_3$-Lösung und wiederum mit Eiswasser gewaschen und im Vakuum bis zur Trockne eingedampft.

Der sirupartige Rückstand kristallisiert unter der Wirkung von warmem Äther. Das Produkt (0,82 g, 82%) ist halogenfrei und schmilzt bei 72—74 °C; $[\alpha]_D = +74{,}3°$ ($c = 1{,}2$, in Chloroform). Die Ausgangsverbindung **2** (das β-Anomere) schmilzt bei 81—82 °C; $[\alpha]_D = -24{,}4°$ (in Chloroform) [18]. Auf Grund des optischen Drehungsvermögens ist das Reaktionsprodukt eine Mischung aus 34% **2** und 66% des α-Anomeren.

$C_{16}H_{24}O_9S$ (392,4). Ber. S 8,17; gef. S 8.07.

Der Anomerengemisch-Charakter des Produkts wird auch durch das in $CDCl_3$ aufgenommene NMR-Spektrum angezeigt. Im Spektrum wurden die Dublette beider anomeren Protonen (H-1_α und H-1_β) beobachtet:

H-1_α 5,76 ppm, $J_{1,2}$ 5,0 Hz
H-1_β 4,58 ppm, $J_{1,2}$ 8,5 Hz

Reaktion der Verbindung 7 mit $ZnCl_2$/Salzsäure

1 g **7** wird in 20 ml Chloroform gelöst und unter den bei **2** angeführten Bedingungen mit $ZnCl_2$/HCl in Reaktion gebracht. Die chloroformische Lösung wird entsäuert und in Vakuum abgedampft. Der sirupartige Rückstand wird in warmem Äther gelöst. Beim Stehen der Lösung im Kühlschrank kristallisieren 0,8 g (80%) unverändertes **7** aus; Schmp. 118 °C, $[\alpha]_D = -40{,}5°$ ($c = 0{,}74$, in Toluol). (Lit. Schmp. 118 °C, $[\alpha]_D = -40{,}1°$ (in Toluol) [22].) Im Gemisch mit dem Ausgangsmaterial zeigt sich keine Schmelzpunkterniedrigung.

LITERATUR

[1] F. Szabó, I., Farkas, I., Bognár, R., Gross, H.: Acta Chim. Acad. Sci. Hung. **64,** 67 (1970)
[2] Bognár, R., Farkas-Szabó, I., Farkas, I., Gross, H.: Carbohyd. Res. **5,** 241 (1967)
[3] Capon, B.: Chem. Rev. **69,** 4 (407) (1969)
[4] Bonner, W. A.: J. Am. Chem. Soc. **70,** 3491 (1948)
Weygand, F., Ziemann, H., Bestmann, H. J.: Chem. Ber. **91,** 2534 (1958)
Wolfrom, M. L., Garg, H. G., Horton, D.: J. Org. Chem. **28,** 2989 (1963)
Hengstenberg, W., Wallenfels, K.: Carbohyd. Res. **11,** 85 (1969)
[5] Weygand, F., Ziemann, H.: Liebigs Ann. Chem. **657,** 179 (1962)
Wolfrom, M. L., Groebke, W.: J. Org. Chem. **28,** 2986 (1963)
[6] Horton, D., Hutson, D. H.: Advan. Carbohydrate Chem. **18,** 123 (1963)
Wood, H. B. Jr., Coxon, B., Diehl, H. W., Fletcher, H. G. Jr.: J. Org. Chem. **29,** 461 (1964)
[7] Farkas, I., Menyhárt, M., Bognár, R., Gross, H.: Chem. Ber. **98,** 1419 (1965)
[8] Rieche, A., Gross, H.: Chem. Ber. **92,** 83 (1959)
[9] Pfäffli, P. J., Hixson, S. H., Anderson, L.: Carbohyd. Res. **23,** 195 (1972)
[10] Pacsu, E.: Ber. **61,** 1508 (1928)
[11] Fischer, E., Armstrong, E. F.: Ber. **34,** 2885 (1901)
[12] Skraup, Z. H., Kremann, R.: Monatsh. f. Chem. **22,** 375 (1901)
[13] Vogel, H., Georg, A.: Tabellen der Zucker und ihrer Derivate. 228 Seiten. Springer-Verlag, Berlin, 1931
[14] Hudson, C. S., Kunz, A.: J. Am. Chem. Soc. **47,** 2052 (1925)
[15] Brauns, D. H.: J. Am. Chem. Soc. **51,** 1820 (1929)
[16] Sakata, M., Haga, M., Tejima, S.: Carbohyd. Res. **13,** 379 (1970)
[17] Purves, C. B.: J. Am. Chem. Soc. **61,** 3619 (1929)
[18] Černý, M., Pacák, J.: Coll. Czechoslov. Chem. Commun. **24,** 2566 (1959)
[19] Černý, M., Staněk, J., Pacák, J.: Monatsh. f. Chem. **94,** 290 (1963)

[20] STENHAGEN, E., ABRAHAMSSON, S., MCLAFFERTY, F. W.: Atlas of Mass Spectral Data, Interscience Publishers, New York, 1969, Vol. I, 18, 36 Seiten.
[21] BAX, P. C., STEVENS, W.: Rec. Trav. Chim. Pays-Bas **1970**, 89 (3), 265
[22] FISCHER, E., DELBRÜCK, K.: Ber. **42**, 1476 (1909)

István FARKAS
Rezső BOGNÁR
Márta M. MENYHÁRT
Anna K. TARNAI
4010 Debrecen, Egyetem tér 1. Pf. 20. Ungarn.

Mária BIHARI
József TAMÁS
1088 Budapest, Puskin u. 11—13. Ungarn.

Acta Chimica Academiae Scientiarum Hungaricae, 84 (3), pp. 335—342 (1975)

THE REACTIVITY OF THE CARBONYL GROUP IN FLAVONOID COMPOUNDS, I

KINETIC STUDIES ON THE FORMATION OF 2,4-DINITROPHENYLHYDRAZONES

É. R. DÁVID and R. BOGNÁR

(Organic Chemistry Department of the Kossuth Lajos University, Debrecen)

Received January 12, 1974

The reactivity of the C=O group in flavonoid compounds as a function of the structure (degree of oxidation) and the substitution conditions were studied in their reactions with 2,4-dinitrophenylhydrazine by means of the ultraviolet spectrophotometry. The carbonyl group of the unsubstituted flavanone was found to exhibit the greatest reactivity. The hydroxyl substituent at the carbon atom adjacent to the carbonyl group will lower the reactivity of both the flavanone and 2'-hydroxychalcone derivatives, owing to chelate formation. Substituents in para position related to the carbonyl group will modify the rate of the 2,4-dinitrophenylhydrazone-formation reaction in accordance with their $+I$ or $-I$ effects.

Several methods have been known for the analytical detection and determination of the carbonyl group [1—4]. The most frequently applied one is the measurement accomplished in the form of the 2,4-dinitrophenylhydrazone derivative, since aldehydes and ketones form poorly soluble coloured precipitates with 2,4-dinitrophenylhydrazine in aqueous or alcoholic solutions, which can be measured gravimetrically or by back-titration [2, 5].

Particularly in the determination of carbonyl compounds available in small amounts only, the spectrophotometry is very advantageous, since 2,4-dinitrophenylhydrazones have a characteristic absorption band in the 340—420 nm range with a high molar absorbance; it shows a considerable bathochromic shift in alkaline medium [5—10].

In the investigation on the reactivity of the carbonyl group in flavonoid compounds with different oxidation levels [11, 12] as a function of their structures and substitution conditions, the favourable properties of the 2,4-dinitrophenylhydrazone-formation reaction have been utilized. The 2,4-dinitrophenylhydrazones of the flavonoid compounds examined have not been isolated, but extracted with *n*-hexane and the factors influencing the reactivity of the carbonyl group have been evaluated from the reaction rate constants calculated from the kinetic curves constructed on the basis of the increase in the absorbance measured at the actual λ_{max}.

Quantitative and unambiguous accomplishment of the reaction [13, 14, 15] was ensured by adjusting a proper ratio of the concentrations of the acid, the reagent and the flavonoid compound.

The data obtained were checked by comparing the spectroscopic data of some 2,4-dinitrophenylhydrazones prepared in pure state previously, which were also utilized in establishing the quantitative accomplishment of the reaction.

Experimental

1. *Preparation of 2,4-dinitrophenylhydrazones*

The flavonoid parent compounds were prepared according to literature prescriptions. Their 2,4-dinitrophenylhydrazones were prepared by the diglyme method of H. J. SHINE [7]. The majority of the 2,4-dinitrophenylhydrazones precipitated immediately from the reaction mixture, they were filtered off, then washed with ethanol with aqueous ethanol. The crystals were dried at room temperature and identified on the basis of the melting-point values and the elemental-analysis data.

2. *Spectrophotometric studies on 2,4-dinitrophenylhydrazones*

The UV spectra were recorded with a Unicam SP 800 recording spectrophotometer in $5 \cdot 10^{-5} M$ concentration. The spectral data are given in Table II. (Since the substances are poorly soluble in ethanol, the λ_{max} values given for ethanolic solutions refer to cold-saturated solutions.)

Table I

Melting-point and elemental-analysis data of 2,4-dinitrophenylhydrazones of flavonoid compounds

2,4-Dinitrophenyl-hydrazone derivative	Colour	Calcd.	Found
		M.p. °C	N%	
flavanone-	orange	251—52*	13.86	13.98
3-hydroxyflavanone-	red	256—8**	13.33	13.46
5-hydroxyflavanone-	orange-red	258—9	13.33	13.50
7-hydroxyflavanone-	dark red	245—6	13.33	13.05
1-thiaflavanone-	yellow	234—35	13.33	13.90
flavone-	red	280—1	12.69	12.78
chalcone-	orange	247—8***	14.44	14.8
2'-hydroxychalcone-	orange-red	235—7	13.86	13.72
4-hydroxychalcone-	dark red	239—41	13.86	14.05
4'-hydroxychalcone-	ochre-yellow	232—5	13.86	13.88
4-nitrochalcone-	red	230—5	16.13	16.30
2'-benzyoxychalcone-	orange	246—7	11.36	10.96

* R. MOZINGO, H. ADKINS: J. Am. Chem. Soc. **60**, 669 (1938). M.p. 254—55°C
F. KÁLLAY, G. JANZSÓ, I. KOCZOR: Tetrahedron **23**, 4317 (1967). M.p. 252—55°C
** F. RAMIREZ, C. D. TELEFUS: J. Org. Chem. **34**, 377 (1969). M.p. 257°C
*** J. D. ROBERTS, CH. GREEN: J. Am. Chem. Soc. **68**, 214 (1946). M.p. 247—8°C

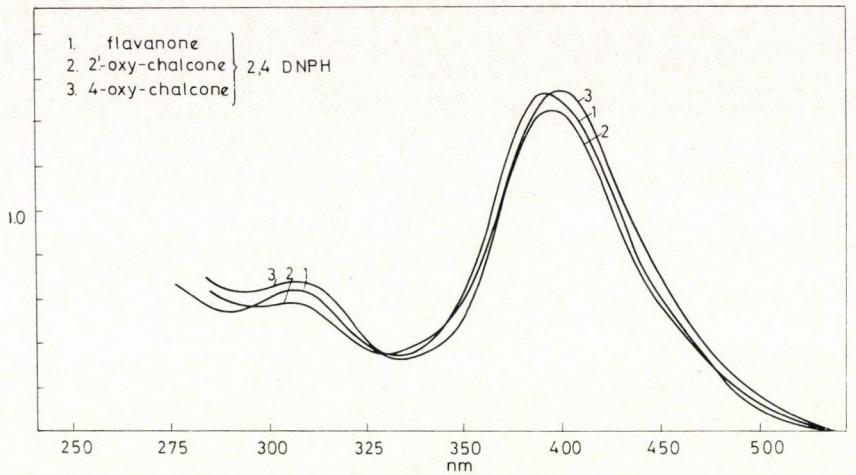

Fig. 1. Spectra of 2,4-dinitrophenylhydrazones of flavonoid compounds in $5 \cdot 10^{-5}$ *M* dioxane solutions

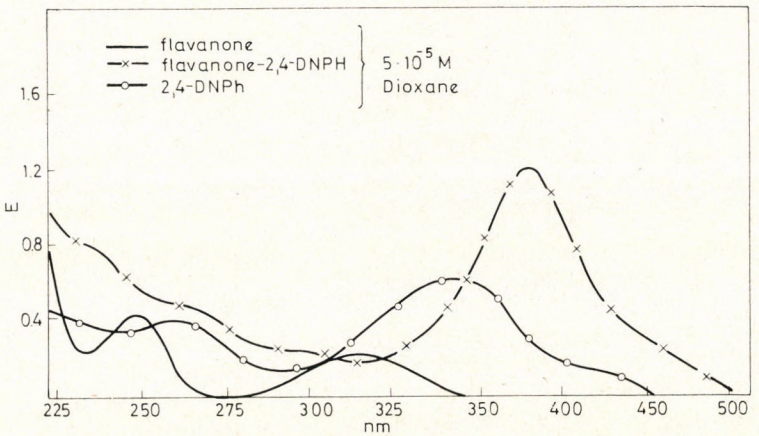

Fig. 2. Spectra of flavanone, flavanone 2,4-dinitrophenylhydrazone and 2,4-dinitrophenylhydrazone in $5 \cdot 10^{-5}$ *M* dioxane solutions

The data in Table II, as well as Figs 1 and 2 show that the spectra of the 2,4-dinitrophenylhydrazones of flavonoid compounds are almost independent of the structure of the starting material (flavanone, chalcone, etc.), but can clearly be distinguished from those of the starting materials and the reagent, 2,4-dinitrophenylhydrazine, as well. Substituents in various positions will also modify the spectrum to an insignificant extent only (Figs 1, 2).

3. *Kinetic runs*

In the kinetic runs the difference in the solubilities of the reagent and the products in *n*-hexane was utilized [6]. The 2,4-dinitrophenylhydrazones

formed could easily be separated from the reagent present in a great excess by extracting the sulfuric acid–ethanolic solution with *n*-hexane. The coloured hexane solution proved to be quite stable, thus the spectra of the neutral, pure 2,4-dinitrophenylhydrazones could be measured with satisfactory reproducibility.

Table II

Spectral data of 2,4-dinitrophenylhydrazones of flavanoids in different solvents

2,4-Dinitrophenyl-hydrazones	Dioxane		Chloroform		Ethanol
	λ_{max}	ε	λ_{max}	ε	λ_{max}
2,4-dinitrophenylhydrazine	346	16 400	347	15 100	348.5
flavanone-	386	30 500	390	31 500	390
5-hydroxyflavanone-	375	29 750	375	29 000	376
3-hydroxyflavanone-	384	30 000	390	29 000	392
7-hydroxyflavanone-	389	30 000	395	29 500	398
1-thioflavanone-	380	29 500	382	29 000	382
chalcone-(benzalacetophenone)	392	32 000	396*	32 500	396*
2'-hydroxychalcone-	388	31 000	392	30 500	392
2'-benzyloxychalcone-	393	31 500	394	30 500	394
4'-hydroxychalcone-	390	32 500	398	32 500	400
4-hydroxychalcone-	398	30 700	400	30 500	405
4,4'-dibromochalcone-	391	31 800	390	31 500	395

* J. D. ROBERTS, CH. GREEN: J. Am. Chem. Soc. **68**, 214 (1946). λ_{max} [EtOH] = 395 nm. C. DJERASSI, E. RYAN: J. Am. Chem. Soc. **71**, 1000 (1949). λ_{max} [$CHCl_3$] = 398 nm

Therefore, the initial concentrations of the flavonoid compounds were chosen so as to achieve quantitative extraction of the 2,4-dinitrophenylhydrazones formed with *n*-hexane, even at the end of the reaction.

For this purpose, $5 \cdot 10^{-4} M$ ethanolic solutions of the flavonoid compounds were used, to which a sulfuric acid–ethanolic solution of the reagent was added in 1 : 1 volume ratio. (Optimum acid concentration was $1.5 M$.) The time elapsed from combining the solutions was clocked with a stop-watch and, depending on the rate of the reaction, 1 ml samples were pipetted into 10 ml of *n*-hexane in 1-, 5-, 10- or 20-minute periods. After shaking the mixture, the absorbance of the *n*-hexane phase was measured at 390 nm. The reference solution was the reagent treated in the same way. (1 ml of the reagent + 1 ml of pure ethanol extracted with 10 ml of *n*-hexane showed $E_{390} = 0.2$.) The reagent can be used for about one weak only; its absorbance was checked daily.

The $1 \cdot 10^{-1} M$ 2,4-dinitrophenylhydrazine reagent was prepared with various acid constants (0.5, 1.0, 1.5, 2.0, 2.5, 3.0, 4.0 and 5.0 M), and the reaction rate was found to be almost identical with acid contents in the 1.5 —

2.5 *M* range. Below and above these acid concentrations, however, the rate of reaction decreased considerably. In less acid solutions, the reagent separated on storage, while at higher acid concentrations the decrease in the free base concentration presumably hindered the rapid accomplishment of the reaction. In addition to these facts, the absorbance of the reference solution was increased by the higher acid content. Thus the optimum acid content was considered to be 1.5 *M*. The measurements were carried out at 23 $\pm$ 0.05°C.

Reagent for the kinetic runs

Reagent-grade 2,4-dinitrophenylhydrazine (1.980 g) was dissolved in reagent-grade concentrated sulfuric acid (15 ml). Distilled water (20 ml) was added to it. After cooling, its volume was made up to 100 ml with purified ethanol.

Evaluation of the results

It can be seen in Fig. 3 that, in addition to the 2,4-dinitrophenylhydrazone formed in the reaction, the chalcone was also transferred from the sulfuric acid-ethanolic solution into the *n*-hexane extract. The well-defined isosbestic point in the spectrum confirms the presence of an equilibrium system, in which the decrease in the chalcone concentration with time is in equilibrium with the increase in the concentration of the 2,4-dinitrophenylhydrazone formed.

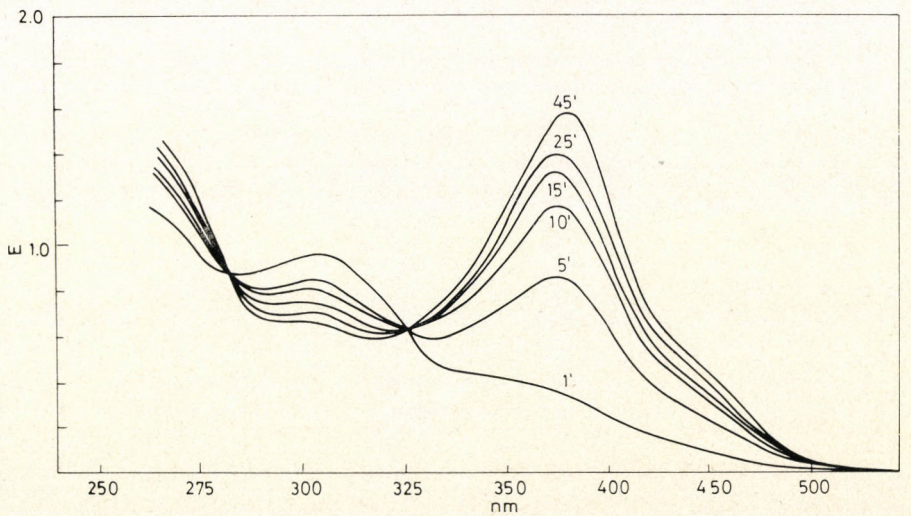

Fig. 3. The equilibrium system of chalcone 2,4-dinitrophenylhydrazone in the *n*-hexane extract, as a function of time

Similar equilibria have generally been observed in the formation of 2,4-dinitrophenylhydrazones of other chalcone derivatives examined.

In the case of flavone and flavanone derivatives, only the 2,4-dinitrophenylhydrazones formed are soluble in *n*-hexane, thus the isosbestic point could not be utilized and only the absorption spectrum of the dinitrophenylhydrazone was measured, being proportional to the concentration.

On the basis of spectrophotometric data, the kinetic curves have been constructed and the half-times and rate constants calculated (Table III).

Table III

Rate constants of 2,4-dinitrophenylhydrazones of some flavonoids at 23 ± 0.05°C

Compound	$K\ (min^{-1}) \cdot 10^{-3}$	Compound	$K\ (min^{-1}) \cdot 10^{-3}$
flavone-	255.00	chalcone	155.00
1-thiaflavanone-	153.00	2'-benzyloxychalcone-	153.00
3-hydroxyflavanone-	15.00	2'-hydroxy-4-methylchalcone-	9.48
5-hydroxyflavanone-	3.82	2'-hydroxy-4-chlorochalcone-	9.0
flavone-	0.18	2'-hydroxychalcone-	6.95
5-methoxyflavanone-	43.6	2'-hydroxy-4-methoxychalcone-	
		2',4-dihydroxychalcone-	0.38

Since the changes in the concentration of the acid and that of the reagent being in a large excess were negligible as compared to the change in the concentration of the dinitrophenylhydrazone formed, considered as a function of time, the reaction was found to follow a pseudo first-order kinetics, which was verified by the identical half-times of flavonoid compounds with different initial concentrations.

The evaluation of the rate constants suggests that the 2,4-dinitrophenylhydrazone derivative is formed in a well-measurable, relatively rapid reaction, in both the flavanone and the chalcone series. In the case of flavone and the sterically hindered ortho-substituted flavonoids, the reaction is very slow. (For example, the amount of the flavone 2,4-dinitrophenylhydrazone derivative was only 50% even after a 260-hr reaction period.)

The substituents in para position will (Fig. 4), of course, affect the rate of the reaction in accordance with their enhancing or lowering action on the electron density of the α-carbon atom with decreased electron concentration, brought about by the polarization of the carbonyl group, depending on their positive or negative inductive and mesomeric effects. When, however, the reaction-rate values are plotted against the constants δ and δ^+, total and unambiguous linearity cannot be established, which makes necessary the determination of new substitution constants in the flavonoid series.

The plot of the logarithm of the reaction-rate values of the 2,4-dinitrophenylhydrazone-formation reaction as a function of the basicity constants (pK^{+}_{BH}) determined by us previously [16, 17], shows that the substitution and structural effects equally appear in the case of both constants, but in opposite ratios. That is, the less basic the carbonyl group of a compound (*e.g.* flavanone), the higher the rate of the formation of the 2,4-dinitrophenylhydrazone derivative, while with increasing basicity (*e.g.* flavone) the reaction rate will decrease.

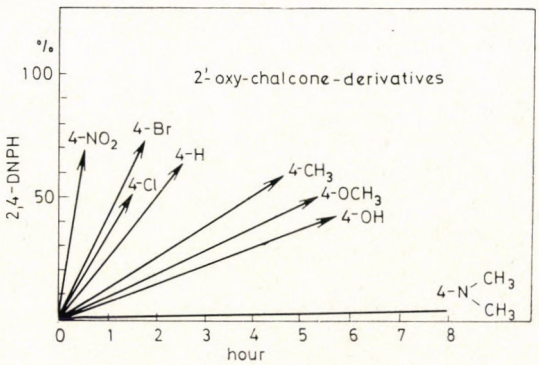

Fig. 4. Reaction rate curves of substituted 2'-hydroxychalcone 2,4-dinitrophenylhydrazone derivatives

The reaction will be quite hindered below a certain limit, that is, where the electron cloud of the oxygen atom will completely shield the positive charge at the α-carbon atom, owing to the high polarity (cross-conjugation, substitution effect), and where no positive charge can develop at the α-carbon atom, because of the cross-conjugation effect (*e.g.*, 7-hydroxyflavone, 4-dimethylaminochalcone). In the formation of dinitrophenylhydrazones, the steric effects hinder the nucleophilic addition reaction to a far larger extent than the solvolytic action in the basicity (Fig. 5, compounds 2, 3, 4, 5, 6, 7).

This is also confirmed by the decreased reaction rate of 3-hydroxy- and 5-hydroxyflavanone and 2'-hydroxychalcone. By all means, when the basicity constant values, pK_{BH^+}, are plotted as a function of the logarithms of the rate constants of the 2,4-dinitrophenylhydrazones formed, the inverse proportionality is apparent (Fig. 5).

The method developed for kinetic measurements seems, according to the experiences, to be suitable for investigating the reactivity of the carbonyl groups in not only flavonoid, but in other types of compounds, too, as well as for the determination of new substitution and steric constants in the knowledge of the basicity constants. These comparative studies can be accomplished relatively simply with 2—3-mg samples.

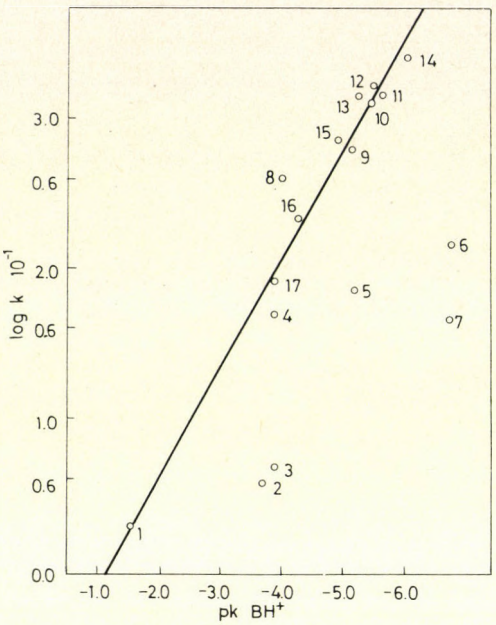

Fig. 5. The logarithms of 2,4-dinitrophenylhydrazone reaction rates as a function of the basicity constants

REFERENCES

[1] FRITZ, J. S., YAMAMURA, S. S., BRADFORD, E. C.: Anal. Chem. **31,** 260 (1959)
[2] BALDINUS, J. G., ROTHBERG, J.: Anal. Chem. **34,** 924 (1962)
[3] WEISS, F. T.: Determination of Organic Compounds: Methods and Procedures. Wiley-Interscience, New York 1970
[4] LÉGRÁDI, L.: Microchimica Acta **1971,** 380
[5] VULTERIN, J., ZYKA, H.: Chem. Listy **50,** 364 (1956)
[6] LAWRENCE, R. C.: Nature **205,** 1313 (1965)
[7] SHINE, H. J.: J. Org. Chem. **24,** 253 (1959)
[8] LOHMAN, F. H.: Anal. Chem. **30,** 972 (1958)
[9] COWELL, D. B., SELBY, B. D.: Analyst **88,** 974 (1963)
[10] JORDAN, D. E.: Anal. Chim. Acta **37,** 379 (1967)
[11] BOGNÁR, R.: MTA Kém. Tud. Oszt. Közl. **6,** 227 (1955)
[12] FREUDENBERG, K., WEINGES, K.: Tetrahedron **16,** 4317 (1967)
[13] KÁLLAY, F., JANZSÓ, G., KOCZOR, I.: Tetrahedron **23,** 4317 (1967)
[14] JENKS, W. P.: J. Am. Chem. Soc. **81,** 475 (1959)
[15] PATAI, S.: The Chemistry of the Carbonyl Group. Interscience Publishers, John Wiley and Sons, London 1966, 1970, Vol. I and II
[16] DÁVID, É. R., RÁKOSI, M., BÁLINT, J., BOGNÁR, R.: Acta Univ. Debr. Phys. et Chim. **XV–XVI,** 163 (1969)
[17] DÁVID, R. É., LITKEI, GY., BOGNÁR, R.: Acta Univ. Debr. Phys. et Chim. **XVII,** 215 (1971)

Éva R. DÁVID
Rezső BOGNÁR } 4010 Debrecen, Hungary.

Acta Chimica Academiae Scientiarum Hungaricae, 84 (3), pp. 343—351 (1975)

СИНТЕЗ И ИССЛЕДОВАНИЕ СВОЙСТВ РАСТВОРОВ ПРИВИТЫХ СОПОЛИМЕРОВ ПОЛИВИНИЛОВОГО СПИРТА С ПОЛИВИНИЛПИРРОЛИДОНОМ

ТАШМУХАМЕДОВ С. А., КАРАБАЕВ А. Ш., ФУЗАИЛОВ Ш., ЛАРИН П.П., ТИЛЛАЕВ Р. С. и УСМАНОВ Х. У.

(СССР, Ташкентский Государственный университет им. В. И. Ленина)

16. IV. 1973

Радиационно-химическим методом синтезированы привитые сополимеры поливинилового спирта с поливинилпирролидоном в зависимости от дозы облучения, природы и концентрации растворителя. Полученные продукты идентифицированы методом ИК-спектроскопии.

При изучении температурной зависимости вязкости растворов привитых сополимеров обнаружены аномальные изменения вязкости, выражающиеся в появлении экстремальных точек на кривой вязкости. Подобное явление объяснено с точки зрения возможности конформационного перехода макромолекул привитых сополимеров от агрегированной формы в форму статистического клубка.

Сорбционным и калориметрическим исследованием показано, что акт прививки винилпирролидона к поливиниловому спирту приводит к уплотнению структуры полимера

Среди привитых сополимеров поливинилового спирта (ПВС) определенный научный и практический интерес представляет система ПВС-поливинилпирролидон (ПВП). В литературе сведения об этой системе отсутствуют. Данные привитые сополимеры, будучи составленными из водорастворимых полимеров, представляют интересный объект с точки зрения исследования свойств растворов ввиду возможности значительного межцепного взаимодействия сегментов различной химической природы. Поэтому в данной работе приводятся результаты синтеза привитых сополимеров ПВС—ПВП и изучения свойств их растворов с привлечением ряда физико-химических методов.

Экспериментальная часть.

Использовали промышленный образец ПВС производства Ереванского завода «Поливинилацетат» с характеристической вязкостью $[\eta]$ в воде при 25°С, равной 0,74, и содержанием ацетатных групп 4,2%. Винилпирролидон очищали вакуумной перегонкой при 82—84°С 8 мм. рт. ст., n_D^{22} 1,5070, d^{25} 1,0448. Синтез привитых сополимеров осуществляли радиационным методом с использованием гамма лучей источника Co^{60} путем одновременного облучения смеси полимера и мономера в интервале доз облучения от 0,1 до 0,5 Мрад при мощности дозы 67 рад/сек. Прививку проводили в вакууме, в присутствии растворителей, в качестве которых использовали метанол и диоксан, так как предварительно была установлена низкая эффективность прививки при проведении реакции в массе. Привес в весе исходного полимера определяли

после экстракции реакционной смеси хлороформом, в результате которого удалялся гомо-ПВП.

ИК-спектры образцов снимали на двухлучевом спектрофотометре UR—10 в областях 3800—2600 $см^{-1}$ (призма из LiF), 2000—700 $см^{-1}$ (призма из NaCl) и 700—400 $см^{-1}$ (призма из KBr). Образцы для снятия ИК-спектров готовили прессованием с KBr по общепринятой методике.

Характеристические вязкости образцов измеряли в капиллярном вискозиметре типа Уббелоде, допускающем последовательное разбавление исследуемого раствора в самом вискозиметре [1]. Характеристическую вязкость находили по данным приведенной вязкости 3-х—4-х разбавлений, экстраполяцией к нулевому значению концентрации раствора.

Сорбционные свойства исследовали на высоковаккумной установке типа Мак—Бэна с кварцевыми пружинами [2].

Тепловые эффекты определяли при помощи микрокалориметра типа Шотки [3]. Все исследования проводили термостатированием при 25°C.

Результаты и их обсуждение

Данные привитой сополимеризации при исходном соотношении ПВС : : ВП = 1 : 2 и 30% концентрации растворителя от веса мономера в зависимости от дозы облучения представлены на рис. 1. Как видно, привес после экстракции гомо-ПВП повышается в интервале доз 0,2—0,5 Мрад и значительная конверсия мономера, израсходованного для привитой сополимеризации, наблюдается при дозе 0,5 Мрад. Судя по результатам, прививка в присутствии метанола протекает значительно эффективнее, чем в случае диоксана. Так, при дозе облучения 0,5 Мрад привесы составляют 147 и 19% соответственно, что можно объяснить различиями в полярности и радиационно-

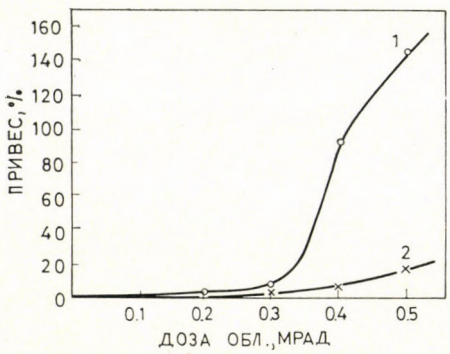

Рис. 1. Влияние дозы облучения и природы растворителя на прививку ВП к ПВС. ПВС : ВП = 1 : 2, Мощность обл. 67 рад/сек. 1- метанол, 2-диоксан (концентрация растворителя 30% от веса мономера).

химических выходов свободных радикалов для этих растворителей. Однако, в обоих случаях высокая радиационная чувствительность мономера по сравнению с ПВС приводит к образованию значительных количеств гомополимера, особенно при низких дозах облучения, когда эффективность прививки низкая. Использование же доз облучения свыше 0,5 Мрад дает нерастворимые продукты, так как ПВС и особенно ПВП относятся к сшивающимся под действием излучения полимерам [4]. На рис. 2 приведены данные по синтезу при дозе 0,4 Мрад в зависимости от концентрации растворителя. Эти данные показывают, что с увеличением концентрации метанола привес сначала растет до концентрации растворителя 30%, а затем плавно падает. Естественно, что

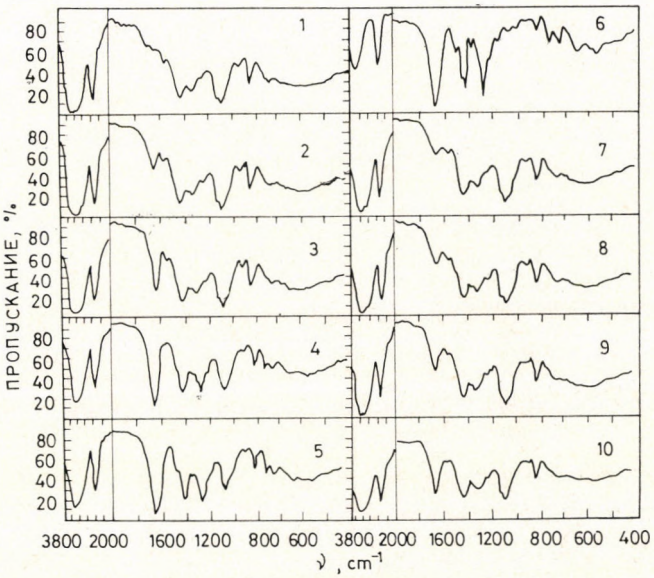

Рис. 2. Влияние концентрации растворителя на прививку ВП к ПВС. ПВС : ВП = 1 : 2. Мощность обл. 67 рад/сек. Доза обл. 0,4 Мрад. 1- метанол, 2- диоксан (концентрация растворителя в процентах от веса мономера)

уменьшение привеса с увеличением концентрации растворителя связано с разбавлением реакционной смеси. В случае диоксана низкая эффективность прививки указывает, что данный растворитель не может служить сенсибилизатором прививки ВП к ПВС.

На рис. 3 приведены ИК-спектры привитых сополимеров ПВС—ПВП, а также ПВС и ПВП. Полное отнесение частот для ПВС к соответствующим видам колебаний сделано в [5]. В спектре ПВП имеются полосы поглощения валентных колебаний гидроксильных групп, включенных в водородную связь, максимум поглощения которых находится при 3500 $см^{-1}$, валентные CH —2980 $см^{-1}$, в области 1680 $см^{-1}$ проявляются валентные C = O колебания, в области 1495 и 755 $см^{-1}$ проявляются колебания цикла ВП. Дефор-

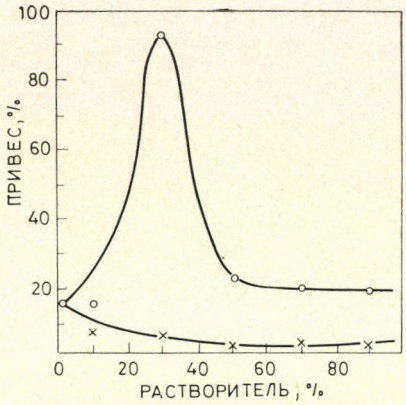

Рис. 3. ИК-спектры ПВС, ПВП и их привитых сополимеров. 1— ПВС; сополимеры, синтезированные в присутствии метанола; 2—0,2 Мрад; 3—3,0 Мрад; 4—0,4 Мрад, 5—0,5 Мрад; 6—ПВП; сополимеры, синтезированные в присутствии диоксана; 7—0,2 Мрад; 8—0,3 Мрад; 9—0,4 Мрад; 10—0,5 Мрад.

мационные колебания CH_2, CH групп имеют характерные поглощения в области 1500—31 300 $см^{-1}$. Область 1292 $см^{-1}$ относится к деформационным колебаниям цикла, а область 855 $см^{-1}$ к валентным CC колебаниям. Характерной особенностью в ИК-спектре ПВП является наличие поглощения в области гидроксильных групп (3700—3200 $см^{-1}$), которое связано, по-видимому, с присоединением гидроксильных групп на концах макромолекул гомополимера вследствие большой гидрофильной способности ПВП. Деформационные колебания OH групп проявляются в области 1100—1000 $см^{-1}$. При прививке ВП к ПВС в ИК-спектрах полученных продуктов имеются полосы поглощения, характерные как для ПВС, так и для ПВП. Как видно, с увеличением дозы облучения растет интенсивность валентных колебаний C = O групп и несколько уменьшается интенсивность валентных колебаний OH групп, включенных в водородную связь. Незначительное уменьшение интенсивности полосы поглощения гидроксильных групп можно объяснить тем, что в процессе прививки, вследствие наличия примесей воды в реакционной среде, происходит увеличение скорости обрыва цепи с образованием на концах привитого ПВП OH группы, поглощение которых накладывается на поглощение OH группы ПВС. Для образцов, полученных при одной и той же интегральной дозе облучения, интенсивность полос поглощения привитого ПВП несколько ниже в случае применения в качестве растворителя диоксана, чем метанола, что подтверждает данные синтеза. Ввиду того, что полосы поглощения 1680 и 1100 $см^{-1}$ очень чувствительны к содержанию ПВП и ПВС в сополимере, эти полосы могут быть использованы в качестве аналитических для количественного определения состава сополимеров.

Качественное изучение растворимости показало, что синтезированные привитые сополимеры ПВС—ПВП растворяются при нагревании в воде,

моноэтаноламине, диметилформамиде, в смеси воды и метанола (1 : 1), воды и уксусной кислоты (1 : 1), а в муравьиной кислоте растворяются при комнатной температуре. Характеристическую вязкость $[\eta]$ привитых сополимеров измеряли в воде, муравьиной кислоте и смеси воды с диметилформамидом.

Как видно из рис. 4, $[\eta]$ привитых сополимеров в воде меньше $[\eta]$ исходного ПВС. Очевидно, это связано с тем, что в водных растворах гидрофобность углеводородного скелета макромолекул ПВС по отношению к воде приводит к потере их гибкости. Поэтому при прививке более гибких цепей ПВП жесткость основных цепей уменьшается и $[\eta]$ привитых сополимеров сначала уменьшается, а затем остается постоянной, что может служить указанием на существование в растворе компактных макромолекулярных клубков. При добавлении же диметилформамида (ДМФ) в водный раствор вязкость исходного ПВС (рис. 5) вначале несколько уменьшается, а затем растет до максимального значения, после чего имеет место падение вязкости. Хорошо известно, что ПВС представляет собой жесткоцепный полимер, скелетная жесткость которого обусловлена внутри- и межмолекулярными водородными связями. В присутствии ДМФ гибкость макромолекул ПВС, по-видимому,

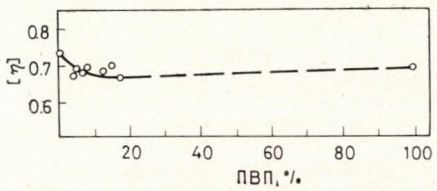

Рис. 4. Изменение $[\eta]$ растворов привитых сополимеров ПВС—ПВП в воде.

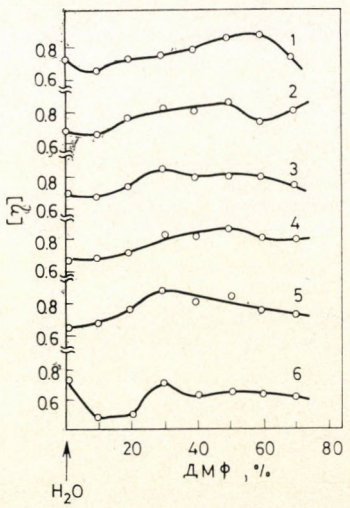

Рис. 5. Изменение $[\eta]$ ПВС, ПВП и их привитых сополимеров в смешанных водно-диметилформамидных растворителях. 1 — ПВС, 2—5,5% ПВП, 3—10,5% ПВП, 4—14,0% ПВП, 5—17,5% ПВП, 6 — ПВП.

должна увеличиваться, так как ДМФ имеет группы, способные взаимодействовать как с метиленовыми группами ПВС, так и группу $= N - C \langle {}^{O}_{H}$, способную образовывать водородные связи с гидроксильными группами полимера. Поэтому первоначальное введение ДМФ будет способствовать повышению гибкости, и вязкость несколько уменьшается. Дальнейшее увеличение ДМФ в смеси увеличит сольватацию ПВС молекулами растворителя, в результате чего объем макромолекулярного клубка увеличится и тем самым вязкость также увеличится. Такие эффекты наблюдаются и для ПВП. В случае же привитых сополимеров $[\eta]$ начинает расти сразу при добавлении ДМФ, очевидно, за счет одновременной сольватации основных и боковых цепей привитого сополимера. Снижение же вязкости при больших содержаниях ДМФ является следствием стремления макромолекул привитых сополимеров к образованию компактных структур, так как избыток ДМФ начинает играть роль осадителя.

В водных растворах данных привитых сополимеров возможно также внутримолекулярное взаимодействие между гидроксильными группами основных цепей и карбонильными группами лактамных циклов боковых цепей. Возможно, что именно этим обстоятельством объясняются данные рис. 6, согласно которым $[\eta]$ механических смесей этих полимеров в воде совпадают с аддитивными значениями, а увеличение молекулярного веса ПВП в смеси почти не изменяет $[\eta]$ водного раствора смеси полимеров, как это видно из рис. 7.

На рис. 8 представлена температурная зависимость $[\eta]$ ПВС, ПВП, их механической смеси и привитых сополимеров ПВС—ПВП в воде. Из рисунка видно, что для гомополимеров и их смеси $[\eta]$ линейно изменяется с неболь-

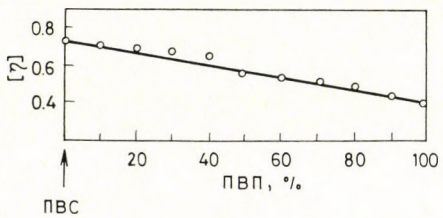

Рис. 6. Изменение $[\eta]$ механической смеси ПВС с ПВП в воде, от соотношения ПВС и ПВП.

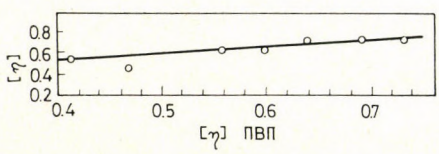

Рис. 7. Изменение $[\eta]$ механической смеси ПВС с ПВП (соотношение (1 : 1) от молекулярного веса ПВП, в воде.

шим отрицательным температурным коэффициентом. Для привитых сополимеров эта зависимость выражена сильнее и характеризуется наличием излома прямых при 30°C. Обращает на себя внимание, что после достижения точки излома вязкость почти не изменяется. Очевидно, что наличие такой точки свидетельствует об определенном конформационном превращении в структуре макромолекул привитых сополимеров. Дондос [6] в ряде работ показал, что наличие экстремальных точек на кривых температурной зависимости вязкости привитых сополимеров обусловлено разрушением агрегированной структуры макромолекул привитых сополимеров с последующим приобретением структуры статистического клубка. Действительно, в растворах муравьиной кислоты кривая температурной зависимости вязкости привитых сополимеров ПВС—ПВП характеризуется четко выраженным минимумом и максимумом в области 35—40°C (рис. 9).

Естетственно, что различный характер проявления конформационного перехода в воде и муравьиной кислоте связан с различной природой этих растворителей.

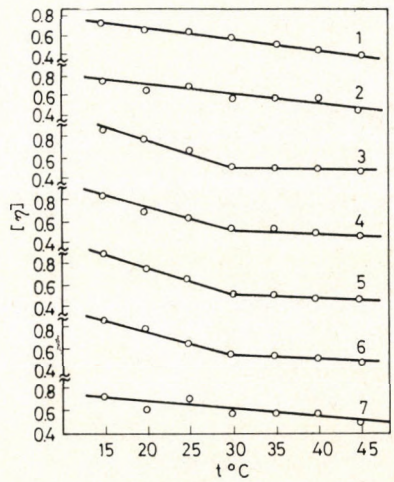

Рис. 8. Изменение $[\eta]$ ПВС, ПВП, их механической смеси и привитых сополимеров от температуры, в воде. 1— ПВС, 2—механическая смесь ПВС с ПВП 1 : 1), 3—5,5% ПВП, 4—10,5% ПВП, 5—14,0 ПВП, 6—17,5% ПВП, 7 — ПВП.

На рис. 10 приведены изотермы сорбции паров воды привитыми сополимерами ПВС—ПВП, из которого видно, что сорбционная способность ПВС близка к таковой для ПВП. Однако сорбция паров воды привитыми сополимерами меньше по сравнению с гомополимерами, что более заметно при больших содержаниях ПВП в привитом сополимере. В тоже время ПВС растворяется в воде с положительным тепловым эффектом несколько большим, чем ПВП, как это следует из рис. 11. Привитые сополимеры растворяются с

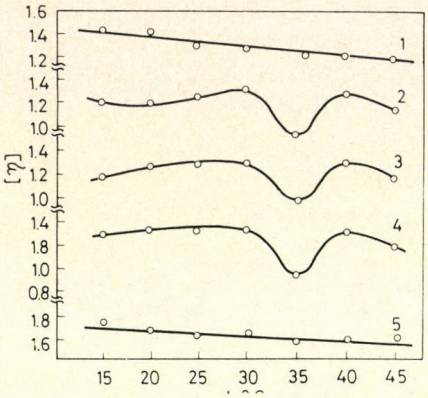

Рис. 9. Изменение $[\eta]$ ПВС, ПВП и их привитых сополимеров от температуры, в муравьиной кислоте. 1 — ПВС, 2—5,5% ПВП, 3—10,5% ПВП, 4—17,5% ПВП, 5 — ПВП.

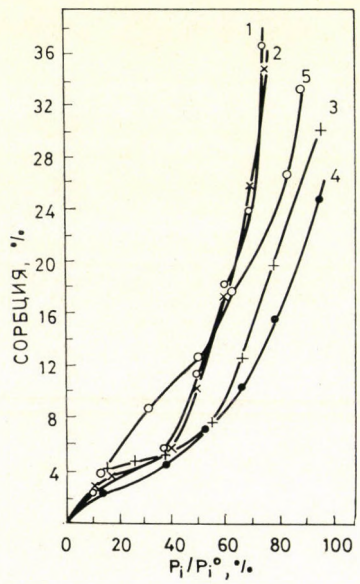

Рис. 10. Изотермы сорбции паров воды ПВС, ПВП и их привитыми сополимерами. 1 — ПВС, 2—9,0% ПВП, 3—12,5% ПВП, 4—17,5% ПВП, 5—ПВП.

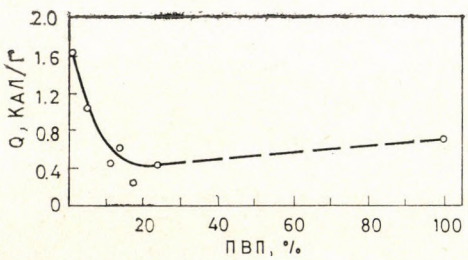

Рис. 11. Изменение теплот растворения привитых сополимеров ПВС—ПВП в воде.

менее положительным тепловым эффектом, чем гомополимеры. Таким образом, сорбционные данные и тепловые эффекты коррелируют друг с другом и указывают на уплотнение структуры полимера с увеличением степени прививки.

Summary

Graft copolymers of polyvinyl alcohol with polyvinylpyrrolidone have been synthesized by a radiation-chemical method, varying the irradiation dose, the nature and concentration of the solvent. The products obtained have been identified by IR spectroscopy.

The temperature dependence of the viscosity of the graft copolymers is anomalous; viscosity curves revealing extrema are observed. This phenomenon is interpreted in terms of a possible change in the conformation of the graft copolymer, from an aggregative form to a random coil state.

Sorption and calorimetric experiments have shown that in the process of grafting vinylpyrrolidone to polyvinyl alcohol, a more compact polymer structure is obtained.

ЛИТЕРАТУРА

1. Усманов Х. У., Тиллаев Р. С., Мусаев У. Н., Заводская лаборатория, № *12*, 1943 (1961)
2. Ташмухамедов С. А., Кандидатская диссертация. Ташкент, 1966 г.
3. Ташмухамедов С. А., Усманов Х. У., Тиллаев Р. С. Высокомолек. соед. (А) *10*, 379 (1968)
4. Чарлзби А., Ядерные излучения и полимеры. М., ИЛ., 1959 г.
5. KRIMM, S., LIANG, C. Y., SUTHERLAND, L. B.: J. Polym. Sci. **22**, 227 (1956)
6. DONDOS, Q.: J. Chim. Phys. et Phys. Chim. Biol. **62**, 1023 (1965)

S. A. TASHMUKHAMEDOV
A. Sh. KARABAEV
Sh. FUZAILOV
P. P. LARIN
R. S. TILLAEV
Kh. U. USMANOV

Ташкентский Государственный университет им. В. И. Ленина
Вузгородок, Химфак, Ташгу Ташкент 700095, СССР.

INDEX

ANALYTICAL CHEMISTRY — ANALYTISCHE CHEMIE — АНАЛИТИЧЕСКАЯ ХИМИЯ

IKRÉNYI, K.: Tandem Titrator 229

PHYSICAL AND INORGANIC CHEMISTRY — PHYSIKALISCHE UND ANORGANISCHE CHEMIE — ФИЗИЧЕСКАЯ И НЕОРГАНИЧЕСКАЯ ХИМИЯ

SÁRKÁNY, A., GUCZI, L. und TÉTÉNYI, P.: Über den Mechanismus der an Nickelpulver katalysierten Hydrogenolyse von Butan (On the Mechanism of the Hydrogenolysis of Butane Over Nickel-Dust Catalyst) 245

MARTIN, A. and KISS, Á. I.: Calculation of the π-Electronic Structure and Spectra of Hetero-disubstituted Halobenzenes by the MIM and PPP Methods 259

SZOTYORY, L., UJHIDY, A. und SZABÓ, I.: Reaktionskinetische Beiträge zur Untersuchung der Ringschlußreaktion von Carbäthoxy-2-(3-Chlorphenylamino)-äthylacrylat (Reaction Kinetic Contributions to the Investigation of The Ring-closing Reaction of Carbethoxy-2-(3-chlorophenylamino)-ethylacrylate) 279

GÉCZY, I.: Synthetic Linear Polymers, XXXII. Changes in the Dipole Moment of Polymer Homologous Compounds as a Function of the Molecular Weight 289

CSER, F., HARDY, GY.: Structural Studies on Polyacenaphthylene 297

WOJCIECHOWSKA, M., FIEDOROW, R. and KUCZYNSKI, W.: Catalytic Properties of Magnesium Fluoride 313

ORGANIC CHEMISTRY — ORGANISCHE CHEMIE — ОРГАНИЧЕСКАЯ ХИМИЯ

ELKASCHEF, M. A.-F., ABDEL-MEGEID, F. M. E., MOKHTAR, K.-E. M. and GAD, F. A.: 4-Pyrones, VII. Further Reactions of 4-Pyrones 319

FARKAS, I., BOGNÁR, R., MENYHÁRT, M. M. TARNAI, A. K. BIHARI, M. und TAMÁS, J.: Selektive Spaltung von Thioglykosiden mit Dichlormethyl-Methyläther (On the Selective Splitting of Thioglycosides with Dichloromethyl-methylether) 325

DÁVID, É., BOGNÁR, R.: The Reactivity of the Carbonyl Group in Flavonoid Compounds, I Kinetic Studies on the Formation of 2,4-Dinitrophenylhydrazones 335

CHEMICAL TECHNOLOGY — CHEMISCHE TECHNOLOGIE — ХИМИЧЕСКАЯ ТЕХНОЛОГИЯ

Ташмухамедов С. А., Карабаев А. Ш., Фузаилов Ш., Ларин П. П., Тиллаев Р. С. и Узманов Х. У.: Синтез и исследование свойств растворов привимых сополимеров поливинилового спирта с c_i поливинилпирролидоном (TASHMUKHAMEDOV, S. A., KARABAEV, A. SH., FUZAILOV, SH., LARIN, P. P., TILLAEV, R. S. and USMANOV, KH. U.: Synthesis and Study of Polyvinyl Alcohol — Polyvinylpyrrolidone Graft Copolymer Solutions) 343

Printed in Hungary

A kiadásért felel az Akadémiai Kiadó igazgatója. Műszaki szerkesztő: Zacsik Annamária

A kézirat nyomdába érkezett: 1974. XII. 9. — Terjedelem: 11,2 (A/5) ív, 80 ábra

75.1197 Akadémiai Nyomda, Budapest — Felelős vezető: Bernát György

ACTA CHIMICA

ТОМ 84—ВЫП. 3

Разностный „tandem" титрометр

К. ИКРЕНИ

РЕЗЮМЕ

Конструирован прибор для титрования, позволяющий расширить область определения электропроводности при кислотно-основном, осадительном, комплексо- или хелатометрическом и окислительно-восстановительном титрованиях. В целях создания кондуктометрического титрометра с конструкцией регистрации разности электропроводностей (т. н. Разностного или «tandem» титрометра) нами изготовлены: разностный кондуктометр, две ячейки для измерения электропроводности и поршневые проточные бюретки с внутренней смазкой. Новые методы обозначения (регистрации) конца титрования при «tandem» системе позволяют значительное устранение влияния исходных веществ, а также определение двух компонентов при одном титровании.

Механизм гидрогенолиза бутана на порошкообразном никелевом катализаторе

А. ШАРКАНЬ, Л. ГУЦИ и П. ТЕТЕНИ

Был изучен гидрогенолиз н-бутана и 2-метилпропана на порошкообразном никелевом катализаторе в интервале температур 160—260°С. Отношение водород/углеводород изменялось в пределах от 3 до 10. Селективность образования продуктов реакции исследовалась в зависимости от парциального давления водорода, температуры и активности катализатора. Селективность гидрогенолиза ($S_{P_Г}$) увеличивается с увеличением парциального давления водорода, а активность катализатора с уменьшением температуры. На основе меченого промежуточного продукта пропан-1-C^{14} было доказано, что неселективный гидрогенолиз н-бутана и 2-метилпропана может быть объяснен отсутствием адсорбционного равновесия промежуточного продукта. На основе экспериментальных данных было установлено, что на никеле образуются «сильно» дегидрированные углеводородные радикалы, которые затем быстро реагируют на поверхности.

Расчет π-электронного спектра и электронного строения гетеро-дигалогенбензолов

А. МАРТИН и А. И. КИШ

С помощью методов MIM и PPP были рассчитаны π-электронная структура и спектр дизамещенных бензолов, содержащих два различных галоидных атома.

Полученные энергии MIM и волновые функции, а также спектральные данные PPP, плотность заряда, порядок связи и вклад π-электронов в дипольный момент сравнивались с результатами, полученными для моно- и гомо-дизамещенных галогенбензолов.

Было установлено, что параметры, разработанные для расчета галогенбензолов и едино использованные, дают результаты с почти одинаковой точностью как в случае гетеродизамещенных производных, так и в случае моно- и гомо-дизамещенных производных.

Кинетические данные для циклизации 1-карбетокси-2-/3-хлорфениламино/-этилакрилата

Л. СОТЁРИ, А. УЙХИДИ и И. САБО

Кинетика реакции циклизации 1-карбетокси-2-(3-хлорфениламино) - этилакрилата была исследована при различных концентрациях и температурах. Средой реакции служил дифенил, содержащий 10% парафинового масла. За ходом реакции следили по изменению во времени веса выделяющегося твердого вещества. Концентрация конечного продукта реакции 3-карбетокси-4-гидрокси-7-хлорхинолина была изображена в зависимости от времени. Были получены кривые с максимумом, указывающие на протекание последовательных реакций. Отсюда тремя различными методами были определены аррениусовские постоянные. Было проверено предположение о том, что причиной отклонения полученных результатов в случае 5 и 10%-ых концентраций является солевой эффект.

Синтетические линейные полимеры, XXXII

Изменение дипольного момента полимергомологических соединений в зависимости от молекулярного веса

И. ГЕЦИ

Удельный квадратичный дипольный момент поли-(трифторхлорэтилена) и полиеновых олигомеров с концевой группой C_6H_5 изменяются линейно в зависимости от обратной величины молекулярного веса. Поэтому в данных условиях эти полимеры не образуют вторичной структуры. Средний дипольный момент звена, повторяющегося в этих полимерах, равен 0,12 D для (—CFCl—CF_2—) и 1,02 D для (—CH = CH—). В случае полиеновых олигомеров с диметиламинной концевой группой, поли-γ-бензил-L-глутамата и полимеров фенилсилоксана подобное графическое изображение приводит к отклонению от линейности. На основе этого, в случае этих соединений следует считаться с образованием вторичных структур.

Структурные исследования полиаценафтиленов

Ф. ЧЕР и ДЬ. ХАРДИ

Была определена плотность олиго- и полиаценафтиленов, полученных различным способом. Рентгеновская диффрактограмма олигомера, с наибольшей плотностью, приготовленного в твердой фазе иодовым инициированием, разделялась на гауссовские пики. Диффракционные углы, соответствующие максимумам, индексировались соответственно моноклинным кристаллам с размерами ячейки a = 11,70, b = 7,62 и c = 9,82 Å и с углом наклона $\beta \simeq 90°$. Пространственная группа $P2_1$.

С помощью минимализации конформационной энергии были рассчитаны атомные координаты эритро и трео мономерных единиц. Исходя из сегментов двух типов, был построен полимер с изо- и синдиотактической цепочкой, а также была рассчитана конформационная энергия полимерной цепочки в зависимости от углов искажения основной цепи (φ_1, φ_2). Из эритро сегментов — вследствие стерических препятствий — не удалось построить полимерную цепочку. В случае трео изотактических цепей конформационная энергия обладает четырьмя местными минимумами. Полимерная цепочка, относящаяся к наиболее глубокому минимуму, представляет собой 2_1 геликс. В случае синдиотактических полимеров получена цепочка с 3 минимальными энергиями: геликс 2_1, геликс 4_1 и с рядом центра симметрии. Геликс 2_1 — абсолютный минимум энергии — соответствует ячейке олигомера. Геликс 2_1 и ряд центра симметрии приводит к цепочкам подобного строения. Эти цепочки могут быть получены из строения кристалла мономера с помощью трансляционного движения небольшой степени; геликс 2_1 может быть изоморфным с кристаллом мономера.

Комбинация эритро и трео сегментов также может привести к геликсу 2_1. Однако, содержание энергии значительно превышает энергию чистых трео цепочек.

Каталитические свойства фтористого магния

М. ВОЙЦИКОВСКА, Р. ФЕДОРОВ и В. КУЦИНСКИ

Были описаны свойства пористого фторида магния, полученного действием гидрофтористой кислоты на раствор сульфата магния. Образцы фтористого магния, кальцинированные при различных температурах, были исследованы с точки зрения их каталитических свойств в некоторых модельных реакциях. Приводятся некоторые заключения относительно природы кислотных мест на поверхности фтористого магния.

4-Пироны, VII

Некоторые реакции 4-пиронов

М. А. Ф. ЭЛЬКАШЕФ, Ф. М. Е. АБДЕЛЬ-МЕГЕЙД, К. Е. М. МОХТАР и Ф. А. ГАД

4-Алкилиден(4Н)пиран может быть получен взаимодействием диазоалканов с 4-тиопиронами. 5,6-Бензофлавон, реагируя с галогенидами фенил- или бензилмагния, дает 4,4-дифенил- или 4,4-дибензил-производные. Взаимодействие с бромидом п-метоксифенилмагния этого соединения, а также 2-метилхромона с бромидом фенилмагния приводит к образованию соответствующих 4-гидрокси-соединений.

Селективное расщепление тиогликозидов с помощью дихлорметил-метилового эфира

И. ФАРКАШ, Р. БОГНАР, М. М. МЕНЬХЕРТ, А. К. ТАРНАИ, М. БИХАРИ и Й. ТАМАШ

Ацетилированные алкил- и арил-1-тио-β-D-глюко- и -галактопиранозиды (1—13) с помощью дихлорметил-метилового эфира /$ZnCl_2$ расщепляются до α-ацетохлор-D-глюкозы (III) и α-ацетохлор-D-галактозы (IV).

Согласно исследованиям с дисахаридными производными расщепление является селективным: с хорошим выходом может быть изолировано ацетохлор-производное незатронутого сахарного компонента.

При расщеплении гликозида единственным побочным продуктом, содержащим серу, — в зависимости от агликона — является S-алкил- и S-атилтиоформиат (VII и IV); последний, однако, в применяемых условиях реакции количественно галогенизируется до S-дихлорметилтиофенола (VIII). Побочные продукты были идентифицированы с помощью комбинированного газовохроматографического и масс-спектрометрического метода. На этой основе кажется вероятным, что тиогликозиды под влиянием дихлорметил-метилового эфира /$ZnCl_2$ — независимо от природы агликона — разлагаются с «S-алкильным отщеплением», образуя соответствующие ацетогалогеновые сахара через, по всей вероятности, комплекс типа сульфониума (X).

Исследования на модельных соединениях показывают, что соляная кислота, выделяющаяся в побочной реакции, практически не играет роли реагента, расщепляющего гликозид.

Исследование реакционной способности карбонильной группы флавоноидных соединений, I

Исследование кинетики образования 2,4-динитрофенилгидразона

Е. Р. ДАВИД и Р. БОГНАР

Реакционная способность флавоноидных соединений, зависящая от структуры группы C = O (от степени окисления) и от заместителей, была исследована на примере взаимодействия с 2,4-динитрофенилгидразином с помощью метода УФ спектроскопии. Было найдено, что наибольшая реакционная способность карбонильной группы наблюдается в случае незамещенного флаваона. Замещение гидроксилом положения, соседнего с карбонилом, — вследствие образования внутреннего хелата — уменьшает реакционную способность как флаванона, так и 2'-гидроксихалкона. Заместители, находящиеся в параположении к карбонильной группе, в соответствии с их +1 или —1 эффектами, изменяют скорость реакции образования 2,4-динитрофенилгидразона.

JOURNAL OF THERMAL ANALYSIS

An international forum for communications on thermal investigations

Journal of THERMAL ANALYSIS has an international Editorial Board, the members of which are distinguished specialists from all over the world.

AIMS AND SCOPE

The main subjects covered are: thermogravimetry, derivative thermogravimetry, differential thermal analysis, dilatometry, differential scanning calorimetry, thermometry, evolved gas detection, evolved gas analysis, multiple techniques and miscellaneous thermal methods (including the thermal method with various instrumental techniques), instrumentation for the thermal method. Papers dealing with these subjects are published in the following sections: Original Research Papers, Short Communications, Special Reviews, Bibliography Section, Modern Instruments. The Special Reviews section is reserved for papers that have been published in greater detail in some journal for a special branch of scientific field or industry.

Papers submitted to the journal may deal with any field of chemistry, metallurgy or mineralogy, e.g. they may deal with inorganic, organic or polymeric materials and they may cover biochemical, mineralogical or metallurgical applications.

Journal of THERMAL ANALYSIS is published bimonthly comprising about 720 pages per year. Size: 17×25 cm.

Journal of THERMAL ANALYSIS is published jointly by

AKADÉMIAI KIADÓ
Budapest

HEYDEN & SON LIMITED
London

ABSORPTION SPECTRA IN THE ULTRAVIOLET AND VISIBLE REGION

Series edited by L. LÁNG

According to international book reviews, this series is highly useful in both structure research and chemical analysis. This applies especially to problems of analytical character or structure determination encountered in the pharmaceutical, dye and other industries, i.e. in organic chemical industry in general. A great advantage of this collection is that the spectra published may, in many cases, directly be used for solving the particular problems in question.

The series dealing with *ultraviolet and visible spectra* was started by the Publishing House of the Hungarian Academy of Sciences in 1959, and by now the project has got as far as Vol. 18. The editors invite the users of the collection to contribute to the success of this work by submitting for publication spectra of new compounds.

Each volume contains about 400 pages spectra graphs and tables of about 190 compounds + indexes.

Cumulative index: I–V, VI–X, X–XV

AKADÉMIAI KIADÓ
Budapest

ACADEMIC PRESS
New York

The whole series is a co-edition, – distributed on the American Continent by ACADEMIC PRESS, New York, in all other countries by KULTURA, H-1389 Budapest, P. O. B. 149

The Acta Chimica publish papers on chemistry, in English, German, French and Russian.

The Acta Chimica appear in volumes consisting of four parts of varying size, 4 volumes being published a year.

Manuscripts should be addressed to

Acta Chimica
Budapest 112/91 Műegyetem

Correspondence with the editors should be sent to the same address.

The rate of subscription is $ 32.00 a volume.

Orders may be placed with "*Kultúra*" Foreign Trade Company for Books and Newspapers (1389 Budapest 62, P.O.B. 149. Account No. 218 10990) or with representatives abroad.

Les Acta Chimica paraissent en français, allemand, anglais et russe et publient des mémoires du domaine des sciences chimiques.

Les Acta Chimica sont publiés sous forme de fascicules. Quatre fascicules seront réunis en un volume (4 volumes par an).

On est prié d'envoyer les manuscrits destinés à la rédaction à l'adresse suivante:

Acta Chimica
Budapest 112/91 Műegyetem

Toute correspondance doit être envoyée à cette même adresse.

Le prix de l'abonnement est de $ 32,00 par volume.

On peut s'abonner à l'Entreprise pour le Commerce Extérieur de Livres et Journaux «*Kultúra*» (1389 Budapest 62, P.O.B. 149 Compte-courant No. 218 10990) ou à l'étranger chez tous les représentants ou dépositaires.

«*Acta Chimica*» издают трактаты из области химической науки на русском, французском, английском и немецком языках.

«*Acta Chimica*» выходят отдельными выпусками разного объема. 4 выпуска составляют один том. 4 тома публикуются в год.

Предназначенные для публикации рукописи следует направлять по адресу:

Acta Chimica
Budapest 112/91 Műegyetem

По этому же адресу направлять всякую корреспонденцию для редакции.

Подписная цена – $ 32,00 за том.

Заказы принимает предприятие по внешней торговле книг и газет «*Kultúra*» (1389 Budapest 62, P.O.B. 149. Текущий счет № 218 10990) или его заграничные представительства и уполномоченные.

Reviews of the Hungarian Academy of Sciences are obtainable at the following addresses:

ALBANIA

Drejtorija Qändrone e Pärhapjes
dhe Propagandimit tä Librit
Kruga Konferenca e Päzes
Tirana

AUSTRALIA

A. Keesing
Box 4886, GPO
Sydney

AUSTRIA

GLOBUS
Höchstädtplatz 3
A-1200 Wien XX

BELGIUM

Office International de Librairie
30, Avenue Marnix
Bruxelles 5
Du Monde Entier
162. rue de Midi
1000 Bruxelles

BULGARIA

HEMUS
11 pl Slaveikov
Sofia

CANADA

Pannonia Books
2, Spadina Road
Toronto 4, Ont.

CHINA

Waiwen Shudian
Peking
P. O. B. 88

CZECHOSLOVAKIA

Artia
Ve Směčkách 30
Praha 2
Poštovní Novinivá Služba
Dovaz tisku
Vinohradská 46
Praha 2
Mad'arská Kultura
Václavské nám. 2
Praha 1
SLOVART A. G.
Gorkého
Bratislava

DENMARK

Ejnar Munksgaard
Nörregade 6
Copenhagen

FINLAND

Akateeminen Kirjakauppa
Keskuskatu 2
Helsinki

FRANCE

Office International de Documentation
et Librairie
48, rue Gay-Lussac
Paris 5

GERMAN DEMOCRATIC REPUBLIC

Deutscher Buch-Export und Import
Leninstraße 16
Leipzig 701
Zeitungsvertriebsamt
Fruchtstraße 3—4
1004 Berlin

GERMAN FEDERAL REPUBLIC

Kunst und Wissen
Erich Bieber
Postfach 46
7 Stuttgart S.

GREAT BRITAIN

Blackwell's Periodicals
Oxenford House
Magdalen Street
Oxford
Collet's Subscription Import
Department
Dennington Estate
Wellingsborough, Northants.
Robert Maxwell and Co. Ltd.
4—5 Fitzroy Square
London W. 1.

HOLLAND

Swetz and Zeitlinger
Keizersgracht 471—487
Amsterdam C.
Martinus Nijhof
Lange Voorhout 9
The Hague

INDIA

Hind Book House
66 Babar Road
New Delhi 1

ITALY

Santo Vanasia
Via M. Macchi 71
Milano
Libreria Commissionaria Sansoni
Via La Marmora 45
Firenze
Techna
Via Cesi 16.
40135 Bologna

JAPAN

Kinokuniya Book-Store Co. Ltd.
826 Tsunohazu 1-chome
Shinjuku-ku
Tokyo
Maruzen and Co. Ltd.
P. O. Box 605
Tokyo-Central

KOREA

Chulpanmul
Phenjan

NORWAY

Tanum-Cammermeyer
Karl Johansgt 41—43
Oslo 1

POLAND

Ruch
ul. Wronia 23
Warszawa

ROUMANIA

Cartimex
Str. Aristide Briand 14—18
Bucureşti

SOVIET UNION

Mezhdunarodnaya Kniga
Moscow G—200

SWEDEN

Almquist and Wiksell
Gamla Brogatan 26
S—101 20 Stockholm

USA

F. W. Faxon Co. Inc.
15 Southwest Park
Westwood Mass. 02090
Stechert Hafner Inc.
31. East 10th Street
New York, N. Y. 10003

VIETNAM

Xunhasaba
19, Tran Quoc Toan
Hanoi

YUGOSLAVIA

Forum
Vojvode Mišića broj
Novi Sad
Jugoslavenska Knjiga
Terazije 27
Beograd

30. IV. 1975 Index: 26.007

ACTA CHIMICA

ACADEMIAE SCIENTIARUM HUNGARICAE

ADIUVANTIBUS

V. BRUCKNER, GY. DEÁK, K. POLINSZKY,
E. PUNGOR, G. SCHAY, Z. G. SZABÓ

REDIGIT

B. LENGYEL

TOMUS 84 FASCICULUS 4

AKADÉMIAI KIADÓ, BUDAPEST

1975

ACTA CHIM. (BUDAPEST) ACASA 2 84 (4) 353–479 (1975)

ACTA CHIMICA

A MAGYAR TUDOMÁNYOS AKADÉMIA KÉMIAI TUDOMÁNYOK OSZTÁLYÁNAK IDEGEN NYELVŰ KÖZLEMÉNYEI

SZERKESZTI

LENGYEL BÉLA

TECHNIKAI SZERKESZTŐK

DEÁK GYULA és HARASZTHY-PAPP MELINDA

Az Acta Chimica német, angol, francia és orosz nyelven közöl értekezéseket a kémiai tudományok köréből.

Az Acta Chimica változó terjedelmű füzetekben jelenik meg, egy-egy kötet négy füzetből áll. Évente átlag négy kötet jelenik meg.

A közlésre szánt kéziratok a szerkesztőség címére (Budapest 112/91 Műegyetem) küldendők.

Ugyanerre a címre küldendő minden szerkesztőségi levelezés. A szerkesztőség kéziratokat nem ad vissza.

Megrendelhető a belföld számára az „Akadémiai Kiadó"-nál (1363 Budapest Pf 24 Bankszámla 215 11488), a külföld számára pedig a „Kultúra" Könyv- és Hírlap Külkereskedelmi Vállalatnál (1389 Budapest 62, P.O.B. 149 Bankszámla: 218 10990) vagy annak külföldi képviseleteinél és bizományosainál.

Die Acta Chimica veröffentlichen Abhandlungen aus dem Bereiche der chemischen Wissenschaften in deutscher, englischer, französischer und russischer Sprache.

Die Acta Chimica erscheinen in Heften wechselnden Umfanges. Vier Hefte bilden einen Band. Jährlich erscheinen 4 Bände.

Die zur Veröffentlichung bestimmten Manuskripte sind an folgende Adresse zu senden:

Acta Chimica
Budapest 112/91 Műegyetem

An die gleiche Anschrift ist auch jede für die Redaktion bestimmte Korrespondenz zu richten. Abonnementspreis pro Band: $ 32,00.

Bestellbar bei dem Buch- und Zeitungs-Außenhandels-Unternehmen »*Kultúra*« (1389 Budapest 62, P.O.B. 149 Bankkonto Nr. 218 10990) oder bei seinen Auslandsvertretungen und Kommissionären.

Acta Chimica Academiae Scientiarum Hungaricae, 84 (4), pp. 353—379 (1975)

STUDY OF THE VISCOSITY OF METAL CHLORIDE–H_2O AND METAL CHLORIDE–HCl–H_2O SYSTEMS

E. BERECZ

(Department of General and Physical Chemistry, Technical University of Heavy Industries, Miskolc)

Received April 2, 1973

The results are given of a comparative study of the viscosity of ternary metal chloride (mainly alkali metal and alkaline earth metal chloride)–HCl–H_2O systems, and of their constituent binary systems. From the course of the viscosity *vs.* concentration curves for the individual binary aqueous systems, and from the extent and trend of the changes in the viscosity of the binary systems when the third component (salt or acid) is added, conclusions are drawn on the structure and their concentration dependence in the binary and ternary systems. An analytical correlation and a method of relatively high accuracy, applicable on the basis of the proposed binary equation $[\eta = f(m_{salt})]$ are given for the calculation of the viscosity in ternary metal chloride–HCl–H_2O systems.

This work involves the study of ternary electrolyte systems of the type metal chloride–HCl–H_2O with the aim of gaining a deeper insight into their structural properties. Appropriately selected properties are investigated experimentally in the whole of the stable concentration interval up to saturated solutions. In this way it is hoped to throw light on the structural conditions, mainly of moderately concentrated and concentrated solutions, for which relatively few data are available. It was considered that, besides the present state of structural research on ternary solutions, the best possibilities are provided by suitable, reliable comparative examinations permitting a uniform systematization on a fixed experimental basis. The model systems were chosen so as to contain either a given anion (alkali metal chloride, alkaline earth metal chloride, $MnCl_2$, HCl; or $MnSO_4$, $NiSO_4$, $MgSO_4$, H_2SO_4) or the same cations ($MnSO_4$–$MnCl_2$, $MgCl_2$–$MgSO_4$, H_2SO_4–HCl). In this way the effects of cations or anions with different charges, radii and electronic structures can be distinguished from one another.

At the same time, the study of ternary solutions is treated as a method of obtaining more detailed information on the structure of the constituent binary systems. A study is made of how the addition of a third component affects the properties of the original binary system, as a function of the concentration of the latter. Further, a comparison is made of the interrelations of the property changes resulting from temperature variation in the binary system, or from the addition of the third component.

Our conclusions based on such results and relating to the viscosity were published earlier [1]. The present publication describes a comparative study of the viscosity of ternary metal chloride (mainly alkali and alkaline earth, metal chloride)–HCl–H_2O systems and their binary constituent systems earlier investigated in the whole of the concentration interval for which the system is stable at the given temperature [2]. In addition to conclusions on the structure of the solutions, a method and equation of relatively high accuracy, applicable on the basis of the binary η *vs.* m_{salt} equation found, are given for the calculation of the viscosity of the ternary metal chloride–HCl–H_2O systems.

General study of the viscosity of metal chloride–H_2O systems

Figures 1 and 2 present the viscosities of the individual metal chloride solutions at 25 °C as a function of concentration* [2—4]. It can be seen that the course of the η *vs.* m curves depends very strongly on the nature of the metal ion, and mainly on its charge and size.

In this respect the charge of the ions is the decisive factor. For cations of a given charge, and with a given anion, the viscosity *vs.* concentration curves each run in close and similar, definite bands, even when there are fairly large differences in cation radius (see the shaded bands in Fig. 1). Naturally, for a given concentration a larger viscosity generally relates to a smaller metal ion; this is always the case for univalent cations at not too high concentrations. The smaller cation has a higher field, and can thus exert a relatively larger effect on the water molecules in its vicinity. It is an obvious consequence of this that at a given concentration the smaller metal ion, together with the larger hydrate sheath developing around it, can move only with more difficulty and with a relatively higher activation energy as a result of a mechanical shear force acting on the solution.

Figures 1 and 2 show that the curve depicting the concentration dependence of the viscosity of HCl runs in the band of the curves for the univalent metal chlorides. This indicates that, as regards the viscosity, the H_3O^+ ion behaves to a certain extent like any other univalent cation (this is supported by the fact that the viscosity *vs.* concentration curve for the H_2SO_4, for instance, lies in the band of the η *vs.* m curves for the sulfates of the univalent metal cations). Nevertheless, particularly as regards the concentration dependence, the effect of the H_3O^+ ion differs from those of univalent monoatomic ions with inert gas configurations. For example, although the m_{HCl} curve remains within the band, its course is so much flatter that, similarly to

* This means in practice the concentration interval from $m = 0.2$ to saturation, since we do not deal with a detailed investigation of the very dilute solutions.

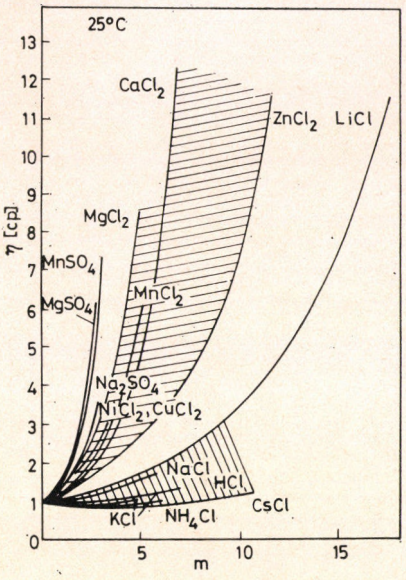
25°C
CaCl2
ZnCl2
LiCl
MgCl2
MnSO4
MnCl2
MgSO4
Na2SO4
NiCl2
CuCl2
NaCl
HCl
CsCl
KCl
NH4Cl
η [cp]
m

Fig. 1

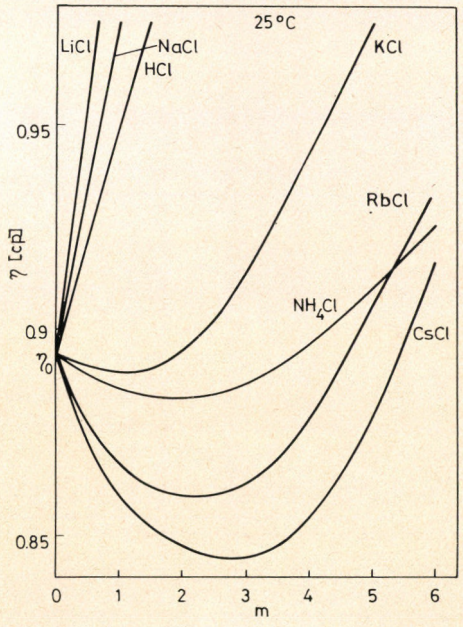
25°C
LiCl
NaCl
HCl
KCl
RbCl
NH4Cl
CsCl
η [cp]
η0
m

Fig. 2

the η *vs.* m_{NH_4Cl} curve, it no longer corresponds to the dimensions of the H_3O^+ ion (r_{ion} = 1.12 Å).

In the case of the chlorides of the univalent monoatomic ions with inert gas configurations the conditions are quite clear: the situation of the viscosity curves within the band is a monotonous function of the cation radius at all concentrations (see Fig. 3, which shows the variation of the viscosities of the individual univalent metal chlorides as a function of the cation radius at m = = 0.5). This points to the fact that for a given charge the hydration effect too must be an unambiguous function of the size of the cation with an inert gas electron configuration. This is also the case for the chlorides of divalent monoatomic ions with inert gas configurations.

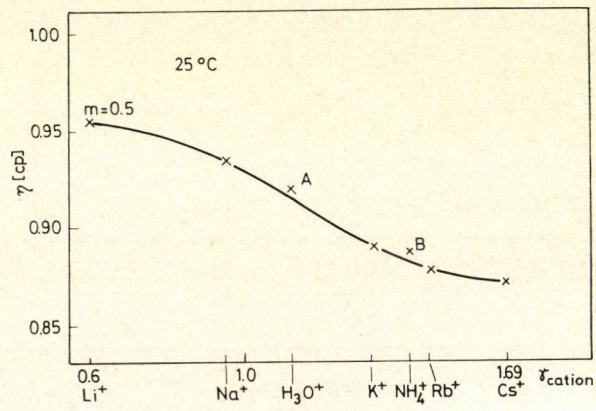

Fig. 3

At the individual concentrations, however, the η values corresponding to the radii of the complex cations (NH_4^+, H_3O^+) do not lie on the η *vs.* r_{cation} curves for the chlorides of the univalent monoatomic ions with inert gas configurations (see *e.g.* points A and B in Fig. 3), and the situation is the same for the monoatomic ions with non-inert gas configurations. As a consequence, although the viscosity curves for the complex cations lie in the appropriate band, in dilute solution they are situated in positions corresponding to a smaller cation size. Thus, for HCl the η *vs.* m curve does not lie in the position corresponding to the radius of H_3O^+, but runs closer to the curve for NaCl. This effect is even more pronounced for NH_4Cl, where the η *vs.* m curve lies close to that for KCl. Indeed, at higher concentrations the curves for both of these complex cations assume a different character from those for the monoatomic ions with inert gas configurations (Fig. 2).

Thus, in the case of complex ions the hydration number (however this is defined or determined) cannot simply be calculated from the charge and the ionic size, and even in the case of the same ionic size, the hydration of complex

ions differs from that of monoatomic ions with the same charge. It is obvious, therefore, that in these cases the hydration depends not only on the charge and the ionic size, but also on the shapes of the ions, determined by electronic structures which no longer have inert gas configurations.

In this respect there is also a certain difference between H_3O^+ and NH_4^+. Of these two, only the NH_4^+ is the ion in advance existent and truly composite ion; H_3O^+ comes about only in solution, where it is always present, as a monohydrated primary complex of H^+. The further hydration of H_3O^+, therefore, is essentially the hydration of a 'positively-charged water molecule'; this breaks up the water structure to a relatively greater extent, being more positively hydrated* than some monoatomic ions of the same size. At the same time NH_4^+ is a truly composite ion, which may exist in solution in a non-hydrated form too. The hydration of NH_4^+ can proceed 'regularly', at most being more strongly directed to a definite extent by the electron configuration developed. In practice in the first hydrate sphere this means more water molecules than the maximum number which can fit geometrically into a layer of spheres with a thickness equal to the diameter of the water molecule, beginning at a distance determined by the radius; the reason is that there is a possibility for the deeper penetration of 4 water molecules in the direction of the faces of the tetrahedron.

As a result of these factors, at least in more dilute solutions, H_3O^+ behaves as a more structure-breaking and more positively hydrating ion than can be expected from its size; on the other hand, compared to its size and charge, NH_4^+ behaves as a less structure-making, and less negatively hydrating ion.

The situation is similar with the monoatomic ions with non-inert gas configurations, *e.g.* Ni^{2+}, Cu^{2+}, Zn^{2+}, Mn^{2+}, etc. As regards the concentration dependence in these cases the charge is similarly the fundamental factor; the individual η *vs.* m curves for the chlorides (and sulfates) of the divalent metals are much steeper (Fig. 1) than those for the univalent metal ions. The size is not the only other factor, however: a role is also played by the effect of the electronic structure. All this is well illustrated by the set of curves in Fig. 1. The viscosity relating to identical concentrations of the chlorides (and sulfates) of divalent metal cations with non-inert gas configurations (Ni^{2+}, Mn^{2+}, Zn^{2+}, Cu^{2+}), does not vary according to the sequence corresponding to the simple increase in ionic radius: $Mg^{2+} \rightarrow Cu^{2+} \rightarrow Zn^{2+} \rightarrow Ni^{2+} \rightarrow Mn^{2+} \rightarrow Ca^{2+}$; the observed variation is in accordance with the sequence Mg^{2+} [Ne] $\rightarrow$

* The different terminologies applied to structure-breaking or positive hydration, and structure-making or negative hydration result from the different attempts by various authors to approximate and interpret the phenomenon of hydration [5]; even if they are not identical, at least they relate to similar or very close physical concepts (breaking and making of the water structure refer to the hydrate layer more distant from the ion, while positive and negative hydration to the hydrate layer closest to the ion, but at the same time the heat of hydration is characteristic of the interaction of the ion with the entire bulk of water).

$\rightarrow Ni^{2+}[Ar]3d^8 \rightarrow Mn^{2+}[Ar]3d^5 \rightarrow Ca^{2+}[Ar] \rightarrow Zn^{2+}[Ar]3d^{10}$. For the ions with non-inert gas configurations, therefore, the $3d$ electron number sequence clearly passes through a minimum. As a consequence, at given concentrations the viscosity curve for $ZnCl_2$ strongly deviates from the band between the curves for $MgCl_2$ and $CaCl_2$, into the region of lower viscosities. This indicates that in the case of the different cations with non-inert gas configurations there arise various forces and hence possibilities of ion–solvent coupling (these control the hydration conditions, and accordingly the ordering and viscosity conditions for a given charge and concentration), in which the smaller ion has not a larger, but a smaller force than the larger ion. Similarly as for the composite ions, the ion–solvent interactions will be much more directed than in the case of the ions with inert gas configurations. Consequently, the correlation between the ionic size and the viscosity may exhibit a different, and even opposite tendency to that observed in the ions with inert gas configurations.

It is clear from Fig. 1 that strong effects are exerted on the viscosity not only by the charge, size and electronic structure of the cations, but also by the charge and size of the anion, and also its electronic structure in relation to its nature as a complex ion or a monoatomic ion with a non-inert gas configuration. This is shown by the fact that, as already pointed out above, at a given concentration the viscosity sequence of the individual cations is different for the sulfates (complex anion) from that for the chlorides (monoatomic anion). Further, the line of the η *vs.* m curves are very different in the case of 1—1 type (*e.g.* NaCl) and 1—2 type (*e.g.* Na_2SO_4) electrolytes containing the same cation.

Equation relating to the concentration dependence of the viscosity of aqueous metal chloride solutions

To a good approximation the following relation has been found to hold for the dependence on concentration* of the viscosity of binary aqueous metal chloride solutions under isothermal conditions:

$$\eta_{\text{specific}} = \frac{\eta - \eta_0}{\eta_0} = Am\,(m + B)\,e^{Cm^3} = (ABm + Am^2)\,e^{Cm^3} = (Dm + Am^2)\,e^{Cm^3} \tag{1}$$

In terms of the molal specific viscosity η', Eq. (1) assumes the form

$$\eta' = \frac{\eta_{sp}}{m} = \frac{\eta - \eta_0}{m\eta_0} = A\,(m + B)\,e^{Cm^3} \tag{2}$$

* In these investigations the concentration is always expressed in molality, so that the numerical concentration values be independent of the temperature.

Table I

Compound	Cation radius (Å)	$A \times 10^3$	B	$D \times 10^3 = AB \times 10^3$	$C \times 10^3$
LiCl	0.65	9.0	14.78	133	0.19
NaCl	0.95	13.5	5.41	73	0.14
HCl	1.12	—	—	61.5	0
	(1.03)				
KCl	1.33	5.26	—1.77	—9.3	0
NH_4Cl	1.43	3.75	—0.32	—12	0
	(1.35)				
RbCl	1.48	6.94	—4.76	—33	—0.60
CsCl	1.69	7.78	—5.4	—42	—0.25
$MgCl_2$	0.65	108	3.24	350	5.59
$CaCl_2$	0.99	66	3.94	260	3.42
$MnCl_2$	0.80	77.5	4.65	360	2.72
$MnSO_4$	0.80	240	2.17	520	22.32
H_2SO_4	1.12	9.26	19.44	180	0

where η_0 is the viscosity of the solvent. The values of the constants in the equation for a temperature of 25 °C are given in Table I.

Similarly to the equation of LENGYEL [6], which operates with concentration units of mol/l, Eq. (1) gives an exponential dependence on the concentration. It differs from LENGYEL's equation in that it contains one constant more (although as we shall see, two of its constants, A and B, are related by the expression $AB = D$), and the concentration exponent in the exponential term appears not to the first, but to the third power.

Table II illustrates the accuracy of Eqs (1) and (2), based on our own data [2], and on those of LENGYEL *et al.* [3] and of other authors [4].

In addition to apparently having three constants, the use of Eqs (1) and (2) also has other advantages: the isothermal dependence of the viscosity on the concentration is described as a temperature-independent function of the molality; because of the smallness of constant C, it is worth taking into consideration only at higher concentrations (and essentially only in the case of strongly positive hydration); and most important of all, in dilute or moderately concentrated solutions the equations can be brought into very simple forms, and the constants can be determined graphically from only two measured viscosity data (indeed, this is also so for ternary systems, to which, as will be seen later, the equations can readily be applied).

Table II

m		HCl	LiCl	NaCl	KCl	NH_4Cl	CsCl	$MgCl_2$	$CaCl_2$
	measd.	0.948	1.021	0.978	0.890	0.886	0.869	1.312	1.189
1	calcd.	0.949	1.021	0.971	0.890	0.887	0.864	1.303	1.186
	Δ%	0.11	0	—0.68	0	0.11	—0.58	—0.69	—0.25
	measd.	0.998	1.164	1.077	0.896	0.884	0.850	1.996	1.591
2	calcd.	1.004	1.164	1.073	0.896	0.886	0.847	1.952	1.614
	Δ%	0.60	0	—0.37	0	0.23	—0.35	—2.20	1.45
	measd.	1.051	1.323	1.199	0.913	0.888	0.846	3.005	2.240
3	calcd.	1.059	1.325	1.200	0.911	0.892	0.844	2.991	2.242
	Δ%	0.76	0.15	0.08	—0.22	0.45	—0.24	—0.46	0.09
	measd.	1.103	1.496	1.349	0.939	0.896	0.855	4.902	3.219
4	calcd.	1.114	1.505	1.352	0.937	0.905	0.856	4.893	3.227
	Δ%	1.00	0.60	0.22	—0.21	1.00	0.12	—0.18	0.25
	measd.	1.157	1.695	1.525		0.910	0.882	8.41	4.81
5	calcd.	1.169	1.709	1.533		0.924	0.881	8.89	4.93
	Δ%	1.04	0.83	0.52		1.54	—0.11	5.71	2.49
	measd.	1.212	1.927				0.918		
6	calcd.	1.224	1.939				0.918		
	Δ%	1.00	0.63				0		
	measd.		2.512				1.014		
8	calcd.		2.507				1.021		
	Δ%		—0.20				0.69		
	measd.		3.335						
10	calcd.		3.307						
	Δ%		—0.84						
	measd.		4.524						
12	calcd.		4.488						
	Δ%		—0.79						
	measd.		6.250						
14	calcd.		6.340						
	Δ%		1.44						

In not too concentrated solutions $e^{Cm^3} \simeq 1$, and to a good approximation

$$\eta_{rel} = \frac{\eta}{\eta_0} = 1 + ABm + Am^2$$

and

$$\eta' = \frac{\frac{\eta}{\eta_0} - 1}{m} = \frac{\eta - \eta_0}{\eta_0 m} = AB + Am = D + Am \tag{4}$$

which is the equation of a straight line.

In essence, therefore, Eq. (4) linearizes the η *vs.* m viscosity equation, and makes possible the determination of the value of $D = AB$ by linear extrapolation of the η *vs.* m straight line to infinite dilution ($m \to 0$), where

$$AB = D = \eta_\infty \tag{5}$$

the molal specific viscosity relating to infinitely dilute solution. Its value and its dependence on the radii of the monoatomic cations practically agree with the coefficients of the Jones-Dole equation for alkali metal chloride solutions at 25 °C [7]. Similarly,
for $m = 1$ we have

$$(\eta')_{m=1} = D + A = AB + A \tag{6}$$

and this means that the value of the coefficient B is

$$B = \frac{(\eta')_{m=1}}{A} - 1 \tag{7}$$

In the above sense, therefore, the values of A, B and $AB = D$ can be obtained for an aqueous solution of any metal chloride if the value of η' is determined at $m = 1$ and at some other m value*, and $\eta'_\infty = D = AB$ is determined by linear extrapolation after joining of the two points with a straight line.

Fig. 4 presents the η' *vs.* m straight lines, their courses relative to one another, and the η'_∞ sequence.

Of course, all that has been said above holds not only for the metal chlorides, but also for other salts. This is illustrated by the straight lines for various salts to be seen in Fig. 5.

* It is obvious from Eq. (4) that the relatively low difference of η and η_0 in dilute solutions leads to the error in the value of η' being the greatest in such solutions. In the calculations it is reasonable to take the other m as larger than 1, and to select it in the range of medium viscosities and concentrations (for not too positive or negative hydration: $m \simeq 1$—5; for very positive hydration in the case of univalent ions: $m \simeq 1$—4; and for divalent ions: $m = 0.6$—2).

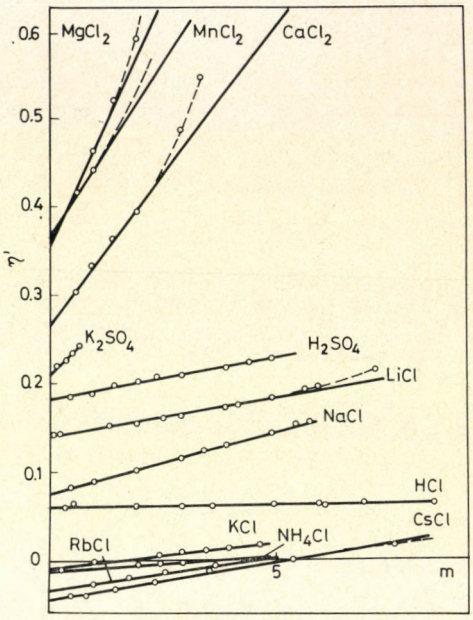

Fig. 4

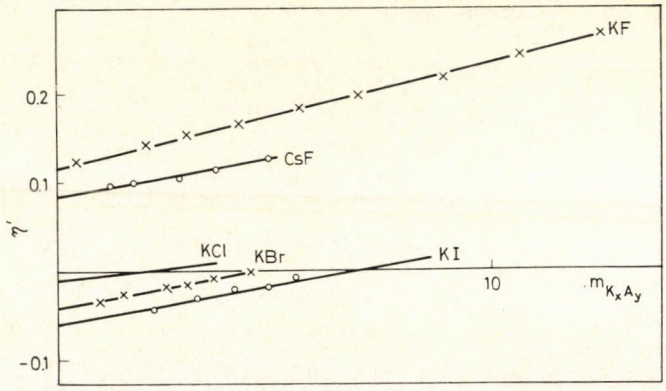

Fig. 5

Once A and B have been calculated in the above simple manner, C too can be calculated. From Eq. (2) for any $m \neq 1$ (preferably $m > 1$):

$$\ln (\eta')_m = \ln [A(m + B)] + Cm^3$$

from which

$$C = \frac{\ln \dfrac{\eta'}{A\,(m + B)}}{m^3} = \frac{\ln \dfrac{\eta'}{Am + D}}{m^3} = \frac{2.303}{m^3} \log \frac{\eta'}{Am + D} \qquad (8)$$

The signs of the η'_∞ values relating to the chlorides of different metal cations obviously provide useful and clear-cut information on the structure-breaking or structure-making nature of the metal cation for a given anion: the values of the former lie in the range of positive η'_∞, and those of the latter in the negative η'_∞ region.

At the same time, from the relative sequence of the individual η'_∞ values and from the magnitude of their values it is similarly possible to estimate the extents of the hydrating abilities of the cations, again for a given anion. This is mainly of importance as regards the complex ions, in the present case H_3O^+ and NH_4^+.

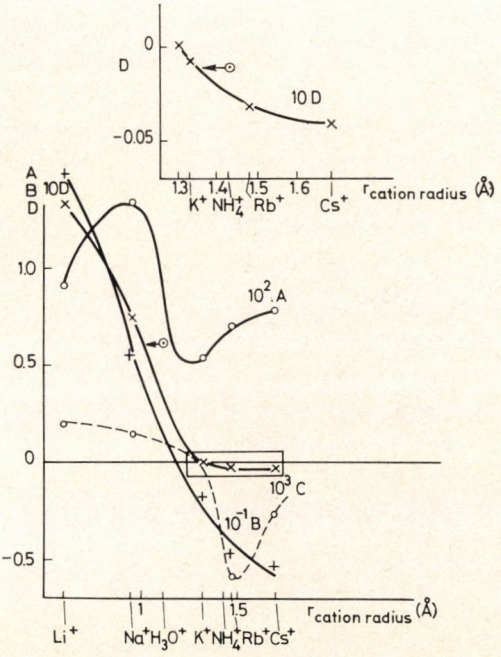

Fig. 6

The D_{HCl} and D_{NH_4Cl} values do not lie on the monotonous D *vs.* monoatomic ion radius curve (Fig. 6) (in the same way as seen above for the viscosity values of NH_4Cl and HCl, which did not lie on the monotonous viscosity *vs.* monoatomic ion radius curve for solutions with $m = 0.5$ plotted in Fig. 3); the D values for HCl and NH_4Cl lie on the curve only if a smaller ionic radius is taken. All this permits the conclusion that, at least as far as the viscosity is concerned, the values of the 'effective' ionic radii of H_3O^+ and NH_4^+ are not the generally accepted 1.12 and 1.43 Å [12], but the lower values of 1.03 and 1.35 Å, respectively.

In this way, therefore, it is possible to express an opinion as to the 'effec-

Table III

	$\eta'_\infty = D$		$\Delta H_{hydration\ energy}$ (kcal/mol)
LiCl	0.133	Li^+	—121 (120—136)
NaCl	0.07	Na^+	—98 (94—114))
KCl	—0.01	K^+	—80 (75— 94)
NH_4Cl	—0.013	NH_4^+	—79 (87)
RbCl	—0.033	Rb^+	—71 (69— 87)
CsCl	—0.043	Cs^+	—63 (61— 80)
$MgCl_2$	0.35	Mg^{2+}	—470 (490)
$CaCl_2$	0.26	Ca^{2+}	—375 (410)

tive' ionic radius (which, in addition to the charge, is now the exclusive determining factor as regards the hydration) of those ions for which the radius cannot be calculated from simple considerations of geometry and electronic structure.

At the same time, the η' *vs.* m straight lines are also of use inasmuch as they can give a certain amount of information on the tendency of the concentration dependence of the structure-breaking or structure-making behaviour of the individual ions, and in relation to one another too.

It is clear from Fig. 2 that the dependences of the η' values on the concentration for the chlorides of H_3O^+ and NH_4^+ differ from those for the chlorides of the univalent monoatomic ions with inert gas configurations. The curves for HCl and NH_4Cl solutions are flatter than those for the other salts, showing the difference already referred to above, between the viscosities of the composite and the not composite univalent cations.

That the sequence and values of $\eta'_{\infty,i}$ are in fact measures of the hydrating ability is illustrated by their comparison with the hydration energies, so far regarded as one of the most characteristic measures of the hydrating ability.

Table III lists the $\eta'_{\infty,i} = D_i$ values found for the metal chlorides examined, and the hydration energy values for the corresponding cations [12]. It can clearly be seen from the Table that the tendencies of changes in the $\eta'_{\infty,i}$ values for the individual metal chlorides and the $\Delta H_{hydr.}$ values for the individual corresponding ions agree. The basis of our calculations of the individual hydration energies consisted not only of conclusions drawn from the direct experimental results, but also of speculative considerations setting out from different, of necessity simplifying, assumptions. Accordingly, it may be considered as to whether the $\eta'_{\infty,i}$ data obtained from the direct experimental results can be regarded as more objective than the hydration energies for the characterization of the hydrating ability, in the same way as the mobilities

corresponding to the conductivities of infinitely dilute solutions more objectively characterize the electric migration abilities of the ions as compared to one another.

In order to obtain a better understanding of the physical meaning of the constants A, B and $AB = D$, they have been plotted in Fig. 6 as a function of the ionic radius for the univalent monoatomic ions. It can be seen from the Figure that the value of $AB = D$ changes sign at $r_{\text{cation}} = 1.3$ Å. For metal chlorides this value is the boundary between structure-breaking and structure-making effects.

The change in the sign of D was due to the change in sign of B as a function of the cation radius, and thus it must clearly be characteristic of the ion–solvent interaction. Accordingly, A should be characteristic of the other basic interaction in the electrolyte solutions, the ion–ion interaction. This assumption is supported by the fact that, although its value varies according to a maximum–minimum curve, it always remains positive, the sign not changing with the variation of the cation radius.

This fact is noteworthy from the aspect that if the ion–ion interactions are considered merely as the effects of pointlike charges on one another, then the constant characteristic of this in the η *vs.* m equation should not vary with the ionic radius in the positive range. However, since A does vary with the ionic radius, in the manner shown in Fig. 6, it is our view that we cannot speak of 'pure' ion–ion interactions in the solution. In the consideration of the ion–ion interactions too it is absolutely necessary to reckon with the shielding effect of the hydrate sphere formed by either positive or negative hydration around the ion as a result of the ion–solvent interactions. Because of the different natures of the two types of hydration mechanism, this shielding effect will not be the same for positively and negatively hydrating ions.

For example, Li^+ is the smallest univalent cation and is hydrated the most strongly (positively). The bound water molecules give rise to the greatest extent of shielding. The resulting ion–ion interaction will thus be less than for the larger Na^+. With the increase of the ionic radius, the value of A, characterizing the resulting ion–ion interaction, also increases.

In the case of the negatively hydrating ions, the value of A (*i.e.* the resulting ion–ion interaction) becomes much smaller than for the positively hydrating ions, but this similarly increases to a slight extent with the increase of the ionic radius. In our view the cause of this is that these exert a structure-making effect around their nucleus on their formation from the monomer. Thus, 'structured' [8] water is formed, which is more ordered than the monomer was. The shielding effect of this structure appears to be larger even than for positively hydrating ions. With increasing ionic radius (Rb^+, Cs^+, Cl^-), however, the size of the ion also becomes too large to fit into the cavities in 'structured' water [11], and thus these can no longer develop original 'structured' water.

Instead, their size leads to the distortion of the water structure formed. Consequently, the shielding effect too becomes somewhat smaller, and so the ion–ion interaction increases to a slight extent with the ionic radius.

In essence, therefore, A is not characteristic of the 'pure' ion–ion interaction either, but rather of the ion–ion interaction affected by the hydrate sphere resulting from hydration. Thus, it is even possible to draw conclusions on the extent and nature of the hydration from the dependence of A on the ionic radius. This is also supported by the line of A, since the minimum of the A *vs.* r_{ion} curve lies just on the structure-making — structure-breaking boundary. $D = AB = \eta'_\infty \approx B_{\text{Jones-Dole}}$ is this a function of both ion–ion and ion–solvent interactions, and this can account for the unidirectional deviation of 5—15% in its value from that of the B coefficient in the Jones-Dole equation which is characteristic only of the ion–solvent interaction.

Of the two first, and at the same time main determining constants of viscosity equation (1), therefore, (in contrast with the Jones-Dole equation) only one, A, depends exclusively on one effect, the ion–ion interaction in solution. The other main determining constant, D, is a function of two effects. Thus, neither of the two main determining constants of the equation relates exclusively to the ion–solvent interaction.

At the same time, as seen from Table I and Figure 6, the value of C for univalent monoatomic ions varies as a function of the ionic radius in a similar way as does A, with the difference that the sign too is changed. This indicates that C cannot be a term characteristic of either only the ion–ion or only the ion–solvent interaction. In the first case, even if it does not always increase monotonously, the value of C should at least always be positive. In the other case, in solutions so concentrated that the value of C becomes appreciable, there is no longer any free water present; indeed, in general the geometrically possible first hydrate sphere is no longer always complete. Here, therefore, similarly to the model of LENGYEL [5], a more complex cation–solvent–anion interaction must be assumed. This is characterized by the fact that with the increase of the concentration the water molecules in the hydrate sheath, which are bound increasingly more strongly and which have an increasing permanent dipole moment, come increasingly under the effects of two ions. Some schematic possibilities for this are depicted in Figure 7. With regard to the orientation and displacement polarizations too, they act and exert their field-decreasing effects increasingly as polarized dielectrics, and as permanent dipoles fixed ever more strongly between the two charges. This field-decreasing effect is relatively the strongest when small ions of high charge (and thus of high field) are present. The value of C is visibly the greatest in the case of $MnSO_4$ (Table I), where both ions are divalent and in addition the cation is still relatively small, being the smaller when the charge is lower and the ion is larger. In this case negative C values appear.

It was earlier mentioned that effects are also exerted on the viscosity *vs.* concentration function by the charge and size of the anion accompanying the metal cations. This is illustrated by Figs 1 and 2, and by a comparison of the η'_∞ values of the corresponding salts. It can be seen from the Fig. 4 that the η' *vs.* m straight line for KCl lies below that for HCl, and in more dilute solutions is in the negative range. At the same time, in the case of K_2SO_4 (containing a divalent anion) the straight lines lie above those for H_2SO_4, while even in dilute solutions they are only in the positive range. The negative hydration effect of K^+ is thus compensated, and even outweighed by the positive hydra-

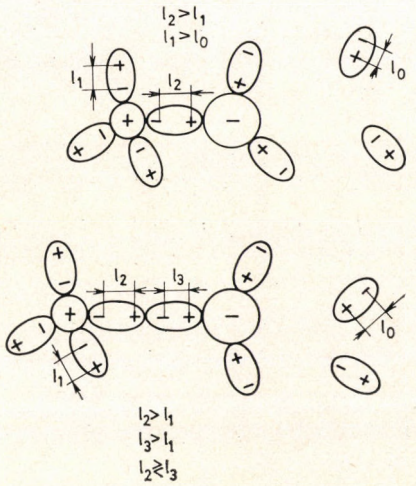

Fig. 7

tion effects of the univalent F^-, which has the same size, and of the divalent SO_4^{2-}, similarly of the same size. That the charge is in fact a stronger factor than the size, as regards the viscosity, is clearly shown by the fact that an increase of ca. 75% in the ionic radius as observed from the ratio $r_{F^-}/r_{SO_4^{2-}} = 1.36/2.30 \approx 0.6$ would rather promote the negative hydration effect, but nevertheless the η'_∞ value for K_2SO_4 (0.205) is roughly twice as large as that for KF (0.11).

All this shows that the viscosity of electrolyte solutions cannot in essence be interpreted on the basis of only the properties of the individual ions [7]. They cannot be broken down merely to increments from the individual ions, as can be done in the case of the conductivity of dilute solutions, for these measurable, and possibly calculable viscosities depend on the combined effects of the two ions on each other and on the solvent water; parts are played in this by the charge, size and electronic structure of each of the individual ions involved, and also by their concentrations. All this points to the conclusion

that the negative and positive hydration of the individual cations, and the assessment of this, cannot be separated completely from the properties of the accompanying anion (or cation). Nor can they be separated completely from those properties of the solvent system, the concentration dependence of which is under investigation. It thus appears that the structure-breaking or structure-making nature of the given ion cannot be regarded as a characteristic feature of absolute validity from every point of view; it can be considered only as a good, essentially qualitative factor, which is not entirely independent of the conditions.

General study of concentration and temperature dependences of the viscosity of ternary solution systems of the type metal chloride–HCl–H_2O

The viscosity *vs.* concentration diagrams of the ternary electrolyte solution systems of the type metal chloride–HCl–H_2O can be classified in three types (Fig. 8). As regards the ternary systems examined here at 25 °C, the hydrochloric acid solutions of chlorides containing positively hydrating cations are included in type I. Within this, the hydrochloric acid solutions of those metal chlorides whose metal ions hydrate positively to only a weak or a moderate extent are included in type I/*a* (*e.g.* Na^+), whereas if the metal ion shows strong positive hydration, the solution is classified in type I/*b* (*e.g.* Li^+, Mg^{2+}, Ca^{2+}). For both binary and ternary solutions of these:

$$\Delta\eta = \eta - \eta_{\text{solvent}} = f(m_{\text{salt}}, m_{\text{acid}}) > 0 \tag{9}$$

At the same time, the hydrochloric acid solutions of the chlorides of negatively hydrating cations (*e.g.* K^+, NH_4^+, Cs^+) are classified in type II. For these solutions:

$$\Delta\eta = \eta - \eta_{\text{solvent}} = f(m_{\text{salt}}, m_{\text{acid}}) \leqslant 0 \tag{10}$$

However, the outlined types of ternary viscosity *vs.* concentration diagrams are of more general validity: they refer not only to hydrochloric acid solutions of metal chlorides, but also to other salt–acid–water systems of the type K_xA_y–H_zA_v–H_2O.

Apart from the simple systematization, the classification into types has a deeper aim and use. On this basis, ions can be unambiguously categorized from the view point of their positive or negative hydration. This is of importance practically, as regards the possible pre-estimation of ternary concentration dependences and values of the viscosity for systems which have not been examined in the complete concentration interval. This is also possible on the basis

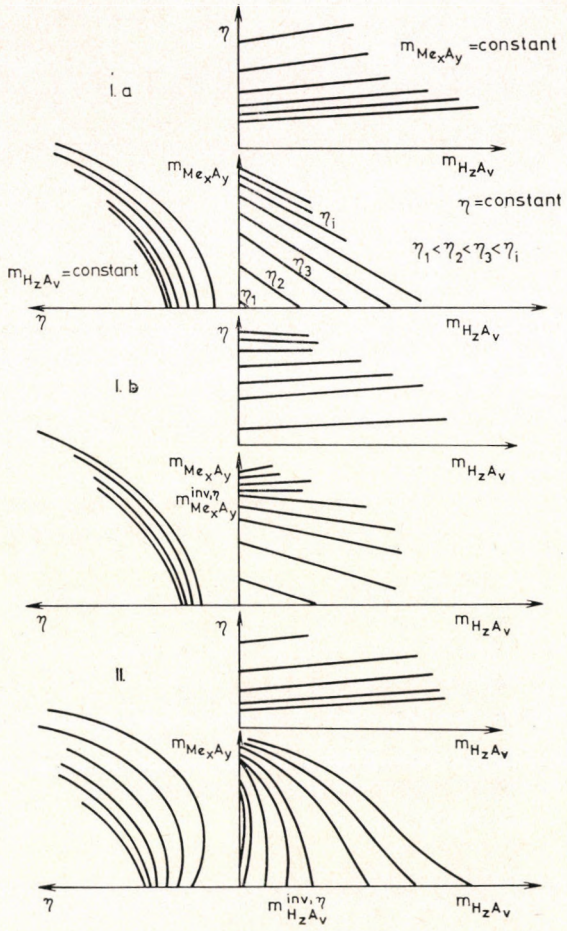

Fig. 8

of several viscosity data for the ternary system if by chance (particularly for ions which are complex or of a non-inert gas configuration), for which it was shown above that the extent of hydration does not depend exclusively on the charge and the geometry of the ions sufficient, or sufficiently accurate data are not available in the constituent binary systems, or if the conclusions to be drawn from the various properties or from the property *vs.* concentration diagrams do not unambiguously give the possibility of classification into one or the other group.

In the manner to be seen from the basic diagram of the classification into types (Fig. 8), in the metal chloride–HCl–H_2O systems of type I/*a* the addition of a third component to an aqueous solution of any concentration always increases the original viscosity of the initial binary solution in the entire ternary

concentration interval. In the event of the addition of a salt as the third component, the increase is relatively the stronger, the greater the concentration of the initial binary hydrochloric acid solution. At the same time, in the case of types I/*b* and II the addition of HCl or salt to binary aqueous salt or hydrochloric acid solutions, respectively, does not unconditionally increase the viscosity of the initial binary aqueous solution. Depending on the line of the viscosity curve, which is determined by the nature of the salt the addition can also lead to a decrease.

In metal chloride–hydrochloric acid–water solution systems of types I/*b* and II, therefore, there will be an inversion of the viscosity change induced by the HCl (salt) added as third component, as a function of the concentration of the original binary salt (acid) solution.

If the concept of the isothermal concentration coefficient is introduced to characterize the viscosity conditions prevailing in complete generality in ternary systems of the type M_xA_y–H_zA_v–H_2O, then the *isothermal salt concentration coefficient* of the viscosity change for the binary aqueous solution of the acid H_zA_v is

$$\alpha_\eta = \left(\frac{\partial \eta}{\partial m_{M_xA_y}}\right) m_{H_zA_v,\, t} \tag{11}$$

and the *isothermal acid concentration coefficient of* the viscosity change for the binary aqueous solution of the salt M_xA_y is

$$\beta_\eta = \left(\frac{\partial \eta}{\partial m_{H_zA_v}}\right) m_{M_xA_y,\, t} \tag{12}$$

Both α and β are functions of the nature of the dissolved compounds, the salt concentration, the acid concentration and the temperature. For every binary acid concentration for systems of types I/*a* and I/*b*:

$$\alpha > 0 \tag{13}$$

For every binary salt concentration for systems of types I/*a* and II:

$$\beta > 0 \tag{14}$$

For systems of type II:

$$\alpha \gtreqless 0 \text{ if } m_{H_zA_v} \lesseqgtr m^{\text{inv},\,\eta}_{H_zA_v} \tag{15}$$

and for systems of type I/b:

$$\beta \gtreqless 0 \text{ if } m_{M_xA_y} \lesseqgtr m^{\text{inv},\,\eta}_{M_xA_y} \tag{16}$$

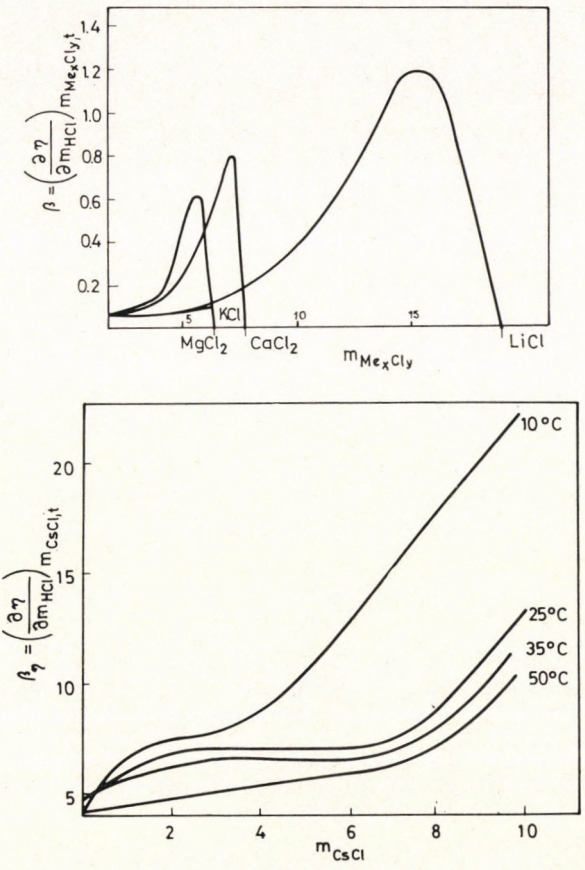

Fig. 9

where $m^{\text{inv},\,\eta}_{H_zA_v}$ ($m^{\text{inv},\,\eta}_{M_xA_y}$) is the *isothermal inversion acid concentration (salt concentration) referring to the viscosity, i.e.* that concentration of the binary aqueous $H_zA_v(M_xA_y)$ solution where the isothermal salt (acid) concentration coefficient $\alpha(\beta)$ changes sign.

In the examined systems of type metal chloride–HCl–H_2O an $m^{\text{inv},\,\eta}_{H_zA_v}$ concentration is observed for the systems KCl–HCl–H_2O, NH_4Cl–HCl–H_2O and CsCl–HCl–H_2O, and an $m^{\text{inv},\,\eta}_{M_xA_y}$ concentration for the systems LiCl–HCl–H_2O, $MgCl_2$–HCl–H_2O and $CaCl_2$–HCl–H_2O, for the latter at concentrations close to saturation (at 25 °C $m^{\text{inv},\,\eta}_{M_xA_y}$ is 18.9, 5.1 and 6.6 for LiCl, $MgCl_2$ and $CaCl_2$, respectively).*

* In the classification into types, and correspondingly in the examination of the $m^{\text{inv},\,\eta}$ values too, it is always necessary to take into consideration the effect of temperature. For example, our studies under polythermal conditions on the $MgCl_2$–HCl –H_2O system show that $m^{\text{inv},\,\eta}_{MgCl_2}$ increases with the temperature. At 35 °C it can still be found in the unsaturated concentration range stable at the given temperature, but at 50 °C it lies outside this range. For the $MgCl_2$–HCl–H_2O system at 50 °C, therefore, $\beta > 0$.

Comparisons between systems containing different cations and evaluations can be performed very descriptively if, for example, the isothermal acid concentration coefficient β_η is plotted as a function of the salt concentration (Fig. 9/a). It can be seen from the Figure that the β_η *vs.* m_{salt} curves can be broken down into practically linear sections.

The linear sections with different slopes show up particularly clearly in the cases of LiCl, $MgCl_2$ and $CaCl_2$, *i.e.* the chlorides containing the very positively hydrating cations, where the point of intersection of the descending third section with the $\beta_\eta = 0$ axis is the isothermal inversion salt concentration $m^{inv,\,\eta}_{M_xA_y}$. However, they can also be observed unambiguously in the case of chlorides containing negatively hydrating metal ions (*e.g.* Cs^+) which exhibit smaller relative changes (Fig. 9/b).

The line of the binary η *vs.* m_{salt} curves themselves (Figs 1 and 2) has already shown that the structure of the solution, which determines the value of η, varies constantly from dilute solution up to saturation. The curves in Fig. 9, indicating the extent of the viscosity change on the addition of the third component, and which can be broken down sharply into three linear sections, clearly demonstrate that the change in the structure of the binary salt solution is not uniform, even if the salt concentration is uniformly increased. Within a given, definite concentration interval the extent of the structural change is constant, but the extents of the structural changes corresponding to the individual concentration intervals are not the same in the different concentration intervals. In our case, therefore, each of the three linear sections observed in the $\beta_\eta = f(m_{salt})$ curves points to the structure dominating in that given binary solution concentration interval. At certain limiting concentrations, these structures transform into other dominating solution structures, characterized by different slopes of the straight lines $\beta_\eta = f(m_{salt})$.

The fact that various dominating structure intervals can exist in binary metal chloride solutions as the concentration varies, and that the structure does not change monotonously as a function of concentration, is supported by other evidence. Thus, in concentrated solutions sharp and sudden changes are observed too in the concentration dependences of other properties similarly providing information on the solution structure. Examples are the M and N functions [1] characterizing the mutual connection of the addition of the third component and the activation enthalpy, activation entropy and temperature change. In addition to all this, it must be emphasized that the effect of the decrease of β_η and the inversion in the third section occurs only in the cases of those salts the viscosities of which are very high in concentrated solution, and which separate from their saturated solutions with crystal water ($LiCl.H_2O$, $MgCl_2.6\,H_2O$, $CaCl_2.6\,H_2O$). The third, descending sections of the β_η *vs.* m_{salt} curves for these solutions indicate, therefore, that in the corresponding concentration interval of these systems there appears to begin a new prearrangement

of a solution structure similar in a statistical sense to the solid phase separating from the solution.

It is clear from the above that an isothermal inversion salt concentration $m^{\text{inv.}\,\eta}_{M_xA_y}$ relating to the viscosity occurs when HCl is added to a very concentrated aqueous solution of a metal chloride the cation of which has a very high hydration ability (Li^+, Mg^{2+}, Ca^{2+}), and for which, as a consequence of this and of the dielectric effects discussed, the viscosity of aqueous solutions increases very strongly in the more concentrated range as a result of the increase of the salt concentration.

The isothermal inversion in viscosity change observed in solutions of such high concentration and viscosity can be explained as follows. In these concentrated solutions, which contain strongly positively hydrating cations, the original water structure has completely disappeared, *i.e.* there is no longer any "free water" at all present. Thus, when HCl is added to the ion–hydrate structure it can less dissociate. It rather undergoes physical dissolution, and remains as a charge-free, quasi-inert gas complex. This loosens the structure which has formed, and at the same time, by increasing the distance between the ions, decreases the ion–ion interactions. Indeed, it also decreases both factors of the dielectric polarization, and thus a viscosity-decreasing effect arises.

This interpretation is supported by a number of observations. (1) With such ions and in such a high concentration range the value of the specific electric conductivity is increased by added HCl to only a very slight extent, and the molar conductivity too barely changes. This indicates that the HCl fails to dissociate, and thus there is no increase in the number of charge carriers and no possibility of proton conduction. (2) In contrast to what is observed with moderately concentrated salt solutions, on the addition of HCl the overall molar volume of the binary salt solution will no longer increase, but will decrease to a slight extent, or at least hardly change [8], in the same way as for any other physical dissolution (*e.g.* when an inert gas dissolves in water, etc.). (3) The vapour pressure [9] indicates that in this very concentrated solution the original total (here $P_{H_2O} = P_{\text{total}}$) vapour pressure of the binary salt solution will increase on the addition of HCl, and not decrease as happens in dilute and moderately concentrated salt solutions. This is a sign that, as the dissociation of HCl is slight, a process occurs similar to the salting-out phenomenon observed on the dissolution of inert gases in salt solutions.

Method for calculating the viscosity of ternary metal chloride–HCl–H_2O systems

Many attempts have been made to devise viscosity equations by means of which the values of the viscosity can be given for concentrations at which measurements have not been carried out. This is of great importance as regards technological practice. At the same time, the validity of the equations obtained, or in many cases the deviations from them, can lead to a deeper understanding of the structure of the given solution.

In our earlier investigations [10] use was made of the method of ZDANOVSKII, based on the additivity of kinematic fluidities, for the calculation of the viscosity of ternary solution systems. We developed this method so as

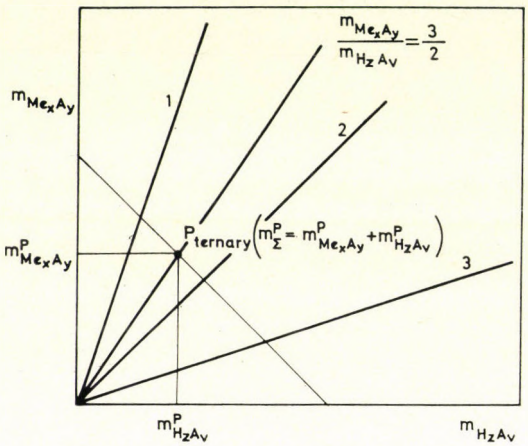

Fig. 10

to eliminate the use of the troublesome volume fraction for simpler practical application. We were able to derive an equation of simple form, by means of which the viscosity of a given three-component solution can be calculated to a good approximation in the knowledge of the density of the solution and the viscosities and densities of the two-component solutions with the same concentrations as the concentrations of all the dissolved substances.

The equation has the very great advantage that it contains no terms at all which have no physical meaning. The basic relation used is the equation on the basis of which measurement is performed with the flow viscosimeter. Further, the viscosity of the three-component solutions can be given in the knowledge of the density and viscosity data for the binary solutions.

A basic condition of the calculation of the viscosity of the ternary solution with this method, however, is the effective knowledge of the viscosities of the component binary systems in the possible full binary concentration intervals. At the same time, the method is no longer applicable for certain

ternary concentrations; these are the concentrations for which the corresponding binary salt solutions do not exist, the solubility of the salt in water being too low at the given temperature [10].

However, this latter drawback can also be eliminated, and in the above method a much higher accuracy can be attained by applying to the ternary systems the viscosity equations of types (1) and (2) relating to the binary systems. This has the added advantage that it does not necessitate the cumbersome use of volume fractions either, but operates with the molality in the ternary solution too.

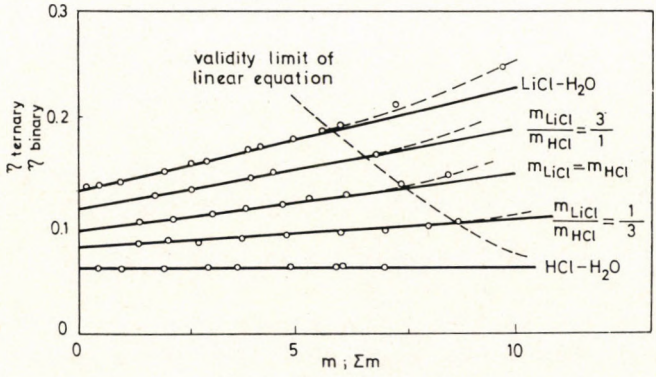

Fig. 11

Equation (2) is applied to the ternary systems by regarding the individual ternary solutions of concentration $m_{M_xA_y} + m_{H_zA_v} = m_\Sigma$ as quasi-binary solutions for which the ratio $m_{M_xA_y}/m_{H_zA_v}$ is constant (see the quasi-binary curves relating to points 1, 2, 3 and to the ternary point P in Fig. 10, for which the ratios $m_{M_xA_y}/m_{H_zA_v}$ are in turn 3/1, 1/1, 1/3 and 3/2). Equation (2) can thus be written for any such quasi-binary curve, or similarly to (4) for a moderately concentrated solution

$$\eta_t' \approx D_t + A_t m_\Sigma \tag{17}$$

where

$$\eta_{\infty,t}' = D_t = A_t B_t \tag{18}$$

and subscript t refers to the ternary solution.

In connection with the system LiCl–HCl–H_2O, Fig. 11 presents the η *vs.* m functions for the binary LiCl–H_2O and HCl–H_2O systems, and also the η'_{ternary} *vs.* m_Σ functions for the quasi-binary systems corresponding to the ratios $m_{M_xA_y}/m_{H_zA_v} = 3/1$, 1/1 and 1/3 (similar results are given by the other M_xCl_y–HCl–H_2O systems too). The Figure shows that on analogy with (4), expression (17) does in fact hold, and for moderately concentrated ternary

solutions, where C can still be neglected, the function η'_{ternary} *vs.* m_Σ is a straight line. The limiting value of this, obtained by linear extrapolation to $m_\Sigma = 0$, gives $D_t = \eta'_{t,\infty}$ relating to the given value of $m_{M_xCl_y}/m_{HCl}$

Both D_t and A_t (and thus naturally B_t too) are obtained from the individual binary D and A values as mean values weighted according to the concentrations $m_{M_xA_y}$ and $m_{H_zA_v}$ relating to the ternary solutions under examination:

$$D_t = \frac{m_{MxAy} \cdot D_{MxAy} + m_{HzAv} \cdot D_{HzAv}}{m_{MxAy} + m_{HzAv}} \tag{19}$$

and

$$A_t = \frac{m_{MxAy} \cdot A_{MxAy} + m_{HzAv} \cdot A_{HzAv}}{m_{MxAy} + m_{HzAv}} \tag{20}$$

where $m_{M_xA_y} + m_{H_zA_v} = m_\Sigma$.

This means, therefore, that if we wish to calculate the viscosity of any ternary solution (*e.g.* that with the concentration denoted by point P_t in Fig. 10) in the knowledge of the binary A and D values, then the values of A_t and D_t must be determined from (19) and (20), and substituted into (17). (The effective knowledge of the binary viscosities is thus not necessary.)

In the knowledge of the molal specific viscosity η'_t in the equation, the other ternary η' values for this same $m_{M_xA_y}/m_{H_zA_v}$ can be obtained by a simple graphical method. The points relating to the η'_t value obtained by calculation and the $\eta_{t,\infty} = D_{t,\infty}$ value referring to zero m_Σ according to (17) are joined by a straight line. In this manner, therefore, taking into account what was said in the derivation of the binary viscosity equation, the η'_t values can be determined by a simple graphical procedure for the complete ternary system. Two isothermal viscosity measurements are made for each of the two binary systems constituting the ternary system, in the range of moderately high concentrations, when C is not appreciable. It is advantageous for one of these measurements to be made in the vicinity of $m_\Sigma = 1$, and the other at a moderately high ternary concentration.

$$\eta'_t = \frac{\eta_t - \eta_0}{\eta_0, m\Sigma}$$

while the viscosity η_t of any ternary solution of appropriate concentration is given on the basis of

$$\eta_t = \eta'_t m_\Sigma \eta_0 + \eta_0 = \eta_0 (\eta'_t m_\Sigma + 1) \tag{21}$$

Table IV gives an insight into the relatively high accuracy, the good applicability and the limitations of the graphical method in the ternary system.

Table IV

	m_{salt}	m_{acid}	m_Σ	$\eta_{measd.}$	$\eta_{calcd.}$			
					[17]	Δ%	[25, 21]	Δ%
	2	8	10	1.70	1.73	1.76	1.73	1.76
	5	5	10	2.18	2.17	—0.46	2.28	4.59
	8	2	10	2.85	2.60	—8.77	2.86	0.35
	2	6	8	1.60	1.59	—0.62	1.61	0.62
	4	4	8	1.80	1.85	2.78	1.89	5.00
	6	2	8	2.10	2.10	0.00	2.19	4.29
$LiCl—HCl—H_2O$	1	5	6	1.32	1.34	1.51	1.34	1.51
	3	3	6	1.55	1.56	0.65	1.57	1.29
	5	1	6	1.77	1.79	1.13	1.81	2.26
	1	3	4	1.21	1.21	0.00	1.21	0.00
	2	2	4	1.31	1.31	0.00	1.31	0.00
	3	1	4	1.40	1.40	0.00	1.41	0.71
	1	1	2	1.08	1.08	0.00	1.08	0.00
	2	8	10	1.50	1.398	—6.80	1.373	—8.47
	5	5	10	1.36	1.329	—2.28	1.276	—6.18
	8	2	10	1.20	1.260	5.00	1.188	—1.00
	2	6	8	1.28	1.260	—1.56	1.249	—2.42
	4	4	8	1.20	1.186	—1.17	1.168	—2.67
$CsCl—HCl—H_2O$	6	2	8	1.09	—1.113	2.11	1.092	0.18
	1	5	6	1.17	1.173	0.26	1.171	0.09
	3	3	6	1.07	1.072	0.19	1.067	—0.28
	5	1	6	0.96	0.970	1.04	0.967	0.73
	1	3	4	1.05	1.049	—0.10	1.049	—0.10
	2	2	4	0.98	0.985	0.51	0.984	0.41
	3	1	4	0.92	0.920	0.00	0.920	0.00
	1	1	2	0.93	0.925	—0.54	0.925	—0.54

Of course, if the concentration is so high that the simple graphical solution can no longer be applied, the goal can be achieved analytically; in this case the C_t value must also be taken into consideration. On analogy with (2), we can here arrive at a general equation suitable for the calculation of the viscosity of the ternary solution system. In accordance with (2), for any quasi-binary ratio $m_{M_xA_y}/m_{H_zA_v}$ we have for a ternary system

$$\eta'_t = (D_t + A_t m_\Sigma)\, e^{C_t m_\Sigma^3} \qquad (22)$$

If it is taken into account that in the expanded series all terms to the power two or more can to a good approximation be neglected, then we obtain the relation

$$\eta_t' = D_t e^{C_t m_\Sigma^3} + A_t m_\Sigma e^{C_t m_\Sigma^3} = D_t (1 + C_t m_\Sigma^3) + A_t (1 + C_t m_\Sigma^3) m_\Sigma =$$
$$= D_t + A_t m_\Sigma + D_t C_t m_\Sigma^3 + A_t C_t m_\Sigma^4 \tag{23}$$

If, for simplicity's sake, the binary salt solution system is denoted by the subscript 1 and the binary hydrochloric acid system by subscript 2, and C_t too is calculated on the analogy of (19) and (20), then we arrive at the equation

$$\eta_t' = \frac{m_1 D_1 + m_2 D_2}{m_\Sigma} + \left(\frac{m_1 A_1 + m_2 A_2}{m_\Sigma}\right) m_\Sigma +$$
$$+ \left[\left(\frac{m_1 D_1 + m_2 D_2}{m_\Sigma}\right)\left(\frac{m_1 C_1 + m_2 C_2}{m_\Sigma}\right)\right] m_\Sigma^3 +$$
$$+ \left[\left(\frac{m_1 A_1 + m_2 A_2}{m_\Sigma}\right)\left(\frac{m_1 C_1 + m_2 C_2}{m_\Sigma}\right)\right] m_\Sigma^4 \tag{24}$$

From this, the desired ternary viscosity equation is

$$\eta_t' = \frac{m_1 D_1 + m_2 D_2}{m_\Sigma} + m_1 A_1 + m_2 A_2 +$$
$$+ [D_1 C_1 m_1^2 + D_2 C_2 m_2^2 + (D_2 C_1 + D_1 C_2) m_1 m_2] m_\Sigma +$$
$$+ [A_1 C_1 m_1^2 + A_2 C_2 m_2^2 + (A_2 C_1 + A_1 C_2) m_1 m_2] m_\Sigma^2 \tag{25}$$

The first two terms on the right-hand side of Eq. (25) are identical with the linear ternary viscosity equation (17). If this is denoted by X:

$$X = \frac{m_1 D_1 + m_2 D_2}{m_\Sigma} + m_1 A_1 + m_2 A_2 \tag{26}$$

Equation (25) can then be written in the following form:

$$\eta_t' = X + X (m_1 C_1 + m_2 C_2) m_\Sigma^2 \tag{27}$$

In our case, for the ternary metal chloride–HCl–H_2O systems, taking into account that $C_2 = C_{HCl-H_2O} = 0$, we have

$$\eta_t' = X + X C_1 m_1 m_\Sigma^2 = X (1 + C_1 m_1 m_\Sigma^2) \tag{29}$$

The accuracy and applicability of the ternary viscosity equations (25) and (29) are similarly illustrated for several metal chloride–HCl–H_2O systems by the data in Table IV.

REFERENCES

[1] BERECZ, E., BÁDER, I.: Acta Chim. (Budapest) **74,** 213 (1972)
[2] BERECZ, E., ANDRÁS, L., GEIGER, I.: Magy. Kém. Foly. **66,** 291 (1960)
BERECZ, E., HORÁNYI, GY.: Magy. Kém. Foly. **67,** 152 (1961)
BERECZ, E., VÉRTES, GY.: Magy. Kém. Foly. **70,** 106 (1964)
BERECZ, E.: Z. Phys. Chem., **229,** 173 (1965)
BERECZ, E.. NAGY-CZAKÓ, J.: Proc. 16th Meeting of CITCE 165 (1965)
BERECZ, E., BÁDER, I.: Magy. Kém. Foly. **79,** 106 (1973)
[3] LENGYEL, S., TAMÁS, J., GIBER, J.: Magy. Kém. Foly. **70,** 66 (1964)
[4] LANDOLT-BÖRNSTEIN: Zahlenwerte u. Funktionen. 6th Ed., vol. II. Part 5. Springer Verlag, 1969
[5] SAMOILOV, O. YA.: Struktura vodnikh rastvorov elektrolitov i gidratatsiya ionov. Izd. AN SSSR, Moscow 1957
LEE KAVANAU, J.: Water and Solute–Water Interactions. Holden-Day Inc. 1964
[6] LENGYEL, S.: J. Chim. Phys., **72** 28 (1969)
[7] ERDEY-GRÚZ, T.: Transport processes in aqueous solutions (in Hungarian) Akadémiai Kiadó, Budapest 1971
[8] BERECZ, E., BÁDER, I.: Magy. Kém. Foly. **79,** 31 (1973)
[9] BERECZ, E.: C. Sc. Dissertation, Leningrad, 1954
BERECZ, E.: Acta Chim. Acad. Sci. Hung., **15,** 301 (1958)
[10] BERECZ, E., VÉRTES, GY.: Acta Chim. Acad. Sci. Hung., **39,** 437 (1963)
[11] LYASHCHENKO, A. K.: Zh. Strukt. Khim., **9,** 781 (1968)
[12] MISCHCHENKO, K. P., RAVDIEL, A. A.: Kratkii spravochnik fizikokhimisheskikh velichin. Gos. n. techn. izdat. khim. lit. Leningrad 1955

Endre BERECZ; 3515 Miskolc-Egyetemváros, Hungary.

Acta Chimica Academiae Scientiarum Hungaricae, 84 (4), pp. 381—384 (1975)

DISTINCTION BETWEEN *SYN* AND *ANTI* KETOXIMES OF 2-ACYL-FURANS AND THEIR CONDENSED ANALOGUES BY THEIR NMR SPECTRA

P. SOHÁR, GY. OCSKAY* and L. VARGHA†

*(Research Institute for Pharmaceutical Chemistry, *Research Institute for Organic Chemistry, Budapest)*

Received October 31, 1973

The *syn* and *anti* isomers of 2-acylfuranoximes, being unsubstituted at C-3, can be easily distinguished by their PMR spectra. The anisotropic effect of the oxime group brings about a strong paramagnetic shift of the H-3 singlet in the relative to the *anti* isomer ($\Delta\delta \simeq 0.75$ ppm).

In our previous publications we described the synthesis [1] and structure determination [2] of the isomeric ketoximes of different 2-acylfuran derivatives (**I**) by their UV and IR spectra. In the present paper the possibility of distinguishing the stereoisomers by their PMR spectra is discussed.

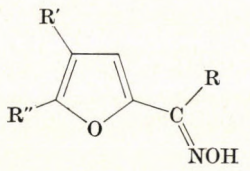

I

The theoretical possibility is based on the observation that the PMR spectra reveal the paramagnetic shift of those protons which are sterically closed to the oxime group. This phenomenon is a consequence of the anisotropic effect of the adjacent oxime group [3, 4], as can be seen *e.g.* in the case of the dioximes **IIa–c**, where the signal of the H-4 and/or H-10 protons is shifted [4].

According to these data, first of all the signal of H-3 and that of the protons of the R group should be shifted differently in the *syn* and *anti* isomers of the ketoximes **I**.

As an example the spectra of the two isomeric benzofuryl-2-methyl-ketoximes (**IIIa, b**) are discussed. In the 60 MHz spectra — taken in hepta-deuterodimethylformamide on a VARIAN 60D spectrometer — the chemical shift of the methyl group is practically identical in both isomers ($\delta = 2.47$ ppm), but the signal of the H-3 ring-proton is shifted differently (Figs 1 and 2).

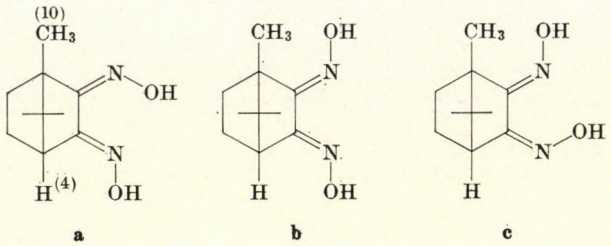

a b c

II

$\delta CH_3(10)$ [ppm]	0.99	1.32	1.31
δCH (4) [ppm]	3.07	2.99	2.38

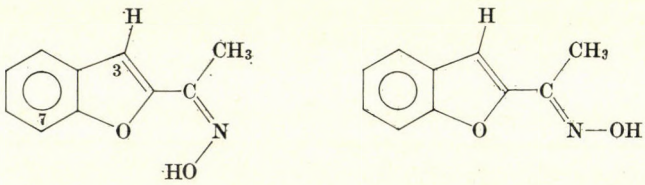

a b

III

In the *syn* isomer **IIIa** the chemical shift of this proton is $\delta = 7.95$ ppm, whereas in the *anti* isomer **IIIb** $\delta = 7.20$ ppm. This difference of 0.77 ppm makes an unambiguous identification of the structures possible. The relative value of the shifts δH-3 (*syn*) $\geqslant$ δH-3 (*anti*) corresponds to the expectation, as the anisotropic effect of the oxime group causes a strong paramagnetic shift in the *syn* isomer.

A weaker paramagnetic shift of the signal of the H-7 proton can be observed too in the spectrum of the *syn* isomer, shown by the extension of the complex ABCD multiplet (which can be analyzed by a computer only) towards higher frequencies. In the spectrum of **IIIa** the multiplet appears between 425 and 475 Hz, whereas in the spectrum of **IIIb** between 425—470 Hz (Figs 1 and 2).

The shift and the shape of the OH signal differs in these spectra too (in the case of the *syn* isomer the sharp signal appears at $\delta = 4.0$ ppm and in the *anti* isomer the broad signal appears at $\delta = 4.15$ ppm). Nevertheless this difference cannot be used for determining the structure, as in the case of mobile protons both the chemical shift and the shape of the signal are temperature- and concentration-dependent and are altered by the water content of the solvent too.

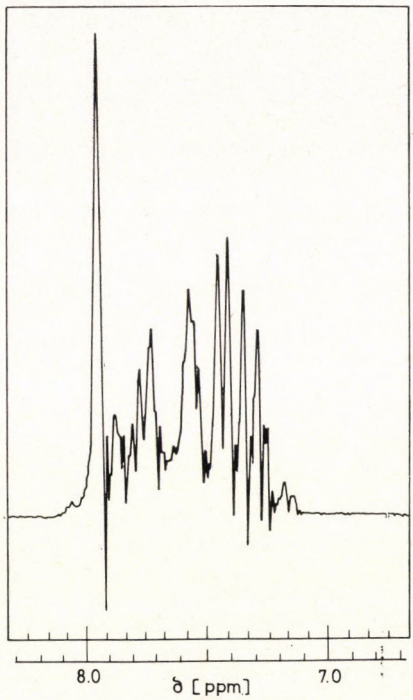

Fig. 1. Part of the 60 MHz PMR spectrum of *syn* benzofuryl-2-methylketoxime **(IIIa)** with the signals of ring protons 3—7 in DMF-d_7

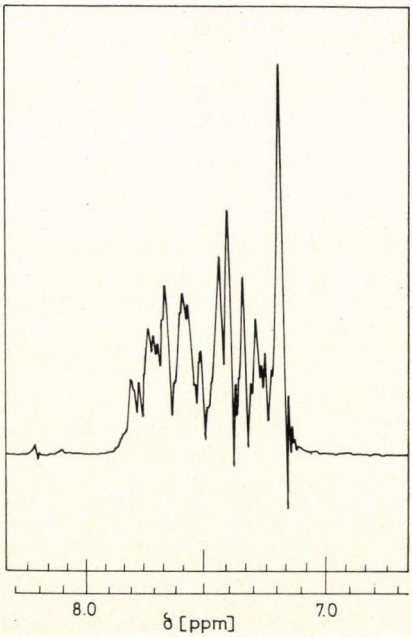

Fig. 2. Part of the 60 MHz PMR spectrum of *anti* benzofuryl-2-methylketoxime **(IIIb)** with the signals of ring protons 3—7 in DMF-d_7

REFERENCES

[1] OCSKAY, G., VARGHA, L.: Tetrahedron, **2,** 140 (1958)
[2] SOHÁR, P., VARSÁNYI, G., VARGHA, L., OCSKAY, G.: Acta Chim. Acad. Sci. Hung., **40,** 431 (1964)
[3] DANIEL, A., PAVIA, A. A.: Tetrahedron Letters, 1145 (1967)
[4] HUITRIC, A. C., ROLL, D. B., DEBOER, J. R.: J. Org. Chem., **32,** 1661 (1967)

Pál SOHÁR; 1325 Ujpest, P. O. B. 82.
György OCSKAY; 1085 Budapest, Stáhly u. 13, Hungary.

Acta Chimica Academiae Scientiarum Hungaricae, 84 (4), pp. 385—392 (1975)

ELECTRODEPOSITION OF COBALT, II

CATHODE POLARIZATION AND GRAIN SIZE OF THE DEPOSIT

R. D. SRIVASTAVA and SUSHIL KUMAR

(Chemical Laboratories, University of Lucknow, India)

Received July 9, 1973
In revised form March 25, 1974

The influence of current density, temperature and pH on cathodic polarization, the corrosion resistance of the electrodeposit towards atmosphere and the grain size of the deposit have been studied on electrodeposited cobalt from some cobalt baths. Increase of C. D. increases the polarization and decreases the grain size of the deposit. The rise of temperature of the bath is found to decrease the polarization and corrosion resistance but to increase the grain size. Lowering of the pH of the bath causes the deposit to become less corrosion resistant and bigger in grain size.

It has been shown earlier that there exists a relation between cathodic polarization and the structure of the deposit [1—4]. It is generally agreed that electrodeposited metals are crystalline, and the external appearance and size of the grains depends mainly on the rate at which the crystals grow and on the rate of the formation of fresh nuclei. If the conditions are such as to favour the rapid formation of crystal nuclei, the deposits will be fine-grained, if the tendency is for the nuclei to grow rapidly, relatively large crystals form and the deposits become rough in appearance.

Some work on the electrodeposition of copper and cobalt has been done in this laboratory in which the impurity content [5], porosity, adherence and microstructure [6] of the deposits as well as the plating characteristics [7] of various electroplating baths under different conditions have been studied. Not much work on the electrodeposition of cobalt in terms of polarization measurements and structural studies seems to have been done as compared to nickel [8—12] and other electrodeposited metals. The relation between cathodic polarization and texture of an iron-cobalt alloy electrodeposit has been studied by ROTINYAN [13] and others. The growth textures of cobalt electrodeposits in relation to magnetic properties [14], the orientation types which can exist in cobalt electrodeposits [15], structure and mechanism of the cobalt metal obtained by electrocrystallization [16, 17] have been previously studied.

In the present study the cathodic polarization, the grain size of cobalt electrodeposits and their interrelation as well as the corrosion resistance of

the deposits have been investigated using various electrolytic baths. The variable parameters were current density, temperature and pH of the electrolytic solutions.

Experimental

All chemicals used were Analar (B. D. H.) products. Fresh solutions prepared in doubly distilled water were used for each experiment. The cathodes of copper strips of 10×2 cm, were etched, washed, dried and then dipped in carbon tetrachloride for some time and again washed and dried before being used for plating purposes. Carbon anodes impregnated with paraffin wax were used throughout the entire study of electrodeposition. Polarization measurements were made in a HARING cell [18] made of perspex which provided better means for measuring the electrode potential. The cell was immersed in a thermostat. Potential and current measurements were made with the potentiometer and 1 ohm standard resistor.

For measuring cathodic polarization, the connection to the cathode was made by an agar-agar bridge, whose tip, drawn into a capillary of approximately 1 mm diameter, was pressed lightly against the electrode. Thus, the error due to the potential drop through the electrolyte was minimized. All the measurements were made with unstirred solutions. After 25 min of deposition, cathodic polarization was observed to attain a steady value and it was measured then. The value was considered steady if it did not change more than 1 mV in 10 min. The cathodic polarization was determined by noting the difference of cathode potential at the given current density and the potential when no current was flowing through the electrolytic bath.

X-ray powder diffraction photographs of the cobalt electrodeposits were taken using a Philips X-ray tube and a powder camera with circular film for determining the grain size of the deposits, but the patterns showed sharp, smooth diffraction rings, indicating grain sizes of the order of 10^{-5} to 10^{-3} cm. Within this range the rings were insensitive to size changes, making exact measurements of the diameters impossible. Consequently, an optical microscope was used to measure the grain size (or the size of more than one crystal looking like one unit system and appearing as a grain) of the deposit. For each sample of the electrodeposit observations at five different places were taken and the mean value was taken for the average grain size of the deposit.

Corrosion resistance of the deposits is expressed as the reciprocal of the number of spots revealed by the ferroxyl test per square centimeter of the tested deposit.

The compositions of the plating baths used were as follows:

Nos	Bath	Symbol of bath	Composition of bath (g/l)
1	All sulfate bath	S	332 $CoSO_4 \cdot 7\ H_2O$ and 30 H_3BO_3
2	All chloride bath (Wesley type)	C	298 $CoCl_2 \cdot 6\ H_2O$ and 30 H_3BO_3
3	Watt's bath	W	319 $CoSO_4 \cdot 7\ H_2O$, 45 $CoCl_2 \cdot 6\ H_2O$ and 30 H_3BO_3
4	Sulfate bath with Mg present	SM	165 $CoSO_4 \cdot 7\ H_2O$, 85 Na_2SO_4, 17.5 $MgSO_4 \cdot 7\ H_2O$ and 35 H_3BO_3
5	Sulfate bath with glycerol	SG	332 $CoSO_4 \cdot 7\ H_2O$, 30 H_3BO_3 and 20 glycerol
6	Sulfate bath without boric acid (H_3BO_3)	SWB	332 $CoSO_4 \cdot 7\ H_2O$ only

The volume of the solution was always selected so that it covered cathode area of $2.5 \times 2\ cm^2$ in the electrolytic cell.

Results and discussion

The cathodic polarization observed in the all sulfate bath (S) was greater than that in the all chloride bath (C) for each value of the current density (Table I).

Polarization is due to any slowness of the electrode process and usually in the deposition of metals on the cathode. It is mainly a concentration polarization [19] produced by the decrease of the cations concentration in the cathode

Table I

Cathodic polarization data for different elecrolytic baths

Copper; cathode pH of baths (S), (C) and (W) 2.0, 2.5 and 1.9, respectively

No.	Cathode current density (A/dm^2)	Temperature (°C)	Cathodic polarization (V)		
			All sulfate bath (S)	All chloride bath (C)	Watt's bath (W)
1	1.192	35	0.3333	0.1992	0.2808
2	2.221	35	0.3662	0.2307	0.3250
3	3.110	35	0.3997	0.2593	0.3464
4	6.016	35	0.4549	0.3105	0.3902
5	9.104	34	0.4980	0.3417	0.4213
6	12.028	35	0.5233	0.3609	0.4502
7	3.110	20	0.4712	0.3219	0.4268
8	3.110	50	0.3207	0.1957	0.2702

compartment. As the C. D. is increased, the rate of discharge of ions at the cathode is enhanced, resulting in more diminution of the cation concentration near the cathode, which increases the polarization. This is supported by the results obtained for baths (S), (C) and (W) for the electrodeposition of cobalt (Nos 1—6, Table I). The thickness of the diffusion layer adjacent to the cathode surface is appreciably decreased by increasing temperature, thus the rate of diffusion of metal ions (*i.e.* Co^{2+} ions) to the cathode is increased, consequently, the polarization is decreased (Nos 7 and 8, Table I).

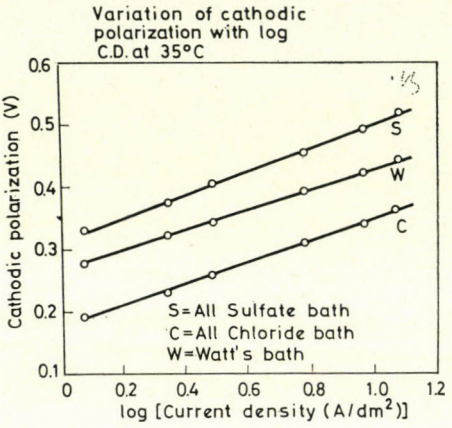

Fig. 1

The deposition of Ni, Co and Fe is always accompanied by the discharge of hydrogen at the cathode and the observed deposition overvoltage is said to be due to hydrogen overvoltage. The large polarizations in the case of iron group metals are attributed besides concentration polarization, to some slow stage in the discharge process occurring between hydrated ions in the vicinity of the cathode and stable atoms on the electrode surface. The variation of cathodic polarization with the logarithm of the current density is found to be a linear function (Fig. 1), suggesting that in the electrodeposition of cobalt the rate-determining step for polarization is the discharge of the ions at the cathode. Either the dehydration of the ions is slow or the actual neutralization of the cation is slow. According to GLASSTONE [20], the metal is first deposited in a metastable state; the conversion of this form of the metal to the stable state is the rate-determining process.

The value of Table Slope b has been calculated for different electrolytes (Table II), using the following equation

$$W = a + b \log I$$

where W is the overpotential, I is the current density and the constant a is the intercept of the overpotential *vs.* log (current density) curve (Fig. 1).

Table II

Nos	Plating bath	Intercept (*a*)	Tafel slope (*b*)
1	All sulfate bath (S)	0.3125	0.1769
2	All chloride bath (C)	0.1750	0.1710
3	Watt's bath (W)	0.2700	0.1550

The protective value of the electrodeposited coating depends to a large extent on the porosity of the deposit. The corrosion resistance data (Table III) have been calculated in terms of the spots revealed by the ferroxyl test method and expressed as follows

$$\text{Corrosion resistance} \quad \frac{100}{\text{No. of spots per cm}^2}$$

Deposits obtained from bath (C) are found to show a high degree of resistance to corrosion, even up to thickness of 9.36 μ (Nos 2 and 13, Table III). The minimum corrosion resistance is obtained in the case of the deposit from bath (SG) (No. 6, Table III). The addition of glycerol to the sulfate bath (S) increases the viscosity of the solution, thus the diffusion of cobalt ions to the cathode is retarded and the rate of formation of crystal nuclei is considerably

Table III

Corrosion resistance of cobalt electrodeposits

Current density used = 3.110 A/dm^2

No.	Plating bath	pH of bath	Temperature (°C)	Thickness of the deposit (μ)	Corrosion resistance
1	S	2.0	35	56.20	1.25
2	C	2.5	35	56.20	Approaching to ∞ (very high)
3	W	1.9	35	56.20	3.57
4	SWB	2.0	35	56.20	3.12
5	SM	2.9	35	56.20	0.48
6	SG	2.1	35	56.20	0.23
7	S	2.0	50	56.20	0.83
8	S	2.0	20	56.20	1.66
9	S	1.1	35	56.20	0.42
10	C	1.1	35	56.20	0.42
11	S	6.0	35	56.20	Approaching to ∞ (very high)
12	S	2.0	35	9.36	0.83
13	C	2.5	35	9.36	Approaching to ∞ (very high)

Table IV

Microscopic examination of grain size and nature of cobalt electrodeposit

No.	Plating bath	$C.D_2$ (A/dm^2)	Temperature (°C)	pH of bath	Grain size (μ)	Nature of electrodeposit
1	S	1.192	35	2.0	3.00	Smooth surface with bulbs of average size 27.5 μ uniformly distributed over the entire surface
2	S	3.110	35	2.0	2.50	Smoother and more even than No. 1
3	S	0.016	35	2.0	2.14	Smoother and more even than No. 2, having pits of average size 27.5 μ distributed over entire surface
4	S	12.028	35	2.0	2.14	Similar to No. 3, having pits over entire area
5	C	3.110	35	2.5	1.87	Much smoother and more even than No. 2, no bulbs or pits on the surface
6	C	6.016	35	2.5	1.50	Smoother than No. 5, maximum smoothness and evenness among deposits 1—14
7	W	3.110	35	1.9	2.14	Smoother than No. 2, almost similar to No. 3
8	SWB	3.110	35	2.0	3.00	Clusters of bulging bulbs of average size 30 μ almost uniformly distributed over entire surface
9	S	3.110	20	2.0	2.14	Smoother and more even than No. 2 and 11
10	W	3.110	20	1.9	1.87	Smoother and more even than Nos 7, 9 and 12
11	S	3.110	50	2.0	3.00	Coarser and more uneven than No. 9
12	W	3.110	50	1.9	2.50	Coarser and more uneven than No. 10
13	S	3.110	35	1.1	3.33	Coarser and more uneven than No. 2, nodules of average size 15 μ almost uniformly distributed over entire surface
14	C	3.110	35	1.1	2.14	Coarser and more uneven than Nos 5 and 6

affected, giving more porous deposits. Therefore, the corrosion resistance decreases enormously.

The electrode-posited film obtained from Watt's bath (W) is found to show a rather good resistance to corrosion (No. 3, Table III) and is less resistant than the deposit from the chloride bath (C). Deposits from the sulfate bath without boric acid (SWB) are much more corrosion resistant than deposits from sulfate baths with added boric acid (S) (No. 4, Table III). Deposits from the electrolytic bath (SM), with magnesium are found to show a poor resistance to corrosion (No. 5, Table III).

Lowering the temperature of the bath is found to cause the deposits to become more corrosion resistant (No. 8, Table III). This might be due to the decrease in the rate of crystal growth with the decrease of temperature of the bath, producing less porous deposit. The lowering of the pH of the bath inhibits the precipitation of basic salts, therefore, the deposits will be more porous as only an insufficient amount of colloidal oxides will be available for adsorption on the crystal nuclei [21], which leads to the production of smooth deposits, hence the corrosion resistance is expected to decrease (Nos 9, 10, Table III). Deposits at pH 1.1 from bath (C) show deterioration to a large extent in the corrosion resistance in comparison to deposits at pH 2.5 from bath (C), and deposits at pH 6.0 from bath (S) give an enormous improvement in corrosion resistance in comparison to deposits at pH 2.0 from bath (S) (No. 11, Table III).

The relationship between overpotential and log (C. D.) is linear for baths (S), (C) and (W) (Fig. 1), indicating the frequent formation of new nuclei [9], therefore, smooth and fine-grained deposits are produced (Table IV).

The relatively higher values of cathodic polarization suggest nucleation and lower values the crystal development as the predominant process [22]. As the C. D. is increased, cathodic polarization is found to increase (Table I), hence the rate of formation of fresh nuclei is increased, giving smoother and finer grained deposits. Thus, reduction in grain size is distinctly observed (Nos 1—3, Table IV). The minimum value of grain size is found in the deposits from chloride bath (C), consequently, an extremely smooth and even surface is obtained (No. 6, Table IV).

The decreasing of the bath temperature increases the polarization (No. 7, Table I), hence smoother deposits are obtained and the grain size is reduced (Nos 9, 10, Table IV). The decrease of the pH of the bath increases the grain size of the deposits, therefore, coarser and rougher deposits are produced (Nos 13, 14, Table IV).

*

Grateful acknowledgements are made to the State Council of Scientific and Industrial Research, U. P., for the award of a research grant.

REFERENCES

[1] Bancroft, W. D.: Trans. Am. Electrochem. Soc., **23,** 261 (1913)
[2] Aten, A. H. W., Boerlage, L. M.: Rec. Trav. Chim. Pay-Bas **39,** 720 (1920)
[3] Blum, W., Rawdon, H. S.: Trans. Am. Electrochem. Soc., **44,** 397 (1923)
[4] Kohlschutter, V.: Trans. Am. Electrochem. Soc., **45,** 229 (1924)
[5] Srivastava, R. D., Kumar, S.: Trans. Inst. Metal Finishing London, **50,** 102 (1972)
[6] Srivastava, R. D., Kumar, S.: Plating, **60,** 487 (1973)
[7] Srivastava, R. D., Kumar, S.: Acta Chim. (Budapest) **78,** 139 (1973)
[8] Yuza, V., Kopyl, L.: J. Phys. Chem. U.S.S.R., **14,** 1074 (1940)

[9] GAVDAM, G. E.: Discuss. Faraday Soc. **1,** 182 (1947)
[10] REISER, H., FISHER, H.: Z. Electrochem., **58,** 668 (1954)
[11] BRENNER, A., ZENTNER, V., JENNINGS, C.: Plating **39,** 857 (1952)
[12] BANERJEE B. C., GOSWAMI, A.: J. Electrochem. Soc., **106,** 20 (1959)
[13] ROTINYAN, A. L., MOLOTKOVA, E. N., DANILOVITCH, O. M.: Tsvet. Metall., **4,** 49 (1960)
[14] POLUKAROV, V. M., Russ. J. Phys. Chem., **34,** 68 (1960)
[15] SARD, R., SCHWARTZ, C. D., WEIL, R.: J. Electrochem. Soc., **113,** 424 (1966)
[16] EPELBOIN, I., FROMENT, M., MAURIN, G.: Plating, **56,** 1356 (1969)
[17] EPELBOIN, I., WIART, R.: J. Electrochem. Soc., **118,** 1577 (1971)
[18] HARING, H. E.: Trans. Electrochem. Soc., **49,** 417 (1926)
[19] AGAR, J. N., BOWDEN, F. P.: Proc. Roy. Soc. London **169** A, 206 (1938)
[20] GLASSTONE, S.: J. Chem. Soc., 2887 (1926)
[21] O'SULLIVAN, J. B.: Trans. Faraday Soc., **26,** 89 (1930)
[22] SHREIR, L. L., SMITH, J. W.: J. Electrochem. Soc., **99,** 450 (1952)

R. D. SRIVASTAVA
Sushil KUMAR
} Chemical Laboratories, University of Lucknow, India.

Acta Chimica Academiae Scientiarum Hungaricae, 84 (4), pp. 393—407 (1975)

INFRARED VIBRATIONAL FREQUENCIES OF REDUCED TUNGSTEN OXIDES WO_{3-x} $(1 \geq x > 0)$

A. B. Kiss

(Tungsram Research Institute, Budapest)

Received December 18, 1973

The infrared spectra of tungsten oxides of the composition WO_{3-x} $(1 \geq x > 0)$ have been investigated. In the range of $x < 0.1$, oxides with triclinic, monoclinic, orthorhombic and tetragonal lattices are formed, and in spite of their deviation from the composition WO_3, these oxides are generally called the polymorphous modifications of WO_3. All the four oxide types of different symmetry may be stable at room temperature, depending on the thermal treatment and impurities. Since the spectra of the various modifications differ more or less from each other, an infrared spectrophotometric investigation of the oxide generally called WO_3 must determine the modification of the substance in question.

The number and the symmetry type of the possible vibrations have been determined by a factor group analysis of the oxides of D_{4h}, D_{2h}, C_{2h} and C_i symmetry. The two strong bands in the spectra of the oxide modifications are indicative of the fact that the molecular vibrations of the WO_6 octahedral element dominate in the oxides, thus, in first approximation the oxides can be considered as distorted modifications of the ideal RO_3 lattice (O_h). Accordingly, the character of the infrared bands has been determined by means of the correlation $O_h \rightarrow D_{4h} \rightarrow D_{2h} \rightarrow C_i$. The extent of splitting of the $2F_{1u}$ mode increases in the direction of tetragonal → triclinic transformation, *i.e.* with increasing distortion.

The frequency shift of the νW—O vibrational bands of highest frequency is in close relationship with the value of x, *i.e.* with the number of oxygen vacancy sites, so that conclusions can be drawn from the spectra on the kind and structure of the oxide. Moreover, the correlation between frequency and oxygen deficiency represents that borderline which separates the series of WO_{3-x} $(1 \geq x > 0)$ oxides with regard to the mode of incorporation and structure of the oxygen vacancy sites. The IR spectrum also indicates sensitively the development of the so-called super-lattice $2 \times W_{20}O_{58} = W_{40}O_{116}$.

One of the decisively important technological steps in production of tungsten filaments is the reduction with hydrogen of ammonium paratungstate-5.hydrate, and of the tungsten trioxide formed from it, to metallic tungsten. During this process, several stable, intermediate oxides appear between the WO_3 and the W states. Considerable research efforts are extended on elucidating the conditions of their formation, and on crystallographic and morphological study of their structures. It is common knowledge that the composition of the substance called tungsten trioxide does not correspond in general exactly to the ratio of 1W : 3 O, the number of oxygen atoms being always somewhat less than three. Accordingly, the general formula can be written as WO_{3-x}. Since a certain oxygen deficit is needed for the formation of the various crystal modifications, and, in essence, this means reduction,

the "polymorphous modifications of tungsten trioxide" too will be regarded in our discussion as reduced oxides. The conform with the general terminology use in the literature, the expression 'polymorphous modifications of WO_3' will be used, keeping in mind, however, that the oxides in question can in fact be fitted into the series of the reduced oxides WO_{3-x} $(1 \geq x > 0)$.

The polymorphous modifications of WO_3 are more or less distorted variants of the ReO_3 type cubic lattice ($Pm3m$) [1]. The elementary unit of the various modifications is the octahedron, with the metal atom in its center being surrounded by six oxygen atoms, in an arrangement deviating more or less from regular. The polymorphism of WO_3 has been widely studied [2—10]. These studies show that between —40 and 17 °C the triclinic, between 17 and 330 °C the monoclinic, between 330 and 640 °C the orthorhombic, and above 740 °C the tetragonal modifications are formed. Thus, the symmetry of the WO_3 crystal lattice is considerably influenced by the temperature.

It is also known that contaminations shift the characteristic temperatures of polymorphous transformations in the direction of lower temperatures, so that modifications forming at higher temperatures can be made stable also at room temperature by the incorporation of an appropriate amount of foreign ions [10]. Consequently, all four crystal forms of WO_3 may be stable at room temperature.

In practice, the differentiation of the orthorhombic from the monoclinic modification is rather important since, when cooled to room temperature, the ammonium salts used for the preparation of WO_3, *e.g.* ammonium paratungstates, afford in general a substance of monoclinic or orthorhombic structure, depending on the contaminant and on the ignition temperature. However, upon thermal treatment above 1000 °C or in the case of sufficiently high contaminant concentrations, triclinic or tetragonal forms may also occur at room temperature.

Therefore, when investigating WO_3, *e.g.* by infrared spectrophotometry, the modification in which the substance is present must be definitely established, because, as will be seen, the spectra of the various modifications differ more or less from each other. On the other hand, the infrared spectra are known, conclusions can be drawn on the modification of the WO_3 investigated, and this can be used when studying the transformation properties of WO_3.

Though the infrared and Raman spectra of WO_3 have been studied by several authors [11—15], in the predominant part of these works the X-ray diffraction background is missing, *i.e.* it remains obscure which modification is present. Rocchiccioli–Deltcheff and Lecomte [11] only assumes that the WO_3 for which the spectrum has been recorded is present in the monoclinic form, Mattes and Schröder [14] indicate a rhombic structure, while other works [12, 13, 15] do not at all specify the modification of WO_3. With the aim of eliminating the uncertains connected with the structures and the

spectra, the infrared spectra of the WO_3 modifications have been studied. These investigations were extended also to the more strongly reduced intermediate oxides.

Experimental

The oxide modifications were made available by Dr. GADÓ. The samples were crystallographically well defined test substances of X-ray diffraction studies [10]

Preparation procedures

Triclinic: Thermal treatment of monoclinic WO_3 in air, for 50 hrs in a sealed quartz tube at 1200 °C. On mild crushing the larger crystal grains formed gave a pure triclinic modification.

Monoclinic: Ignition of purity ammonium paratungstate-5.hydrate, product Tungsram, in a stream of air at 950 °C for 5 hrs.

Orthorhombic: Ignition of ammonium paratungstate-5.hydrate, product Tungsram, at 600 °C for 5 hrs.

Tetragonal: Ignition of WO_3 with 0.08 mol SiO_2 content at 540 °C for 2 hrs.

Reduced oxides: Tungsram products formed in the reduction of tungsten trioxide with hydrogen.

The infrared spectra of the samples were recorded with a Model Perkin-Elmer 225 spectrophotometer in a KJ pellet. Spectra are shown in Figs 1 and 2, and the wavenumbers of the absorption bands are listed in Tables I and II.

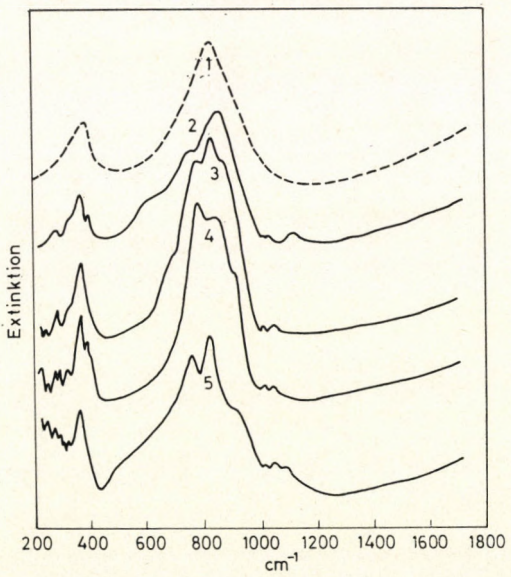

Fig. 1. Infrared spectra of WO_3 modifications 1. Cubic, 2. Tetragonal, 3. Orthorhombic, 4. Monoclinic, 5. Triclinic

Table I

Infrared wavenumbers of the different WO_3 modifications

Cubic C_h [15]		Tetragonal D_{4h}		Orthorhombic D_{2h}		Monoclinic C_{2h}		Triclinic C_i	
cm^{-1}	assign.	cm^{-1}	assign.	cm^{-1}	assign.	cm^{-1}	assign.	cm^{-1}	assign.
				230	B_{1u}	226	A_u		
				250	B_{2u}	252		250	
				286	B_{3u}	280		278	
		288	E_u δW—O—W			290	B_u	292	
					δW—O—W	307	δW—O—W	305	δW—O—W
		320	?	325	?	322		322	
(362)	(F_{2u} δW—O)					340			
		370	A_{2u} δW—O—W	370	B_{1u}	360	A_u	358	
390	F_{1u} δW—O	400	E_u			386			A_u
								500	
		650	$A_{2u}+E_u$						
		755	A_{2u}	770	B_{1u}	775	A_u	755	
815	F_{1u} νW—O	832	E_u νW—O	820	B_{2u} νW—O	835	B_u νW—O	810	νW—O
				870	B_{3u}	900	B_u	905	
		1000		1005		1010		1005	
		1038		1030		1035		1040	
		1110	νSi—O (SiO_2)						

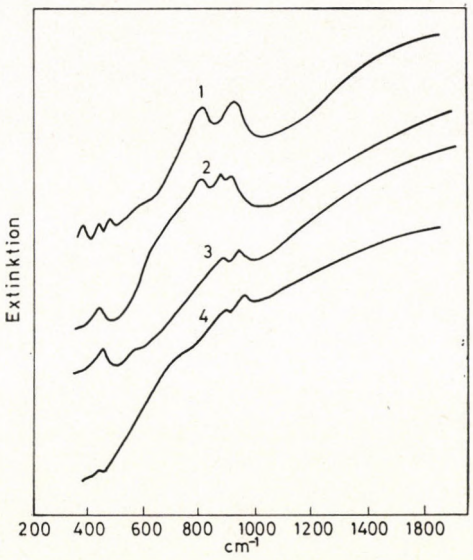

Fig. 2. Infrared spectra of reduced tungsten oxides 1. $W_{20}O_{58}(WO_{2.90})$, 2. $W_{40}O_{116}(WO_{2.90})$, 3. $W_{18}O_{49}(WO_{2.72})$, 4. WO_2

Table II

Infrared wavenumbers of reduced tungsten oxides

$W_{20}O_{58}$ $WO_{2,90}$	$W_{40}O_{116}$ $WO_{2,90}$	$W_{18}O_{49}$ $WO_{2,72}$	WO_2
390			
450	450	455	450
490			
650	650	580	
818	810		
	890	900	890
925	920	940	955

Interpretation of the infrared spectra of tungsten oxides

In the lattice of tungsten trioxide, the tungsten atoms are not in the center of octahedra but are dislocated in the direction of one of the axes, thus causing a waviness of the planes in which the tungsten atoms are arranged, as *e.g.* in the tetragonal modification [10]. If the dislocation has finite components in two or in all three directions, a waviness in space is developed, and the orthorhombic or the monoclinic and triclinic modifications of still lower symmetry are formed [10]. Table III summarizes the characteristic structural

Table III

Crystallographic data of WO_3 modifications

Modification	Cubic*	Tetragonal	Orthorhombic	Monoclinic	Triclinic
Cell parameters		a=5.25 Å c=3.91 Å	a=3.740 Å b=7.546 Å c=3.837 Å	a=3.835 Å b=7.517 Å c=7.285 Å β=90° 90′	a=7.30 Å b=7.52 Å c=7.69 Å α=88.9° β=90.9° γ=90.9°
Space group	$Pm3m$—O_h^1	$P_4/_{nm}$—D_{4h}^7	P_{mab}—D_{2h}^{11}	$P2_{1/a}$—C_{2h}^5	$P\bar{1}$—C_i^1
Number of molecules, Z	1	2	4	4	8
From Wyckoff's table Tungsten positions Oxygen positions	 1(a) 3(d)	 2(c) 2(c), 4(d)	 4(d) 4(d), 8(e)	 4(e) 12(e)	 8(*i*) 24(*i*)
Site symmetry Tungsten Oxygen	 O_h D_{4h}	 C_{4v} C_{4v}, C_{2h}	 C_S C_S, C_1	 C_1 C_1	 C_1 C_1
References		[10] [16]	[10] [17]	[10] [18]	[10] [19]

* Fictive data obtained by assuming an ideal RO_3 type structure

data of the WO_3 modifications, with special regard to the requirements of the infrared spectroscopic study.

No WO_3 built up from perfectly regular WO_6 polyhedra, *i.e.* WO_3 of cubic structure, has been prepared so far. However, as will be seen later, since the spectroscopic characteristics of all modifications can be traced back eventually to the cubic structure, Table III contains also those data which would be characteristic of cubic WO_3, if such a modification existed.

As in other crystalline systems the number and symmetry type of the vibrations in the case of tungsten trioxide can be determined by the method of BHAGAVANTAM and VENKATARAYUDU [20], under the assumption that the homologous atoms of the crystal lattice vibrate in-phase ($k = 0$), which makes possible counting on a single lattice. Using the correlation method recommended by FATELEY *et al.* [21] in the factor group analysis of the various WO_3 modifications (Tables IV—VIII), it is found that, according to the selection rules valid for crystalline systems, with the decrease in symmetry of the WO_3 crystal lattice, theoretically 3, 14, 45, and 93 normal vibrations are to be expected in the given order, disregarding the acoustic modes arising from the translation of the crystal as a whole.

Table IV

Factor group analysis of cubic WO_3

O_h Factor group species	Transl. species	Acoustic species	Crystal coeff.	Vibrational coeff.	Activity IR	Activity R
A_{1g}	—	—	—	—		+
A_{1u}	—	—	—	—		
A_{2g}	—	—	—	—		
A_{2u}	—	—	—	—		+
E_g	—	—	—	—		
E_u	—	—	—	—		
F_{1g}	—	—	—	—		
F_{1u}	3	1	3	2	+	
F_{2g}	—	—	—	—		+
F_{2u}	—		1	1		

Correlation: $D_{4h} \rightarrow O_h$ (oxygen)

$\Gamma_{vibr} = 2F_{1u} + 1F_{2u}$

Table V

Factor group analysis of tetragonal WO_3

D_{4h} Factor group species	Transl. species	Acoustic species	Crystal coeff.	Vibration. coeff.	Activity IR	Activity R
A_{1g}	—	—	2	2		+
A_{1u}	—	—	1	1		
A_{2g}	—	—	—	—		
A_{2u}	$T(z)$	1	3	2	+	
B_{1g}	—	—	—	—		+
B_{1u}	—	—	1	1		
B_{2g}	—	—	—	—		+
B_{2u}	—	—	1	1		
E_g	—	—	2	2		+
E_u	$T(x, y)$	1	6	5	+	

Correlation: $C_{4v} \rightarrow D_{4h}$ (tungsten, oxygen)

$C_{2h} \rightarrow D_{4h}$ (oxygen) The results of C_2, C_2', C_2'' correlations are identical

$\Gamma_{vibr} = 2A_{1g} + 1A_{1u} + 2A_{2u} + 1B_{1u} + 1B_{2u} + 2E_g + 5E_u$

Table VI

Factor group analysis of orthorhombic WO_3

D_{2h} Factor group species	Transl. species	Acoustic species	Crystal coeff.	Vibrational coeff.	Activity IR	Activity R
A_g	—	—	7	7		+
A_u	—	—	5	5		
B_{1g}	—	—	7	7		+
B_{1u}	$T(z)$	1	5	4	+	
B_{2g}	—	—	5	5		+
B_{2u}	$T(y)$	1	7	6	+	
B_{3g}	—	—	5	5		+
B_{3u}	$T(x)$	1	7	6	+	

Correlation: $C_S \xrightarrow{\delta xy} D_{2h}$ (tungsten, oxygen)

$C_1 \rightarrow D_{2h}$ (oxygen)

$\Gamma_{vibr.} = 7A_g + 5A_u + 7B_{1g} + 4B_{1u} + 5B_{2g} + 6B_{2u} + 5B_{3g} + 6B_{3u}$

Table VII

Factor group analysis of monoclinic WO_3

D_{2h} Factor group species	Transl. species	Acoustic species	Crystal coeff.	Vibrational coeff.	Activity IR	Activity R
A_g	—	—	12	12		+
B_g	—	—	12	12		+
A_u	$T(z)$	1	12	11	+	
B_u	$T(x, y)$	2	12	10	+	

Correlation: $C_1 \rightarrow C_{2h}$ (tungsten, oxygen)

$$\Gamma_{vibr.} = 12A_g + 12B_g + 11A_u + 10B_u$$

Table VIII

Factor group analysis of triclinic WO_3

C_i Factor group species	Transl. species	Acoustic species	Crystal coeff.	Vibrational coeff.	Activity IR	Activity R
A_g	—	—	48	48		+
A_u	$T(x, y, z)$	3	48	45	+	

Correlation: $C_1 \rightarrow C_i$ (tungsten, oxygen)

$$\Gamma_{vibr.} = 48A_g + 45A_u$$

Table IX

Activity of the vibrational species of tungsten trioxides

WO_3	Infrared active	Raman active	Inactive
Cubic O_h	$2F_{1u}$	—	$1F_{2u}$
Tetragonal D_{4h}	$2A_{2u} + 5E_u$	$2A_{1g} + 2E_g$	$1A_{1u} + 1B_{1u} + 1B_{2u}$
Orthorhombic D_{2h}	$4B_{1u} + 6B_{2u} + 6B_{3u}$	$7A_g + 7B_{1g} + 5B_{2g} + 5B_{3g}$	$5A_u$
Monoclinic C_{2h}	$11A_u + 10B_u$	$12A_g + 12B_g$	—
Triclinic C_i	$45A_u$	$48A_g$	—

It is apparent from Table IX that of the vibrations obtained many are inactive, however, particularly in the case of the modifications of lower symmetry, a great number of infrared-active normal vibrations are left, compared to which substantially fewer bands appear in the spectra.

An inspection of Fig. 1 immediately reveals a common feature of the spectra of the polymorphous modifications, *viz.* that essentially the absorption curves consist of two intense bands. On the other hand, their shape and splitting, *i.e.* the fine structure of the spectra, is characteristic of the given modification.

This is not surprising: it has been shown in connection with the study of the infrared spectra of molybdates and tungstates built up from octahedra [22, 23] that the normal frequencies of polymetallogenates consisting of MO_6 elements, can also be deduced from the normal vibrations of the octahedral XY_6 molecules, under consideration of the symmetry degradation determined by the polyanion and its crystal group, and the corresponding changes in the spectra, *e.g.* splitting, *etc.* Thus, regardless of the crystal point group of the WO_3 modification, the vibrations of the elementary unit, the octahedron, will dominate the spectra. Therefore, as a first approximation, the two intense bands exhibited in the spectra of all polymorphous modifications, can be considered in essence as corresponding to the cubic lattice of the ReO_3 type, *i.e.* to the infrared active modes $F_{1u}(\nu X-Y)$ and $F_{1u}(\delta X-Y)$ connected with the vibration of a single octahedron. With decreasing symmetry, or rather with increasing distortion, these bands are split, and the lower is the symmetry of the given modification, the higher will be extent of splitting.

Let us now consider spectrum 1 in Fig. 1. In the plotting of this spectrum, the frequencies calculated by OHWADA [15] have been taken as a basis. These calculations assume an ideal structure of the ReO_3 type, *i.e.* a cubic lattice. Accordingly, Table I contains the frequencies of 815 and 390 cm^{-1} corresponding to the two F_{1u} modes of 'cubic WO_3', calculated by normal co-ordinate analysis [15].

For the assignment of the bands of the different modifications and for the determination of the vibrational species, first the correlation table must

Table X

Splitting of the species of the O_h point group in the various factor groups

Cubic O_h	Tetragonal D_{4h}	Orthorhombic $D_{2h}(C_2')$	Monoclinic $C_{2h}(C_2(z))$	Triclinic C_i
A_{1g}	A_{1g}	A_g	A_g	A_g
A_{1u}	A_{1u}	A_u	B_g	A_u
A_{2g}	A_{2g}	B_{1g}	A_u	
A_{2u}	A_{2u}	B_{1u}	B_u	
E_g	B_{1g}	B_{2g}		
E_u	B_{1u}	B_{2u}		
F_{1g}	B_{2g}	B_{3g}		
F_{1u}	B_{2u}	B_{3u}		
F_{2g}	E_g			
F_{2u}	E_u			

Table XI

Correlation table of infrared active vibrations

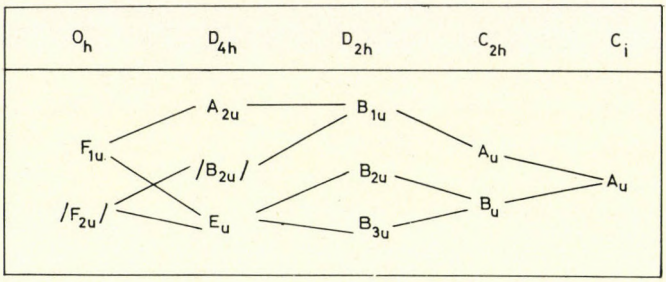

be constructed, which gives the splitting of the irreducible representations of the O_h point group, corresponding to the cubic lattice, in the factor groups D_{4h}, D_{2h}, C_{2h} and C_i, characteristic of the WO_3 modifications. The number of these species in Table X can be further reduced by neglecting the Raman and inactive modes, to obtain thus Table XI, which corresponds to the correlation table containing only infrared-active representations.

With the aid of correlation Table XI, conclusions can be drawn on the species of the vibrational modes produced by the two active (F_{1u}) and the one inactive (F_{2u}) modes of the cubic lattice in the crystal lattice of new symmetry, formed in the course of transformation. Accordingly, orientative information may be obtained from Table I on the possible character of band splittings in the spectra of the modifications of lower symmetry. At the same time, the table gives an illustrative picture on the band systems characteristic of the modifications, on the basis of which a possibility offers itself for the determination of the crystal structure, or more exactly, of the cell symmetry of tungsten trioxides of unknown origin and structure.

As has already been shown, the stretching frequencies of the terminal W–O bands are closely connected with the structural properties of tungstates and molybdates built up from octahedra, and any structural change will result primarily in a change of the frequencies in question [22—24]. It can be seen from Table I that the νW–O vibrational bands of highest frequency in the polymorphous WO_3 modifications are gradually shifted towards higher frequencies, namely in the direction corresponding to the tetragonal → triclinic transformation. Before any conclusions are drawn from this phenomenon, it should be recalled that the composition of the modifications prepared by thermal treatment from pure WO_3, does not correspond in any of the cases exactly to the ratio of W/O = 1/3, and thus, neither is the valency of tungsten in these modifications exactly six. It could also be said that the expression tungsten trioxide is not exact since the oxygen deficit in the crystal lattice

Table XII

Numerical values characteristic of rhe oxygen index of tungsten oxides

Oxide	Valency range of tungsten	x in WO_{3-x}	Oxygen/tungsten
Triclinic	6 —5.995	0 —0.005	3 —2.995
Monoclinic	5.995—5.97	0.005—0.015	2.995—2.985
Orthorhombic	5.97 —5.94	0.015—0.030	2.985—2.970
Tetragonal	5.94 —5.78	0.030—0.10	2.970—2.89
$W_{20}O_{58}$	5.80	0.10	2.90
$W_{18}O_{49}$	5.44	0.28	2.72
WO_2	4.00	1.0	2.0

of the oxide modifications increases in the direction of the transformation triclinic → tetragonal, and the composition varies within the limits $WO_{2\cdot999} \longleftrightarrow WO_{2\cdot890}$.

Let us now try to correlate the above frequency shift to the tungsten valency ranges corresponding to the different WO_3 modifications, or, in WO_{3-x}, to the changes of the limits of x, *i.e.* to the vacancy concentrations calculated from these. The valency ranges characteristic of the triclinic, monoclinic, orthorhombic and tetragonal modifications and the values of x are summarized in Table XII, whereas the vacancy concentration ranges have been given by GADÓ [10]. These values were taken as basis for the plotting of Figs 3 and 4.

From the course of the curves in the figures, determined by the change in frequency, it can be easily understood, why the cubic WO_3 could not be prepared so far. The figures indicate clearly that the stability ranges of the triclinic, monoclinic, orthorhombic and tetragonal forms are well defined, while the range corresponding to the formation of the regular cubic lattice falls into an undefined area. Indeed, in the cubic WO_3 the valency range of tungsten would involve values of $5.78 \rightarrow 0$, and on the other side, vacancy concentration would also exceed all limits, which, naturally, is impossible.

If WO_3 with oxygen vacancy sites is regarded as an A_xWO_3 'tungsten bronze', the polymorphous modifications can be considered according to GADÓ [10] as $(A)_xWO_3 \equiv WO_{3-x}$ hole-bronzes. However, according to this concept and under consideration of Figs 2 and 3, it becomes evident that for the formation of cubic WO_3 at least $x = 0.12$ vacancy sites are needed, *i.e.* the valency of tungsten should decrease below 5.76. However, the corresponding oxygen deficit would presumably produce a stress in the WO_{3-x} lattice, so that it would disintegrate before the last member of the oxide series, the cubic O_h lattice, can be formed. Instead of this, an oxide structure is formed according to an older concept is the blue oxide or $W_{20}O_{58}$, however, actually it is

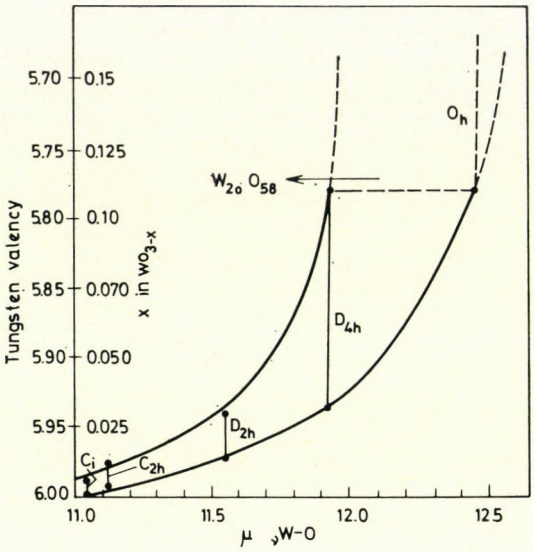

Fig. 3. Relationship between the ranges of x in WO_{3-x} and the νW—O vibrational frequencies of the modifications

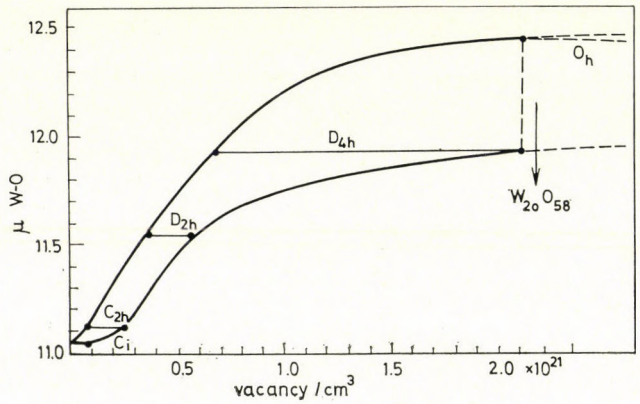

Fig. 4. Shift of the νW—O vibrational frequencies depending on vacancy concentration

characterized by a sheared crystallographic structure and differs slightly from the above composition [10], but is more stable under the given conditions.

The infrared spectra of the reduced tungsten oxides are substantially poorer in bands (Fig. 2) than the spectra of the tungsten trioxide modifications. With decreasing tungsten valency, the transmittance of the KJ pellets prepared from an identical amount of the sample decreases gradually, and the base line approaches per cent transmission zero with increasing steepness. The emergence of the bands from the base line, *i.e.* the intensity of the bands decreases also gradually, and is the lowest for WO_3. However, the frequency

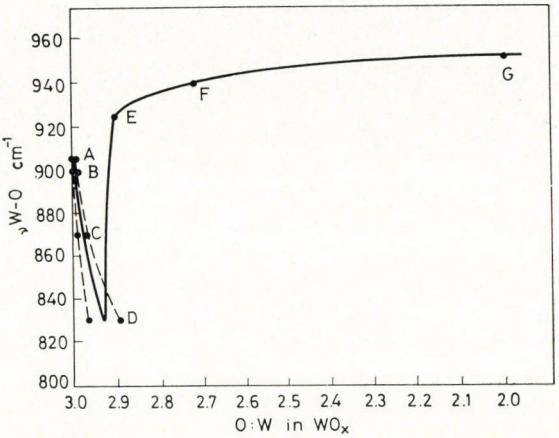

Fig. 5. Change of the W—O stretching vibration frequencies as a function of the change in the oxygen index:
A) Triclinic
B) Monoclinic
C) Orthorhombic
D) Tetragonal
} WO_3
E) Blue oxide $W_{20}O_{58}$
F) $W_{18}O_{49}$
G) WO_2

of the band maxima can be established even in the case of WO_2 with satisfactory accuracy (Table II).

Characterizing the oxides with the general formula $WO_{3-x}(1 \geq x > 0)$, the valency regions and the corresponding x values are given in Table XII. Thus, from the point of view of oxygen deficiency, tungsten trioxide modifications and reduced oxides have been arranged in a unified system. Naturally, it does not mean any difference in principles that oxygen deficiency ranges have been assigned to the trioxide modifications [10], while definite values to the reduced oxides.

As has been done in the case of WO_3 modifications, we shall now examine how the changes in the oxide structure can be characterized by the stretching frequencies of the terminal W–O bonds, which are most sensitive to the changes of structural properties [22—24], considering now all the tungsten oxides falling into the $1 \geq x > 0$ range as a unified system. When the highest frequency bands of the W–O stretching vibrations are plotted against one of the oxygen indexes, *e.g.* the O : W ratio, the relationship shown in Fig. 5 is obtained. The total range relevant to the trioxide modifications is marked with a dotted line. When the mean value of this region, marked with a solid line, is taken as basis, it can be seen that the frequency decreases gradually from the triclinic to the tetragonal modification, *i.e.* to $x \approx 0.06$, and starting from the reduced oxides, the frequency increases rapidly. The νW–O vibrational frequency belonging to the phases changes according to a distinct maximum curve. Remarkably, some of the known physical properties of tungsten oxides exhibit a behaviour similar to that shown in Fig. 5, from which it might be

Table XIII

Change of some physical characteristics of the oxide series

Oxide	Density g/cm³ [25]	Thermal dilatation (30—350 °C) 10^{-6}/°C [26]	W—O cm^{-1}
Triclinic	7.29 (WO_3)		905
Monoclinic	7.17 ($WO_{2.98}$)	15.30 (WO_3)	900
Orthorhombic			870
Tetragonal	7.14 ($WO_{2.96}$)		832
$W_{20}O_{58}$	7.16	0.2	925
$W_{18}O_{49}$	7.78	1.2	940
WO_2	10.82	3.3	950

assumed that the phenomena can be traced back to some common cause, *e.g.* to a property of material structure. According to Table XIII, the minima of the density [25] and thermal dilatation [26] similarly fall into a region near the composition of the tetragonal oxide.

Figure 5 divides the $1 \geq x > 0$ range into two sections, and this, as will be seen, can be correlated with detailed structural information gained mainly from X-ray investigations. According to GADÓ and MAGNÉLI [27], WO_3 can dissolve oxygen deficiencies in small concentrations as point vacancies and, according to Fig. 5, between x-values of 0 and 0.06 this distorts the basic ReO_3 type lattice. On the other hand, in the $1 > x > 0.06$ region, the higher oxygen deficiency results in a more extensive lattice rearrangement. Thus, when oxygens are withdrawn from the stoichiometric WO_3, isolated defect sites are first created, and the polymorphous modifications of the trioxide are formed. Subsequently, the vacancies are ordered in the lattice of tungsten trioxide, producing the so-called sheared structures [10,28]. The first independent phase of this region is $W_{20}O_{58\pm0.02}$ [10]. The formula of the blue oxide has been given in this way, because the composition can vary actually from $WO_{2.92}$ to $WO_{2.88}$ [29, 30], and the composition $W_{20}O_{58}$ belongs to the idealized structure of the oxides between these limits. As a summary, the conclusion has finally been drawn that the minimum exhibited in Fig. 5 constitutes a partition from the aspect of the mechanism and structure of the incorporation of oxygen deficiency.

The oxide of composition $W_{40}O_{116}$, corresponding to spectrum 2 in Fig. 2, has not been discussed so far. In this oxide the valency of tungsten and the oxygen deficiency are identical with those in the blue oxide, therefore, as far as Fig. 5 is concerned, the conclusions relevant to the blue oxide remain valid. According to the X-ray investigations of GADÓ [10], it differs from $W_{20}O_{58}$ in that the elementary cell has doubled in direction *b*. Its formation might be

caused by the ordering of oxygen vacancy sites or impurities. The infrared spectrum support the assumption that the structure of $W_{40}O_{116}$ is in essence the same as that characteristic of $W_{20}O_{58}$, but its νW–O vibrational band at 925 cm^{-1} has split, owing to effects accompanying the doubling of the cell.

It can be seen, therefore, that even if no concrete structural information can be obtained from the infrared spectra recorded in this narrow region, with the aid of suitably selected spectral characteristics, or rather their changes, orientative information may be gained about certain problems. Thus, it can be established among others, at what compositions does some structural modification occur in the substance. Curves similar to those in Fig. 5 can readily be interpreted with the aid of subsequent X-ray data, and thus, curves of this type often complement the results of X-ray diffraction studies [22—24].

REFERENCES

[1] Braekken, H.: Z. Krist., **78,** 484 (1931)
[2] Wyart, J., Foex, M.: Compt. rend., **232,** 2459 (1951)
[3] Ueda, R., Ichinokawa, T.: Phys. Rev., **82,** 563 (1951)
[4] Hirakawa, K.: J. Phys. Soc. Japan, **7,** 331 (1952)
[5] Perri, A. J., Banks, E., Post, B.: J. Appl. Phys., **28,** 1272 (1957)
[6] Tanasaki, S.: J. Phys. Soc. Japan, **14,** 680 (1959)
[7] Tanasaki, S.: J. Phys. Soc. Japan, **15,** 566, 573 (1960)
[8] Crowdwer, B. L., Sienko, M. J.: Inorg. Chem., **4,** 73 (1965)
[9] Braekken, H.: J. Appl. Phys., **37,** 3635 (1966)
[10] Gadó, P.: Dissertation, 1970.
[11] Rocchiccioli-Deltcheff, C., Lecomte, M. J.: Compt. rend., **268,** 45 (1969)
[12] Krasser, W.: Naturwiss., **56,** 213 (1969)
[13] Beattie, I. R., Gilson, T. R.: J. Chem. Soc. (A) **2322** (1969)
[14] Mattes, R., Schröder, F.: Naturforsch. **24b,** 1095 (1969)
[15] Ohwada, K.: Spectrochim. Acta, Part A, **26,** 1035 (1970)
[16] Wilson, A. J. C.: Structure Reports **16,** 229 (1959)
[17] Wilson, A. J. C.: Structure Reports **15,** 190 (1957)
[18] Pearson, W. B.: Structure Reports **19,** 369 (1963)
[19] Pearson, W. B.: Structure Reports **23,** 359 (1968)
[20] Bhagavantam, S., Venkatarayudu, T.: Proc. Ind. Acad. Sci., **9A,** 224 (1939)
[21] Fataley, W. G., McDevitt, N. T., Bentley, F. F.: Appl. Spect., **25,** 155 (1971)
[22] Kiss, B. A., Holly, S., Hild, E.: Acta Chim. (Budapest) **72,** 147 (1972)
[23] Kiss, B. A.: Acta Chim. (Budapest), **75,** 351 (1973)
[24] Kiss, B. A., L. Chudik-Major: Acta Chim. (Budapest), **75,** 237 (1973)
[25] Gébert, E., Ackermann, R. J.: Inorg. Chem., **5,** 136 (1966)
[26] Takamori, T.: Amer. Cer. Soc., **47,** 534 (1964)
[27] Gadó, P., Magnéli, A.: Mat. Res. Bull., **1,** 33 (1966)
[28] Gadó, P.: Acta Phys. Acad. Sci. Hung., **18,** 111 (1965)
[29] Hegedüs, J. A., Millner, T., Neugebauer, J., Sasvári, K.: Z. anorg. allg. Chem., **281,** 64 (1955)
[30] Glemser, O., Sauer, H.: Z. anorg. Chem., **252,** 144 (1943)

András B. Kiss; 1044 Budapest, Váci ut 77, Hungary.

Acta Chimica Academiae Scientiarum Hungaricae, 84 (4), pp. 409—418 (1975)

MASS SPECTRA OF SOME α-AMINOOXY ACID DERIVATIVES

J. TAMÁS*, J. HEGEDÜS-VAJDA*, L. DANCSI** and L. KISFALUDY**

*(*Central Research Institute for Chemistry of the Hungarian Academy of Sciences, Budapest, and ** Gedeon Richter Chemical Works, Ltd., Budapest)*

Received January 28, 1974

The mass spectrometric behaviour of aminooxy-acetic acid and some of its derivatives is discussed.

The fragmentation of the free aminooxy acid is more complicated than that of glycine. In the derivatives, the fragmentation of every bond of the straight chain occurs, providing detailed information about the sequence of atoms in the molecule.

In the case of anilides numerous rearrangements have been observed, among them methylene and methyl group migration.

Introduction

The mass spectrometric study of α-aminooxy acids and their derivatives is interesting owing to the practical importance of these compounds: 1. certain derivatives have pronounced tuberculostatic effects [1]; 2. incorporation into chains of peptides with biological activity permits studies on "structure-effect" correlations [2]. A detailed study of the mass spectral behaviour may help to elucidate structural problems of this group of compounds by mass spectrometry.

In the present paper the electron impact-induced fragmentation and rearrangement of eight representative compounds of approximately 200 derivatives prepared so far, described by the general formula XYN-O-CH_2-CO-R are discussed.

Results and discussion

The mass spectra of the simplest member of this group, aminooxyacetic acid, and of the analogous α-amino acid, glycine [3], are shown in Fig. 1. The mass spectrum of the latter is very simple owing to the fragmentation directing effect of the amino group, and the fragments arise from a single fission of the C–C bond leading to alternative fragments from which the charge is preferentially localized in the 'aminopart'. The fragmentation of compound **I** results in a number of fragment ions, which are produced from the molecular ions in competitive and consecutive dissociation processes. The decomposition pattern based on the elemental composition of the fragment ion determined by exact mass measurements is presented in Scheme 1.

Compounds examined:

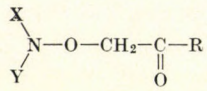

	X	Y	R
I	H	H	OH
II	H	H	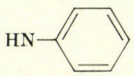
III	H	CH_3CO	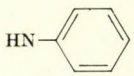
IV	H	H	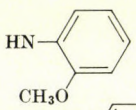
V	H	H	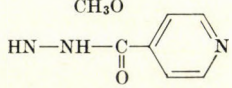
VI	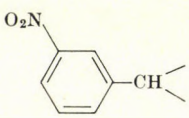		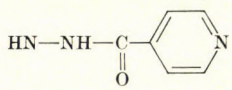
VII	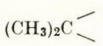		$HN-NH_2$
VIII	H	H	$HN-O-(CH_2)_{11}CH_3$

It is characteristic for the fragmentation that, beside water elimination, fissions 'a' and 'c' occur as competitive primary fragmentation pathways, while fission 'd' (loss of NH and NH_3) takes place only in secondary dissociation processes (leading to ions at m/e 31 and 29). The m/e 60 ion is produced from the molecular ion *via* a McLafferty rearrangement (γ-H migration) process.

The presence of the diverse fragmentation pathways is in accordance with the weaker basicity of the aminooxy group in α-aminooxy acids: the localization of the positive charge on this group is less frequent than that on the amino group of amino acids, and thus the fragmentation is not directed exclusively by the aminooxy group even in the case of the free acid [4].

This is true even more for the derivatives, which show considerably different mass spectrometric behaviour than does compound **I**. The molecular ion of the anilide of aminooxyacetic acid (**II**) shows a high stability (Fig. 2a).

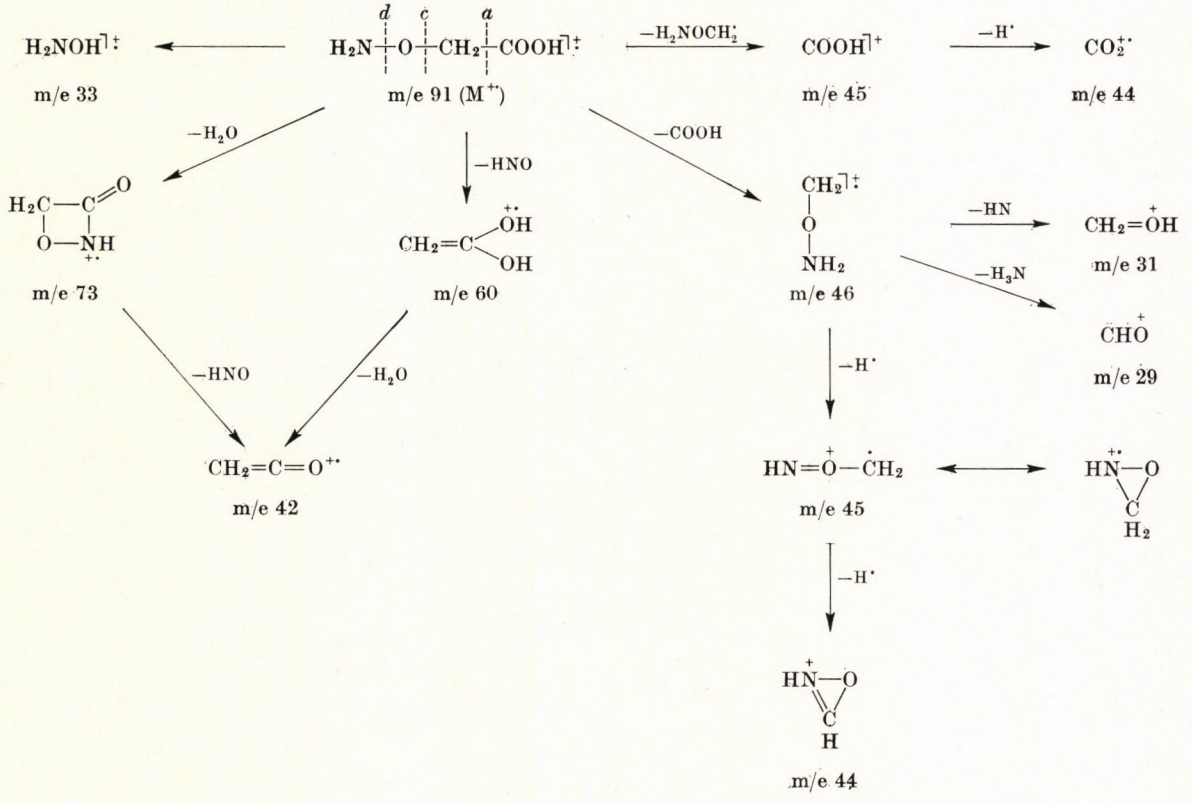
m/e 33
m/e 91 (M+·)
m/e 45
m/e 44
m/e 73
m/e 60
m/e 46
m/e 31
m/e 29
m/e 42
m/e 45
m/e 44

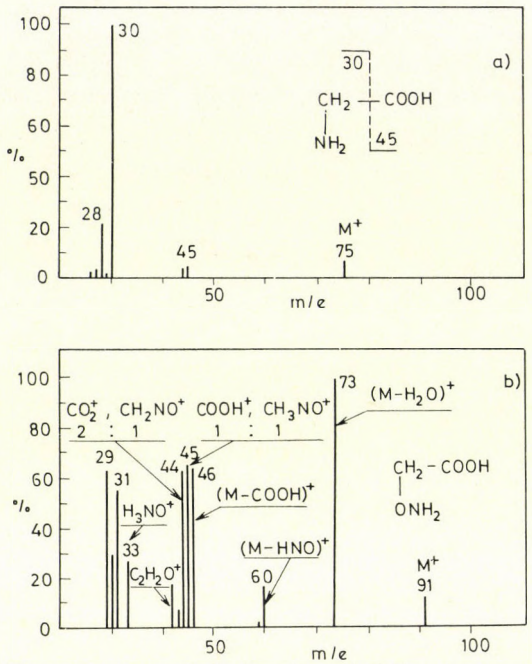

Fig. 1. 70 eV mass spectra of glycine *(a*, ref. [3]*)* and compound **I** *(b)*
(Isotope peaks are not shown in the figures)

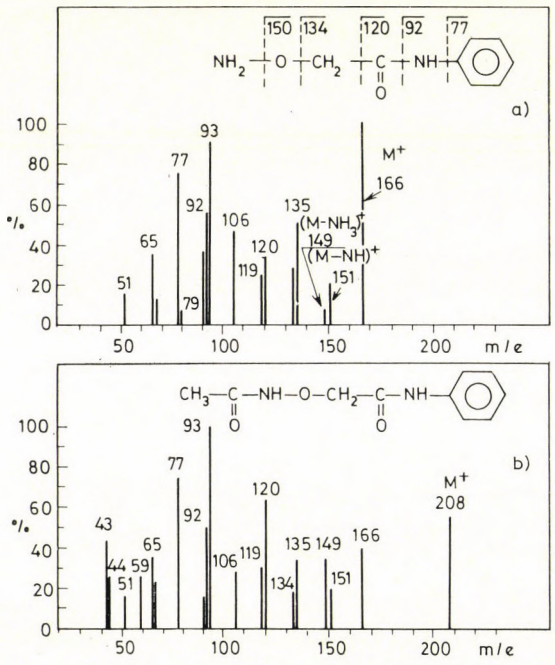

Fig. 2. 70 eV mass spectra of compounds **II** *(a)* and **III** *(b)*

Here, similarly to acetanilide, the main fragmentation pathway is the formation of the aniline molecular ion at m/e 93. Furthermore, fission 'd' (loss of NH or NH_3) takes place as a primary process. In the formation of the m/e 135 ion arising from cleavage 'c' with H migration, the proton transfer most probably occurs through a six-membered cyclic transition state (γ-H transition). Hence the structure of the resulting ions differs from that of the molecular ion of acetanilide. The homolytic version of fission 'c' leads to the ion at m/e 134. Owing to its radical character, this ion is less stable and decomposes in a number of fragmentation pathways (see Fig. 2a). Among these processes the elimination of a CO molecule also occurs, indicating its strong tendency to rearrangement. The latter process leading to the m/e 106 ion can be rationalized in terms of methylene group migration:

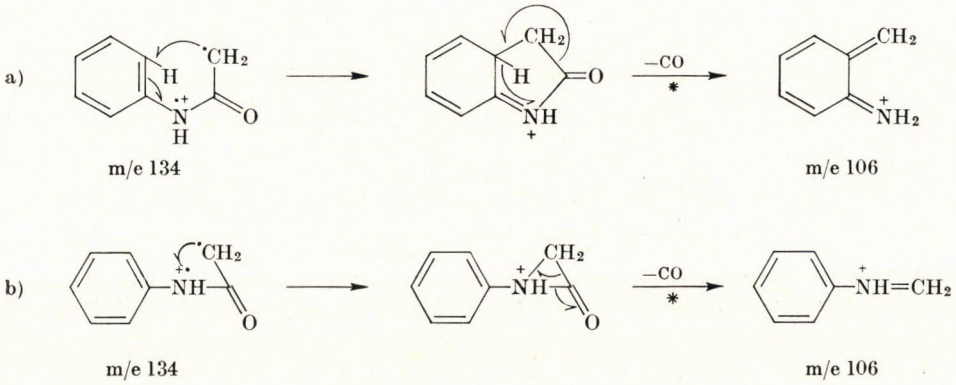

Further decomposition of the m/e 106 ion (loss of HCN) renders route *a* more probable.

In the mass spectrum of acetanilide the m/e 106 ion does not appear, indirectly supporting that the structure of the $(M-1)^+$ ion of acetanilide (1%) differs from that of the m/e 134 ion observed in the mass spectrum of compound **II**.

The ion at m/e 119 corresponds to the molecular ion of phenylisocyanate and by elimination of CO gives rise to the $C_6H_5N^+$ nitronium cation at m/e 91.

For compound **III** the main primary fragmentation process is the elimination of ketene from acetyl group. Further decompositions lead to the same ions as does the fragmentation of compound **II** (see Fig. 2b). The differences in the relative abundances of the common ions of compounds **II** and **III** may be due to the different pathways of their origins and to the different stabilities of the neutral parts produced.

In the mass spectrum of compound **IV** an exceedingly large number of peaks appear (see Fig. 3), owing to the presence of the *ortho*-methoxy group (*ortho* effect). Several peaks are found to be doublets, *e.g.* the peaks at m/e 134 and 121 correspond to ions $C_8H_8NO^+$ and $C_7H_4NO_2^+$ in an abundance ratio of 2 : 1 and to ions $C_7H_7NO^+$ and $C_8H_9O^+$ in the ratio of 3 : 1, respectively. Using the numerous metastable peaks detected in the mass spectrum, a detailed fragmentation scheme and a number of interesting decomposition pathways

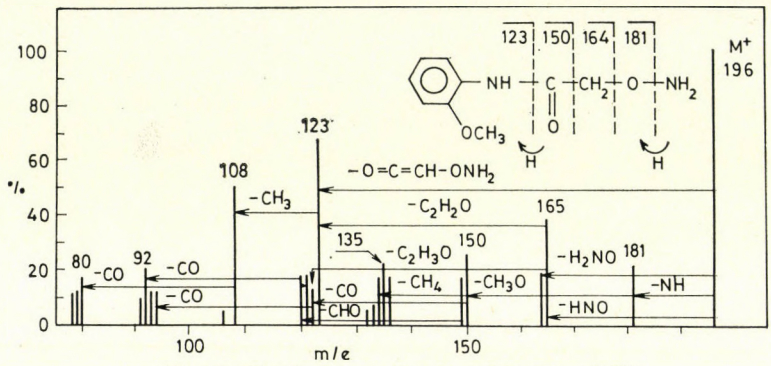

Fig. 3. 70 eV mass spectrum of compound **IV**

were deduced. Part of the main dissociation processes is completely analogous to those for compound **II**: from the m/e 164 ion, which is the methoxy substituted version of the m/e 134 ion observed for compound **II**, the elimination of CO also occurs, giving rise to an ion at m/e 136. The loss of CH_2O from the m/e 164 ion yields the ion at m/e 134 corresponding to that of compound **II**. The known fragmentation series characteristic for *o*- and *p*-anisidines [5] is also present in the spectrum:

$$123 \xrightarrow[*]{-CH_3} 108 \xrightarrow[*]{-CO} 80$$

Some particular rearrangements have also been observed. The m/e 150 is capable of losing a methane molecule:

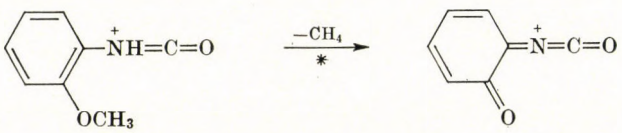

m/e 150 m/e 134

The loss of CHO from the ion at m/e 149 is followed by the elimination of CO. This process appears to involve methylene migration:

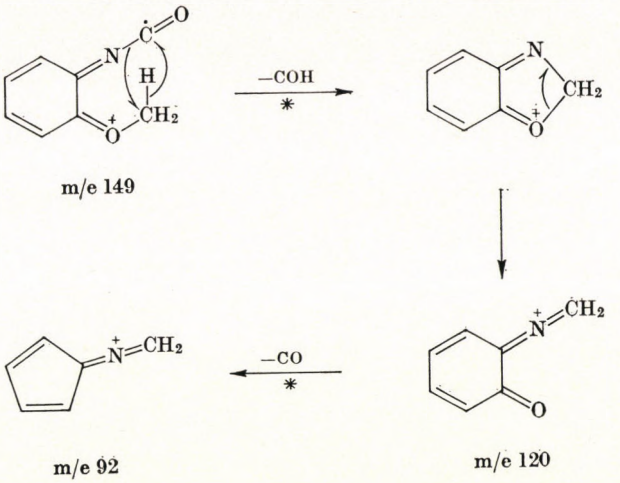

The following process is interpreted by methyl group transfer:

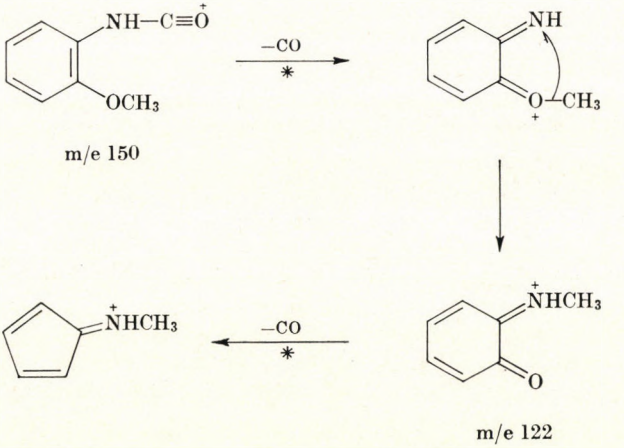

These rearrangements cannot be observed in the mass spectrum of *o*-methoxyacetanilide.

The mass spectra of compounds **V** to **VIII** show molecular ions but their abundances depend strongly on the nature of substituents (Figs 4 to 7). The fragmentation of these compounds is much simpler than that of the former. Although some of the spectra contain a great number of fragment peaks, *e.g.* the mass spectrum of compound **VIII**, most fragments are formed by simple homolytic cleavage of the skeleton or by fission with H-transfer. As none of

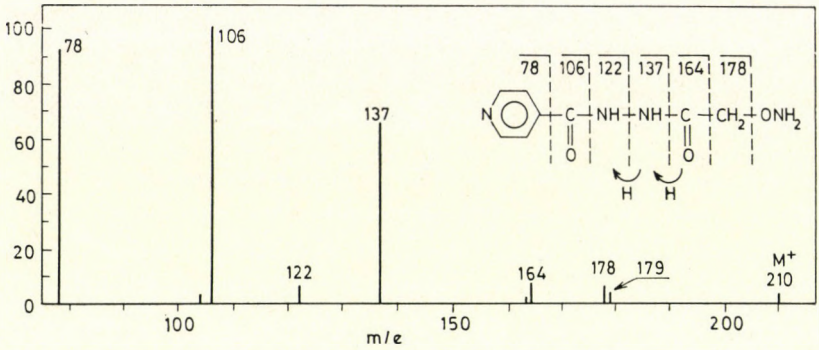

Fig. 4. 70 eV mass spectrum of compound **V**

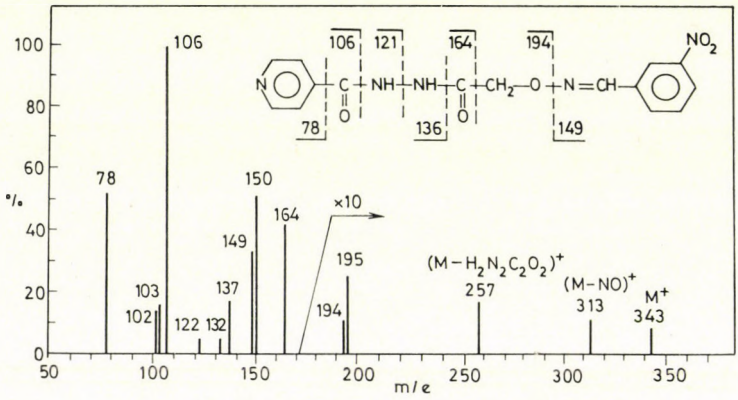

Fig. 5. 70 eV mass spectrum of compound **VI**

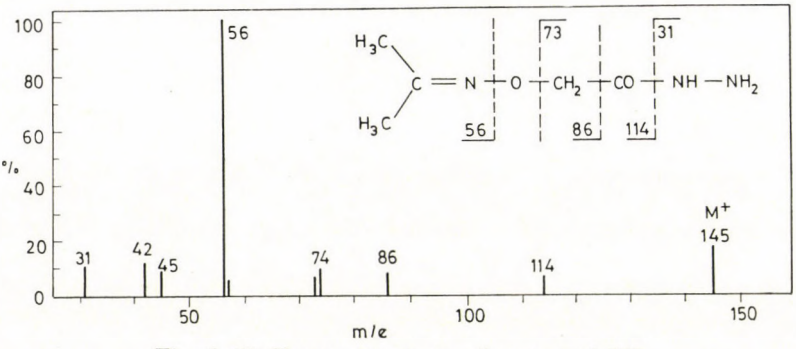

Fig. 6. 70 eV mass spectrum of compound **VII**

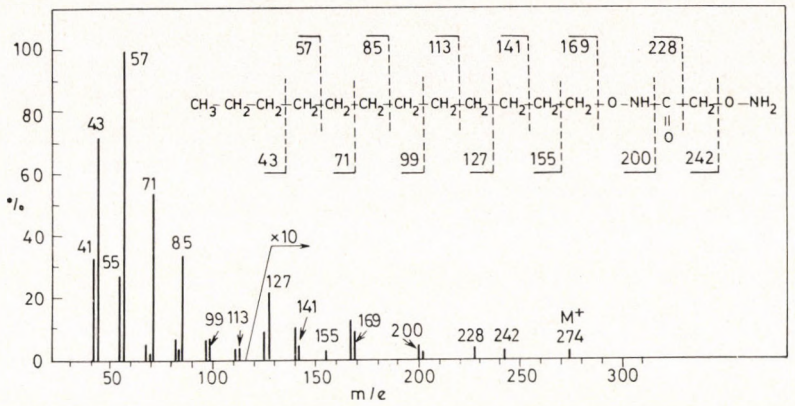

Fig. 7. 70 eV mass spectrum of compound **VIII**

the groups exerts a dominant fragmentation-directing effect, the splitting of almost every bond of the straight chain may occur.

Therefore, detailed information about the sequence of atoms in the molecule can be obtained from the high resolution mass spectra of these compounds. The mass spectra of compounds **II** and **IV** also contain a large amount of information, but the structural correlations are more complicated because of the great number of rearrangements.

Some rearrangement reactions were also found in the mass spectra of compounds **V** to **VIII**, of which the following are worth mentioning. In the case of compound **VI** the ion at m/e 257 is formed from the molecular ion *via* elimination of a neutral part of elemental composition $C_2H_2N_2O_2$. This process involves a skeletal rearrangement similar to the observed loss of SO_2 with arylsulfonamides [6].

Experimental

The mass spectra were obtained on an AEI MS-902 double focusing instrument, operating at 70 eV. The compounds were introduced *via* the direct insertion probe, the temperature of the ionization chamber was 160°—180 °C. The exact mass measurements were carried out with an accuracy of 2—3 ppm. Compounds **I** to **VIII** were prepared according to Ref. [7].

REFERENCES

[1] Kisfaludy L., Dancsi L., Patthy Á., Fekete Gy., Szabó I.: Experientia, **27,** 1055 (1971)
[2] Kisfaludy L., Lőw M., Dancsi L., Patthy Á., Nyéki O., Sárközi M.: Peptides 1972; Proc. 12th Eur. Peptide Symp; p. 409; H. Hanson and H. D. Jakubke Eds., North-Holland Publ. Co., Amsterdam 1973
[3] Junk G., Svec H.: J. Amer. Chem. Soc., **85,** 839 (1963)

[4] TAMÁS J., HEGEDÜS-VAJDA J., DANCSI L., KISFALUDY L.: Org. Mass Spectrom., **9**, 672 (1974)
[5] SPITELLER G., SPITELLER-FRIEDMANN M.: Mh. Chem., **93**, 1395 (1962)
[6] SPITELLER G., KASCHNITZ R.: Mh. Chem., **94**, 964 (1963)
[7] KISFALUDY L., DANCSI L., PATTHY Á., FEKETE GY., SZABÓ I.: Hung. Pat. No. 160. 181; 160.182; 162.469; RI-528; RI-529; RI-530

József TAMÁS
Judit HEGEDÜS-VAJDA } 1088 Budapest, Puskin utca 11—13.
Lajos DANCSI
Lajos KISFALUDY } 1103 Budapest, Gyömrői út 19/21, Hungary.

Acta Chimica Academiae Scientiarum Hungaricae, 84 (4), pp. 419—430 (1975)

pH-METRIC STUDIES ON THE MIXED-LIGAND CHELATES OF OXOVANADIUM(IV) WITH PICOLINIC ACID AND SOME DICARBOXYLIC ACIDS

S. P. SINGH and J. P. TANDON

(Chemical Laboratories, University of Rajasthan, Jaipur-302004, India)

Received February 2, 1974

pH-metric studies are described on the interaction of oxovanadium(IV) with picolinic acid in the absence and presence of some dicarboxylic acids (oxalic, phthalic and maleic acids) at 30 ± 0.5 °C ($\mu = 0.1$ KNO_3). The formation of 1 : 1 as well as 1 : 2 (VO^{2+} : picolinic acid) complexes (log $K_{MA} = 5.93 \pm 0.02$ and log $K_{MA2} = 5.24 \pm 0.11$) are indicated by these studies. The equilibrium constant for the reaction, $VOA^+ + H_2O \rightleftarrows VO(OH)A + H^+$ has been calculated as 3.97 ± 0.08 in the 1 : 1 VO^{2+}–picolinic acid system. The formation of 1 : 1 : 1 mixed ligand complexes is shown in the ternary systems studied and their formation constants have been evaluated.

Introduction

pH-metric studies on the systems, VO^{2+}–aminopolycarboxylic acids and VO^{2+}–dicarboxylic acids were described in earlier communications [1, 2] from these laboratories. In the present communication, potentiometric studies on the interaction of vanadyl ion with picolinic acid in the absence and presence of an equimolar concentration of dicarboxylic acids (oxalic, phthalic and maleic acids) have been described. Such studies do not appear in the literature, although spectrophotometric and polarographic studies on the 1 : 1 VO^{2+}–picolinic acid system have been reported [3].

Experimental

A stock solution of vanadyl sulphate (BDH) was prepared with bidistilled water and standardized as described in an earlier communication [1]. Solutions of picolinic (Fluka purum), oxalic (AnalaR BDH), phthalic (BDH) and maleic (Burgoyne) acids were prepared by direct weighing and standardized potentiometrically against a standard KOH solution. The pH-titrations were carried out at 30 ± 0.5 °C with a Cambridge pH-meter standardized against a 0.05 *M* solution of potassium hydrogen phthalate (AnalaR BDH). The ionic strength of all the solutions was kept constant ($\mu = 0.1$ KNO_3) by adding 5 ml of 1 *M* potassium nitrate to each solution and using low concentrations of the ligand and the metal ion. The final volume was always kept constant (50 ml) by diluting with required volume of bidistilled water.

Results and discussion

Curve 1, Fig. 1 represents the potentiometric titration of picolinic acid with 0.1 *M* KOH and exhibits a sharp inflection at m = 1 (where m represents the No. of moles of base added per mole of the metal ion). The dissociation constant *k* of the acid was calculated by the method of CHABEREK and MARTELL [4]. The *pk* was found to be 5.28 ± 0.02.

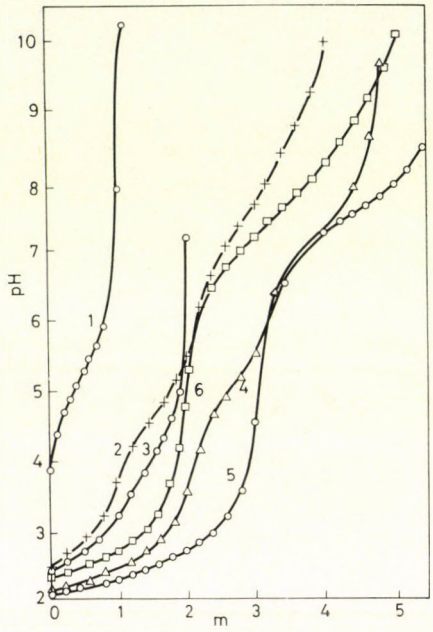

Fig. 1. Potentiometric titration curves of the normal and mixed-ligand chelate systems of oxovanadium(IV) with picolinic and oxalic acids as ligands. Curve 1, picolinic acid; 2,1 : 1 VO(IV)–picolinic acid; 3, oxalic acid; 4, 1 : 1 VO(IV)–oxalic acid; 5, 1 : 1 : 1 VO(IV)–oxalic acid–picolinic acid; 6, 1 : 2 VO(IV)–picolinic acid; m = moles of base added per mole of metal ion

Curve 2, Fig. 1 represents the potentiometric titration of the solution containing equimolar quantities of vanadyl sulphate and picolinic acid and exhibits a weak inflection at $m = 1$ followed by a buffer region terminating in a second inflection at $m = 2$. The first inflection may be attributed to the formation of a 1 : 1 complex and the reaction may be represented as:

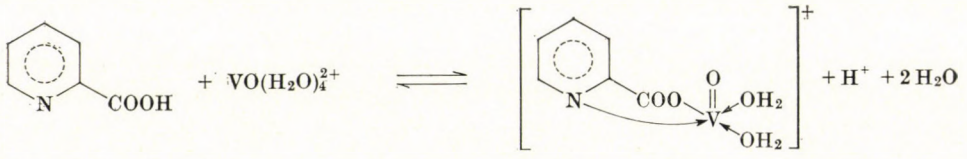

The second inflection at $m = 2$ probably indicates the formation of a hydroxo derivative and the reaction may be indicated as:

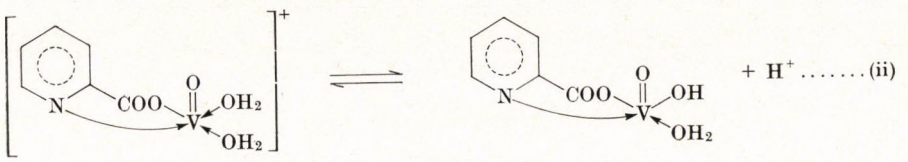

The poor inflection at $m = 1$ shows that the formation of 1 : 1 chelate and its hydrolysis overlap with each other. The formation of the above species is supported by the analysis of the potentiometric data given below:

In the initial stages the reaction may be represented as:

$$VO^{2+} + HA \rightleftharpoons VOA^{+} + H^{+} \qquad \text{(iii)}$$

where HA stands for the picolinic acid. The equilibrium constant, K_1 of the reaction may be expressed as:

$$K_1 = \frac{[VOA^{+}]\,[H^{+}]}{[VO^{2+}]\,[HA]} \qquad (1)$$

The formation constant, K_{MA} of the chelate may be given by:

$$K_{MA} = \frac{[VOA^{+}]}{[VO^{2+}]\,[A^{-}]} \qquad (2)$$

The dissociation constant k of the acid may be expressed as:

$$k = \frac{[H^{+}]\,[A^{-}]}{[HA]} \qquad (3)$$

If T_M represents the total concentration of all the metal species, T_A that of various ligand species and if T_{OH} be the concentration of the base added to the reaction mixture during the titration, it may be shown that:

$$T_M = [VO^{2+}] + [VOA] \qquad (4)$$

$$T_{OH} + [H^{+}] = [VOA] + [A^{-}] \qquad (5)$$

$$T_A = [HA] + [A^{-}] + [VOA] \qquad (6)$$

In the pH range studied, concentration of OH^{-} and the hydrolyzed species of the vanadyl ion were negligible as compared to other species present in the

reaction mixture. From the above relations it may be shown that:

$$[HA] = T_M - T_{OH} - [H^+] \tag{7}$$

and

$$[VO^{2+}] = (T_M - T_{OH} - [H^+])\left(1 + \frac{k}{[H^+]}\right) \tag{8}$$

The concentrations of other species present in the solution may be determined algebraically from equations (4)—(6) and also the values of K_1 and K_{MA}. The calculated values are $pK_1 = \bar{1}.35 \pm 0.02$ and $\log K_{MA} = 5.93 \pm 0.02$.

Hydrolysis of the (1 : 1) chelate

A gradual increase in the values of $\log K_{MA}$ at $m > 0.2$, probably indicates that the normal 1 : 1 chelate undergoes hydrolysis with the formation of a hydroxo complex and the solution becomes more acidic than it would be in the absence of hydrolyzed species. The hydrolytic reaction may be represented as:

$$VOA^+ + H_2O \rightleftharpoons VO(OH)A + H^+ \tag{iv}$$

The hydrolysis constant, K_h may be expressed as:

$$K_h = \frac{[VO\,(OH)\,A]\,[H^+]}{[VOA^+]} \tag{9}$$

The overall reaction in the system may be written as:

$$VO^{2+} + HA + H_2O \rightleftharpoons VO(OH)A + 2\,H^+ \tag{vi}$$

The equilibrium constant for this reaction may be given by:

$$K_H = \frac{[VO\,(OH)\,A]\,[H^+]^2}{[VO^{2+}]\,[HA]} \tag{10}$$

The following equations are obtained from the usual material balance:

$$T_M = [VO^{2+}] + [VOA^+] + [VO(OH)A] \tag{11}$$

$$T_{OH} + [H^+] = [VOA^+] + 2[VO(OH)A] + [A^-] \tag{12}$$

$$T_A = [HA] + [A^-] + [VOA^+] + [VO(OH)A] \tag{13}$$

Combination of equations (1), (3) and (11)—(13) gives:

$$a[VO^{2+}]^{+} + b[VO^{2+}] - c = 0 \tag{14}$$

$$\text{where } a = \frac{K_1}{[H^+]}, \qquad b = 2 + \frac{k}{[H^+]} \text{ and}$$

$$c = (2T_M - T_{OH} - [H^+]) \left(1 + \frac{k}{[H^+]}\right)$$

After determining the concentration of free vanadyl ions, concentrations of other species present in the equilibrium mixture can be calculated from the above equations and also the values of K_h and K_H($-\log K_h = 3.97 \pm 0.08$ and $-\log K_H = 3.32 \pm 0.08$).

When two moles of picolinic acid are titrated in the presence of a single mole of vanadyl sulphate (Fig. 1, curve 6), a sharp inflection at $m = 2$ is observed and this may be attributed to the formation of 1 : 2 (metal : ligand) complex in accordance with the equation:

$$VOA^{+} + HA \rightleftharpoons VOA_2 + H^{+} \tag{vi}$$

Equilibrium constant K_2 of the reaction may be expressed as:

$$K_2 = \frac{[VOA_2]\,[H^+]}{[VOA^+]\,[HA]} \tag{15}$$

K, the equilibrium constant of the overall reaction:

$$VO^{2+} + 2\,HA \rightleftharpoons VOA_2 + 2\,H^{+} \tag{vii}$$

may be defined as:

$$K = \frac{[VOA_2]\,[H^+]^2}{[VO^{2+}]\,[HA]^2} \tag{16}$$

Assuming that only mononuclear metal chelate species are formed in the system, the following equations are obtained for maintaining the material balance:

$$T_M = [VO^{2+}] + [VOA^+] + [VO(OH)A] + [VOA_2] \tag{17}$$

$$T_{OH} + [H^+] = [VOA^+] + 2[VO(OH)A] + 2[VOA_2] + [A^-] \tag{18}$$

$$T_A = [HA] + [A^-] + [VOA^+] + [VO(OH)A] + 2[VOA_2] \tag{19}$$

In the pH range studied, concentrations of OH^- and hydrolyzed species of the vanadyl ion were negligible in comparison with those of other species

present in the solution. Using the equations (1), (3), (10) and (17)—(19), it may be shown that:

$$a[VO^{2+}]^2 - b[VO^{2+}] + c = 0 \tag{20}$$

where $a = \dfrac{2K_H}{[H^+]^2}$, $b = 2 + (2T_M - T_{OH} - [H^+])\left(\dfrac{K_1}{[H^+]} + \dfrac{K_H}{[H^+]^2}\right)$

and $c = (2T_M - T_{OH} - [H^+])\left(1 + \dfrac{k}{[H^+]}\right)$

Computation of the equilibrium concentration of the free vanadyl ions present in the solution could be made by solving equation (20). The concentration of other species can then be calculated and the values of $-\log K = 1.39 \pm 0.11$ and $-\log K_2 = 0.04 \pm 0.11$ could thus be determined from the various points of the titration curve.

Stability of (1 : 2) chelate

Formation constant, K_{MA_2} of the 1 : 2 complex and the overall stability constant β_2 of the metal chelate may be defined as:

$$K_{MA_2} = \frac{[VOA_2]}{[VOA^+]\,[A^-]} \tag{21}$$

and

$$\beta_2 = \frac{[VOA_2]}{[VO^{2+}]\,[A^-]^2} \tag{22}$$

Using expressions (3), (15) and (16), it may be shown that,

$$K_{MA_2} = \frac{K_2}{k} \tag{23}$$

and

$$\beta_2 = \frac{K}{k^2} \tag{24}$$

The values of $\log K_{MA_2}$ and $\log \beta_2$ were found to be 5.24 ± 0.11 and 11.17 ± 0.11 respectively.

Mixed ligand chelates

Curve 3, Figs 1, 2 and 3 represents the potentiometric titration of the dicarboxylic acids with KOH and curve 4, Figs 1, 2 and 3 of vanadyl sulphate in the presence of an equimolar concentration of oxalic, phthalic or maleic

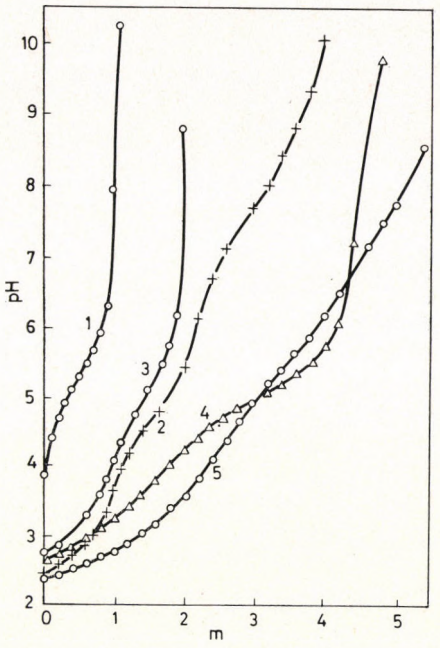

Fig. 2. Potentiometric titration curves of the normal and mixed-ligand chelate systems of oxovanadium(IV) having picolinic and phthalic acids as ligands. Curve 1, picolinic acid; 2, 1 : 1 VO(IV)–picolinic acid; 3, phthalic acid; 4, VO(IV)–phthalic acid; 5, 1 : 1 : 1 VO(IV)–picolinic acid–phthalic acid; m = moles of base added per mole of metal ion

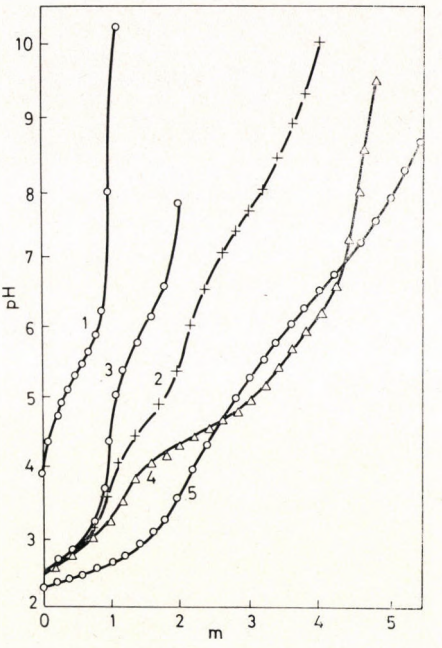

Fig. 3. Potentiometric titration curves of the normal and mixed-ligand chelate systems of oxovanadium(IV) with picolinic and maleic acids as ligands. Curve 1, picolinic acid; 2, 1 : 1 VO(IV)–picolinic acid; 3, maleic acid; 4, VO(IV)–maleic acid; 5, 1 : 1 : 1 VO(IV)–picolinic acid–maleic acid; m = moles of base added per mole of metal ion

acids, respectively. The calculation of dissociation constants of acids, equilibrium, chelate formation and hydrolysis constant for 1 : 1 VO^{2+} — dicarboxylic acid systems have been described in an earlier communication [2] (Table I).

Curve 5, Figs 1, 2 and 3 represents the potentiometric titration of vanadyl sulphate in the presence of an equimolar concentration of picolinic acid and one of the dicarboxylic acids (H_2L) used. It can be inferred from the comparison

Table I

Dissociation constants of the ligands and equilibrium and hydrolysis constants of 1 : 1 VO^{2+}–oxalic acid chelate

Ligand	pk_1	pk_2	$-\log K_1$	$-\log K_H$
Oxalic acid	1.66±0.05	3.90±0.02	0.91±0.07	4.49±0.02
Phthalic acid	2.89±0.02	5.04±0.01	—	—
Maleic acid	2.23±0.02	5.97±0.04	—	—

of curve 5 with the composite curve representing the titrations of the free ligand and the binary system that the formation of a mixed ligand chelate, MAL, is the only possibility in the mixed systems studied. Further, from the analysis of the potentiometric curves and the stability constants determination of the chelates VOA^+, VOL and $VOAL^-$, it may be shown that at the initial stages of the titration of 1 : 1 : 1 VO^{2+}–oxalic acid–picolinic acid system, the concentration of mixed ligand chelate $VOAL^-$ is lower than that of VOL and the formation of the mixed ligand chelate, therefore, occurs through the formation of 1 : 1 VO^{2+}–oxalic acid chelate. However, in other cases *viz.* VO^{2+}–picolinic acid–phthalic acid and VO^{2+}–picolinic acid–maleic acid systems, the mixed ligand chelate formation occurs through the formation of 1 : 1 VO^{2+}–picolinic acid chelate.

(i) *Calculation of equilibrium constant for* VO^{2+}*–oxalic acid–picolinic acid system*

In the vanadyl sulphate–oxalic acid system, formation of 1:1 VO^{2+}–oxalic acid chelate may be represented as:

$$VO^{2+} + H_2L \rightleftharpoons VOL + 2\,H^+ \qquad \text{(viii)}$$

where H_2L represents the dicarboxylic acid. The equilibrium constant of the reaction may be expressed as:

$$K_1' = \frac{[VOL]\,[H^+]^2}{[VO^{2+}]\,[H_2L]} \qquad (25)$$

The hydrolytic reaction may be represented as:

$$VOL + H_2O \rightleftharpoons VO(OH)L^- + H^+ \qquad \text{(ix)}$$

and the overall reaction in the system may be written as

$$VO^{2+} + H_2L + H_2O \rightleftharpoons VO(OH)L^- + 3\,H^+ \qquad \text{(x)}$$

The equilibrium constant for this reaction may then be given by

$$K_H' = \frac{[VO(OH)L^-]\,[H^+]^3}{[VO^{2+}]\,[H_2L]} \qquad (26)$$

The acid dissociation constants, k_1 and k_2 of the dicarboxylic acids may be given by

$$k_1 = \frac{[HL^-]\,[H^+]}{[H_2L]} \qquad \text{and} \qquad k_2 = \frac{[L^{2-}]\,[H^+]}{[HL^-]}$$

The formation of the mixed ligand chelate may be represented as

$$VOL + HA \rightleftharpoons VOAL^- + H^+ \qquad \text{(xi)}$$

and the overall reaction for the formation of the mixed ligand chelate may be written as:

$$VO^{2+} + H_2L + HA \rightleftharpoons VOAL^- + 3\,H^+ \qquad \text{(xii)}$$

If K' and K'' be the equilibrium constants of the reactions (xi) and (xii) respectively then

$$K' = \frac{[VOAL^-]\,[H^+]}{[VOL]\,[HA]} \qquad (27)$$

and

$$K'' = \frac{[VOAL^-]\,[H^+]^3}{[VO^{2+}]\,[H_2L]\,[HA]} \qquad (28)$$

Other pertinent equations are

$$T_M = [VO^{2+}] + [VOL] + [VO(OH)L^-] + [VOAL^-] \qquad (29)$$

$$T_{OH} + [H^+] = 2[VOL] + 3[VO(OH)L^-] + 3[VOAL^-] + [HL^-] + \\ + 2[L^{2-}] + [A^-] \qquad (30)$$

$$T_A = [HA] + [A^-] + [VOAL^-] \qquad (31)$$

$$T_L = [H_2L] + [HL^-] + [L^{2-}] + [VOL] + [VO(OH)L^-] + \\ + [VOAL^-] \qquad (32)$$

where T_L represents the total concentration of the oxalic acid. In a 1 : 1 : 1 reaction mixture of vanadyl sulphate, oxalic acid and picolinic acid, it may be shown from the above equations that

$$a[VO^{2+}]^2 + b[VO^{2+}] - c = 0 \qquad (33)$$

where $a = \frac{K_1'}{[H^+]^2} - \frac{kK_H'}{[H^+]^4}$, $b = 2\,XY + Y\left(1 - \frac{k_1k_2}{[H^+]^2}\right) - \frac{k}{[H^+]} \cdot X$

and $c = (3\,T_M - T_{OH} - [H^+])\,XY$

here $X = \left(1 + \frac{k_1}{[H^+]} + \frac{k_1k_2}{[H^+]^2}\right)$ and $Y = \left(1 + \frac{k}{[H^+]}\right)$

(ii) *Calculation of formation equilibrium for the systems,* VO^{2+}*–picolinic acid–phthalic or maleic acids*

As shown above, the formation of 1 : 1 VO^{2+}–picolinic acid chelate may be represented as

$$VO^{2+} + HA \rightleftharpoons VOA^{+} + H^{+}$$

The formation of the mixed ligand chelate, in these cases, may be represented as:

$$VOA^{+} + H_2L \rightleftharpoons VOAL^{-} + 2\,H^{+} \qquad \text{(xiii)}$$

or overall reaction for the formation of the mixed ligand chelate may be written as

$$VO^{2+} + HA + H_2L \rightleftharpoons VOAL^{-} + 3\,H^{+} \qquad \text{(xiv)}$$

If K' and K'' be the equilibrium constants of the reactions (xiii) and (xiv) respectively then

$$K' = \frac{[VOAL^{-}]\,[H^{+}]^2}{[VOA^{+}]\,[H_2L]} \qquad (34)$$

and

$$K'' = \frac{[VOAL^{-}]\,[H^{+}]^3}{[VO^{2+}]\,[HA]\,[H_2L]} \qquad (35)$$

Other pertinent equations are

$$T_M = [VO^{2+}] + [VOA^{+}] + [VO(OH)A] + [VOAL^{-}] \qquad (36)$$

$$T_{OH} + [H^{+}] = [VOA^{+}] + 2[VO(OH)A] + 3[VOAL^{-}] + [HL^{-}] + 2[L^{2-}] + [A^{-}] \qquad (37)$$

$$T_A = [HA] + [A^{-}] + [VOA^{+}] + [VO(OH)A] + [VOAL^{-}] \qquad (38)$$

$$T_L = [H_2L] + [HL^{-}] + [L^{2-}] + [VOAL^{-}] \qquad (39)$$

where T_L represents the total concentration of the dicarboxylic acids used as secondary ligands. In a 1 : 1 : 1 reaction mixture of vanadyl sulphate, picolinic acid and a secondary ligand, it may be shown that

$$a[VO^{2+}]^2 + b[VO^{2+}] - c = 0 \qquad (40)$$

where $a = \left(2 + \frac{k_1}{[H^{+}]}\right)\frac{K_1}{[H^{+}]} + \left(1 - \frac{k_1 k_2}{[H^{+}]^2}\right)\frac{K_H}{[H^{+}]^2}$

$$b = XY + X + \left(1 - \frac{k_1 k_2}{[H^{+}]^2}\right)Y$$

and $c = (3T_M - T_{OH} - [H^{+}])\,XY$

X and Y have the same notations as indicated earlier. Computation of the equilibrium concentration of free vanadyl ions present in the reaction mixture could be made by solving equations (33) and (40). Concentration of other species can then be determined and the values of K' and K''.

Stability of 1 : 1 : 1 mixed ligand chelates

The stability constant of the ternary complex in the VO^{2+}–oxalic acid–picolinic acid system may be defined as

$$K_{MAL} = \frac{[VOAL^-]}{[VOL]\,[A^-]}$$

and may be determined by the expression

$$K_{MAL} = \frac{K'}{k}$$

However, in case of systems, VO^{2+}–picolinic acid–phthalic or maleic acids, formation constant may be defined as

$$K_{MAL} = \frac{[VOAL^-]}{[VOA^+]\,[L^{2-}]}$$

and may be determined by the expression

$$K_{MAL} = \frac{K'}{k_1\,k_2}$$

The overall stability constant of the mixed ligand chelate

$$K'_{MAL} = \frac{[VOAL^-]}{[VO^{2+}]\,[A^-]\,[L^{2-}]}$$

may be calculated from the expression

$$K'_{MAL} = \frac{K''}{k\,k_1\,k_2}$$

The values of equilibrium and chelate formation constant of the ternary chelates are presented in Table II.

Table II

Equilibrium and chelate formation constants of mixed-ligand chelates

System	$-\log K'$	$-\log K''$	$\log K_{MAL}$	$\log K'_{MAL}$
VO^{2}–oxalic acid–picolinic acid	1.35 ± 0.07	0.44 ± 0.07	5.75 ± 0.07	10.40 ± 0.07
VO^{2+}–picolinic acid–phthalic acid	4.38 ± 0.14	3.73 ± 0.14	3.55 ± 0.14	9.48 ± 0.14
VO^{2+}–picolinic acid–maleic acid	3.60 ± 0.12	2.95 ± 0.14	4.60 ± 0.12	10.53 ± 0.12

In case of VO^{2+}–oxalic acid–picolinic acid system (curve 5, Fig. 1), a sharp inflection at $m = 3$ may be attributed to the complete neutralization of both the protons of oxalic acid and one of picolinic acid liberated as a result of chelation in accordance with the equation:

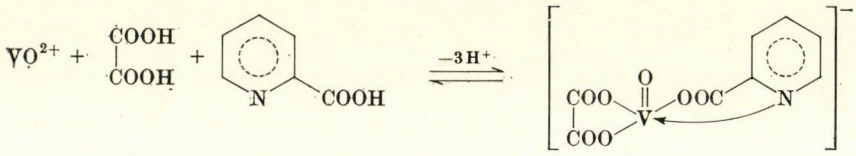

Complete formation of the mixed ligand chelate thus occurs at $m = 3$. However, in other cases no inflection at this stage indicates the decomposition of the mixed ligand chelate into other species, which is also supported by the gradual decrease in the values of the stability constants of the ternary chelates at $m > 1.6$ and 1.4 having phthalic and maleic acids respectively as secondary ligands.

The data show the following order of stability of the mixed ligand chelates in terms of the secondary ligands:

maleic acid > phthalic acid.

This is in accordance with their relative basicities as observed in the case of binary complexes also.

*

The authors are grateful to Prof. R. C. MEHROTRA, Head of the Chemistry Department, University of Rajasthan, Jaipur and the authorities of J. V. College, Baraut (Meerut) for providing the necessary facilities. The financial assistance from U. G. C. New Delhi is also gratefully acknowledged.

REFERENCES

[1] SINGH, S. P., TANDON, J. P.: Prakt. Chem., **315** (1), 23 (1973)
[2] SINGH, S. P., TANDON, J. P.: Acta Chim. (Budapest) **80,** 425 (1974)
[3] MERCIER ROLAND C., BONNET M., PARIS M.: Bull. Soc. Chim. France, **10,** 2926–32 (1965) (Fr.); **12,** 3577–86 (1965) (Fr.)
[4] CHABEREK S., MARTELL, A. E.: J. Amer. Chem. Soc. **74,** 5052 (1952)

S. P. SINGH
J. P. TANDON
Jaipur 302004 India.

Acta Chimica Academiae Scientiarum Hungaricae, 84 (4), pp. 431—443 (1975)

COMPLEX STUDY OF NICKEL SKELETON CATALYSTS, I

THERMAL DESORPTION METHOD AND APPARATUS FOR THE STUDY OF HYDROGENATION CATALYSTS

J. HEISZMAN, K. PAYER*, S. BÉKÁSSY and J. PETRÓ

*(Department of Organic Chemical Technology, Technical University, Budapest, *Central Chemical Research Institute of the Hungarian Academy of Sciences, Budapest)*

Received March 25, 1974

A thermal desorption apparatus involving a furnace and detector of special design was constructed to determine the amount and forms of hydrogen sorbed on hydrogenation catalysts. A commercial platinum resistance thermometer was built into the detector. A special procedure was employed to coat the external surface of the ceramic cover of the resistance in the measuring chamber with a platinum catalyst of high sensitivity and long life-time. The sensitivity of the detector is two orders higher than that of thermal conductivity cells. The reproducibility of the results obtained with the apparatus is good, the differences from the average value being within 10%.

On traditional and copper-promoted Raney nickels both weakly and strongly bound hydrogens were detected, while a third type of hydrogen was also observed on catalysts prepared from Ni–Mg and Ni–Zn alloys. On these latter catalysts the total amount of hydrogen is substantially less than on those prepared from Ni–Al alloys.

Further examinations in this field are in progress.

Introduction

The catalytic properties of hydrogenation catalysts are closely connected with the hydrogen sorbed on their surfaces during their preparation and reactions. Many methods have been developed to determine the amount of hydrogen and to study the nature of sorption. In the chemical [1, 2] and electrochemical [3] procedures the catalyst surface may also undergo chemical transformation, and thus the results can be somewhat uncertain. The hydrogen sorbed on electrically conducting metal filaments has been investigated in vacuum by flash-desorption [4].

The adsorption and desorption properties of granular catalysts have been examined by CREMER *et al.* [5] and SCHAY *et al.* [6], with the material packed in a chromatographic column.

A thermal desorption procedure (TPDM: temperature-programmed desorption method) and apparatus applicable to powder catalysts too have been developed by CVETANOVIČ *et al.* [7—9]. This procedure contains the characteristics of both the gas chromatography and the flash techniques. The catalyst containing the adsorbate is heated at constant rate in an inert-gas flow by

indirect heating, and the desorbed gas is determined by the measurement of thermal conductivity.

With the spreading of the measurement method, many similar apparatuses have been constructed [10—12]. For detection ILLINGER and RIVIN [13] and ERTL and KÜPPERS [14] employed a mass-spectrometer, and RUŽIČKA *et al.* [15] a combustion-chamber detector. UNEMURA [16] and RUŽIČKA *et al.* [15] incorporated a DTA block into the apparatus in order to accommodate the sample under investigation.

The TPDM meant a step forward in adsorption–desorption research, for it permits the quantitative and qualitative determination of the hydrogen sorbed on a catalyst. It also has other advantages:

1. the apparatus is simple;
2. it is applicable to the study of both metallic and non-metallic materials in powder form;
3. it permits the joint kinetic treatment of the chemisorption and the surface reaction;
4. in certain cases it permits the joint kinetic treatment of the desorption and the surface reaction;
5. the conditions approximate better to those of the catalytic reactions than they do in the flash filament method.

Thermal desorption investigations can have two aims:

a) a fundamentally physico-chemical one, the establishment of the kinetics and mechanism of the desorption;

b) the practical understanding of the gas—solid interactions on polycrystalline industrial catalysts.

The second of these aims is substantially the easier to attain; it is merely necessary to ensure several experimental conditions which in practice are readily achieved and reproducible. Examples of these:

constant-rate gas flows;

minimal volume in the sample holder, and between the sample holder and detector;

constant heating rate (and which can be regulated over a wide range);

stable operation of the detector.

Experimental

In accordance with the above requirements, we have designed and built an apparatus with which thermal desorption measurements can be carried out reproducibly and with satisfactory accuracy. An outline of the apparatus is given in Fig. 1.

The flow rates of the gases from the cylinders (A) are stabilized with a

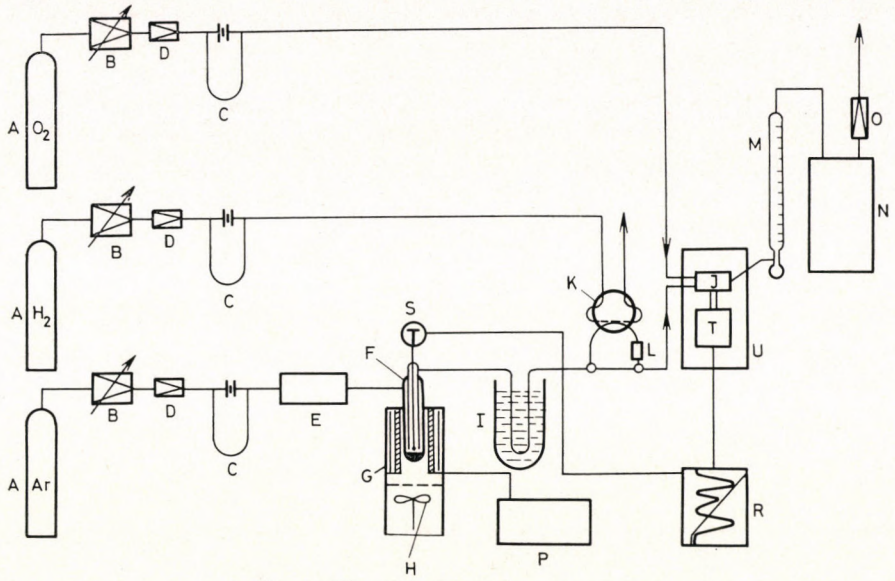

Fig. 1. Thermal desorption apparatus

pneumatic feed-control (B) and a capillary (D) before the differential manometer (C). The argon carrier gas is freed from oxygen with a diatomaceous earth-supported copper–copper(I) oxide catalyst at 200—250 °C. The moisture in the carrier gas is removed by freezing-out, and then by adsorption on columns packed with silica gel and molecular sieve (E).

The carrier gas next passes into the quartz sample holder vessel (F), the form and dimensions of which were determined on the basis of our experimental results. The argon comes into contact with the catalyst sample after passing through the jacket, where it is heated up to the temperature of the sample. The catalyst is arranged in a thin (1—2 mm) layer at the bottom of the tube, so that the diffusion and back-adsorption are decreased to the minimum. Above the catalyst there is just sufficient space for the carrier gas to pass through unimpeded.

The dimensions and thermal insulation of the furnace (G) were chosen so as to allow several measurements daily. The diameter of the ceramic body supporting the heated filaments is only a few mm larger than that of the sample holder vessel. Accordingly, the heat transfer is good, but the thermal capacity of the system is minimal. Thermal radiation outwards is inhibited by three concentric cylinders made of bright aluminium.

During measurement the furnace is covered with an asbestos plate, and thus the air between the cylinders is at rest and acts as an insulator. After the measurement this cover is removed and air is blown through the furnace from below (H). In this way the temperature falls from 1000 °C to room temperature in about 1 hour.

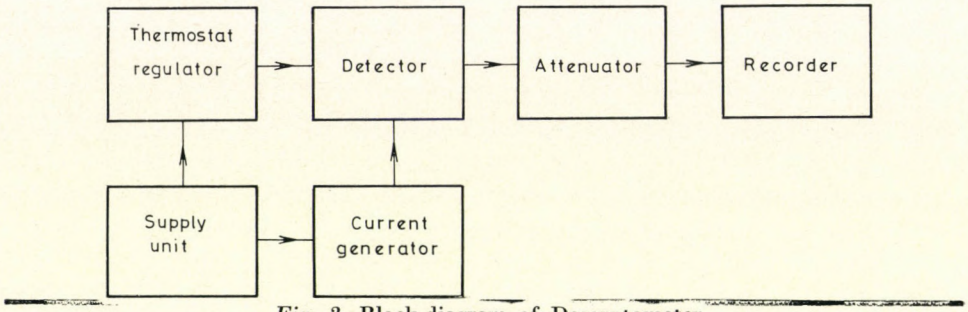

Fig. 2. Block-diagram of Desorptometer

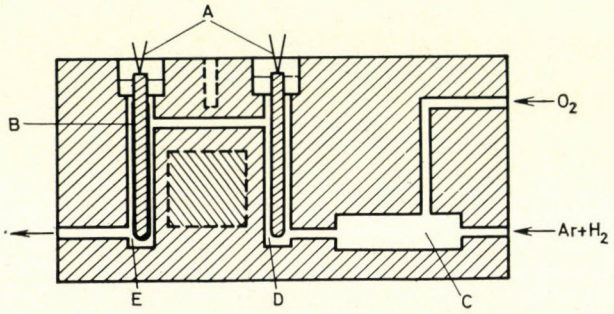

Fig. 3. Construction of the detector

After freezing-out with solid CO_2 (I) the hydrogen-containing carrier gas passes into the detector (J). The known volume of hydrogen necessary to calibrate the detector is passed into the carrier gas flow by means of the gas-meter tap (K). In order that the form of the calibration signal should approximate better to that of the broader desorption peaks, a mixing vessel too (L) was inserted after this tap.

After leaving the detector the gas mixture ($Ar + O_2$) passes into the open air *via* a soap-film flowmeter (M), a buffer vessel (N) and a capillary (O).

The rate of heating of the furnace is regulated with a Programik 2029 (MIKI) temperature-programming apparatus (P).

The detector signal and the catalyst temperature are recorded with a double-pen recorder (R), and so the temperatures of the peak maxima can readily be determined. The temperature of the catalyst is measured with a Pt–Pt/Rh thermocouple (S).

The detector and the related electronic system (T) incorporated are known as the Desorptometer (U).

A block-diagram of the electrical part of the Desorptometer is shown in Fig. 2. The current generator and the regulator of the thermostat are provided with the appropriate potential from a mains D. C. supply feed.

Fig. 3 presents a section of the brass detector block.

A platinum resistance thermometer (A) is used in the detector for the detection and quantitative determination of hydrogen. The external surface of the ceramic cover of the resistance in the measuring arm is coated with platinum black (B) by a special procedure. A Pt filament, possibly coated with platinum black, was earlier employed in combustion chamber detectors. These Pt filaments aged rapidly, they were unstable, and in addition their activities and sensitivities did not attain the desired values. On the sensing device of the combustion chamber constructed there is platinum catalyst of high surface

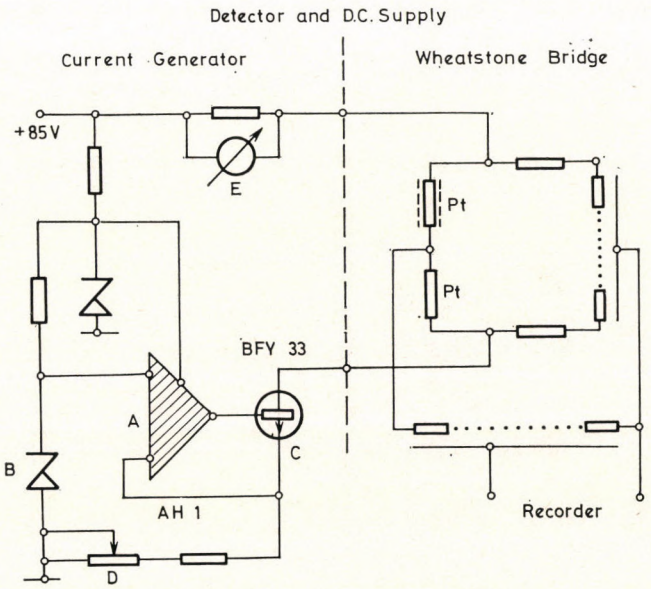

Fig. 4. Detector and D.C. supply

and activity (B), which well endures the relatively high operating temperature. When used under the prescribed conditions its life-time is about 2 years. After this it can be regenerated in about 3 hours.

The argon carrier gas containing the hydrogen to be measured is mixed with oxygen in the mixing chamber (C), and the resulting gas mixture then passes through the comparator (D) and measuring (E) chambers of the detector. In the measuring chamber the hydrogen is oxidized. The heat released causes the temperature, and hence the resistance, of the internal Pt filament thermometer to change.

The thermal resistance couple is connected into a Wheatstone bridge (Fig. 4). The current flowing across the bridge is supplied by a constant-current generator, the main element of which is an integrated-circuit amplifier (A).

The current flowing across the bridge is led through a reference resistance, and the resulting potential drop is compared with the potential of a Zener diode (B). The error signal is increased 100 times by the amplifier, which regulates the current of a power transistor (C) so that the bridge current is constant and independent of the resistance of the bridge elements. The bridge current can be controlled with a potentiometer (D) connected into the emitter of the transistor and can be checked on a read-off meter (E). The output of the null resistances is connected into the recorder arm, and thus the bridge current does not alter during the zero balancing. At the same time the bridge current heats the Pt resistances to ca. 400 °C, and in this way the temperature of the catalyst on the external surface can be maintained at the optimum base value.

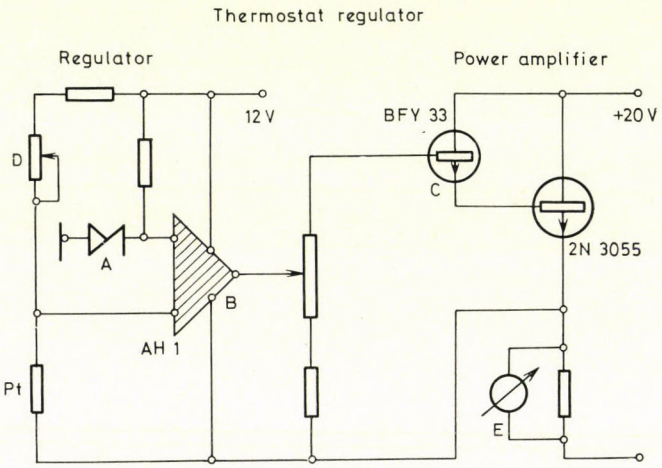

Fig. 5. Thermostat regulator

As mentioned already, the detector is placed in a thermostat. The electrical connection of the thermostat is depicted in Fig. 5. It consists of two main parts: a temperature regulator and an amplifier. The temperature-sensing device is a Pt resistance here too. The potential drop resulting on this is compared with the potential of a Zener diode (A). The error signal is led into an integrated-circuit amplifier (B), the output of which passes to a two-stage transistor power amplifier (C). An interesting feature of the connection is that there is no special heating body, the detector block being heated by the dissipation heat of the power transistor. The temperature of the thermostat can be regulated with a potentiometer (D). The current of the final transistor (and at the same time the operation of the regulator) can be checked on an instrument (E). The temperature of the thermostat is 80 ± 0.1 °C.

Results and discussion

Besides hydrogen, the detector is suitable for the determination of any other combustible gas or vapour. To establish the optimum operating conditions of the detector, we studied the effects of the potential and strength of the heating current and the flow rates of the carrier gas and the oxygen on the size of the detector signal. The results are given in Figs 6—8. With a view to the maximum stability and reproducibility, the apparatus was operated un-

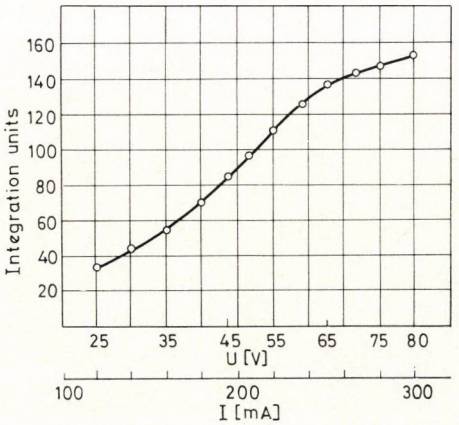

Fig. 6. Variation of the size of the signal corresponding to the addition of 1 cm^3 hydrogen with the heating current of the detector

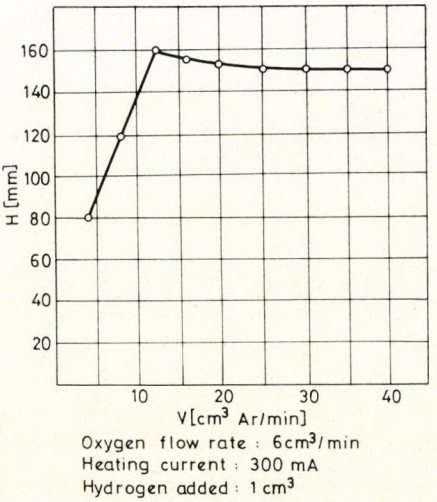

Fig. 7. Variation of the height of the detector signal with the flow rate of the argon carrier gas

der conditions where any change in the conditions was accompanied by the relatively lowest change in the detector signal. Such parameters were

Ar carrier gas flow rate:	30 cm^3/min
O_2 flow rate:	6 cm^3/min
heating current:	80 V =, 300 mA

The detector signal is directly proportional to the amount of hydrogen up to an added volume of hydrogen of 2.5 cm^3 (Fig. 9). The linearity was not investigated at higher hydrogen concentrations, since calibration too was made for every thermal desorption recording, while in addition the lower

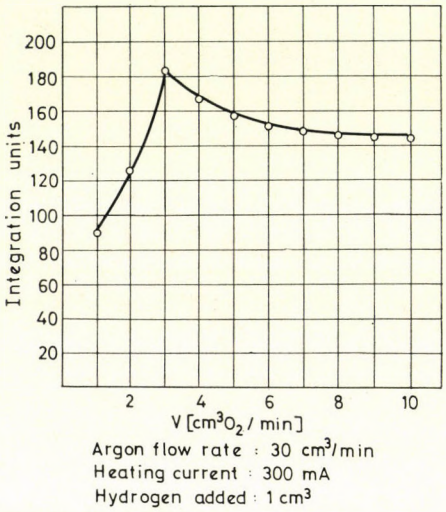

Fig. 8. Variation of the size of the detector signal with the flow rate of the oxygen

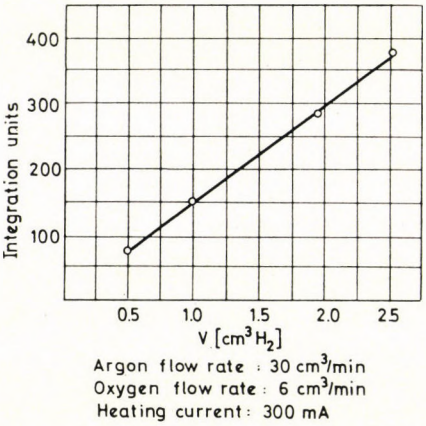

Fig. 9. Variation of the size of the detector signal with the amount of hydrogen added

hydrogen concentration range was selected for additions on the basis of the sensitivity of the apparatus and the hydrogen contents of the catalysts.

According to DIMBAT *et al.* [17], the sensitivity of thermal conductivity detectors in gas-chromatography is given by

$$S = \frac{F \cdot E \cdot V \cdot U}{m} \qquad \left[\frac{\text{mV} \cdot \text{cm}^3}{\text{mg}}\right]$$

where

S = sensitivity
F = area of the signal [cm^2]
E = sensitivity of recording apparatus [mV/cm]
V = flow rate of carrier gas [cm^3/min]
U = reciprocal of paper rate [min/cm]
m = mass of sample [mg].

On this basis the sensitivity of our detector is 2.5×10^5 mV.cm^3.mg^{-1}, whereas that of thermal conductivity measuring cells in general is 2×10^3 mV.cm^3.mg^{-1}, *i.e.* about 2 orders lower.

The performance of the apparatus can be illustrated by the following examples.

A study was made of the hydrogen sorbed on skeleton nickel catalysts prepared from alloys of various compositions. The starting alloys were obtained by melting the appropriate metals together in an induction furnace. Their compositions are listed in Table I.

The alloys were ground, and the 0.124 mm grain fraction from samples 1 and 2, and the 0.063 mm fraction from samples 3 and 4 were taken to prepare catalysts.

Samples 1 and 2 were treated at 50 °C for 2 hours with 20 wt.% NaOH, sample 3 at 115 °C for 15 min with 30 wt.% NaOH, and sample 4 at 60 °C for 20 min with 40 wt.% NaOH. The catalysts were next washed with distilled water until neutral, and then stored under distilled water.

Table I

Composition of the starting alloys

Sample No.	Ni [wt. %]	Al [wt. %]	Other [wt. %]
1	48	52	0
2	46.5	52	1.5 Cu
3	43	0	57 Mg
4	32	0	68 Zn

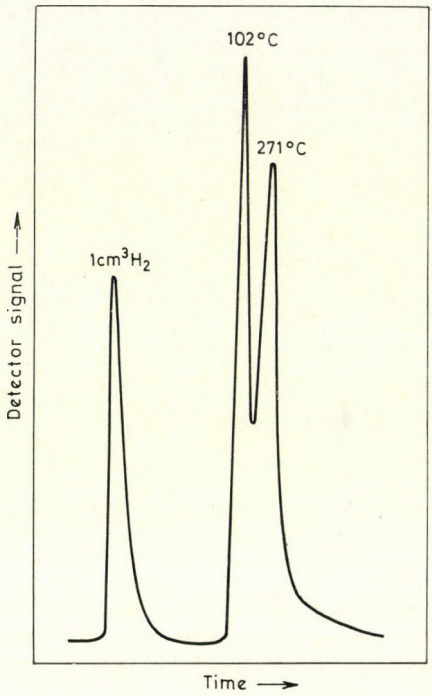

Fig. 10. Desorptogram of nickel skeleton catalyst

The thermal desorption recordings of the samples are presented in Figs 10—13. The conditions of the recordings were as follows:

argon carrier gas flow rate:	30.3 cm^3/min
oxygen flow rate:	6.0 cm^3/min
heating rate:	12 °C/min
detector heating:	300 mA
detector temperature:	80 °C.

The results of the measurements are given in Table II.

In agreement with earlier data [16, 18—21], the experimental data indicate that there is both weakly and strongly bound hydrogen on the traditionally-prepared Raney nickel (Fig. 10). As a result of the presence of a small amount of copper promoter, the amount of the H_{II} form on the catalyst increases considerably (Fig. 11), suggesting that the copper in this concentration is presumably incorporated into the nickel lattice and increases the number of active centres necessary for the existence of the H_{II} sorption phase.

It is striking that the hydrogen contents of the catalysts prepared from alloys containing magnesium and zinc are substantially lower than those of the catalysts prepared from the traditional aluminium alloys (Figs 12—13).

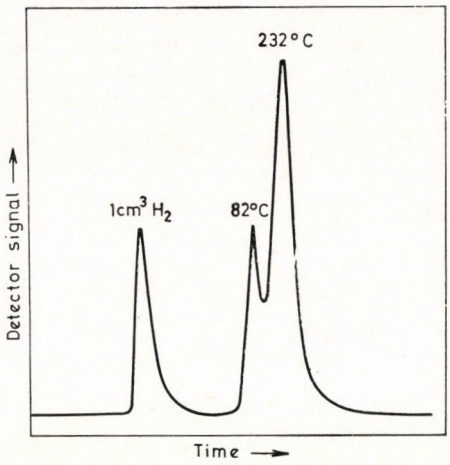

Fig. 11. Desorptogram of copper-promoted nickel skeleton catalyst

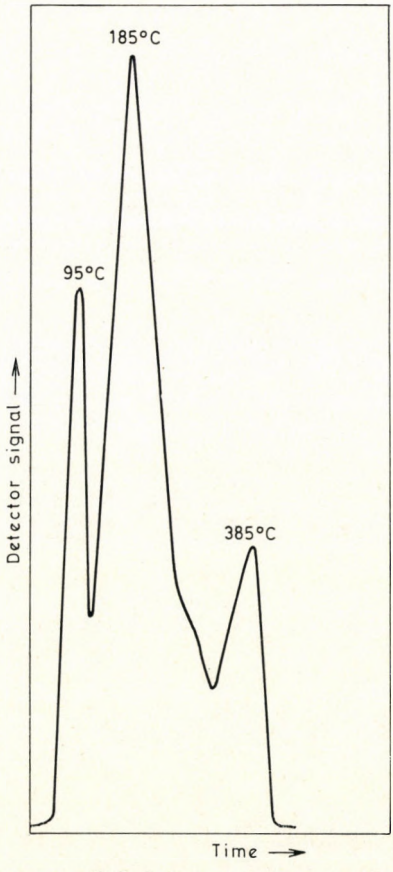

Fig. 12. Desorptogram of skeleton catalyst prepared from Ni–Mg alloy

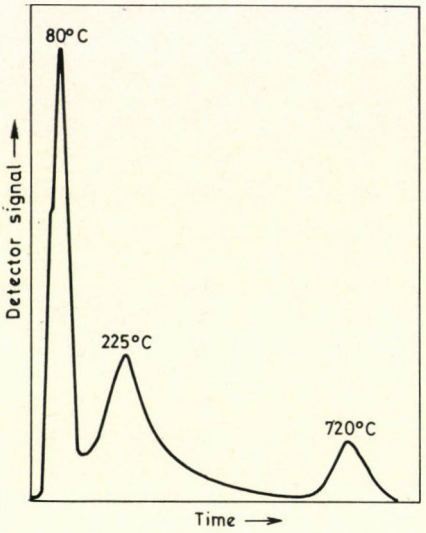

Fig. 13. Desorptogram of skeleton catalyst prepared from Ni–Zn alloy

Table II

Results of thermal desorption measurements on the catalysts

Sample No.	Hydrogen desorbed [cm³/g] / Temperature of peak maximum [°C]			Total hydrogen [cm³/g]
	I	II	III	
1	29/102	25/271	0	54
2	18/82	62/232	0	80
3	6.8/95	19.1/185	4.6/385	30.5
4	3.5/80	2.8/225	0.6/720	6.9

Table III

Reproducibility of thermal desorption results

Catalyst		1	2	3
Raney nickel (freshly prepared here)	Desorbed hydrogen [cm³/g]	43.6	39.9	46.1
	Average [cm³/g]		43.2	
	Diff. from aver. [%]	+0.9	—7.6	+6.7
Degussa B 113_a (age unknown)	Desorbed hydrogen [cm³/g]	62	62	68
	Average [cm³/g]		64	
	Diff. from aver. [%]	—3.1	—3.1	+6.2
Degussa B 113_b (age unknown)	Desorbed hydrogen [cm³/g]	71.5	72.0	75.0
	Average [cm³/g]		72.8	
	Diff. from aver. [%]	—1.8	—1.1	+3.0

It is characteristic for these catalysts that they also contain a third type of hydrogen, which is desorbed at a relatively high temperature.

An examination was made of the reproducibility of the results obtained with the apparatus. The data in Table III show that the difference from the average is less than 10%.

REFERENCES

[1] Freidlin, L. H., Rudneva, K. G.: Dokl. Akad. Nauk SSSR **91,** 569 (1953)
[2] Csűrös, Z., Petró, J., Heiszman, J.: Acta Chim. Acad. Sci. Hung. **22,** 73 (1960)
[3] Sokolskii, D. V.: Zh. Obshch. Khim. **22,** 1934 (1952)
[4] Ehrlich, G.: Advan. Catal. **14,** 256 (1963)
[5] Cremer, E., Roselius, L.: Angew. Chem. **70,** 50 (1958)
[6] Fejes, P., Nagy, F., Schay, G.: Acta Chim. Acad. Sci. Hung. **20,** 451 (1959)
[7] Amenomiya, Y., Cvetanovič, R. J.: J. Phys. Chem. **67,** 144, 2046, 2705 (1963)
[8] Amenomiya, Y., Chenier, J. H. B., Cvetanovič, R. J.: J. Phys. Chem. **68,** 52 (1964)
[9] Amenomiya, Y., Cvetanovič, R. J.: Advan. Catal. **17,** 103 (1967)
[10] Contour, J. P., Pannetier, G.: Bull. Soc. Chim. France **1969,** 2658
[11] Popova, N. M., Babenkova, L. V., Sokolskii, D. V.: Kinet. i Katal. **10,** 1177 (1969)
[12] Yakerson, V. J., Rozanov, V. V., Rubinstein, A. M.: Surf. Sci. **12,** 221 (1968)
[13] Illinger, J. L., Rivin, D.: Surf. Sci. **21,** 169 (1970)
[14] Ertl, G., Küppers, D.: Ber. Buns. Ges. Phys. Chem. **75,** 1017 (1971)
[15] Zapletal, V., Kolomazník, K., Soukup, J., Ružička, V.: Chem. Listy **62,** 210 (1968); Czechoslovak patent no. 131348
[16] Unemura, K.: Nippon Kagaku Kaishi **1973,** 1258
[17] Dimbat, M., Porter, P. E., Stross, F. H.: Anal. Chem. **28,** 290 (1956)
[18] Zapletal, V., Kolomazník, K., Soukup, J., Ružička, V.: Coll. Czech. Chem. Commun. **33,** 2437 (1968)
[19] Sokolskii, D. V., Popov, N. J., Svech, I. S., Kolomichev, L. A., Kan, S. I.: Zh. Fiz. Khim. **47,** 1725 (1973)
[20] Prettre, M.: C. R. Acad. Sci., Paris, Ser. C. **265,** 957 (1967)
[21] Lapujoulade, J.: Vide **24,** 52 (1969)

József Heiszman 1111 Budapest, Műegyetem rkp. 3.
Károly Payer 1125 Budapest, Pusztaszeri út 57—69.
Sándor Békássy, József Petró } 1111 Budapest, Műegyetem rkp. 3. Hungary.

Acta Chimica Academiae Scientiarum Hungaricae, 84 (4), pp. 445–457 (1975)

INTERACTIONS OF UNSATURATED HYDROCARBONS WITH PLATINUM CATALYSTS: INVOLVING REACTIONS, RETENTION, DEACTIVATION, AND REGENERATION

Z. PAÁL*, S. J. THOMSON**, G. WEBB** and N. J. MCCORKINDALE**

(Institute of Isotopes of the Hungarian Academy of Sciences, and ** Chemistry Department, The University, Glasgow, Scotland)*

Received April 1, 1974

Interactions of ethylene, cyclohexene and 1-hexene with platinum catalysts were investigated. The reactions can be interpreted in terms of hydrogen disproportionation, resulting in hydrogenation and hydrogenolysis on the one hand and hydrogen-deficient products, both in the gas phase and on the surface, on the other hand. Unsaturated hydrocarbons suffered dissociative adsorption on the metal displacing a part of retained hydrogen. New evidence has been obtained to suggest that adsorption *via* single bonds leads to hydrogenation–dehydrogenation whereas multiple bonding leads to hydrogenolysis and retention of hydrocarbons. The selectivity of the hydrogenolysis/hydrogenation reactions was different with platinum black and platinum-on-silica catalyst; probably these processes require different active sites. Retention of hydrocarbons was the main cause of catalyst deactivation; removal of retained species required oxygen treatment; hydrogen treatment was less efficient. The extent of all these phenomena was found to be dependent on the hydrocarbon structure. Retention and reactivation were also studied in radiotracer experiments.

Introduction

It is well known that metal catalysts may lose their catalytic activity during interactions with hydrocarbons. This phenomenon may be correlated with the accumulation of carbon-rich species on the surface. Unfortunately, very few systematic studies have been carried out in this field, and even fewer studies have been made under conditions of catalytic reaction, although processes of deactivation are inseparable from other surface processes occurring on the catalyst and the problem is of great practical importance.

It is reasonable to assume that retained surface species shown by radiotracer studies [1] on supported metal catalysts represent the first step in the formation of carbonaceous surface residues. It has been suggested that carbon–metal triple bonds may play an important role in the primary carbonizing process [2]. The formation of C_4- and C_6 species has been detected during studies of ethylene retention on metal films [3] and it is clear that, with the further polymerization of these species, the products soon reach a state where the size of the molecule alone could prevent it being desorbed into the gas phase.

Very little is known about the precise nature of surface carbonaceous

residues. Surface polymers of graphitic and non-graphitic structure have been observed by LEED [4, 5] and electron microscopic studies [6, 7]. There is data on the influence of the structure of the hydrocarbon reactants on the rate of deactivation; it is considerably more rapid with stretched chain (all-*trans)* polyenes, indicating that they combine more readily with each other than those of *cis-* or cyclic structures [8].

Methods of preventing the accumulation of surface deposits and of effecting their removal have been studied in order to preserve catalytic activity: these studies have not been systematic. It is known that the presence of hydrogen may result in the maintenance of a fairly constant level of catalytic activity [8, 9].

The *removal* of irreversibly adsorbed species may require more vigorous treatment. This depends on the nature of the surface species to be removed; *e.g.* irreversibly chemisorbed benzene can be desorbed by hydrogen treatment [10]; similar treatment may be of use in restoring catalytic activity lost during interactions with ethylene [11]. Surface polymers usually require extensive oxygen treatment, which results in a more complete and rapid restoration of activity [12]: this is the common practice in large scale industrial processes.

It is obvious that phenomena concerning deactivation, retention and reactivation are closely related to the more general problem of the interaction of hydrocarbons with the catalyst surface. Thus we present our results in this field which were obtained essentially by the same methods and under the same conditions as were applied to the study of hydrocarbon reaction mechanisms [8] and to hydrogen interactions over platinum catalysts [13]. Our interpretation and discussion are therefore on a common basis. Thus, the study of different aspects of the same phenomenon may help towards a better understanding of the central problem, *i.e.* hydrocarbon reactivity on platinum catalysts.

Our studies comprised the investigation of the effect of small amounts of oxygen present during catalytic reactions and the influence of hydrocarbon structure and type of reaction, hydrogen-consuming or hydrogen-producing, on deactivation and reactivation phenomena. Our studies also included the comparison of the behaviour of supported and unsupported platinum catalysts, in an attempt to determine whether spillover hydrogen had any marked effect, and some radiotracer experiments concerning accumulation and removal of retained species. The results of these studies together with earlier data serve as a basis for discussion.

Experimental

Apparatus: Experiments were carried out in a pulse-flow microcatalytic reactor coupled directly to a gas chromatograph as described in detail in [13]. In the radiotracer experiments the gas phase radioactivity was measured by using a proportional counter [13] while catalyst radioactivity was monitored by a liquid scintillation method reported earlier [14]. All experiments were performed at 360 °C.

Catalysts: A platinum black catalyst prepared from H_2PtCl_6 [13] as well as a 5% Pt/SiO_2 [11] catalyst were used. The catalysts were pretreated by heating in oxygen and then hydrogen as described previously [13].

Materials: Ethylene, cyclohexene and 1-hexene were used as model compounds [13]. The size of the hydrocarbon pulses was selected so that they contained approximately identical numbers of molecules.

Results

Ethylene was selected for the study of the effect of oxygen and of the support. Self-hydrogenation, hydrogenolysis and retention of ethylene were observed which resulted in the formation of ethane, methane and carbonaceous residues. Evaluation of the results has been made by calculating the amounts of individual products as well as the ratio of ethane to methane; thus we obtained data on both activity and selectivity of the catalysts.

a) *The effect of oxygen on the catalytic activity*

The last stage of the standard pretreatment of the catalysts was usually their treatment with hydrogen which should remove any oxygen present on the platinum surface and replace it by hydrogen. It was of interest to learn whether the presence of oxygen caused any change in the direction of reaction. This was done by comparing the composition of products from ethylene reactions in the presence of pure and oxygen-containing helium.

With each successive 0.5 ml (N.T.P.) injection of ethylene on to the catalyst the activity decreased in a similar manner to that observed previously [11, 15]. The results in Fig. 1 show that with freshly-prepared platinum black (0.06 g), deactivation, as determined by yields of methane and ethane, for

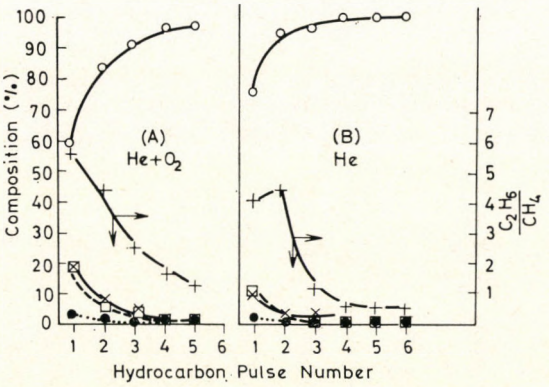

Fig. 1. Deactivation of Pt-black by 0.5 ml pulses of ethylene at 360 °C: 0.06 g catalyst: fresh sample for A and B. A, helium flow 60 ml min^{-1} containing 0.25% O_2; B, helium flow 60 ml min^{-1}, pure. ● CH_4, □ C_2H_6, ○ C_2H_4, × retention, + selectivity, $\frac{C_2H_6}{CH_4}$

ethylene self-hydrogenation and hydrogenolysis was slower when a helium carrier-gas stream containing 0.25 vol.% of oxygen was used, than with pure helium. A slight decrease in the catalyst selectivity, as defined by the C_2H_6/CH_4 ratio in the product, was observed during deactivation; the only difference worth mentioning was between the first two pulses: in the absence of oxygen, more methane was produced on the fresh catalyst.

b) *The comparison of platinum black and platinum-on-silica catalysts*

The essentially identical phenomena observed with and without 0.25% oxygen in the carrier gas allowed this study to be performed using oxygen-containing gas. Since deactivation was slow the detailed behaviour of the systems could be observed. Fig. 2 presents the sequence of the deactivation at 360 °C for a platinum-on-silica catalyst. It can be seen that apart from a relatively rapid loss of activity (by the tenth injection 93% of the ethylene was recovered unchanged — *cf.* 0% for the first injection), a marked change in selectivity was observed during deactivation. On clean catalysts initial pulses of ethylene produced mainly ethane by self-hydrogenation. The proportion of ethane increased in the next pulse and subsequently decreased from pulse to pulse (Fig. 2). We propose that the reason for this maximum in the ethane yield is the availability of hydrogen, for hydrogenation, resulting from the further breakdown of species derived from the initial dissociative adsorption.

The composition of the products resulting from the injection of ethylene on to platinum black (0.16 g) was remarkably similar to that observed with the 5% Pt/SiO_2 catalyst (Fig. 3), although the platinum black differed from the supported catalyst in that small quantities of hydrogen were always observed after ethylene injections (not shown in the figure).

A striking difference manifests itself in the selectivity (C_2H_6/CH_4) of the two types of catalyst. With platinum black, the extent of self-hydrogenation was considerably higher even with freshly regenerated catalysts. On supported platinum, the selectivity passed through a maximum with deactivation. The decrease of selectivity after the maximum was similar to that observed with unsupported platinum during deactivation.

The injection of 10 ml of air on to any of the deactivated catalysts resulted in a considerable restoration of the catalytic activity for self-hydrogenation, hydrogenolysis and retention (Figs 2 and 3). Further injections of ethylene resulted in a progressive deactivation of the catalyst to approximately the same level of activity and selectivity as for each fresh catalyst. When deactivated Pt black or Pt/SiO_2 catalysts were treated at 360 °C in a flow of hydrogen (25 ml min^{-1}) for 10 min, only partial restoration of the activity for self-hydrogenation and hydrogenolysis was achieved. It may be noted that both catalysts

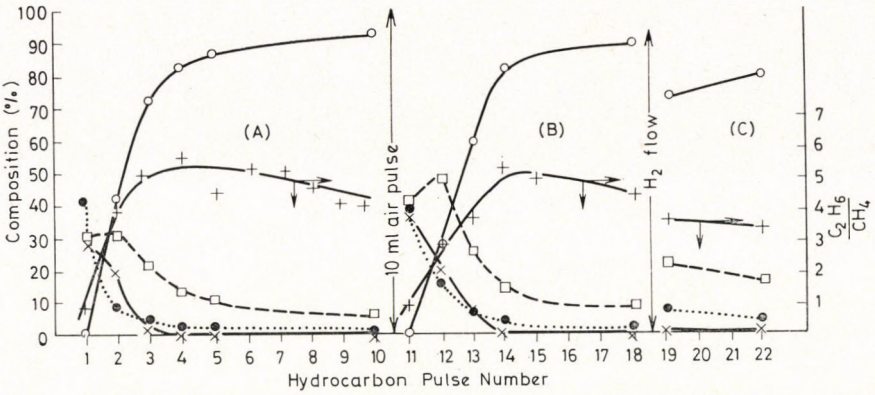

Fig. 2. Deactivation and regeneration of 5% Pt/SiO_2 catalyst during its interaction with ethylene. $t = 360$ °C; 0.05 g catalyst; 0.5 ml ethylene pulses: pretreatment, catalyst in air, then 10 min H_2 flow, 20 min He flow. A, fresh catalyst; B, after 10 ml pulse of air; C, after 10 min H_2 flow. ● CH_4, □ C_2H_6, ○ C_2H_4, × retention, + selectivity, $\frac{C_2H_6}{CH_4}$

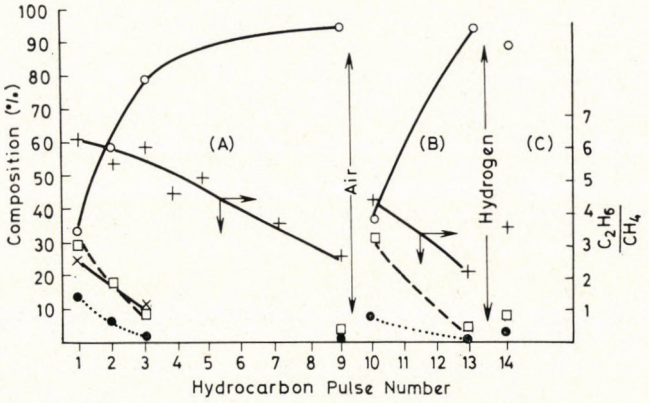

Fig. 3. Deactivation and regeneration of Pt-black in reaction with ethylene. $t = 360$ °C: carrier gas He, containing 0.25% O_2 at 60 ml min^{-1}. Pulses of 0.5 ml ethylene: pretreatment, 2×10 ml air then H_2 flow for 10 min. A, fresh catalyst; B, after 10 ml air; C, after H_2 flow for 11 min. H_2 present among products in all cases. Traces CO_2 after B. ● CH_4, □ C_2H_6, ○ C_2H_4, + selectivity, $\frac{C_2H_6}{CH_4}$

maintained their characteristic behaviour with regard to product composition and selectivity during repeated treatments. However with platinum black, traces of carbon dioxide were observed following the injection of a pulse of air on to the catalyst. Because of the presence of small amounts of oxygen in the carrier gas, prolonged exposure of the catalyst in a carrier gas stream at elevated temperature also brought about the restoration of catalytic activity. No regeneration of activity was observed at room temperature using the

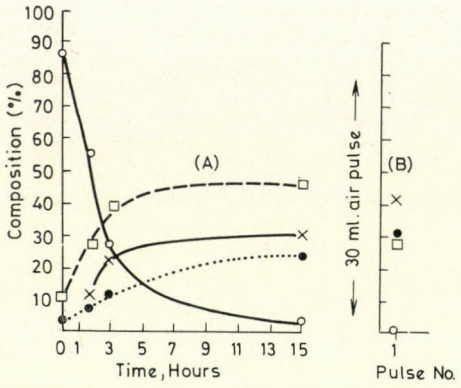

Fig. 4. Regeneration of the Pt/SiO_2 catalysts used for Fig. 1 by prolonged He containing 0.25% O_2 at 360 °C. A, helium + oxygen; B, effect of 30 ml air pulse. ● CH_4, □ C_2H_6, ○ C_2H_4, × retention

flow of oxygen-containing helium. In Fig. 4, the effect of different durations of carrier gas flow on the activity and selectivity of a platinum-on-silica catalyst is shown together with the effect of a 30 ml pulse of air. Continuous treatment by oxygen at a low partial pressure was less efficient in regenerating a catalyst than was a smaller volume of oxygen at a higher partial pressure. Similar results were obtained with platinum black.

c) *Radiotracer studies of retention and regeneration phenomena*

It can be seen that retention of hydrocarbons accompanied catalyst deactivation. This phenomenon was investigated by using [^{14}C]-ethylene as a tracer. A fresh sample of platinum black was deactivated in the usual manner by injection of [^{14}C]-ethylene. The extent of deactivation can be seen in Table I.

Table I

Reaction and retention of [^{14}C]-ethylene on a Pt-black catalyst

Catalyst: 0.06 g Pt-black, No pretreatment: heating to 50 °C in air, then in He-flow to 360 °C: t = 360 °C (except when specified): Hydrocarbon: 0.5 ml $^{14}C_2H_4$ with radioactivity: 4650 counts in proportional gas counter

Pulse No.	Product composition, %			Retention	Radioactivity (counts)	
	CH_4	C_2H_6	C_2H_4		recovered	retained (%)
I	10.8	25.5	32.5	31.2	2740	41
II	0.8	5.7	87.9	5.6	4450	4.5
III*	0.2	0.3	99.5	—	4630	—
IV	0.3	0.8	96.3	2.6	4460	4
V	0.2	0.4	96.7	2.7	3800**	—

* 300 °C
** CH_4 flow increased; radioactive counts only approximate

Table II

Deactivation of platinum black catalyst with alternate pulses of [^{14}C]-ethylene and inactive ethylene

Catalyst: 0.06 g Pt, pretreated with 10 ml air, 6 min. H_2 flow at 360 °C. Temperature: 360 °C. Hydrocarbon: 0.5 ml [^{14}C]-ethylene, radioactivity: appr. 19500 counts in a proportional gas counter

No. of pulse and starting hydrocarbon	Product composition, % / Radioactivity, counts		
	CH_4	C_2H_6	C_2H_4
I $^{14}C_2H_4$	*1.9*	*9.8*	*88.2*
	300	1400	15,600
II C_2H_4	*0.5*	*2.1*	*97.4*
	background		
III $^{14}C_2H_4$	*0.5*	*1.2*	*98.3*
	—	200	17,600
IV C_2H_4	*0.6*	*0.7*	*98.7*
	background		

These results also show the retention of radioactive hydrocarbon on unsupported platinum. The retention data calculated from the chromatographic traces are closely similar to those calculated from radioactivity measurements using a proportional counter coupled to the exit from the chromatograph [11, 15].

The problem of whether species retained by the catalyst might interact with gas phase hydrocarbons [16] was studied by introducing alternate radioactive and inactive pulses of ethylene on to a platinum black catalyst. Table III shows that while deactivation proceeded in the usual manner, the radioactivity of the products leaving the catalyst corresponded exactly to that of hydrocarbon which had been introduced, *i.e.* an inactive pulse of ethylene introduced after a radioactive pulse acquired *no* radioactivity from retained surface species.

It has been shown recently [14] that tritium retained by platinum black catalysts can be detected by immersing samples in a liquid-scintillator and counting the radioactivity. A similar procedure, using [^{14}C]-C_2H_4 as tracer, was used to determine whether carbon still remained on the catalyst after it had been reactivated in air.

Following deactivation with five 0.5 ml pulses of [^{14}C]-ethylene, the catalyst was cooled to room temperature and a few mg placed in a standard scintillation counting liquid [14]. Retained radioactive surface species caused counting with an observed rate of 1470 counts min^{-1} mg^{-1}. The remainder

Table III

Comparison of catalyst deactivation and regeneration with ethylene, cyclohexene and 1-hexene

t = 360 °C; 0.16 g Pt-black, carrier gas: 60 NTP ml/min He + 0.25% O_2

Experiment	Starting hydrocarbon		
	Ethylene One pulse: 0.5 ml = 22 μmole	Cyclohexene One pulse: 2.5 μl = 24 μmole	1-Hexene One pulse: 3 μl = 24 μmole
Pulse 1. (on fresh Pt-black)			
Starting material, %	28.6	0	77.7
Reacted %	41.1 (5.8+35.3)*	88.8 (0.1+88.7)*	22.3 (3.3+9.2+10.8)*
Retention %	30.3	11.2	—
Relative extent of reaction:	1.0	1.0	1.0
Pulse No. 10			
Starting material, %	96.0	26.5 (1.5+73.5)*	98.0
Reacted %	4.0 (1.2+2.8)*	73.5	2.0 (1.2+0.4+0.4)*
Retention %	0	0	—
Relative extent of reaction:	0.10	0.83	0.09
Pulse No. 18			
Starting material, %	—	93.0	—
Reacted %	—	7.0 (0.04+7.0)*	—
Retention %	—	0	—
Relative extent of reaction:	—	0.08	—
Deactivated Pt			
Starting material, %	95.1	91.6	98.0
Reacted %	4.9 (1.6+3.3)*	8.4 (0.1+8.3)*	2.0 (1.2+0.4+0.4)*
Retention %	0	—	—
Relative extent of reaction:	0.12	0.095	0.056
Regenerated with 10 min H_2 flow			
Starting material, %	90.0	35.9	95.6
Reacted %	10.0 (2.4+7.6)*	64.1 (0.6+63.5)*	4.4 (1.4+0.9+2.1)*
Retention %	0	—	0
Relative extent of reaction:	0.25	0.72	0.20
Deactivated Pt			
Starting material, %	94.7	97.4	97.3
Reacted %	5.3 (1.5+3.7)*	2.6 (0+2.6)*	2.7 (1.7+0.4+0.6)*
Retention %	—	—	—
Relative extent of reaction:	0.13	0.03	0.12
Regenerated with air slug:	10 ml	15 ml	10 ml
Starting material, %	37.0	0.7	74.6
Reacted %	39.4 (7.8+31.6)*	99.3 (0.7+98.2)*	25.4 (3.5+10.3+11.6)*
Retention %	23.6	—	—
Relative extent of reaction:	0.98	1.1	1.10

Table III. (continued)

Experiment	Starting hydrocarbon		
	Ethylene One pulse: 0.5 ml = 22 μmole	Cyclohexene One pulse 2.5 μl = 24 μmole	1-Hexene One pulse: 3 μl = 24 μmole
Deactivated Pt			
Starting material, %	96.0	85.2	96.8
Reacted %	4.0 (1.2+2.8)*	14.8 (0.1+14.7)*	3.2 (1.6+0.7+0.8)*
Retention %	—	—	—
Relative extent of reaction:	0.10	0.165	0.14
Regenerated with air slug and 10 min H_2 flow	20 ml	15 ml	10 ml
Starting material, %	30.9	0.03	69.5
Reacted %	43.8 (13.9+29.9)*	96.7 (0.1+96.6)*	30.5 (4.7+15.4+10.4)*
Retention %	25.3	3.3	—
Relative extent of reaction:	1.1	1.07	1.36

* The "reacted" values mean the sum of transformation products observed. In parentheses, individual types of products are shown. The meaning of numbers in the parentheses is as follows:
for ethylene: (methane% + ethane%);
for cyclohexene: (cyclohexane% + benzene%);
for 1-hexene: (hydrogenolysis products% + hexane% + dehydrogenated products%)

of the platinum catalyst was heated to 360 °C in air and maintained at this temperature for 5 min. Although this treatment was more severe than when pulses of air were used to regenerate the catalyst, subsequent scintillation counting of the catalyst showed that it still gave an activity of 90 counts min^{-1} mg^{-1}, thus clearly indicating that some carbon-14 still remained on the catalyst.

Radioactivity measurements determined by gas-proportional counting of [^{14}C]-ethylene and liquid scintillation counting of the catalyst could not be directly compared with each other, due to different counting efficiencies in the two systems. Electron microscopic studies of carbon depositions from C_6-olefins [6] indicated that 'amorphous' carbon tends to accumulate in 'patches' on the catalyst and consequently, self-absorption of the [^{14}C]-*beta*-particles would affect the final counts obtained for the regenerated catalyst.

d) *The effect of substrate structure on deactivation and regeneration*

Catalyst deactivation and reactivation were also investigated with two other olefins, namely cyclohexene and 1-hexene. Cyclohexene gave substantial yields of benzene but only a small amount of cyclohexane with little or no hydrogenolysis; the products from 1-hexene contained lower molecular weight hydrocarbons, hexane, hexadienes and benzene formed in hydrogenolysis,

hydrogenation, dehydrogenation and cyclization reactions, respectively. It was shown previously that 1-hexene deactivates platinum black much more rapidly than cyclohexene [6]. The results shown in Table III indicate that identical numbers of moles of the straight-chain olefins, ethylene and 1-hexene, brought about similar deactivation. Much more cyclohexene was necessary for the same loss of activity, and hydrogen was much more effective in reactivation of the catalyst than was the case with ethylene or 1-hexene. Air and air + hydrogen treatments had similar efficiency in restoring catalytic activity. In the latter case, the activity might even reach a higher level than the initial value. It has to be noted that whereas high retention was observed with ethylene much lower retention was found with C_6-hydrocarbons, although the very complex character of the gas chromatogram made strict quantitative evaluation difficult in the case of 1-hexene.

Discussion

All three olefins introduced on to platinum catalysts underwent significant reaction. All reactions observed represented some sort of *hydrogen disproportionation* resulting in hydrogen-rich and hydrogen-deficient products by comparison with the hydrocarbon reactants.

The fact that hydrogen disproportionation reactions occur implies *dissociative adsorption* of hydrocarbons. Hydrogen removed from the hydrocarbon during this process form a common pool with the residue of the originally retained hydrogen. The surface at this stage can be visualized as covered partly by hydrocarbon residues and by partly hydrogen atoms. The catalyst surfaces always contained hydrogen at 360 °C as shown by radioactive tracer studies [13], even after oxygen treatment. The surface reaction represented the combination of these fragments in ratios which depart from the initial ratio.

This proposal is supported by experiments with tritiated catalysts [13]. When hydrocarbons reacted over them, each fraction contained radioactivity. Tritium in *dehydrogenated* species proves that extensive dissociation occurred: surface species may lose more hydrogen than is necessary to form a particular dehydrogenated product; tritium in the *hydrogenated* products supports our suggestion of a common hydrogen pool on the surface and disproves direct hydrogen transfer from one molecule to another without participation of the surface hydrogen.

When ethylene was introduced on to a tritiated platinum black the small hydrogen peak was radioactive [17]. This indicated that retained surface hydrogen did participate in forming molecular hydrogen (which represents a peculiar sort of recombination of surface fragments), in other words, ethylene interaction with the surface involved also *displacement of hydrogen.*

The analysis of the product distributions yields further information. The amounts of dehydrogenated and hydrogenated products should according to our postulate correspond to each other. Unfortunately no exact material balance could be calculated because both hydrogen supply and products involve surface species for which the amounts can only be estimated approximately. With ethylene, no hydrogen deficient product appeared in the gas phase: the absence of acetylene was confirmed experimentally. The hydrogen-deficient products must, therefore, have been surface residues, and this explains the high retention values for ethylene when compared with C_6-hydrocarbons. With the latter, benzene (or hexadienes) represent(s) a thermodynamically favoured dehydrogenation product.

The specific radioactivity of the methane formed on a tritiated catalyst is about twice as high as that of ethane (and about five times as high as that of molecular hydrogen) [17]. This suggests that most of the H_2 molecules must have originated from dissociated ethylene and approximately twice as much of hydrogen came from the common pool to one molecule methane as to ethane. This leads to the conclusion that whereas ethane formation may be represented by associative adsorption followed by the uptake of two hydrogens, methane was formed from species multiply bonded to the surface formed as a result of extensive dissociation. This, in turn, is evidence that the two types (at least) of adsorption suggested previously [1, 2] may have occurred under the present conditions as shown schematically in Fig. 5. The participation of dissociatively adsorbed ethylene species in ethane formation (*i.e.* the interconversion shown in brackets in Fig. 5) is not excluded in this argument.

On the basis of literature data, multiple-bonded species may be regarded as responsible for both hydrogenolysis [18, 19] and retention or deactivation [1, 2].

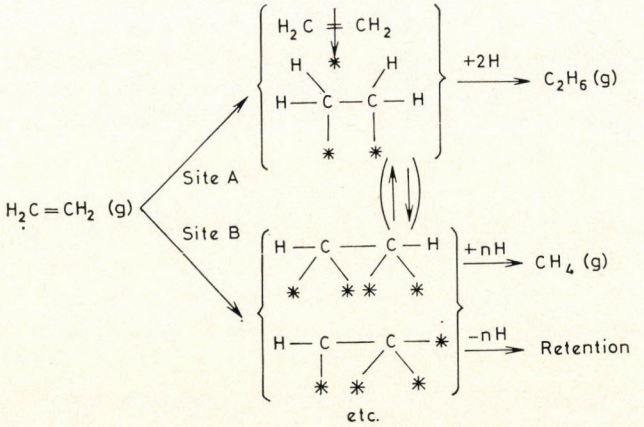

Fig. 5. Schematic representation of reaction possibilities of ethylene on platinum. ✳ denotes active sites without their exact specification

It is reasonable to assume that hydrogenation and hydrogenolysis occur at two types of sites (Fig. 5). It has been suggested that there is a preference for the formation of multiple-bonded species on 'edges' and 'corners' [20]. It is reasonable to suggest that these two types of site were present on our catalysts. Their amounts were different on supported and unsupported platinum. Pt/SiO_2 having smaller distribution of metal particle sizes must have more 'edges' and 'corners' and it exhibits much higher methane formation at about the same overall conversion of olefin than unsupported platinum. The deactivation of these sites is more rapid than that of 'flat plane sites'; this causes a change in selectivity during subsequent reactions. It is not yet clear how these two types of site are correlated with the different catalytic activities of various crystal planes observed by SOMORJAI *et al.* [5].

The presence of hydrogen during the initial stages of dissociative hydrocarbon adsorption slows down the production of multiple-bonded surface species [8]. Spillover hydrogen from supported platinum is ineffective in this respect. Figs 2 and 3 show essentially identical courses of deactivation in both cases.

Cyclic hydrocarbon structures do not favour the formation of multiple-bonded surface species; therefore deactivation is much slower with cyclohexene and virtually no hydrogenolysis occurs. Residues formed from cyclohexene are, presumably, of singly bonded to the surface and hydrogen is much more effective in removing them, than in the case of linear hydrocarbons, see Table III.

It has been shown that retained species can be displaced by gas phase hydrocarbons only to a limited extent [16]. Under our conditions, gas phase ethylene was not able to cause detectable displacement of retained ethylene species (see Table II).

The effects of oxygen are, by comparison, opposite to those observed with hydrogen. The presence of small amounts of oxygen in the helium carrier gas caused only a minor decrease in the rate of deactivation, whereas oxygen injections had a marked effect on the removal of retained species. Oxygen may perhaps act according to a Rideal-Eley mechanism arriving from the gas phase and oxidizing carbonaceous residues. This effect was practically independent of the catalyst type and hydrocarbon substrate; thus results obtained in the presence of small amounts of oxygen were essentially the same as those using pure helium.

As indicated by radiotracer experiments, oxygen treatment may leave some surface carbon which is present in thick patches and/or carbon 'whiskers' [7]; the presence of such strongly bonded carbon does not, to any larger degree, influence the catalytic activity.

The decrease of selectivity on both catalysts during deactivation shows that — after a certain amount of hydrocarbon had been converted — dehydrogenation activity decreases somewhat faster. This may be due partly to the

growth of carbonaceous species from the corners on to the flat plane regions, partly to the depletion of hydrogen on the surface, preventing desorption. Little retention accompanies deactivation in this region. The similar behaviour of ethylene and 1-hexene suggests that, in both cases, adsorbed species may combine with each other, giving perhaps polyenic type polymer species as proposed earlier [8].

*

The experimental work serving as a basis of this paper has been carried out in the Chemistry Department, The University, Glasgow. One of us (Z. P.) thanks the IAEA for a Fellowship. The authors express their gratitude to Professor P. TÉTÉNYI for valuable discussions.

REFERENCES

[1] TAYLOR, G. F., THOMSON, S. J., WEBB, G.: J. Catal. **12,** 150 (1968)
[2] REID, J. U., THOMSON, S. J., WEBB, G.: J. Catal. **30,** 378 (1973)
[3] MCCARROLL, J. J., THOMSON, S. J.: J. Catal. **19,** 144 (1970)
[4] EDMONDS, T., MCCARROLL, J. J., PITKETHLY, R. C.: Paper presented to Symposium on Low Temperature Carbon Formation, Glasgow, March 1973
[5] SOMORJAI, G. A.: Catalysis Reviews, **7,** 87 (1972)
[6] PAÁL, Z., FRYER, J., THOMSON, S. J.: Symposium on the Mechanism of Hydrocarbon Reactions, P-31 Siófok, June 1973.
[7] FRYER, J. R., PAÁL, Z.: Carbon, **11,** 665 (1973)
[8] PAÁL, Z., TÉTÉNYI, P.: J. Catal. **30,** 350 (1972)
[9] ROHRER, J. C., SINFELT, J. H.: J. Phys. Chem. **66,** 1193 (1962)
[10] TÉTÉNYI, P., BABERNICS, L.: J. Catal. **8,** 215 (1967); BABERNICS, L., TÉTÉNYI, P., KERTÉSZ, L.: Z. Phys. Chem. N. F. **89,** 237 (1974)
[11] ALTHAM, J. A., WEBB, G.: J. Catal. **18,** 133 (1970)
[12] PAÁL, Z., TÉTÉNYI, P.: Acta Chim. Acad. Sci. Hung. **53,** 193 (1967)
[13] PAÁL, Z., THOMSON, S. J.: J. Catal. **30,** 96 (1973)
[14] PAÁL, Z., THOMSON, S. J.: Radiochem. Radioanal. Letters, **12,** 1 (1972)
[15] TAYLOR, G. F., THOMSON, S. J., WEBB, G.: J. Catal. **12,** 191 (1968)
[16] REID, J. U., THOMSON, S. J., WEBB, G.: J. Catal. **30,** 372 (1973)
[17] PAÁL, Z., THOMSON, S. J.: Kémiai Közlemények, (in press)
[18] KEMBALL, C.: Proc. IVth Internat, Congress on Catalysis, Moscow, 1968, Akadémiai Kiadó, Budapest 1971, vol. I., p. 424
DOWIE, R. S., KEMBALL, C., KEMPLING, T. C., WHAN, D. A.: Proc. Roy. Soc. London, A**327,** 491 (1972)
[19] GUCZI, L., SÁRKÁNY, A., TÉTÉNYI, P.: J. C. S. Faraday Trans. I, **70,** 1971 (1974)
[20] ANDERSON, H. R.: Adv. Catalysis, **23,** 1 (1973)

Zoltán PAÁL; H-1525 Budapest 114, P. O. B. 77, Hungary.
Samuel J. THOMSON
Geoffrey WEBB
Norman J. MCCORKINDALE } Glasgow G12 8QQ, Scotland.

Acta Chimica Academiae Scientiarum Hungaricae, 84 (4), pp. 459—465 (1975)

TIN(IV) COMPLEXES OF SCHIFF BASES DERIVED FROM *o*-HYDROXYACETOPHENONE AND AMINOALCOHOLS

O. P. SINGH*, R. N. PRASAD and J. P. TANDON

(Chemical Laboratories, University of Rajasthan, Jaipur-302004, India)

Received July 12, 1974

Derivatives of the type $SnCl_4.SBH_2$ and $SnCl_4(SBH_2)_2$ have been synthesized by the reaction of tin(IV) chloride with the title Schiff bases in 1 : 1 and 1 : 2 molar ratios, respectively, in dry benzene. The products have been obtained in almost quantitative yields and in a state of sufficient purity. Their IR spectra have been recorded and conductance data show them to be non-electrolytes.

Introduction

In recent years, the preparation and characterization of several tin(IV) complexes with monodentate, bidentate and multidentate Schiff bases have been reported [1—10]. However, reactions of tin(IV) chloride with the Schiff bases derived from the condensation of *o*-hydroxyacetophenone with aminoalcohols such as 2-aminoethanol, 1-amino-2-propanol, 3-aminopropanol, 2-aminobutanol and 2-methyl-2-aminopropanol having the donor system, HO—N—OH, do not seem to have been studied so far. In the present paper, reactions of tin tetrachloride with these Schiff bases are described. The Schiff bases may be structurally represented by the following general formula (**I**):

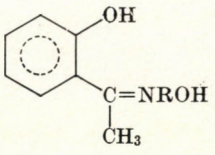

I

(where R = $-(CH_2)_2-$, $-CH_2\underset{|}{\overset{CH_3}{C}}H-$, $-(CH_2)_3-$, $-CH(C_2H_5)CH_2-$ or $-C(CH_3)_2CH_2-$).

* Chemistry Department, R. B. S. College, Agra, India.

Experimental

Materials and methods

The reactions were carried out under strictly anhydrous conditions. Benzene (BDH) was first refluxed over sodium wire for several hours and then distilled azeotropically with ethanol. Tin(IV) chloride (Reidel) was kept over copper turnings and redistilled before use. Dimethylformamide (BDH) was fractionally distilled under reduced pressure and the distillate mixed with about 12% (by volume) of dry benzene. After removal of the benzene–water azeotrope, the DMF was again distilled under reduced pressure (55 ± 1 °C/35 mm) to obtain benzene-free DMF. It was first shaken with pre-ignited, anhydrous alumina powder (BDH chromatographic grade) and then decanted. The middle fraction boiling at 55 ± 1 °C/35 mm was collected and stored in dark, stoppered pyrex flasks. The specific conductivity of the solvent was found to be $0.5—1.5 \cdot 10^{-7}$ ohm^{-1} cm^{-1} at 25 ± 1 °C.

Preparation of Schiff bases

Schiff bases from *o*-hydroxyacetophenone were prepared by dissolving equimolar amounts of the appropriate hydroxyalkylamine and *o*-hydroxyacetophenone in benzene and refluxing the solution for several hours, followed by the removal of water–benzene azeotrope. The products were distilled before use; their analyses and physical characteristics are recorded in Table I.

Preparation of tin(IV) complexes

Reactions of tin(IV) chloride with the Schiff bases in 1 : 1 and 1 : 2 molar ratios have been carried out. Tin(IV) chloride was dissolved in benzene and the calculated amount of the Schiff base was slowly added with constant shaking. An exothermic reaction took place and the solid compound separated immediately. In the cases where the Schiff base was found to be insoluble in cold benzene, it was first dissolved by refluxing and the solution was then cooled. After decanting the solvent, the resulting solids were repeatedly washed with benzene. The solvent was then removed under reduced pressure and the products were finally dried at 40—60°/0.5 mm for 2—3 hrs. The resulting derivatives were insoluble in most common organic solvents, but soluble in DMF. Analyses, physical properties and molar conductance values of these compounds are given in Table II.

Analyses and physical measurements

Tin was estimated in the compounds gravimetrically as tin oxide. Chlorine was determined as silver chloride and nitrogen by the Kjeldahl method.

Conductance measurements were made with a Tesla RLC bridge using a cell having the cell constant 0.74 cm^{-1}.

The infrared spectra of the Schiff bases and their complexes in nujol mulls were recorded on a UR-10 double beam IR Spectrophotometer in the region 4000—400 cm^{-1}.

Results and discussion

The molar conductance values, as determined in DMF at 10^{-3} *M* concentration and 25 ± 1 °C, fall in the range 8.31—9.87 ohm^{-1} cm^2 mole^{-1} (Table II), indicating that these derivatives behave as non-electrolytes in DMF. Their molecular weights could not be determined on account of their scarce solubility in common organic solvents.

The 1 : 1 and 1 : 2 molar ratio reactions have been found to yield $SnCl_4 . SBH_2$ and $SnCl_4(SBH_2)_2$ derivatives, respectively (where SBH_2 = Schiff

Table I

Schiff bases and their analyses

No.	Schiff base	Physical characteristics			Analysis, %		
		Appearance	M. p., °C	B. p. °C/mm	C Found (Calcd.)	H Found (Calcd.)	N Found (Calcd.)
1.	2-Hydroxy-N-(α-methyl-salicylidene) ethylamine ($C_{10}H_{13}NO_2$)	yellow solid	94—96	149—152/0.1—0.2	67.15 (67.01)	7.85 (7.31)	7.60 (7.81)
2.	2-Hydroxy-N-(α-methyl-salicylidene) propylamine ($C_{11}H_{15}NO_2$)	yellow solid	89—92	164/1.2	68.85 (68.37)	8.50 (7.82)	7.40 (7.25)
3.	3-Hydroxy-N-(α-methyl-salicylidene) propylamine ($C_{11}H_{15}NO_2$)	yellow solid	75—76	160/0.5—0.6	68.18 (68.37)	7.65 (7.82)	7.45 (7.25)
4.	1-Hydroxymethyl-N-(α-methylsalicylidene) propylamine ($C_{12}H_{17}NO_2$)	highly viscous yellow liquid	—	137—138/0.3—0.6	69.72 (69.55)	8.45 (8.27)	6.93 (6.76)
5.	1-Hydroxy-1-methyl-N-(α-methylsalicylidene) propylamine ($C_{12}H_{17}NO_2$)*	yellow liquid	—	91—92/0.1—0.2	69.64 (69.55)	8.43 (8.27)	6.64 (6.76)

* Used to distinguish the products having the same molecular formula

Table II

Synthesis and characteristics of tin(IV) Schiff base complexes

No.	Tin tetra-chloride, g	Schiff base, g	Molar ratio	Compound, yield (g), appearance	Analysis (%) Sn Found (Calc.)	Cl Found (Calc.)	N Found (Calc.)	Molar conductance ($ohm^{-1}cm^2$ $mole^{-1}$)
1.	1.84	$C_{10}H_{13}NO_2$ 1.26	1 : 1	$SnCl_4$ ($C_{10}H_{13}NO_2$) (3.11), reddish white solid	26.60 (27.00)	32.43 (32.29)	3.21 (3.18)	8.31
2.	1.14	$C_{10}H_{13}NO_2$ 1.57	1 : 2	$SnCl_4$ ($C_{10}H_{13}NO_2$)$_2$ (2.62), reddish white solid	19.01 (19.18)	22.87 (22.95)	4.60 (4.52)	8.60
3.	2.93	$C_{11}H_{15}NO_2$ 2.17	1 : 1	$SnCl_4$ ($C_{11}H_{15}NO_2$) (5.09), yellow solid	26.61 (26.16)	30.99 (31.30)	2.97 (3.08)	8.36
4.	1.34	$C_{11}H_{15}NO_2$ 2.00	1 : 2	$SnCl_4$ ($C_{11}H_{15}NO_2$)$_2$ (3.30), yellow solid	18.63 (18.35)	22.11 (21.96)	4.16 (4.32)	8.60
5.	2.26	$C_{11}H_{15}NO_2$* 1.67	1 : 1	$SnCl_4$ ($C_{11}H_{15}NO_2$)* (3.67), yellow solid	25.86 (26.16)	31.27 (31.30)	3.04 (3.08)	8.41
6.	1.40	$C_{11}H_{15}NO_2$* 2.09	1 : 2	$SnCl_4$ ($C_{11}H_{15}NO_2$)$_2$* (3.49), yellow solid	18.40 (18.35)	21.91 (21.96)	4.26 (4.32)	9.87
7.	1.80	$C_{12}H_{17}NO_2$ 1.43	1 : 1	$SnCl_4$ ($C_{12}H_{17}NO_2$) (3.23), pale yellow solid	25.22 (25.38)	30.29 (30.36)	2.93 (2.99)	8.31
8.	3.04	$C_{12}H_{17}NO_2$ 4.85	1 : 2	$SnCl_4$ ($C_{12}H_{17}NO_2$)$_2$ (7.90), pale yellow solid	17.77 (17.60)	21.06 (21.05)	4.26 (4.15)	8.60
9.	1.30	$C_{12}H_{17}NO_2$* 1.03	1 : 1	$SnCl_4$ ($C_{12}H_{17}NO_2$)* (2.17), yellow solid	25.17 (25.38)	30.83 (30.36)	2.97 (2.99)	8.50
10.	1.14	$C_{12}H_{17}NO_2$* 1.81	1 : 2	$SnCl_4$ ($C_{12}H_{17}NO_2$)$_2$* (2.95), yellow solid	17.43 (17.60)	21.02 (21.05)	4.03 (4.15)	8.70

* These compounds were used to distinguish the products having the same molecular formula

hase having the donor system HO—N—OH). With increasing concentration of the Schiff base, derivatives of the type $SnCl_4(SBH_2)_2$ could only be isolated.

Co-ordination of the azomethine nitrogen to the tin atom is indicated by the shift of the $\nu C=N$ vibration towards higher frequencies. In the IR spectra of Schiff bases, a strong band due to $\nu C=N$ appears at about 1610 cm^{-1}, whereas in the tin complexes this band is observed at about 1640 cm^{-1} (Table III). A similar shift to higher frequencies has been reported in tin(IV) complexes of salicylideneanilines [3]. If only the nitrogen of the ligand co-ordinates the metal atom in the 1 : 1 complex will be pentaco-ordinated. However, hexaco-ordinated complexes in the case of tin(IV) have been reported to be more stable. KOGAN *et al.* [3] have shown the formation of 1 : 2 complexes only between tin(IV) chloride and the Schiff bases from salicylaldehyde and aromatic amines. In these cases, co-ordination of nitrogen to the metal has been suggested giving an octahedral geometry to the complex and the phenolic OH does not co-ordinate. A similar reaction of tin(IV) chloride with salicylaldehyde has also been reported to yield a 1 : 2 complex only [11]. Co-ordination takes place through the carbonyl oxygen, and the oxygen of the OH group of salicylaldehyde does not co-ordinate. In these cases, lack of formation of the 1 : 1 complex indicates the unstable nature of the pentaco-ordinated state of the tin atom. This leads us to conclude that the 1 : 1 complexes posses octahedral geometry, which is possible if one of the oxygen atoms of the ligand moiety co-ordinates to the metal atom. Since it has already been reported that phenolic oxygen does not co-ordinate, it can be assumed that in these cases the alcoholic oxygen atom takes part in the co-ordination. The 1 : 2 complex of tin(IV) chloride with ethyl alcohol [12] also supports this fact.

Table III

Infrared absorption frequencies (cm^{-1}) of the Schiff bases and their in(IV) complexes

Schiff base	$\nu C=N$	' (IV) complex	$\nu C=N$	Sn ← O
$C_{10}H_{13}NO_2$	1610s	$SnCl_4 \cdot C_{10}H_{13}NO_2$	1644s	405s
		$SnCl_4 \cdot (C_{10}H_{13}NO_2)_2$	1640s	405s
$C_{11}H_{15}NO_2$	1614s	$SnCl_4 \cdot C_{11}H_{15}NO_2$	1640s	407s
		$SnCl_4 \cdot (C_{11}H_{15}NO_2)_2$	1640s	408s
$C_{11}H_{15}NO_2$*	1610s	$SnCl_4 \cdot C_{11}H_{15}NO_2$*	1640s	405s
		$SnCl_4 \cdot (C_{11}H_{15}NO_2)_2$*	1640s	406s
$C_{12}H_{17}NO_2$	1607s	$SnCl_4 \cdot C_{12}H_{17}NO_2$	1642s	405s
		$SnCl_4 \cdot (C_{12}H_{17}NO_2)_2$	1630s	405s
$C_{12}H_{17}NO_2$*	1605s	$SnCl_4 \cdot C_{12}H_{17}NO_2$*	1640s	406s

* Used to distinguish the products having the same molecular formula

In the IR spectra of these complexes, co-ordination of the alcoholic oxygen to the metal can be inferred by the appearance of a strong band in the region 405 cm^{-1} (Table III). Similar bands in the region 460—400 cm^{-1} have been assigned to Sn ← O in the case of tin(IV) complexes with oxygen donor ligands [11, 13—17].

Thus in view of the observed non-electrolyte nature of the products and the predominant hexacovalency of tin(IV), the 1 : 1 complexes may be represented by the general formula **II.**

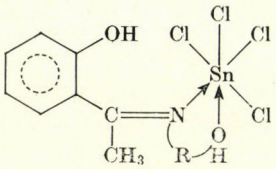

II

The 1 : 2 complexes may similarly be represented by the general structure **III** giving an octaco-ordinated environment to the central tin atom:

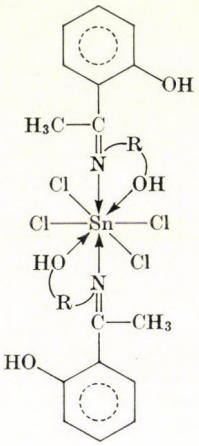

III

Octaco-ordinated complexes of tin(IV) have been reported with a variety of ligands such as 8-hydroxyquinoline [18], tropolone [19] and phthalocyanine [20].

The dodecahedral geometry for tin tetranitrate [21] has been confirmed on the basis of X-ray crystal studies and D_{2d} symmetry has been suggested.

*

The authors are greatly thankful to Prof. R. C. MEHROTA and Prof. K. C. JOSHI for providing all the laboratory facilities. Thanks are also due to Dr. D. R. SINGH, R. B. S. College, Agra, for constant encouragement. The financial assistance to one of us (O. P. S.) by the U. G. C., New Delhi is also gratefully acknowledged.

REFERENCES

[1] BEATTIE, I. R.: Quart. Rev. **17,** 382 (1963)
[2] BEATTIE, I. R., GILSON, T., WEBSTER, M., MCQIULLAN, G. P.: J. Chem. Soc. **1964,** 238
[3] KOGAN, V. A., OSIPOV, O. A., MINKIN, V. I., SOKOLOV, V. P.: Zh. Neorg. Khim. **10,** 83 (1965)
[4] GARNOVSKII, A. D., MINKIN, V. I., OSIPOV, O. A., PANYUSHKIN, V. T., ISAEVA, L. K., KNYAZHANSKII, M. I.: Zh. Neorg. Khim. **12,** 2443 (1967)
[5] MAGGIO, F., BOSCO, R., CEFALU, R., BARBIERI, R.: Inorg. Nucl. Chem. Lett. **4,** 389 (1968)
[6] FARANGLIA, G., MAGGIO, F., BOSCO, R., CEFALU, R., BARBIERI, R.: Inorg. Nucl. Chem. Lett. **5,** 177 (1969)
[7] KOGAN, V. A., SOKOLOV, V. P., OSIPOV, O. A.: Zh. Obshch. Khim. **40,** 332 (1970)
[8] KOGAN, V. A., SOKOLOV, V. P., OSIPOV, O. A.: Zh. Obshch Khim. **40,** 883 (1970)
[9] BIRADAR, N. S., KULKARNI, V. H.: Inorg. Nucl. Chem. **33,** 2451 (1971)
[10] BIRADAR, N. S., KULKARNI, V. H.: J. Inorg. Nucl. Chem. **33,** 3781 (1971)
[11] PAUL, R. C., CHADHA, S. L.: J. Inorg. Nucl. Chem. **32,** 3204 (1970)
[12] SNEED, M. C., BRASTED, R. C.: Comprehensive Inorganic Chemistry, Vol. VII, p. 224, 1961
[13] PAUL, R. C., CHADHA, S. L.: Inorg. Nucl. Chem. **31,** 2753 (1969)
[14] PAUL, R. C., CHADHA, S. L.: Aust. J. Chem. **22,** 1381 (1969)
[15] PAUL, R. C., SINGH, P., CHADHA, S. L., MAKHANI, H. S.: J. Inorg. Nucl. Chem. **32,** 2141 (1970)
[16] TANAKA, T., KAMITANI, T.: Inorg. Chem. Acta **2,** 175 (1968)
[17] HUNTER, S. H., LANGFORD, V. M., RODLEY, G. A., WILKINS, C. J.: J. Chem. Soc. A., **1968,** 305
[18] RAMAIAH, K., MARTIN, D. F.: Chem. Comm. **1965** 130
[19] MEUTTERTIES, E. L., WRIGHT, C. M.: J. Am. Chem. Soc. **86,** 5132 (1964)
[20] KROENKE, W. J., KENNEY, M. E.: Inorg. Chem. **3,** 251 (1964)
[21] GARNER, C. D., SUTTON, D., WALLWORK, S. C.: J. Chem. Soc. A., **1967,** 1949

O. P. SINGH; Chemistry Department, R. B. S. College, Agra, India.
R. N. PRASAD, J. P. TANDON } Chemical Laboratories, University of Rajasthan, Jaipur-302004 India.

Acta Chimica Academiae Scientiarum Hungaricae, 84 (4), pp. 467—469 (1975)

ACETOLYSIS OF *O*-TETRAACETYL-1-DEOXY-1-(2',4'-DINITROPHENYLHYDRAZINO)-D-GLUCOPYRANOSE

(SHORT COMMUNICATION)

Á. GERECS

(Department of Chemical Technology, Eötvös Loránd University, Budapest)

Received March 1, 1974

In the acetolysis of 2,3,4,6-O-tetraacetyl-1-deoxy-1-(2',4'-dinitrophenylhidrazino)-β-D-glucopyranose (**I**) (Ac_2O, AcOH, NaOAc, 100 °C), 2,3,4,5,6-O-pentaacetyl-D-glucose-2',4'-dinitrophenylhydrazone (**II**) is not the only product. O-Tetraacetyl-D-gluconic $\prec 1.5 \succ$ lactone-2',4'-dinitrophenylhydrazone is formed as a by-product and anomerization also takes place, depending on the acetic acid content of the reaction mixture; this process is fast in acetic acid but slow in acetic anhydride. The β-anomer of **I** is a chromatographically pure, crystalline substance, the α-anomer could be detected by means of paper chromatography only in amorphous mixtures. They suffered acetolysis in acetic anhydride yielding compound **II**; the reaction is fast in the case of the former substance, and slow for the latter, as shown paper chromatographically.

In a previous paper [1] we have reported on the possibility of the conversion of 2,3,4,6-O-tetraacetyl-1-deoxy-1-(2',4'-dinitrophenylhydrazino)-D-glucopyranose (**I**) into O-pentaacetyl-D-glucose-2',4'-dinitrophenylhydrazone (**II**) with acetic anhydride in the presence of sodium acetate catalyst. Subsequently the progress of the reaction was followed by measuring the change in specific rotation, which permitted a comparison of the stabilities of the pyranose ring in different 1-deoxy-1-(arylhydrazino)-pyranose derivatives [2].

In the acetolysis of **I**, the specific rotation is always lower than expected *i.e.* that of **II**. It has been established that the acetic acid content of acetic anhydride affects the rate of the reaction, but the cause of this was not investigated then. Some recent experimental observations related to this phenomenon are described here.

Some results of the experiments carried out at various acetic anhydride to acetic acid ratios are shown in Fig. 1.

It can be seen from the results that the overall reaction rate decreases with increasing acetic acid content and, slower process becomes predominant after the initial faster reaction.

The acetolysis experiments were carried out in a reaction mixture with the following composition: paper chromatographically pure compound **I** (0.200 g), acetic anhydride or a mixture of acetic anhydride and acetic acid (20 ml), anhydrous sodium acetate (0.100 g). Temperature 100 °C. The specific rotation of **I** and **II** are $[\alpha]_D^{20} = 0.0°$ ($c = 1$) and $[\alpha]_D^{20} = +83.0°$ ($c = 1$), respectively, in the given reaction mixture.

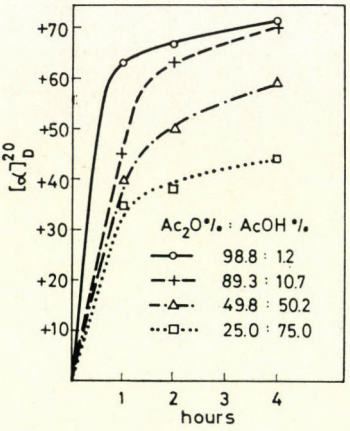

Fig. 1

In acetic acid medium (in the absence of sodium acetate), compound **I** is converted at 100 °C within 15—20 min into an equilibrium mixture (**III**) having a specific rotation of $[\alpha]_{20}^{D} = +30°$ (Fig. 2). This is evidently the equilibrium mixture of the two anomers. The anomerization also takes place in acetic anhydride at 100 °C, but at a significantly lower rate, as shown in Fig. 2. The curve representing the course of the reaction indicates presumably the sum of the increase in specific rotation brought about by the anomerization and a limited acetolysis reaction.

The formation of an equilibrium mixture was confirmed by the following experiments, too. A solution of **I** (1.00 g) in acetic acid (100 ml) was heated at 100 °C for 2 hrs, thus $[\alpha]_D^{20} = 0.0° \rightarrow 31°$. The solution was concentrated in vacuum and mixed with water; the product was separated and dried, yielding **III** (1.00 g). This was extracted with ice-cold methanol (3×3 ml). The insoluble residue was **IV** (0.45 g), $[\alpha]_D^{20} = +0.04°$ (AcOH, $c = 1$). The residue from the methanolic solution was an amorphous substance (**V**), with $[\alpha]_D^{20} = +43°$ (AcOH, $c = 1$). Based on the composition of **I** ($C_{20}H_{24}O_{13}N_4$), calcd. N 10.60; found N 10.54; 10.57%. Compound **IV**, like **V**, is converted within 30 min in acetic acid at 100 °C into a mixture of specific rotation $[\alpha]_D^{20} = +30°$.

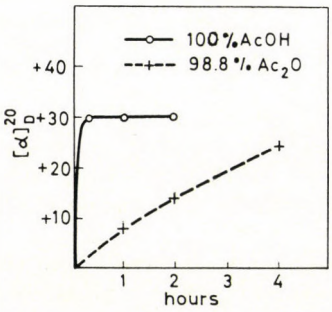

Fig. 2

The above substances and mixtures have been subjected to paper chromatographic examination, using Whatman 3 paper, and a developing mixture consisting of *n*-hexane and methyl ethyl ketone in 100 : 16 volume ratio. 0.1 ml of a 0.1% solution of the substance to be tested was applied at the starting line, and the dried paper was sprayed with 1*N* NaOH after developing for a 5 1/2 hr period. Compound **I** produced an elongated brown spot, $R_f = 0.49$, while **II** gave a circular brown spot, $R_f = 0.83$. In the chromatograms of **III**, **IV**, **V**, characteristic circular red spots with $R_f = 0.76$, 0.73 and 0.74, respectively, were observed indicating the presence of the α-anomer, in addition to the spot due to **I**.

The anomer mixture **V** has been subjected to further fractionation by dissolving it in benzene, then precipitating the various fractions from the solution with carbon tetrachloride. The pure α-anomer could not be obtained in this way either, only a mixture enriched in the α-anomer, as indicated by the value of specific rotation and the paper chromatographic test. **V** (1.60 g) yielded an amorphous fraction (**VI**) (0.167 g) with a specific rotation of $[\alpha]_{20}^{D} = +51.5°$ (AcOH, $c = 1$).

After the acetolysis of **V** (99.73% Ac_2O, NaOAc, 4 hrs at 100 °C), the red spot indicating the presence of the α-anomer did not disappear. On the contrary, in the acetolysis of **I** (98.35% AcO_2, NaOAc, 4 hrs at 100 °C), this red spot was not observed, while a brown spot with $R_f = 0.67$ representing by-product **VII** appeared. This proved to be identical with O-tetraacetyl-D-gluconic-⟨1,5⟩-lacton-2',4'-dinitrophenylhydrazone obtained as the by-product in the acetylation of **I** carried out in the presence of quinoline or pyridine [3], and this was the main product in the oxidation of **I** [4]. Its structure has been verified by NMR investigations [4].

Lactone-hydrazone **VII** was also isolated in the following way: the raw product (5.1 g) obtained on acetolysis of **I** (5 g) (97.77% Ac_2O, NaOAc, 4 hrs at 100 °C) was dissolved in ethyl acetate (20.4 ml) and petroleum ether (27 ml) was added to it, resulting in the separation of crystalline raw **VII** (0.63 g, 12.5%). M.p. 190—193 °C, $[\alpha]_D^{20} = +46.7°$ ($CHCl_3$, $c = 1.00$). After recrystallization from methanol, m. p. 193—194.5 °C, mixed m. p. with authentic sample 194 °C. The R_f value was also identical with that of the authentic sample.

$C_{20}H_{22}O_{13}N$ (526.428). Calcd. C 45.63; H 4.21; N 10.64. Found C 45.38; 45.42; H 4.40; 4.48; N 10.65; 10.60%.

After isolating **VII**, the raw hydrazone **II** was obtained (3.9 g, 71%). M. p. 108—112 °C, $[\alpha]_D^{20} = +87.5°$ ($CHCl_3$, $c = 1$).

*

The author thanks Mrs. M. BARTA for the valuable technical assistance and to Mrs. Dr. M. BALOGH for the microanalyses.

REFERENCES

[1] GERECS, Á., SOMOGYI, L., KÓNYA, A., BUKOVECZ, M.: Acta Chim. Acad. Sci. Hung., **30,** 95 (1962); Magy. Kém. Foly., **68,** 492 (1962)
[2] FÓTI, A., GERECS, Á., RUFF, F.: Acta Chim. Acad. Sci. Hung., **47,** 221 (1965); Magy. Kém. Foly., **72,** 176 (1966)
[3] GERECS, Á., FÓTI, A., RUFF, F.: Acta Chim. Acad. Sci. Hung., **42,** 145 (1964)
[4] RUFF, F., SCHUSTER, I., GERECS, Á.: Acta Chim. Acad. Sci. Hung., **57,** 111 (1968)

Árpád GERECS; 1088 Budapest, Múzeum krt. 6—8, Hungary.

Acta Chimica Academiae Scientiarum Hungaricae, 84 (4), pp. 471—475 (1975)

SYNTHESIS OF *THREO-* AND *ERYTHRO-β-o-* TOLYLSERINE AND THEIR DERIVATIVES

A. HAJÓS

(Pharmaceutical Research Institute, Budapest)

Received March 1, 1974

The main product of the addition of glycine to *o*-tolualdehyde in the presence of aqueous sodium hydroxide is *threo-β-o*-tolylserine, while the by-product formed in small amounts is *erythro-β-o*-tolylserine. The ester derivatives of both compounds can be reduced to the corresponding aminoalcohols with boron hydrides in high yield.

The derivatives of β-phenylserine and the corresponding aminoalcohols have been extensively studied because of the similarity of their structures to those of biologically active compounds. It has been known for more than 80 years that the addition of glycine to benzaldehyde in the presence of aqueous sodium hydroxide leads to β-phenylserine *via* the corresponding Schiff base [1, 2, 3], but the actual configuration of the compound, which is identical with that of threonine [4], was determined only in 1950. According of subsequent studies, *erythro-β*-phenylserine can also be isolated in small amounts [5, 6]; during the first hour of the reaction period, its amount is nearly equal to that of the *threo* isomer, but on further standing the *erythro*-isomer is converted into the *threo* compound almost completely [7]. This interesting phenomenon is probably due to an isomerization process taking place *via* retrograde aldol addition [8]. Direct addition of glycine to hydroxybenzaldehydes cannot be carried out; the hydroxy and dihydroxy-β-phenylserines can be prepared only in the reaction of the appropriate benzyloxybenzaldehydes with glycine in the presence of potassium hydroxide. Here the main product of the reaction is again the *threo* isomer [9]. Addition of glycine to *p*-nitrobenzaldehyde can be achieved in the presence of calcium hydroxide, however, in this case only the *threo* isomer has been isolated [10].

In the knowledge of these results, our aim was to study the reaction of tolualdehydes with glycine.

In the case of *o*-tolualdehyde the reaction proceeds in a manner quite similar to that of benzaldehyde, and 48% *threo-* and 4.5% *erythro-β-o*-tolylserine are formed under the usual conditions. The configuration of the diastereomers can be assigned on the basis of the characteristic R_f values, being higher for the *threo* isomer [7, 8] in the system applied, as well as by the IR spectra,

in which a band characteristic of the *erythro* isomer appears at 840—834 cm^{-1} [9].

In order to prepare the appropriate aminoalcohol, *threo-β-o*-tolylserine (**I**) was converted into the crystalline N-acetyl-*threo-β-o*-tolylserine ethyl ester (**II**), and the product was reduced with complex hydrides. Lithium aluminium hydride suggested for the reduction of phenylserine esters in the literature [6, 11] could not be utilized here, since even in inverse application of the reducing agent the main product formed was *threo*-1-(*o*-methylphenyl)-2-ethyl-amino-1,3-propanediol. By the use of calcium or sodium borohydride, however, the desired product, *threo*-1-(*o*-methylphenyl)-2-acetyl-amino-1,3-propanediol (**III**) could be obtained in high yield; subsequent hydrolysis with

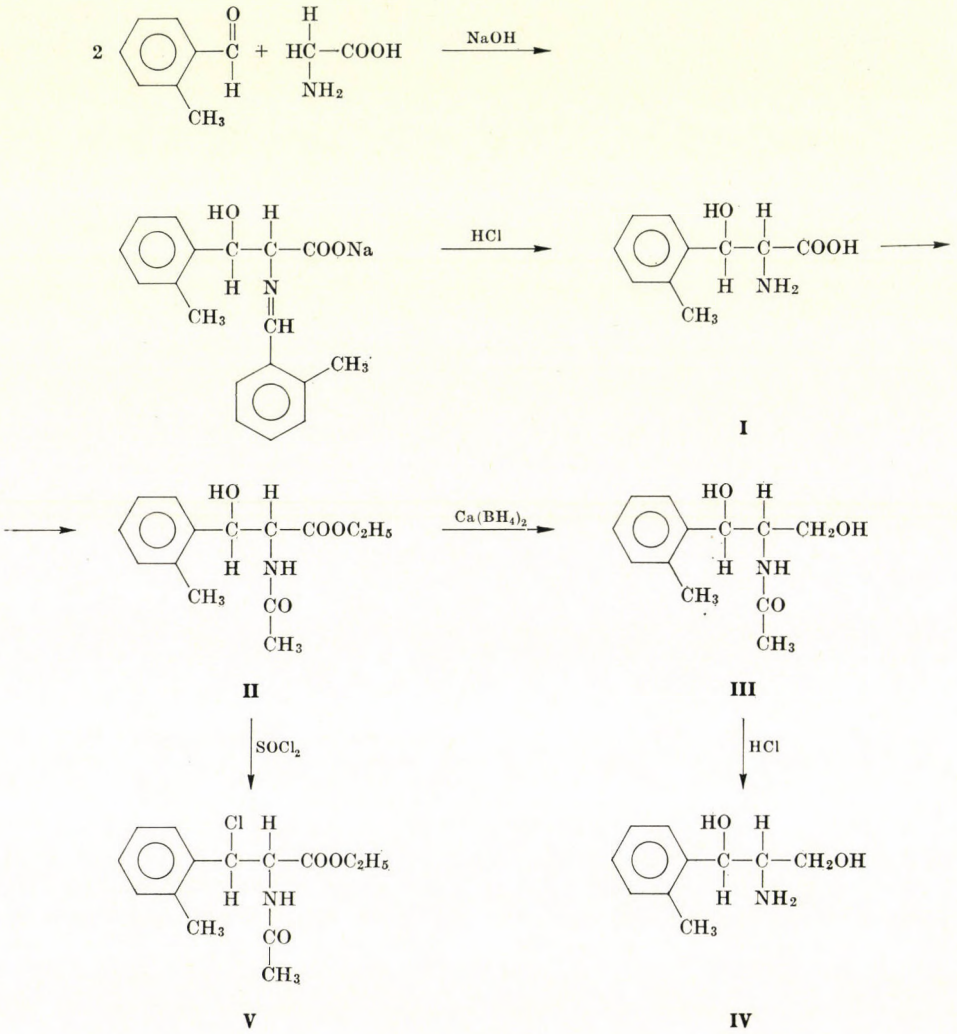

hydrochloric acid resulted in *threo*-1-(*o*-methylphenyl)-2-amino-1,3-propanediol (**IV**). In the reaction of **II** with thionyl chloride *threo*-3-chloro-3-(*o*-methylphenyl)-2-acetyl-amino-propionic acid ethyl ester (**V**) was formed in a manner characteristic of the *threo* isomer, similarly to the corresponding phenylserine derivative [5] but in a higher yield, with presumably unchanged configuration [12]. It is well known that N-acetyl-*erythro*-β-phenylserine ethyl ester forms oxazoline with inversion under similar conditions [13]. It is noteworthy that in the threonine series, both diastereomers can be converted into oxazoline [14, 15].

The 2,3-di- and triacetyl derivatives of **IV** have also been prepared. *Erythro*-β-*o*-tolylserine, like the *threo* isomer, can be converted into N-acetyl-*erythro*-β-*o*-tolylserine ethyl ester (**VI**), which yields *erythro*-1-(*o*-methylphenyl)-2-amino-1,3-propanediol (**VII**) on reduction with calcium borohydride and subsequent hydrolysis of the raw product:



VI **VII**

Experimental

Threo- and erythro-β-O-tolylserine

Sodium hydroxide (3.62 g) and glycine (4.55 g) were dissolved in a mixture of water (15 ml) and ethanol (2 ml) at 0 °C, then *o*-tolualdehyde (14.7 g) was added to it and stirred at 0 °C for 15 min. The mixture solidified into a crystalline mass; this was heated to 30 °C and the homogeneous melt obtained was refrigerated overnight followed by the addition of concentrated hydrochloric acid (7.4 ml). The crystals separated were filtered off; 9.67 g of product was obtained. M. p. 192—195 °C (d.) The substance was dissolved in water (100 ml) and precipitated with ethanol (100 ml); the precipitate was filtered off, yielding *threo*-β-*o*-tolylserine (5.70 g). M. p. 203—204 °C (d.). Yield: 48%. The R_f value is 0.56 on a Kieselgel-HF layer, in a developing mixture consisting of butanol, acetone, ammonia and water (8 : 1 : 1 : 6).

$C_{10}H_{13}NO_3$ (195.2). Calcd. C 61.53; H 6.71; N 7.17. Found C 61.45; H 6.24; N 7.29%.

The product (1 g) separated from the mother liquor was dissolved in water (10 ml). Addition of ethanol (20 ml) afforded *erythro*-β-*o*-tolylserine (0.53 g). M. p. 201 °C (d.). Yield: 4.5%. The R_f value is 0.44 on a Kieselgel-HF layer, in a developing mixture consisting of butanol, acetone, ammonia and water (8 : 1 : 1 : 6).

$C_{10}H_{12}NO_3$ (195.2). Calcd. C 61.53; H. 6.71; N 7.17. Found C 61.55; H 6.63; N 7.16%.

N-Acetyl-threo-β-*o*-tolylserine ethyl ester

Threo-β-*o*-tolylserine (26.8 g) was refluxed in absolute ethanol (500 ml) for 5 hrs while introducing hydrochloric acid into the solution. This was evaporated to dryness in vacuum, then the oily product obtained (48.9 g) was dissolved in water (100 ml), then 1% sodium carbonate solution (450 ml) and acetic anhydride (25 ml) were added dropwise during a 15 min period while stirring vigorously at 0 °C. After stirring for 1 hr the precipitate separated was

filtered off. 23.80 g of product was obtained after drying. M. p. 161—165 °C. After recrystallization from ethanol (150 ml) 20.85 g of the substance was obtained. M. p. 174—175 °C. Yield: 57%.

$C_{14}H_{19}N_2O_4$ (265.3). Calcd. C 63.38; H 7.22; N 5.28. Found C 63.18; H 7.42; N 5.37%.

Threo-1-(*o*-methylphenyl)-2-ethylamino-1,3-propanediol

A solution of $LiAlH_4$ (1.30 g) in absolute ether (60 ml) was added dropwise to a solution of N-acetyl-*threo-β-o*-tolylserine ethyl ester (2.65 g) in ether (60 ml) under nitrogen atmosphere while stirring. A slight increase in the temperature of the solution could be observed. The mixture was stirred at room temperature for 3 hrs, then water (5 ml) was added; the precipitate separated was filtered off and the ethereal mother liquor was evaporated to dryness, the residue (1.25 g) was filtered with benzene. Weight after drying: 0.90 g. M. p. 91—93 °C. Yield: 43%. After recrystallization from benzene, m. p. 95—96 °C.

$C_{12}H_{19}NO_2$ (209.3). Calcd. C 68.89; H 9.14; N 6.68. Found C 68.41; H 9.24; N 6.26%.

The inorganic precipitate was dissolved in 2*N* hydrochloric acid (100 ml), the solution was made alkaline, filtered, then extracted with 3×50 ml of ethyl acetate; the extract was evaporated to dryness, the crystalline residue (0.35 g) was filtered with benzene. 0.25 g of *threo*-1-*o*-methyl-phenyl-2-acetylamino-1,3-propanediol was obtained. M. p. 194—195 °C. Yield: 11%.

Threo-1-(*o*-methylphenyl)-2-acetyl-amino-1,3-propanediol

(a) $CaCl_2 \cdot 2\,H_2O$ (2.2 g) was dissolved in absolute ethanol (75 ml) and a solution of $NaBH_4$ (1 g) in absolute ethanol (75 ml) was added dropwise at —50 °C under cooling with dry ice-acetone and stirring. N-Acetyl-*threo-β-o*-tolylserine ethyl ester (2.65 g) was added to the mixture, and it was stirred at —20 °C for 7 hrs, then refrigerated overnight. The sodium chloride precipitate was filtered off, the mother liquor was evaporated to dryness, and the residue was taken up with 1*N* hydrochloric acid (20 ml). The crystals separated were filtered off and washed with ethanol. 2.22 g of the product was obtained. M. p. 200—201 °C. Yield: 100%. After recrystallization from absolute ethanol, m. p. 203—204 °C.

$C_{12}H_{17}NO_3$ (223.3). Calcd. C 64.58; H 7.67; N 6.27. Found C 64.24; H 7.73; N 6.19%.

(b) When the reduction was carried out in tetrahydrofuran (100 ml) with the same amounts of reagents at 30 °C for 8 hrs, 1.90 g of the product was obtained. M. p. 198—200 °C. Yield 85%.

(c) A solution of $NaBH_4$ (0.5 g) and N-acetyl-*threo-o*-tolylserine ethyl ester (1.33 g) in absolute ethanol (100 ml) was stirred at room temperature for 8 hrs, then allowed to stand overnight at room temperature and evaporated to dryness in vacuum. The crystalline residue was mixed with 1*N* hydrochloric acid (15 ml) and filtered off. After drying the weight of the product was 1.01 g. M. p. 193—194 °C. Yield 91%. After recrystallization from absolute ethanol, m. p. 203—204 °C.

Threo-1-(*o*-methylphenyl)-2-amino-1,3-propanediol

Threo-1-*o*-methylphenyl-2-acetylamino-1,3-propanediol (1 g) was hydrolyzed with 2*N* hydrochloric acid (10 ml) on a boiling water bath for 1 hr, the solution was clarified with carbon, made alkaline with 2*N* sodium hydroxide solution (13 ml), extracted with ethyl acetate (3×20 ml) and the extract evaporated to dryness. A crystalline substance (0.74 g) was obtained, it was filtered with benzene. After drying the weight of the product was 0.61 g. M. p. 102—106 °C. After recrystallization from benzene (60 ml), the weight of the product was 0.45 g. M. p. 115—117 °C. Yield 56%.

$C_{10}H_{15}NO_2$ (181.2). Calcd. C 66.30; H 8.34; N 7.75. Found C 66.26; H 8.38; N 8.04%.

N,N,O-Triacetyl-threo-1-(*o*-methylphenyl)-2-amino-1,3-propanediol

Threo-1(*o*-methylphenyl)-2-acetylamino-1,3-propanediol (0.2 g) was dissolved in absolute pyridine (1 ml), and acetic anhydride (1 ml) was added while cooling with ice. The solution was allowed to stand overnight at room temperature, evaporated to dryness in vacuum, the residue was dissolved in ether (40 ml), washed with 1*N* hydrochloric acid (2×10 ml) and water (2×10 ml), and the ethereal solution was concentrated after drying. 0.16 g of crystalline product was obtained. M. p. 114—115 °C. Yield 58%.

$C_{16}H_{21}NO_2$ (307.3). Calcd. C 62.54; H 6.89; N 4.56. Found C 61.91; H 6.85; N 4.45%.

Threo-1-(*o*-methylphenyl)-2-acetyl-amino-3-acetyl-oxy-propanol

Threo-1-(*o*-methylphenyl)-2-amino-1,3-propanediol (0.5 g) was suspended in absolute benzene (22 ml) and acetyl chloride (0.74 ml) was added while stirring at room temperature. The mixture was stirred at room temperature for 1 hr, and ice-water (19 ml) was added. The aqueous phase was separated, the pH was adjusted to 8 with concentrated ammonia solution (1 ml) under cooling, and extracted with ether (3×25 ml). The ethereal solution was dried, then evaporated to dryness; the residue was crystallized from benzene. 0.31 g of the product was obtained. M. p. 136—137 °C. Yield 43%.

$C_{14}H_{19}NO_4$ (265.3). Calcd. C 63.36; H 7.22; N 5.28. Found C 63.47; H 7.05; N 4.99%.

N-Acetyl-erythro-β-*o*-tolylserine ethyl ester

The substance was prepared from *erythro-β-o*-tolylserine similarly to the procedure applied for the corresponding *threo* isomer. Yield 61%. M. p. 126—127 °C (ethanol).

$C_{14}H_{19}N_2O_4$ (265.3). Calcd. C 63.38, H 7.22; N 5.28. Found C 63.48; H 7.38; N 5.39%.

Erythro-1-(*o*-methylphenyl)-2-amino-1,3-propanediol

It was prepared from N-acetyl-*erythro-β-o*-tolylserine ethyl ester similarly to the procedure used for the corresponding *threo* isomer. The reduction step was carried out with calcium borohydride in ethanol. Yield 45%. M. p. 102—103 °C (from benzene).

$C_{10}H_{15}NO_2$ (181.2). Calcd. C 66.30; H 8.34; N 7.75. Found C 66.50; H 8.42; N 7.86%.

Threo-3-chloro-3-(*o*-methylphenyl)-2-acetyl-amino-propionic acid ethyl ester

N-Acetyl-*threo-β-o*-tolylserine ethyl ester (0.5 g) was stirred with thionyl chloride (5 ml) at room temperature for 30 min, then the solution was poured into 10% sodium carbonate (50 ml) under cooling. The precipitate separated was filtered off, dried and crystallized from benzene–petroleum ether. Weight: 0.20 g. M. p. 95—97 °C. Yield 38%.

$C_{14}H_{18}ClNO_3$ (283.7). Calcd. C 59.27; H 6.39; Cl 12.46; N 4.93. Found C 58.98; H 6.36; Cl 12.15; N 5.14%.

*

The author thanks the Microanalytical Department of the Institute for the microanalyses, and Dr. P. SOHÁR for recording the infrared spectra.

REFERENCES

[1] ERLENMEYER, E.: Ber., **25,** 3445 (1892)
[2] ERLENMEYER, E., FRÜSTÜCK, E.: Liebigs Ann. Chem., **284,** 36 (1894)
[3] ERLENMEYER, E., BADE, F.: Liebigs Ann. Chem., **337,** 222 (1904)
[4] VOGLER, K.: Helv. Chim. Acta, **33,** 2111 (1950)
[5] FONES, W. S.: J. Org. Chem., **17,** 1534 (1952)
[6] SHAW, K. N. F., FOX, S. M.: J. Amer. Chem. Soc., **75,** 3417 (1953)
[7] SHAW, K. N. F., FOX, S. M.: J. Amer. Chem. Soc., **75,** 3421 (1953)
[8] HAJÓS, A., KOLLONITSCH, J.: Acta Chim. Acad. Sci. Hung., **17,** 449 (1958)
[9] BOLHOFER, W. A.: J. Amer. Chem. Soc., **76,** 1322 (1954)
[10] ERHART, G.: Chem. Ber., **86,** 483 (1953)
[11] CARRARA, G., WEITNAUER, G.: Gazz. Chim. Ital., **79,** 856 (1949)
[12] INGOLD, C. K.: Structure and Mechanism in Organic Chemistry, Cornell University Press, Ithaca, New York 1953, p. 393
[13] BOLHOFER, W. A.: J. Amer. Chem. Soc., **74,** 5459 (1952)
[14] ELLIOT, D. F.: J. Chem. Soc., **62,** (1950)
[15] PFISTER, K., ROBINSON, C. A., SHABICA, A. C., TISHLER, M.: J. Amer. Chem. Soc., **71,** 1101 (1949)

Andor HAJÓS; 1045 Budapest, Szabadságharcosok útja 47. Hungary.

Acta Chimica Academiae Scientiarum Hungaricae, 84 (4) pp. 477—479 (1975)

SYNTHESIS OF ARYLIDENE-*BIS* (PHENYLACETAMIDES)

(SHORT COMMUNICATION)

GY. DEÁK, K. GÁLL-ISTÓK and L. HAZAI

(Institute for Medical Research of the Hungarian Academy of Sciences, Budapest)

Received August 20, 1974

Arylidene-*bis*(phenylacetamides) [2] are key compounds in the synthesis of 1-aryl-1,4-dihydro-3(2H)-isoquinolinones [1] having significant biological activity. Previously, extensive investigations dealt with the formation of these compounds from arylacetonitriles or arylacetamides [3]. The aim of the present study was to elucidate whether the method is also suitable for the synthesis of derivatives carrying alkyl group(s) at the methylene groups of the *bis*-amide. On the basis of kinetic measurements [2], an unfavourable effect of the chain branching at the α-position could be expected on the reaction proceeding between the aromatic aldehyde and the nitrile, presumably because of steric reasons:

$$\mathrm{ArCHO} + 2\ \mathrm{Ar'CR^1R^2CN} \xrightarrow[\mathrm{H_2SO_4}]{\mathrm{AcOH}} \mathrm{ArCH(NH{-}CO{-}CR^1R^2{-}Ar')_2}$$

The reaction was accomplished in anhydrous acetic acid, in the presence of concentrated sulfuric acid catalyst. The data of the new *bis*-amide derivatives are shown in Table I.

As it can be seen in the Table, alkyl substitution in the α-position significantly reduces the yield of the *bis*-amide. The hindering effect is particularly striking in the case of disubstitution, when a prolonged reaction period is necessary for the formation of the product with benzaldehyde. It is worth noting that the chain length of the alkyl substituent strongly influences the extent of conversion. Another interesting feature of this reaction is that methyl and phenyl substituents give rise to nearly the same reduction in yield.

Benzylidene-*bis*(phenylisobutyramide) has also been synthesized from isobutyramide by GILBERT's method [4], but the yield was even lower (29%) than in the acetic acid procedure.

Table I

$$Ar-CH\begin{cases}NH-CO-CR^1R^2-C_6H_5\\NH-CO-CR^1R^2-C_6H_5\end{cases}$$

Arylidene bis (phenylacetamides)

R^1	R^2	Ar	Reaction time, hr	Reaction temp. °C	Yield %	M p.* °C (Solvent of cryst.)	Analysis Calcd./found C	H	N
H	H	C_6H_5 (3)	24	20	75	—	—	—	—
Me	H	C_6H_5	24	20	35	224 (DMF)	77.69 77.59	6.79 6.75	7.25 7.24
Me	Me	C_6H_5	168	20	31	167—68 (EtOAc)	78.22 78.14	7.29 7.44	6.76 6.71
Me	Me	*p*-NO_2—C_6H_5	24	20	25	183—85 (EtOH)	75.16 74.96	6.77 6.37	3.15 3.14
iPr	H	C_6H_5	24	40	26	260—62 (MeOH)	78.70 78.77	7.77 8.14	6.33 6.52
iPr	H	*p*-NO_2—C_6H_5	48	40	17	279 (DMF)	71.44 71.53	6.83 7.06	8.62 8.75
iPr	Me	C_6H_5	48	40	—	—	—	—	—
Bu	H	C_6H_5	72	20	8	226—28 (DMF–EtOH)	79.09 78.82	8.14 8.16	5.95 6.16
C_6H_5	H	C_6H_5	48	20	36	271—72 (PrOH)	82.34 82.54	5.92 6.38	5.49 5.29
C_6H_5	H	*p*-NO_2—C_6H_5	48	20	33	302—03 (DMF)	75.66 75.70	5.26 5.51	7.56 7.44

* Melting points are uncorrected

Experimental

Materials α-Phenylpropionitrile was prepared according to the procedure proposed by MOHASZA [5]. The other nitriles were synthesized TARANKO and PERRY's [6] method in DMSO solution.

Bis amides

These were synthesized as described formerly [3].

REFERENCES

[1] Hung. Pat. 5,372; C. A. **78,** 159458 (1972)
[2] DEÁK, GY., GÁLL-ISTÓK, K., KÁLMÁN, ZS., HASKÓ-BREUER, J.: Acta Chim. (Budapest) **76,** 299 (1973)

[3] CSŰRÖS, Z., DEÁK, GY., HARASZTHY-PAPP, M., HOFFMANN, I.: Acta Chim. Acad. Sci. Hung. **59,** 119 (1969)
[4] GILBERT, E. E.: Synthesis, **1972,** 30
[5] MOHASZA, H.: Rocz. Chem. **39,** 1401 (1965)
[6] TARANKO, L. B., PERRY, R. H.: J. Org. Chem., **34,** 226 (1969)

Gyula DEÁK
Klára GÁLL-ISTÓK
László HAZAI
1083 Budapest, Szigony u. 43. Hungary.

INDEX

PHYSICAL AND INORGANIC CHEMISTRY – PHYSIKALISCHE UND ANORGANISCHE CHEMIE – ФИЗИЧЕСКАЯ И НЕОРГАНИЧЕСКАЯ ХИМИЯ

BERECZ, E.: Study of the Viscosity of Metal Chloride–H_2O and Metal Chloride–HCl–H_2O Systems 353

SOHÁR, P., OCSKAY, GY., VARGHA, L.: Distinction between *Syn* and *Anti* Ketoximes of 2-Acyl-Furans and Their Condensed Analogues by Their NMR Spectra 381

SRIVASTAVA, R. D., SUSHIL KUMAR: Electrodeposition of Cobalt, II. Cathode Polarization and Grain Size of the Deposit 385

KISS, A. B.: Infrared Vibrational Frequencies of Reduced Tungsten Oxides WO_{3-x} $(1 \geq x > 0)$ 393

TAMÁS, J., HEGEDÜS-VAJDA, J., DANCSI, L., KISFALUDY, L.: Mass Spectra of Some α-Aminooxy Acid Derivatives 409

SINGH, S. P., TANDON, J. P.: pH-Metric Studies on the Mixed-Ligand Chelates of Oxovanadium(IV) with Picolinic Acid and Some Dicarboxylic Acids 419

HEISZMAN, J., PAYER, K., BÉKÁSSY, S., PETRÓ, J.: Complex Study of Nickel Skeleton Catalysts, I. Thermal Desorption Method and Apparatus for the Study of Hydrogenation Catalysts 431

PAÁL, Z., THOMSON, S. J., WEBB, G., MCCORKINDALE, N. J.: Interactions of Unsaturated Hydrocarbons with Platinum Catalysts: Involving Reactions, Retention, Deactivation and Regeneration 445

SINGH, O. P., PRASAD, R. N., TANDON, J. P.: Tin(IV) Complexes of Schiff Bases Derived from *o*-Hydroxyacetophenone and Aminoalcohols 459

ORGANIC CHEMISTRY – ORGANISCHE CHEMIE – ОРГАНИЧЕСКАЯ ХИМИЯ

GERECS, Á.: Acetolysis of *o*-Tetraacetyl-1-deoxy-1-(2′,4′-Di-nitrophenylhydrazino)-D-Glucopyranose (Short Communication) 467

HAJÓS, A.: Synthesis of *Threo-* and *Erythro-β-o*-Tolylserine and Their Derivatives 471

DEÁK, GY., GÁLL-ISTÓK, K., HAZAI, L.: Synthesis of Arylidene-*bis*(phenylacetamides) (Short Communication) 477

Printed in Hungary

A kiadásért felel az Akadémiai Kiadó igazgatója — Műszaki szerkesztő: Zacsik Annamária

A kézirat nyomdába érkezett: 1974. XII. 23. — Terjedelem: 11,9 (A/5) ív 67 ábra

75.1260 Akadémiai Nyomda, Budapest — Felelős vezető: Bernát György

ACTA CHIMICA

ТОМ 84—ВЫП. 4

РЕЗЮМЕ

Исследование вязкости систем хлорид металла – H_2O и хлорид металла – $HCl – H_2O$

Э. БЕРЕЦ

Исследованы вязкости водных и солянокислых растворов хлоридов щелочных и редкоземельных металлов.

На онове сравнительного изучения хода кривых вязкость — концентрация для бинарных смесей, а также на основе величины и направления изменений вязкости, происходящих при добавлении третьего компонента к бинарным растворам, были сделаны заключения относительно структуры растворов, а также их зависимости от концентрации в бинарных и тройных системах.

Исходя из полученной зависимости вязкости от концентрации для бинарных смесей, были предложены аналитические и графические методы расчета вязкости для тройных систем.

Отличие син-кетоксимов 2-ацилфуранов от их анти-изомеров, а также их конденсированных аналогов с помощью спектров ЯМР

П. ШОХАР, ДЬ. ОЧКАИ и Л. ВАРГА

Син- и *анти*-изомеры 2-ацилфураноксимов, незамещенных в положении 3, могут быть легко различены с помощью спектров ЯМР. Синглет H-3 сильно смещен парамагнитно в случае *син*-изомера по сравнению с *анти*-изомером ($\Delta\delta \cong 0{,}75$ ppm), вследствие анизотропного эффекта оксимной группы.

Электропокрытие кобальта, II

Поляризация катода и размеры зерен покрытия

Р. Д. СРИВАСТАВА и С. КУМАР

Было исследовано влияние плотности тока, температуры и pH на поляризацию катода, стойкость к коррозии электропокрытия под влиянием атмосферы и на размеры зерен электропокрытия кобальта в некоторых ваннах электропокрытия кобальта. Увеличение плотности тока увеличивает поляризацию и уменьшает размеры зерен покрытия. Повышение температуры ванны уменьшает поляризацию и стойкость к коррозии и увеличивает размеры зерен. Уменьшение pH ванны вызывает понижение стойкости к коррозии и увеличение размеров зерен.

ИК колебательные частоты восстановленных окислов WO_{-x} $(1 \geq x > 0$

А. Б. КИШ

Были исследованы ИК спектры окислов вольфрама с составом WO_{3-x} $(1 \geq x > 0)$. В интервале $0 < x < 0{,}1$ образуются окислы с триклинной, моноклинной, орторомбической и тетрагональной кристаллической решеткой, и, несмотря на отклонение от состава WO_3, их обычно называют полиморфными модификациями «WO_3». Все эти четыре типа окислов с такой симметрией — в зависимости от термической обработки и примесей — могут быть стабильными и при комнатной температуре. Т. к. спектры различных модификаций в большей или меньшей степени различаются, то поэтому при ИК спектрофотометрическом исследовании окисла, обычно называемого WO_3, необходимо выяснить, с какой модификацией имеем дело.

С помощью анализа фактора групповой симметрии D_{4h}, D_{2h}, C_{2h} и C_i могут быть определены возможное число колебаний и тип симметрии. Две сильные полосы поглощения этих окислов указывают на то, что в окислах доминируют молекулярные колебания октаэдерного элемента WO_6, и, т. о., в первом приближении окислы могут рассматриваться как искаженные модификации идеальной решетки типа ReO_3. В соответствии с этим характер ИК полос может быть определен с помощью корреляции $O_h \rightarrow D_{4h} \rightarrow D_{2h} \rightarrow C_i$. Степень расщепления частоты $2F_{1u}$ в направлении трансформационного превращения тетрагональной в триклинную структуру, т. е. в соответствии с увеличением искажения, повышается.

Сдвиг наивысших частот полос колебания ν_{W-O} строго связан со значением x, т. е. с числом мест дефектов W—O кислорода. Т. о., на основе спектра можно заключить о типе окисла, т. е. о строении. Одновременно с этим, зависимость между частотой и дефектом кислорода указывает на различия в способе встраивания дефектов кислорода и их строении в ряду окислов WO_{3-x} $(1 \geq x > 0)$. ИК спектр оказывается чувствительным и для образования т. наз. сверхрешетки $2 \times W_{20}O_{58} = W_{40}O_{116}$.

Масс-спектрометрическое исследование производных α-аминооксикарбоновых кислот

Й. ТАМАШ, Ю. ХЕГЕДЮШ-ВАЙДА, Л. ДАНЧИ и Л. КИШФАЛУДИ

Приводится масс-спектрометрическое поведение О-аминооксиуксусной кислоты и ее некоторых производных, замещенных на карбоксиле, а также на карбоксиле и аминогруппе. Фрагментация свободной кислоты протекает гораздо сложнее, чем фрагментация глицина. Масс-спектр производных — вследствие распространения фрагментации на все связи скелета открытой цепочки — снабжает подробными сведениями относительно порядка атомов в молекуле. В случае анилидов были обнаружены многие процессы перегруппировок, среди которых следует упомянуть миграцию метилена и метила.

pH-Метрическое исследование смешанных лигандных хелатов оксованадия (IV) с пиколиновой и некоторыми дикарбоксильными кислотами

С. П. СИНГ и Й. П. ТАНДОН

Описываются pH-метрические исследования взаимодействия оксованадия(IV) с пиколиновой кислотой в присутствии и отсутствии некоторых дикарбоксильных кислот (щавелевая, фталевая, малеиновая кислоты) при $30 \pm 0{,}5°C$ ($0 = 0{,}1$ KNO_3). Было обнаружено образование комплексов с составом как 1 : 1, так и 1 : 2 (VO^{+2}: пиколиновая кислота) и определены их константы стабильности: $\log K_{MA} = 5{,}93 \pm 0{,}02$ и $\log K_{MA_2} = 10{,}52 \pm \pm 0{,}11$. Константа равновесия реакции $VOA^+ + H_2O \rightleftarrows VO(OH)A + H^+$ была рассчитана в системе с составом 1 : 1 (VO^{+2}:пиколинова кислота) и равна $3{,}97 \pm 0{,}08$. В трехкомпонентных системах было обнаружено образование комплексов со смешанными лигандами с составом 1 : 1 : 1. Были определены их константы стабильности.

Комплексное исследование катализаторов с никелевым скелетом, I

Термодесорбционный метод и установка для исследования гидрирующих катализаторов

Й. ХЕЙСМАН, К. ПАЙЕР, Ш. БЕКАШИ и Й. ПЕТРО

Была разработана термодесорбционная установка для определения количества и форм водорода, сорбированного на гидрирующих катализаторах. В ней были использованы печь, специальной конструкции, и детектор со встроенными торговыми термометрами сопротивления платины. На внешнюю поверхность керамического покрытия сопротивления, находящегося в измерительной ячейке, специальным методом наносили платиновый катализатор высокой чувствительности и продолжительного времени жизни. Чувствительность детектора на два порядка превышает чувствительность ячеек теплопроводности. Воспроизводимость результатов, получаемых на установке, удовлетворительна и отклонения от средних величин не превышают 10%-ов.

На обычном и модифицированном медью никеле Ренея был обнаружен слабо и сильно связанный водород, а на катализаторах, приготовленных из сплавов Ni—Mg и Ni—Zn, было обнаружено три различных типа водорода. Общее количество водорода на последних катализаторах значительно меньше, чем на образцах из сплавов Ni—Zn.

Проводятся дальнейшие исследования в этой области.

Взаимодействие незамещенных углеводородов с платиновыми катализаторами: протекающие реакции, ретенция, дезактивация и регенерация

З. ПААЛ, С. Дж. ТОМСОН, Дж. ВЕББ и Н. Дж. МЭККОРКИНДЕЙЛЬ

Было исследовано взаимодействие этилена, циклогексана и 1-гексена с платиновыми катализаторами. Протекающие реакции объясняются, с одной стороны, диспропорционированием водорода, приводящим к гидрированию и гидрогенолизу, а с другой сторны, к образованию водородно-убедненных продуктов как в газовой фазе, так и на поверхности. Нанасыщенные углеводороды претерпевают диссоциативную адсорбцию на металле, вытесняя часть удерживаемого водорода. Были получены новые доказательства в пользу того, что адсорбция на одинарной связи приводит к гидрированию-дегидрированию, в то время Как многократные связи приводят к гидрогенолизу и задерживанию углеводородов. Селективность к реакциям гидрогенолиза и гидрования была различной на катализаторах платиновой черни и платины на силикагеле; вероятно, для протекания этих процессов требуются различные активные центры. Задерживание углеводородов является основной причиной дезактивации катализатора; удаление удерживаемых частиц требует обработки кислородом. Обработка водородом является менее эффективной. Было найдено, что протекание всех этих процессов зависит от структуры углеводородов. Задерживание и реактивация были исследованы также с помощью радиоактивной метки.

Комплексы олова(IV) с шиффовыми основаниями, полученными из о-гидроксиацетофенона и аминоспиртов

О. П. СИНГ, Р. Н. ПРАСАД и И. П. ТАНДОН

Производные типа $SnCl_4 \cdot SBH_2$ и $SnCl_4(SBH_2)_2$ были синтезированы на основе реакции хлорида олова(IV) с шиффовыми основаниями с молярными отношениями компонентов 1 : 1 и 1 : 2, в среде сухого бензола. Результирующие продукты были получены с почти количественным выходом и в состоянии с пригодной чистотой. Были сняты их ИК спектры. Данные по проводимости указывают на то, что они являются неэлектролитами.

Синтез трео- и эритро-β-о-толилсерина и его производных

А. ХАЙОШ

При присоединении глицинов к о-толуальдегиду в присутствии натриевой щелочи, в качестве главного продукта образуется трео-, а в качестве побочного продукта, в небольшом количестве, — эритро-β-о-толилсерин. Сложные эфиры этих двух соединений с боргидридными комплексами восстанавливаются с хорошим выходом до соответствующих аминоспиртов.

According to international book reviews the series
ABSORPTION SPECTRA IN THE ULTRAVIOLET AND VISIBLE REGION
started in 1959 – is highly useful in both structure research and chemical analysis.
Our Publishing House now offers you a new series on *infrared spectra!*

ABSORPTION SPECTRA IN THE INFRARED REGION

Editor of the series L. LÁNG
Introductory volume written by S. HOLLY and P. SOHÁR

Though the scientific literature has several series dealing with the same field, naturally none of them strives for completeness, and overlapping is very small. The present series is concerned with very recent spectra, including those which are not given in the original papers. The *Introductory Volume* gives a detailed discussion of the characteristic frequencies affording ample guidance for the practical spectroscopist. The most important technical information is also included.

In English. Approx. 320 pages per volume
17 × 23 cm. Loose-leaf cloth binders

AKADÉMIAI KIADÓ
Budapest

BUTTERWORTH LIMITED
London

A co-edition, – distributed in the socialist countries by *Kultura*, H-1389 Budapest P. O. B. 149; in all other countries by *Butterworth Limited*, London

ABSORPTION SPECTRA IN THE ULTRAVIOLET AND VISIBLE REGION

Series edited by L. LÁNG

According to international book reviews, this series is highly useful in both structure research and chemical analysis. This applies especially to problems of analytical character or structure determination encountered in the pharmaceutical, dye and other industries, i.e. in organic chemical industry in general. A great advantage of this collection is that the spectra published may, in many cases, directly be used for solving the particular problems in question.

The series dealing with *ultraviolet and visible spectra* was started by the Publishing House of the Hungarian Academy of Sciences in 1959, and by now the project has got as far as Vol. 18. The editors invite the users of the collection to contribute to the success of this work by submitting for publication spectra of new compounds.

Each volume contains about 400 pages spectra graphs and tables of about 190 compounds + indexes.

Cumulative index: I–V, VI–X, X–XV

AKADÉMIAI KIADÓ
Budapest

ACADEMIC PRESS
New York

The whole series is a co-edition, – distributed on the American Continent by ACADEMIC PRESS New York, in all other countries by KULTURA, H-1389 Budapest, P. O. B. 149

JOURNAL OF THERMAL ANALYSIS

An international forum for communications on thermal investigations

Journal of THERMAL ANALYSIS has an international Editorial Board, the members of which are distinguished specialists from all over the world.

AIMS AND SCOPE

The main subjects covered are: thermogravimetry, derivative thermogravimetry, differential thermal analysis, dilatometry, differential scanning calorimetry, thermometry, evolved gas detection, evolved gas analysis, multiple techniques and miscellaneous thermal methods (including the thermal method with various instrumental techniques), instrumentation for the thermal method. Papers dealing with these subjects are published in the following sections: Original Research Papers, Short Communications, Special Reviews, Bibliography Section, Modern Instruments. The Special Reviews section is reserved for papers that have been published in greater detail in some journal for a special branch of scientific field or industry.

Papers submitted to the journal may deal with any field of chemistry, metallurgy or mineralogy, e.g. they may deal with inorganic, organic or polymeric materials and they may cover biochemical, mineralogical or metallurgical applications.

Journal of THERMAL ANALYSIS is published bimonthly comprising about 720 pages per year. Size: 17×25 cm.

Journal of THERMAL ANALYSIS is published jointly by

AKADÉMIAI KIADÓ
Budapest

HEYDEN & SON LIMITED
London

RADIOCHEMICAL AND RADIOANALYTICAL LETTERS

An International Journal for RAPID Communication in Radiochemistry and Radioanalytical Chemistry

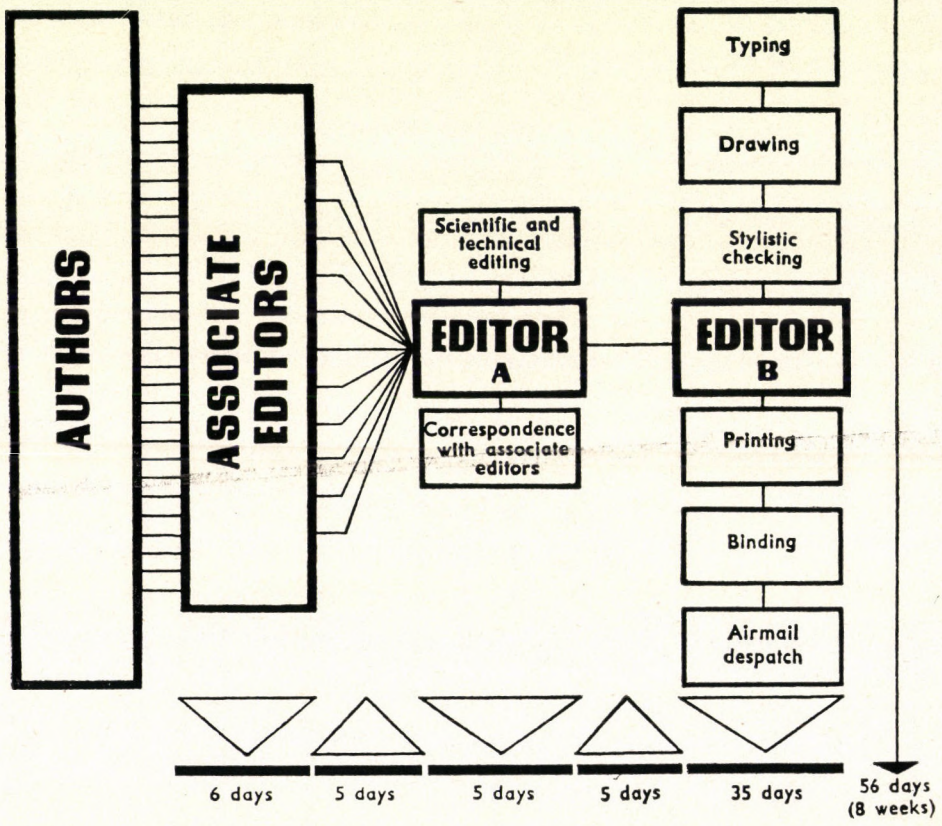

ELSEVIER SEQUOIA S.A.
LAUSANNE

AKADÉMIAI KIADÓ
BUDAPEST

ACTA ALIMENTARIA

ACADEMIAE SCIENTIARUM HUNGARICAE

publishes original papers in the field of food science and technology (physico-chemistry, chemistry, analysis, biology, microbiology, enzymology, engineering, automation and economics related to fundamental principles of the production, preparation, preservation, packaging and examination of foods) in English.

Contributions to ACTA ALIMENTARIA are regularly abstracted or indexed in all reference journals.

ACTA ALIMENTARIA is as a rule a quarterly. Four issues make up a volume of some 400 to 500 pages yearly.
Subscription rate per volume: US $32.00

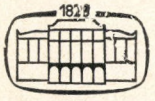

AKADÉMIAI KIADÓ
Publishing House of the
Hungarian Academy of Sciences
BUDAPEST

AKADÉMIAI KIADÓ, H-1363 Budapest, P.O.B. 24

☐ Please enter my/our subscription for ACTA ALIMENTARIA for one volume

☐ Please enter a standing order for ACTA ALIMENTARIA, beginning with

DATE . . . . . .

☐ Please send a specimen-copy free of charge

NAME . . . . . .

ADDRESS . . . . . .

JOURNAL OF RADIOANALYTICAL CHEMISTRY

International journal dealing with all aspects of nuclear analytical methods

Journal of Radioanalytical Chemistry has an international Editorial Board, whose members are distinguished specialists from all parts of the world – from Moscow to San Diego, from Prague to Tokyo.

The main subjects covered are:

Activation analysis
Radiometric analysis
Radioreagent analysis
Radiometric titration
Isotope dilution analysis
Beta, gamma X-ray and neutron absorption and backscattering
Analytical separations involving radionuclides
Instrumentation and automation for radioanalytical chemistry

Journal of Radioanalytical Chemistry provides the reader with important and up-to-date information on research being carried out all over the world. Data and Bibliography Sections and a section entitled Laboratory of the Issue help to serve this purpose.

Journal of Radioanalytical Chemistry appears generally in three or four volumes per year of some 480 to 500 pages each, published in several issues in English, French or German. Size: 17 × 25 cm.

Journal of Radioanalytical Chemistry is published jointly by

AKADÉMIAI KIADÓ
Budapest

ELSEVIER SEQUOIA
Lausanne

The Acta Chimica publish papers on chemistry, in English, German, French and Russian.

The Acta Chimica appear in volumes consisting of four parts of varying size, 4 volumes being published a year.

Manuscripts should be addressed to

Acta Chimica
Budapest 112/91 Műegyetem

Correspondence with the editors should be sent to the same address.

The rate of subscription is $ 32,00 a volume.

Orders may be placed with "*Kultúra*" Foreign Trade Company for Books and Newspapers (1389 Budapest 62, P.O.B. 149 Account No. 218 10990) or with representatives abroad.

Les Acta Chimica paraissent en français, allemand, anglais et russe et publient des mémoires du domaine des sciences chimiques.

Les Acta Chimica sont publiés sous forme de fascicules. Quatre fascicules seront réunis en un volume (4 volumes par an).

On est prié d'envoyer les manuscrits destinés à la rédaction à l'adresse suivante:

Acta Chimica
Budapest 112/91 Műegyetem

Toute correspondance doit être envoyée à cette même adresse.

Le prix de l'abonnement est de $ 32,00 par volume.

On peut s'abonner à l'Entreprise pour le Commerce Extérieur de Livres et Journaux «*Kultúra*» (1389 Budapest 62, P.O.B. 149 Compte-courant No. 218 10990) ou à l'étranger chez tous les représentants ou dépositaires.

«*Acta Chimica*» издают трактаты из области химической науки на русском, французском, английском и немецком языках.

«*Acta Chimica*» выходят отдельными выпусками разного объема. 4 выпуска составляют один том. 4 тома публикуются в год.

Предназначенные для публикации рукописи следует направлять по адресу:

Acta Chimica
Budapest 112/91 Műegyetem

По этому же адресу направлять всякую корреспонденцию для редакции.

Подписная цена — $ 32,00 за том.

Заказы принимает предприятие по внешней торговле книг и газет «*Kultúra*» (1389 Budapest 62, P.O.B. 149 Текущий счет № 218 10990) или его заграничные представительства и уполномоченные.

Reviews of the Hungarian Academy of Sciences are obtainable at the following addresses:

ALBANIA

Drejtorija Qändrone e Pärhapies dhe Propagandimit tä Librit
Kruga Konferenca e Päzes
Tirana

AUSTRALIA

A. Keesing
Box 4886, GPO
Sydney

AUSTRIA

GLOBUS
Höchstädtplatz 3
A-1200 Wien XX

BELGIUM

Office International de Librairie
30, Avenue Marnix
Bruxelles 5
Du Monde Entier
162, Rue du Midi
1000 Bruxelles

BULGARIA

HEMUS
11 pl Slaveikov
Sofia

CANADA

Pannonia Books
2, Spadina Road
Toronto 4. Ont.

CHINA

Waiwen Shudian
Peking
P. O. B. 88

CZECHOSLOVAKIA

Artia
Ve Směčkách 30
Praha 2
Poštovní Novinová Služba
Dovoz tisku
Vinohradská 46
Praha 2
Mad'arska Kultura
Václavské nám. 2
Praha 1
SLOVART A. G.
Gorkého
Bratislava

DENMARK

Ejnar Munksgaard
Nörregade 6
Copenhagen

FINLAND

Akateeminen Kirjakauppa
Keskuskatu 2
Helsinki

FRANCE

Office International de Documentation et Librairie
48, rue Gay-Lussac
Paris 5

GERMAN DEMOCRATIC REPUBLIC

Deutscher Buch-Export und Import
Leninstraße 16
Leipzig 701
Zeitungsvertriebsamt
Fruchtstraße 3—4
1004 Berlin

GERMAN FEDERAL REPUBLIC

Kunst und Wissen
Erich Bieber
Postfach 46
7 Stuttgart S.

GREAT BRITAIN

Blackwell's Periodicals
Oxenford House
Magdalen Street
Oxford
Collet's Subscription Import Department
Dennington Estate
Wellingsborough, Northants.
Robert Maxwell and Co. Ltd.
4—5 Fitzroy Square
London W. 1.

HOLLAND

Swetz and Zeitlinger
Keizersgracht 471—487
Amsterdam C.
Martinus Nijhof
Lange Voorhout 9
The Hague

INDIA

Hind Book House
66 Babar Road
New Delhi 1

ITALY

Santo Vanasia
Via M. Macchi 71
Milano
Libreria Commissionaria Sansoni
Via La Marmora 45
Firenze
Techna
Via Cesi 16.
40135 Bologna

JAPAN

Kinokuniya Book-Store Co. Ltd.
826 Tsunohazu 1-chome
Shinjuku-ku
Tokyo
Maruzen and Co. Ltd.
P. O. Box 605
Tokyo-Central

KOREA

Chulpanmul
Phenjan

NORWAY

Tanum-Cammermeyer
Karl Johansgt 41—43
Oslo 1

POLAND

Ruch
ul. Wronia 23
Warszawa

ROUMANIA

Cartimex
Str. Aristide Briand 14—18
Bucureşti

SOVIET UNION

Mezhdunarodnaya Kniga
Moscow G—200

SWEDEN

Almquist and Wiksell
Gamla Brogatan 26
S—101 20 Stockholm

USA

F. W. Faxon Co. Inc.
15 Southwest Park
Westwood Mass. 02090
Stechert Hafner Inc.
31. East 10th Street
New York, N. Y. 10003

VIETNAM

Xunhasaba
19, Tran Quoc Toan
Hanoi

YUGOSLAVIA

Forum
Vojvode Mišića broj
Novi Sad
Jugoslavenska Knjiga
Terazije 27
Beograd

5. V. 1975

Index: 26.007